FACULDADE DE ENGENHARIA DA UNIVERSIDADE DO PORTO

Communication Strategies in Cooperative Intelligent Transport Systems

António Manuel Ribeiro Pereira da Costa



Mestrado Integrado em Engenharia Informática e Computação

Supervisor: Rosaldo José Fernandes Rossetti

Second Supervisor: Pedro Miranda de Andrade de Albuquerque d'Orey

27th July 2021

Communication Strategies in Cooperative Intelligent Transport Systems

António Manuel Ribeiro Pereira da Costa

Mestrado Integrado em Engenharia Informática e Computação

27th July 2021

Abstract

Cooperative Intelligent Transport Systems (C-ITS) are an important area of development for many domains such as the automotive, telecommunication and digital security industries. Road users and traffic managers share information and use it to coordinate their actions in order to improve road safety, traffic efficiency and comfort of driving, allowing the driver to make the right decisions and adapt to the traffic situation.

The effectiveness of C-ITS solutions depends on the user's decision-making process, which is the main source of uncertainty in any mobility system. The communication problems may be diverse and may be affected by many factors, including the quality of sensors that can be used to collect useful information, the Quality of Service (QoS) of the communication infrastructure, and its ability to communicate appropriately, timely and reliably.

In this project it was designed an approach based on microscopic simulation and game theory to evaluate C-ITS solutions, in particular how information should be disseminated to produce a wider reach of demand and produce different strategies to adapt and propagate it according to different mobility scenarios and network configurations.

In a scenario with a binary road network, a game based on the n-Person Prisoner's Dilemma was formalized, in which the traveller information system, the RSU, is one of the participants together with vehicles. Taking place in a dynamic environment, in order to analyze the emergence of cooperation and improve network performance, those "accept" or "reject" a route recommendation. A set of strategies was developed to elaborate and disseminate the RSU recommendation, aiming at a predictive and non-reactive behaviour towards an optimal and fair system state, and the impact of the degradation of the RSU communication was studied. The results highlighted the need to tailor the dissemination to the cooperation rate of the vehicles and the importance of the information system in the performance and fairness of the system.

Keywords: C-ITS, Cooperative Intelligent Transport Systems, V2X, Vehicle-to-Everything Communications, VANET, SUMO, n-Person Prisoner's Dilemma

Resumo

Os Sistemas Inteligentes de Transporte Cooperativos (C-ITS) são uma área importante de desenvolvimento em muitos domínios, tais como as indústrias automóvel, telecomunicações e segurança digital. Os utilizadores das estradas e os gestores de tráfego partilham informações e utilizam-nas para coordenar as suas acções de modo a melhorar a segurança rodoviária, a eficiência do tráfego e o conforto da condução, permitindo ao condutor tomar as decisões correctas e adaptar-se à situação do tráfego.

A eficácia das soluções C-ITS depende do processo de decisão do utilizador, que é a principal fonte de incerteza em qualquer sistema de mobilidade. Os problemas de comunicação podem ser diversos e podem ser afectados por muitos factores, incluindo a qualidade dos sensores que podem ser utilizados para recolher informações úteis, a Qualidade de Serviço (QoS) da infra-estrutura de comunicação, e a sua capacidade de comunicar de forma apropriada, atempada e fiável.

Neste projecto concebeu-se uma abordagem baseada em simulação microscópica e teoria do jogo para avaliar soluções C-ITS, em particular a forma como a informação deve ser divulgada para produzir um maior alcance da procura e produzir diferentes estratégias para a adaptar e propagar de acordo com diferentes cenários de mobilidade e configurações de rede.

Num cenário com uma rede rodoviária binária, formalizou-se um jogo assente no Dilema do Prisioneiro com *n*-Pessoas, no qual o sistema de informação ao viajante, a RSU, é um dos participantes juntamente com veículos. A decorrer num ambiente dinâmico, com o intuito de analisar a emergência da cooperação e melhorar o desempenho da rede, aqueles "aceitam" ou "rejeitam" uma recomendação de rota. Desenvolveu-se um conjunto de estratégias para elaborar e disseminar a recomendação da RSU, visando um comportamento preditivo e não reactivo, no sentido de um estado óptimo e justo do sistema, e estudou-se o impacto da degradação da comunicação da RSU. Os resultados evidenciaram a necessidade de ajustar a disseminação à taxa de cooperação dos veículos e a importância do sistema de informação no desempenho e justiça do sistema.

Keywords: C-ITS, Sistemas Cooperativos de Transportes Inteligentes, V2X, Comunicações Veículo-a-Tudo, VANET, SUMO, Dilema do Prisioneiro *n*-Pessoas

Contents

1 Introduction **1**
- 1.1 Context and Motivation . . . 1
- 1.2 Problem Description . . . 2
- 1.3 Research Questions . . . 2
- 1.4 Goals and Expected Results . . . 2
- 1.5 Methodology . . . 3
- 1.6 Structure of the Document . . . 3

2 Background Knowledge **5**
- 2.1 Introduction . . . 5
- 2.2 Intelligent Transport Systems . . . 5
- 2.3 Cooperative-Intelligent Transport Systems . . . 6
- 2.4 Vehicular Communications . . . 6
  - 2.4.1 Applications . . . 8
  - 2.4.2 Routing . . . 10
  - 2.4.3 Dissemination of Information . . . 11
- 2.5 Social Dilemmas and Cooperation . . . 11
  - 2.5.1 *n*-Person Prisoner's Dilemma . . . 12
  - 2.5.2 Cooperative Behaviour in Prisoner's Dilemma . . . 14
- 2.6 Learning Algorithms . . . 16
  - 2.6.1 Roth-Erev Reinforcement Learning Algorithm . . . 16
  - 2.6.2 Modified Roth-Erev RL Algorithm . . . 18
  - 2.6.3 Variant Roth-Erev RL Algorithm . . . 19
- 2.7 Summary . . . 19

3 Related Work **21**
- 3.1 Introduction . . . 21
- 3.2 Review Methodology . . . 21
  - 3.2.1 Search strategy . . . 21
  - 3.2.2 Inclusion criteria . . . 22
- 3.3 C-ITS Services . . . 23
- 3.4 Vehicular Communications . . . 26
- 3.5 Applications . . . 27
  - 3.5.1 Road Safety Applications . . . 28
  - 3.5.2 Cooperative Traffic Efficiency Applications . . . 28
  - 3.5.3 Cooperative Local Services and Global Internet Services Applications . . . 29
  - 3.5.4 Other Applications . . . 29
- 3.6 Routing . . . 30

3.7 Dissemination of Information . . . 30
3.8 Survey and Review Papers . . . 31
3.9 Simulation . . . 31
3.10 Game Theory in Traffic Contexts . . . 32
3.10.1 Emergence of Cooperative Behaviour . . . 32
3.10.2 Route Choice and Traffic Information . . . 33
3.10.3 Fairness and Efficiency . . . 35
3.11 Summary . . . 36

4 Methodological Approach **37**
4.1 Problem Formulation . . . 37
4.2 Proposed Method . . . 37
4.3 Problem Formalization . . . 37
4.3.1 System Optimality . . . 38
4.3.2 *n*-Person Dilemma . . . 38
4.4 Summary . . . 42

5 Experimental Setup **43**
5.1 Simulation Framework . . . 43
5.1.1 Requirements . . . 43
5.1.2 System Architecture . . . 44
5.2 Test Network . . . 44
5.3 Population . . . 46
5.4 Payoffs . . . 49
5.5 Strategies . . . 50
5.5.1 RSU Route Recommendation Algorithms . . . 50
5.5.2 Vehicle “Personalities” . . . 53
5.6 Parameters . . . 54
5.7 Evaluation Metrics . . . 55
5.8 Preliminary Tests, Calibration and Setbacks . . . 56
5.9 Summary . . . 57

6 Simulation Experiments and Analysis **59**
6.1 Baselines . . . 59
6.2 Stochastic Behaviour . . . 73
6.3 Memory Based Tactics . . . 74
6.4 Reinforcement Learning Based . . . 78
6.4.1 Payoff matrices . . . 79
6.4.2 Roth-Erev algorithms parameters . . . 82
6.5 System Fairness . . . 84
6.6 Providing Additional Information . . . 86
6.7 RSU Dissemination Degrading Over Time . . . 88
6.8 Summary . . . 89

7 Conclusions and Future Work **91**
7.1 Conclusions . . . 91
7.2 Further Developments . . . 92
7.3 Main Contributions . . . 93
7.4 Future Work . . . 93

7.5 Final Remarks . . . 93

A Simulation Runs **95**
A.1 Simulation launcher usage . . . 96
A.2 Parameters . . . 99
A.3 820veh-24h-00060000 . . . 101
A.4 120veh-24h-00061111 . . . 106
A.5 200veh-24h-00061111 . . . 111
A.6 224veh-24h-00061111 . . . 116
A.7 250veh-24h-00061111 . . . 121
A.8 345veh-24h-00061111 . . . 126
A.9 450veh-24h-00061111 . . . 131
A.10 570veh-24h-00061111 . . . 136
A.11 820veh-24h-00061111 . . . 141
A.12 930veh-24h-00061111 . . . 146
A.13 820veh-24h-01060000 . . . 151
A.14 820veh-24h-02060000 . . . 156
A.15 820veh-24h-03060000 . . . 161
A.16 820veh-24h-04060000 . . . 166
A.17 820veh-24h-05060000 . . . 171
A.18 820veh-24h-06060000 . . . 176
A.19 820veh-24h-07060000 . . . 181
A.20 820veh-24h-08060000 . . . 186
A.21 820veh-24h-09060000 . . . 191
A.22 820veh-24h-10060000 . . . 196
A.23 820veh-24h-11060000 . . . 201
A.24 820veh-24h-12060000 . . . 206
A.25 820veh-24h-13060000 . . . 211
A.26 820veh-24h-14060000 . . . 216
A.27 820veh-24h-15060000 . . . 221
A.28 820veh-24h-16060000 . . . 226
A.29 820veh-24h-17060000 . . . 231
A.30 820veh-24h-18060000 . . . 236
A.31 820veh-24h-19060000 . . . 241
A.32 820veh-24h-00060001 . . . 246
A.33 820veh-24h-01060001 . . . 251
A.34 820veh-24h-17060001 . . . 256
A.35 820veh-24h-19060001 . . . 261
A.36 820veh-24h-15060001 . . . 266
A.37 820veh-24h-16000001 . . . 271
A.38 820veh-24h-16060001 . . . 276
A.39 820veh-24h-19000001 . . . 281
A.40 820veh-24h-19010001 . . . 286
A.41 820veh-24h-19020001 . . . 291
A.42 820veh-24h-19030001 . . . 296
A.43 820veh-24h-19060001 . . . 301
A.44 820veh-24h-19070001 . . . 306
A.45 820veh-24h-19040001 . . . 311
A.46 820veh-24h-19050001 . . . 316

A.47 820veh-24h-19040003 321
A.48 820veh-24h-19040008 326
A.49 820veh-24h-19040010 331
A.50 820veh-24h-19040011 336
A.51 820veh-24h-19040012 341
A.52 820veh-24h-00049998 346
A.53 820veh-24h-19030003 351
A.54 570veh-24h-19040013 356
A.55 820veh-24h-19040013 361

References **367**

Abbreviations

API	Application Programming Interface
ATIS	Advanced Traveler Information Systems
C-ITS	Cooperative Intelligent Transport Systems
C2C-CC	CAR 2 CAR Communication Consortium
I2V	Infrastructure-to-Vehicle
ICT	Information and Communications Technology
ITS	Intelligent Transport Systems
ITS-S	Intelligent Transport Systems Station
MANET	Mobile Ad hoc Network
OBU	On Board Unit
RL	Reinforcement Learning
RSU	Road Side Unit
SUMO	Simulation of Urban MObility
TraCI	Traffic Control Interface
VANET	Vehicular Ad hoc Network
VCI	Via de Cintura Interna
V2I	Vehicle-to-Infrastructure
V2V	Vehicle-to-Vehicle
V2X	Vehicle-to-Everything
WWW	*World Wide Web*

Chapter 1

Introduction

1.1 Context and Motivation

Worldwide, more people live in urban areas than in rural areas, with 55% of the world's population living in urban areas by 2018. In 1950, only 30% of the world's population was urban, but by 2050, it is projected that about two thirds of the world's population will live in urban centres [332].

At the same time, there has been an increase in the number of cars in large cities and suburbs, also contributing to an increasing need for vehicle mobility in urban centres, resulting in growing traffic congestions, accompanied by unpredicted emergencies and accidents, and causing significant changes in transport infrastructures. Inefficiencies cause considerable waste of time, reduced safety levels for both vehicles and pedestrians, high pollution, degradation of quality of life, and enormous waste of non-renewable fossil energy [90].

Applications of Intelligent Transport Systems (ITS) are getting attention from the research community and will directly impact the smart city life. Vehicles equipped with onboard communication units for on-demand vehicle-to-vehicle (V2V) or infrastructure-to-vehicle (I2V), and roadside units for vehicle-to-infrastructure (V2I) communications will be a reality in the near future, with a key role in improving efficiency, safety, public security, and management of a transport system [146].

Cars are gradually becoming networked devices, interacting directly with each other and with the road infrastructure. This interaction is the domain of Cooperative Intelligent Transport Systems (C-ITS) and will enable road users and traffic managers to share information and use it to coordinate their actions in order to increase road safety and improve the flow of traffic, as well as to help drivers in their decision-making and to adapt to the traffic situation.

Therefore, C-ITS solutions heavily rely on Information and Communication Technologies (ICTs) to support a range of new services, where both supply (i.e. infrastructure and services) and demand (end-users) will interact as peers. Vehicle-to-vehicle (V2V), vehicle-to-infrastructure (V2I) or infrastructure-to-vehicle (I2V), and vehicle-to-everything (V2X) communications are, in fact, the underlying infrastructure that enables C-ITS.

However, this dependence on ICTs may lead to a number of constraints. C-ITS solutions are only effective when they can actually help improve the decision-making process of users, the main source of uncertainty in a mobility system.

1.2 Problem Description

A transport network is the support of urban activities, usually designed to accommodate the movement of people and goods in metropolitan areas. The dynamics of cities and their consequences on traffic flows imply a continuous updating and readjustment of the system. An imbalance between transport demand and network capacity results in congestion, with economic, environmental and social impact.

In the domain of C-ITS, vehicles equipped with sensors and actuators interact with each other and with the road infrastructure, making it possible to share information between users and network managers in order to coordinate their actions. However, the system must obtain and provide the most appropriate information to the exact users in a timely way, to the proper place and at the intended recipient, in order to allow informed decision-making and to influence users towards an optimal condition.

1.3 Research Questions

To guide this research, the following questions were raised:

- *Q1:* Does communication have impact on reaching and maintaining the System Optimum of an urban transport network supported by an intelligent transport infrastructure?
- *Q2:* How does communication interfere with reaching and maintaining the System Optimum from an urban transport network supported by an intelligent transport infrastructure?
- *Q3:* What is the impact of communication on reaching and maintaining the System Optimum of an urban transport network supported by an intelligent transport infrastructure?
- *Q4:* What options could be considered to mitigate the impact of communication on reaching and maintaining the System Optimum of an urban transport network supported by an intelligent transport infrastructure?

1.4 Goals and Expected Results

In this research work, the main goal is to devise a simulation-based approach to assess C-ITS solutions in terms of their ability to influence drivers' decision-making in different scenarios of an urban environment, and the impact of communication failures on these services. It will focus in particular on how the information should be disseminated in order to achieve a wider range of demand and to produce the desired impact on the quality of mobility services.

The aim is to test different strategies to adapt and disseminate information to produce the most effective influence on demand modelling according to different mobility scenarios and network configurations.

In the end, it is expected to contribute to a systematic study and analysis of information percolation strategies to improve C-ITS services, taking into account the topology of the road network, the characteristics of the communication network, the composition of demand, and the uncertainty inherent in human decision-making process.

1.5 Methodology

Methodologically, this work is mostly empirical, relying mainly on simulation methods for implementation and quantitative methods for the analysis of results.

Following the literature review on topics related to the project, namely C-ITS, V2X, CAVs, information theory in ITS, demand modelling, communication networks for ITS, and game theory, the identification and definition of dissemination strategies in C-ITS scenarios will be undertaken, as well as the identification of C-ITS services and selection of case studies.

Upon the formalization of a model for driver's decision-making in C-ITS scenarios, the simulation environment is set up, resorting to microscopic simulation in SUMO [100], enriched with agent-based models of drivers' decision-making, in particular using game theory, in its social dilemma aspects in the context of car traffic.

The final stage comprises the simulation runs, tests, and analysis of results.

1.6 Structure of the Document

The structure this document includes seven chapters.

Chapter 1 provides an introduction to the work and includes the description of context and motivations as well as the objectives to be pursued in this research.

Chapter 2 introduces the background knowledge, the concepts of C-ITS and VANETs.

Chapter 3 includes the review of the state of the art on C-ITS, services and strategies, vehicular communications, and aspects of game theory related to social dilemmas, namely the n-Person Prisoner's Dilemma.

Chapter 4 is dedicated to the problem and the proposed solution, including the mathematical formalization.

Chapter 5 considers the experimental set-up, in particular the system architecture and scenario designed, strategies and variables, and the metrics employed.

Chapter 6 contains the results obtained and their analysis.

Chapter 7 consists of the conclusions of this study, the expected scientific contributions and the prospects for future work.

Chapter 2

Background Knowledge

2.1 Introduction

This chapter introduces the main topics discussed in this work, namely the concepts of intelligent transport systems, vehicle networks and related services, mainly from seminal works and papers, European legislation, regulations and standards, as well as topics related to social dilemmas, in particular the Prisoner's Dilemma, in its *n*-Person variant, and learning algorithms used in this domain.

2.2 Intelligent Transport Systems

According to the European Union directive 2010/40/EU [117], Intelligent Transport Systems (ITS) are advanced applications that aim to provide road users with a set of innovative services related to different modes of transport and traffic management, without incorporating intelligence *strictu sensu*, allowing them to be better informed and making the use of transport more coordinated and "smarter", improving transport safety and mobility, with an increase in productivity and a reduction in the harmful effects of traffic [153]. Figure 2.1 illustrates a typical ITS architecture.

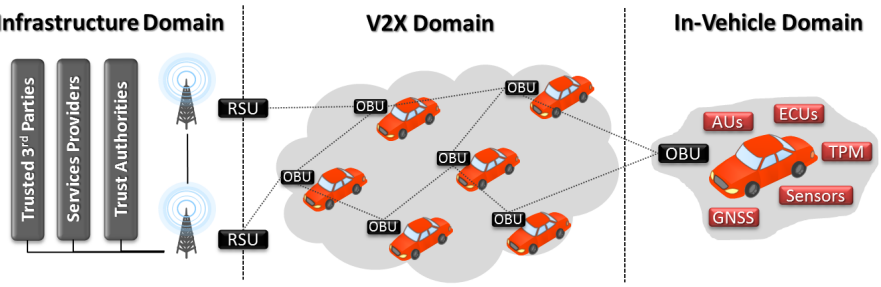


Figure 2.1: ITS Architecture [142].

2.3 Cooperative-Intelligent Transport Systems

While ITS focuses on digital technologies that provide information within the vehicle or on the roadside, C-ITS introduces the idea of cooperation and targets communication between those systems. Vehicles communicate with each other, with the infrastructure or with other C-ITS systems [116, 118] to achieve better road safety, traffic efficiency and comfort of road users.

The development of the co-operative component has been made possible mainly by the advancement of sensor and communication technologies [356, 61], implementing a cooperative behaviour based on communication between two or more actors in the system. This behaviour exists when two or more actors work towards a common or mutually beneficial goal, purpose, or benefit and it is enabled by interaction and information exchange between them [19]. C-ITS conceptual architecture is depicted in Figure 2.2.

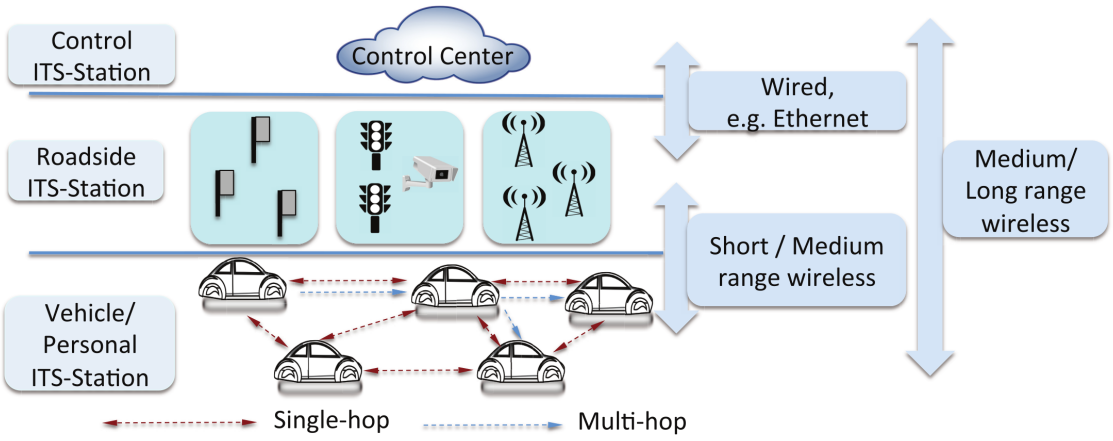


Figure 2.2: C-ITS Conceptual Architecture [61].

2.4 Vehicular Communications

Ad hoc vehicle networks (VANETs) are created by applying the principles of ad hoc mobile networks (MANETs), i.e. the spontaneous creation of a wireless network [327]. VANETs are mainly characterized by dynamic topologies and limited bandwidth and energy, and therefore are a special case of ad hoc mobile networks [330].

The ITS environment comprises ITS stations that will allow direct communication between vehicles (V2V) or between vehicles and an infrastructure (V2I) [112]. The ITS infrastructure is accessed through a fixed ITS station (ITS-S) at the roadside. V2X, in turn, is a general term that includes all possible forms of communication involving vehicles and an external environment.

Self-configuring mobile networks, in which road side units (RSUs) and vehicles equipped with on-board units (OBUs) are mobile nodes, VANETs constitute a key element for C-ITS. Figure 2.3 illustrates a typical vehicular network scenario.

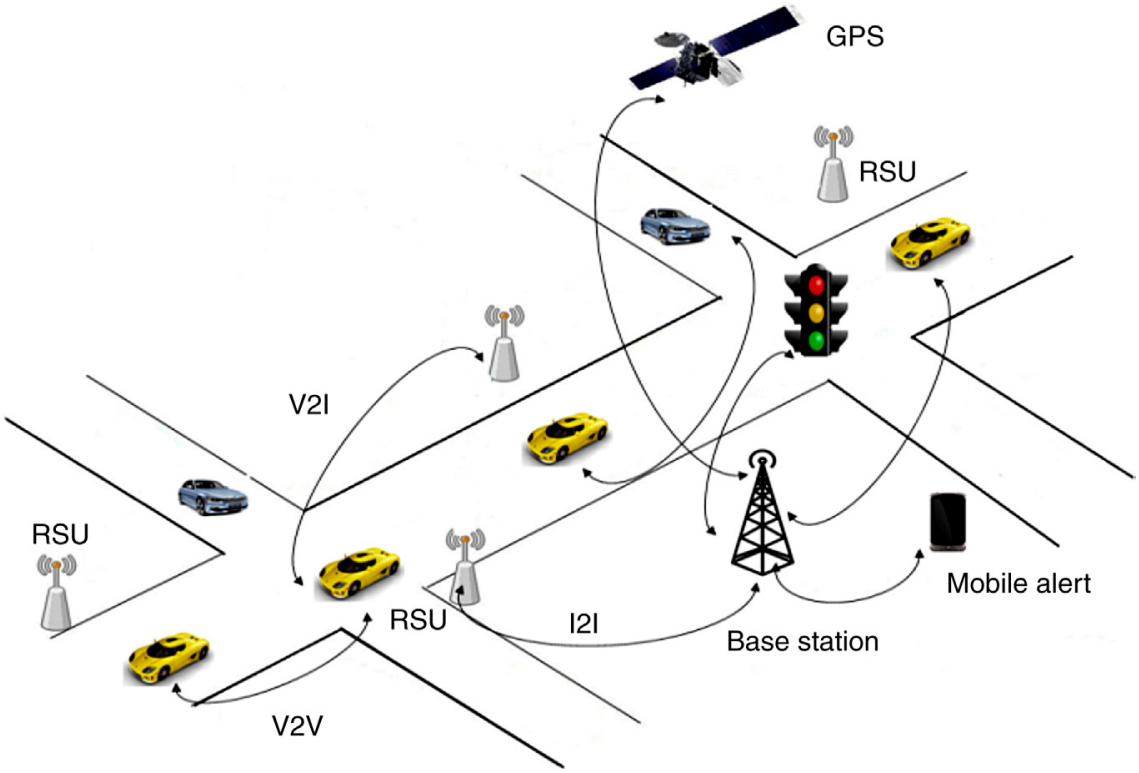


Figure 2.3: A vehicular network scenario (VANET) [254].

The creation of a cooperative environment, in turn, depends on a number of subsystems, as illustrated in Figure 2.4:

- *In-vehicle subsystem,* through the OBU, connected to the vehicle's communication buses, which are installed by the vehicle manufacturer to enable both V2V and V2I communications along properly equipped roads and regions, in motion or parked;

- *Roadside subsystem,* via RSUs, such as beacons on gantries, poles, smart traffic lights, etc., allowing V2I communications along specific road sections;

- *Personal subsystem,* consisting of hand-held devices like mobile phones, tablets, satellite navigation devices, and others not connected to the vehicle communication bus, which will allow only V2I communications over cellular networks.

- *Central subsystem,* a C-ITS entity enabling macro traffic management, which may be part of a centralized traffic management system and used to manage the road infrastructure.

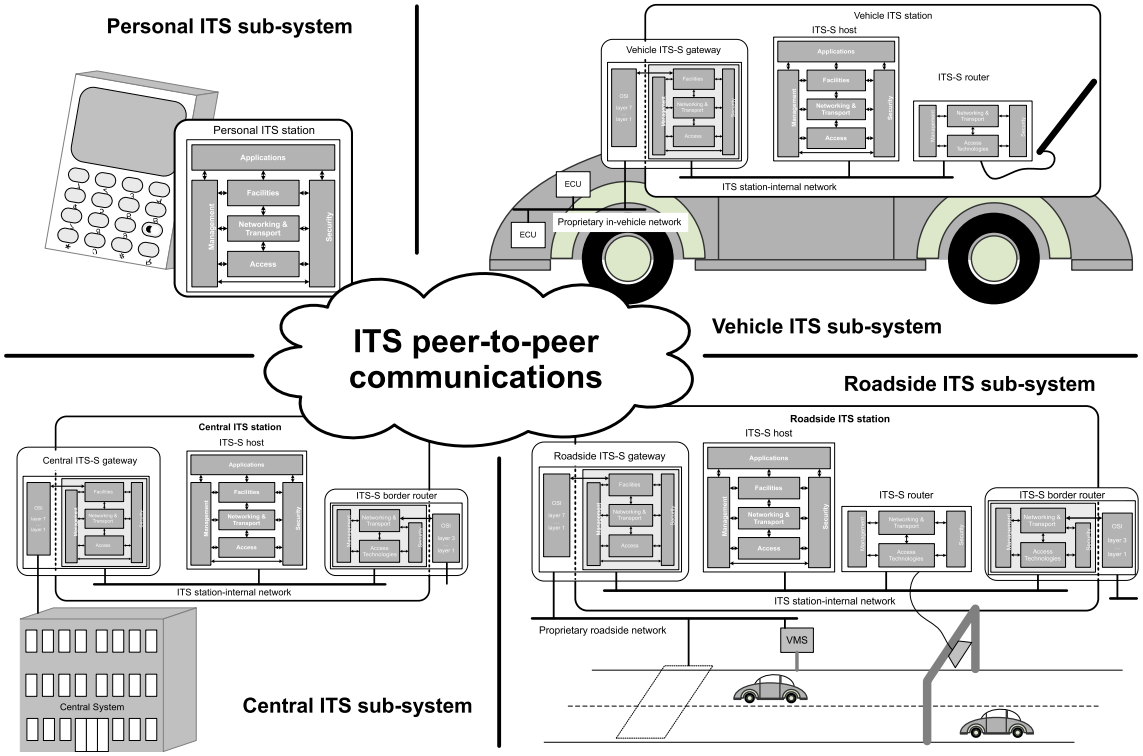


Figure 2.4: C-ITS sub-systems [113].

2.4.1 Applications

The vehicles that constitute a VANET are equipped with a set of wireless sensors and OBUs, which allow them to communicate with other vehicles in their vicinity and with the environment around them (v. Figure 2.5).

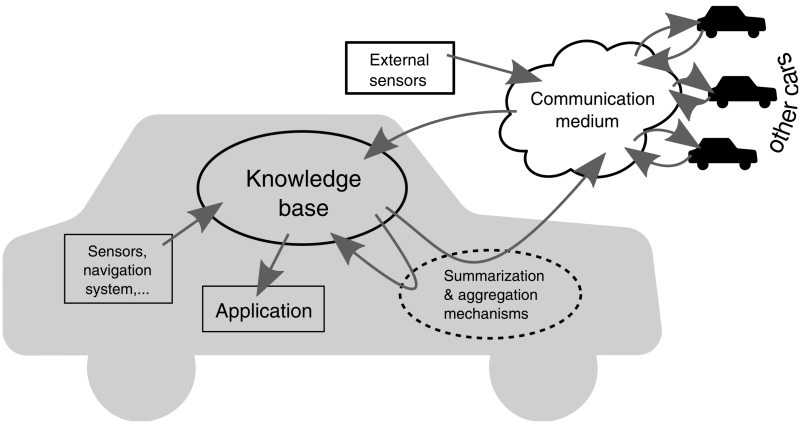


Figure 2.5: Vehicle data dissemination in VANETs [145].

VANET applications were divided into three main categories [55, 114]: safety applications, which aimed to increase vehicle safety on the roads; convenience or traffic related applications that share information between road infrastructure, vehicles on the road, and traffic control systems,

increasing traffic efficiency but also convenience for drivers [191]; and business applications, which provide value-added services, or infotainment, with information, advertisements and entertainment during travel [330], to improve driver productivity, and satisfaction [191].

Figure 2.6 illustrates some VANET applications.

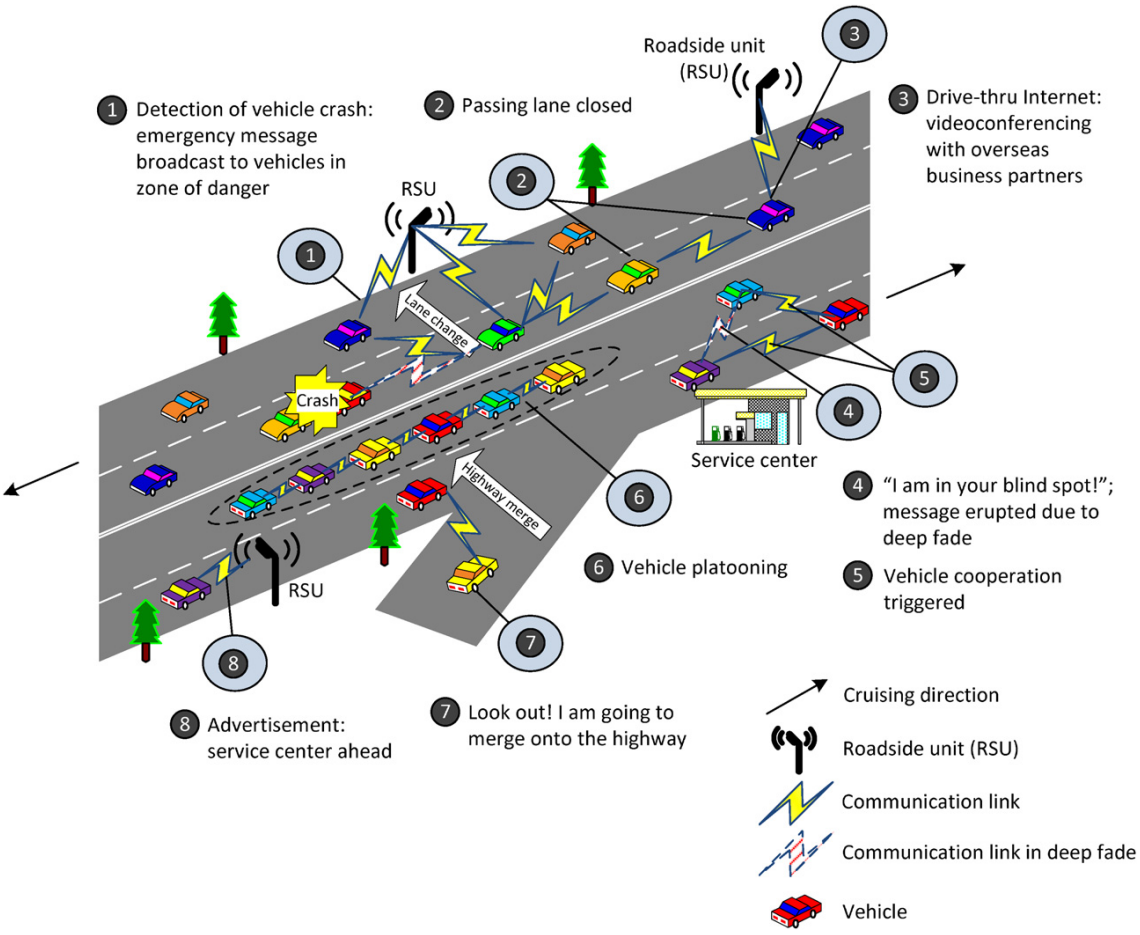


Figure 2.6: VANET applications [64].

2.4.1.1 Safety Applications

Safety applications are intended to have a direct impact on reducing road accidents, particularly in three scenarios: traffic accidents, intersections and road congestions [330, 59, 194].

Due to the speed at which one travels on the main roads, the reaction time to stop in face of an occurrence is very high. Safety applications provide drivers with early alerts and could prevent a collision.

At intersections, where drivers are confronted with two or more traffic flows as well as blind spots, these applications can also give a warning of an eminent collision.

Finally, in road congestions, these can provide drivers with alternative routes to their destinations, reducing road congestion and maintaining a smooth flow of traffic and comfort, thereby increasing the capacity of roads and preventing traffic jams.

2.4.1.2 Convenience or Traffic Related Applications

Traffic management or convenience applications aim to increase traffic efficiency by enhancing the degree of convenience for drivers [225]. These include, among others, planning and diverting routes; electronic tolls, using the vehicle's OBU and sensors to determine distance travelled; notification of parking availability in urban centres, which can help to find parking spaces in a given geographical area; and active prediction of road topography, allowing fuel consumption to be optimized and cruising speed to be adjusted [194].

2.4.1.3 Business Applications

Business oriented applications can provide road users with information, advertising and entertainment during their journey [330]. The most basic ones were related to Internet connection, an essential requirement in today's information society, providing this facility to vehicle occupants and other VANET applications. It can also make use of peer-to-peer techniques, allowing real-time video relay, as well as mobile services such as instant messaging, content download, service announcements and point-of-interest notifications [191].

2.4.2 Routing

Routing schemes for vehicular networks depended on the type of applications and were divided according to their suitability to safety applications, user applications (which include convenience traffic related and business oriented), and Internet connectivity [330]. Protocols are differentiated based on path discovery, seeking to provide efficient and reliable packet transmission between nodes [203]:

- Unicast: point-to-point;
- Multicast: for multiple vehicles, but not all;
- Geocast: for nodes in specific geographic areas;
- Broadcast: for all vehicles in transmission range.

Safety applications require locally broadcast routing schemes, with useful information to multiple vehicles in the nearby vicinity [269], occasionally with some directional information (geocast) [348]. User applications, in turn, could rely only on multicast routing or unicast routing [191].

Furthermore, VANETs are usually linear communication networks, with highly mobile nodes and some predictability of movements. However, mobility poses a number of challenges, notably related to the speed of nodes, from 0 km/h in RSUs or vehicles stuck in traffic jams, up to more than 150 km/h for vehicles travelling on highways [291], as well as with the density of nodes, which may vary between the dense city road network, motorways and rural roads [359]. The number of vehicles per area unit, the obstacles to wireless communication that exist in the surroundings, traffic flows and models, and the predictability of node movement are key factors for the design of routing protocols.

2.4.3 Dissemination of Information

Regarding the dissemination of information in vehicle networks, CAR 2 CAR Communication Consortium distinguished between receiver-centred and transmitter-centred dissemination [55], as opposed to conventional communications, typically receiver-centred.

In receiver-centred dissemination, the source node distributes the information to its neighbours upon detection of a dangerous situation, who in turn redistribute it, aggregating their own state and local information. The spatial distribution is controlled by the receiving node, which determines the relevance of the information received and decides whether it should be redistributed.

In emitter-centred dissemination, the source node routes the information to all neighbours inside a defined geographical area, who upon reception checks whether they are located within it and relays the message.

Done at the network layer, data dissemination can be restricted to an area of relevance defined by the sender, so that data packets are retransmitted until they reach all vehicles in the target geographical area.

Another perspective for dissemination in C-ITS is information-centred, with adaptability to the context and optimized for cooperative use of the radio bandwidth [270]. The high number of nodes sharing a limited channel bandwidth implies a careful selection of information for dissemination according to its value to the recipients, taking into account the conditions of the communication channel [214].

2.5 Social Dilemmas and Cooperation

Situations that involve conflict between immediate self-interest and longer-term collective interests give rise to social dilemmas [336].

Although it is a well-known concept in human ecology and the study of the environment, the "tragedy of the commons" can be perceived in other systems or contexts of society [144]. It states the existence of a resource to which a large number of people have access. As its overuse can create problems and compromise its sustainability, each usufructuary is faced with the decision about how much to use it. Selfish behaviours of individuals within this system lead to its degradation and depletion. The resource can be sustained if everyone has made responsible utilization. But avoiding its usufruct when others continue to exploit it does not prevent its extinction and the share of short-term benefits will be lost anyway [238].

Tanimoto [316] and Hagishima [317] suggest the existence of various social dilemma structures, represented by n-Person Prisoner's Dilemma games, at certain phases of the traffic flow, notably in high-density areas. Urban road traffic in major cities is a modern example of the "tragedy of the commons" [165, 154]. In fact, several parallel concepts can be found between Game Theory and traffic theory. *User Equilibrium,* when a driver cannot unilaterally improve his travel time by changing routes, resembles a *Nash equilibrium* (cf. [235]), the state in which no player has anything to gain by changing only his own strategy. On the other hand, the *System Optimum,*

in which the aggregate utility of all players is maximized, bears resemblance to *Kaldor-Hicks Efficiency* [cf. 170, 149].

2.5.1 *n*-Person Prisoner's Dilemma

The Prisoner's Dilemma is one of the bases for research on social dilemmas—and the best-known and studied models in game theory—, in which individuals are faced with the choice between their own outcome (*defect* option) and the promotion of the collective interest (*cooperation* option) [334, 197]. It appears in a range of group contexts (economic, ecological, sociological, among others), when self-interest is at odds with community benefit [347, 84, 78].

Also in this frame of reference, Nash equilibrium emerged within analytical game theory as a theoretical tool for analysis of cooperation and defection in interdependent decision making. In such equilibrium, when no one has an incentive to unilaterally change his strategy in the face of the expected utility of the alternatives [235], the model predicts mutual defection in the Prisoner's Dilemma [95, 56]. That is, from an individual perspective, not cooperating is always the best strategy, although mutual cooperation is better than not cooperating unilaterally,... hence the dilemma!

By simulating collective actions and behaviours in social groups, *n*-Person Prisoner's Dilemma models have been referred to as *social dilemma games* [290, 86, 210]. During the game, individual players may cooperate with each other for the collective good of their social surroundings, or, on the contrary, they may prefer to nurture their own selfish interests. The incentives to cooperate depend on the number of players contributing to the group and the effect of their actions. However, even though cooperation and social cohesion emerge from the consensual behaviours of the social unit, the dominant strategy of an individual player remains defection.

Social dilemmas formalized as an n-person game ($N \geq 2$) are characterized by the following properties [140, 42, 85, cf. 351, 71]:

a) non-cooperation dominates cooperation, i.e., regardless of what other members of society do, the social payoff to each individual is higher for defecting behaviour than the payoff for cooperative behaviour;

b) universal non-cooperation benefits everyone less than universal cooperation, i.e., all individuals in the social unit receive a lower payoff if all defect than if all cooperate.

Each player can choose to cooperate (C) or defect (D), but has the same preferred option, which does not change despite other players' actions, and the same payoff structure. The payoff of each defecting player is represented as $D(k)$, where k is the number of players in a social unit who cooperate ($0 \leq k \leq N-1$), and that of each cooperating player is given by $C(k)$. The game is then defined by the following conditions [42, 9]:

1. $D(k-1) > C(k), 1 \leq k \leq N$
   (each player is better off choosing to defect rather than cooperate, no matter how many players choose to cooperate on a given turn in the game);
2. $D(0) < C(N)$
   (if everyone cooperates, each player is better off if everyone defects);
3. $D(k+1) > D(k)$ and $C(k+1) > C(k)$
   (the more players cooperate, the better it is for each of them, regardless of whether they choose to cooperate or not);
4. $(k+1) \cdot C(k+1) + (N-k-1) \cdot D(k+1) > k \cdot C(k) + (N-k) \cdot D(k)$
   (society as a whole is better off the more players cooperate).

$C(0)$ and $D(N)$ are undefined, and then the value of k falls between 0 and $(N-1)$. The game therefore has $(N+1)$ distinguishable outcomes, since $0, 1, 2, \ldots, (N-1), N$ participants can choose cooperation [313].

The payoff matrix has the format:

	C	D
C	R R	T S
D	S T	P P

	C	D
C	a a	b c
D	c b	d d

Figure 2.7: Two representations of payoff matrix for 2-person game.

where R is the *reward* for mutual cooperation and P is the *punishment* for mutual defection; T is the *temptation* to defect when the other player cooperates, and S is the *sucker*'s payoff for cooperating when the other player defects. The condition $T > R > P > S$ must hold for Prisoner's Dilemma, with an equilibrium at DD, meaning that if either of the two players abandon this situation, their position will not improve [314].

From the right matrix of Figure 2.7, one obtain the payoff functions for the general case of a compound symmetric game, where n is the number of players choosing C and N the population:

$$\begin{aligned} C(n) &= (a-b)n + bN - a \\ D(n) &= (c-d)n + dN - d \end{aligned} \tag{2.1}$$

Transitioning from 2-person to n-person games, the two-dimensional matrix is then replaced by Equation (2.1), resulting in a graph similar to that of Figure 2.8. According to Hamburger, "any separable, 2-alternative, common-intervally symmetric game has a monotonic average-payoff function", whose " implies parallel linear payoff functions" [140, cf. *Theorem* 10]. The horizontal axis (X) represents the ratio between the number of cooperators and the number of neighbours; and the vertical axis is the reward/punishment provided by the environment [314].

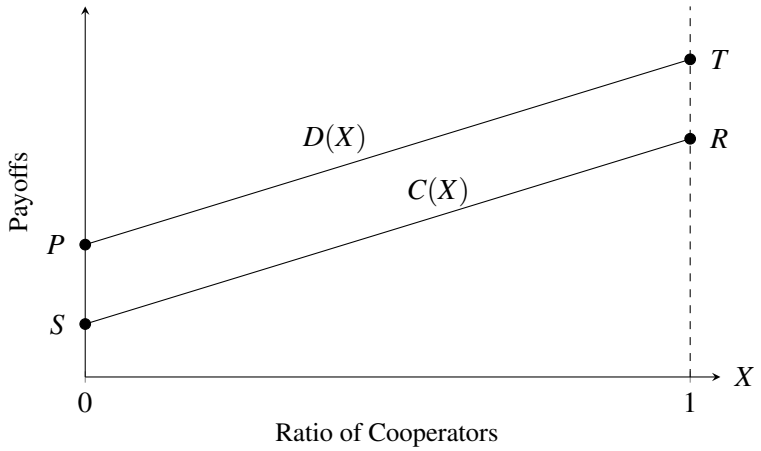


Figure 2.8: Reward/punishment functions for defectors (D) and cooperators (C).

About the payoffs, Macy and Flache [218] define a social dilemma when the order of the four values satisfy the following conditions:

1. $R > P$
   (players prefer mutual cooperation (CC) over mutual defection (DD))
2. $R > S$
   (players prefer mutual cooperation over unilateral cooperation (CD))
3. $2R > T + S$
   (players prefer mutual cooperation over an equal probability of unilateral cooperation and defection)
4. $T > R$
   (players prefer unilateral defection (DC) to mutual cooperation (greed)) or
   $P > S$
   (players prefer mutual defection to unilateral cooperation (fear))

2.5.2 Cooperative Behaviour in Prisoner's Dilemma

Within n-person game models two classes can be distinguished, which are based on the conditions of communication allowed between players [134]. In negotiable games, players can communicate with each other and form coalitions. On the other side we have the non-negotiable games, where communication is limited or not allowed, as in the case where the agents do not even know each other.

Psychology's research into the iterated Prisoner's Dilemma has found that the amount of cooperation achieved, as well as the pattern for achieving it, depends on a wide variety of factors, both related to the context of the game itself, the individual attributes of individual players, and the relationship between them, hence it has become a standard way of approaching issues of social psychology [28].

Each individual is characterized by a certain combination of selfishness and some form of altruism, and this does not change over time. For this reason, individual preferences in interactions of public goods and collective action problems, goods or services that have a certain degree of indivisibility and non-excludability, are generally those of a Prisoners' Dilemma game [319].

The problem of cooperation in the Prisoner's Dilemma has been addressed by means of repetition since Luce and Raiffa [217], in 1957. If it is repeated infinitely, cooperation can be achieved by the selfish behaviour of individuals, through a mechanism of mutual punishment built into each player's strategy [131].

Axelrod [27], after 1984, also uses this approach, from the point of view of the evolutionary stability of cooperation, through computer tournaments, in which he has investigated how it can emerge and be developed over iterations, using a wide variety of different strategies and their distribution over time according to their success.

However, even if conditional cooperative equilibrium strategies in n-Person Prisoner Dilemma were theoretically proven and experimentally investigated, it is more difficult to produce and maintain in an environment of hostile strategies than in the 2-person game, since punishments do not specifically hit defective players, but all members of the cooperative group [222].

Several studies have focused on how agents achieve cooperation, but by modifying the Prisoner's Dilemma (2-person and n-person): e.g., Okada [248], who explored the possibility of cooperation within the framework of institutional arrangements, in which he assumes that the individuals involved in the dilemma can create, by free consent, an institutional order to enforce an agreement or promise of cooperation; Nishihara, showed that, under a given information and payoff structure, cooperation in an n-Person Prisoner's Dilemma can be achieved [244] and maintained [245] as a Nash equilibrium. The latter author was experimentally examined by Vyrastekova and Funak [341], but some doubts were raised about the behavioural relevance in the cooperative equilibrium.

These papers, however, implicitly assumed that an agent's utility equals its payoff—as do several other works that analyzed the emergence of cooperation in such scenarios—, i.e., their social preferences depend only on their payoff, ignoring the payoff of others, something that does not happen in many real-world situations [315].

Another approach was to endow the agents with some learning mechanisms, that can exert the emergence of cooperation if those are equipped with some kind of social attachment, such as spatial relations or group affiliations, through hierarchical organizations and coalitions [33, cf. 284].

Individuals with memory to store a given history size can improve their cooperative behaviour, even in networks with dynamic topology changes [123], or, on the other hand, undergo an evolutionary optimization of cooperation strategies, using population-based genetic algorithms, whose members have distinct goals, evolving according to fitness functions [124].

2.6 Learning Algorithms

Analytic game theory assumes that players have sufficient cognitive capacity and knowledge about the consequences of the alternatives in play to make accurate predictions and decisions. Learning theory, on the other hand, downplays the cognitive significance and allows players to base their predictions on experiential induction rather than logical deduction, considering two entirely separate cognitive mechanisms—*approach* and *avoidance*—that guide decisions towards better outcomes. Rewards induce *approach* behaviour and a tendency to repeat the associated decisions, while punishments induce *avoidance,* leading to a search for other results [218]. Reinforcement learners interact with the environment and make choices based on their experience and the consequences of their actions.

The learning model proposed by Roth and Erev [278], used in sociological theory, conceives agents as adaptive learners who will choose between alternatives in a ratio that corresponds to the reward ratio. The Roth-Erev model leads to the *Matching Law* [362], which, in the context of social dilemmas, predicts that players will learn to cooperate until the payoff for cooperation exceeds that for defection, only possible, given $R > P$, if both players cooperate and defect at the same time [127].

2.6.1 Roth-Erev Reinforcement Learning Algorithm

In the mid-1990s, Roth and Erev devoted some studies [278, 110] to understanding individual learning in a game with multiple participants interacting strategically, and developed a reinforcement learning algorithm with three parameters.

The underlying principle of any reinforcement learning algorithm is to strengthen the tendency to implement an action if it produces favourable results and to weaken it if it produces unfavourable results. Taking this principle from the *Law of Effect,* proposed in the literature of Psychology by Edward L. Thorndike in 1911 [326], those authors focus on individual learning in strategic environments with multiple decision-makers, rather than the direction taken by psychologists, who gave primacy to individual learning in *games against nature,* in which there is only one decision-maker.

In addition, they also adhered to the *Power Law of Practice,* proposed by G. S. Snoddy in 1928 [303, cf. 128], which postulates that the logarithm of reaction time for a task decreases linearly with the logarithm of the number of trials performed, i.e., learning curves tend to be initially steep and then flatten.

Based on observations of learning in multi-agent games, Roth and Erev added two psychological assumptions to capture responsiveness: *experimentation (or generalization) effect,* which states that successful choices in the past are more likely to be employed in the future and similar choices will be employed more often as well; and *recency (or forgetting),* whereby more recent experience generally plays a larger role in determining behaviour than a past experience.

The assumptions were quantified in the Equation (2.2):

$$\begin{aligned} q_{nj}(t+1) &= (1-\phi)q_{nj}(t) + E_j(\varepsilon,N,k,t) \\ E_j(\varepsilon,N,k,t) &= \begin{cases} R_k(j)(1-\varepsilon) & : \ j = k \\ R_k(j)\frac{\varepsilon}{N-1} & : \ j \neq k \end{cases} \end{aligned} \tag{2.2}$$

where:

- n is the n^{th} player
- a_k is the last action chosen
- $q_{nj}(0)$ is the initial propensity of action a_j at $t = 0$ (aspiration level)
- $q_{nj}(t)$ is the propensity of action a_j at time t
- $R_k(t)$ is the reward obtained for taking action a_k at time t
- t is the current time step
- ε is the *experimentation* parameter
- ϕ is the *recency* parameter
- N is the number of actions

The experimentation parameter, set between 0 and 1, is about the necessity to "dilute" initial rewards and encourage experimentation in order to avoid premature fixation on a chosen action. By increasing ε, there is more spillover to the remaining alternative action, resulting in less divergence between propensities. Approaching 0, the reward resulting from the choice is assigned only to that action, implying that only its propensity is updated.

The recency parameter, in turn, is also set between 0 and 1 and allow to "forget" rewards received in the distant past in environments susceptible to change over time. By setting ϕ near 1, it gives more weight to recent rewards, while near 0, equal weight is given to all rewards received to date.

From action propensities, action choice probabilities are calculated by the Equation (2.3):

$$p_{nk}(t) = \frac{q_{nk}(t)}{\sum_{i=1}^{N-1} q_{ni}(t)} \tag{2.3}$$

where:

- $p_{nj}(t)$ is the *choice probability* of action a_j at t
- $\frac{q_{nk}(t)}{\sum_{i=1}^{N-1} q_{ni}(t)}$ is the sum of the propensities associated to the actions available to player n, at time t

The algorithm follows the sequence illustrated in the figure 2.9.

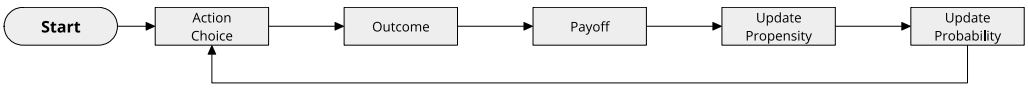


Figure 2.9: Roth-Erev Algorithm sequence.

Equation (2.2) presents the propensity of player n to choose action j at time $(t+1)$. The action j taken by the learning agent in that iteration then becomes action k and the propensities of the set of actions are updated according to the second term of the equation, as well as the associated probabilities for the next iteration, in accordance with the Equation (2.3), thereby generating the so-called reinforcement learning. The pseudocode is presented in Algorithm 1.

Algorithm 1: Roth-Erev Learning Algorithm

Require: $\varepsilon \in (0,1)$ Exploration rate
$\phi \in (0,1)$ Recency
A Set of actions

Input: a_j Current action choice
$q_{nj}(t)$ Propensity for action a_j at time t
a_k Last action chosen
$R_k(t)$ Reward for action a_k at time t
N Number of actions

Parameters: $q_{nj}(0)$ Initial propensity
ε Experimentation
ϕ Recency

1: t $\leftarrow$ 0
2: initialize $q_{nj}(0) \leftarrow 1$, for all $j \in A$
3: **repeat**
4: t $\leftarrow$ t + 1
5: $\left\{ p_{nk}(t) = \frac{q_{nk}(t)}{\sum_{j=1}^{N} q_{nj}(t)} \right\}_{k \in A}$
6: choose action $X_t \leftarrow k \in A$ randomly, using the probabilities $p_{nk}(t)$
7: collect reward $R_t(j)$
8: $q_{nk}(t+1) \leftarrow (1-\phi)q_{nk} + R_k(t)(1-\varepsilon)$
9: **forall** $j \neq k$ **do**
10: $q_{nj}(t+1) \leftarrow (1-\phi)q_{nj} + R_j(t)\frac{\varepsilon}{N-1}$
11: **end**
12: **until** *termination*;

2.6.2 Modified Roth-Erev RL Algorithm

When using the Roth-Erev algorithm described above, Nicolaisen, Petrov and Tesfatsion [243] mentioned what they considered a problematic feature, which consists in the absence of updating propensities in cases of reward equal or close to zero, since only the current propensity weighted by the forgetting parameter will remain.

Another flaw to the algorithm was also pointed out by Koesrindartoto [189], who mentioned that no learning occurs for certain combinations of the ε (*experimentation*) and N (number of actions) parameters.

In view of this, the authors proposed a new formulation for the algorithm, now called Modified Roth-Erev RL, changing the second term, as stated in Equation (2.4):

$$q_{nj}(t+1) = (1-\phi)q_{nj} + E_j^*(\varepsilon, N, k, t)$$
$$E_j^*(\varepsilon, N, k, t) = \begin{cases} R_k(j)(1-\varepsilon) & : \ j = k \\ q_{nj}(t)\frac{\varepsilon}{N-1} & : \ j \neq k \end{cases} \tag{2.4}$$

The coefficient $R_k(j)$ is replaced by $q_{nj}(t)$ when $j \neq k$.Through this formulation, the propensity update is perceived even when the chosen action results in zero reward. The calculation of the probability of choice, in turn, remains according to Equation (2.3) presented above.

2.6.3 Variant Roth-Erev RL Algorithm

The second variation found for the original algorithm was developed by Sun and Tesfatsion [311], who proposes a modification in the calculation of choice probabilities with a *cooling parameter* that affects the degree to which the agent makes use of propensity values, cited by Weidlich and Veit [346] as shown in Equation (2.5), where T is the Gibbs-Boltzmann temperature parameter, based on a Boltzmann distribution.

$$p_{nk}(t) = \frac{e^{\frac{q_{nk}(t)}{T}}}{\sum_{j=1}^{N} e^{\frac{q_{nj}(t)}{T}}} \tag{2.5}$$

It concentrates the focus on actions with high propensity values that correspond, consequently, to actions with high reward values. The formulation maintains, however, the same characteristics of the Modified Roth-Erev algorithm for the updating of the propensities.

2.7 Summary

This chapter introduced the main topics covered in this project, based on seminal works and documents. The concepts of intelligent transport systems, in particular in their cooperative dimension, and the vehicular networks which enable it, have been addressed, as well as the subjects related to social dilemmas because of their application in car traffic management.

The applications running in the context of these networks were distinguished into three categories (safety, traffic-related and business-oriented), with implications for the choice of routing protocols (broadcast, geocast, multicast and unicast) as well as data dissemination strategies (receiver-centred, emitter-centred or information-centred).

The prisoner's dilemma as a multi-person game was also analysed, as it has great practical importance and its study leads to a better understanding of the factors that stimulate or inhibit cooperative behaviour within social systems. Moreover, for its application in behavioural and sociological context, Roth-Erev's reinforcement learning algorithm is analysed as an option to model vehicle decision-making in this project.

Chapter 3

Related Work

3.1 Introduction

The aim of this chapter is to provide state-of-the-art information on the concepts and a perspective of the research conducted in recent years by the scientific community on C-ITS services and strategies through a literature review.

3.2 Review Methodology

The review focused on existing C-ITS services and information exchanged in inter-vehicular communications, asking the following review questions:

- *Q1:* What are the existing C-ITS services?
- *Q2:* What kind of information flows in the various V2X communications?
- *Q3:* Which routing and information dissemination strategies are used?

After the development of review questions, databases were explored during which relevant studies, publications and research work were identified. The material was first assessed for adequate quality, then only relevant data was extracted and summarized.

3.2.1 Search strategy

The bibliographic research was mainly conducted at *Scopus* [107] to collect data using the following queries, in title, abstract and keywords (`TITLE-ABS-KEY ( )`), to answer the review questions mentioned above:

- `( C-ITS OR "Cooperative Intelligent Transport* Systems" )`
- `( SUMO OR "Simulation of Urban MObility" )`
- `( V2X )`

- `( "communication network?" AND "intelligent transport* systems" )`
- `( percolat* W/4 information )`
- `( "information theory" AND "intelligent transport* systems" )`
- `( demand W/4 model?ing AND transport* )`
- `( ( communication W/4 issues ) AND transport* )`
- `( ( decision W/0 mak* ) AND transport* AND intelligent )`
- `( ( decision W/2 mak* ) AND C-ITS )`
- `( C-ITS AND services )`
- `( VANET? AND services )`
- `( ( information W/2 dissemination ) AND VANET? )`
- `( ( ( information OR data ) W/1 dissemination ) AND (C-ITS OR "Cooperative Intelligent Transport* Systems" ) )`
- `( ( ( information OR data ) W/1 dissemination ) AND transport* )`
- `( ( ( "information" OR "data" ) W/1 dissemination ) AND VANET? )`

Bibliographic items (research papers, books or articles) were searched in the digital libraries:

- IEEE Explorer;
- Science Direct;
- ACM Digital Library;
- Springer;
- Elsevier.

In addition to the mentioned sources, technical reports, books, patents, and online literature relevant to present topic of review are included. Several articles have not been identified considering the research phrases mentioned above, due to various reasons, such as not appearing in the title, abstract or keywords. In order to identify more related articles, a manual search was performed on paper and book references, and with certain keywords in digital repositories.

3.2.2 Inclusion criteria

Resources considered in the review are based on the following inclusion and exclusion criteria.

Inclusion:

- Date from 2015-2021
- Journals and conference papers which discuss ITS and V2X dissemination strategies and communications, and urban mobility simulation.

Exclusion

- Resources that include strategies and solutions not related to ITS or vehicular communications.
- Non-journal and non-conference articles;
- All digital resources which do not discuss the ITS and V2X.

3.3 C-ITS Services

The development of C-ITS has played a key role in achieving the European Commission's objectives to tackle the increasing volumes of road transport and transport network load, notably traffic congestion and the consequent energy consumption and CO_2 emissions, relying in particular on the advancement of information technologies to improve its efficiency, safety and environmental performance [25].

The difference introduced by the addition of "cooperative" to ITS is that C-ITS rely on interaction with other vehicles and or the road infrastructure, as well as on the exchange of dynamic data to enable their systems to function [312].

C-ITS are based mainly on vehicular ad-hoc networks, VANETs, the term commonly used by the scientific community to refer to the underlying technologies (architecture, data, and protocols), characterized by highly dynamic changes in the topology of communication nodes, and which are developed and standardized under the working title of ITS and its cooperative counterpart, C-ITS [126].

ERTICO, in March 2015 [111], published the list of **'Day 1 use cases'** and applications, agreed between Amsterdam Group and CAR 2 CAR Communication Consortium (C2C-CC):

- Hazardous location
- Slow vehicle warning
- Traffic Jam ahead warning
- Road works warning
- Stationary vehicle warning
- In vehicle signage
- Probe Vehicle Data
- Signal Phase and time
- Emergency vehicle warning
- Emergency brake light
- Motorcycle approaching indication

On the publication of the report of The Platform for the Deployment of Cooperative Intelligent Transport Systems in the European Union [51], a distinction was made between **'Day 1 services'**, which, given their expected social benefits and the maturity of the technology, were expected to be available in the short term; and **'Day 1.5 services',** considered as mature and highly desired by the market, for which, however, specifications or standards might not yet be completely ready.

List of **'Day 1 services':**

- **Hazardous location notifications:**
  - Emergency brake light;
  - Emergency vehicle approaching;
  - Road works warning;
  - Slow or stationary vehicle(s);
  - Traffic jam ahead warning;
  - Weather conditions.
- **Signage applications:**
  - Green Light Optimal Speed Advisory (GLOSA);
  - In-vehicle signage;
  - In-vehicle speed limits;
  - Probe vehicle data: CAM aggregation;
  - Shockwave Damping (also has other names, falls under the general ETSI category "local hazard warning");
  - Signal violation / Intersection Safety;
  - Traffic signal priority request by designated vehicles.

List of **'Day 1.5 services':**

- **Hazardous location notifications:**
  - Cooperative Collision Risk Warning;
  - Motorcycle Approaching Indication.
- **Other:**
  - Connected & Cooperative navigation into and out of the city (first & last mile, parking, route advice, coordinated traffic lights);
  - Information on fuelling & charging stations for alternative fuel vehicles
  - Off street parking information;
  - On street parking management and information;
  - Park & Ride information;
  - Traffic information & Smart routing;
  - Vulnerable Road User protection;
  - Loading zone management;

In a first analysis, the urban working group of the C-ITS Platform concluded that, to be successful, C-ITS services in an urban context should correspond to local policy objectives, address the problems faced by local authorities and be tailored depending on their local context [52], which is unique, in particular because of:

- The general objective of reducing traffic, pollution and congestion to create more liveable towns;
- Priorities for certain transport modes and intersections, such as public transport, emergency vehicles, etc.
- Cultural and behavioural characteristics;
- Geographical location and configuration of existing road network;
- Robustness of networks;
- Technical and operational characteristics of the public transport network;
- Multitude of road operators, particularly in inter-urban areas;
- Parking availability and policy;
- Multimodality/mixed traffic and safety implications of vulnerable road users.

In terms of implementation priority, the C-ITS Platform has distinguished a number of services according to their application, either from a safety point of view or by enhancing traffic management [52].

Therefore, among the services with the highest safety potential, they prioritized, as **'Day 1 services':**

- In-vehicle speed limits (including dynamic speed limits);
- Emergency electronic braking light;
- Road works warning;
- Weather conditions;
- Hazardous location notification.

and, as **'Day 1.5 services':**

- Intersection safety;
- Vulnerable Road Users protection.

For the Enhancing Traffic Management services, the priority was, for **'Day 1 services':**

- In-vehicle signage;
- In-vehicle speed limits;
- Probe Vehicle Data.

and, the **'Day 1.5 services':**

- Traffic information & smart routing;
- Zone access control for urban areas.

A project conducted in 2018 [101] to quantify the impact of deploying a C-ITS infrastructure in several cities has already shown a sustained improvement in CO_2 emissions and efficiencies in both heavy and light vehicles, as well as in intersection crossing times and average stop numbers, despite some variation depending on site-specific conditions. Therefore, the results indicated potential for significant contributions to environmental policy objectives, given certain road configurations and beneficiaries.

3.4 Vehicular Communications

Vehicular communications are the area that allows the implementation of C-ITS, making it possible to share information through real-time communications between vehicles and roadside communication infrastructures. These networks define different modes of communication to automate the wireless data transmission, as depicted in figure 3.1.

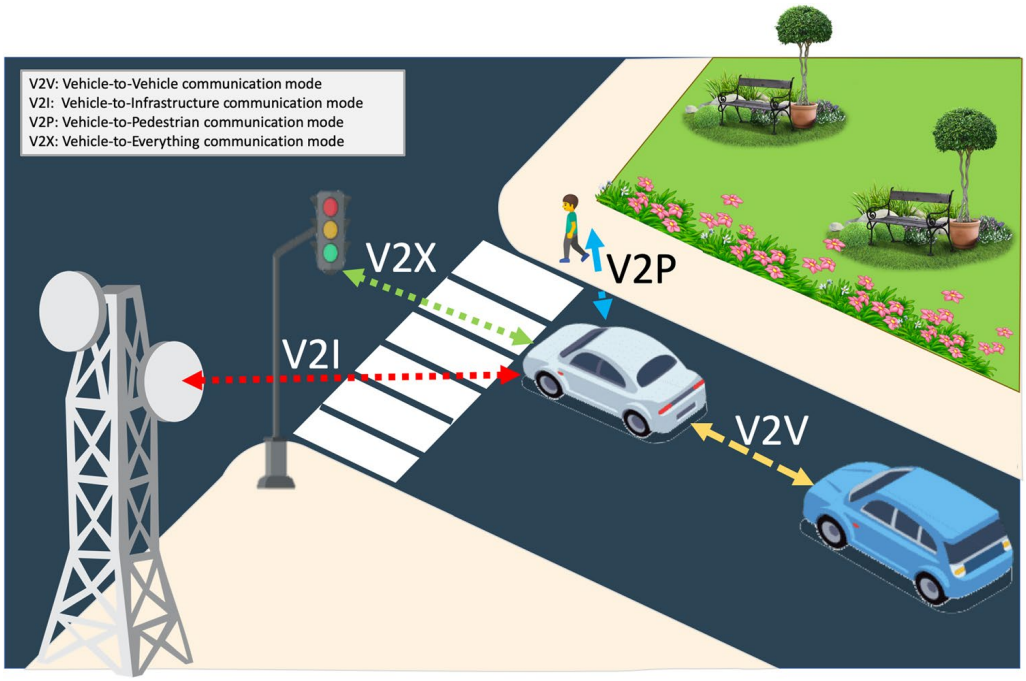


Figure 3.1: Vehicular Communications [354].

The communication models are identical to those mentioned in the previous chapter (section 2.4), but over the past few years some work has been done in order to get the best performance out of each one, according to their respective requirements (see table 3.1).

Communication Model	Research Works
Vehicle-to-Vehicle (V2V)	89, 152, 338, 340, 6, 213, 321, 322, 10, 17, 68, 261
Vehicle-to-Infrastructure (V2I)	89, 183, 344
Vehicle-to-Pedestrian (V2P)	156, 31, 228
Vehicle-to-Everything (V2X)	39, 167, 337, 166, 274, 133, 234

Table 3.1: Research works that address vehicular communication models.

3.5 Applications

The implementation of the applications in the context of C-ITS has been prioritized according to a set of relevant services chosen through a score assigned by the stakeholders [52] (see section 3.3).

Of the research articles gathered in this paper, we have identified and classified them according to the main application to which they refer and their respective class (table 3.2).

Application Class	Application	Research Works
Active Road Safety	Driving Assistance – Cooperative Awareness	49, 97, 283, 357, 198, 73, 182, 231
	Driving Assistance – Road Hazard Warning	257, 182
	Cooperative collision avoidance or mitigation	228, 292, 26, 57, 224, 68, 234
Cooperative Traffic Efficiency	Speed Management	253
	Cooperative Navigation	169, 186, 74, 304, 161, 164
	Cooperative Traffic Management	63, 75, 310, 92, 220, 230, 263, 337, 53, 262, 40, 76, 190, 236, 289, 229
Cooperative Local Services	Location based services	
Global Internet Services	Communities Services	
	ITS Station Life Cycle Management	

Table 3.2: Research works that address vehicular communication applications (based on ETSI Basic Set of Applications list [112]).

Besides the applications in the framework of the basic set defined in the ETSI specifications, the following also deserve mention (table 3.3):

Application	Research Works
Traffic Estimation	211, 227, 247, 162
Services Advertisement	195, 143

Table 3.3: Research works that address other vehicular communication applications.

3.5.1 Road Safety Applications

The main objective of applications in the active road safety class is the improvement of road safety, through driving assistance, both by cooperative awareness and road hazard warnings, as well as collision avoidance or mitigation.

3.5.1.1 Driving assistance – Cooperative awareness

In this application, there are projects related to the use cases *dynamic vehicle warnings* [49, 283, 357] and *cooperative flexible lane change* [97].

3.5.1.2 Driving assistance – Road Hazard Warning

Traffic hazard warnings [257, 182]

3.5.1.3 Cooperative collision avoidance or mitigation

The use case with the most examples in this application is *collision risk warning* [26, 68, 182, 234]

3.5.2 Cooperative Traffic Efficiency Applications

The main objective of the applications in the cooperative traffic efficiency class is the improvement of traffic flow, using speed management and cooperative navigation and traffic management.

3.5.2.1 Speed Management

This application includes the use case *traffic light optimal speed advisory* [253]

3.5.2.2 Cooperative Navigation

This application includes the use cases of *traffic information and recommended itinerary* [169, 186, 74] and *enhanced route guidance and navigation* [304, 161, 164]

3.5.2.3 Cooperative Traffic Management

The most frequent use cases in this application are *intersection management* [75, 92, 337, 53, 262, 40, 76, 289] e *cooperative vehicle-highway automation system* (platooning) [63, 220, 190, 236, 229]. There is also an example of *cooperative adaptative cruise control* [230] and another of *electronic toll collect* [263]

3.5.3 Cooperative Local Services and Global Internet Services Applications

Applications in the classes of cooperative local services and global Internet services advertise and provide on-demand information for vehicles in transit, on both a commercial and non-commercial basis [112]. These services include Infotainment, productivity, ride comfort and vehicle life cycle management. Local cooperative services are provided by ITS network infrastructure itself, while global Internet services are usually purchased from third party Internet providers.

The use cases include:

- Point of Interest notification;
- Automatic access control and parking management;
- ITS local electronic commerce;
- Media downloading;
- Insurance and financial services;
- Fleet management;
- Loading zone management;
- Vehicle software / data provisioning and update;
- Vehicle and RSU data calibration.

3.5.4 Other Applications

Traffic management and prediction is a key factor in improving the traffic efficiency of intelligent transport, in which the knowledge of current and forecasted traffic states play an essential role for route planning. However, the actual traffic status is determined from sensors, which may provide missing or incomplete data due to communication problems or faulty sensors. A proposed particle-based approach with Kriging interpolation allows mitigating the effect of missing data in a large road network, reducing the effects of computational overload through a distributed approach with a central control unit [247].

However, at each intersection, it is possible to consider a continuous adaptation of the routes for each vehicle, in a distributed and server-less way, minimizing the driving time and balancing the vehicles along the road network, with the algorithm proposed by [227], based on a Linear Prediction (LP) model that uses real-time traffic information gathered from vehicle communications.

An alternative is the use of an on-board camera to capture road videos and thereby make estimates of traffic conditions, using wireless communication to share, through a V2X network, traffic information with other vehicles and road infrastructures, which can also provide extra computing resources. Traffic density estimation is done on the basis of a vehicle count through YOLO-based vehicle detection and Hough-based lane detection [211].

The collected data, in addition to enabling real-time evaluation, also constitutes historical information that can be used by an extreme learning machine (ELM) algorithm to design an accurate model to predict hourly road traffic fluidity. A hybrid model called ELM-EBDM [162] showed a good performance both in terms of accuracy and stability, representing an important and reliable tool for traffic managers.

C-ITS environments may, in addition to services directly related to improving traffic safety and efficiency, provide a range of commercial, productivity and entertainment services. However, users must be aware of these in order to request them if they are interested to do so. In this sense, a solution has been proposed for advertising services in C-ITS environments [195, 143], in compliance with existing ETSI CAM standard, through the periodic transmission of a specific message by ITS roadside station, called CAM-Infrastructure Message (CAM-I).

3.6 Routing

Routing is the procedure to determine a path for traffic on a computer network, or between or across multiple networks [50]. Given the specificities and requirements of a vehicular network, we have classified the collected research articles according to the communication model, further distinguishing those that give more emphasis to communication protocols and communication systems or standards (table 3.4).

Routing Context	Research Works
V2V	89, 184, 255, 152, 340, 6, 322, 321, 13, 17, 261
V2I	89, 31, 183, 79
V2P	31, 228, 57
V2X	39, 167, 209, 274, 47, 202, 260
Communication Systems	120, 29, 201
Protocols	156, 233, 139, 307, 2, 12, 15, 172, 77, 213, 221, 181, 259

Table 3.4: Research works related to C-ITS communication models and systems.

3.7 Dissemination of Information

Data dissemination refers to the transport of data to the intended recipients, while meeting certain requirements such as quality of service, delay, reliability, confidentiality, etc., which depend on the applications and data to be disseminated.

Dissemination	Research Works
	87, 281, 288, 46, 69, 249, 14, 258, 271, 3, 5, 30, 77, 79, 91, 161, 215, 300, 320, 1, 68, 94, 138, 151, 199, 259, 260, 306, 333, 339
	232, 41, 18, 168, 2, 328, 358, 102, 208, 219, 325, 1, 157, 329, 223, 246, 287, 352

Table 3.5: Research works related to C-ITS dissemination strategies.

3.8 Survey and Review Papers

A number of survey, review and overview papers have also addressed these issues (table 3.6).

Subject	Papers
Vehicular Communications Applications	62, 119, 159, 265, 11, 21, 22, 160, 298, 301, 130, 141, 200, 354, 196
Vehicular Routing Protocols	353, 119, 159, 265, 7, 8, 22, 251, 285, 298, 305, 130, 141
Vehicular Communications Systems	119, 349, 350, 282, 355
Data/Information Dissemination	297, 130, 60, 132, 141, 266
Cooperative Intersection Management	62, 231
Congestion Detection and Control	252
Vulnerable Road User Safety	80
Public Transport Systems	294
Policies and Practices	43

Table 3.6: Survey, review and overview works related to C-ITS applications and vehicular networks.

3.9 Simulation

Traffic simulation is an invaluable tool for research, allowing to evaluate or test traffic management strategies and their impacts. The SUMO simulator provides a framework with useful tools for the generation, validation and evaluation of high traffic scenarios, from a macroscopic to a submicroscopic level [216].

Vehicles in C-ITS interact with each other to achieve safety and efficiency goals, but include the behavioural uncertainty inherent in human nature. Simulation techniques can mimic the dynamics resulting from the choices of individual human decision makers [226], including with agent-based models—a computational model representing individual agents and their collective behaviour [295] and capture possible macroscopic regularities in a model population of heterogeneous autonomous agents generated from the bottom up [109]—for a collaborative approach to the driving problem [88]. One way to extend the simulation was to combine a traffic simulator, a network simulator and a driving simulator, in which a platooning application was evaluated [20].

Another concern of the simulation in C-ITS context is about the integrated environment with a traffic simulator, a network simulator and an application simulator, in order to test V2X protocols and applications [66]. This type of simulation must take into consideration a set of requirements, namely the need for synchronization between the simulators to produce results for the same instant of time and with the same resolution. The network simulator must be appropriate to the mobility model and allow the dynamic addition and removal of nodes. The simulated scenarios include a channel congestion at highly congested road junctions, the management of traffic flows in the presence of vehicle failures or road accident, and assistance to emergency vehicles [65].

The integration of multi-agent cooperative traffic modelling in a traffic simulator allows to evaluate the potential benefits of cooperative traffic control strategies in different traffic configurations [137, cf. 32], such as on-ramp and lane closure scenarios, or of drivers' interaction with pre-trip information systems in a commuting scenario [276, 277].

On the other hand, simulation-based laboratory experiments have proved capable of replicating travel choices, with better control of the context and the setting of decisions, and at lower cost [96].

3.10 Game Theory in Traffic Contexts

In the parallelism between Game Theory and the study of car traffic it is possible to identify a social dilemma, which explains the stable condition of User Equilibrium with the natural behaviour of drivers, although a System Optimum is rarely reached without the intervention of an information service [187, 188]. However, even if User Equilibrium is optimal for the user, this does not necessarily mean that it is optimal for the system.

3.10.1 Emergence of Cooperative Behaviour

Increasing road capacity is not a viable solution for reducing congestion, as the Braess's Paradox has shown [cf. 45], hence the importance of rational and efficient management of existing resources. Selfishness is an innate characteristic of human beings [250], whereby pure rationality threatens social dilemmas. However, while consistent with selfishness, so is rationality with altruism [108]. Several experiments [155, 72, 135, 125, 34, 99, 150, 98] have shown cooperation in social dilemmas without external controls, suggesting that their origin lies in human nature, but also that its emergence rate has a strong causal link with payoffs [54]. Studies in the field of behavioural economics, with public goods games, have revealed some situations in which cooperation can thrive, namely when there is a positive framing [16]—a cognitive bias based on how the options to a dilemma are presented to people, with a positive or negative connotation—, or a system of sanctions, in which individuals can reduce the outcomes of those who have not contributed, albeit at a cost to the sanctioner [121]. Yet, social approval, when players' outcomes are transparent to others, encourages cooperation and increases contributions [267].

Selfish, rational behaviour leads to suboptimal outcomes and the Nash Equilibrium of the Prisoner's Dilemma of mutual defection is not socially efficient. Nevertheless, the concept of partial cooperation will allow the system to achieve an optimum by inducing some players to act cooperatively, while others decide on the rational action of defecting. When implemented in an iterated fashion, an adequate, Pareto-efficient solution is alternating decision making (turn-taking), in a permanent anti-coordination between the two actions, even though in finitely repeated games it is not an equilibrium state, since players are tempted to abandon this strategy [308]. This concept has been the subject of several studies [239, 48, 318, 70, 171] and empirically verified in a route choice experiment [148, 309], in which alternative cooperation emerged among the players, who had been informed that they would be able to achieve maximum time savings by coordinating their actions. The results showed that players learn to coordinate after a certain period of adaptation,

suggesting that cooperation between small groups can emerge spontaneously through the gradual acquisition of information [cf. 36]. However, as the size of the group increases, there is more difficulty in triggering cooperation, and it seems that learning, although necessary, is not enough to encourage a large number of players to cooperate over a long period of time [44, cf. 279]. In addition, a public goods games experiment further showed that the greater the heterogeneity of the group composition, the lesser the extent of cooperation [302].

Considering a 2x2 game with two participants and a binary choice of congestion-sensitive routes, but where one of them is faster than the other, User Equilibrium occurs when both players choose the faster route, although the social optimum only exists when one player is on the fast route and the other on the slow route, something hardly achievable by two rational players in a one-time game. With repetition, on the contrary, if players learn to cooperate by alternating between faster and slower routes, fairly sharing the time savings between them, partial cooperation can become a game equilibrium [188]. With several interactions of the same commuter community (particularly at peak hours), a social encounter defined as a repeated game can be established [148, 293, cf. 185]. A sufficient number of route alternations between drivers and a certain degree of altruism, gives rise to a self-organizing formation of a fair equilibrium that may keep the network in the optimal system [207]. Also, in a repeated game, fostering cooperation to use alternately better and worse routes, the travel costs of each driver can become on average lower than in User Equilibrium [185].

3.10.2 Route Choice and Traffic Information

One of the management strategies to improve traffic flow towards an optimal network system state is to influence single drivers' route selection. The concept was studied in the form of altruistic route recommendations for small-scale detours using a driving simulator [268]. Although compliance with the suggestions to reach a System Optimum is possible, the results are not directly transferable to real traffic, as it focused on one-shot interactions and the drivers' behaviour might be different, since they were in a laboratory environment.

Cooperative lane changing manoeuvres were also studied using driving simulators, with a repeated interaction to test the effect of indirect reciprocity on participants' tendency to change lanes [361]. Although played in single player and there was no social interaction between participants, the study showed that the concept of social status as a function of prior behaviour promoted reciprocity and the effectiveness of rewards and sanctions in cooperative driving. However, it is necessary to be judicious in designing agent utility/payoff functions since they lead to better outcomes when aligned with, and sensitive to, system metrics than purely local or global agnostic rewards [331].

Another approach in a simple binary network was to provide feedback to agents with the overall daily travel time of the system, to which they responded with a route change when their last action had increased it [206]. The result was a stable and equitable optimal system, with all agents contributing to the common good. However, the model assumed a completely altruistic society, quite difficult to maintain with human drivers.

The benefits of providing travel time information to rational travellers would depend on their knowledge and ability to predict times based on external factors [115], making them able to make

optimal choices and thereby contributing to a reduction in traffic congestion and an improvement in the level of service of the road infrastructure [205]. Despite that, prevailing travel information can have three adverse impacts on the network: over-saturation, overreaction and concentration [35].

In effect, because of the cognitive and affective value of information, many travellers rely on it to make their choices, whether for routes or commuting modes [38, 37, 173]. However, from a social perspective, the increased provision of information at the individual level leads to a state of User Equilibrium [186], as rational agents with full knowledge will compete for the shortest paths in the road network [23, 24]. Moreover, not all drivers would comply with the recommendations, given the rational traits and cognitive limitations associated with human behaviour[212, 264], particularly when the outcome is less than optimal for them [335]. As Roughgarden [280] pointed out, route selection is a selfish act, since it is done in the sense of getting to the destination as quickly as possible, without thinking about the consequences of that choice for others.

With the introduction of Advanced Traveller Information Systems (ATIS), it has become possible to provide current or even predictive information on traffic flow to road users [cf. 4]. By testing different types of messages, it was noted that besides the quantity and validity of the information, its nature also plays a relevant role [343, 342]. Travel time is not a good indicator as it introduces not only concentration but also oscillations in the system, and it is suggested as a better criterion, for traffic control purposes, the overall density, as it optimizes the flow.

A state of perfect information brings road networks closer to the User Equilibrium state, but this is generally sub-optimal and quite different from System Optimum, where the aggregation of travel times of all travellers is minimized. ATIS already speeds up that process by providing faster route recommendations to drivers, yet it could be used to provide the most optimal route for the system, and in this way the road network could converge on System Optimum rather than User Equilibrium, if widely embraced by road users [187].

In addition to travel information provided by external sources, there is also that generated by travellers themselves during their usual travels and based on the experience of previous trips, disseminated through information-sharing services. The study of this model revealed a positive correlation between percolation rate and convergence to User Equilibrium [296].

Another line of research was towards understanding the effects of providing traffic recommendations on driver behaviour, i.e. its impact on implicit cooperation in self-interested players. The provision of information in the form of optimally assigned route recommendations and extrinsic incentives—penalties and rewards for compliance —, on a simple binary road network, allowed cooperation to emerge more efficiently [186]. Recommendations were considered a necessary condition for cooperation and incentives increased their acceptance rate, but the existence of *indifferent* participants, who kept route preference despite being severely penalized, was observed, suggesting the need for some kind of coordination in a realistic road network.

The coordination of players' actions could be implemented within the framework of ATIS technology, although the System Optimum would only be reached when all drivers follow it. In the direction of alternating cooperation, the recommendations should be changed to ensure that all drivers receive suggestions for the best and worst routes with about the same frequency. The results

showed that agents learn to cooperate without incentives, even though punishments or rewards are useful incentives, especially when cooperation between agents requires a change in behaviour against natural propensities [188].

ATIS success in helping travellers to make informed decisions, however, depends heavily on their acceptance, so it is important to be able to predict and understand their response to the information provided. This led to a study about travellers' response to a Variable Message Signs (VMS), integrating a Technology Acceptance Model (TAM), adapted from the traditional model [cf. 83] to a route-switching model. To the TAM variables of *perceived usefulness, perceived ease of use,* and *behavioural intention* [cf. 81, 82], the model includes latent variables specific to travellers' response to VMS, such as *perceived quality of information, attitude towards route switching,* and *familiarity with the network* [93]. The results showed that attitude towards diversions and intention have a lot of influence on behaviour about route change, but also positive perceptions about the VMS itself have an effect on the acceptance of the information provided.

3.10.3 Fairness and Efficiency

As User Equilibrium, in general, does not minimize the total travel time in the system, obtaining a theoretical optimal traffic pattern for the system may cause discrimination of some users in favour of others, which has prompted the creation of unfairness measures of a traveller, relating its metrics to those of the most efficient traveller in the same origin-destination pair [158, cf. 122].

An approach to address this issue was based on a linear programming formulation that produces a lower bound of a simultaneously efficient and fair system state, capable of taking into account dynamic departure time and route choice in a generalized multi-origin-destination network, and providing personalized journey guidance in a dynamic traffic assignment environment [360].

With a more game theory-oriented perspective, some works [206, 207, 188] have considered the emergence of cooperation also from an equity (i.e., fairness) viewpoint. The features and possibilities of the new ATIS technologies now allow the route recommendation to be specific to each user rather than a general message to all drivers on a given stretch of road. Even though the individual-centric information enhances a sub-optimal state of User Equilibrium, it can also lead in the long run to a System Optimum by spreading the optimal system routes, managed to maintain high levels of equity between the agents [188].

Nevertheless, with a route choice model based on n-person games, it was possible to verify how, even without any form of communication, the network manages to reach a System Optimum, while preserving equity among road users. Cooperation emerges of particular interest for modelling scenarios and strategies from the inherent dynamics of the iterated game, even though fairness and altruism are important attributes to maintain it in the long run [207]. The use of C-ITS and V2V and V2I communication systems could also contribute to more efficient cooperative congestion management strategies based on fair and optimized routing of the system.

Game Theory has been used in the study of social dilemmas, namely the one arising in traffic

congestion, to understand the emergence of cooperation among players and its effect on system optimization. Some extrinsic strategies were also tested to alter its growth rate, such as providing traffic information. The scenarios are mainly based on a simple binary network, where one route is faster than the other, but the models analysed are mostly static or one of the routes has fixed parameters, i.e. it is always the best option, while the world is dynamic.

3.11 Summary

This chapter covered the research conducted on C-ITS issues in the most recent years, since 2015, taking special attention to services and their applications, as well as network routing and information dissemination strategies. Moreover, in the context of Game Theory, the literature about modelling the route choice problem as a social dilemma and the strategies to arouse cooperation among drivers was reviewed, and simulation technique was analyzed from the perspective of a tool for implementing those models.

Chapter 4

Methodological Approach

4.1 Problem Formulation

"*Does communication have impact in reaching and maintaining the System Optimum of an urban transport network supported by an intelligent transport infrastructure?*"

Intelligent transport systems are based on a network of sensors and communications between vehicles, road infrastructure and traffic management entities. Various types of data are exchanged between these agents, varying with their topology and hierarchy within the system.

4.2 Proposed Method

In the study of this problem, the situation was reduced to an elementary scenario, composed of an origin-destination pair, connected by two routes with different travel costs, with a configuration of a double arc parallel network (also known as *Pigou's example* (cf. [256])). Agents choose, on each trip, between their preference (the one that, *a priori,* has the lower cost) and the suggestion that is given by the system. The performance of the traffic network is analyzed according to the behaviour of the vehicles and their acceptance or refusal of the route suggestion and information provided by a roadside communication unit.

A microscopic simulation [216] technique has been selected, despite the high computational consumption it requires, as it allows traffic and its behaviour to be simulated realistically.

4.3 Problem Formalization

Regarding the formalization of this work, two parts are distinguished: the optimality of the system, i.e., the most favourable conditions for the traffic network; and the agents' cooperation towards the system, modelled according to the n-Person Prisoner's Dilemma game, which considers a situation where each of n persons has to make a binary decision.

4.3.1 System Optimality

Based on Wardrop's first principle [345, 299, 192], no driver can unilaterally reduce its own travel costs by shifting to another route. This behavioural assumption leads to a deterministic User Equilibrium (UE).

$$\begin{aligned} \underset{X}{\text{minimize}} \quad & Z = \sum_a \int_0^{x_a} t_a(x_a)\mathrm{d}x \\ \text{subject to} \quad & \sum_k f_k^{rs} = q_{rs} : \forall (r,s) \\ & x_a = \sum_r \sum_s \sum_k \delta_{a,k}^{rs} f_k^{rs} : \forall a \\ & f_k^{rs} \geq 0 : \forall k, r, s \\ & x_a \geq 0 : \forall a \in A \end{aligned}$$

In a link a, the variable x_a is equilibrium flows, t_a is the travel time, f_k^{rs} the flow on path k connecting an origin/destination pair $\langle r,s \rangle$, and q_{rs} the trip rate between r and s.

According to Wardrop's second principle [345, 299, 192], an optimal traffic assignment pattern, called the System Optimum (SO), drivers cooperate with each other in order to minimize the total journey time of the system.

$$\begin{aligned} \underset{X}{\text{minimize}} \quad & Z = \sum_a x_a t_a(x_a) \\ \text{subject to} \quad & \sum_k f_k^{rs} = q_{rs} : \forall (r,s) \\ & x_a = \sum_r \sum_s \sum_k \delta_{a,k}^{rs} f_k^{rs} : \forall a \\ & f_k^{rs} \geq 0 : \forall k, r, s \\ & x_a \geq 0 : \forall a \in A \end{aligned}$$

4.3.2 *n*-Person Dilemma

In the *n*-Person Prisoner's Dilemma game each of *n* players has a choice between two actions: to cooperate with the others for the "common good"; or to defect, pursuing their own short-term selfish interests. The participants—who can be individuals, organizations, or other types of agents—, receive a reward or punishment (the *payoff*) that depends simultaneously on their choice and that of all the others. This paradox of decision-making illustrates that the rational collective acting in self-interest is the opposite of the socially optimum.

For the purpose of this project, the dilemma is formulated as a normal-form game, in which vehicles make a binary decision to *accept* or *reject* the suggestion of the RSU, and the payoff function is based on the socially beneficial outcomes that result from choosing a higher cost route, thus contributing to reduce the total cost to the system.

The intuition of this formalization follows, *mutatis mutandis*, directly from the theory (vd. Subsection 2.5.1), the works of Khun [193] and Chremos, Beaver, and Malikopoulos [67]

4.3.2.1 Mathematical Concepts

Within the framework of non-cooperative game theory, the following definitions shall apply:

Definition 1. A finite normal-form game is a tuple $\mathcal{G} = \langle \mathcal{I}, \mathcal{A}, (u_i)_{i \in \mathcal{I}} \rangle$, where:

- $\mathcal{I} = \{1, 2, \ldots, n\}$ is a finite set of n players, with $n \geq 2$;
- $\mathcal{A} = A_1 \times \cdots \times A_n$, where A_i is a non-empty finite set of actions available to player $i \in \mathcal{I}$, whereby $a = (a_1, \ldots, a_n) \in \mathcal{A}$ is an action profile;
- $u = (u_1, \ldots, u_n)$, where $u_i : \mathcal{A} \to \mathbb{R}$, is a real-valued utility function for player $i \in \mathcal{I}$.

Definition 2. Let A_i be the the action profile of player i, let $a_i, a_i' \in A_i$ be two actions of player i, and let A_{-i} be the set of all action profiles of the remaining players. Then, a_i strictly dominates a_i' if $\forall a_{-i} \in A_{-i} : u_i(a_i, a_{-i}) > u_i(a_i', a_{-i})$. An action is strictly dominant if it (strictly) dominates any other action.

Definition 3. A player i's best response to the action profile $a_{-i} = (a_1, \ldots, a_{i-1}, a_{i+1}, \ldots, a_n)$ is the action $a_i^* \in A_i : u_i(a_i^*, a_{-i}) \geq u_i(a_i, a_{-i}), \forall a_i \in A_i$. An action profile a is a Nash equilibrium if, for each player i, a_i is a best response to a_{-i}. An outcome of a game is any action profile $a \in \mathcal{A}$.

Definition 4. Let $\mathcal{G}$ and $a', a \in \mathcal{A}$. Then an action profile a' Pareto dominates action a if $u_i(a') \geq u_i(a), \forall i \in \mathcal{I}$, and $\exists j \in \mathcal{I} : u_j(a') > u_j(a)$

4.3.2.2 Assumptions

Assumption 1. The participants in the game—the vehicles, in this case—, are *rational,* meaning that individual players will do what is profitable to them and try to maximize their expected value.

Assumption 2. Road users have only the knowledge they have gathered through their journeys on the infrastructure, and solely about travel times and rewards received. They have no information about the current status of the network other than the information provided directly to them by the infrastructure (RSU).

Assumption 3. Each vehicle has a predefined preferred route, which corresponds to the route with the lowest cost, the one with the shortest travel time at free-flow speed.

Assumption 4. There is a society of $n \in \mathbb{N} : n \geq 2$ uncooperative players induced with a shared-resource, which is open-access to all.

Assumption 5. The resource is limited, but since each player is rational, they are expected to behave selfishly towards its use.

Assumption 6. The common resource is road infrastructure, and stakeholders use the roads by travelling either on a direct route or an alternative route, thus using road capacity.

Assumption 7. Each traveller/player may choose either to travel in a direct route or use an alternative route, thereby not contributing to congestion.

Assumption 8. In a game-theoretical context, each traveller represents a rational player who has two possible actions, namely D (defect) by rejecting the suggestion provided by the infrastructure and following his preferred/predefined route, or C (cooperate) by accepting the recommendation and taking the proposed route.

Assumption 9. The RSU is also a participant in the game, playing against all vehicles with a fixed strategy to cooperate (C). The payoff depends on the action of the other players accepting or rejecting its recommendation.

Assumption 10. All players receive a benefit (utility) $b \in \mathbb{R}_{>0}$ for their decision to accept the RSU's recommendation and contribute to the social optimum.

Assumption 11. As choosing the preferred route is a selfish choice, and exploits the resources of the common good, each player who decides to reject the suggestion pays a cost $c \in \mathbb{R}_{<0}$.

4.3.2.3 Payoffs

Taking the matrix of payoffs that characterizes the original version of the Prisoner's Dilemma (vd. Subsection 2.5.1), the following matrix is established:

	more than n choose **C**	n or fewer choose **C**
C	$C+B$	C
D	B	0

where **C** and **D** stand for **C***ooperate* and **D***efect* respectively, just as B and C, in turn, mean *Benefit* and *Cost*.

Thus, the payoffs are ordered $B > (B+C) > 0 > C$. In this formulation, based on the "tragedy of the commons", the assumed cost C is represented by a negative number. **T**emptation means getting the benefit without cost, **R**eward is gaining the benefit with a cost, **P**unishment is not obtaining either, and **S**ucker is paying a cost without realizing the benefit. As in the two-player version of the Prisoners' Dilemma, *defecting* dominates strongly over *cooperating* for all players, so rational players would choose **D** in order to achieve 0, even though they would prefer that everyone choose **C** in order to obtain $C+B$ [cf. 147, 308, 193].

The payoff function of player i is given by:

$$f_i(a_i,h), a_i = C_i \text{ or } D_i,\ h = \{0,1,...,n-1\} \subset \mathbb{N}$$

where a_i is player i's action and h is the number of other cooperators.

In the payoff functions it is assumed:

Assumption 12.

1. The payoff difference $f(D,h) - f(C,h)$ is positive and constant for all values of $h = \{0,1,...,n-1\} \subset \mathbb{N}$, and denoted by α;
2. $f(C,h)$ is monotonically increasing in $h = \{0,1,...,n-1\} \subset \mathbb{N}$;
3. $f(C,n-1) > f(D,0)$.

By the first condition of the above assumption, any player i will get a better reward by selecting defection (D) than by choosing cooperation (C), regardless of what all other players select, i.e., defection is the dominant action for each player. The payoff difference α is interpreted as the player's incentive to defect. The second condition means that the payoff of a cooperator becomes increasingly larger as more players select cooperation. By the last condition, if all players choose the dominant defection you will have a non-cooperative equilibrium that will be Pareto-inferior to the outcome if they select the cooperative dominated actions [cf. 248].

Considering the payoffs hold the condition $T > R > P > S$, with $n \in \mathbb{N} : n \geq 2$, the following utility functions result:

$$\begin{aligned} C(h) &= \frac{h \cdot R + (N-h) \cdot S}{h} \\ D(h) &= \frac{h \cdot T + (N-h) \cdot P}{h} \end{aligned} \tag{4.1}$$

plotted as:

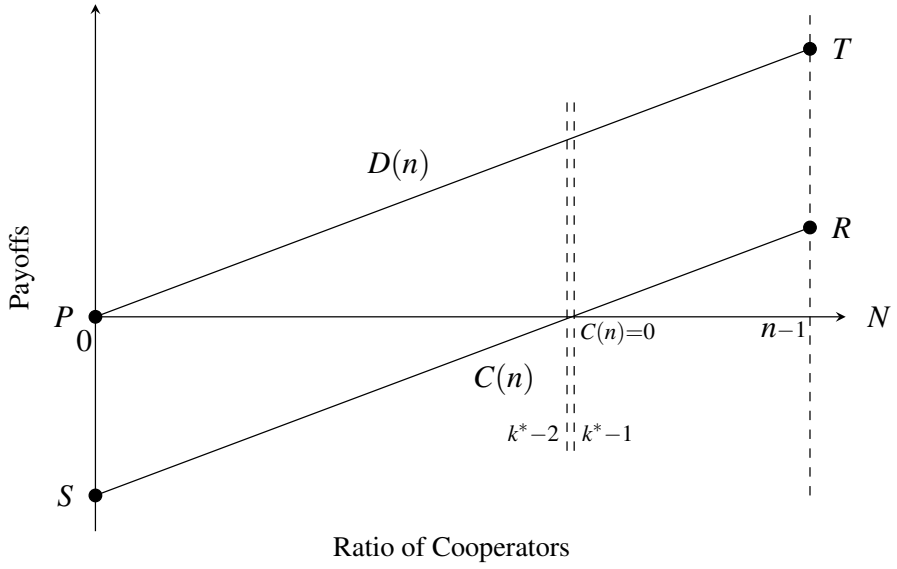


Figure 4.1: Reward/punishment functions for defectors (D) and cooperators (C).

From assumption 12:

$$\exists! k^*(2 \leq k^* \leq n) \in \mathbb{N} : f(C, k^* - 2) < f(D, 0) \leq f(C, k^* - 1)$$

where k^* is the minimum number of cooperators that guarantees that the cooperative payoff can be greater than or equal to the non-cooperative payoff in case no one selects cooperation, i.e, that the overall utility of cooperators is greater than the utility of those who reject suggestion, hence the social dilemma in this context of traffic recommendation and route selection.

4.4 Summary

This chapter dealt with the methodological aspects of the work, namely the formulation of the problem. From a mathematical perspective, the theoretical issues of formalization of the system optimality, with the concepts of User Equilibrium and System Optimum, and the n-Person Iterated Prisoner's Dilemma, characterized as a social dilemma in the context of road traffic, were addressed, with the respective definitions, assumptions and utility functions.

Chapter 5

Experimental Setup

This chapter describes the experimental framework, scenario, and evaluation metrics. The experiment was based on a microscopic simulation through SUMO, controlled via TraCI API from a logic unit written in Python.

5.1 Simulation Framework

5.1.1 Requirements

The SUMO simulator is configured with a set of base scenarios, including traffic flow monitoring sensors. Applications developed in Python implement an external logic control unit and the C-ITS services, which communicate with it through the TraCI interface. This access to the road traffic simulation in progress, retrieve values from simulated objects and manipulate their behaviour in real time.

5.1.1.1 Functional Requirements

Functions	**Requirement**
FR1	System should be able to connect to SUMO via the TraCI API.
FR2	User should be able to define the simulation parameters (number of vehicles, algorithms used and their parameters, random seed, simulation time, ...).
FR3	User should be able to log the data generated by the simulation, step by step, of both the network status and the simulated vehicles.
FR4	User should be able to record travel times and traffic density at various points in the network where sensors are defined.
FR5	User should be able to run the Roth-Erev reinforcement learning algorithm.

Functions	Requirement
FR6	User should be able to run an instance of the n-Person Prisoner's Dilemma.
FR7	User should be able to run different data collection and route selection strategies to create the RSU recommendation.
FR8	User should be able to run different strategies of choosing actions by vehicles.

5.1.1.2 Structural Requirements

Structure	Requirement
Storage	The system should provide storage for scenarios and collected data
Network	The system should operate on a TCP/IP network

5.1.2 System Architecture

Regarding the system architecture to be implemented (Figure 5.1), the SUMO simulator is configured with a set of scenarios stored on disk, and controlled through the TraCI interface. This interface allows access to the simulation of ongoing traffic, obtaining values from the simulated objects and manipulating their behaviour in simulation time.

Two modules written in Python, represented at the bottom of the diagram, constitute the external logic control unit, where the decision models for drivers and road infrastructure as well as the selected C-ITS services will be implemented.

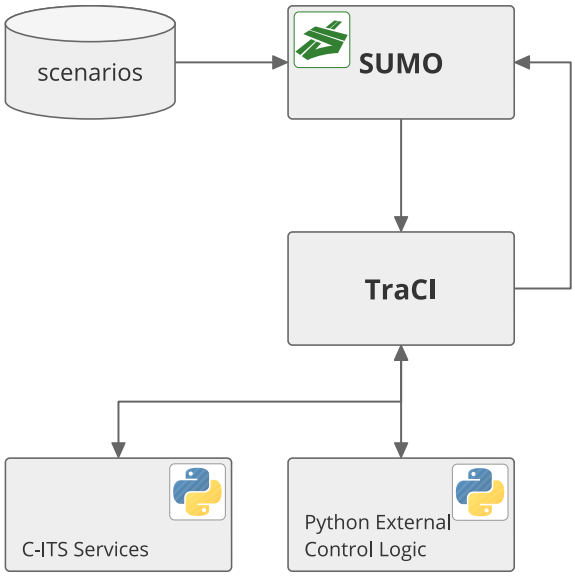


Figure 5.1: Proposed simulation architecture.

5.2 Test Network

The test network for the study is illustrated in Figure 5.2. It consists of a binary network with a 300 m feedback loop and buffer zone, to reinsert the simulated vehicles and be able to maintain a

network overload. There are two possible routes between an origin-destination pair: the main one, designated *direct* (lower cost), with 6000 m, and the *alternative* (higher cost), with 9000 m. RSU sector and feedback edge are two-lane roads, while the *direct* and *alternative* routes are single-lane. The default maximum speed on the network is 25 m/s (90 km/h).

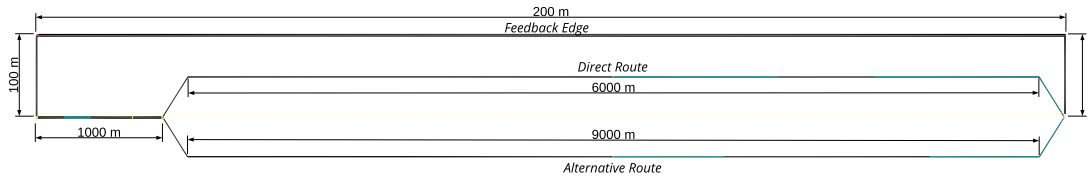


Figure 5.2: Network diagram of the scenario, with the two monitored routes (direct and alternative, with 6000m and 9000m, respectively), the initial zone where the RSU and inductive loop detectors for route selection are located, and the edge for feedback loop. *(Diagram is not to scale.)*

Before the choice node (vd. Figure 5.3), marked as the origin of the chronometry, there is a 1000 m section in which the RSU is located, with a coverage of 150 m, whose zone begins at 250 m of this sector. At 750 m there is an inductive loop detector to carry out route selection, as already chosen by the vehicle. This initial configuration was due to the need to have an area to study the RSU dissemination and, on the other hand, to create a traffic merging zone, to allow vehicles to switch to the most suitable one for the chosen route, without causing too much parasitic noise in the simulation.

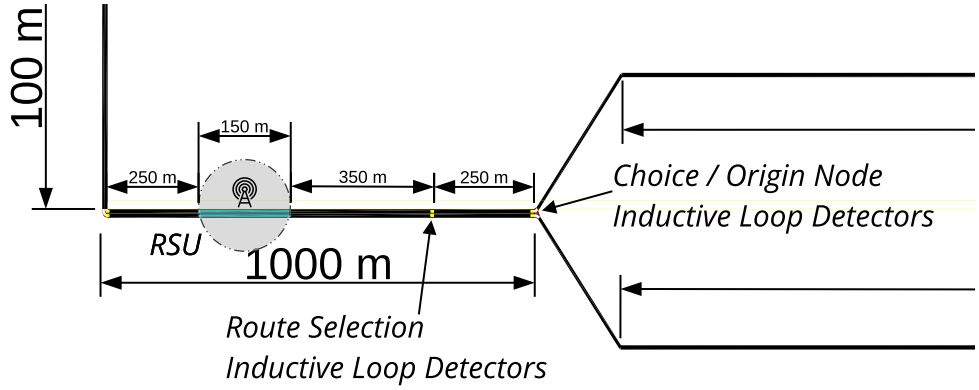


Figure 5.3: Beginning of the network, with the location of the RSU and its coverage, the selection validation inductive loop detector, and another at the choice node at the bifurcation, for the start of timekeeping. *(Diagram is not to scale.)*

On the destination node side (vd. Figure 5.4), there are 1000 m long lane areas for monitoring traffic density, in the middle of the route and for end of queue determination, as well as inductive loop detectors to record intermediate travel times (in the middle of the route) and time to destination (at the destination node).

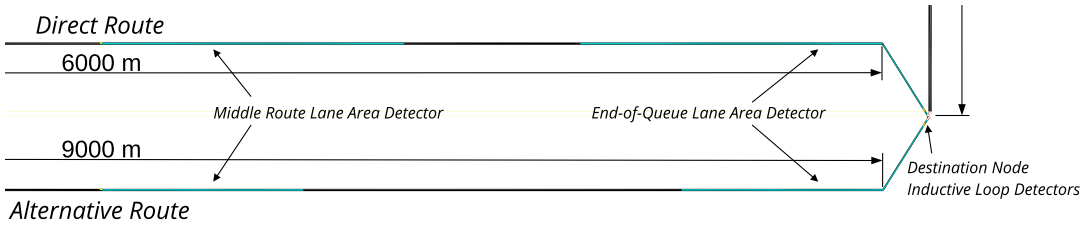


Figure 5.4: Second half of the surveyed area of the two routes, with 1000 m long lane areas and inductive loop detectors for monitoring traffic density in the middle of the route and for end of queue determination, as well as intermediate travel times and time to destination. *(Diagram is not to scale.)*

The feedback edge has lane change prohibition to mitigate parasitic noise in the simulation due to premature vehicle insertion manoeuvres leading to significant instantaneous speed changes.

5.3 Population

To obtain a heterogeneous population, the scenario was populated with four different classes of vehicles, capable of travelling at full network speed, as shown in the table 5.1 and given their respective probabilities. The ceiling on the number of vehicles to be used in the simulation aimed to place the network in a state of congestion on the main (*direct*) route, with traffic moving at a pedestrian-like speed. Thus, the theoretical value were determined analytically considering the *passenger* class, and then verified in a sensitivity analysis by gradually increasing the number of vehicles, diverting all traffic to the *direct* route, until the average speed of the system dropped to 1.50 m/s (5.40 km/h). The floor, in turn, corresponds to the maximum number of vehicles that places the system at critical density, i.e. the maximum achievable density under free flow*.

vClass (SVC)	**Length Width Height**	**minGap**	a_{max} **accel**	b **decel**	b_e **emergency decel**	v_{max} **maxSpeed**	**speed deviation**	**probability**
passenger	4.30 m 1.80 m 1.50 m	2.50 m	2.90 m/s^2	7.50 m/s^2	9.00 m/s^2	180 km/h	0.10	0.70
motorcycle	2.20 m 0.90 m 1.50 m	2.50 m	6.00 m/s^2	10.00 m/s^2	10.00 m/s^2	200 km/h	0.10	0.10
truck	7.10 m 2.40 m 2.40 m	2.50 m	1.30 m/s^2	4.00 m/s^2	7.00 m/s^2	130 km/h	0.10	0.15
bus	12.00 m 2.50 m 3.00 m	2.50 m	1.20 m/s^2	4.00 m/s^2	7.00 m/s^2	85 km/h	0.10	0.05

Table 5.1: Different vehicle types used in the simulation, with their respective characteristics and probabilities.

*The concepts used in this subsection are defined according to the *Highway Capacity Manual* [237].

To determine the maximum number of vehicles [cf. 323]:

$$\begin{aligned} networkLength &= directRoute + rsuSector + feedbackEdge \\ &= 6000 + 1000 + 300 \\ &= 7300\,\mathrm{m} \end{aligned}$$

$$vehicleLength^{*} = 5.00\,\mathrm{m}$$

$$minGap^{*} = 2.50\,\mathrm{m}$$

$$minNetworkSpeed = 1.50\,\mathrm{m/s}$$

$$stationaryState^{\dagger} \sim minNetworkSpeed$$

$$\tau = 1\,\mathrm{s} \qquad \text{(Desired time headway excluding } minGap\text{)}$$

$$\begin{aligned} remainingSpace^{\ddagger} &= stationaryState \cdot \tau \\ &= 1.50\,\mathrm{m} \end{aligned}$$

$$\begin{aligned} spacePerVehicle &= remainingSpace + (vehicleLength + minGap) \\ &= 1.5 + (5.0 + 2.5) \\ &= 9.00\,\mathrm{m} \end{aligned}$$

$$\begin{aligned} density &= \frac{1}{spacePerVehicle} \\ &= \frac{1}{9.0} \\ &= 0.111\,\mathrm{veh/m} \quad (111.111\,\mathrm{veh/km}) \end{aligned}$$

$$\begin{aligned} numVehicles &= density \cdot networkLength \\ &= 0.111 \cdot 7300 \\ &= 811.111\,\mathrm{veh} \end{aligned}$$

And at free flow:

$$freeFlowSpeed = 25.00\,\mathrm{m/s}$$

$$stationaryState \sim freeFlowSpeed$$

$$\begin{aligned} remainingSpace &= stationaryState \cdot \tau \\ &= 25.00\,\mathrm{m} \end{aligned}$$

*As per SUMO defaults.
†State in which origin demands, route choices ratio, and destination supplies are constant, time-independent [cf. 163].
‡The same as *headway*

$$\begin{aligned} spacePerVehicle &= remainingSpace + (vehicleLength + minGap) \\ &= 25 + (5.0 + 2.5) \\ &= 32.50\,\text{m} \end{aligned}$$

$$\begin{aligned} density &= \frac{1}{spacePerVehicle} \\ &= \frac{1}{32.5} \\ &= 0.0308\,\text{veh/m} \quad (30.769\,\text{veh/km}) \end{aligned}$$

$$\begin{aligned} numVehicles &= density \cdot networkLength \\ &= 0.0308 \cdot 7300 \\ &= 224.615\,\text{veh} \end{aligned}$$

After the sensitivity analysis, and also taking into account the mitigation of parasitic noise on the network, a ceiling of 820 vehicles and a floor of 250 vehicles were chosen. The launch speed, during the warm-up phase, is calculated as a function of density so as to obtain a stable traffic flow along the network and a balanced distance between vehicles, i.e. a *stationary state,* when origin demands, route choices ratio, and destination supplies are constant, time-independent [cf. 163]. However, to avoid SUMO keeping some vehicles too long in backlog, making the process very time consuming, the launch phase is done for both routes, thus considering the whole length of the network.

$$\begin{aligned} networkLength &= directRoute + alternativeRoute + 2 \cdot rsuSector + 2 \cdot feedbackEdge \\ &= 6000 + 9000 + 2 \cdot 1000 + 2 \cdot 300 \\ &= 17\,600\,\text{m} \end{aligned}$$

$$numVehicles = 820\,\text{veh}$$

$$\begin{aligned} spacePerVehicle &= \frac{networkLength}{numVehicles} \\ &= \frac{17600}{820} \\ &= 21.463\,\text{m} \end{aligned}$$

$$\begin{aligned} remainingSpace &= spacePerVehicle - (vehicleLength + minGap) \\ &= 21.463 - (5.0 + 2.5) \\ &= 13.963\,\text{m} \end{aligned}$$

$$\begin{aligned} stationaryState &\sim \frac{remainingSpace}{\tau} \\ &\sim \frac{13.963}{1.0} \\ &\sim 13.963\,\text{m/s} \end{aligned}$$

$$\begin{aligned} launchSpeed &\Leftrightarrow stationaryState \\ &= 13.963\,\text{m/s} \end{aligned}$$

5.4 Payoffs

The payoffs chosen were based on the cost of the routes, taking into account their travel times in free flow. Considering only the independent monitored two single-lane edges *direct* and *alternative,* the journey times are respectively 240 s and 360 s.

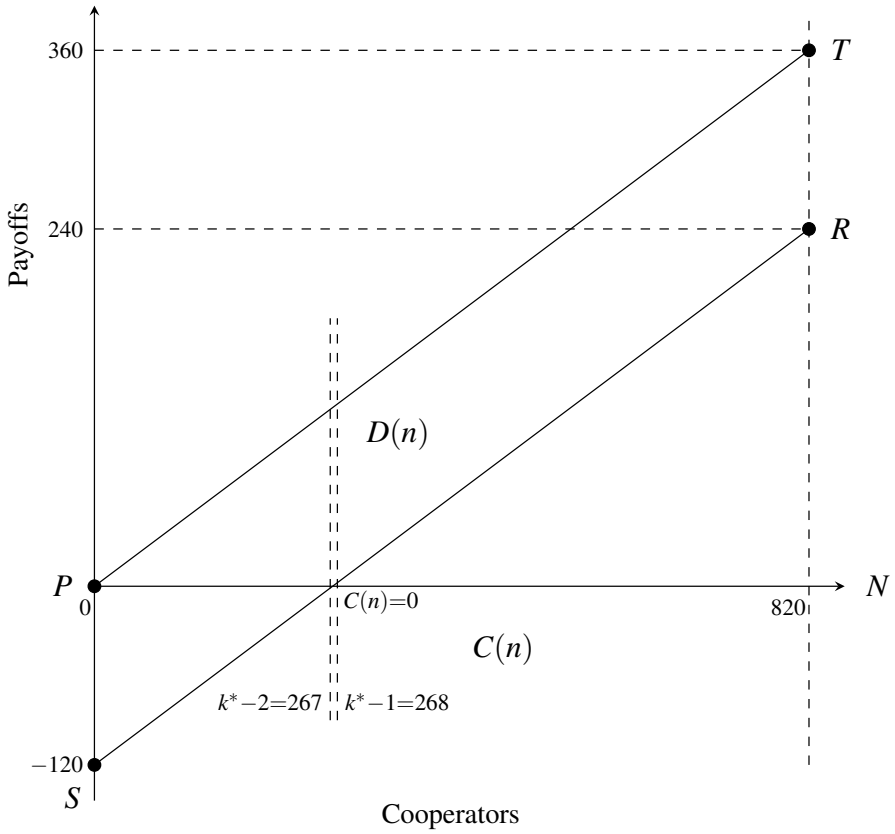


Figure 5.5: Reward/punishment functions for defectors (D) and cooperators (C), with the values $T = 360$, $R = T + S = 240$, $P = 0$, $S = -120$, obtaining $k^* = 269$ for 820 vehicles plus RSU (cf. Subsection 4.3.2.3)

In view of the formalization of the Subsection 4.3.2.3, the *Punishment* value is $P = 0$. The *Sucker* is the cost of taking the *alternative* route, hence the negative value $S = -120$. The value of *Temptation* is significant for the slope of the payoff functions and, consequently, for the cooperation rates. Therefore, two values were chosen to do the experiment with two complementary cooperation ratios: $T = 360$, with which we get *Reward* value $R = T + S = 240$, and $T = 180$, that give $R = 60$ (cf. Subsection 4.3.2.3), obtaining, respectively, $k^* = 549$ and $k^* = 269$ for 820 the vehicles plus the RSU, which always cooperates, its payoff being a reflex of the vehicles' cooperation. The graphs of the respective functions are plotted in Figures 5.6 and 5.5.

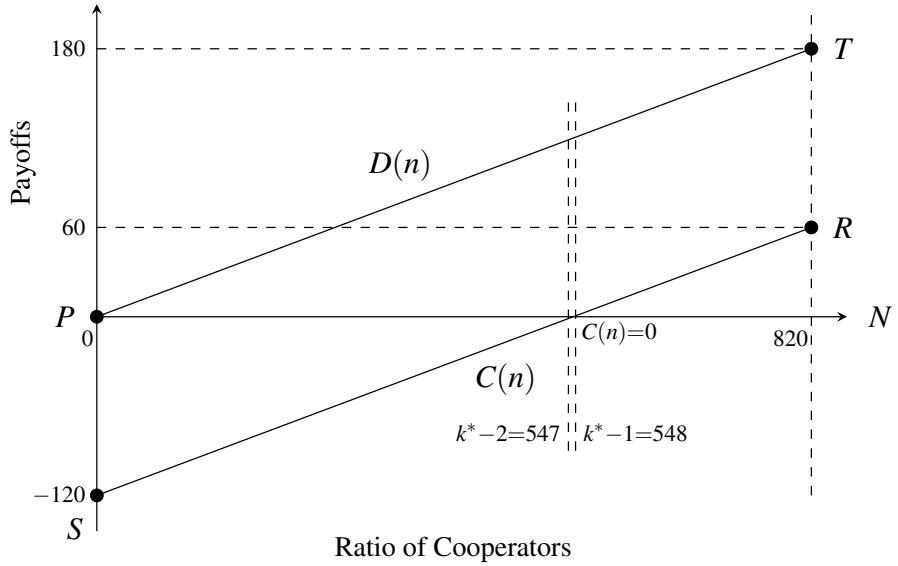


Figure 5.6: Reward/punishment functions for defectors (D) and cooperators (C), with the values $T = 180$, $R = T + S = 60$, $P = 0$, $S = -120$, obtaining $k^* = 549$ for 820 vehicles plus RSU (cf. Subsection 4.3.2.3)

.

5.5 Strategies

In this implementation of a n-Person Prisoner's Dilemma, the RSU is part of the game along with the vehicles, providing them with a recommendation (cf. Subsection 4.3.2.2, Assumptions 8 and 9). About the strategies created, the RSU always cooperates in terms of the game, but there is a set of distinct algorithms to build and disseminate the recommendations. The vehicles, in turn, act according to their "personality", that determines their willingness to cooperate.

5.5.1 RSU Route Recommendation Algorithms

In order to induce the system to an optimal state, there is an RSU at the beginning of the circuit, before the bifurcation at the *choice node*, which delivers recommendations to vehicles on the most appropriate route to take, which they may or may not follow. The construction of the suggestions is based on a set of measurements obtained by the inductive loop and lane area detectors, in an approximation to the reality, as well as some from the system itself for simulation comparison purposes.

A total of 20 algorithms were implemented, which can be categorized into four groups: *travel time based, occupancy/density based, system data based,* and *proportional*, the latter aiming at a differentiated dissemination, i.e. a part of the vehicles under RSU coverage receive a route suggestion, and the rest receive the complementary route. Some variations were being added as the experiences revealed inconsistencies and instabilities.

5.5.1.1 Travel Time Based

The straightforward suggestion uses travel times captured at destination node:

- `travel_time_simple`: compares the journey times taken by the vehicles arriving at the destination and recommend the fastest route in the attempt to equalize both;
- `travel_time_free_flow_tt`: a variation on the previous, includes the free flow time in the comparison, so that when there are no recorded times for one of the routes, the time of the complementary route can be assessed against its theoretical estimate.

As during the preliminary tests the calculations with the times captured at the end of the route showed a significant time lag compared to the anticipation needed to compensate the trip distance, the travel time at mid-route was considered, thus distinguishing two sections of each road. As such:

- `intermediate_travel_time_free_flow_tt`: implements the previous approach of comparing to free-flow times, but with the times captured at mid-distance;
- `travel_time_product`: uses the product of the values captured at destination and mid-distance, on each route, in order to give preference to the one with at least one faster section.

In addition to the last recorded journey time, the RSU keeps a memory of successive readings, and the averages of the last n values are compared in algorithm variants, similar to the above-mentioned counterparts:

- `travel_time_moving_average_simple`;
- `travel_time_moving_average_product`.

Linked to the recording of travel times is a time-to-live (TTL) mechanism, to discard values when they are no longer relevant.

5.5.1.2 Occupancy/Density Based

Other useful metrics for analyzing the state of traffic is road occupancy or density, which is linearly related to the former. Lane area detectors capture these values in the middle of the route and at the end, the latter so-called end-of-queue, as it aims to determine the formation of congestion when approaching the destination.

Thus, in line with the travel time-based algorithms, were implemented:

- `occupancy_simple`: compares the occupancy on both routes, taken at mid-distance and normalized according to the ratio between them;
- `end_of_queue_occupancy`: compares the occupancy in the lane areas at the end of both routes, near the destination node, normalized according to the ratio between them;
- `occupancy_product`: uses the product of the values captured in the lane-areas at destination and mid-distance, on each route, in order to give preference to the one with at least one less denser section.

Attending both to travel times and occupancy:

- `travel_time_occupancy`: builds the recommendation on the comparison of the products of the measured values of travel time and occupancy, the latter normalized according to the ratio between the two routes.

5.5.1.3 System Data Based

From a more theoretical perspective, we consider the values provided by the system itself, both of average speed, estimated travel time and occupancy on the edges:

- `mean_speed`: suggests the route along the edge with the highest mean speed;
- `lane_estimated_travel_time`: recommends the route with the lowest estimated journey time;
- `lane_occupancy`: compares the average of the last n lane occupancy values of the total for each of the monitored routes.

5.5.1.4 Proportional

Lastly, a series of proportionality-oriented algorithms about the vehicles sent by one and another route, these assuming that the RSU is in a mode other than broadcast, such as multicast or even unicast, which can be implemented by means of a subscription service.

- `proportional`: the basis, theoretical, only considering the ratio between the lengths of both routes, and distributing the vehicles so as to achieve balance;
- `proportional_ dynamic`: with four distinct versions, adjusting the proportion at runtime by means of predictions based on metrics both captured and provided by the system:
  - `_v1`: uses an average of the last n recorded values, according to statistical averaging by dividing n values by n;
  - `_v2`: as the previous one, uses an average of the last n recorded values, although calculated differently, by dividing, in turn, $m \leq n$ values by n;
  - `_v3`: considers a ratio of the products of the averages of the last n values of travel times at the halfway point and at the end;
  - `_v4`: similar to the previous one, calculating a ratio of the products of the averages of the last n values, but with the respective occupancies.

The remaining two algorithms take also values provided by the system, rather than those captured:

- `pigou_example`: inspired by the model set out in Pigou's theories [cf. 256], the proportion is obtained from the product of the normalization of occupancies and the average travel time of the last n trips;

- `pigous_example_cooperation_weighted`: follows the principle of the previous one, where the proportion results from the products of the normalization of occupancies and the average travel time of the last n trips, and reinforces its weight according to the cooperation rate as measured by the RSU.

5.5.2 Vehicle "Personalities"

For the purpose of analysing the emergence of cooperation and its impact on system performance and RSU strategies, some player (vehicle) "personalities" [cf. 313, 314] were considered, as described below:

- *Greedy:* selects the action that gave it the highest reward.
- *Accountant:* its choice of action depends on the average payoffs for previous actions.
- *Stochastic:* the probability (p) of taking a certain action is constant and the agent is not influenced by the environment. These particular cases were considered:
  - *Submissive:* always cooperates ($p = 1$).
  - *Stubborn:* never cooperates ($p = 0$).
  - *Undecided:* acts randomly ($p = 0.5$).
- *Pavlovian:* the probability of electing a particular action changes by an amount proportional to the reward or punishment it has received from the environment. If the action is followed by a satisfactory state, then the agent's propensity to choose that particular action is reinforced. In this study the Modified Roth-Erev reinforcement learning algorithm was implemented (cf. Subsection 2.6.2)

5.5.2.1 Action Selection Tactics

The above personalities are realized using a set of tactical algorithms.

As an elementary case, the one with the same name as the personality, `stochastic`, whose variants are adjusted by means of probability parameters.

The *greedy* personality will choose the most advantageous action from the last n trips, however according to different metrics:

- `best_travel_time`: values the action in which he completed the journey in the shortest time;
- `best_payoff`: chooses the action that earned it the highest payoff;
- `best_payoff_utility`: selects the action based on a utility function with obtained payoffs and respective travel times.

The *accountant,* in turn, compares the reward of his last action with the average of the rewards previously received:

- `mean_payoff`: chooses to defect while the payoff is higher than average;

- `mean_payoff_v2`: elects the last action if it was higher than average, or the complementary one otherwise.

In the case of *Pavlovian,* which learns to react to the environment, the Modified Roth-Erev reinforcement learning algorithm is used:

- `roth_erev`: implements the Modified Roth-Erev reinforcement learning algorithm;
- `roth_erev_utility`: variation of the previous one, with a utility function based on payoff and a comparison between the last and the best travel time.

5.6 Parameters

To increase the flexibility of the implemented framework, simulation runs can be launched by command line or by bash scripts, with a set of parameters that allow to create variations, which are described below:

– `step-length`: defines the step duration in seconds;

– `seed`: initializes the random number generator with the given value, both for SUMO and the Python module;

– `output-prefix`: specifies the prefix that is applied to all output files, allowing different simulation runs to be distinguished, or a timestamp is entered otherwise;

– `sim-run-time`: passes the simulation execution time, in hours, which is counted from the end of the warm-up phase;

– `num-vehicles`: sets the number of vehicles to be loaded in simulation, i.e the population;

– `warmup-speed`: determines the maximum allowed speed during the warm-up phase;

– `warmup-routes-weight`: a pair of integers that specifies the weights of each route in the calculation of the proportions during the warm-up phase;

– `network-speed`: provides the maximum speed of the network, otherwise it will be 25 m/s as defined above;

– `change-behavior-probability`: a pair of integers with the weights used to calculate the probabilities that a vehicle will change its behaviour and accept the suggestion against the best action previously chosen;

– `cooperation-probability`: a pair of integers with the weights used to calculate the probabilities of a vehicle choosing the actions of *cooperating* or *defecting,* if there is no defined strategy that overrides it;

– `vehicle-selection-strategy`: provides the vehicle's action selection strategy/algorithm, which will be chosen based on its "personality", as defined above;

- `turn-rsu-off`: switches off suggestions by the RSU and vehicles choose the route based on their individual preference or their journey history, if a probability of behavioural change has been set and they have experienced the *alternative* route;
- `rsu-dynamic-dissemination`: activates a dynamic dissemination interval by the RSU, being adjusted at runtime as a function of the average speed of the vehicles passing through its coverage area;
- `rsu-dissemination-interval`: specifies the dissemination/transmission interval of the RSU, in seconds, or the minimum interval if dynamic dissemination is active;
- `rsu-suggestion-strategy`: passes the RSU algorithm used to build the recommendation, as specified in Subsection 5.5.1;
- `rsu-routes-weight`: a pair of integers with the route weights for proportionality calculation in case it is intended to override the values defined in the scenario;
- `rsu-moving-avg-size`: defines the number of RSU and vehicle history elements that will be used to calculate the last n values in the various strategies/algorithms, otherwise the last 5 elements will be considered;
- `travel-times-ttl`: sets the time-to-live of the values recorded in the history of the RSU and vehicles, i.e. the time during which they are relevant;
- `payoff-matrix`: tuple of floats that define the Prisoner's Dilemma payoff matrix (in the T,R,P,S sequence), employed in some algorithms;
- `roth-erev-parameters`: pair of floats in the range [0, 1], with specific parameters passed to the Roth-Erev algorithm (when used), namely the *Recency* and *Experimentation*.
- `rsu-change-dissemination`: changes the range of MSW dissemination over the simulation time, in accordance with the lists provided in the parameters below.
- `rsu-change-dissemination-steps`: list of the simulation steps, in seconds (s), at which a change of the RSU dissemination interval occurs.
- `rsu-change-dissemination-intervals`: list of the RSU dissemination intervals, in seconds (s), activated at the times defined in the previous parameter.

5.7 Evaluation Metrics

To evaluate the performance of the various strategies implemented for both RSU and vehicles, the following metrics were considered:

- *Mean network speed* (m/s): the average speed across all vehicles in the network, to give an insight into the system's performance and stability.

- *Mean speed* (m/s): mean speed on each route, both taken in the 1000 m long mid-distance lane areas detectors of the (*direct* and *alternative* routes), and obtained from output files with aggregated edge/lane based network performance measures.
- *Travel times* (s): travel times for each vehicle, measured on the two edges after the bifurcation (*direct* and *alternative* routes), by inductive loop detectors, between the *choice node* and the *destination node,* as well as between the *choice node* and the *middle* of the route. To calculate individual travel time averages and obtain the best recorded time, personal records of each vehicle are used.
- *Occupancy* (%): the occupancy of the lane on each route, both taken in the 1000 m ling mid-distance lane areas detectors of the (*direct* and *alternative* routes), and obtained from output files with aggregated edge/lane based network performance measures.
- *Number of Cooperators/Defectors* (#): number of *cooperators* and *defectors* in the system at each simulation step.
- *Degree of Cooperativeness* (#): a cumulative sum, calculated at each iteration, based on the complement of the ratio of cooperators, i.e., the higher the number of cooperators the less it increases, but the defectors are more penalized, and vice-versa. It varies inversely with the size of the group to which the player belongs, and reflects of how much the vehicle stands out from the majorities.
- *Number of trips* (#): number of trips that the vehicle was able to complete during the simulation period, obtained from the individual vehicle logs.

Data are collected at each step of the simulation run, as well as aggregated using inductive loop and lane area detectors, at 1 min and 5 min. Some of these metrics are also used at runtime for the purposes of route recommendation strategies. Each vehicle also keeps an individual log where it collects the number of journeys and their times, the decisions made and routes taken, as well as the payoffs obtained.

5.8 Preliminary Tests, Calibration and Setbacks

At the beginning of this work, some tests were carried out to design the scenario according to the purposes of the study, and then a sensitivity analysis and calibration of the network were performed.

Taking into consideration the characteristics found in the microscopic simulation of SUMO, there was a need to create the feedback edge to achieve the overload of the system. In an attempt to re-feed the network using teleportation, in order to maintain the vehicles' travel history, but SUMO would put them in backlog until it could reinsert them, and, furthermore, they would circulate in free flow to the destination node. One solution would be to create a slower section at the end of the route in order to cause congestion, but this would impose limiting the speed to a specific fixed number, which would introduce an artificial value into the system. With the feedback edge, the network naturally goes into overload when all vehicles are inserted in simulation according to the intended and calculated density.

Another issue pertinent to the design of the network was the SUMO lane change model, which gives rise to premature slowdowns on two-lane sections. Therefore, the feedback edge has the two lanes separated so as to create a buffer zone and prevent one of the lanes from causing unilateral congestion near the destination node. The buffer length allows mitigation of those parasitic values in the monitored lanes (*direct* and *alternative*). The common section where the RSU is located was also configured in this sense, keeping the two lanes and giving space for traffic to switch after making a decision, already according to the route it is going to take.

Nevertheless, SUMO is configured with the `time-to-teleport` option to infinity, since in the event that a vehicle is longer almost stationary than a given threshold value, it is assumed to be grid-locked and teleported to the next free edge on its route, thereby escaping the feedback process and as such would be removed from the simulation as having arrived.

5.9 Summary

This chapter covered the aspects related to the experimental setup. The framework to be implemented, its architecture and requirements were taken into account, as well as the design and configuration of the network under analysis. Then, it was addressed the simulated population, the values of the payoffs matrix, along with the strategies and algorithms used by the RSU and vehicles. Finally, the evaluation metrics were defined and some of the issues that led to decisions made about the design and implementation were briefly discussed.

Chapter 6

Simulation Experiments and Analysis

This chapter presents the results obtained and the respective analysis, taking into consideration the taxonomy of the various strategies, tactics, and algorithms implemented. A number of metrics are assessed, relating both to the speed and journey times achieved and to traffic density and flow, taking into due consideration the fundamental diagrams.

In each section, the most representative situations are examined and discussed, with the corpus of results of all the experiments under assessment being provided in Appendix A.

6.1 Baselines

The three fundamental characteristics of traffic flow are *flow*, *speed*, and *density* [241]. In this study the density is taken as an independent variable, controlled by the number of vehicles inserted in each simulation.

As reference values, one takes the *critical density* and the *jam density*, i.e. respectively the maximum density achievable under free flow and the maximum density achieved under congestion [58], whose theoretical values will be calculated [cf. 323] considering the free-flow speed $v_f = 25.00\,\mathrm{m/s}$ and jam speed $v_{jam} = 0.00\,\mathrm{m/s}$, which means a complete stop.

At free flow:

$$freeFlowSpeed = 25.00\,\mathrm{m/s}$$

$$vehicleLength^{*} = 5.00\,\mathrm{m}$$

$$minGap^{*} = 2.50\,\mathrm{m}$$

$$stationaryState^{\dagger} \sim freeFlowSpeed$$

$$\tau = 1\,\mathrm{s} \qquad \text{(Desired time headway excluding } minGap\text{)}$$

$$
\begin{aligned}
remainingSpace^{\ddagger} &= stationaryState \cdot \tau \\
&= 25.00\,\mathrm{m} \\
spacePerVehicle &= remainingSpace + (vehicleLength + minGap) \\
&= 25 + (5.0 + 2.5) \\
&= 32.50\,\mathrm{m}
\end{aligned}
$$

$$
\begin{aligned}
density &= \frac{1}{spacePerVehicle} \\
&= \frac{1}{32.5} \\
&= 0.0308\,\mathrm{veh/m} \quad (30.769\,\mathrm{veh/km})
\end{aligned}
$$

$$
\begin{aligned}
flow &= density \cdot freeFlowSpeed \\
&= 0.0308 \cdot 25.00 \\
&= 0.769\,\mathrm{veh/s} \quad (2769.231\,\mathrm{veh/h})
\end{aligned}
$$

And at traffic jam:[‡]

$$
jamSpeed = 0.00\,\mathrm{m/s}
$$

$$
stationaryState \sim jamSpeed
$$

$$
\begin{aligned}
remainingSpace &= stationaryState \cdot \tau \\
&= 0.00\,\mathrm{m} \\
spacePerVehicle &= remainingSpace + (vehicleLength + minGap) \\
&= 0.0 + (5.0 + 2.5) \\
&= 7.50\,\mathrm{m}
\end{aligned}
$$

$$
\begin{aligned}
density &= \frac{1}{spacePerVehicle} \\
&= \frac{1}{7.5} \\
&= 0.1333\,\mathrm{veh/m} \quad (133.333\,\mathrm{veh/km})
\end{aligned}
$$

$$
\begin{aligned}
flow &= density \cdot speed \\
&= 0.1333 \cdot 0.00 \\
&= 0.000\,\mathrm{veh/s} \quad (0.000\,\mathrm{veh/h})
\end{aligned}
$$

The critical density is therefore 0.0308 veh/m (30.769 veh/km), which gives a theoretical maximum flow of 0.769 veh/s (2769.231 veh/h). For the length of the network, it represents 224 vehicles, although due to the RSU sector with two lanes, this value could rise to 255 vehicles. In jam condition, traffic is standstill, vehicles occupy their length and a minimum interval between them,

[*] As per SUMO defaults.

[†] State in which origin demands, route choices ratio, and destination supplies are constant, time-independent [cf. 163].

[‡] The same as *headway,* wich represents the time (in seconds (s)) between successive vehicles, so the remaining space represents the free space in front of the vehicle, calculated as a function of the speed..

giving a density of 0.1333 veh/m (133.333 veh/km) —although having the flow of 0.00 veh/s (0.00 veh/h) —, which, in this network, represents 973 vehicles.

Physical infrastructure of a transport supply system have a finite *capacity,* i.e. a maximum number of vehicles that can be served in a given time interval, the maximum flow [103, 324]. The fundamental traffic flow diagram (Figure 6.1) illustrates the relationship between road traffic flow (vehicles per time unit) and traffic density (vehicles per length unit).

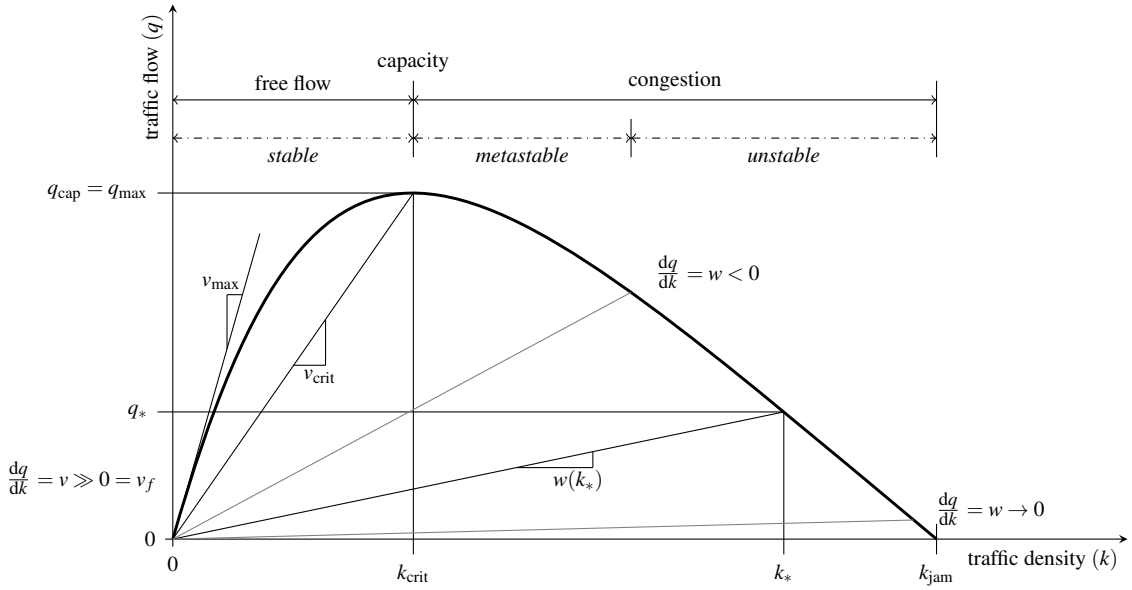


Figure 6.1: Fundamental diagram of traffic flow and its properties (adapted from [178, cf. 204, 286, 275, 176, 177]), where q is the traffic flow, k the traffic density, v the free-flow upstream wave velocity, and w the congested downstream wave velocity.

According to this diagram [cf. 58], there are two conditions under which the traffic flow can be zero: when the traffic density is zero, i.e. there are no vehicles on the road and the speed is assumed to be the maximum theoretical value, the *free-flow speed,* $v_0 = v_f$; or when the speed is zero, i.e. the vehicles are not moving and the traffic density is at its maximum theoretical value, the *jam density,* k_{jam}. The peak of the *density-flow* curve is reached at the theoretical maximum flow, the *capacity* of the road.

This diagram also depicts the three stages into which the traffic flow is divided, according to the *Three-Phase Traffic theory* [174, 176]: *stable* stage, *metastable* stage and *unstable* stage. During the *stable* phase, the traffic flow is a *free-flow,* there is barely any traffic congestion and vehicles are moving close to maximum speed. In the metastable phase, there is already some congestion and the flow may experience slight disruptions, although the traffic state remains stable. The *unstable* phase is when traffic is congested much of the time and vehicles move slowly.

The relationship between the three fundamental characteristics of traffic flow can be analyzed in the Greenshields model diagram [104, 242, cf. 175] (Figure 6.2). From this graph, it can be inferred that the theoretical maximum flow or capacity occurs simultaneously at the peaks of the *velocity-flow* and *density-flow* curves, with the corresponding *critical velocity* (v_{crit}) and *critical*

density (k_{crit}). The sections of the curves represented in solid line correspond to non-congested conditions, while the dashed line sections are congested conditions.

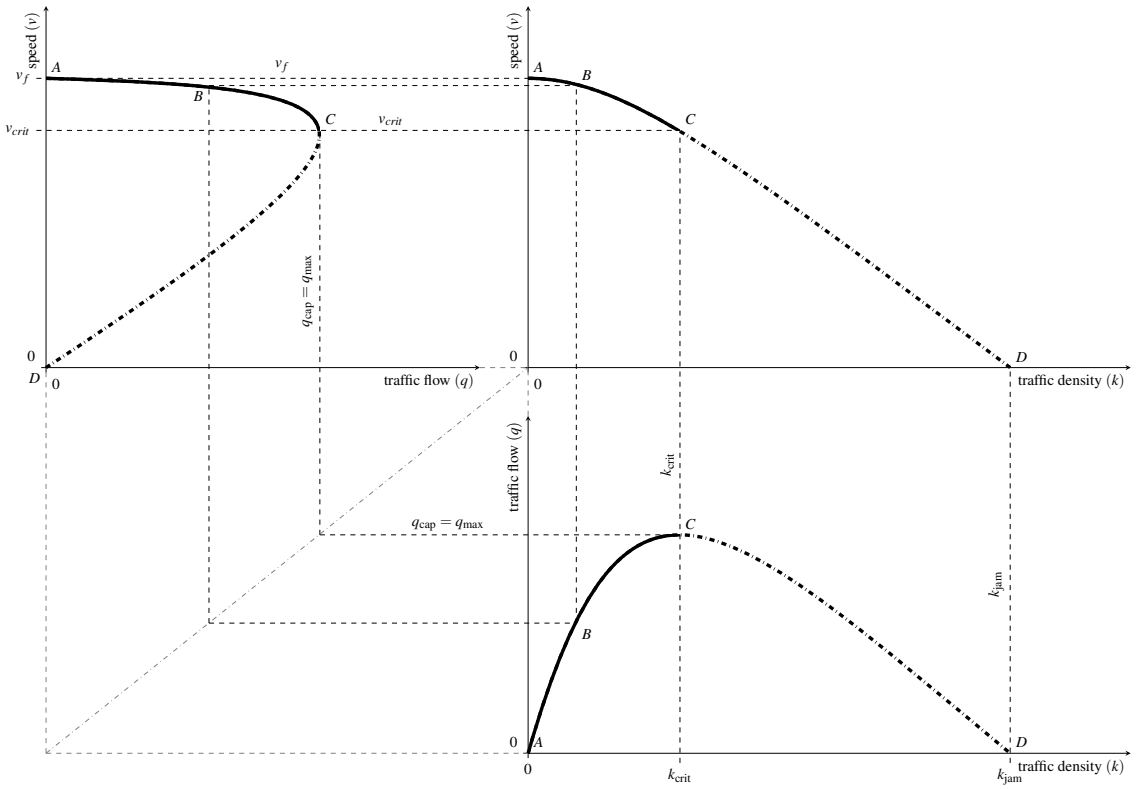


Figure 6.2: Greenshields model for Speed-Flow-Density Relationship (based on [104, 273, 272, cf. 136]), where q is the traffic flow, k the traffic density, and v the speed.

From the *speed-flow* diagram (top left), under non-congested conditions ($\overline{AC}$ section), when the traffic flow is very low, the speed is at its highest level (free-flow speed), and vehicles can travel at the desired speed. Velocity gradually decreases as flows increase, until capacity is reached, where the transition from uncongested to congested conditions occurs, and the optimal speed is reached. As flow decreases due to congestion ($\overline{CD}$ section), so does speed, and for very severe congestion, both flow and speed approach zero.

Correspondingly, in the flow density curve (bottom right), the maximum flow corresponds to the critical (optimal) density. In severe congestion conditions, the jam density is reached when vehicles become standstill, and the flow is close to zero.

In the *velocity-density* relationship (top right), it is observed that the velocity, theoretically maximum for density equal to zero, gradually decreases and approaches zero at jam density, the maximum density.

Despite the extensive use of the Greenshields model, experimental observations do not support its form [104], hence some revisions, such as Greenberg's model (Figure 6.3). Since under zero to light traffic conditions there is sufficient space for vehicles to maintain the desired speed, the free flow speed v_f can be sustained up to a critical density k_{crit}, and traffic flow grows linearly in

this phase. However, as the traffic density increases, the speed starts to decrease until it approaches zero, when the density reaches the maximum, i.e., the jam density k_{jam} [240]. Traffic flow, in turn, increases a bit more until it peaks at capacity density k_{cap}, and then tends to zero at the jam density, just as in Greenshields' model (cf. 6.2).

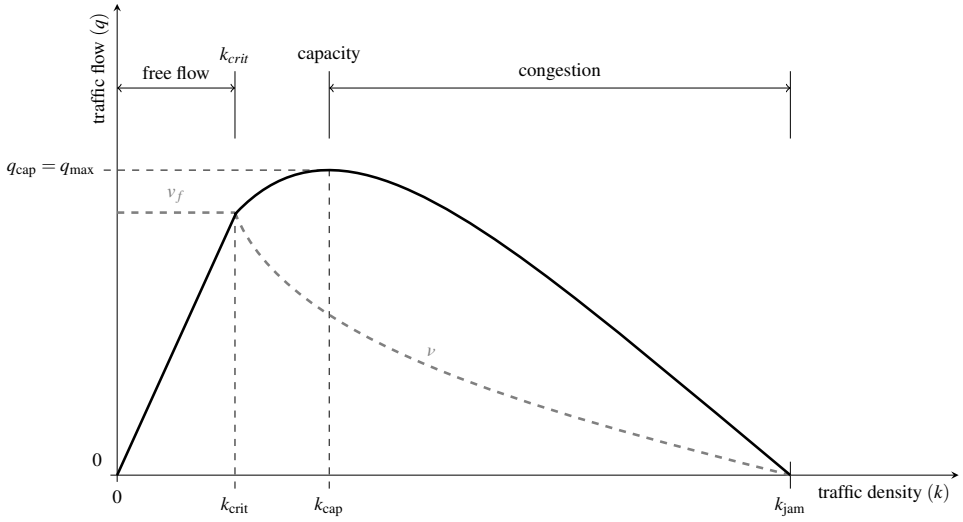
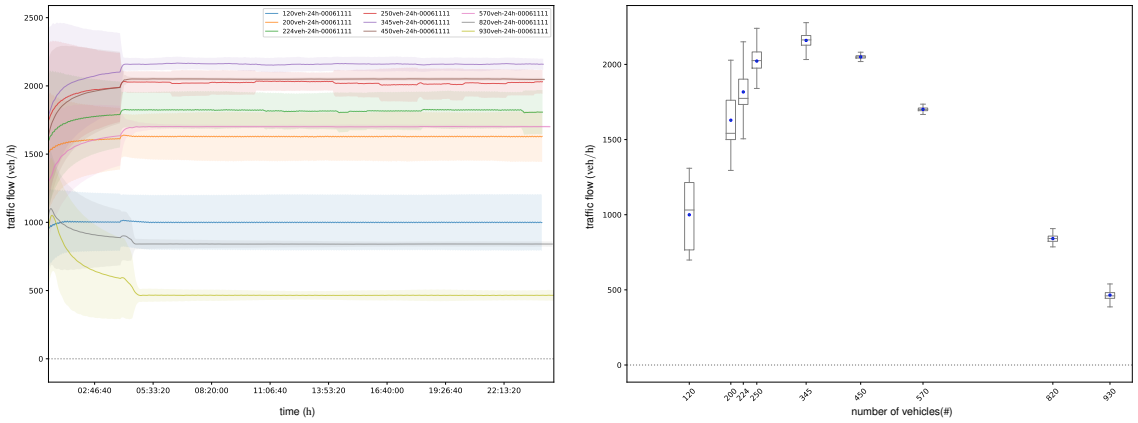


Figure 6.3: Greenberg model of *flow-density* relationship (adapted from [240, cf. 104]), where q is the traffic flow, k the traffic density, and v identifies the underlying *speed-density* curve (plotted as a dashed line) to show how it relates to the *flow-density* curve.

In the experiments performed the independent variable was the density, so variations were made in the population taking into account the theoretical values calculated, choosing 120, 200, 224, 250, 345, 450, 570, 820 and 930 vehicles. In order to analyze congestion on the main (*direct*) route, the "personality" of the vehicles was selected so that they all chose the preferred route, ignoring any system recommendation.

The recorded traffic flows are shown in the Figure 6.4. After the warm-up period, during which vehicles circulated on both routes in order to facilitate the insertion process in simulation, there was a phase of stabilization of flow as they converged on the *direct* route, and then the network maintained a constant average traffic flow until the end of the 24 h. However, at lower densities (`120veh-...`, `200veh-...`, `224veh-...` and `250veh-...`) the standard deviation (Figure 6.4a, shaded) indicates greater variability of the flow, in contrast to the *metastable* stage (`450veh-...` and `570veh-...`), where the variation is minimal. At the densities analyzed within the *unstable* phase (`820veh-...` and `930veh-...`), there was a slight increase in the variability of the flow, which is mainly due to the approach of severe congestion, which already generates some shock waves, as will be seen in more detail below.

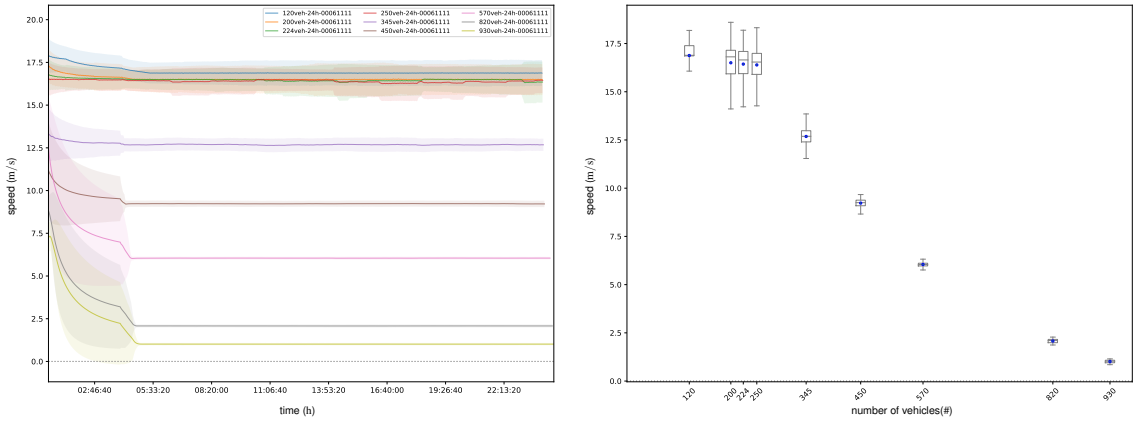
This analysis is corroborated by the boxplot chart (Figure 6.4b), where it is possible to observe this convergent stabilization of flow (by the size of the box) until the peak is reached, and a slight increase in variation when the flow tends towards zero at the end. Furthermore, plotted against the number of vehicles (as a function of density), it evidences the characteristic curve of the *flow-density* diagram (cf. Figure 6.1), with peak traffic flow at 345 vehicles.



a) Traffic flow over 24 h, SMA.

b) Boxplot of traffic flow against number of vehicles in simulation.

Figure 6.4: Traffic flow on the *direct* route, in vehicles per hour (veh/h), for the various populations considered: a) during a 24 h period, 4 h Simple Moving Average, mean (line) and standard deviation (shaded); and b) a boxplot of the variation of the traffic flow according to the number of vehicles in simulation. These comprise the free-flow period (120 and 200 vehicles), maximum capacity (224 vehicles) —in fact, the theoretical peak may occur at ≈ 250 vehicles because of the 1000 m with two lanes in the RSU sector—, congested downstream wave velocity (345, 450 and 570 vehicles), and near jam density (820 and 930 vehicles), when they are of the *stubborn* personality. Nevertheless, it was observed that the average flow increased until we had 345 vehicles on the network, and then it started to decrease. By the standard deviation (shaded), it is possible to notice that by increasing the number of vehicles (and consequently the density) the flow gradually became more stable, due to the decrease in the average speed (cf. Figure 6.5 and Greenshield Model diagrams, on Figure 6.2). During the beginning of the simulation, after the warm-up, there is still a moment of speed variation, as the vehicles converge to that route, with pronounced instability, as can be observed by the standard deviation. *Legend identifies the simulation runs (cf. Appendix A for details).*



a) Network mean speed over 24 h, SMA.

b) Boxplot of network mean speed against number of vehicles in simulation.

Figure 6.5: Mean speed in the network, in meters per second (m/s), for various populations considered (120, 200, 224, 250, 345, 450, 570, 820 and 930 vehicles), when they are of the *stubborn* personality, i.e., they invariably opt for the preferred route, the *direct* one, faster when in free-flow: a) during a 24 h period, 4 h Simple Moving Average, mean (line) and standard deviation (shaded); and b) a boxplot of the variation of the network speed according to the number of vehicles in simulation. During the beginning of the simulation, after the warm-up, there is still a moment of speed decrease, as the vehicles converge to that route, with pronounced instability, as can be observed by the standard deviation. *Legend identifies the simulation runs (cf. Appendix A for details).*

Considering speed against density, in the same populations (Figure 6.5), there is a gradual decrease with increasing density, although those below 250 vehicles have very close average values. Moreover, with the decrease in speed there was also less variation, as can be seen by the standard deviation (Figure 6.5a, shaded). As with the analysis of traffic flows, this is corroborated by the boxplot chart, which highlights speed values with a very slight decrease up to 250 vehicles (indicating a plateau) and a steeper decrease as density increases.

Although the velocity decreases with increasing density, the curve perceived in this graph has some dissimilarity with the characteristic curve of the Greenshields model (cf. 6.2). Nevertheless, given the populations and the resulting curves, the findings, both flow-density and velocity-density, are in full accordance with Greenberg's model (cf. 6.3). Compared to the calculated theoretical value of $\{224, 250\}$ vehicles for the critical density, the speed sustained with only a slight decrease in this range, followed by a sharp decrease; traffic flow, for its part, rose sharply to 250 vehicles, but continued to increase, peaking at 345 vehicles, after which it began a descent tending towards zero in jam density.

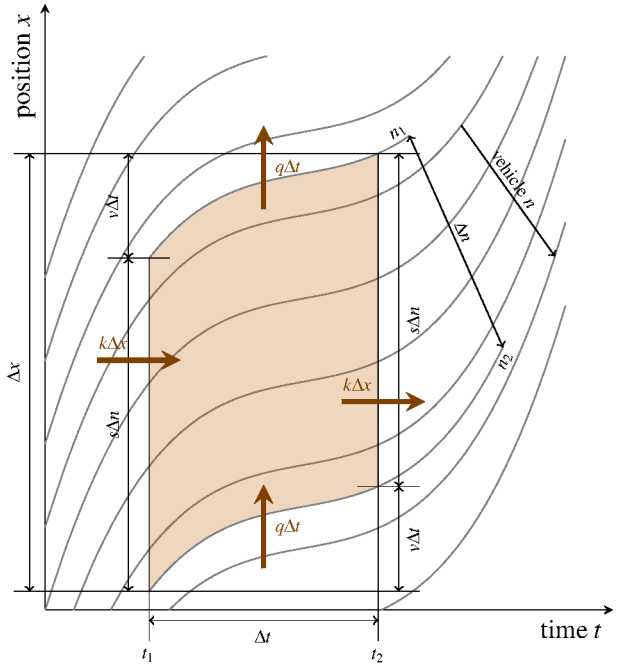
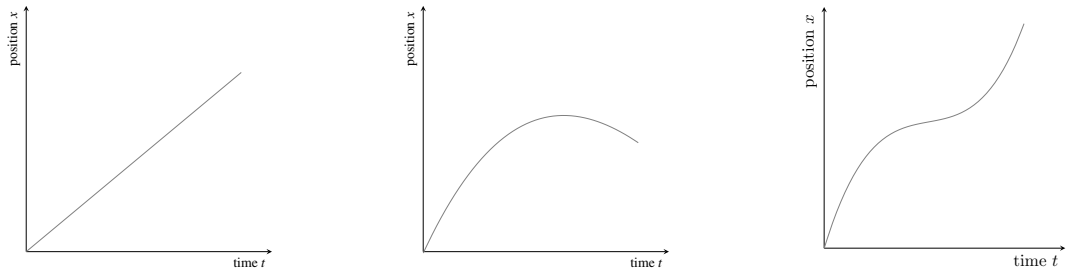


Figure 6.6: Graphical derivation of the conservation equation in the kinematic wave model in Lagrangian coordinates (adapted from [180, cf. 179]), where position x increases over time t for a fixed number of vehicles n; and s represents the space occupied by vehicles, v the speed, q the traffic flow and k the traffic density. The density-flow relationship is shown by the number of vehicles entering the control volume (shaded) —*inflow*—, which is equal to the number of vehicles leaving it—*outflow*.

Another relevant tool in car traffic analysis is the time-space diagram [cf. 241] (Figure 6.6), in which the trajectories of individual vehicles in space are plotted against time, describing the relationship between their position in a traffic flow and the time as they progress along the road. The vehicles in motion are depicted by sloping lines, and stationary ones by horizontal lines. The slope of the line corresponds to the vehicle speed and the curved sections of the trajectories represent

those changing speed, i.e. accelerating or decelerating. Reductions in speed flatten the slope of the lines, and increases in speed accentuate the slopes.



a) Movement with constant speed

b) Reversal of the direction of movement

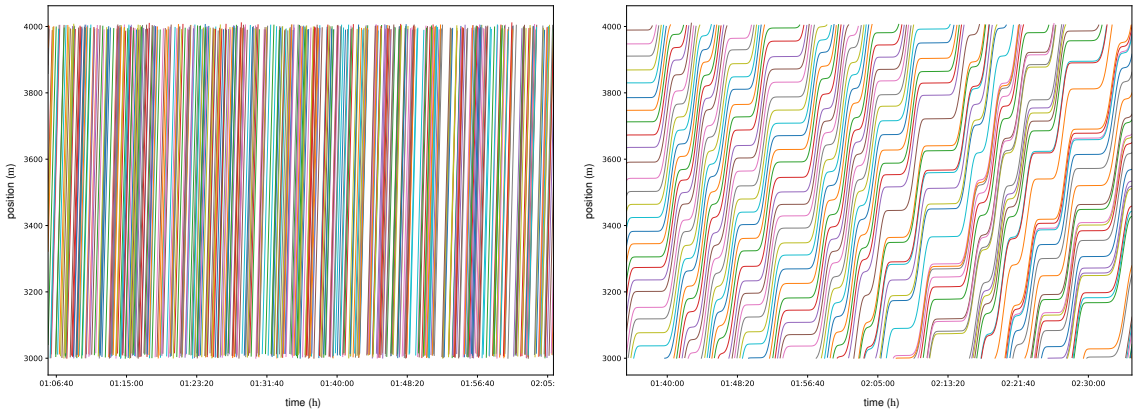
c) Movement interspersed with a stationary state

Figure 6.7: Primary patterns in the space-time diagram for a single vehicle. The left-hand figure shows the distance x increasing linearly with respect to the origin as time progresses, and the vehicle moves smoothly along the road. In the middle figure, the vehicle initially moves at a smooth pace until it reaches a position and then reverses its direction of motion. Finally, the figure on the right shows a vehicle whose motion becomes stationary halfway through the trajectory, and maintaining the same position, and resuming movement.

In Figure 6.7, the primary patterns appearing in a space-time diagram for a single vehicle are illustrated, distinguishing a vehicle with constant speed (Figure 6.7a), i.e. the distance increases linearly with respect to the origin as time progresses; the vehicle that reverses its direction of motion (Figure 6.7b); and lastly, a vehicle whose motion undergoes a stationary period in the middle of the trajectory (Figure 6.7c). From those figures [cf. 106], steeply rising sections of $x(t)$ describe a rapidly advancing vehicle and horizontal sections of $x(t)$ characterize a stationary vehicle, while weakly sloping sections represent a slow moving vehicle. Straight lines indicate a constant speed movement and curved sections show an accelerated movement: acceleration if the curve is concave downwards, deceleration if the curve is convex upwards. The propagation of a change in flow and density gives rise to shock waves [105].

Plots of two key moments of the simulations carried out (Figure 6.8), the *capacity* density and a density close to the *jam density*, show a very high traffic flow with the 345 vehicles (Figure 6.8a), manifested in the very close lines (vehicles), but the speed is still constant or with a very high slope (straight lines). However, with 930 vehicles (Figure 6.8b) and the network overloaded, the density approaches the *jam density* and the traffic flow starts tending towards zero, causing the lines to be further apart. The slope of the lines—*speed*—, shows stationary periods, with flat lines, and a congestion shockwave pattern results, a consequence of the propagation of vehicle states.

The analyzes performed with the vehicles of the *stubborn* "personality", i.e., non-cooperating and invariably opting for the preferred (*direct*) route, provides a baseline of the system, changing the traffic density and reaching a congestion, as everyone takes the same way and ignores the recommendations. At the other extreme of this situation is the fully cooperating *submissive* vehicles, which will give a baseline for the functionality and performance of the various recommendation and dissemination strategies/algorithms by the RSU.



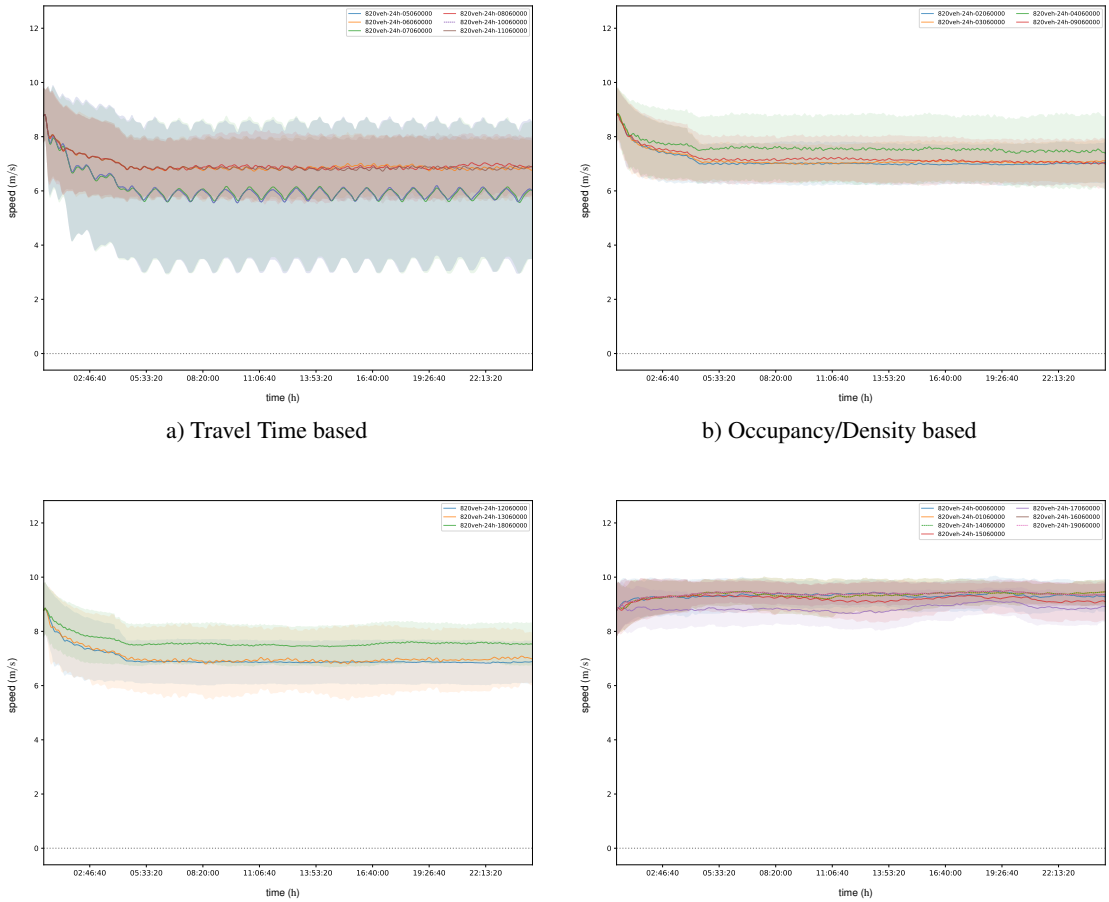
a) Time-space diagram for simulation run `345veh-24h-00061111`.

b) Time-space diagram for simulation run `930veh-24h-00061111`.

Figure 6.8: Time-Space diagram of simulation runs `345veh-24h-00061111` (A.8) and `930veh-24h-00061111` (A.12), for the one hour period after the end of the warmup, from 1:00:00 to 2:00:00 simulation time, plotted for the data from the sensor placed in the middle of the *direct* route (between 3000 m and 4000 m). In the diagram on the left, with a density corresponding to the *capacity,* we observe a very high traffic flow, with the lines (vehicles) very close together, and a constant speed (straight lines). In turn, the diagram on the right, with the network overloaded and the density approaching the *jam density,* already shows a very low flow (tending towards zero) and stationary periods (horizontal lines). The resulting pattern in this one also illustrates the propagation of vehicle states, i.e. the congestion shockwave.

The algorithms were divided into four categories (Figure 6.9), taking into account the metrics used and their origin, as well as the mode of dissemination. With the data provided by the sensors installed in the network, the lane areas and the inductive loops, there are the algorithms *based on travel time* and those *based on density/occupancy.* In addition to these data, and for the purposes of the simulation, there are the global measurements provided by the simulator itself (*based on system data*). Finally, there is a set of *proportional* algorithms, which, also based on those previous measures, disseminate two different recommendations to two groups of vehicles, according to the calculated proportions.

The population considered in these simulation runs was 820 vehicles, a density that causes moderate-high congestion (pedestrian speed, when all are diverted to the main route), but without creating too much parasitic noise in the network. The non-proportional approaches (Figures 6.9a, 6.9b and 6.9c) almost all achieved an average network speed of about 7.00 m/s (25.20 km/h), with exception of `travel_time_moving_average_simple (820veh-24h-07060000)` and `travel_time_free_flow_tt (820veh-24h-10060000)`, which were not only lower (around 6.00 m/s (21.60 km/h)), but also with higher instability and variability, as can be seen by the standard deviation (shaded). Indeed, when at the highest values it is higher than the others, but it gave rise to heavy congestion, with strong speed drops and variations in flow (cf. Appendices A.19 and A.22). Since both are based only on travel time captured at the destination, this variation and amplitude is mainly due to the lag between the generation of the recommendation and its dissemination, as diverting traffic to the complementary route at this point no longer avoids the accumulation of traffic on the route (due to its length) and consequent congestion. This can be seen



a) Travel Time based

b) Occupancy/Density based

c) System data based

d) Proportional

Figure 6.9: Mean speed in the network, in meters per second (m/s), during a 24 h period, 4 h Simple Moving Average, mean (line) and standard deviation (shaded), in the various algorithms implemented to build the RSU recommendation (cf. Subsection 5.5.1), with which all the vehicles comply. *Legend identifies the simulation runs (cf. Appendix A for details).*

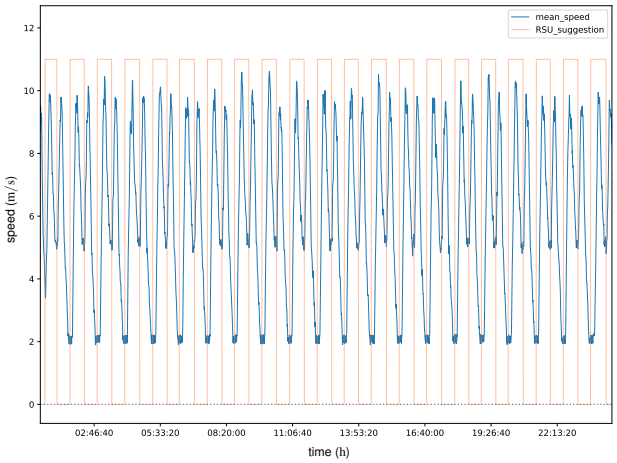


Figure 6.10: Mean speed in the network, for simulation run `820veh-24h-07060000` (A.19), in meters per second (m/s), over a 24 h period, superimposing (vertically, in orange) the instants at which the RSU issued a recommendation to follow the *alternative* route.

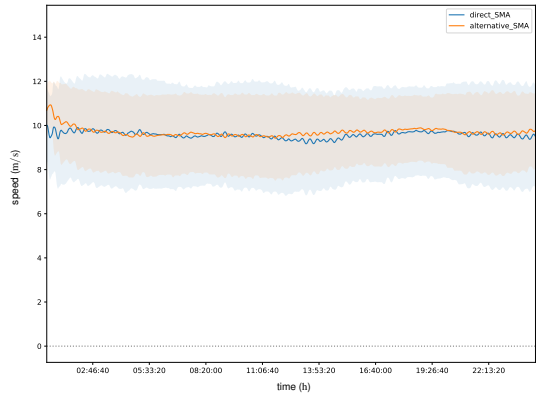
in Figure 6.10, where the sharp variations in the average velocity are directly related to the change in RSU recommendation.

Using values provided by the system (Figure 6.9c), the average network speed was similar, except the edge occupancy-based recommendation (`820veh-24h-18060000`), which is not only the most stable, but also obtained a slightly higher average speed (about 7.75 m/s (27.90 km/h). In the other two, relying on the mean speed (`820veh-24h-12060000`) of the monitored edges was also more stable than the one that uses the predicted travel time (`820veh-24h-13060000`).

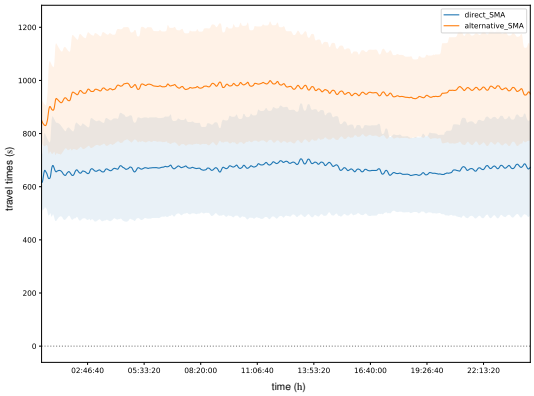
About the proportional strategies (Figure 6.9d), in which the RSU performs a multicast dissemination instead of broadcast, separating distinct groups by the two routes, average speeds above 9.00 m/s (32.40 km h) were registered. Albeit with close but consistently higher values, the best results were achieved by the algorithms inspired by Pigou's example (`pigous_example` and `pigous_example_cooperation _weighted`, in which the proportion is calculated on the basis of both travel time and traffic density; and `proportional_dynamic` and `proportional _dynamic_v2` with calculations based on the average of the travel times of the last n vehicles. These two pairs, moreover, have coincident curves, because the seed values for pseudo random generation used in the simulation are identical in each run for the purpose of comparison between the strategies. In the case inspired by Pigou's example, both start from the same calculation formula, only varying the weight of the proportion according to the cooperation ratio recorded by the RSU which, is total cooperation is equal to one. In the other pair the difference is in the ratio calculation, where it calculates a pseudo-average considering the total memory defined by the simulation parameter, even when some values were removed due to time-to-live, and the other is an accurate average of the last values up to a maximum of n passed as argument.

In this analysis, the theoretical ratio based on the ratio between the two routes (`proportional`) also achieved a good performance, but it should be noted that the cooperation was full from the beginning and even during the warmup period this strategy is used to distribute the vehicles evenly on the network. Slightly below these was `proportional_dynamic_v3`, which uses the final and intermediate travel time values, although it shows a little more stability.

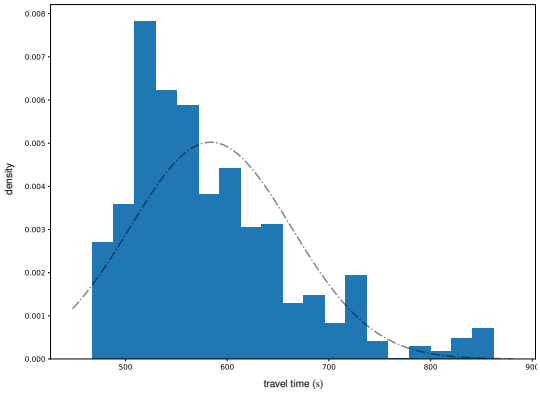
Along with the metric of average network speed, one can also observe the status of the monitored routes and their impact on vehicles over the simulated 24 h. Simulation run `820veh-24h-17060000` (A.29) relies on the algorithm `proportional_dynamic_v4`, which has as variables a moving average of the last n occupancy values of the intermediate lane area and the end-of-queue lane area, near the destination. The moving average of the mean speed (Figure 6.11a) was similar on the two routes, although the *direct* route had a greater amplitude of variation and reached higher values. As a consequence, travel times (Figure 6.11b) registered on the *alternative* route—which is lengthier—, were also elevated. The average travel time recorded by each vehicle followed a normal distribution centred around 790 s (Figure 6.11d), however, when looking at the best time recorded over the 24 h (Figure 6.11c) it was found that the distribution is positively/right skewed, centred around 530, although the shape of the histogram denotes a multi-modal distribution, with modes at 600 s, 720 s and 850 s.



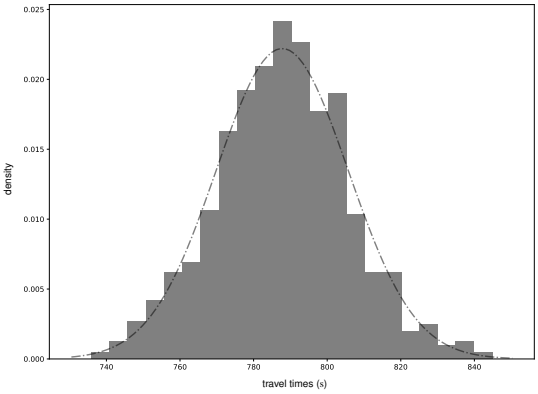
a) Mean speed 4 h SMA.



b) Travel times 4 h SMA.



c) Best travel times histogram.

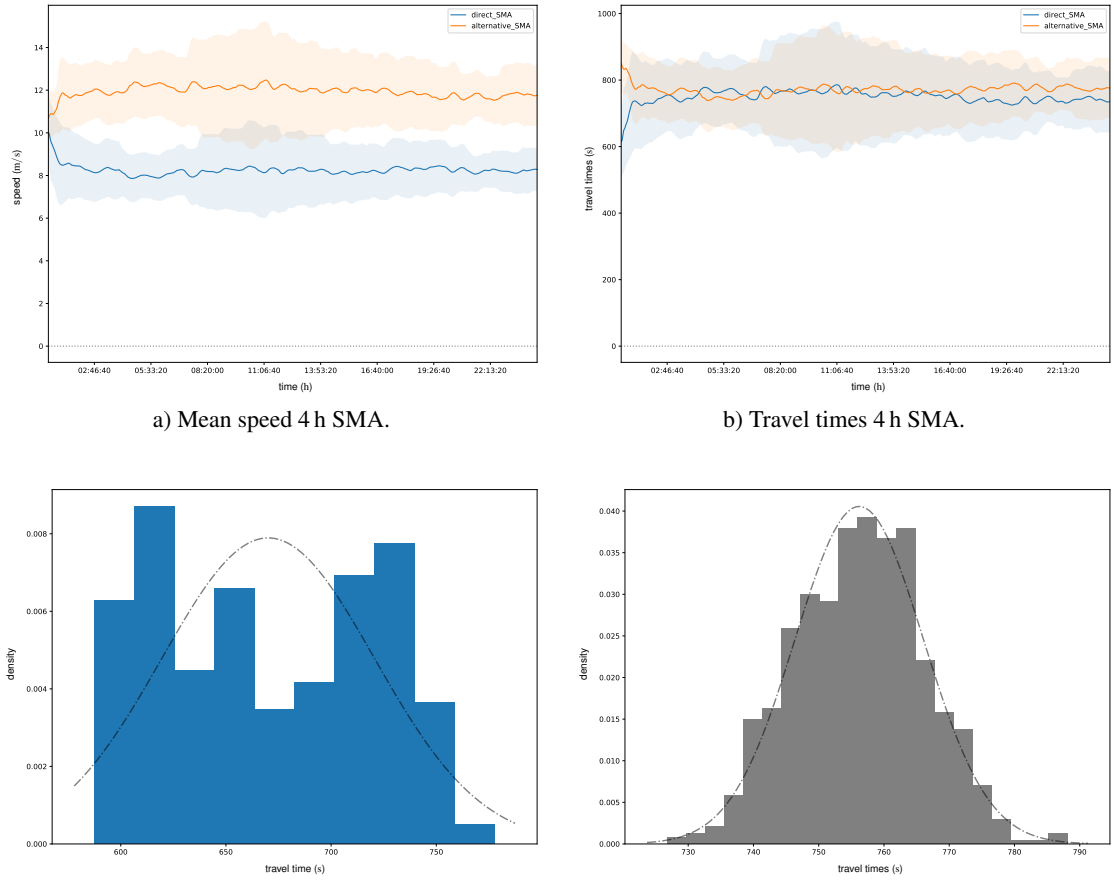


d) Average travel times histogram.

Figure 6.11: Mean speed, in meters per second (m/s), and travel times in seconds (s), on each route, for simulation run `820veh-24h-17060000` (A.29), aggregated to 1 min, over a 24 h period, 4 h Simple Moving Average, mean (line) and standard deviation (shaded); and density histograms of best travel time and average travel times for the population, in seconds (s), during the simulation of a 24 h period, superimposing the normal density curve. The number of bins was calculated by the Freedman Diaconis rule.

In the simulation run `820veh-24h-01060000` (A.13), on the other hand, based on the algorithm `proportional_dynamic`, whose variables are the moving average of the last n travel time values, the mean speed (Figure 6.12a) on the *alternative* route is higher than on the *direct* route, leading to travel times (Figure 6.11b) that are similar between the two routes. The distribution of the average travel times (Figure 6.11d) for each vehicle is centred on 760 s, with a smaller standard deviation than in the previous case. About the best travel times of each vehicle (Figure 6.11c), the shape of the density histogram suggests a multimodal distribution with a higher peak around 620 s and another around 720 s, however contained in the range $[600, 760]$ s.

Finally, simulation run `820veh-24h-19060000` (A.31) also shows the average speed (Figure 6.13a) of the *alternative* route higher than the *direct* route, however, the same happens with travel times (Figure 6.13b). Nevertheless, the differences between the values of the *direct* and *alternative* route are lower when compared to the aforementioned dissimilarities and, in addition, they are more stable values, as can be seen by the respective standard deviations (shaded). The distribution of average journey times centres on 755 s and although most vehicles achieved best



a) Mean speed 4 h SMA.

b) Travel times 4 h SMA.

c) Best travel times histogram.

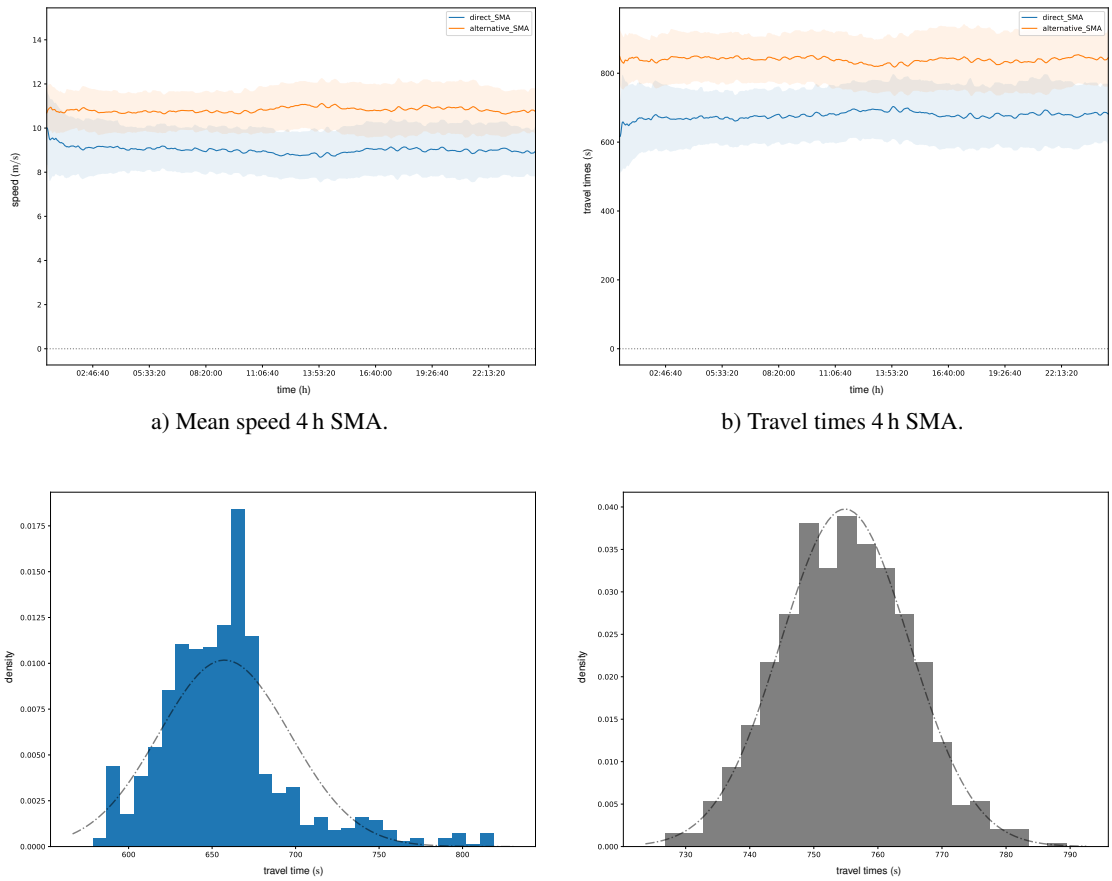
d) Average travel times histogram.

Figure 6.12: Mean speed, in meters per second (m/s), and travel times in seconds (s), on each route, for simulation run `820veh-24h-01060000` (A.13), aggregated to 1 min, over a 24 h period, 4 h Simple Moving Average, mean (line) and standard deviation (shaded); and density histograms of best travel time and average travel times for the population, in seconds (s), during the simulation of a 24 h period, superimposing the normal density curve. The number of bins was calculated by the Freedman Diaconis rule.

times between $[640, 670]$ s, this distribution is positively/right skewed, with some vehicles whose best times were 750 s and 800 s.

Considering the number of laps taken by the vehicles over the 24 h simulation (Figure 6.14), `820veh-24h-17060000` (Figure 6.14a), based on travel times, had a distribution centred on 87 trips, while `820veh-24h-01060000` (Figure 6.14b), focusing on mean speed, was centred on [92,93] and `820veh-24h-19060000` (Figure 6.14c), combining travel time and traffic density, centred on 93 trips.

From these results, it was noted that proportionality is important in the diffusion of the recommendation, giving it a predictive rather than merely reactive character. The best performance was achieved with the combination of travel times and traffic density, since, although similar in terms of average network speed to the use of travel times alone, their values were more stable, with smaller deviations over time. On the other hand, these two strategies relying on travel time allowed vehicles to perform more laps during the 24 h than the one using only traffic density values.



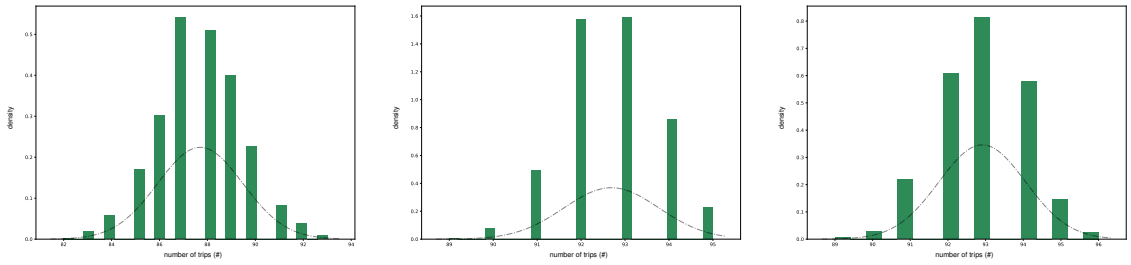
a) Mean speed 4 h SMA.

b) Travel times 4 h SMA.

c) Best travel times histogram.

d) Average travel times histogram.

Figure 6.13: Mean speed, in meters per second (m/s), and travel times in seconds (s), on each route, for simulation run `820veh-24h-19060000` (A.31), aggregated to 1 min, over a 24 h period, 4 h Simple Moving Average, mean (line) and standard deviation (shaded); and density histograms of best travel time and average travel times for the population, in seconds (s), during the simulation of a 24 h period, superimposing the normal density curve. The number of bins was calculated by the Freedman Diaconis rule.



a) `820veh-24h-17060000`

b) `820veh-24h-01060000`

c) `820veh-24h-19060000`

Figure 6.14: Density histogram of the number of trips made by each vehicle, during the simulation of a 24 h period, superimposing the normal density curve. The number of bins was calculated by the Freedman Diaconis rule. They all follow a normal distribution, but `820veh-24h-17060000` (A.29), is centred on 87 trips, while `820veh-24h-01060000` (A.13), is centred on [92,93] trips and `820veh-24h-19060000` (A.31), on 93 trips.

6.2 Stochastic Behaviour

After analyzing the results of the recommendation algorithms of the RSU in a situation of full cooperation, tests were carried out with *undecided* "personality", stochastic vehicles, i.e. with 50 % probability of accepting the suggestion, in order to assess the resilience and adaptability of the RSU to the dynamism of the population. The strategies that had given the best results in full cooperation were chosen, namely `proportional (820veh-24h-00060000)`, `proportional_dynamic_v3 (820veh-24h-15060000)`, `proportional_dynamic_v4 (820veh-24h-17060000)`, `pigous_example (820veh-24h-16060000)`, and `pigous_example_cooperation_weighted (820veh-24h-19060000)` (respectively, Appendices A.3, A.27, A.29, A.28, and A.31).

Although these algorithms gave close results in terms of average network speed in full cooperation, as seen above, when subjected to stochastic population some differences were evident. From Figure 6.15 one notices a group of three algorithms with average speeds around 7 m/s (25.20 km/h), while `820veh-24h-19060000` reached around 8 m/s (28.80 km/h) m/s, but `820veh-24h-01060000` was only around 5 m/s (18 km/h) and `820veh-24h-00060000` slightly below 4 m/s (14.40 km/h).

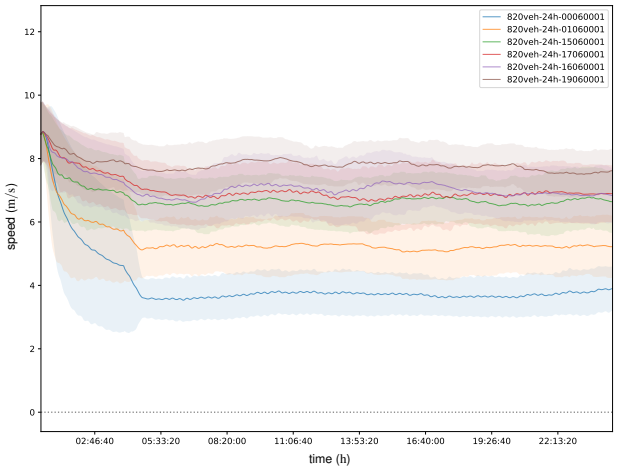


Figure 6.15: Mean speed in the network, in meters per second (m/s), during a 24 h period, 4 h Simple Moving Average, mean (line) and standard deviation (shaded), for a population of 820 vehicles, when they are of the *undecided* personality, i.e., there is a 50 % probability probability of cooperating and accepting the suggestion of the RSU, built and disseminated according to the proportional algorithms (cf. Subsection 5.5.1). *Legend identifies the simulation runs (cf. Appendix A for details).*

Looking at the remaining metrics, it was found that the number of vehicles was invariably higher on the *direct* route, increasing density and consequently decreasing speed on this path. `820veh-24h-15060000` (A.27), based on an algorithm averaging the last n travel times, captured both at destination and mid-distance, had mean travel times of about 1400 s on the *direct* route 500 s on the *alternative*. Nevertheless, the average of the times recorded by each vehicle follows a normal distribution centred on 1000 s, although the best recorded times follow a multimodal distribution with the highest mode centred on 480 s, despite a lower mode around 1300 s.

With an identical algorithm but relying on the densities of the final and intermediate lane areas, `820veh-24h-17060000` (A.29) registered similar travel times, although with the average vehicle travel times following a positively/right skewed distribution centred on 950 s and the best times with the highest mode around 460 s and a lower one also at about 1300 s. The same happened in `820veh-24h-16060000` (A.28), which combines the travel time and density metrics to build the recommendation, with only slight divergence in the highest modes of the mean and best travel times distributions, about 960 s and 450 s respectively.

The best performance with stochastic vehicles was obtained in `820veh-24h-19060000` (A.31), whose algorithm is similar to the previous one, inspired by Pigou's example and based on travel times and density, but in this implementation with the proportions affected by a factor of the cooperative ratio recorded by the RSU. The difference between the journey times captured on the *direct* and *alternative* routes were 1200 s and 600 s respectively, narrowing the gap between them, and the average vehicle travel times centred on 880 s, while the best times had the highest peak at 500 s despite a second, rather lower mode at 1150 s.

Finally, `820veh-24h-01060000` (A.13) whose algorithm is based only on the average of the last n travel times, showed similar characteristics to the preceding ones, but the inequality between the routes and among the best times recorded by the vehicles was accentuated, these with multimodal distribution, a very high peak at 450 s but a mode also at 1450 s. The average travel time of the vehicles follows a normal distribution, though centred at about 1200 s. `820veh-24h-00060000` (A.3), which recorded the lowest values, is a theoretical proportion, from the ratio between the two paths. Despite a good performance with full cooperation, it proved inadequate to deal with the dynamism of the network when the vehicles have a stochastic behaviour.

A prominent aspect of this experiment was the number of recommendations issued by the RSU (*see* graph of average speed with superimposed recommendations in the respective Appendices), which generated large oscillations and instability in the speeds registered in the *alternative* route. On the *direct* route, where more vehicles were concentrated, and therefore with lower speeds, it was not as noticeable. The exception was the algorithm used in `820veh-24h-19060000`, which not only obtained the best result but also recorded more stable values, highlighting, therefore, the need to observe the cooperation of vehicles to accept the suggestion of the RSU when constructing the proportion, in order to counterbalance those who reject. In addition, it is also worth noting the convenience of using not only the values captured at the destination, but combining them with others recorded at intermediate points along the path to be more predictive.

6.3 Memory Based Tactics

The interaction of the vehicles with the RSU in order to accept or not its recommendation relies on a set of personalities modelled to determine their choices (cf. Subsection 5.5.2). To support decision making, some personalities resort to the data collected from previous trips, such as travel time and payoffs against chosen actions, but under the assumption of only own knowledge, i.e. each vehicle knows only its own history, and uses a limited number of the last records, adjusted to five

in the case of this experiment. *Greedy* and *accountant* characters were considered (Figure 6.16), the former with a utility function that tries to maximise the outcome by re-selecting the action that gave the best return, the other by analyzing the last option taken compared to the average of its outcomes.

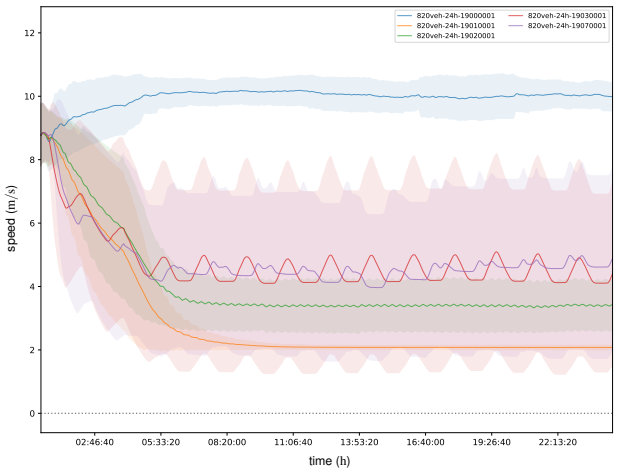
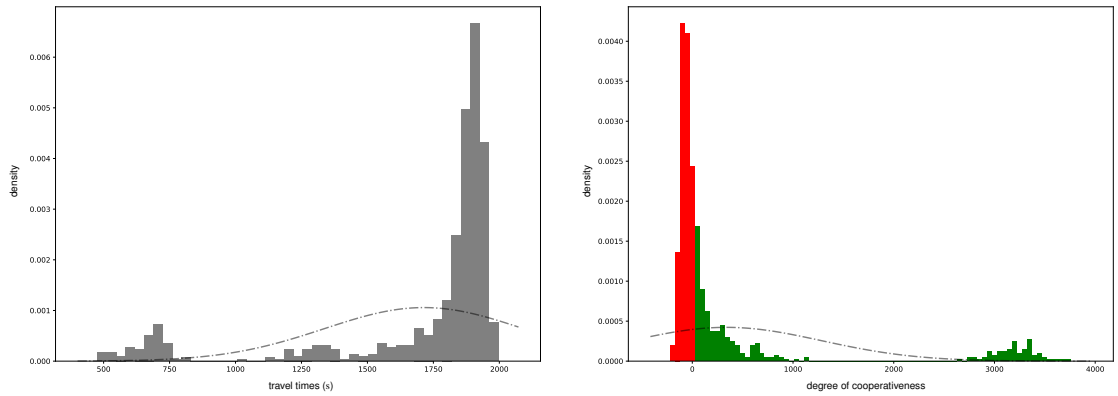


Figure 6.16: Mean speed in the network, in meters per second (m/s), during a 24 h period, 4 h Simple Moving Average, mean (line) and standard deviation (shaded), for a population of 820 vehicles, whose tactics are based on memory (*greedy* and *accountant*, cf. Subsection 5.5.2), i.e. the data that each one has collected in the last trips made, both in travel time, payoff and chosen actions. *Legend identifies the simulation runs (cf. Appendix A for details).*

Within the *greedy* ones, the simplest strategy, used in the simulation run `820veh-24h-19000001` (A.39), consisted in minimizing the travel time, accepting the recommendation of the RSU if it had already contributed to it in the past, or rejecting it otherwise, that is, from the last n actions the one in which the shortest time had been recorded was chosen. This was also the one that obtained the best result in terms of average speed in the network, widely standing out from the others. However, the metric used for the decision was travel time only. The values obtained were relatively stable, as can be seen by the standard deviations, but failed to equalize the times between the two routes, holding a difference of 300 s. On the other hand, both the average and the best travel time per vehicle followed bimodal distributions, both with modes around 500 s and 900 s. Indeed, an analysis of the vehicle history revealed that the cooperation ratio remained identical to the initial distribution at launch, and the RSU always had the same group of cooperators following its recommendations (comparing the result with simulation `820veh-24h-16000001` (A.37) reinforces the need to use that ratio in the RSU dissemination proportion).

In the remaining *greedy* tactics, the option for the best payoff, `820veh-24h-19010001` (A.40), achieved an average network speed of only about 2 m/s (7.20 km/h), in a situation of congestion on the *direct* route. In effect, the inflexible selfish search for the best reward led to a population of defectors, turning the RSU useless. Adopting a utility function together with the payoff, in `820veh-24h-19020001` (A.41), helped improve the result, but the group of cooperators remained small. However, in the face of congestion on the *direct* route, they were diverted to the *alternative* route, with very low density, and therefore achieving travel times close

to free-flow. Consequently, analyzing the histogram of average travel times per vehicle against that of the *degree of cooperativeness** (Figure 6.17), we find that the former is negatively/left skewed, with the one peaking around 1950 s, and the other is almost symmetric, positively/right skewed, with the peak around 0. A mode with centre around 700 s in average travel times has its reflection in cooperativeness at around 3250, meaning that the most cooperative (i.e. those who accepted the RSU recommendation) were rewarded with considerably shorter travel times over the simulated 24 h.



(a) Average travel times histogram.

(b) Degree of cooperativeness histogram.

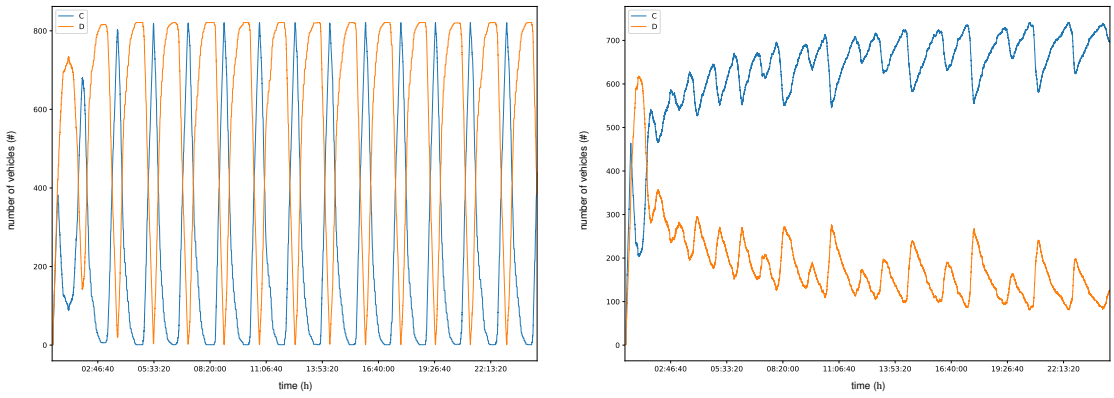
Figure 6.17: Density histograms of average travel times, in seconds (s), and *degree of cooperativeness** for the population, simulation run `820veh-24h-19020001` (A.41), during the simulation of a 24 h period, superimposing the normal density curve. The number of bins was calculated by the Freedman Diaconis rule.

The *accountant*'s personality was tested on two tactics, one more altruistic `820veh-24h-19030001` (A.42), cooperating when below its average of the last n payoff values, and the other more selfish `820veh-24h-19070001` (A.44), choosing the action that gives rewards above the mean. Although both obtained average network speed values around 4.50 m/s (16.20 km/h), their values were very unstable, with high standard deviations of around 3 m/s (10.80 km/h), due to a frequent, oscillatory reversal of the number of cooperators in the first case and convergence to the centre in the second. They equally have a normal distribution of the average journey times per vehicle centred on 1360 s, but the former has a bimodal distribution of the best time per vehicle with modes at 400 s and 1100 s, and the latter is multimodal, although with a high peak at 500 s, and a mode with about half the density of that centred on 800 s, and two lower modes at around 400 s and 1100 s.

The above experiments were carried out with vehicles whose decisions were inflexible, and based only on their history. A variation included the susceptibility of 20 % to change decision and accept the suggestion depending on additional information provided by the RSU about the last recorded travel time on the recommended route, with which the vehicle compares its previous performance. In terms of willingness to cooperate, there has been a shift from the cyclical reversal

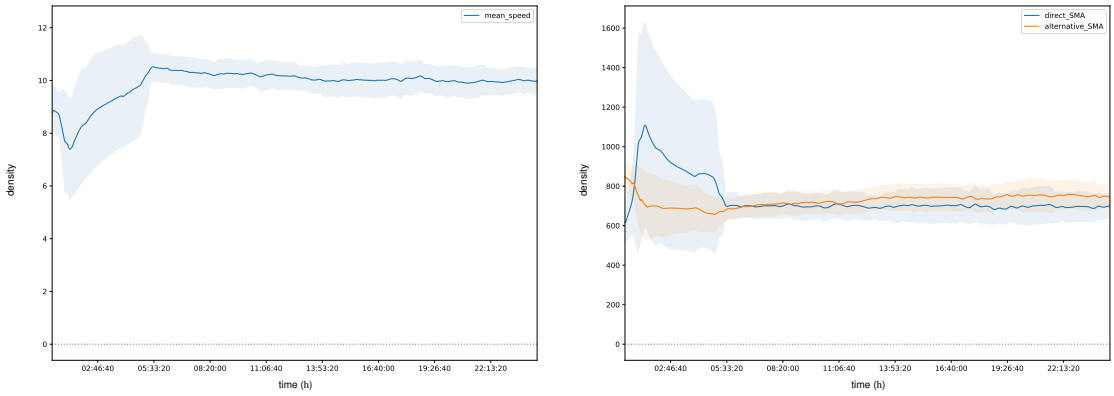
*The degree of cooperativeness is a cumulative sum, calculated at each iteration, based on the complement of the ratio of cooperators, i.e., the higher the number of cooperators the less it increases, but the defectors are more penalized, and vice-versa. It varies inversely with the size of the group to which the player belongs.

of cooperation and defection (Figure 6.18a) to an evolution of cooperation (Figure 6.18b) over the simulated 24 h.



(a) `820veh-24h-19030001` (b) `820veh-24h-19030003`

Figure 6.18: Evolution of the number of *Cooperators* and *Defectors* over a 24 h period, for simulation runs `820veh-24h-19030001` (A.42) and `820veh-24h-19030003` (A.53). The "personality" of the vehicle is *accountant*, using the `mean_payoff` strategy, with an altruistic disposition, cooperating when below its mean of the last n payoff values. In the graph on the left, the vehicle is inflexible to the choice made, while in the right graph, besides a route recommendation, it receives additional information from the RSU about the last recorded travel time on that route, having a 20 % susceptibility to change of decision and accept the suggestion. From the cyclical inversion of cooperation and defection shifted to an evolution of cooperation.

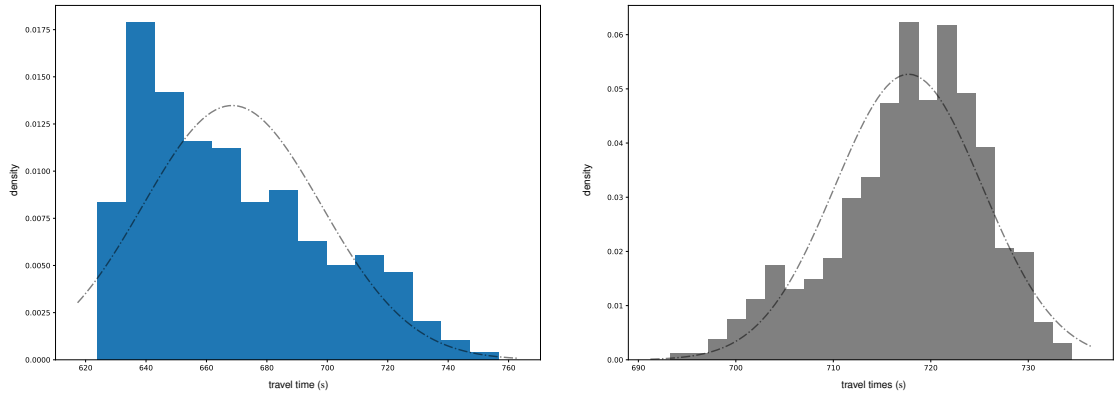


(a) Mean speed in the network 4 h SMA. (b) Travel times on each route 4 h SMA.

Figure 6.19: Mean speed in the network, in meters per second (m/s), and travel times on each route, over a 24 h period, for simulation run `820veh-24h-19030003` (A.53). The personality of the vehicle is *accountant*, using the `mean_payoff` strategy, with an altruistic disposition, cooperating when below its mean of the last n payoff values. By providing the vehicle with additional information about the last recorded travel time on the recommended route, it has a 20 % susceptibility to change of choice and accept the suggestion. The average speed of the network reached a relatively stable value of 10 m/s (36 km/h) (*a*), and travel times on each route converged to around 700 s (*b*).

The most noticeable consequence was the convergence of travel times on both routes to around 700 s (Figure 6.19b), to which also contributed the proportion calculation made by the RSU for dissemination purposes, which in this simulation also considered the ratio of cooperators. Its impact was also experienced in the average speed of the network, reaching around 10 m/s (36 km/h)

(Figure 6.19a). With regard to the average times taken by the vehicles, it followed a slightly negative/left skewed distribution with a centre at around 720 s, and a standard deviation around 10 s. In turn, the best travel time recorded by each vehicle followed a positively/right skewed distribution, with a mode around 640 s, and there were no times worse than 750 s.



(a) Best travel times histogram.

(b) Average travel times histogram.

Figure 6.20: Density histograms of best travel time and average travel times for the population, in seconds (s), for simulation run `820veh-24h-19030003` (A.53), over a 24 h period, superimposing the normal density curve. The number of bins was calculated by the Freedman Diaconis rule.

Tactics based on the agents/vehicles' own memory proved ineffective, with poor performance in terms of average system speed. In the algorithm that achieved higher results this was because the population remained balanced and inflexible in terms of cooperation since launch, giving rise to two distinct groups, as observed by the bimodal distributions of the averages and best travel times recorded by the vehicles.

The low number of cooperators or with wide oscillations did not allow the RSU to make recommendations impacting on system performance. Only the inclusion of additional information and the increased susceptibility to acceptance of the suggestion led to improved results, not only by the average speed on the network, but mainly by the balanced, similar and relatively stable travel times achieved simultaneously on both routes.

6.4 Reinforcement Learning Based

In an approach more consonant with sociological and behavioural theories, based on the reinforcement learning model proposed by Roth and Erev, which conceives agents as adaptive learners with the probability of electing a particular action proportional to the reward or punishment it has received from the environment. The modified Roth-Erev reinforcement learning algorithm was implemented in this study (cf. Subsection 2.6.2), and, in addition, two experiments were performed with respect to the payoff, one—simulation run `820veh-24h-19040001` (A.45)—employing the values obtained directly from the payoff functions given by the matrix (cf. Section 5.4) and another—simulation run `820veh-24h-19050001` (A.46)—where that value is affected by a

utility function based on the ratio between the best vehicle travel time and the last recorded travel time. Notwithstanding, the measures of speed, travel time, flow and cooperation were very close and with very similar patterns, although the latter slightly lower, as can be seen by the result of the average speed on the network over the simulated 24 h (Figure 6.21).

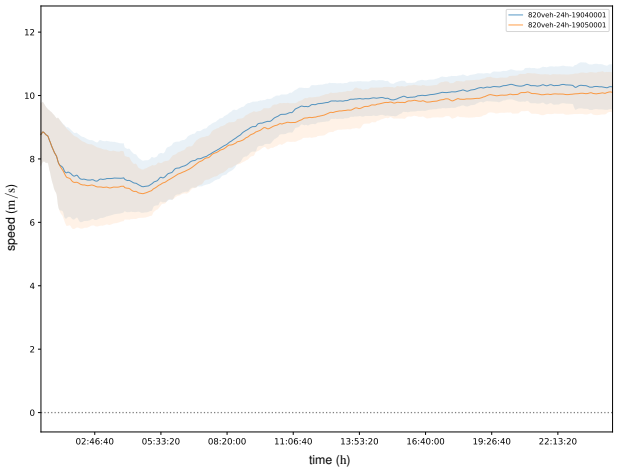


Figure 6.21: Mean speed in the network, in meters per second (m/s), during a 24 h period, 4 h Simple Moving Average, mean (line) and standard deviation (shaded), for a population of 820 vehicles, simulation runs `820veh-24h-19040001` (A.45) and `820veh-24h-19050001` (A.46), which employ different algorithms with respect to payoff. In the first one the payoff value is directly obtained from the payoff functions given by the matrix (cf. Section 5.4) and in the second one it is affected by a utility function based on the ratio between the best travel time of the vehicle and the last recorded one. *Legend identifies the simulation runs (cf. Appendix A for details).*

Therefore, it was decided to proceed with the simple formulation, payoff functions only.

6.4.1 Payoff matrices

As described and specified in Section 5.4, the matrices `[360.0, 240.0, 0.0, -120.0]` and `[180.0, 60.0, 0.0, -120.0]` were used, according to the $[T,R,P,S]$ scheme.

The result obtained, in terms of average network speed (Figure 6.22), evidences higher values with the second matrix, around 10.50 m/s (37.80 km/h) compared to around 10 m/s (36.00 km/h), besides having reached a stable value sooner, around 8 h in the simulation against 14 h with the other one.

At the origin of these findings is the earlier emergence of cooperation and a greater number of cooperators—as can be seen in Figure 6.23—, which allowed the RSU to better distribute the vehicles across the routes, building target recommendations according to the calculated proportions. By reducing the value of the *Temptation* (and therefore the *Reward*), the moment of reversal was brought forward (from about 11 h of simulation to 4 h) and the number of cooperators reached a higher and more stable value, from around 450 to about 550—Figure 6.24—, a number in line with that calculated for k in Section 5.4, Figure 5.6.

Another aspect of this change in payoff matrices has to do with the travel times recorded on each route and the respective traffic flows. In the first case, with higher *Temptation*, flows had a slower

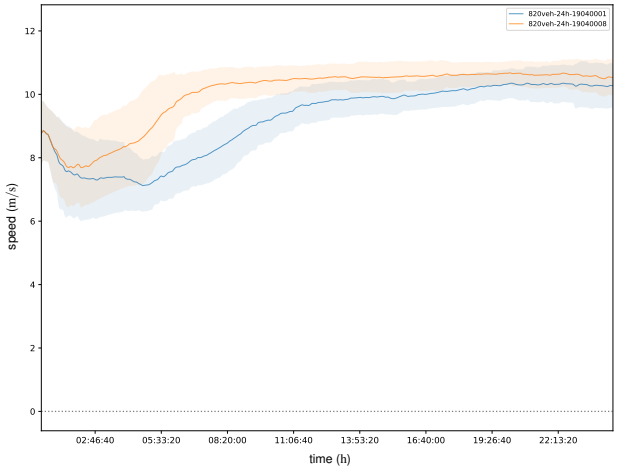
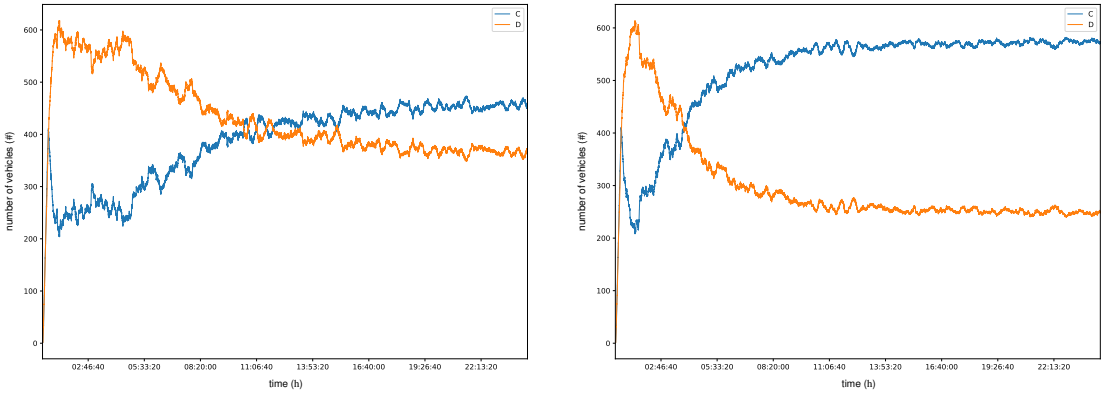


Figure 6.22: Mean speed in the network, in meters per second (m/s), during a 24 h period, 4 h Simple Moving Average, mean (line) and standard deviation (shaded), for a population of 820 vehicles, simulation runs `820veh-24h-19040001` (A.45) and `820veh-24h-19040008` (A.48), in which two different payoff matrices are used, `[360.0, 240.0, 0.0, -120.0]` in the first and `[180.0, 60.0, 0.0, -120.0]` in the second (according to the $[T,R,P,S]$ scheme). The latter obtained an earlier emergence of cooperation and a larger number of cooperators, with an impact on the speed of the system. *Legend identifies the simulation runs (cf. Appendix A for details).*

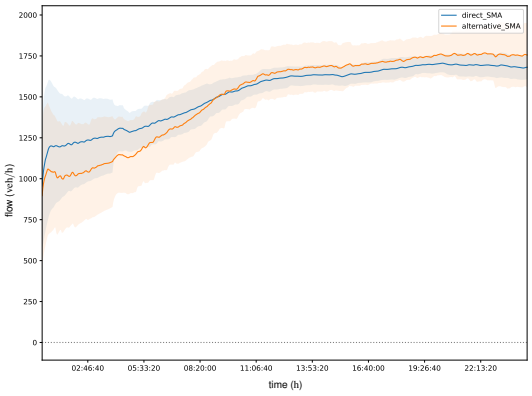


a) `820veh-24h-19040001`: `[360.0, 240.0, 0.0, -120.0]`

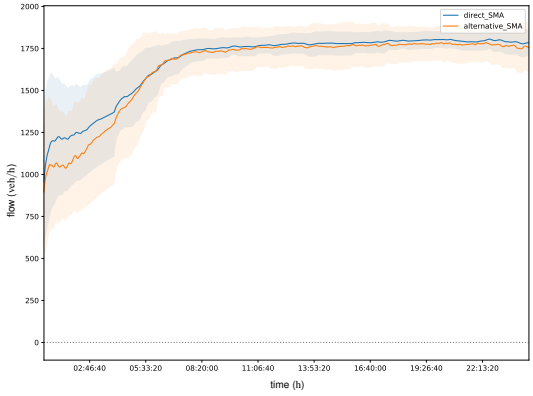
b) `820veh-24h-19040008`: `[180.0, 60.0, 0.0, -120.0]`

Figure 6.23: Evolution of the number of *Cooperators* and *Defectors* over a 24 h period, changing the payoff matrix, for simulation runs `820veh-24h-19040001`: `[360.0, 240.0, 0.0, -120.0]`; and `820veh-24h-19040008`: `[180.0, 60.0, 0.0, -120.0]`. The impact of this change was felt not only in the emergence of cooperation, but also in the number of cooperators. By reducing the *Tempation* value (and therefore the *Reward*, cf. Section 5.4), the time of the inversion was brought forward (from 11 h to 4 h) and the number of cooperants was increased (from around 450 to about 550).

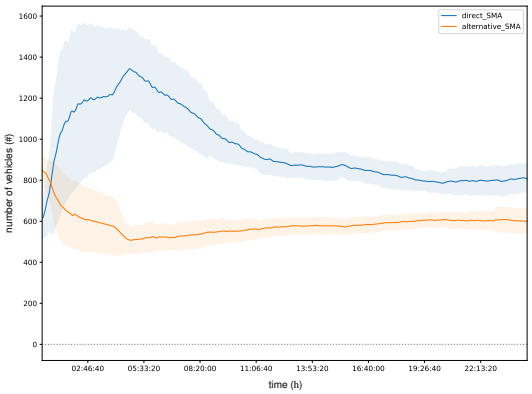
growth, were more unstable, and the average value reached was around 1700 veh/h (Figure 6.24a), while in the second case flows in both routes converged to a similar value, at the moment when the inversion of the number of *Cooperants* versus *Defectors* took place, and continued to grow until a plateau at around 1750 veh/h, reached at 8 h of simulation and which remained relatively stable (Figure 6.24b). As a consequence, travel times converged to a relatively identical value in this situation, around 700 s (Figure 6.24c), while in the previous one the direct route recorded higher times, around 800 s compared to 600 s for the alternative route (Figure 6.24d).



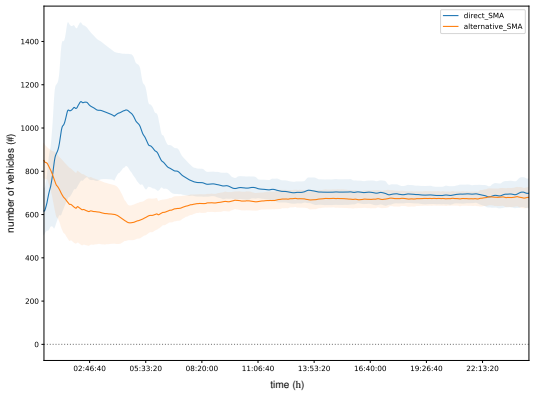
a) `820veh-24h-19040001`: Traffic flows.



b) `820veh-24h-19040008`: Traffic flows.



c) `820veh-24h-19040001`: Travel times.



d) `820veh-24h-19040008`: Travel times.

Figure 6.24: Traffic flows (*top*) and travel times (*bottom*) on each route, in seconds (s), aggregated to 1 min, over a 24 h period, 4 h Simple Moving Average, mean (line) and standard deviation (shaded), changing the payoff matrix, for simulation runs `820veh-24h-19040001`: `[360.0, 240.0, 0.0, -120.0]`; and `820veh-24h-19040008`: `[180.0, 60.0, 0.0, -120.0]`. The impact of the change was felt in the convergence of flows and travel times on each route. By reducing the value of *Temptation* (consequently the *Reward*, cf. Section 5.4), those times became closer and relatively stable from 10 h of the simulation.

On the other hand, regarding the times recorded by the vehicles throughout the simulation, in the first case the averages followed a bimodal distribution, with modes at 660 s and 900 s, as well as the best times, with modes at 550 s and 750 s, which also gave rise to a bimodal distribution of the number of trips with modes at 80 and 105. By reducing the value of *Temptation*, a decrease in the amplitude of those metrics was observed. The average travel time follows a bimodal distribution, with modes at 690 s and 730 s, while the best time follows a multimodal distribution, with modes at

600 s, 630 s and 670 s, and the same happens with the number of trips made by each vehicle, with modes at 98, 102 and 104.

From these experiences, it has been noticed, to some extent, the impact of the payoff matrix on the emergence of cooperation as well as its consequences on the system performance, since the RSU depends on the cooperators, who accept its suggestion, to lead the network to a regime, at least, suboptimal.

6.4.2 Roth-Erev algorithms parameters

By using the Roth-Erev algorithm for agent learning, the variation of its parameters was also tested, assessing its effect on the system's performance.

In the preliminary analysis of the average speed in the network (Figure 6.25), it was observed that, although it stabilized on a plateau at around 10.50 m/s (37.80 km/h) in all tested variations, the evolution during the first 8 h simulated was different, but evidencing a strong correlation of the moment of speed increase with the emergence of cooperation. Simulation run `820veh-24h-19040011` (A.50), which had the earliest cooperation reversal (Figure 6.26d) was the one that progressed sooner in terms of speed, the opposite happening with simulation run `820veh-24h-19040010` (A.49), which was the latest (Figure 6.26b). However, despite the former having a slightly lower plateau of the number of *Cooperators*, this does not seem to have affected the average speed value achieved.

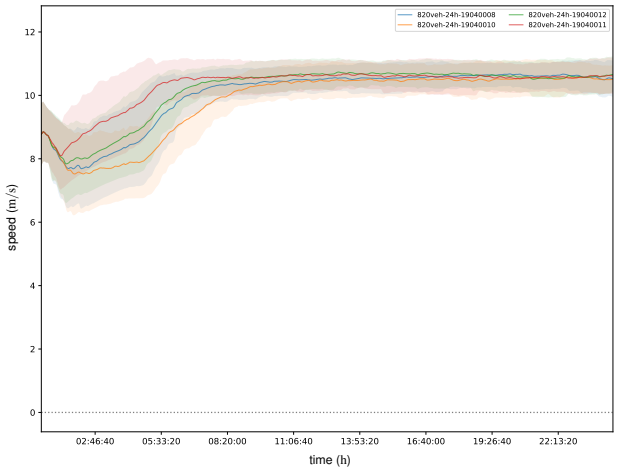
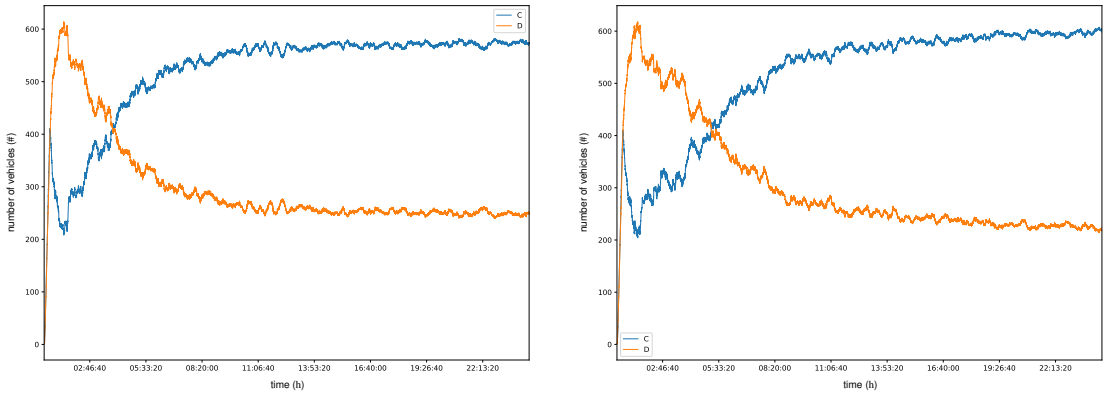


Figure 6.25: Mean speed in the network, in meters per second (m/s), during a 24 h period, 4 h Simple Moving Average, mean (line) and standard deviation (shaded), for a population of 820 vehicles, with the payoff matrix [180, 60, 0, -120] (according to the scheme $[T,R,P,S]$), varying the *Recency* and *Experimentation* parameters of the Roth-Erev reinforcement learning algorithm, which, having an impact on the emergence of cooperation, were reflected in the evolution of the average speed during the first simulated hours. The parameters were: `820veh-24h-19040008` (A.48): $\phi = 0.1$, $\varepsilon = 0.2$; `820veh-24h-19040010` (A.49): $\phi = 0.1$, $\varepsilon = 0.5$; `820veh-24h-19040012` (A.51): $\phi = 0.2$, $\varepsilon = 0.5$; and `820veh-24h-19040011` (A.50): $\phi = 0.5$, $\varepsilon = 0.5$. *Legend identifies the simulation runs (cf. Appendix A for details).*

Comparing the evolution of the number of *Cooperants* and *Defectors* over the 24 h (Figure 6.26), the pattern was similar, with a strong initial growth of the *Defectors* up to about two-thirds of the population followed by a reversal of positions ending in a plateau of the *Cooperants*.

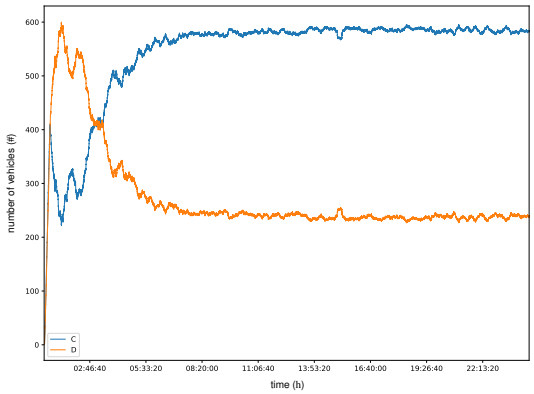
Through *experimentation* (or generalization), successful choices in the past are more likely to be employed again and similar choices are used more frequently. However, in the early stages, it serves to avoid premature fixation on an action. *Recency* (or forgetting), on the other hand, gives the most recent experience a more important role in determining behaviour than a past experience.

By increasing the *experimentation* (Figures 6.26a and 6.26b), the slope in the evolution towards cooperation was smaller, delaying the moment of reversal in the number of cooperators, and even remained positive throughout the 24h, although gradually decreasing. However, when increasing *recency* (Figures 6.26a, 6.26c, and 6.26d), we observed an anticipation of that inversion, with a steeper slope and the effective establishment of a plateau.

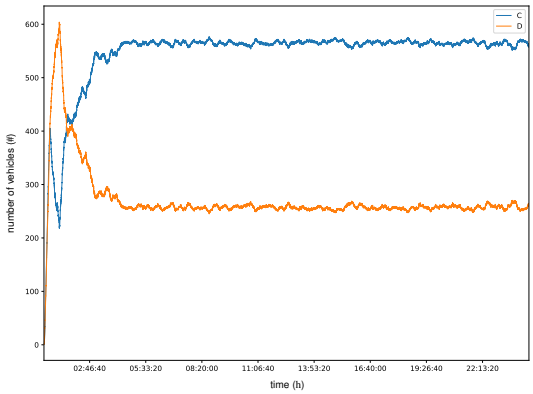


a) `820veh-24h-19040008`: $\phi = 0.1$, $\varepsilon = 0.2$

b) `820veh-24h-19040010`: $\phi = 0.1$, $\varepsilon = 0.5$



c) `820veh-24h-19040012`: $\phi = 0.2$, $\varepsilon = 0.5$



d) `820veh-24h-19040011`: $\phi = 0.5$, $\varepsilon = 0.5$

Figure 6.26: Evolution of the number of *Cooperators* and *Defectors* over a 24 h period, varying the *Recency* and *Experimentation* parameters of the Roth-Erev reinforcement learning algorithm, for simulation runs `820veh-24h-19040008` (A.48): $\phi = 0.1$, $\varepsilon = 0.2$; `820veh-24h-19040010` (A.49): $\phi = 0.1$, $\varepsilon = 0.5$; `820veh-24h-19040012` (A.51): $\phi = 0.2$, $\varepsilon = 0.5$; and `820veh-24h-19040011` (A.50): $\phi = 0.5$, $\varepsilon = 0.5$.

In the analysis of the remaining metrics, both traffic flows and travel times converged to similar

values on both routes, as pointed out in the previous experiment (cf. Subsection 6.4.1), with the timing of convergence being equally related to the moment of emergence of cooperation. The effect of this convergence, however, was felt at an individual level in the average and best journey times recorded by each vehicle over the simulated 24 h.

The base situation, simulation run `820veh-24h-19040008` (A.48), with $\phi = 0.1$ and $\varepsilon = 0.2$, had a bimodal distribution of the average vehicle travel times with modes at 690 s and 730 s, the former with slightly more density, in the interval $[650, 750]$ s. The best travel times obtained by each vehicle, in turn, already had a multimodal distribution, with the densest modes at around 600 s and 630 s, and others at around 670 s and, lowest, at 560 s, contained in the interval $[560, 750]$ s.

When the *experimentation* parameter was increased, simulation run `820veh-24h-19040010` (A.49), with $\phi = 0.1$ and $\varepsilon = 0.5$, the mean travel times followed a bimodal distribution, with modes at 700 s and 730 s and reaching densities closer together, in the interval $[660, 770]$ s, while the best travel times obtained by each also followed a multimodal distribution, but now with a mode denser at 670 s, and the others less than half the density of that at 630 s, 645 s and 685 s, contained in the interval $[630, 695]$ s. Although there was a slight widening in the amplitude of the mean travel times (only 10 s), the amplitude of the interval of the best times had a significant reduction.

With the increase of the *recency* parameter, in simulation run `820veh-24h-19040012` (A.51), with $\phi = 0.2$ and $\varepsilon = 0.5$, the mean travel times continued with a bimodal distribution, but with modes at 690 s and 715 s, in the interval $[660, 725]$ s, and the best travel times obtained equally with a multimodal distribution, but now with a peak at 635 s, slightly lower modes at 620 s and 645 s, and the remaining, much less dense modes at 595 s, 680 s and 700 s, in the interval $[585, 710]$ s, with a reduction in the upper limit of the range.

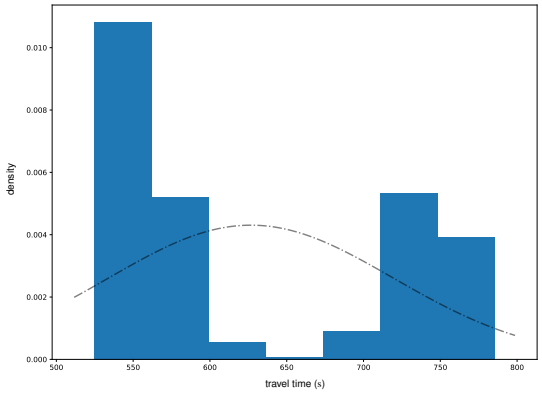
On a final note, simulation run `820veh-24h-19040012` (A.51), with $\phi = 0.5$ and $\varepsilon = 0.5$, had a bimodal distribution of the mean travel times, with modes at 685 s and 715 s, in the interval $[665, 715]$ s, and better travel times with a multimodal but strongly positively/right skewed distribution, peak at 610 s and modes at 600 s and 580 s, and very weakly dense modes at 630 s, 650 s, 670 s and 690 s, in the interval $[665, 715]$ s.

Changing the *recency* and *experimentation* parameters in the Roth-Erev algorithm had a direct effect on the emergence of cooperation. By happening earlier, it led to a decrease in the amplitude of the ranges of the vehicle time distributions, and consequently the modes became closer, with greater equality among all vehicles, regardless of whether they cooperated or not by accepting the RSU recommendation.

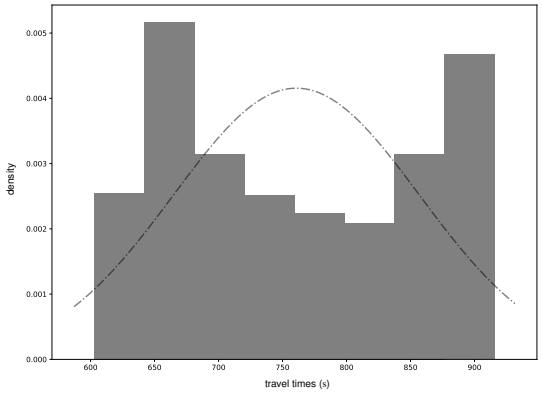
6.5 System Fairness

A system is said to be fair when there is a equitable sharing of resources, impartial and just, without favouritism or discrimination, showing no bias towards some individuals [cf. 129].

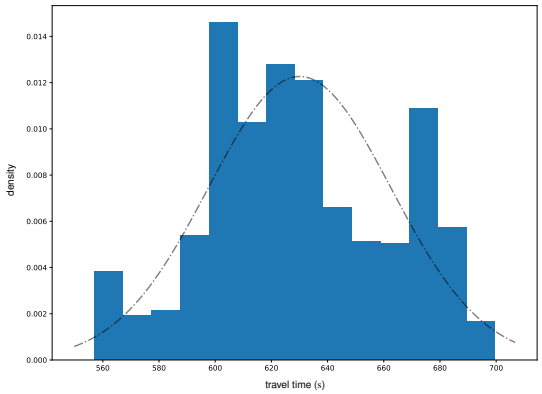
In order to assess the fairness of the implemented game model, where the RSU is one of the players and cooperation is reflected in the acceptance of its suggestion, one will look at the density



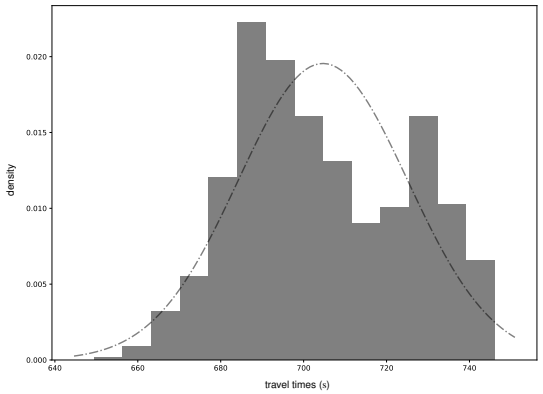
a) `820veh-24h-19040001`:
Best travel times histogram.



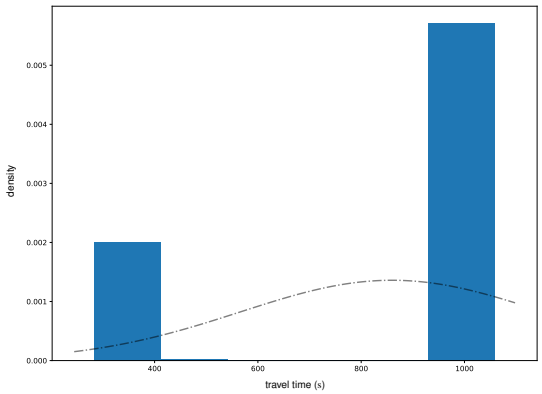
b) `820veh-24h-19040001`:
Average travel times histogram.



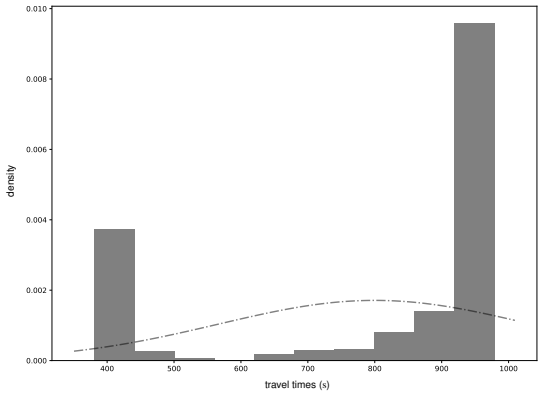
c) `820veh-24h-19040008`:
Best travel times histogram.



d) `820veh-24h-19040008`:
Average travel times histogram.



e) `820veh-24h-19040011`:
Best travel times histogram.



f) `820veh-24h-00049998`:
Average travel times histogram.

Figure 6.27: Density histograms of best travel time and average travel times for the population, in seconds (s), during the simulation of a 24 h period, superimposing the normal density curve, for simulation runs `820veh-24h-19040001` (A.45) (*top*), `820veh-24h-19040008` (A.48) (*middle*), and `820veh-24h-00049998` (A.52) (*bottom*), all with Roth-Erev parameters $\phi = 0.1$ and $\varepsilon = 0.2$, top row with payoff matrix `[360.0, 240.0, 0.0, -120.0]`, and middle/bottom rows with `[180.0, 60.0, 0.0, -120.0]`. The number of bins was calculated by the Freedman Diaconis rule. The two top rows show situations where there was an emergence of cooperation towards accepting the suggestion of the RSU, occurring earlier in the middle one. With the acceptance of the RSU's recommendation there is a tendency to approach a normal distribution of travel times (average and best times per vehicle) and the amplitude of the intervals gets narrower. In the bottom row is an example taken from the literature, where there is no RSU and the effect of cooperation is assumed in relation to the system, giving up the choice of the preferred route, evidencing the inequality between vehicles.

histograms of travel times, the best time and the average obtained by each vehicle of the population. For comparison, a further model is included from the literature, in which there is no RSU and the effect of cooperation is assumed with respect to the system, in which vehicles give up their preferred route choice.

Given the graphs of the Figure 6.27, the two top rows show situations where there was an emergence of cooperation towards accepting the suggestion of the RSU, occurring earlier in the middle one. The first had a different payoff matrix (cf. Subsection 6.4.1), with a late appearance of cooperation and a number of cooperators just over half the population. Travel times showed two groups by the bimodal distributions of both the average and the best times recorded per vehicle, the average with modes at 650 s and 900 s, and the best time at 550 s and 750 s. With the anticipation of cooperation and higher number of cooperators (middle row) the amplitude of the intervals gets narrower, lowering the upper limit in the best times to 690 s and tending towards the centre in the averages, within the range $[650, 750]$ s. The distributions, although still multimodal, also tend to approach a normal distribution. The number of trips made had a similar evolution, from a bimodal distribution with modes at 80 and 105, in the interval $[77, 110]$ s, it also tended to a normal distribution, with a peak at 102, in the interval $[96, 108]$ s.

On the bottom row, with no action of the RSU, even though it reached an average speed in the network of 10 m/s (36 km/h), and with an identical cooperation as in the middle row, the resulting distributions were bimodal, with modes of the best times at 360 s and 1000 s, of the averages at 400 s and 950 s, and in the number of trips at 80 and 170, evidencing the existence of two very distinct groups of vehicles, an inequality in which one is clearly benefited relative to the other.

This analysis denotes the importance of a degree of cooperation for a fairer system, but also the role of RSU recommendations, balancing the distribution of vehicles across the network so that both cooperating and non-cooperating vehicles perform similarly, either in terms of travel time or the number of trips made during the period, i.e. it is not always the same vehicles that get the best times but they tend to an equilibrium.

6.6 Providing Additional Information

The RSU, in order to bring the system to an optimal state, transmits a route recommendation which may or may not be accepted by the driver/vehicle. Besides the suggestion, it was experimented to send additional information concerning the route state in order to influence the driver's behaviour, namely the last recorded travel time on the recommended route. The driver compares it against its own experience and, if it is better, there is a probability of changing its decision and accepting the recommendation. Given the difficulty of modelling this behaviour, a simple probabilistic model was chosen, just to have an insight of the effect.

Comparing simulation runs with identical payoff matrices and parameters (Figure 6.28), `820veh-24h-19040008` (A.48) and `820veh-24h-19040003` (A.47), in terms of mean speed in the system, it was found that the one in which they received the additional information had more

stable values from the beginning, at around 9 m/s (32.40 km/h), while the other, despite dropping and being unstable in the first 5 h of simulation, then reached a stable value around 10.50 m/s (37.80 km/h) which it maintained until 24 h.

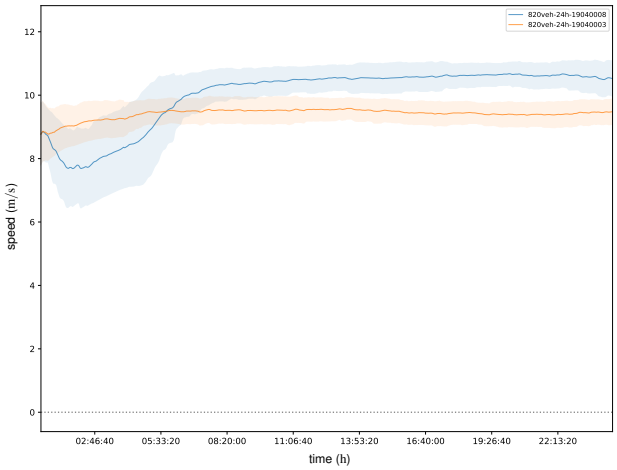
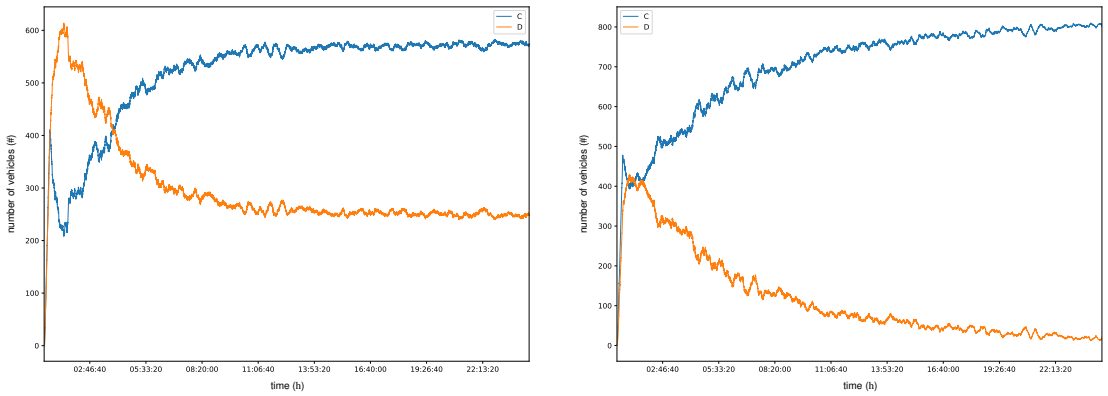


Figure 6.28: Mean speed in the network, in meters per second (m/s), during a 24 h period, 4 h Simple Moving Average, mean (line) and standard deviation (shaded), for a population of 820 vehicles, simulation runs `820veh-24h-19040008` (A.48) and `820veh-24h-19040003` (A.47), with identical payoff matrices and parameters, but the latter provides additional information about the last travel time associated with the recommended route, and it has a 20 % susceptibility to change of choice and accept the suggestion. *Legend identifies the simulation runs (cf. Appendix A for details).*



a) `820veh-24h-19040008` b) `820veh-24h-19040003`

Figure 6.29: Evolution of the number of *Cooperators* and *Defectors* , over a 24 h period, for simulation runs `820veh-24h-19040008` and `820veh-24h-19040003`, with identical payoff matrices and parameters, but the latter provides additional information about the last travel time associated with the recommended route, and it has a 20 % susceptibility to change of choice and accept the suggestion.

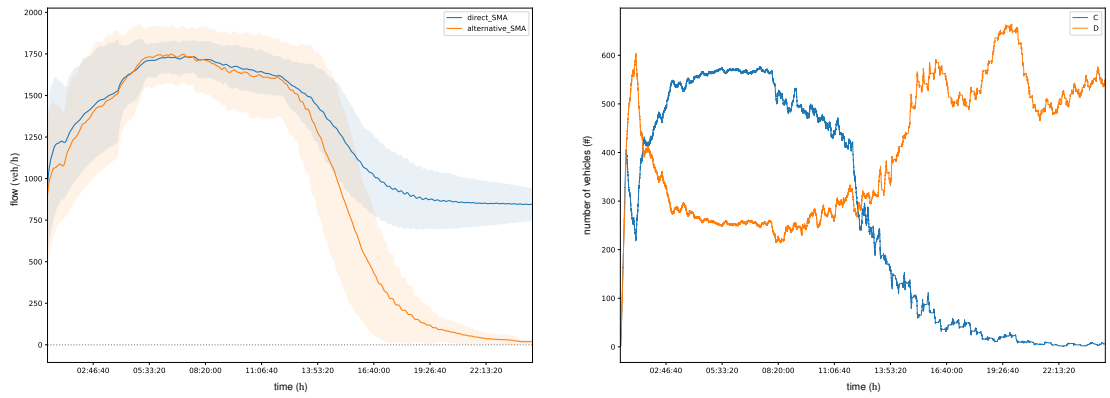
The most noticeable effect was seen in the evolution of cooperation (Figure 6.29), where information contributed to an earlier emergence and a growth throughout the simulation almost to full cooperation (Figure 6.29b), in contrast to the plateau evident in the evolution without additional information (Figure 6.29a). However, this increase in cooperation was not reflected in the system performance, on the contrary, as travel times and number of vehicles became higher in

the *alternative* route, with traffic flows around 1600 veh/h, instead of the convergence seen before, with identical travel times in both routes and traffic flows around 1750 veh/h. As the influence induced on the driver with this extra information depends on a time recorded at the end of the route, the time lag that will occur due to the distance from the destination to the node of choice and, consequently, the moment of congestion formation, the *alternative* (longer) route ended up receiving more vehicles when there was still capacity on the *direct* route, impairing the performance of the system.

Some experiments were also done with changing the information lifetime (time-to-live) by the RSU, discarding older information in variations of 30 s, 60 s or 120 s, but there was no change in the results with these values.

6.7 RSU Dissemination Degrading Over Time

In the previous sections it was considered that the RSU had a dissemination time interval that allowed it to deliver the recommendations to all vehicles passing in the coverage area, throughout the entire simulated period. With the purpose of analyse the effect of a degradation of this service, simulations were conducted in which the dissemination time interval doubled every 4 h, in the sequence $\{5, 10, 20, 40, 80, 160\}$ s, during which an increasing number of vehicles stopped receiving suggestions and continued on their default preferred route.



a) Traffic flow on each route, 4 h SMA.

b) Evolution of Cooperation.

Figure 6.30: Traffic flow on each route, in vehicles per hour (veh/h), 4 h Simple Moving Average, and evolution of the number of *Cooperators* and *Defectors,* over a 24 h period, for simulation run `820veh-24h-19040013`, in which the RSU's dissemination time interval doubled every 4 h, in the sequence $\{5, 10, 20, 40, 80, 160\}$ s.

During the first 8 h the evolution was similar to the previous cases, both in terms of cooperation emergence and traffic flow, i.e. up to 10 s interval the RSU was able to deliver recommendation to all vehicles. However, starting at 8 h of simulation, with 20 s interval, there was witnessed a decreasing trend in the traffic flow (Figure 6.30a), which followed a drop in the number of vehicles in game (both *cooperators* and *defectors* decreased) (Figure 6.30b). The traffic flow on both routes, and consequently the mean speed on the network, had a steeper decrease after 12 h, when the

interval was increased to 40 s, that of the *alternative* route tending to zero, as most of the traffic started to converge to the *direct* route. The cooperation, which had also been decreasing, suffered a strong decline and there was an inversion of trends with an increase in the number of *defectors*, although the sum diminished, since fewer vehicles were left in game.

In subsequent interactions with the RSU, the number of *cooperators* continued to decrease, tending towards zero, while that of *defectors* rose, with only part of the population, there being, however, two peaks, which can be explained with the reduction in speed due to the congestion that was forming as more vehicles converged on the *direct* route. In fact, in simulations carried out with a smaller population (cf. `570veh-24h-19040013` (A.54)), which did not generate congestion, after the inversion, the number of *defectors* reached a peak and then gradually descended in steps.

From what was observed, including by analysing the vehicles' individual history, as they began to receive increasingly sparse recommendations from the RSU, they began to reject more often the few they did receive, even those that were mostly cooperative in the early hours.

6.8 Summary

This chapter analyzed the results of the simulations performed during this study. It began by evaluating the baselines, with the vehicles converging to the main route of the network and the population size as the independent variable, in order to have an insight into the formation of traffic congestion, in comparison with the Greenshields and Greenberg theoretical models of traffic flow and the density-flow-speed relationship.

Then, it proceeded with the vehicles in full cooperation with the information system, the RSU, i.e., they all accepted its route recommendation. In this way, it was possible to analyze the selection and construction strategies of the suggestions and their impact on the system. Several metrics were employed as computation data and the dissemination was varied, sending to all vehicles in the coverage area (broadcast) or distinguishing groups of vehicles (multicast), whereby the need to use a combination of the travel times and traffic density on the routes, as well as the cooperation ratio with the RSU, to define the proportions of the groups was perceived.

After that, it was started to test the vehicle personalities, first the stochastic one, at 50 %, to evaluate the resilience of the RSU algorithms, then the memory-based selection algorithms, choosing the action by the best time or best average in a limit of how much the agent can remember, and, finally with a reinforcement learning algorithm, which gave more successful results, both in terms of cooperation and in terms of average speed reached in the network, as well as in the stability and maintenance of those values, but evidencing the fundamental role of the information system and route recommendations to tend to the system's optimality. These algorithms were also analysed in terms of the fairness of the system, that is, how equitable was the distribution of resources and costs to obtain those results, and it was found that the RSU also plays a very relevant role here along with cooperation to achieve that fairness. The inclusion of travel time information along with the recommendation, in turn, had an impact for increased cooperation, but hampered the performance of the system.

Finally, the system was analyzed against a degradation of the recommendation service, with the RSU increasing the dissemination time intervals, with very evident impact on the cooperation, which tended to zero, since the vehicles started to reject the suggestions when they began to be more sparse, and the network became congested with the convergence to the main route.

Chapter 7

Conclusions and Future Work

This chapter closes the project developed with a summary of the main results obtained and conclusions drawn, also discussing further improvements and future work, and some final remarks.

7.1 Conclusions

The major objective of this work was a systematic study and analysis of information percolation strategies to improve C-ITS services, taking into account the characteristics of the communication network and routing algorithms, the composition of transport demand, and the uncertainty inherent in human decision-making, with the aim of redistributing demand in time and space and promoting sustainable mobility.

During the literature review, the technologies related to inter-vehicular and vehicle-to-infrastructure communication, and advanced traveller information services were surveyed, also taking into account regulations and projects in the European Union context, in order to understand and emulate their operation in the scenarios designed. In addition, game theory and research in behavioural economics were taken into consideration because of the strong relationship between the emergence of cooperation and the resolution of social dilemmas such as that found in the dynamics and complexity of road traffic.

The scenario designed consists of a binary network, with two routes of different cost, of which the one with lower cost is the preferred one for the vehicles. A microscopic simulation runs in SUMO, controlled via TraCI by a program written in Python with the dissemination and decision algorithms, incorporating the interaction of drivers with an information system that makes route recommendations. The decision-making model was implemented based on the n-Person Prisoner's Dilemma and the payoff matrix was grounded on the social dilemma of the "tragedy of the commons". The participants in the game are the vehicles that constitute the population (the independent variable) and the information service, in the form of RSU, which provides a route recommendation to lead the system to an optimal state. The two possible actions of "cooperating"

or “defecting” correspond, respectively, to the options of “accepting” or “rejecting” the suggestion provided by the RSU.

The baseline analysis looked at the formation of traffic congestion in the context of the Greenshields and Greenberg theoretical traffic flow models and the flow density-speed relationship. With full cooperation with the information system, accepting the route recommendation, the selection and construction strategies of the suggestions and their impact on the system were examined, highlighting the need to combine travel time metrics and traffic density in the routes, as well as the cooperation relationship with the RSU, to define group proportions and use a multicast transmission mechanism instead of broadcast.

Using the behaviours defined for the vehicles (personalities), it was assessed the resilience of the RSU algorithms to the dynamic flow in the network and how it is possible to improve its performance with the emergence of cooperation, in particular using Pavlovian agents, modelled with reinforcement learning.

The evaluation metrics were focused on the average speed achieved in the network and cooperation, as also the traffic flows and times achieved in each route, and the respective stability and maintenance of these values, including in a context of fairness and equity of the system in the distribution of resources and costs. The fundamental role of the information system (RSU) and route recommendations for the optimization of the system was prominent.

Variations in the simulation included additional information to the recommendation, with consequences on the increase of cooperation but hindering the performance of the system, and the progressive degradation of the recommendation service, with a strong impact on cooperation, tending towards zero, with a generalized rejection of the increasingly sparse suggestions, and resulting in a network congestion.

7.2 Further Developments

The main objectives of this work were fulfilled, however, because the time-frame for the project and the time-consuming nature of microscopic traffic simulation meant that it was necessary to be judicious in the choice of cases, some aspects could be studied more thoroughly with variations on the model developed, or making use of the tools already implemented, namely through the parameters passed by command line.

Variations could include looking at other networks, with different cost ratios between the main and alternative routes, either in length or in maximum allowed speed, to study their relationship with the evolution of cooperation. On the other hand, given the time it takes for the impact of a measure to manifest itself, due to the distance the vehicles travel before starting a new journey, the simulated period can be extended to several days instead of just 24 h, and include daily demand cycles introducing flow limitation.

Another interesting aspect is to create heterogeneous populations in terms of personalities, to observe interrelationship and inter-influences, and vehicle subscription schemes could be implemented. Regarding cooperation, the RSU could also keep a list of the most cooperative and favour

dissemination by this group. The study of these variations can be confronted with the analyses already made in this work to assess the relevance of these approaches.

7.3 Main Contributions

One of the main contributions of this project is in the context of the emergence of cooperation in a simple road network to improve its performance, based on a game formalized in such a way that the traveller information system, the RSU, is one of the participants and the vehicles are expected to "accept" or "reject" a recommendation from it, performed in a dynamic environment, through the use of a microscopic simulator.

Then, a set of strategies was developed to build and disseminate the recommendation of the RSU, which aim at a predictive rather than reactive behaviour, in the sense of an optimal and fair system state.

Lastly, an analysis of the impact of the RSU communication failures (i.e., what happens when it does not work) was carried out, even without connection to a network simulator.

7.4 Future Work

As vehicular traffic is a complex and adaptive system, with interactions between vehicles whose drivers make decisions and adopt strategies in order to achieve their goal, in a context of conflict and cooperation, game theory concepts play an important role in its analysis. Therefore, possible future work includes studying the vehicle/RSU interaction with other games, namely Minority Games, among others that express cooperation in a social dilemma scenario, to model collective behaviours when users have to compete for limited resources with incomplete information.

7.5 Final Remarks

In this work it was made a simulation of a simple binary network, however, the difficulties experienced in modelling the scenario for a microscopic simulation let one foresee the complexity of managing a real traffic system, by the arbitrariness of human decisions, marked by uncertainty and selfishness, with severe impact on obtaining an optimal state of the system. Within the formalization carried out, with the interaction vehicle *vs* information system, when cooperation emerges, i.e. acceptance of the recommendation, the responsibility for obtaining that optimal state lies in the system itself and its credibility is at stake. But the knowledge of that same cooperation can be a very useful tool for the system, allowing it to deliver the recommendations to the most appropriate users in order to improve performance. Cooperation, connectivity and automation thus become more than complementary technologies, reinforcing each other on the way to a complete fusion. Therefore, an undeniable contribution is expected with clear benefits for road safety, for traffic efficiency, a contribution to the creation of a more sustainable World.

Appendix A

Simulation Runs

A.1 Simulation launcher usage

```
Usage: runner.py [options]

Options:
  -h, --help            show this help message and exit
  --nogui               run the commandline version of sumo
  --step-length=STEP_LENGTH
                        defines the step duration in seconds
  --seed=SEED           initialises the random number generator with the given
                        value
  --output-prefix=OUTPUT_PREFIX
                        prefix which is applied to all output files
  --sim-run-time=SIM_RUN_TIME
                        simulated run time in hours
  --num-vehicles=NUM_VEHICLES
                        number of vehicles to be loaded in simulation
  --warmup-speed=WARMUP_SPEED
                        warm up max speed
  --warmup-routes-weight=WARMUP_ROUTES_WEIGHT
                        routes weight for warmup distribution: (int)<direct>
                        (int)<alternative>
  --network-speed=NETWORK_SPEED
                        network max speed
  --change-behavior-probability=CHANGE_BEHAVIOR_PROBABILITYQ
                        probability of change behavior:
                        (int)<choose_best_action> (int)<accept_suggestion>
  --cooperation-probability=COOPERATION_PROBABILITY
                        vehicle cooperation probability: (int)<defect>
                        (int)<cooperate>
  --vehicle-selection-strategy=VEHICLE_SELECTION_STRATEGY
                        vehicle action selection strategy: best_travel_time,
                        best_payoff, best_payoff_utility, mean_payoff,
                        roth_erev, roth_erev_utility, stochastic,
                        mean_payoff_v2
  --turn-rsu-off        turn off RSU suggestion
  --rsu-dynamic-dissemination
                        turn on RSU dissemination dynamic interval
  --rsu-dissemination-interval=RSU_DISSEMINATION_INTERVAL
                        RSU (minimum) dissemination interval, in seconds
  --rsu-probabilistic-dissemination
                        turn on RSU dissemination dynamic intervallslisting
  --rsu-suggestion-strategy=RSU_SUGGESTION_STRATEGY
                        rsu suggestion strategy: proportional,
                        proportional_dynamic, occupancy_simple,
                        travel_time_simple, travel_time_product,
                        travel_time_moving_average_simple,
                        travel_time_moving_average_product,
                        travel_time_occupancy, travel_time_free_flow_tt,
                        intermediate_travel_time_free_flow_tt, mean_speed,
                        lane_estimated_travel_time, end_of_queue_occupancy,
                        occupancy_product, proportional_dynamic_v2,
                        proportional_dynamic_v3, pigous_example,
                        proportional_dynamic_v4, lane_occupancy,
                        pigous_example_cooperation_weighted
```

```
--rsu-routes-weight=RSU_ROUTES_WEIGHT
                      routes weight for proportional suggestion:
                      (int)<direct> (int)<alternative>
--rsu-moving-avg-size=RSU_MOVING_AVG_SIZE
                      RSU maximum number of elementos for moving average
                      calculation
--travel-times-ttl=TRAVEL_TIMES_TTL
                      travel times TTL (time to live), during which it is
                      available selection functions, in seconds
--payoff-matrix=PAYOFF_MATRIX
                      payoff matrix TRPS: (float)<T> (float)<R> (float)<P>
                      (float)<S>
--roth-erev-parameters=ROTH_EREV_PARAMETERS
                      Roth Erev parameters: (float)<recency>
                      (float)<experimentation>
--rsu-change-dissemination
                      RSU changes dissemination interval over time
--rsu-change-dissemination-steps=RSU_CHANGE_DISSEMINATION_STEPS
                      List of simulation steps (in seconds) in which a
                      change of the RSU dissemination interval occur:
                      [<int>, ..., <int>]
--rsu-change-dissemination-intervals=RSU_CHANGE_DISSEMINATION_INTERVALS
                      List of time intervals (in seconds) for RSU
                      dissemination: "[<int>, ..., <int>]"
```

A.2 Parameters

```
Simulation Run Name Structure

<###>veh-<##>h-########

<###>veh: number of vehicles
<##>h: simulation run time

########: Flags

00000000 base case

[00]000000 rsu strategy
00[00]0000 vehicle strategy
0000[0000] base case (all cooperate, accept suggestion)
0000[1111] base case (all defect, reject suggestion)

RSU suggestion strategy:
   00: proportional
   01: proportional_dynamic
   02: occupancy_simple
   03: occupancy_product
   04: end_of_queue_occupancy
   05: travel_time_simple
   06: travel_time_product
   07: travel_time_moving_average_simple
   08: travel_time_moving_average_product
   09: travel_time_occupancy
   10: travel_time_free_flow_tt
   11: intermediate_travel_time_free_flow_tt
   12: mean_speed
   13: lane_estimated_travel_time
   14: proportional_dynamic_v2
   15: proportional_dynamic_v3
   16: pigous_example
   17: proportional_dynamic_v4
   18: lane_occupancy
   19: pigous_example_cooperation_weighted

Vehicle selection strategy:
   00: best_travel_time
   01: best_payoff
   02: best_payoff_utility
   03: mean_payoff
   04: roth_erev
   05: roth_erev_utility
   06: stochastic
   07: mean_payoff_v2

0000[0001] (50 % initial probability of cooperation [50 50], always choose best action)
0000[0002] (50 % initial probability of cooperation [50 50], 20% change behaviour [80 20])
0000[0003] (50 % initial probability of cooperation [50 50], 20% change behaviour [80 20],
    RSU sends time information, roth-erev parameters to 0.1 0.5, payoff 180 60 0 -120)
```

```
0000[0004] (50 % initial probability of cooperation [50 50], 20% change behaviour [80 20],
    RSU sends time information, increase travel-times-ttl to 120s)
0000[0005] (50 % initial probability of cooperation [50 50], 20% change behaviour [80 20],
    RSU sends time information, reduce travel-times-ttl to 30s)
0000[0006] (50 % initial probability of cooperation [50 50], 20% change behaviour [80 20],
    RSU sends time information, roth-erev parameters to 0.1 0.2)
0000[0007] (50 % initial probability of cooperation [50 50], 20% change behaviour [80 20],
    RSU sends time information, roth-erev parameters to 0.1 0.5)
0000[0008] (50 % initial probability of cooperation [50 50], RSU does not send time
    information, roth-erev parameters to 0.1 0.2, payoff 180 60 0 -120)
0000[0009] (50 % initial probability of cooperation [50 50], RSU does not send time
    information, roth-erev parameters to 0.1 0.5, payoff 360 240 0 -120)
0000[0010] (50 % initial probability of cooperation [50 50], RSU does not send time
    information, roth-erev parameters to 0.1 0.5, payoff 180 60 0 -120)
0000[0011] (50 % initial probability of cooperation [50 50], RSU does not send time
    information, roth-erev parameters to 0.5 0.5, payoff 180 60 0 -120)
0000[0012] (50 % initial probability of cooperation [50 50], RSU does not send time
    information, roth-erev parameters to 0.2 0.5, payoff 180 60 0 -120)
0000[0013] (50 % initial probability of cooperation [50 50], RSU does not send time
    information, roth-erev parameters to 0.5 0.5, payoff 180 60 0 -120), RSU changes
    dissemination interval at steps [14400, 28800, 43200, 57600, 72000] (s), to [10, 20, 40,
    80, 160] (s)
0000[9998] base (all defect, turn off RSU, roth-roth-erev parameters at 0.1 0.2, payoff 180
    60 0 -120)
0000[9999] base (all defect, turn off RSU, roth-roth-erev parameters at 0.1 0.2, payoff 360
    240 0 -120)
```

A.3 820veh-24h-00060000

```
Scenario: scenario-1
Timestamp: 20210521T164208Z
Number of vehicles: 820 vehs
Simulation time: 24.0 h
Warm up end time: 1866.6 s; step 18665
Vehicle selection strategy: stochastic
RSU turned off: False
RSU strategy: proportional
Runner options:
   nogui: True
   step_length: 0.1
   seed: 19750808
   output_prefix: 820veh-24h-00060000
   sim_run_time: 24.0
   num_vehicles: 820
   warmup_speed: 13.96
   warmup_routes_weight: [473, 527]
   network_speed: 25.0
   change_behavior_probability: [0, 100]
   cooperation_probability: [0, 100]
   vehicle_selection_strategy: stochastic
   turn_rsu_off: False
   rsu_dynamic_dissemination: False
   rsu_dissemination_interval: 5
   rsu_probabilistic_dissemination: False
   rsu_suggestion_strategy: proportional
   rsu_routes_weight: [460, 540]
   rsu_moving_avg_size: 5
   travel_times_ttl: 60
   rsu_dissemination_ttl: 0
   rsu_send_travel_time_info: False
   payoff_matrix: [360.0, 240.0, 0.0, -120.0]
   roth_erev_parameters: [0.1, 0.1]
Network Mean speed after warmup:
   Max: 11.13
   Min: 7.14
```

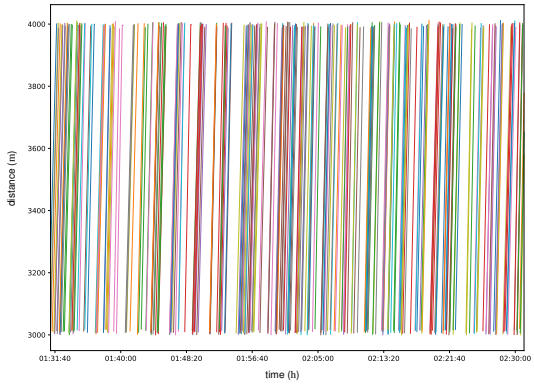


Fig. A.3-1. Time-Space diagram, for the one hour period after the end of the warmup, from 1:00:00 to 2:00:00 simulation time, plotted for the data from the sensor placed in the middle of the *direct* route (between 3000 m and 4000 m). In the case of an overloaded network, congestion shock waves can be observed.

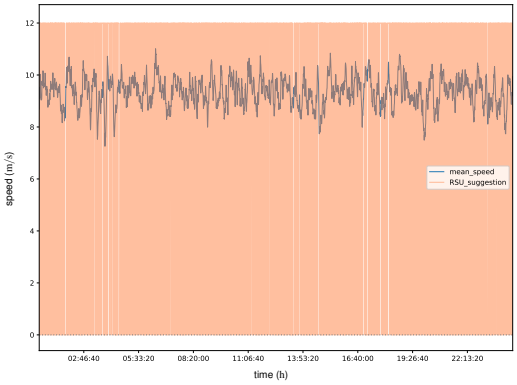


Fig. A.3-2. Mean speed in the network, in meters per second (m/s), over a 24 h period, superimposing (vertically, in orange) the time instants in which the RSU issued a recommendation to follow the *alternative* route.

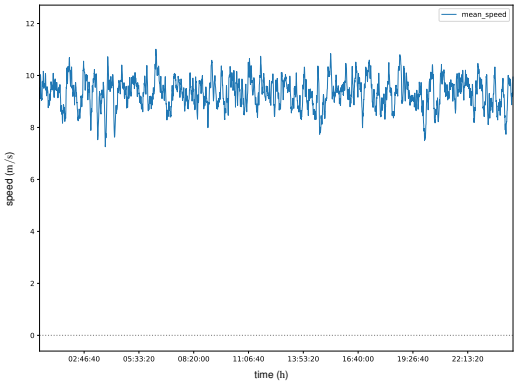


Fig. A.3-3. Mean speed in the network, in meters per second (m/s), over a 24 h period.

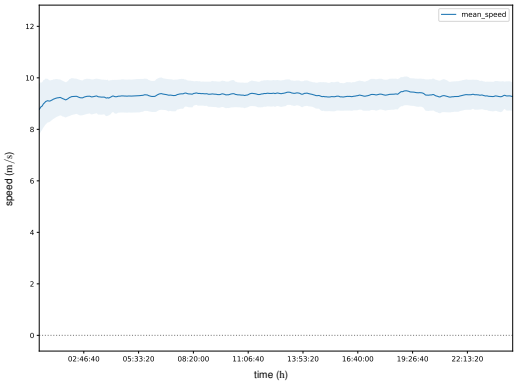


Fig. A.3-4. Mean speed in the network, in meters per second (m/s), over a 24 h period, 4 h Simple Moving Average, mean (line) and standard deviation (shaded).

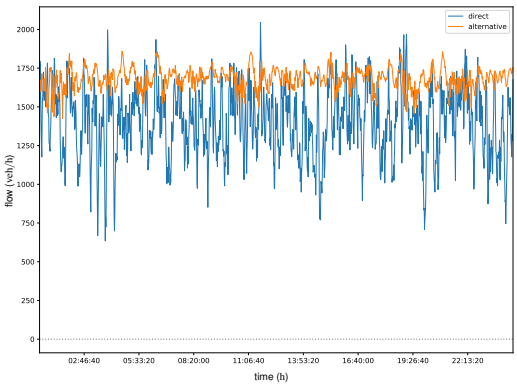


Fig. A.3-5. Traffic flow on each route, in vehicles per hour (veh/h), over a 24 h period.

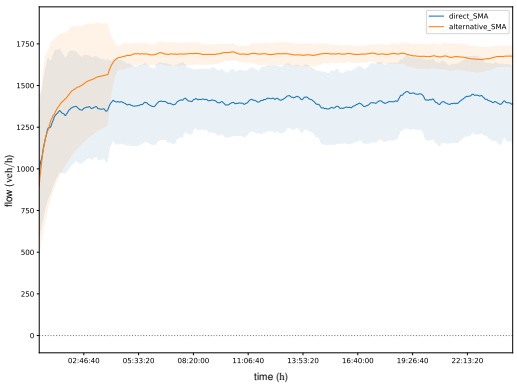


Fig. A.3-6. TrafficTraffic flow on each route, in vehicles per hour (veh/h), over a 24 h period, 4 h Simple Moving Average, mean (line) and standard deviation (shaded).

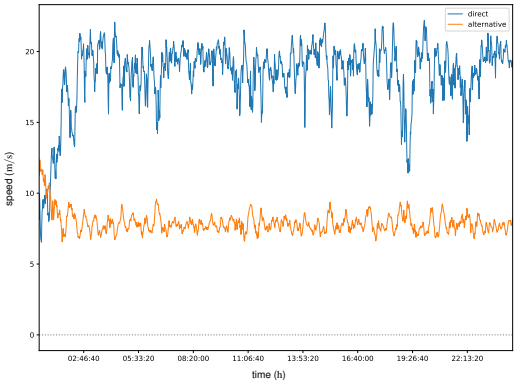


Fig. A.3-7. Mean speed on each route, in meters per second (m/s), aggregated to 1 min, over a 24 h period.

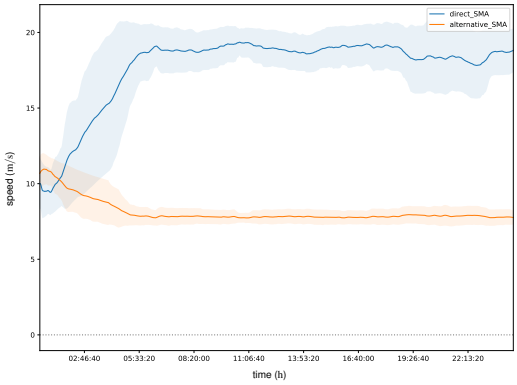


Fig. A.3-8. Mean speed on each route, in meters per second (m/s), aggregated to 1 min, over a 24 h period, 4 h Simple Moving Average, mean (line) and standard deviation (shaded).

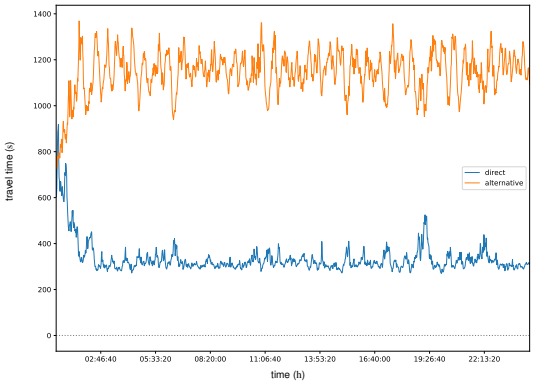


Fig. A.3-9. Travel times on each route, in seconds (s), aggregated to 1 min, over a 24 h period.

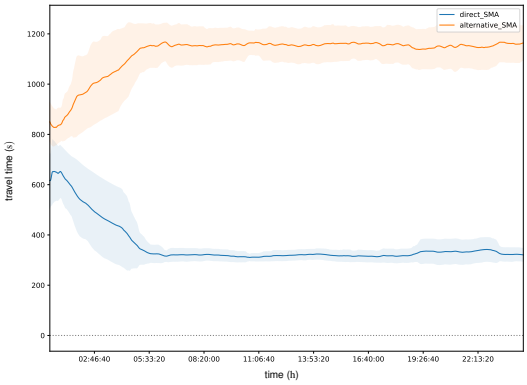


Fig. A.3-10. Travel times on each route, in seconds (s), aggregated to 1 min, over a 24 h period, 4 h Simple Moving Average, mean (line) and standard deviation (shaded).

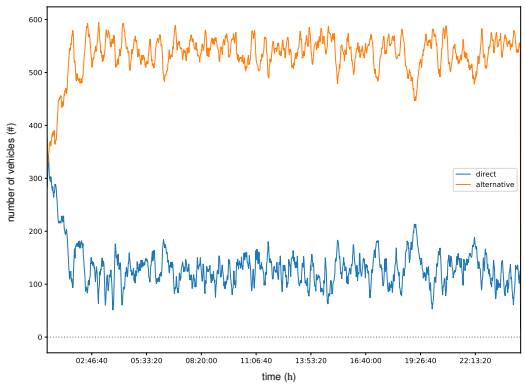


Fig. A.3-11. Average number of vehicles on each route, aggregated to 1 min, over a 24 h period.

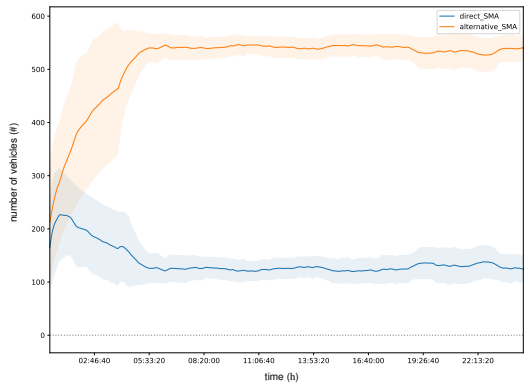


Fig. A.3-12. Average number of vehicles on each route, aggregated to 1 min, over a 24 h period, 4 h Simple Moving Average, mean (line) and standard deviation (shaded).

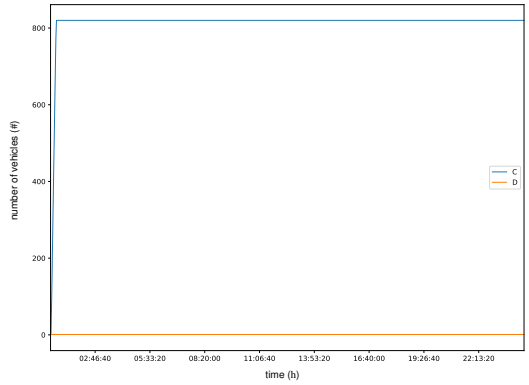


Fig. A.3-13. Evolution of the number of *Cooperators* and *Defectors* over a 24 h period.

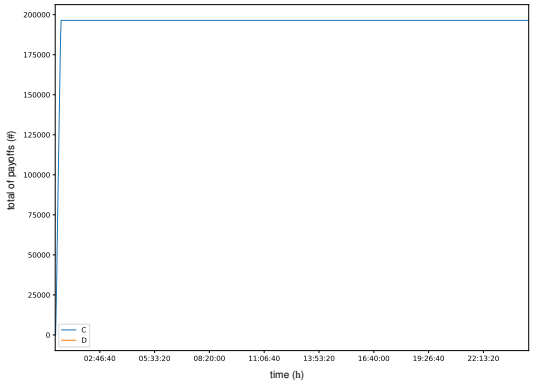


Fig. A.3-14. Evolution of total payoffs for *Cooperators* and *Defectors* (*individual payoff* times the *number of players receiving it*, $C(n) \times n$ and $D(n) \times (N-n)$, where n is the number of *Cooperators*), over a 24 h period.

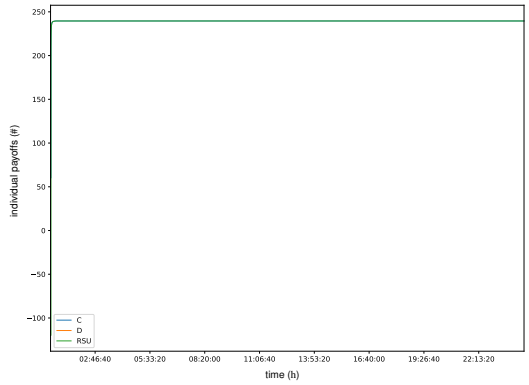


Fig. A.3-15. Evolution of the individual payoffs for *Cooperators, Defectors,* and *RSU* (always cooperating), over a 24 h period.

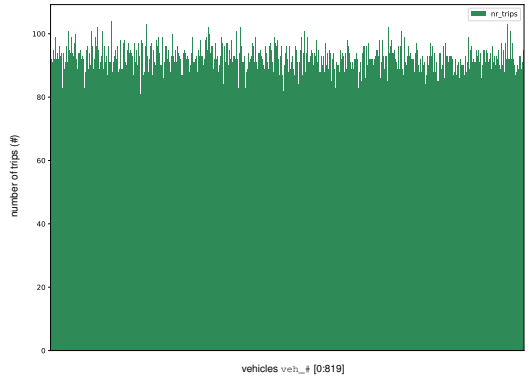


Fig. A.3-16. Number of trips made by each vehicle, during the simulation of a 24 h period.

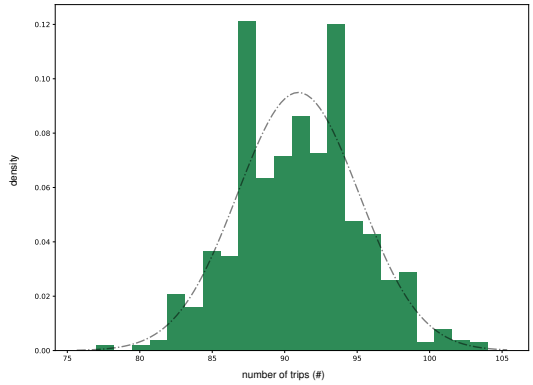


Fig. A.3-17. Density histogram of the number of trips made by each vehicle, during the simulation of a 24 h period, superimposing the normal density curve. The number of bins was calculated by the Freedman Diaconis rule.

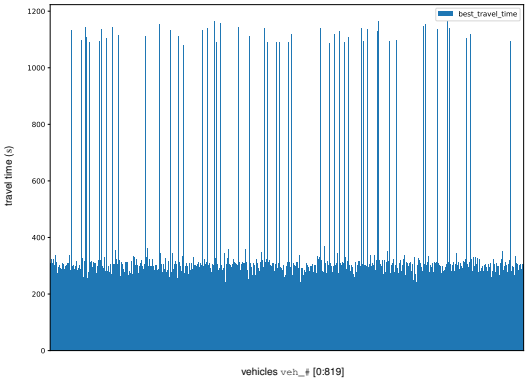


Fig. A.3-18. Best travel time for each vehicle, in seconds (s), during the simulation of a 24 h period.

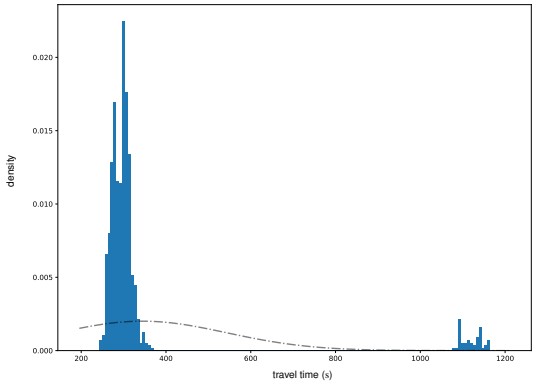


Fig. A.3-19. Density histogram of best travel time for vehicles, in seconds (s), during the simulation of a 24 h period, superimposing the normal density curve. The number of bins was calculated by the Freedman Diaconis rule.

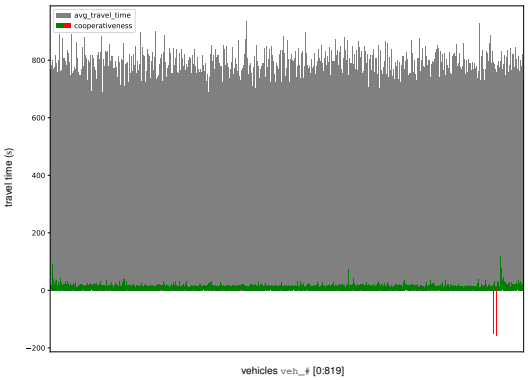


Fig. A.3-20. Average of the travel times, in seconds (s), of individual vehicles, during the simulation of a 24 h period. The bottom graph represents the *degree of cooperativeness**, downscaled by a normalization factor for the purpose of comparison with average times.

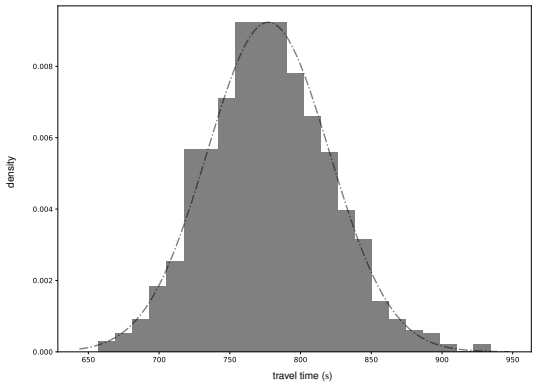


Fig. A.3-21. Density histogram of the average travel times, in seconds (s), of individual vehicles, during the simulation of a 24 h period, superimposing the normal density curve. The number of bins was calculated by the Freedman Diaconis rule.

* The *degree of cooperativeness* is a cumulative sum, calculated at each iteration, based on the complement of the ratio of cooperators, i.e., the higher the number of cooperators the less it increases, but the defectors are more penalized, and vice-versa. It varies inversely with the size of the group to which the player belongs.

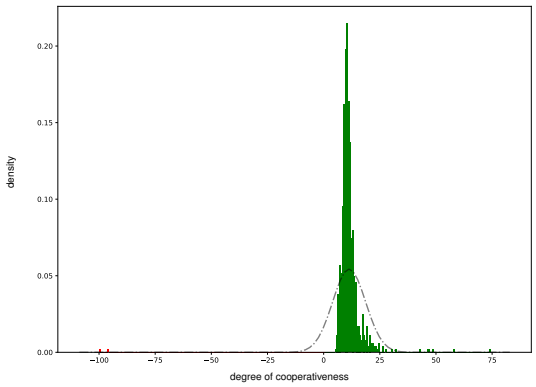


Fig. A.3-22. Density histogram of the *degree of cooperativeness** of individual vehicles, superimposing the normal density curve. The number of bins was calculated by the Freedman Diaconis rule. Generally, when strongly correlated with travel times, it presents a symmetric curve with respect to the *yy*-axis. Because some vehicles choose their preferred route immediately after the end of warmup, due to the gap between the RSU coverage and the route selection point, there may be some outliers.

A.4 `120veh-24h-00061111`

```
Scenario: scenario-1
Timestamp: 20210612T192809Z
Number of vehicles: 120 vehs
Simulation time: 24.0 h
Warm up end time: 98.1 s; step 980
Vehicle selection strategy: stochastic
RSU turned off: False
RSU strategy: proportional
Runner options:
   nogui: True
   step_length: 0.1
   seed: 19750808
   output_prefix: 120veh-24h-00061111
   sim_run_time: 24.0
   num_vehicles: 120
   warmup_speed: 25.0
   warmup_routes_weight: [473, 527]
   network_speed: 25.0
   change_behavior_probability: [100, 0]
   cooperation_probability: [100, 0]
   vehicle_selection_strategy: stochastic
   turn_rsu_off: False
   rsu_dynamic_dissemination: False
   rsu_dissemination_interval: 5
   rsu_probabilistic_dissemination: False
   rsu_suggestion_strategy: proportional
   rsu_routes_weight: [494, 506]
   rsu_moving_avg_size: 5
   travel_times_ttl: 60
   rsu_dissemination_ttl: 0
   rsu_send_travel_time_info: False
   payoff_matrix: [360.0, 240.0, 0.0, -120.0]
   roth_erev_parameters: [0.1, 0.15]
   rsu_change_dissemination: False
   rsu_change_dissemination_steps: [14400, 28800, 43200, 57600, 72000]
   rsu_change_dissemination_intervals: [10, 20, 40, 80, 160]
Network Mean speed after warmup:
   Max: 19.84
   Min: 12.97
```

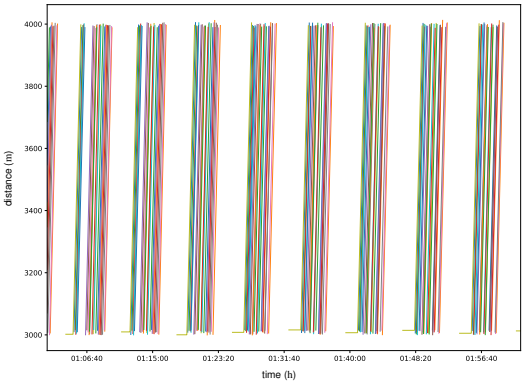


Fig. A.4-1. Time-Space diagram, for the one hour period after the end of the warmup, from 1:00:00 to 2:00:00 simulation time, plotted for the data from the sensor placed in the middle of the *direct* route (between 3000 m and 4000 m). In the case of an overloaded network, congestion shock waves can be observed.

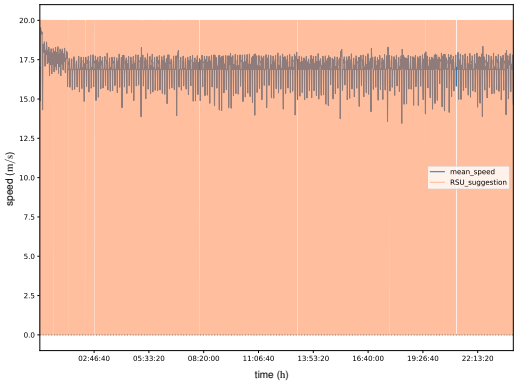


Fig. A.4-2. Mean speed in the network, in meters per second (m/s), over a 24 h period, superimposing (vertically, in orange) the time instants in which the RSU issued a recommendation to follow the *alternative* route.

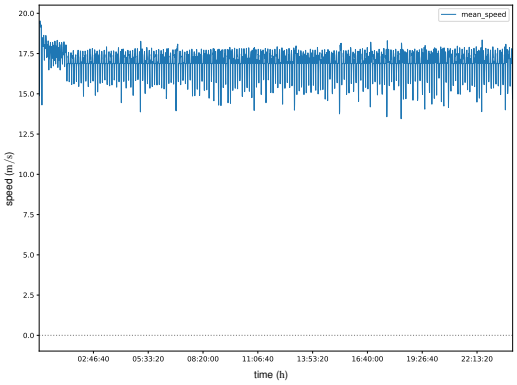


Fig. A.4-3. Mean speed in the network, in meters per second (m/s), over a 24 h period.

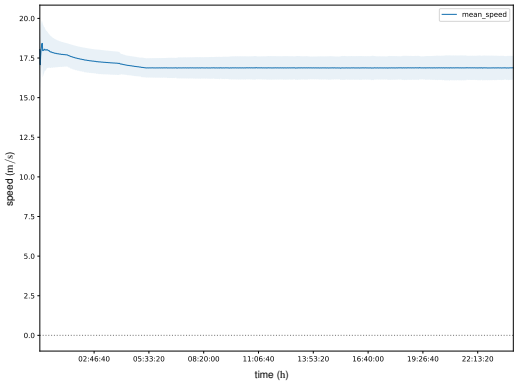


Fig. A.4-4. Mean speed in the network, in meters per second (m/s), over a 24 h period, 4 h Simple Moving Average, mean (line) and standard deviation (shaded).

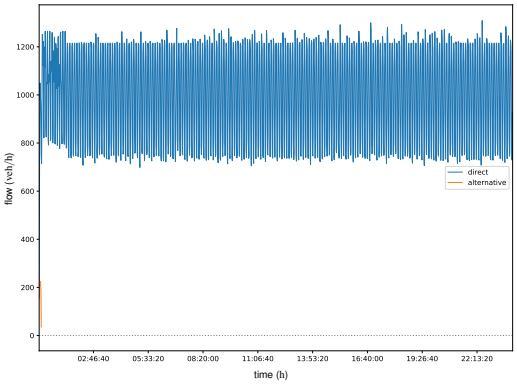


Fig. A.4-5. Traffic flow on each route, in vehicles per hour (veh/h), over a 24 h period.

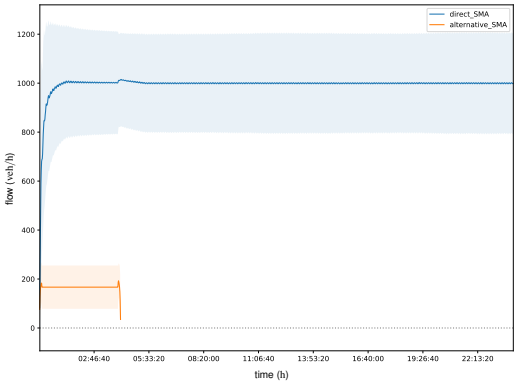


Fig. A.4-6. TrafficTraffic flow on each route, in vehicles per hour (veh/h), over a 24 h period, 4 h Simple Moving Average, mean (line) and standard deviation (shaded).

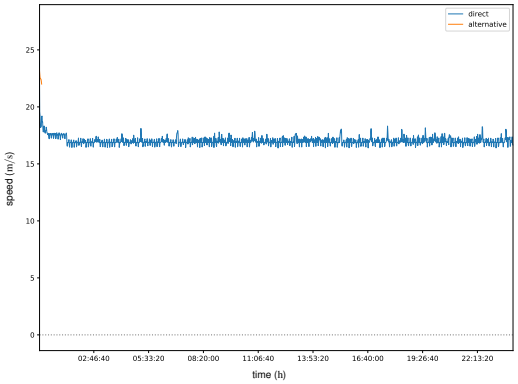


Fig. A.4-7. Mean speed on each route, in meters per second (m/s), aggregated to 1 min, over a 24 h period.

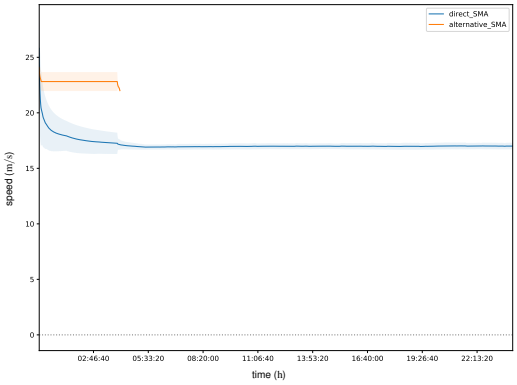


Fig. A.4-8. Mean speed on each route, in meters per second (m/s), aggregated to 1 min, over a 24 h period, 4 h Simple Moving Average, mean (line) and standard deviation (shaded).

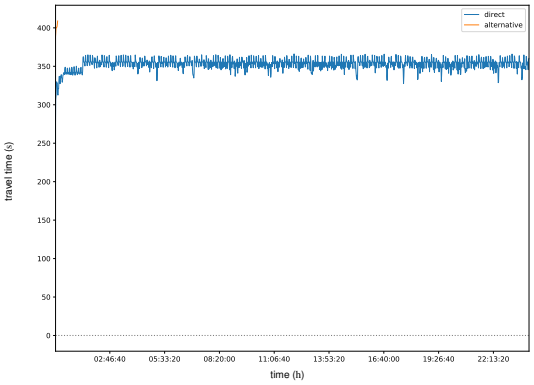


Fig. A.4-9. Travel times on each route, in seconds (s), aggregated to 1 min, over a 24 h period.

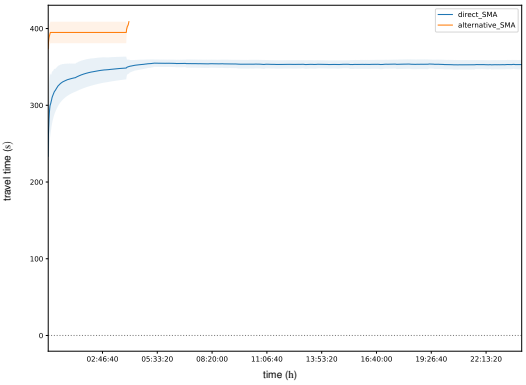


Fig. A.4-10. Travel times on each route, in seconds (s), aggregated to 1 min, over a 24 h period, 4 h Simple Moving Average, mean (line) and standard deviation (shaded).

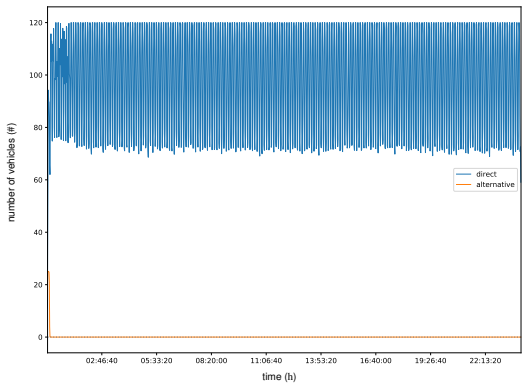


Fig. A.4-11. Average number of vehicles on each route, aggregated to 1 min, over a 24 h period.

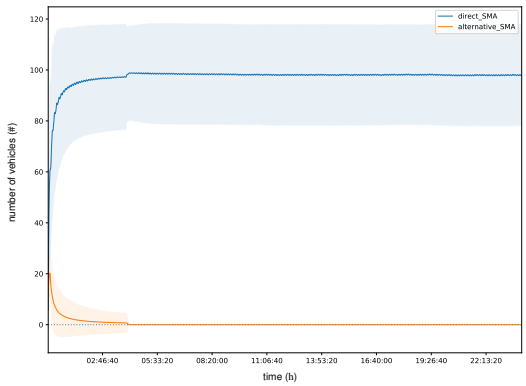


Fig. A.4-12. Average number of vehicles on each route, aggregated to 1 min, over a 24 h period, 4 h Simple Moving Average, mean (line) and standard deviation (shaded).

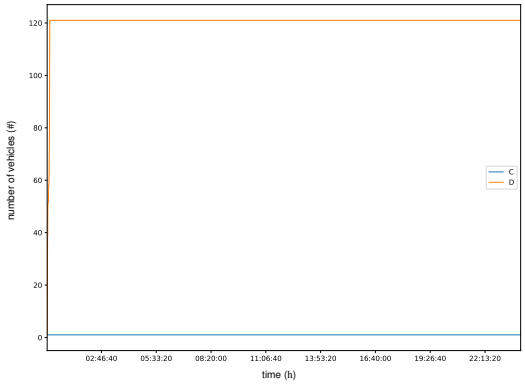


Fig. A.4-13. Evolution of the number of *Cooperators* and *Defectors* over a 24 h period.

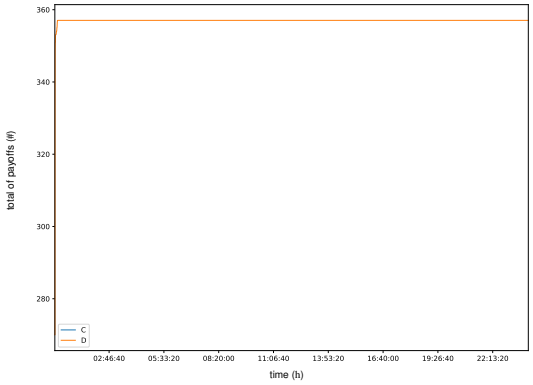


Fig. A.4-14. Evolution of total payoffs for *Cooperators* and *Defectors* (*individual payoff* times the *number of players receiving it*, $C(n) \times n$ and $D(n) \times (N-n)$, where n is the number of *Cooperators*), over a 24 h period.

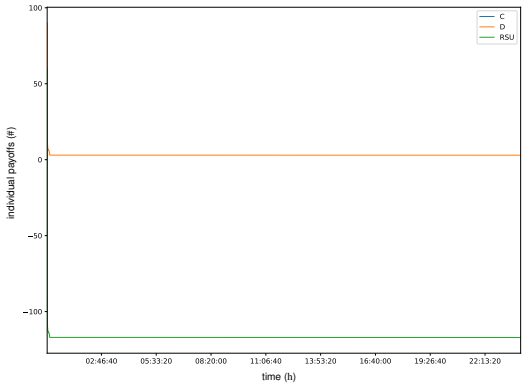


Fig. A.4-15. Evolution of the individual payoffs for *Cooperators, Defectors,* and *RSU* (always cooperating), over a 24 h period.



Fig. A.4-16. Number of trips made by each vehicle, during the simulation of a 24 h period.

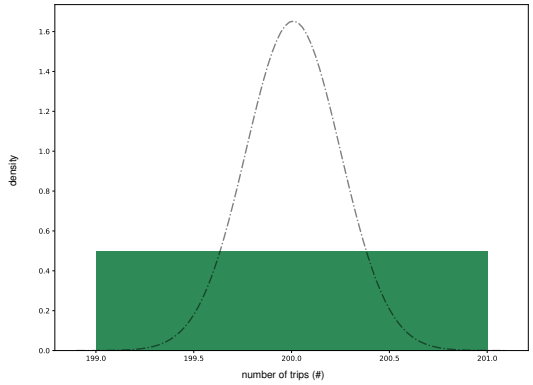


Fig. A.4-17. Density histogram of the number of trips made by each vehicle, during the simulation of a 24 h period, superimposing the normal density curve. The number of bins was calculated by the Freedman Diaconis rule.

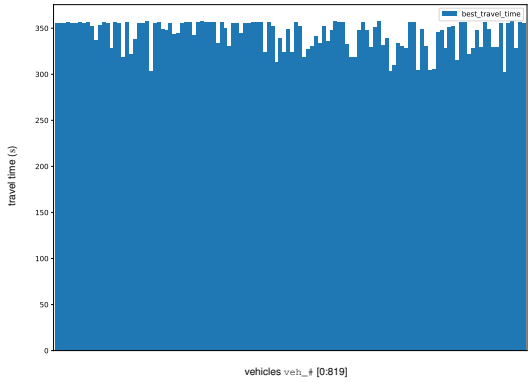


Fig. A.4-18. Best travel time for each vehicle, in seconds (s), during the simulation of a 24 h period.

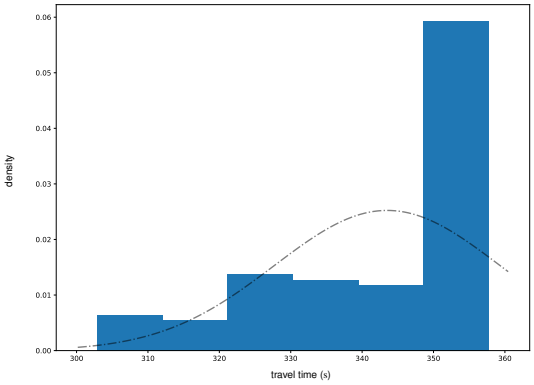


Fig. A.4-19. Density histogram of best travel time for vehicles, in seconds (s), during the simulation of a 24 h period, superimposing the normal density curve. The number of bins was calculated by the Freedman Diaconis rule.

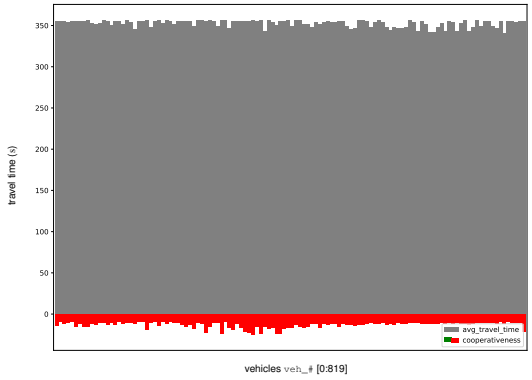


Fig. A.4-20. Average of the travel times, in seconds (s), of individual vehicles, during the simulation of a 24 h period. The bottom graph represents the *degree of cooperativeness**, downscaled by a normalization factor for the purpose of comparison with average times.

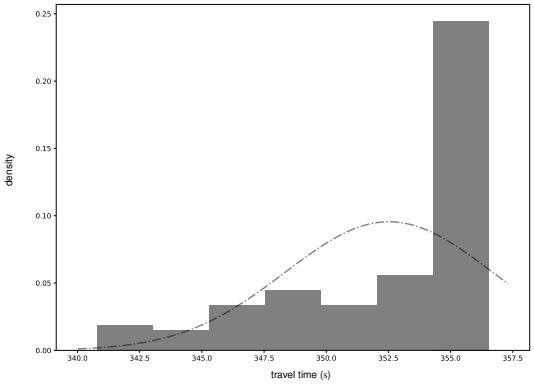


Fig. A.4-21. Density histogram of the average travel times, in seconds (s), of individual vehicles, during the simulation of a 24 h period, superimposing the normal density curve. The number of bins was calculated by the Freedman Diaconis rule.

* The *degree of cooperativeness* is a cumulative sum, calculated at each iteration, based on the complement of the ratio of cooperators, i.e., the higher the number of cooperators the less it increases, but the defectors are more penalized, and vice-versa. It varies inversely with the size of the group to which the player belongs.

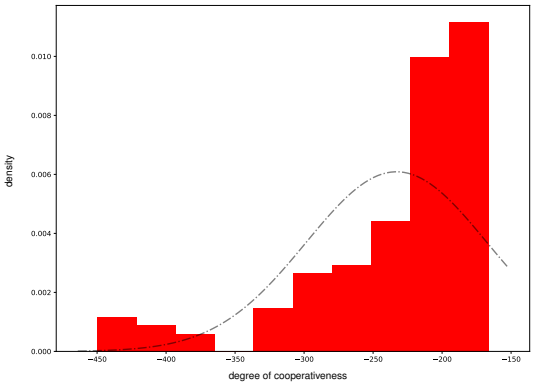


Fig. A.4-22. Density histogram of the *degree of cooperativeness** of individual vehicles, superimposing the normal density curve. The number of bins was calculated by the Freedman Diaconis rule. Generally, when strongly correlated with travel times, it presents a symmetric curve with respect to the *yy*-axis. All vehicles followed the preferred route and rejected the recommendation (all *Defectors*).

A.5 200veh-24h-00061111

```
Scenario: scenario-1
Timestamp: 20210612T192821Z
Number of vehicles: 200 vehs
Simulation time: 24.0 h
Warm up end time: 168.3 s; step 1682
Vehicle selection strategy: stochastic
RSU turned off: False
RSU strategy: proportional
Runner options:
   nogui: True
   step_length: 0.1
   seed: 19750808
   output_prefix: 200veh-24h-00061111
   sim_run_time: 24.0
   num_vehicles: 200
   warmup_speed: 25.0
   warmup_routes_weight: [473, 527]
   network_speed: 25.0
   change_behavior_probability: [100, 0]
   cooperation_probability: [100, 0]
   vehicle_selection_strategy: stochastic
   turn_rsu_off: False
   rsu_dynamic_dissemination: False
   rsu_dissemination_interval: 5
   rsu_probabilistic_dissemination: False
   rsu_suggestion_strategy: proportional
   rsu_routes_weight: [490, 510]
   rsu_moving_avg_size: 5
   travel_times_ttl: 60
   rsu_dissemination_ttl: 0
   rsu_send_travel_time_info: False
   payoff_matrix: [360.0, 240.0, 0.0, -120.0]
   roth_erev_parameters: [0.1, 0.15]
   rsu_change_dissemination: False
   rsu_change_dissemination_steps: [14400, 28800, 43200, 57600, 72000]
   rsu_change_dissemination_intervals: [10, 20, 40, 80, 160]
Network Mean speed after warmup:
   Max: 19.13
   Min: 12.02
```

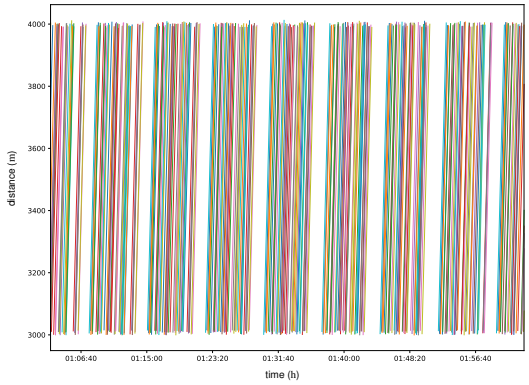


Fig. A.5-1. Time-Space diagram, for the one hour period after the end of the warmup, from 1:00:00 to 2:00:00 simulation time, plotted for the data from the sensor placed in the middle of the *direct* route (between 3000 m and 4000 m). In the case of an overloaded network, congestion shock waves can be observed.

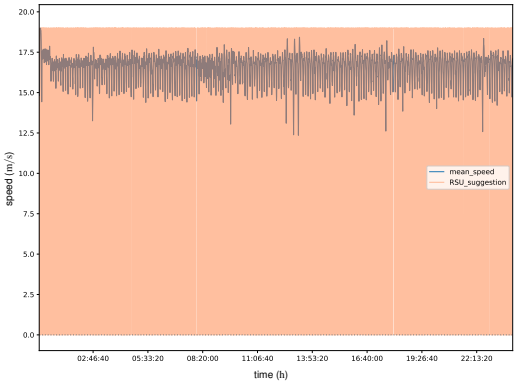


Fig. A.5-2. Mean speed in the network, in meters per second (m/s), over a 24 h period, superimposing (vertically, in orange) the time instants in which the RSU issued a recommendation to follow the *alternative* route.

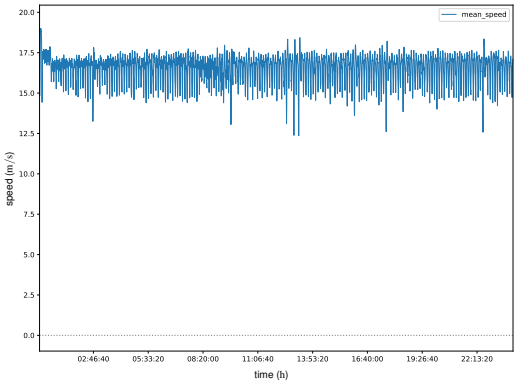


Fig. A.5-3. Mean speed in the network, in meters per second (m/s), over a 24 h period.

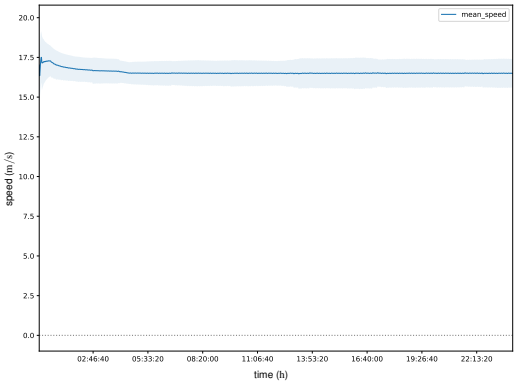


Fig. A.5-4. Mean speed in the network, in meters per second (m/s), over a 24 h period, 4 h Simple Moving Average, mean (line) and standard deviation (shaded).

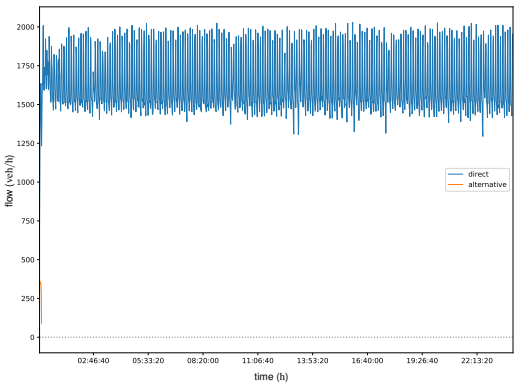


Fig. A.5-5. Traffic flow on each route, in vehicles per hour (veh/h), over a 24 h period.

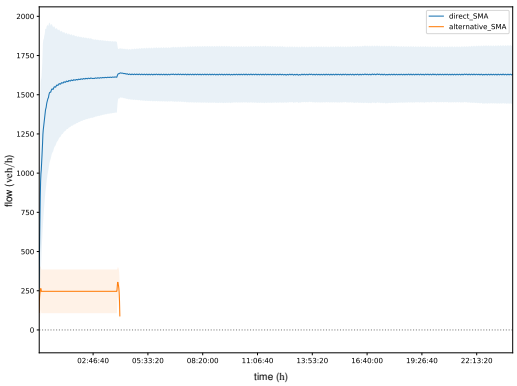


Fig. A.5-6. TrafficTraffic flow on each route, in vehicles per hour (veh/h), over a 24 h period, 4 h Simple Moving Average, mean (line) and standard deviation (shaded).

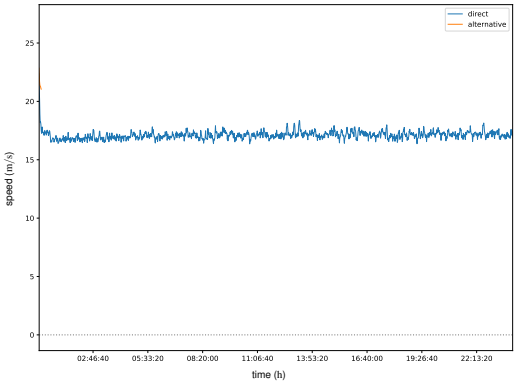


Fig. A.5-7. Mean speed on each route, in meters per second (m/s), aggregated to 1 min, over a 24 h period.

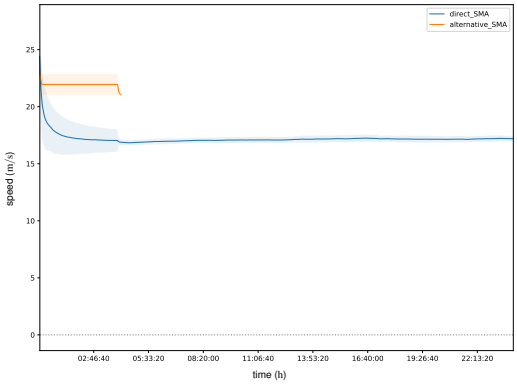


Fig. A.5-8. Mean speed on each route, in meters per second (m/s), aggregated to 1 min, over a 24 h period, 4 h Simple Moving Average, mean (line) and standard deviation (shaded).

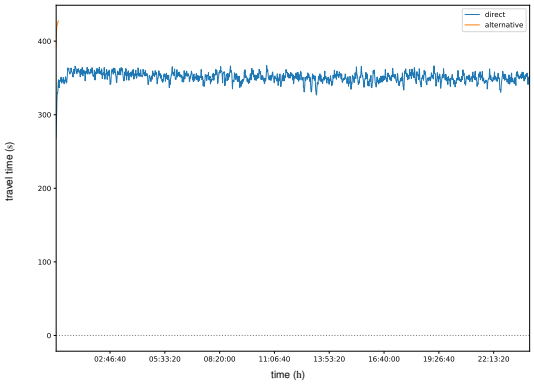


Fig. A.5-9. Travel times on each route, in seconds (s), aggregated to 1 min, over a 24 h period.

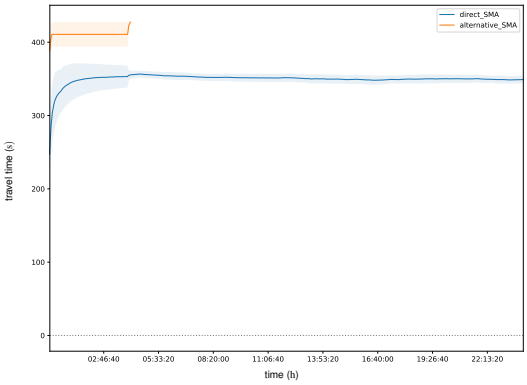


Fig. A.5-10. Travel times on each route, in seconds (s), aggregated to 1 min, over a 24 h period, 4 h Simple Moving Average, mean (line) and standard deviation (shaded).

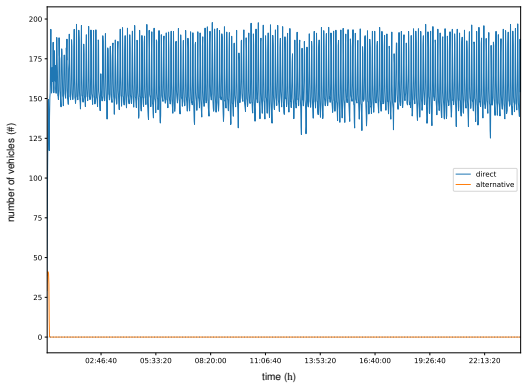


Fig. A.5-11. Average number of vehicles on each route, aggregated to 1 min, over a 24 h period.

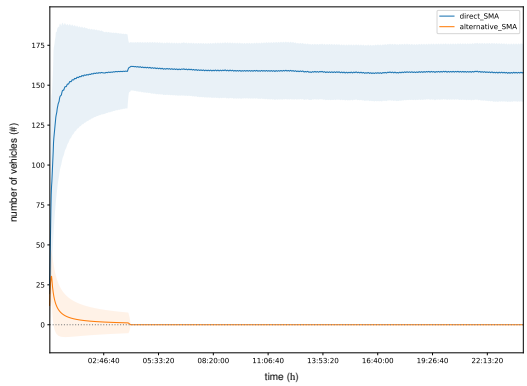


Fig. A.5-12. Average number of vehicles on each route, aggregated to 1 min, over a 24 h period, 4 h Simple Moving Average, mean (line) and standard deviation (shaded).

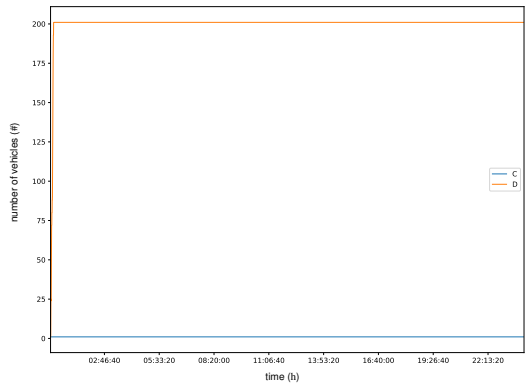


Fig. A.5-13. Evolution of the number of *Cooperators* and *Defectors* over a 24 h period.

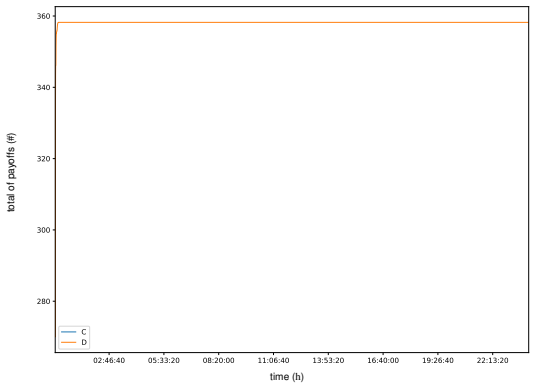


Fig. A.5-14. Evolution of total payoffs for *Cooperators* and *Defectors* (*individual payoff* times the *number of players receiving it*, $C(n) \times n$ and $D(n) \times (N-n)$, where n is the number of *Cooperators*), over a 24 h period.

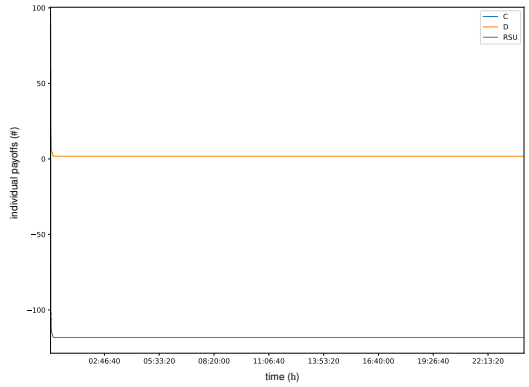


Fig. A.5-15. Evolution of the individual payoffs for *Cooperators, Defectors,* and *RSU* (always cooperating), over a 24 h period.

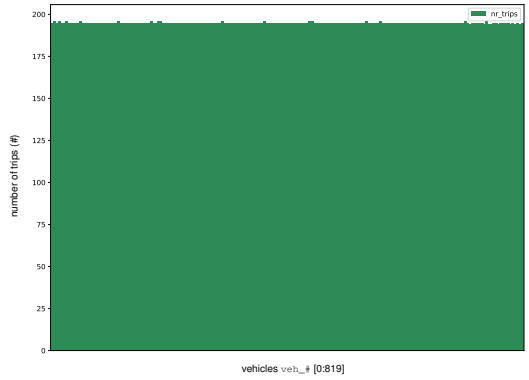


Fig. A.5-16. Number of trips made by each vehicle, during the simulation of a 24 h period.

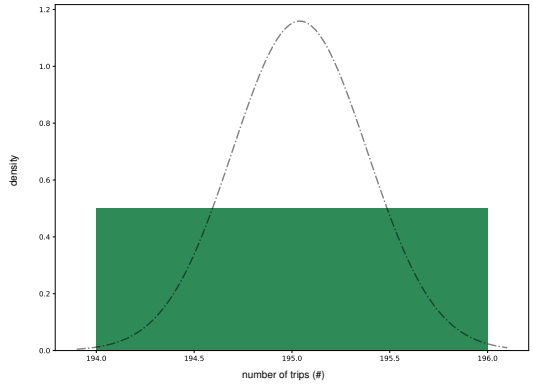


Fig. A.5-17. Density histogram of the number of trips made by each vehicle, during the simulation of a 24 h period, superimposing the normal density curve. The number of bins was calculated by the Freedman Diaconis rule.

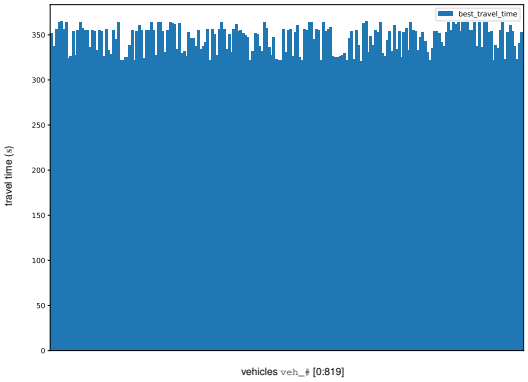


Fig. A.5-18. Best travel time for each vehicle, in seconds (s), during the simulation of a 24 h period.

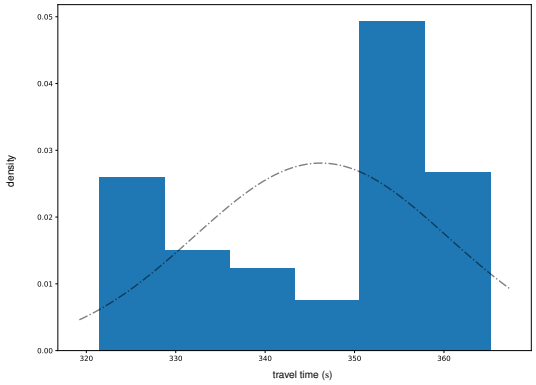


Fig. A.5-19. Density histogram of best travel time for vehicles, in seconds (s), during the simulation of a 24 h period, superimposing the normal density curve. The number of bins was calculated by the Freedman Diaconis rule.

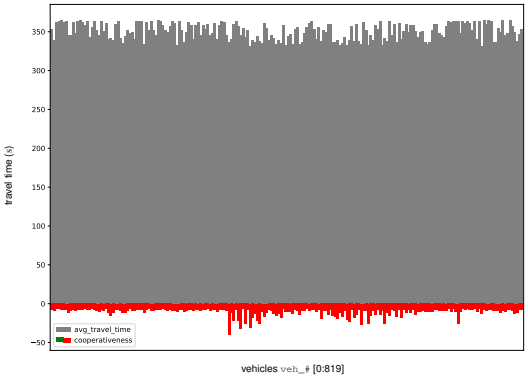


Fig. A.5-20. Average of the travel times, in seconds (s), of individual vehicles, during the simulation of a 24 h period. The bottom graph represents the *degree of cooperativeness**, downscaled by a normalization factor for the purpose of comparison with average times.

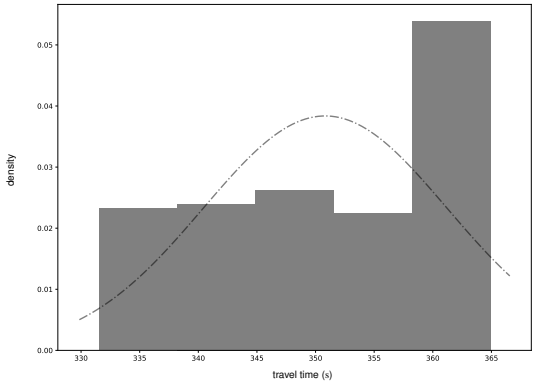


Fig. A.5-21. Density histogram of the average travel times, in seconds (s), of individual vehicles, during the simulation of a 24 h period, superimposing the normal density curve. The number of bins was calculated by the Freedman Diaconis rule.

* The *degree of cooperativeness* is a cumulative sum, calculated at each iteration, based on the complement of the ratio of cooperators, i.e., the higher the number of cooperators the less it increases, but the defectors are more penalized, and vice-versa. It varies inversely with the size of the group to which the player belongs.

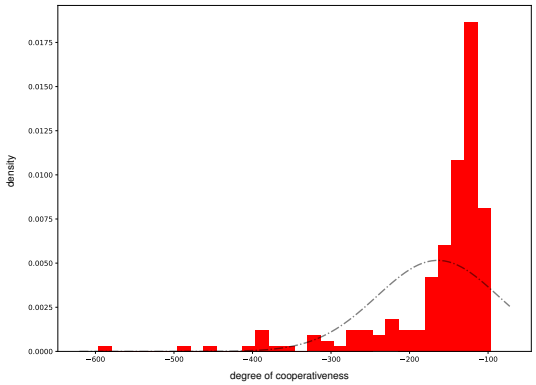


Fig. A.5-22. Density histogram of the *degree of cooperativeness** of individual vehicles, superimposing the normal density curve. The number of bins was calculated by the Freedman Diaconis rule. Generally, when strongly correlated with travel times, it presents a symmetric curve with respect to the *yy*-axis. All vehicles followed the preferred route and rejected the recommendation (all *Defectors*).

A.6 224veh-24h-00061111

```
Scenario: scenario-1
Timestamp: 20210612T192831Z
Number of vehicles: 224 vehs
Simulation time: 24.0 h
Warm up end time: 190.1 s; step 1900
Vehicle selection strategy: stochastic
RSU turned off: False
RSU strategy: proportional
Runner options:
   nogui: True
   step_length: 0.1
   seed: 19750808
   output_prefix: 224veh-24h-00061111
   sim_run_time: 24.0
   num_vehicles: 224
   warmup_speed: 25.0
   warmup_routes_weight: [473, 527]
   network_speed: 25.0
   change_behavior_probability: [100, 0]
   cooperation_probability: [100, 0]
   vehicle_selection_strategy: stochastic
   turn_rsu_off: False
   rsu_dynamic_dissemination: False
   rsu_dissemination_interval: 5
   rsu_probabilistic_dissemination: False
   rsu_suggestion_strategy: proportional
   rsu_routes_weight: [488, 512]
   rsu_moving_avg_size: 5
   travel_times_ttl: 60
   rsu_dissemination_ttl: 0
   rsu_send_travel_time_info: False
   payoff_matrix: [360.0, 240.0, 0.0, -120.0]
   roth_erev_parameters: [0.1, 0.15]
   rsu_change_dissemination: False
   rsu_change_dissemination_steps: [14400, 28800, 43200, 57600, 72000]
   rsu_change_dissemination_intervals: [10, 20, 40, 80, 160]
Network Mean speed after warmup:
   Max: 18.55
   Min: 9.75
```

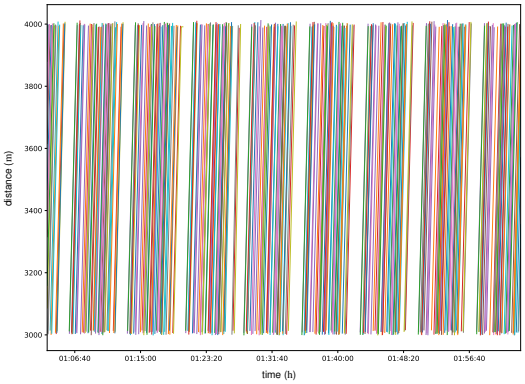


Fig. A.6-1. Time-Space diagram, for the one hour period after the end of the warmup, from 1:00:00 to 2:00:00 simulation time, plotted for the data from the sensor placed in the middle of the *direct* route (between 3000 m and 4000 m). In the case of an overloaded network, congestion shock waves can be observed.

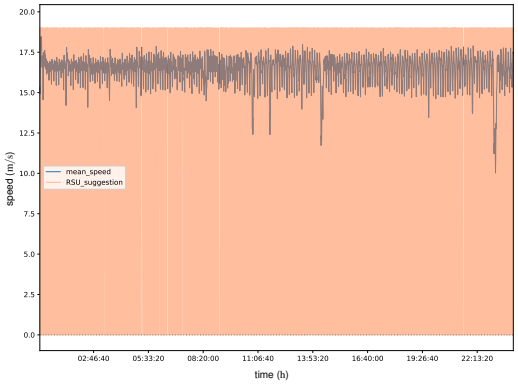


Fig. A.6-2. Mean speed in the network, in meters per second (m/s), over a 24 h period, superimposing (vertically, in orange) the time instants in which the RSU issued a recommendation to follow the *alternative* route.

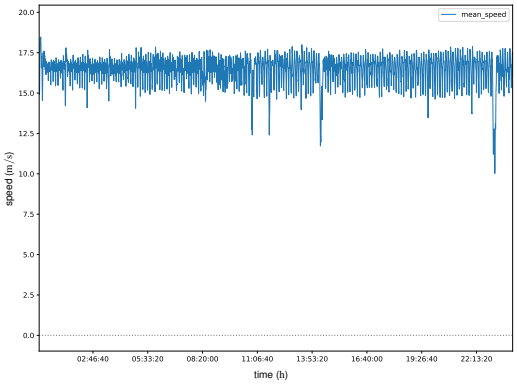


Fig. A.6-3. Mean speed in the network, in meters per second (m/s), over a 24 h period.

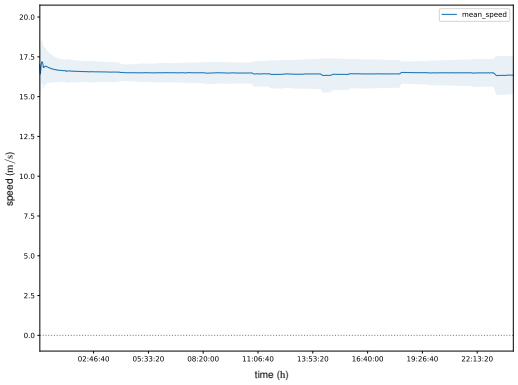


Fig. A.6-4. Mean speed in the network, in meters per second (m/s), over a 24 h period, 4 h Simple Moving Average, mean (line) and standard deviation (shaded).

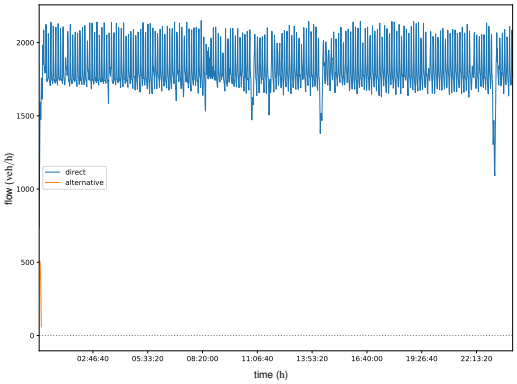


Fig. A.6-5. Traffic flow on each route, in vehicles per hour (veh/h), over a 24 h period.

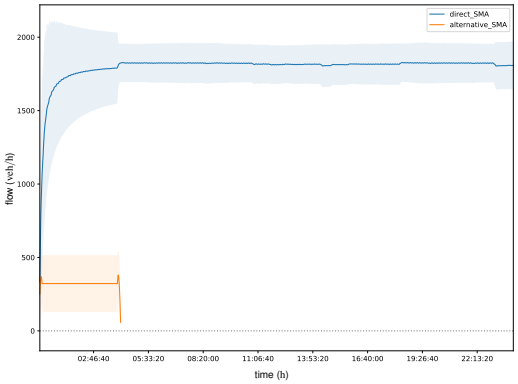


Fig. A.6-6. TrafficTraffic flow on each route, in vehicles per hour (veh/h), over a 24 h period, 4 h Simple Moving Average, mean (line) and standard deviation (shaded).

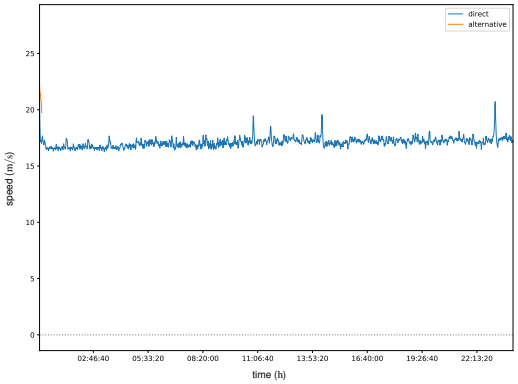


Fig. A.6-7. Mean speed on each route, in meters per second (m/s), aggregated to 1 min, over a 24 h period.

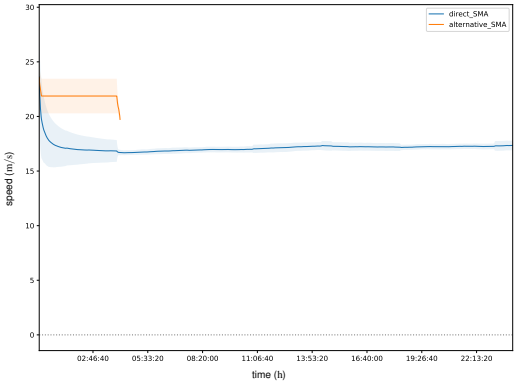


Fig. A.6-8. Mean speed on each route, in meters per second (m/s), aggregated to 1 min, over a 24 h period, 4 h Simple Moving Average, mean (line) and standard deviation (shaded).

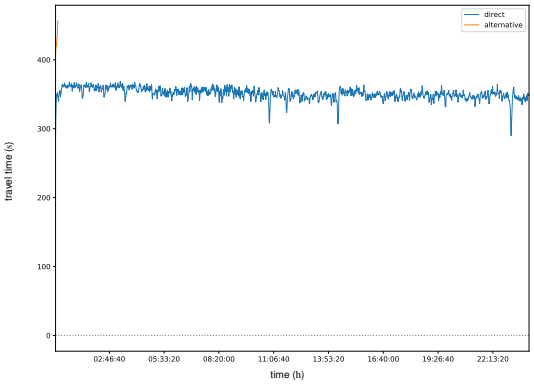


Fig. A.6-9. Travel times on each route, in seconds (s), aggregated to 1 min, over a 24 h period.

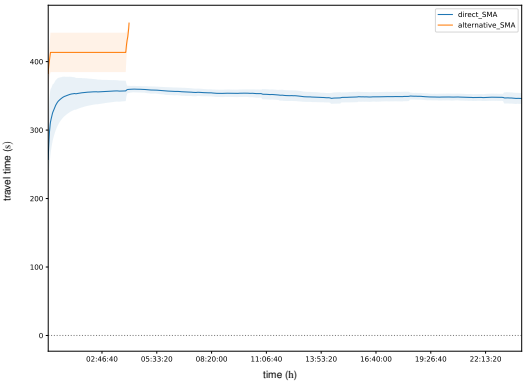


Fig. A.6-10. Travel times on each route, in seconds (s), aggregated to 1 min, over a 24 h period, 4 h Simple Moving Average, mean (line) and standard deviation (shaded).

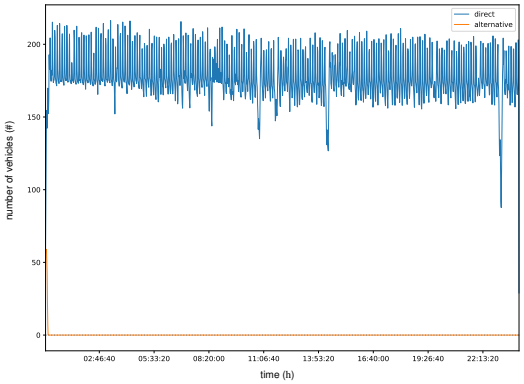


Fig. A.6-11. Average number of vehicles on each route, aggregated to 1 min, over a 24 h period.

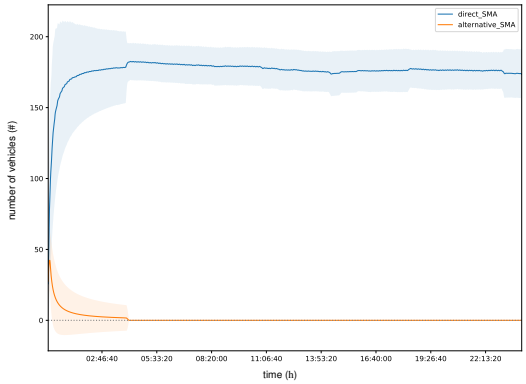


Fig. A.6-12. Average number of vehicles on each route, aggregated to 1 min, over a 24 h period, 4 h Simple Moving Average, mean (line) and standard deviation (shaded).

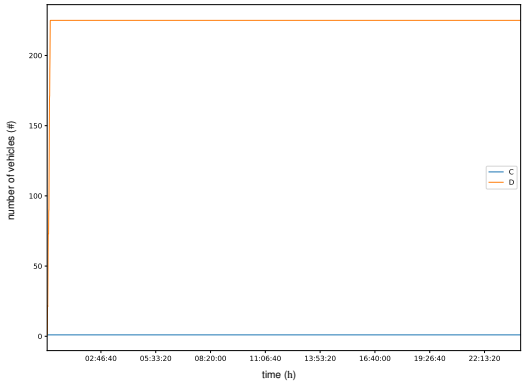


Fig. A.6-13. Evolution of the number of *Cooperators* and *Defectors* over a 24 h period.

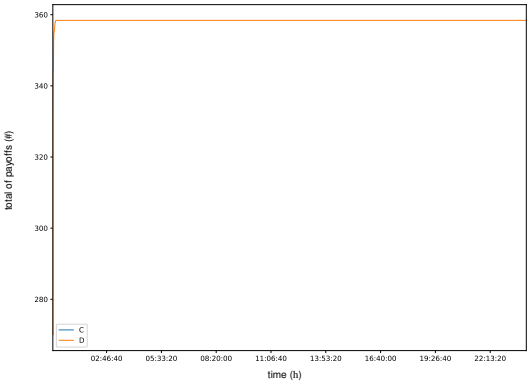


Fig. A.6-14. Evolution of total payoffs for *Cooperators* and *Defectors* (*individual payoff* times the *number of players receiving it*, $C(n) \times n$ and $D(n) \times (N-n)$, where n is the number of *Cooperators*), over a 24 h period.

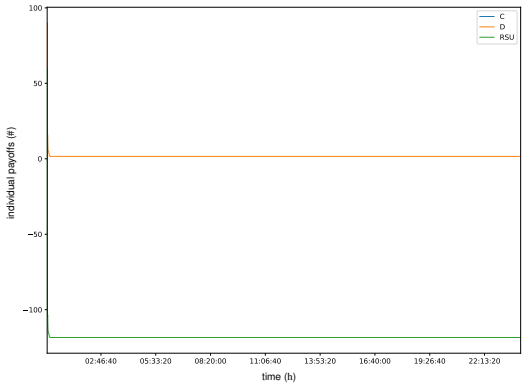


Fig. A.6-15. Evolution of the individual payoffs for *Cooperators, Defectors,* and *RSU* (always cooperating), over a 24 h period.

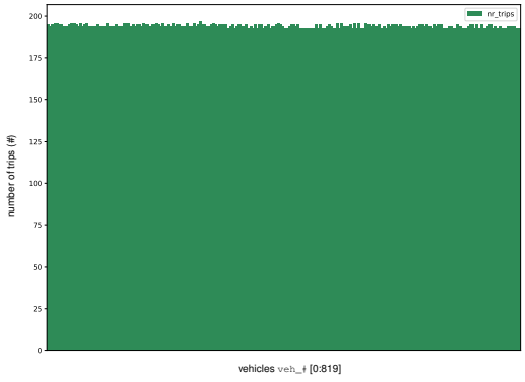


Fig. A.6-16. Number of trips made by each vehicle, during the simulation of a 24 h period.

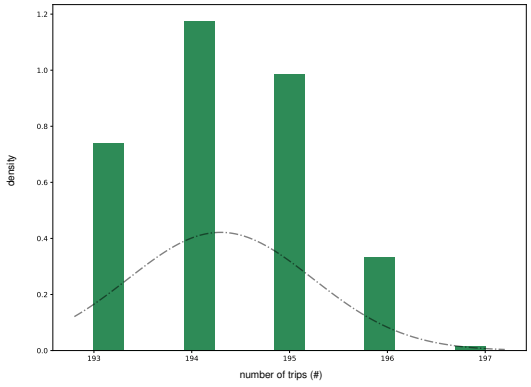


Fig. A.6-17. Density histogram of the number of trips made by each vehicle, during the simulation of a 24 h period, superimposing the normal density curve. The number of bins was calculated by the Freedman Diaconis rule.

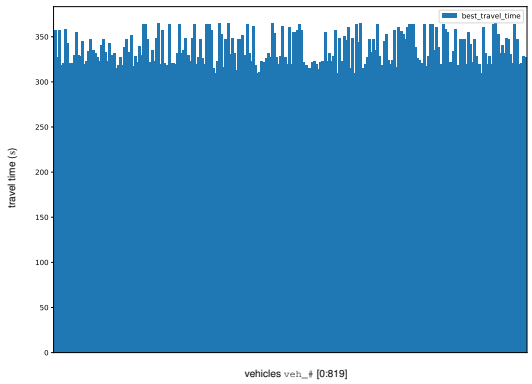


Fig. A.6-18. Best travel time for each vehicle, in seconds (s), during the simulation of a 24 h period.

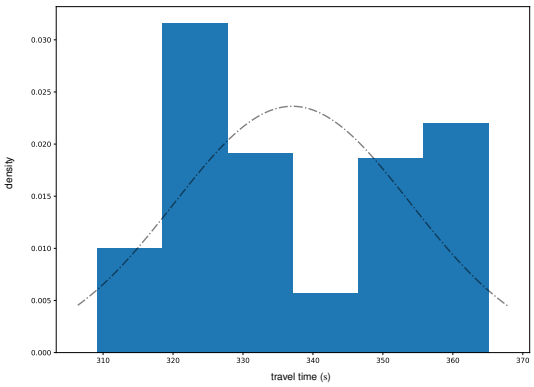


Fig. A.6-19. Density histogram of best travel time for vehicles, in seconds (s), during the simulation of a 24 h period, superimposing the normal density curve. The number of bins was calculated by the Freedman Diaconis rule.

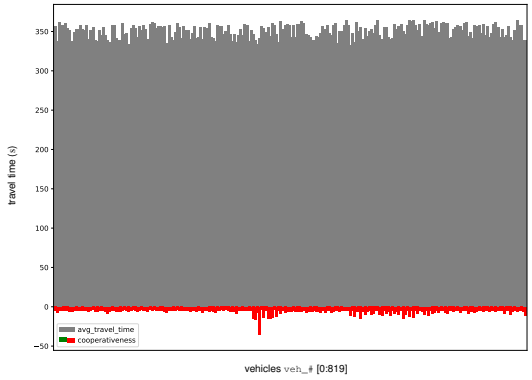


Fig. A.6-20. Average of the travel times, in seconds (s), of individual vehicles, during the simulation of a 24 h period. The bottom graph represents the *degree of cooperativeness**, downscaled by a normalization factor for the purpose of comparison with average times.

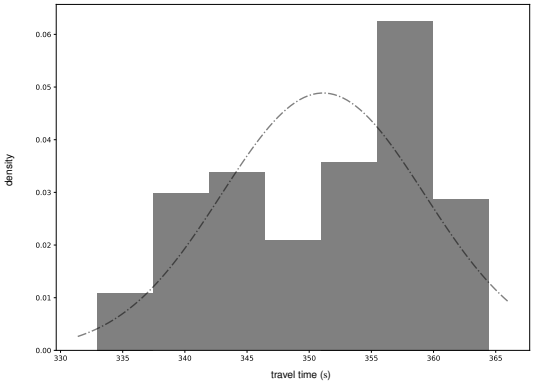


Fig. A.6-21. Density histogram of the average travel times, in seconds (s), of individual vehicles, during the simulation of a 24 h period, superimposing the normal density curve. The number of bins was calculated by the Freedman Diaconis rule.

* The *degree of cooperativeness* is a cumulative sum, calculated at each iteration, based on the complement of the ratio of cooperators, i.e., the higher the number of cooperators the less it increases, but the defectors are more penalized, and vice-versa. It varies inversely with the size of the group to which the player belongs.

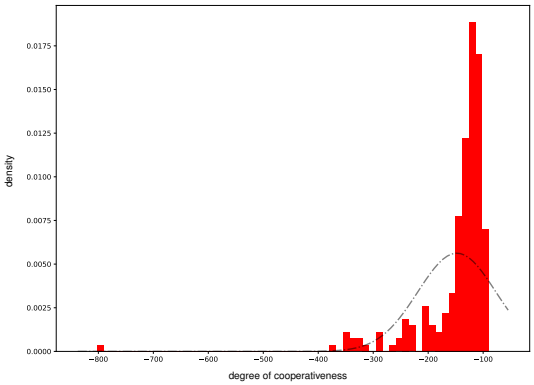


Fig. A.6-22. Density histogram of the *degree of cooperativeness** of individual vehicles, superimposing the normal density curve. The number of bins was calculated by the Freedman Diaconis rule. Generally, when strongly correlated with travel times, it presents a symmetric curve with respect to the *yy*-axis. All vehicles followed the preferred route and rejected the recommendation (all *Defectors*).

A.7 250veh-24h-00061111

```
Scenario: scenario-1
Timestamp: 20210521T113755Z
Number of vehicles: 250 vehs
Simulation time: 24.0 h
Warm up end time: 215.7 s; step 2156
Vehicle selection strategy: stochastic
RSU turned off: False
RSU strategy: proportional
Runner options:
   nogui: True
   step_length: 0.1
   seed: 19750808
   output_prefix: 250veh-24h-00061111
   sim_run_time: 24.0
   num_vehicles: 250
   warmup_speed: 25.0
   warmup_routes_weight: [473, 527]
   network_speed: 25.0
   change_behavior_probability: [100, 0]
   cooperation_probability: [100, 0]
   vehicle_selection_strategy: stochastic
   turn_rsu_off: False
   rsu_dynamic_dissemination: False
   rsu_dissemination_interval: 5
   rsu_probabilistic_dissemination: False
   rsu_suggestion_strategy: proportional
   rsu_routes_weight: [487, 513]
   rsu_moving_avg_size: 5
   travel_times_ttl: 60
   rsu_dissemination_ttl: 0
   rsu_send_travel_time_info: False
   payoff_matrix: [360.0, 240.0, 0.0, -120.0]
   roth_erev_parameters: [0.1, 0.15]
Network Mean speed after warmup:
   Max: 18.32
   Min: 11.11
```

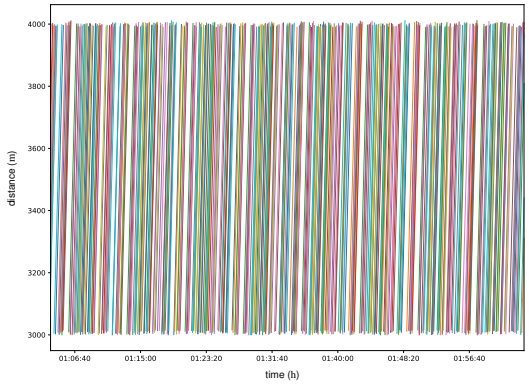


Fig. A.7-1. Time-Space diagram, for the one hour period after the end of the warmup, from 1:00:00 to 2:00:00 simulation time, plotted for the data from the sensor placed in the middle of the *direct* route (between 3000 m and 4000 m). In the case of an overloaded network, congestion shock waves can be observed.

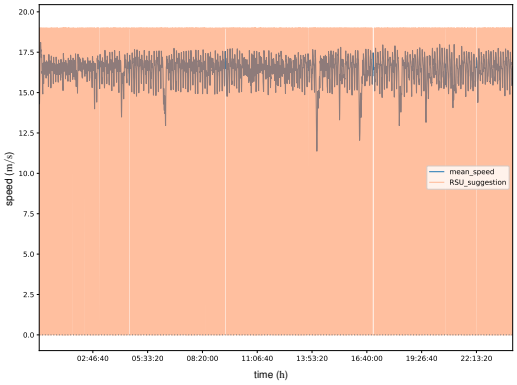


Fig. A.7-2. Mean speed in the network, in meters per second (m/s), over a 24 h period, superimposing (vertically, in orange) the time instants in which the RSU issued a recommendation to follow the *alternative* route.

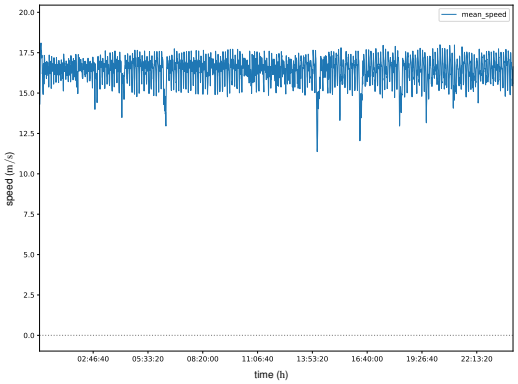


Fig. A.7-3. Mean speed in the network, in meters per second (m/s), over a 24 h period.

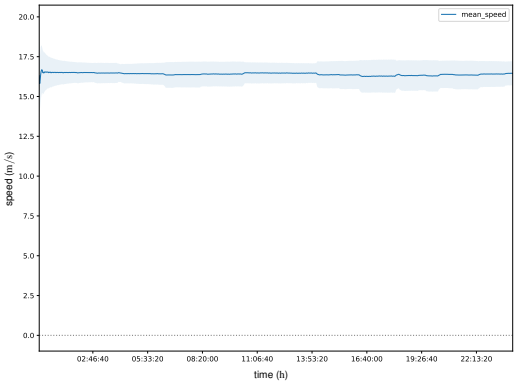


Fig. A.7-4. Mean speed in the network, in meters per second (m/s), over a 24 h period, 4 h Simple Moving Average, mean (line) and standard deviation (shaded).

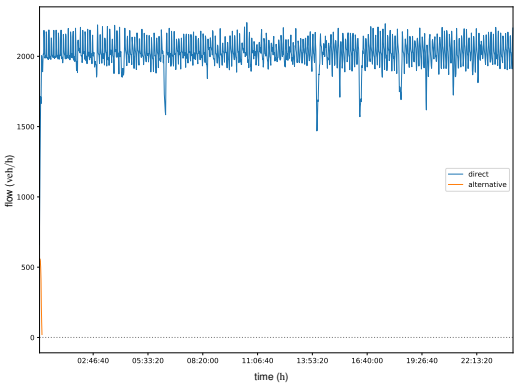


Fig. A.7-5. Traffic flow on each route, in vehicles per hour (veh/h), over a 24 h period.

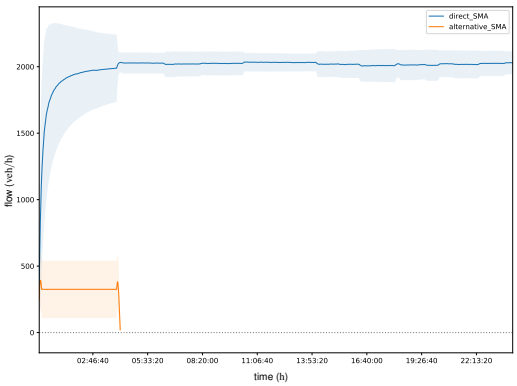


Fig. A.7-6. TrafficTraffic flow on each route, in vehicles per hour (veh/h), over a 24 h period, 4 h Simple Moving Average, mean (line) and standard deviation (shaded).

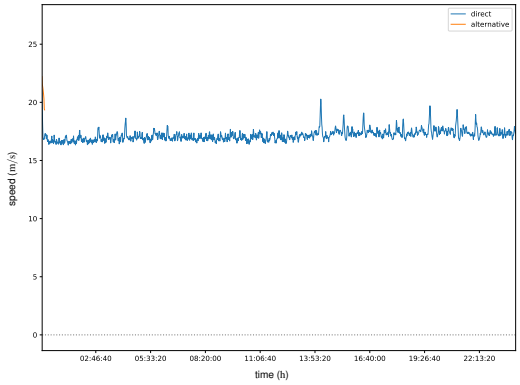


Fig. A.7-7. Mean speed on each route, in meters per second (m/s), aggregated to 1 min, over a 24 h period.

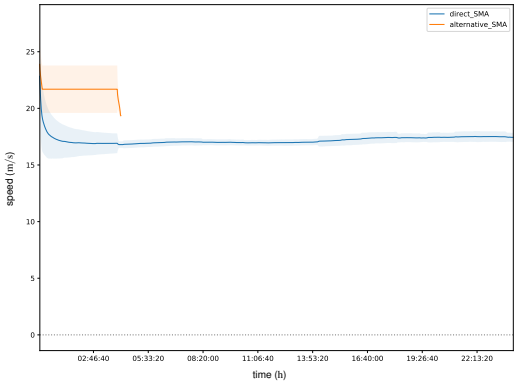


Fig. A.7-8. Mean speed on each route, in meters per second (m/s), aggregated to 1 min, over a 24 h period, 4 h Simple Moving Average, mean (line) and standard deviation (shaded).

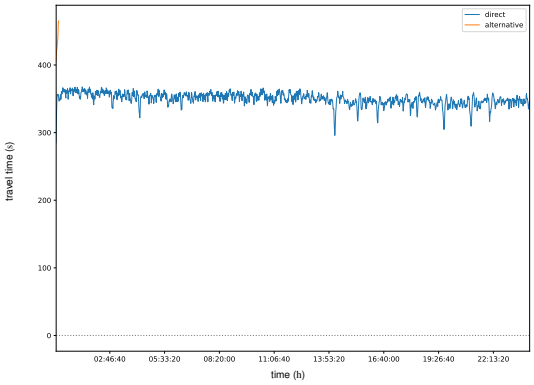


Fig. A.7-9. Travel times on each route, in seconds (s), aggregated to 1 min, over a 24 h period.

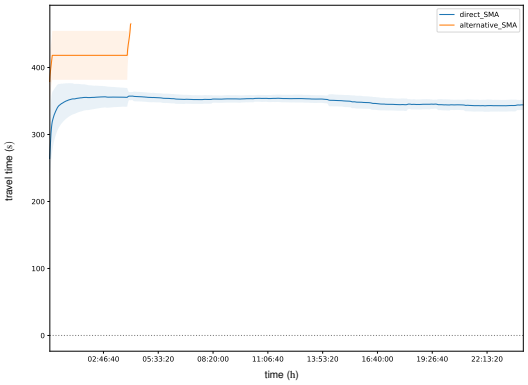


Fig. A.7-10. Travel times on each route, in seconds (s), aggregated to 1 min, over a 24 h period, 4 h Simple Moving Average, mean (line) and standard deviation (shaded).

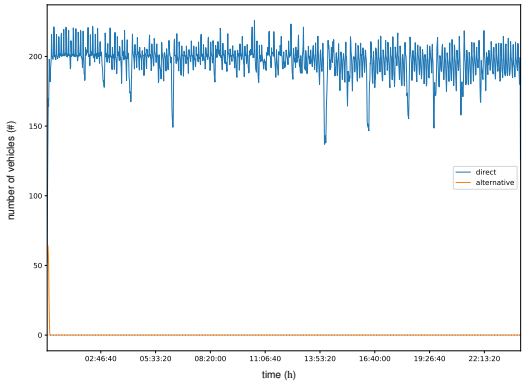


Fig. A.7-11. Average number of vehicles on each route, aggregated to 1 min, over a 24 h period.

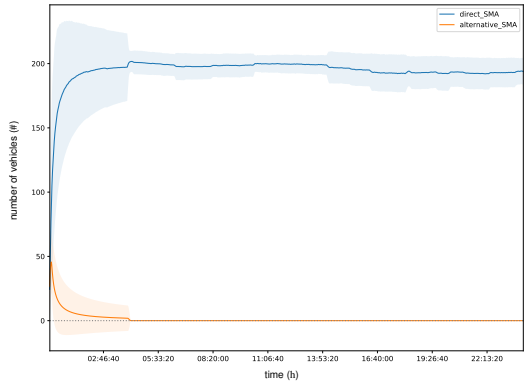


Fig. A.7-12. Average number of vehicles on each route, aggregated to 1 min, over a 24 h period, 4 h Simple Moving Average, mean (line) and standard deviation (shaded).

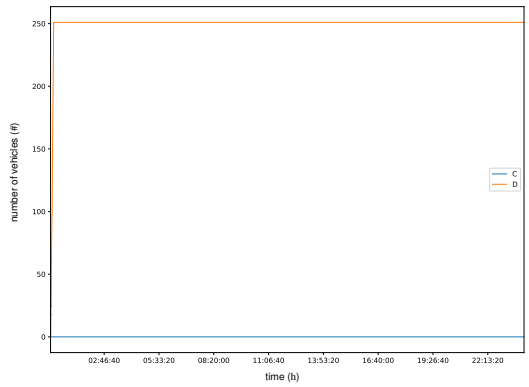


Fig. A.7-13. Evolution of the number of *Cooperators* and *Defectors* over a 24 h period.

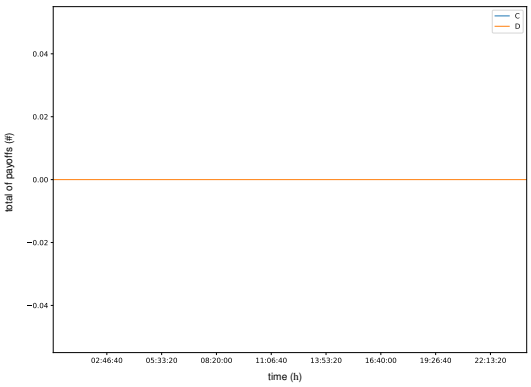


Fig. A.7-14. Evolution of total payoffs for *Cooperators* and *Defectors* (*individual payoff* times the *number of players receiving it*, $C(n) \times n$ and $D(n) \times (N-n)$, where n is the number of *Cooperators*), over a 24 h period.

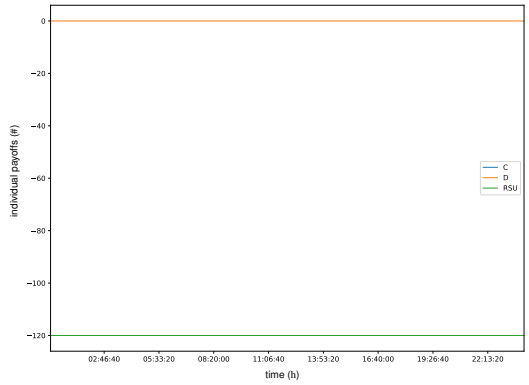


Fig. A.7-15. Evolution of the individual payoffs for *Cooperators, Defectors,* and *RSU* (always cooperating), over a 24 h period.

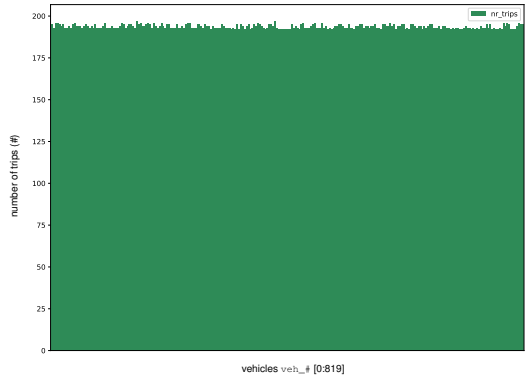


Fig. A.7-16. Number of trips made by each vehicle, during the simulation of a 24 h period.

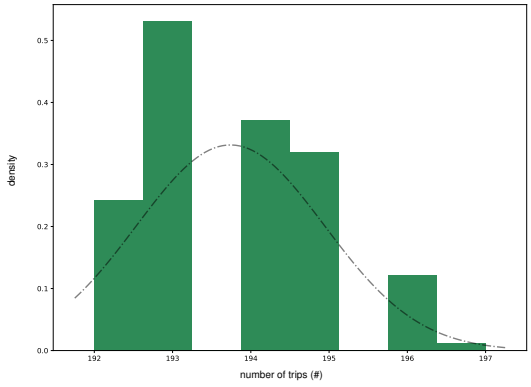


Fig. A.7-17. Density histogram of the number of trips made by each vehicle, during the simulation of a 24 h period, superimposing the normal density curve. The number of bins was calculated by the Freedman Diaconis rule.

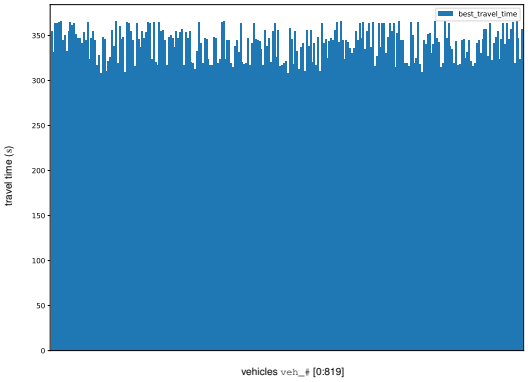


Fig. A.7-18. Best travel time for each vehicle, in seconds (s), during the simulation of a 24 h period.

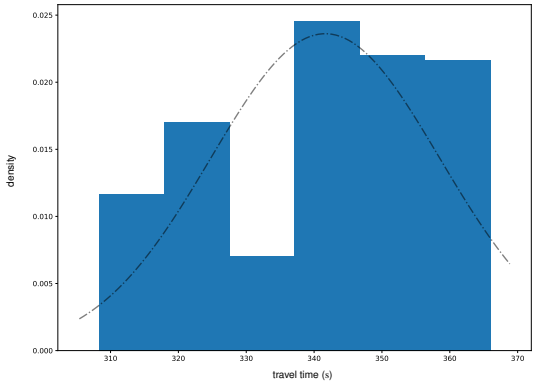


Fig. A.7-19. Density histogram of best travel time for vehicles, in seconds (s), during the simulation of a 24 h period, superimposing the normal density curve. The number of bins was calculated by the Freedman Diaconis rule.

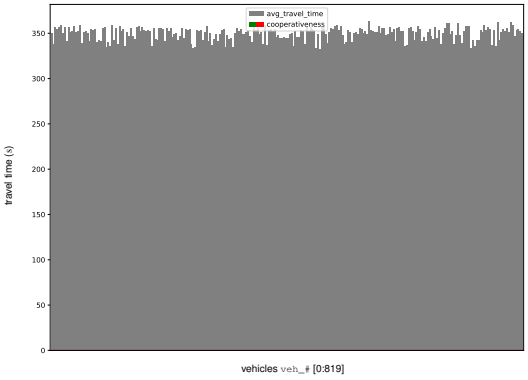


Fig. A.7-20. Average of the travel times, in seconds (s), of individual vehicles, during the simulation of a 24 h period. The bottom graph represents the *degree of cooperativeness**, downscaled by a normalization factor for the purpose of comparison with average times.

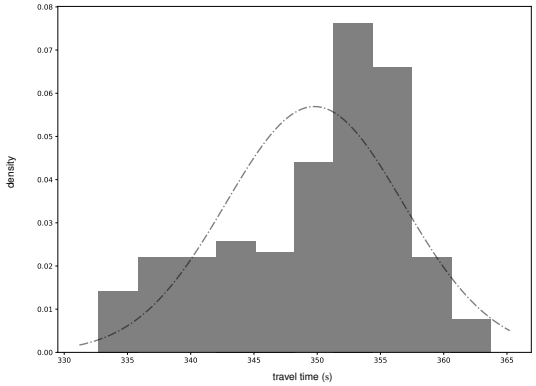


Fig. A.7-21. Density histogram of the average travel times, in seconds (s), of individual vehicles, during the simulation of a 24 h period, superimposing the normal density curve. The number of bins was calculated by the Freedman Diaconis rule.

* The *degree of cooperativeness* is a cumulative sum, calculated at each iteration, based on the complement of the ratio of cooperators, i.e., the higher the number of cooperators the less it increases, but the defectors are more penalized, and vice-versa. It varies inversely with the size of the group to which the player belongs.

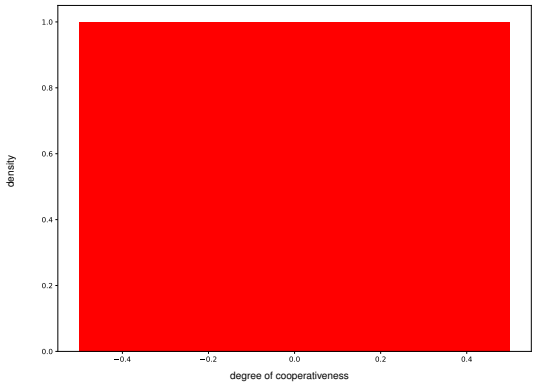


Fig. A.7-22. Density histogram of the *degree of cooperativeness** of individual vehicles, superimposing the normal density curve. The number of bins was calculated by the Freedman Diaconis rule. Generally, when strongly correlated with travel times, it presents a symmetric curve with respect to the *yy*-axis. All vehicles followed the preferred route and rejected the recommendation (all *Defectors*).

A.8 `345veh-24h-00061111`

```
Scenario: scenario-1
Timestamp: 20210613T064608Z
Number of vehicles: 345 vehs
Simulation time: 24.0 h
Warm up end time: 341.3 s; step 3412
Vehicle selection strategy: stochastic
RSU turned off: False
RSU strategy: proportional
Runner options:
   nogui: True
   step_length: 0.1
   seed: 19750808
   output_prefix: 345veh-24h-00061111
   sim_run_time: 24.0
   num_vehicles: 345
   warmup_speed: 25.0
   warmup_routes_weight: [473, 527]
   network_speed: 25.0
   change_behavior_probability: [100, 0]
   cooperation_probability: [100, 0]
   vehicle_selection_strategy: stochastic
   turn_rsu_off: False
   rsu_dynamic_dissemination: False
   rsu_dissemination_interval: 5
   rsu_probabilistic_dissemination: False
   rsu_suggestion_strategy: proportional
   rsu_routes_weight: [482, 518]
   rsu_moving_avg_size: 5
   travel_times_ttl: 60
   rsu_dissemination_ttl: 0
   rsu_send_travel_time_info: False
   payoff_matrix: [360.0, 240.0, 0.0, -120.0]
   roth_erev_parameters: [0.1, 0.15]
   rsu_change_dissemination: False
   rsu_change_dissemination_steps: [14400, 28800, 43200, 57600, 72000]
   rsu_change_dissemination_intervals: [10, 20, 40, 80, 160]
Network Mean speed after warmup:
   Max: 16.65
   Min: 11.31
```

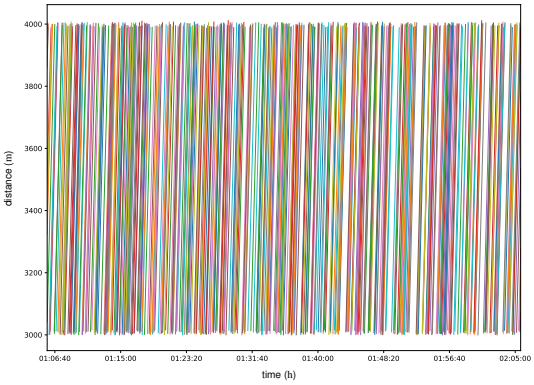


Fig. A.8-1. Time-Space diagram, for the one hour period after the end of the warmup, from 1:00:00 to 2:00:00 simulation time, plotted for the data from the sensor placed in the middle of the *direct* route (between 3000 m and 4000 m). In the case of an overloaded network, congestion shock waves can be observed.

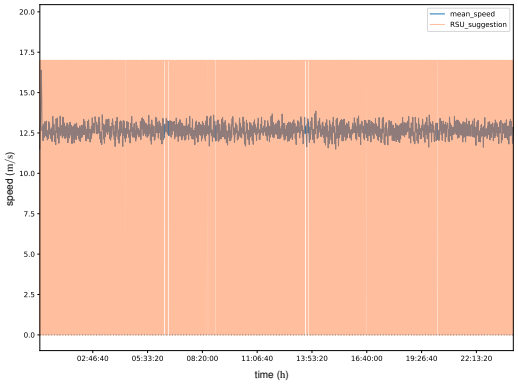


Fig. A.8-2. Mean speed in the network, in meters per second (m/s), over a 24 h period, superimposing (vertically, in orange) the time instants in which the RSU issued a recommendation to follow the *alternative* route.

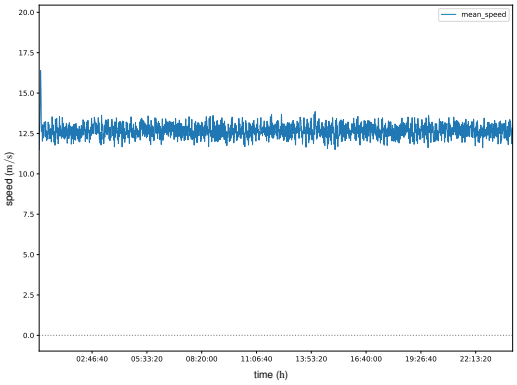


Fig. A.8-3. Mean speed in the network, in meters per second (m/s), over a 24 h period.

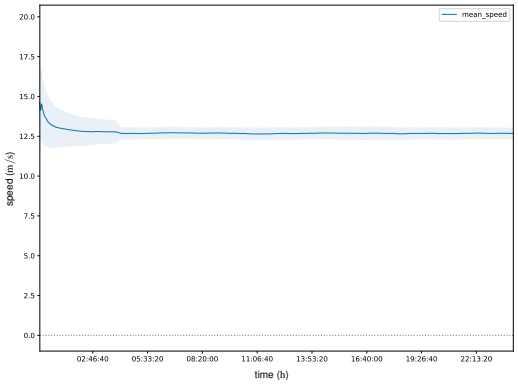


Fig. A.8-4. Mean speed in the network, in meters per second (m/s), over a 24 h period, 4 h Simple Moving Average, mean (line) and standard deviation (shaded).

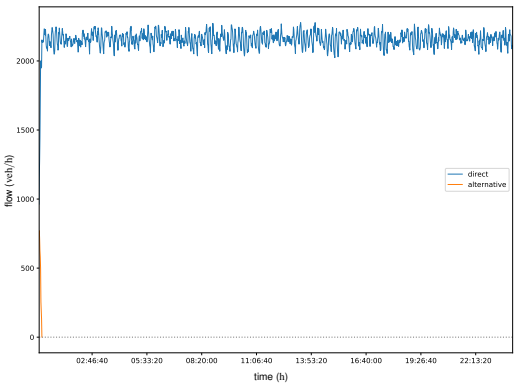


Fig. A.8-5. Traffic flow on each route, in vehicles per hour (veh/h), over a 24 h period.

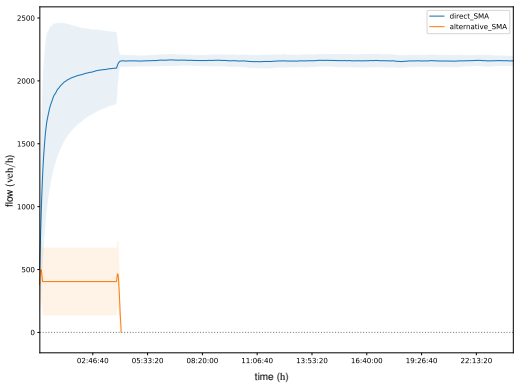


Fig. A.8-6. TrafficTraffic flow on each route, in vehicles per hour (veh/h), over a 24 h period, 4 h Simple Moving Average, mean (line) and standard deviation (shaded).

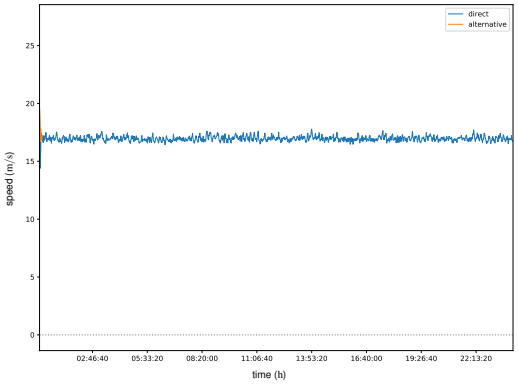


Fig. A.8-7. Mean speed on each route, in meters per second (m/s), aggregated to 1 min, over a 24 h period.

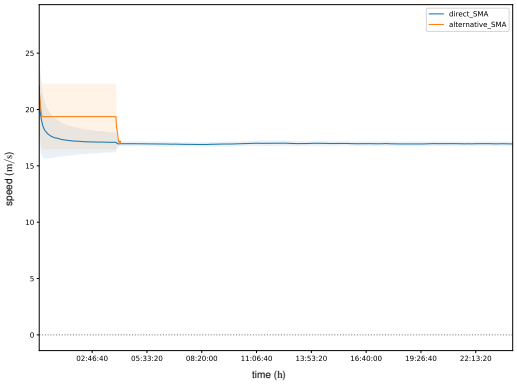


Fig. A.8-8. Mean speed on each route, in meters per second (m/s), aggregated to 1 min, over a 24 h period, 4 h Simple Moving Average, mean (line) and standard deviation (shaded).

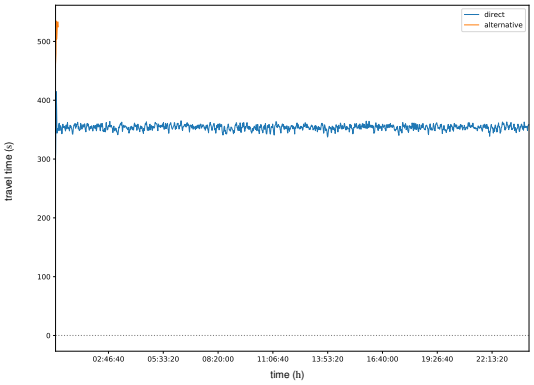


Fig. A.8-9. Travel times on each route, in seconds (s), aggregated to 1 min, over a 24 h period.

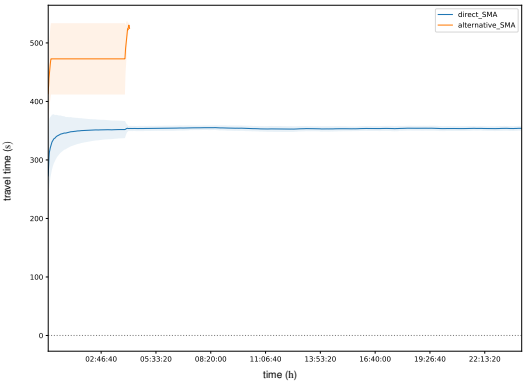


Fig. A.8-10. Travel times on each route, in seconds (s), aggregated to 1 min, over a 24 h period, 4 h Simple Moving Average, mean (line) and standard deviation (shaded).

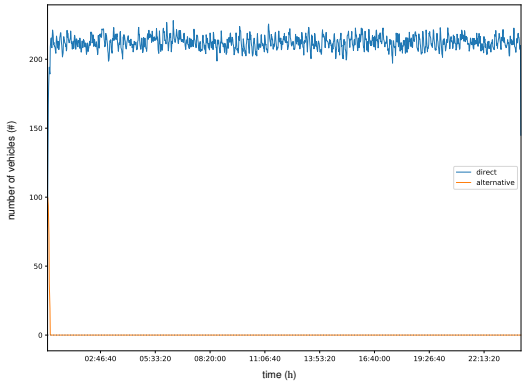


Fig. A.8-11. Average number of vehicles on each route, aggregated to 1 min, over a 24 h period.

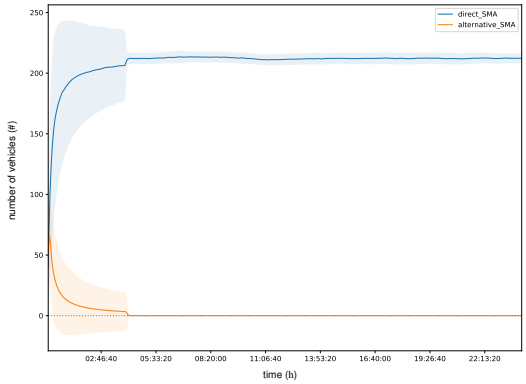


Fig. A.8-12. Average number of vehicles on each route, aggregated to 1 min, over a 24 h period, 4 h Simple Moving Average, mean (line) and standard deviation (shaded).

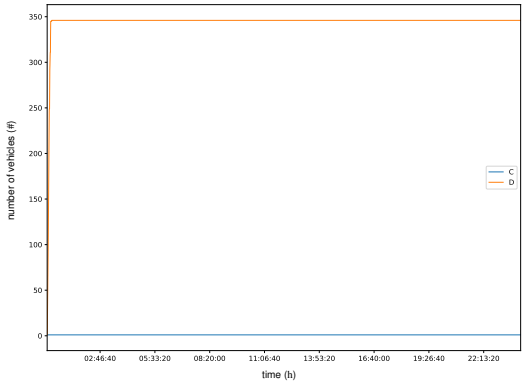


Fig. A.8-13. Evolution of the number of *Cooperators* and *Defectors* over a 24 h period.

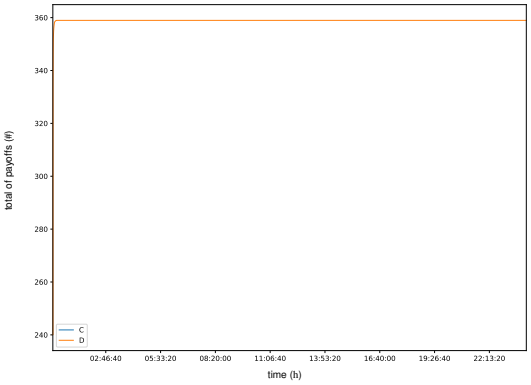


Fig. A.8-14. Evolution of total payoffs for *Cooperators* and *Defectors* (*individual payoff* times the *number of players receiving it*, $C(n) \times n$ and $D(n) \times (N-n)$, where n is the number of *Cooperators*), over a 24 h period.

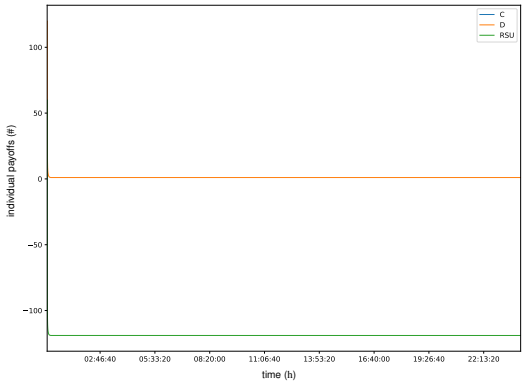


Fig. A.8-15. Evolution of the individual payoffs for *Cooperators, Defectors,* and *RSU* (always cooperating), over a 24 h period.

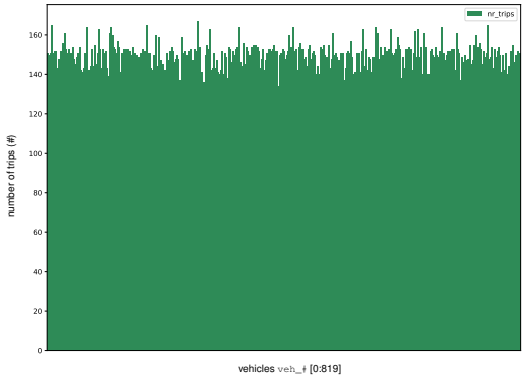


Fig. A.8-16. Number of trips made by each vehicle, during the simulation of a 24 h period.

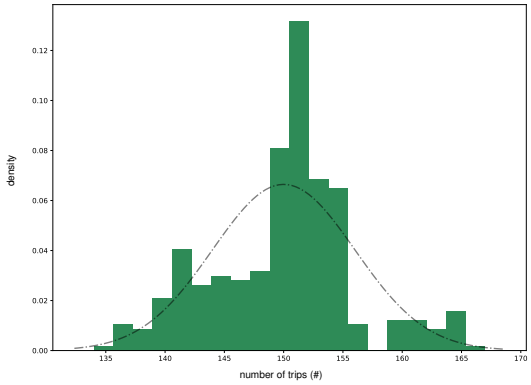


Fig. A.8-17. Density histogram of the number of trips made by each vehicle, during the simulation of a 24 h period, superimposing the normal density curve. The number of bins was calculated by the Freedman Diaconis rule.

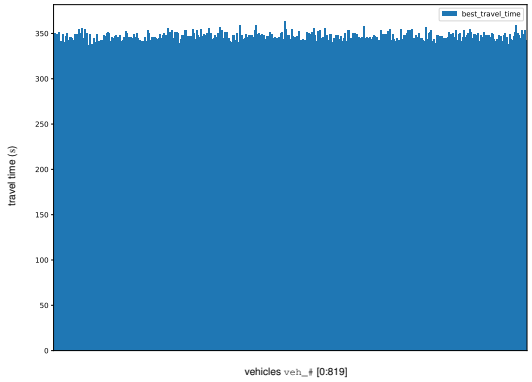


Fig. A.8-18. Best travel time for each vehicle, in seconds (s), during the simulation of a 24 h period.

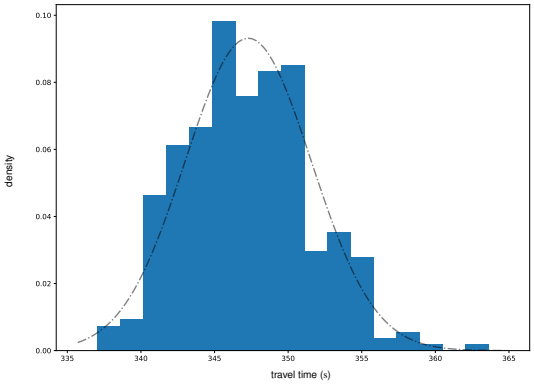


Fig. A.8-19. Density histogram of best travel time for vehicles, in seconds (s), during the simulation of a 24 h period, superimposing the normal density curve. The number of bins was calculated by the Freedman Diaconis rule.

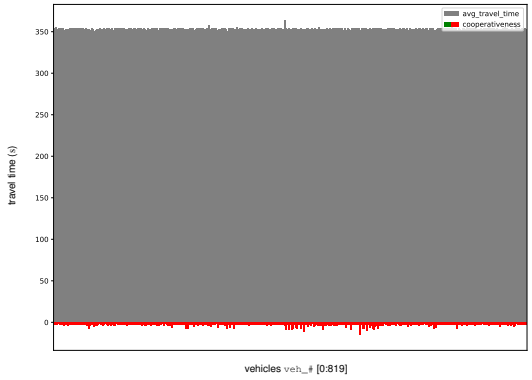


Fig. A.8-20. Average of the travel times, in seconds (s), of individual vehicles, during the simulation of a 24 h period. The bottom graph represents the *degree of cooperativeness**, downscaled by a normalization factor for the purpose of comparison with average times.

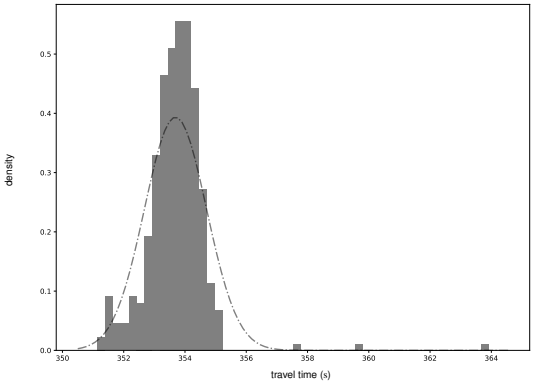


Fig. A.8-21. Density histogram of the average travel times, in seconds (s), of individual vehicles, during the simulation of a 24 h period, superimposing the normal density curve. The number of bins was calculated by the Freedman Diaconis rule.

* The *degree of cooperativeness* is a cumulative sum, calculated at each iteration, based on the complement of the ratio of cooperators, i.e., the higher the number of cooperators the less it increases, but the defectors are more penalized, and vice-versa. It varies inversely with the size of the group to which the player belongs.

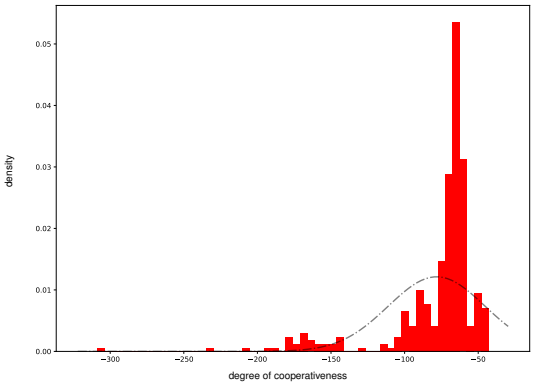


Fig. A.8-22. Density histogram of the *degree of cooperativeness** of individual vehicles, superimposing the normal density curve. The number of bins was calculated by the Freedman Diaconis rule. Generally, when strongly correlated with travel times, it presents a symmetric curve with respect to the *yy*-axis. All vehicles followed the preferred route and rejected the recommendation (all *Defectors*).

A.9 450veh-24h-00061111

```
Scenario: scenario-1
Timestamp: 20210613T081817Z
Number of vehicles: 450 vehs
Simulation time: 24.0 h
Warm up end time: 525.3 s; step 5252
Vehicle selection strategy: stochastic
RSU turned off: False
RSU strategy: proportional
Runner options:
   nogui: True
   step_length: 0.1
   seed: 19750808
   output_prefix: 450veh-24h-00061111
   sim_run_time: 24.0
   num_vehicles: 450
   warmup_speed: 25.0
   warmup_routes_weight: [473, 527]
   network_speed: 25.0
   change_behavior_probability: [100, 0]
   cooperation_probability: [100, 0]
   vehicle_selection_strategy: stochastic
   turn_rsu_off: False
   rsu_dynamic_dissemination: False
   rsu_dissemination_interval: 5
   rsu_probabilistic_dissemination: False
   rsu_suggestion_strategy: proportional
   rsu_routes_weight: [477, 523]
   rsu_moving_avg_size: 5
   travel_times_ttl: 60
   rsu_dissemination_ttl: 0
   rsu_send_travel_time_info: False
   payoff_matrix: [360.0, 240.0, 0.0, -120.0]
   roth_erev_parameters: [0.1, 0.15]
   rsu_change_dissemination: False
   rsu_change_dissemination_steps: [14400, 28800, 43200, 57600, 72000]
   rsu_change_dissemination_intervals: [10, 20, 40, 80, 160]
Network Mean speed after warmup:
   Max: 14.8
   Min: 8.03
```

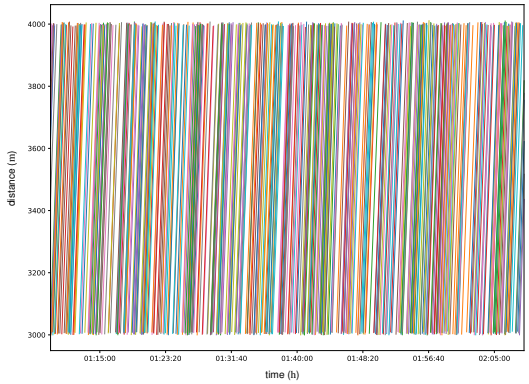


Fig. A.9-1. Time-Space diagram, for the one hour period after the end of the warmup, from 1:00:00 to 2:00:00 simulation time, plotted for the data from the sensor placed in the middle of the *direct* route (between 3000 m and 4000 m). In the case of an overloaded network, congestion shock waves can be observed.

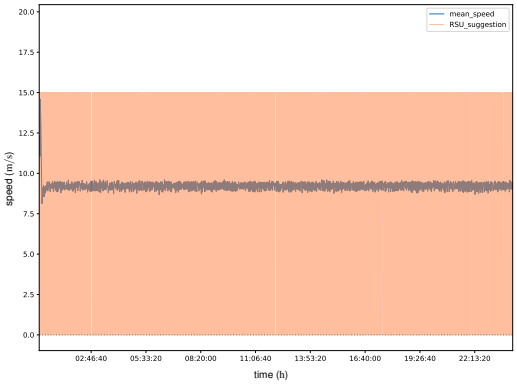


Fig. A.9-2. Mean speed in the network, in meters per second (m/s), over a 24 h period, superimposing (vertically, in orange) the time instants in which the RSU issued a recommendation to follow the *alternative* route.

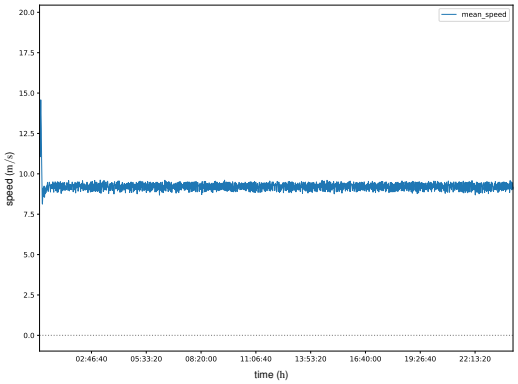


Fig. A.9-3. Mean speed in the network, in meters per second (m/s), over a 24 h period.

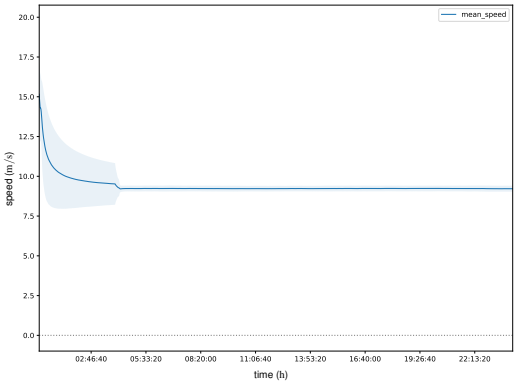


Fig. A.9-4. Mean speed in the network, in meters per second (m/s), over a 24 h period, 4 h Simple Moving Average, mean (line) and standard deviation (shaded).

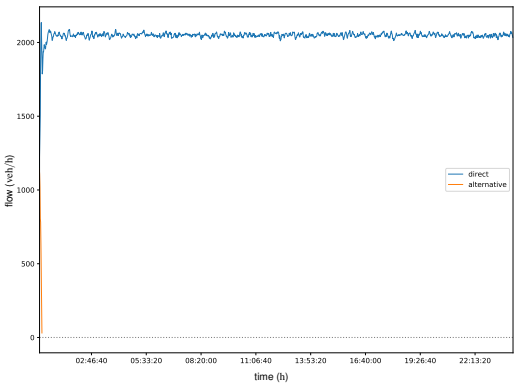


Fig. A.9-5. Traffic flow on each route, in vehicles per hour (veh/h), over a 24 h period.

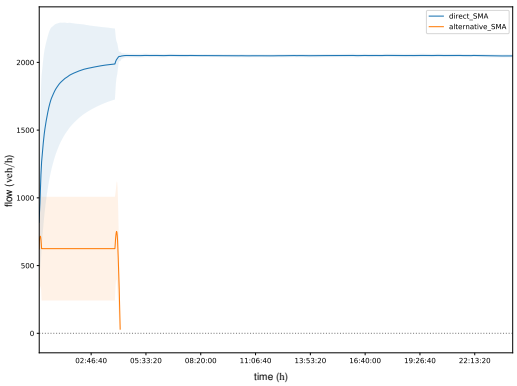


Fig. A.9-6. TrafficTraffic flow on each route, in vehicles per hour (veh/h), over a 24 h period, 4 h Simple Moving Average, mean (line) and standard deviation (shaded).

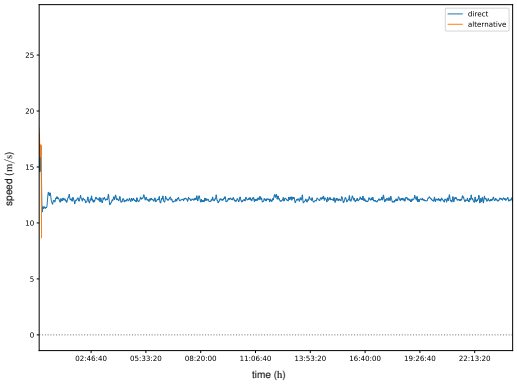


Fig. A.9-7. Mean speed on each route, in meters per second (m/s), aggregated to 1 min, over a 24 h period.

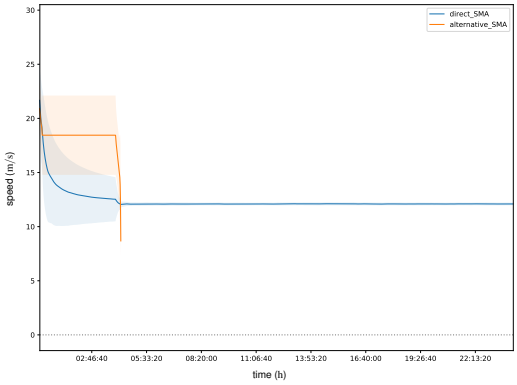


Fig. A.9-8. Mean speed on each route, in meters per second (m/s), aggregated to 1 min, over a 24 h period, 4 h Simple Moving Average, mean (line) and standard deviation (shaded).

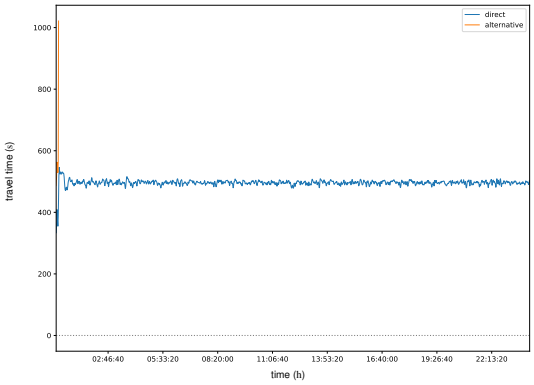


Fig. A.9-9. Travel times on each route, in seconds (s), aggregated to 1 min, over a 24 h period.

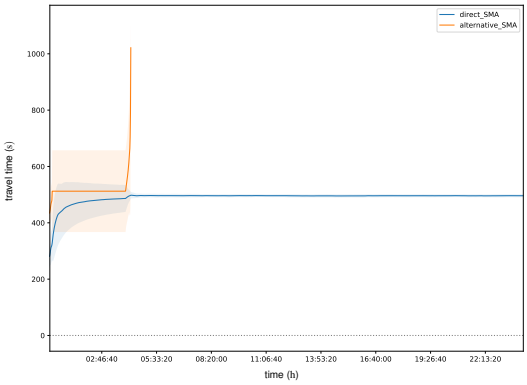


Fig. A.9-10. Travel times on each route, in seconds (s), aggregated to 1 min, over a 24 h period, 4 h Simple Moving Average, mean (line) and standard deviation (shaded).

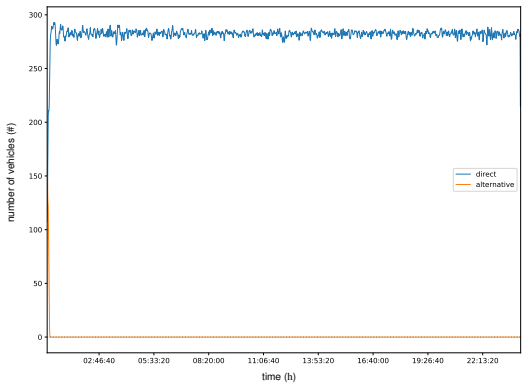


Fig. A.9-11. Average number of vehicles on each route, aggregated to 1 min, over a 24 h period.

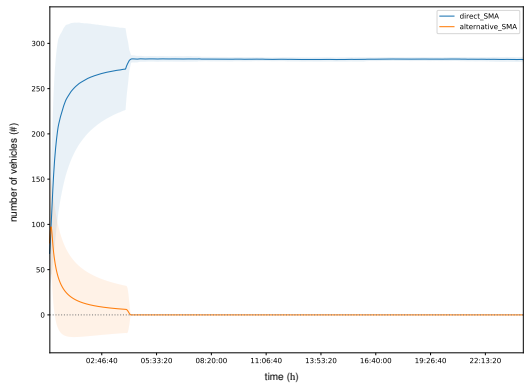


Fig. A.9-12. Average number of vehicles on each route, aggregated to 1 min, over a 24 h period, 4 h Simple Moving Average, mean (line) and standard deviation (shaded).

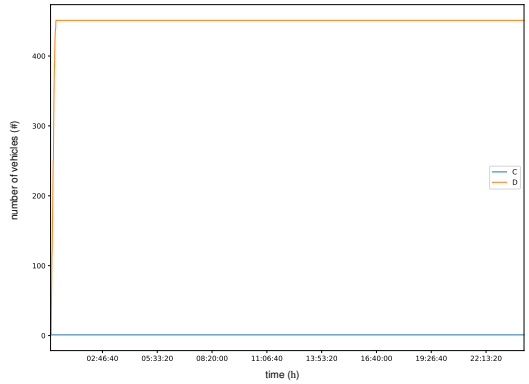


Fig. A.9-13. Evolution of the number of *Cooperators* and *Defectors* over a 24 h period.

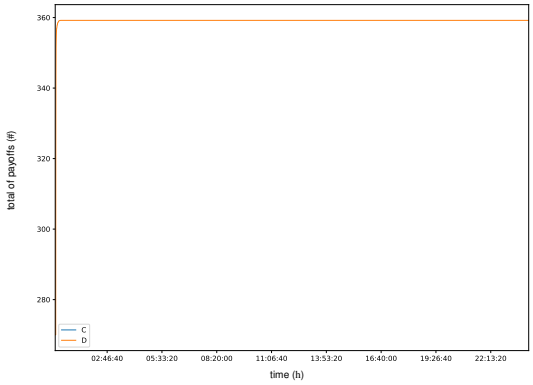


Fig. A.9-14. Evolution of total payoffs for *Cooperators* and *Defectors* (*individual payoff* times the *number of players receiving it*, $C(n) \times n$ and $D(n) \times (N-n)$, where n is the number of *Cooperators*), over a 24 h period.

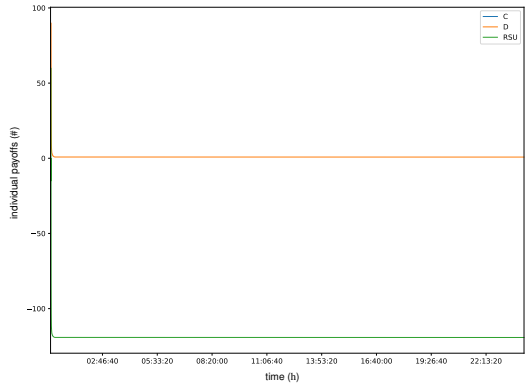


Fig. A.9-15. Evolution of the individual payoffs for *Cooperators, Defectors,* and *RSU* (always cooperating), over a 24 h period.

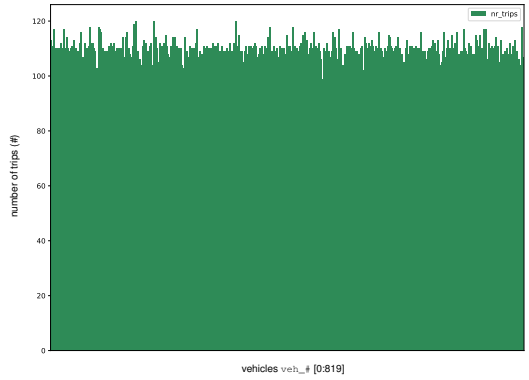


Fig. A.9-16. Number of trips made by each vehicle, during the simulation of a 24 h period.

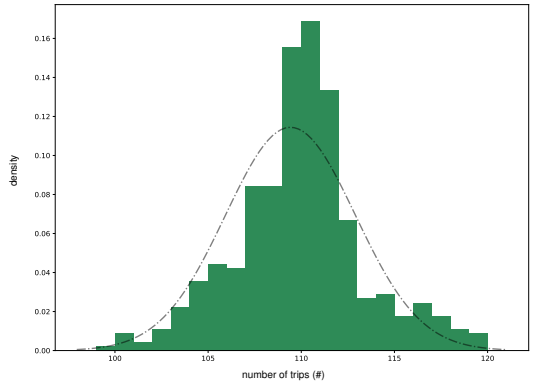


Fig. A.9-17. Density histogram of the number of trips made by each vehicle, during the simulation of a 24 h period, superimposing the normal density curve. The number of bins was calculated by the Freedman Diaconis rule.

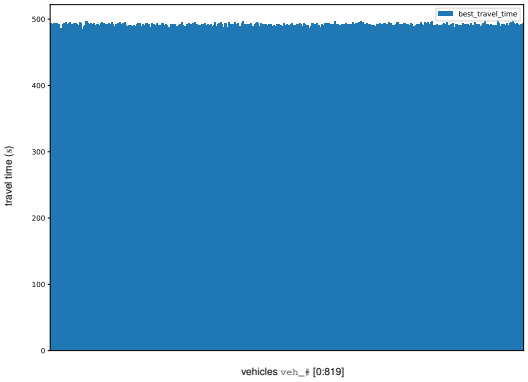


Fig. A.9-18. Best travel time for each vehicle, in seconds (s), during the simulation of a 24 h period.

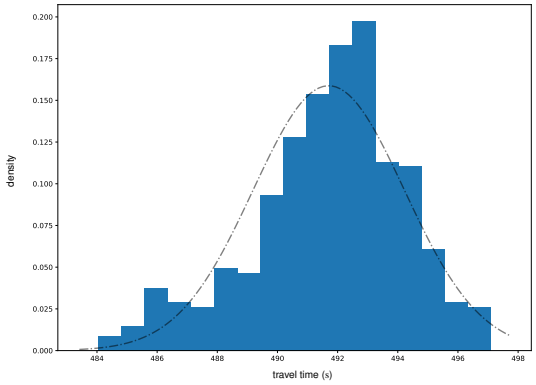


Fig. A.9-19. Density histogram of best travel time for vehicles, in seconds (s), during the simulation of a 24 h period, superimposing the normal density curve. The number of bins was calculated by the Freedman Diaconis rule.

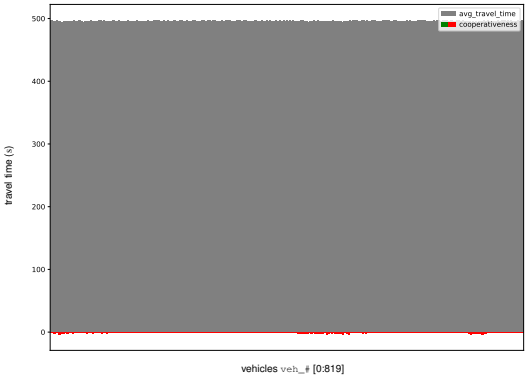


Fig. A.9-20. Average of the travel times, in seconds (s), of individual vehicles, during the simulation of a 24 h period. The bottom graph represents the *degree of cooperativeness**, downscaled by a normalization factor for the purpose of comparison with average times.

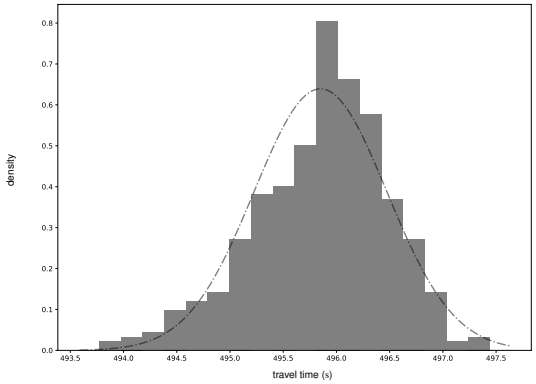


Fig. A.9-21. Density histogram of the average travel times, in seconds (s), of individual vehicles, during the simulation of a 24 h period, superimposing the normal density curve. The number of bins was calculated by the Freedman Diaconis rule.

* The *degree of cooperativeness* is a cumulative sum, calculated at each iteration, based on the complement of the ratio of cooperators, i.e., the higher the number of cooperators the less it increases, but the defectors are more penalized, and vice-versa. It varies inversely with the size of the group to which the player belongs.

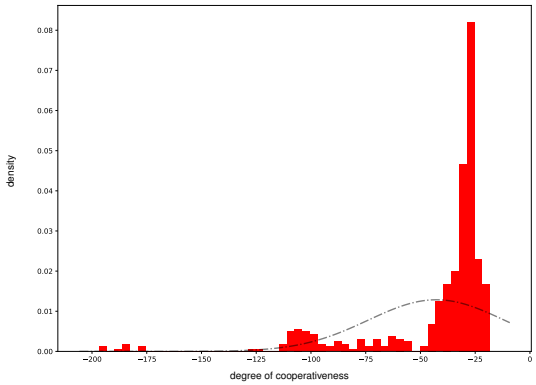


Fig. A.9-22. Density histogram of the *degree of cooperativeness** of individual vehicles, superimposing the normal density curve. The number of bins was calculated by the Freedman Diaconis rule. Generally, when strongly correlated with travel times, it presents a symmetric curve with respect to the *yy*-axis. All vehicles followed the preferred route and rejected the recommendation (all *Defectors*).

A.10 `570veh-24h-00061111`

```
Scenario: scenario-1
Timestamp: 20210521T172548Z
Number of vehicles: 570 vehs
Simulation time: 24.0 h
Warm up end time: 1494.2 s; step 14941
Vehicle selection strategy: stochastic
RSU turned off: False
RSU strategy: proportional
Runner options:
   nogui: True
   step_length: 0.1
   seed: 19750808
   output_prefix: 570veh-24h-00061111
   sim_run_time: 24.0
   num_vehicles: 570
   warmup_speed: 23.38
   warmup_routes_weight: [473, 527]
   network_speed: 25.0
   change_behavior_probability: [100, 0]
   cooperation_probability: [100, 0]
   vehicle_selection_strategy: stochastic
   turn_rsu_off: False
   rsu_dynamic_dissemination: False
   rsu_dissemination_interval: 5
   rsu_probabilistic_dissemination: False
   rsu_suggestion_strategy: proportional
   rsu_routes_weight: [471, 529]
   rsu_moving_avg_size: 5
   travel_times_ttl: 60
   rsu_dissemination_ttl: 0
   rsu_send_travel_time_info: False
   payoff_matrix: [360.0, 240.0, 0.0, -120.0]
   roth_erev_parameters: [0.1, 0.15]
Network Mean speed after warmup:
   Max: 13.59
   Min: 5.37
```

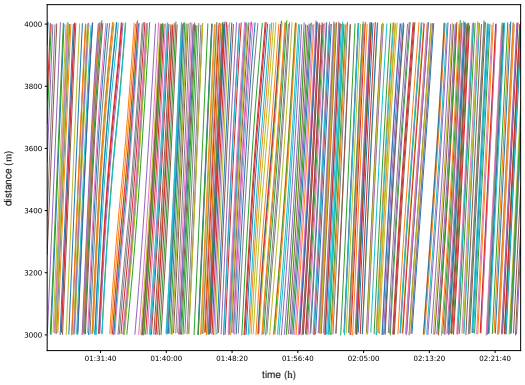


Fig. A.10-1. Time-Space diagram, for the one hour period after the end of the warmup, from 1:00:00 to 2:00:00 simulation time, plotted for the data from the sensor placed in the middle of the *direct* route (between 3000 m and 4000 m). In the case of an overloaded network, congestion shock waves can be observed.

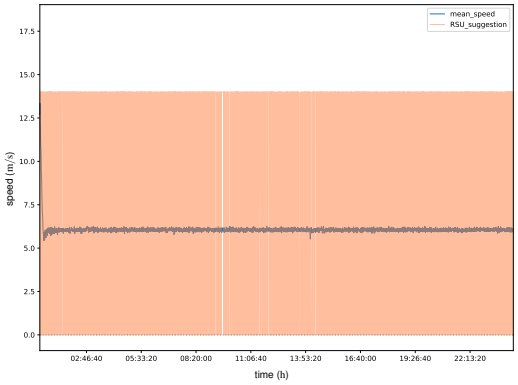


Fig. A.10-2. Mean speed in the network, in meters per second (m/s), over a 24 h period, superimposing (vertically, in orange) the time instants in which the RSU issued a recommendation to follow the *alternative* route.

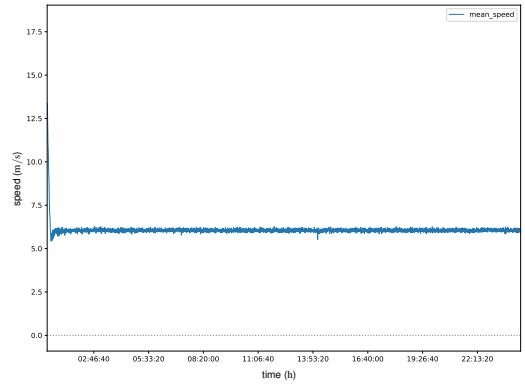


Fig. A.10-3. Mean speed in the network, in meters per second (m/s), over a 24 h period.

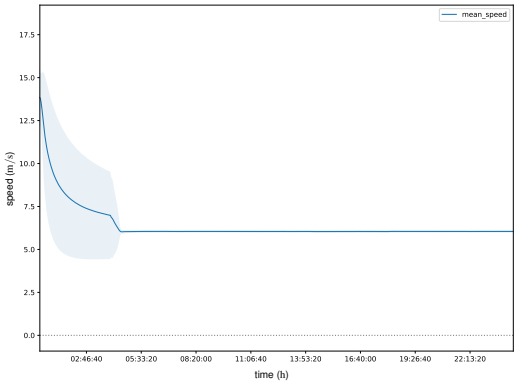


Fig. A.10-4. Mean speed in the network, in meters per second (m/s), over a 24 h period, 4 h Simple Moving Average, mean (line) and standard deviation (shaded).

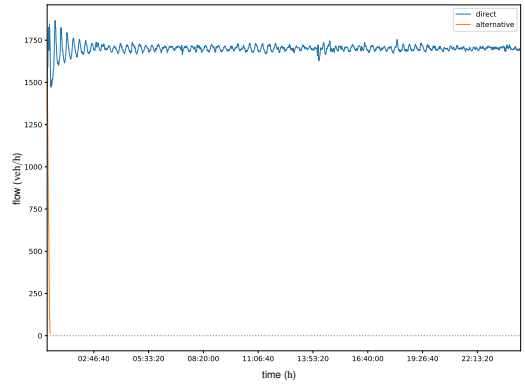


Fig. A.10-5. Traffic flow on each route, in vehicles per hour (veh/h), over a 24 h period.

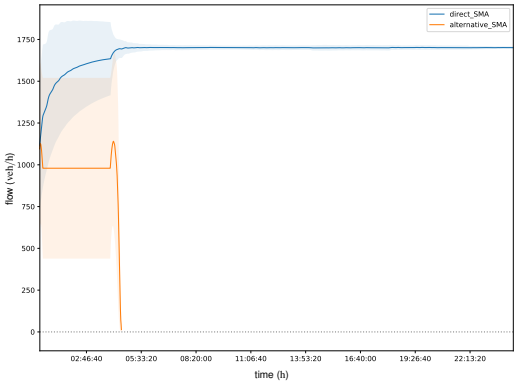


Fig. A.10-6. TrafficTraffic flow on each route, in vehicles per hour (veh/h), over a 24 h period, 4 h Simple Moving Average, mean (line) and standard deviation (shaded).

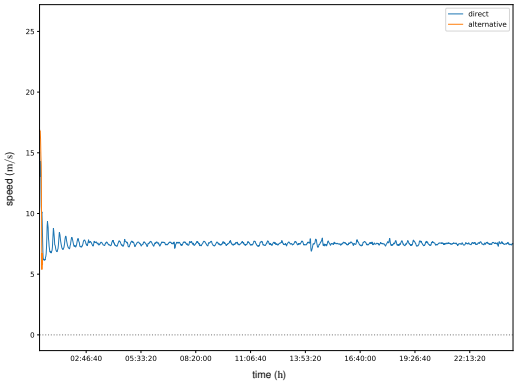


Fig. A.10-7. Mean speed on each route, in meters per second (m/s), aggregated to 1 min, over a 24 h period.

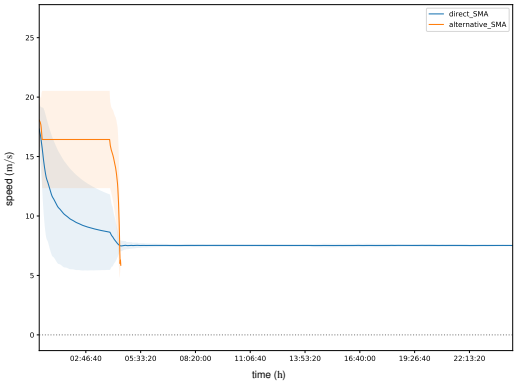


Fig. A.10-8. Mean speed on each route, in meters per second (m/s), aggregated to 1 min, over a 24 h period, 4 h Simple Moving Average, mean (line) and standard deviation (shaded).

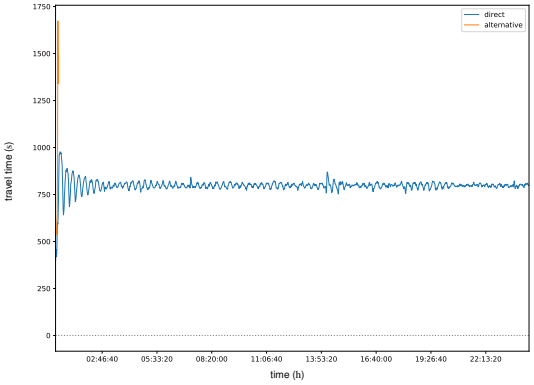


Fig. A.10-9. Travel times on each route, in seconds (s), aggregated to 1 min, over a 24 h period.

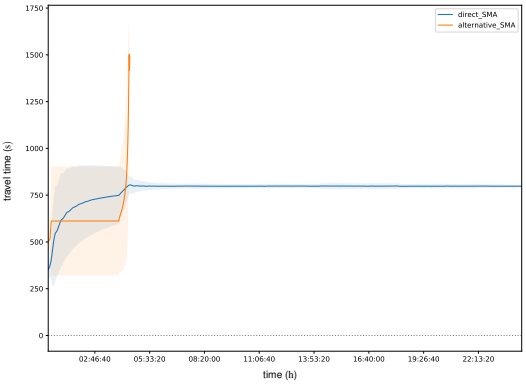


Fig. A.10-10. Travel times on each route, in seconds (s), aggregated to 1 min, over a 24 h period, 4 h Simple Moving Average, mean (line) and standard deviation (shaded).

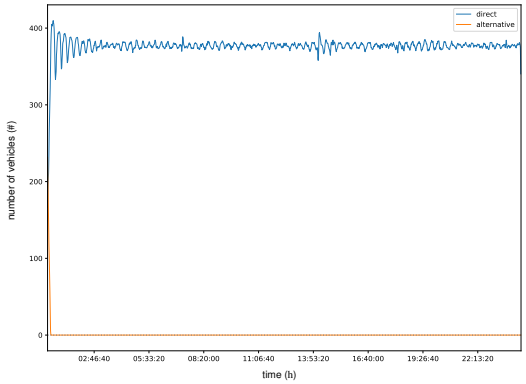


Fig. A.10-11. Average number of vehicles on each route, aggregated to 1 min, over a 24 h period.

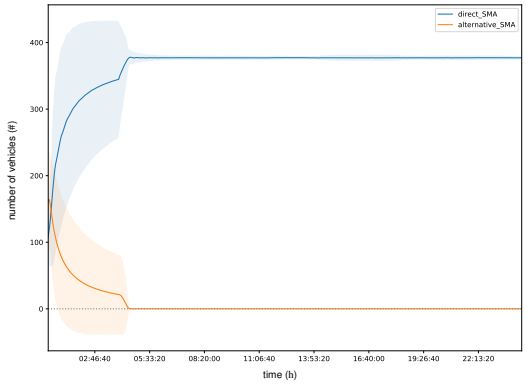


Fig. A.10-12. Average number of vehicles on each route, aggregated to 1 min, over a 24 h period, 4 h Simple Moving Average, mean (line) and standard deviation (shaded).

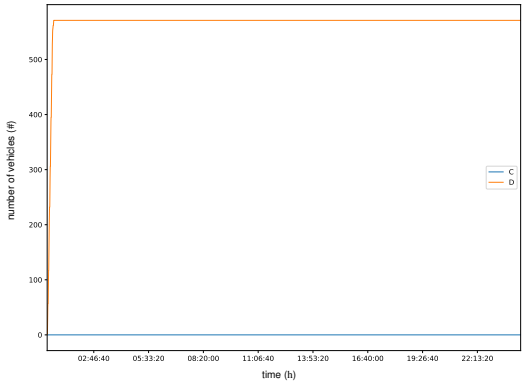


Fig. A.10-13. Evolution of the number of *Cooperators* and *Defectors* over a 24 h period.

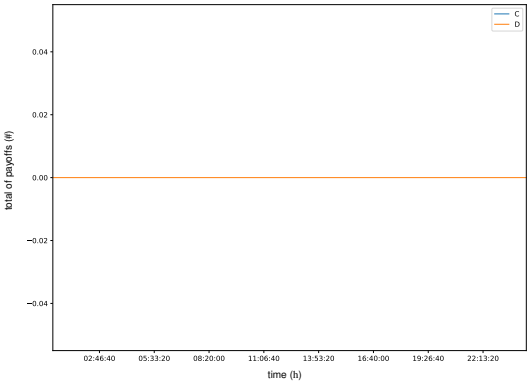


Fig. A.10-14. Evolution of total payoffs for *Cooperators* and *Defectors* (*individual payoff* times the *number of players receiving it*, $C(n) \times n$ and $D(n) \times (N-n)$, where n is the number of *Cooperators*), over a 24 h period.

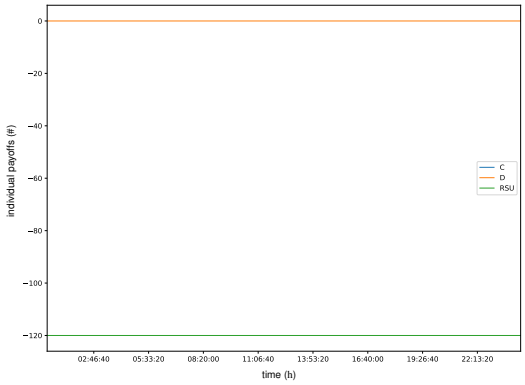


Fig. A.10-15. Evolution of the individual payoffs for *Cooperators, Defectors,* and *RSU* (always cooperating), over a 24 h period.

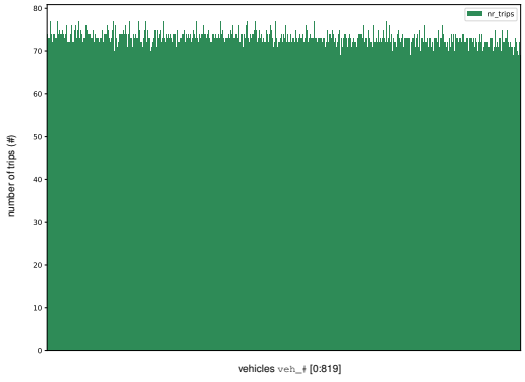


Fig. A.10-16. Number of trips made by each vehicle, during the simulation of a 24 h period.

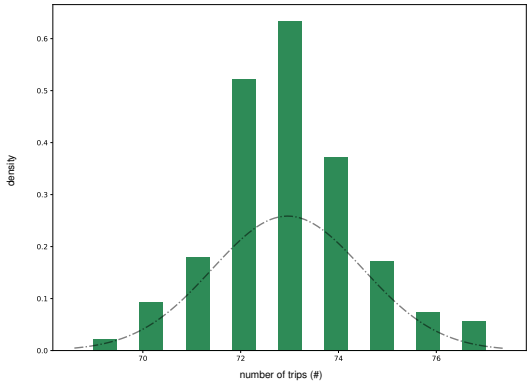


Fig. A.10-17. Density histogram of the number of trips made by each vehicle, during the simulation of a 24 h period, superimposing the normal density curve. The number of bins was calculated by the Freedman Diaconis rule.

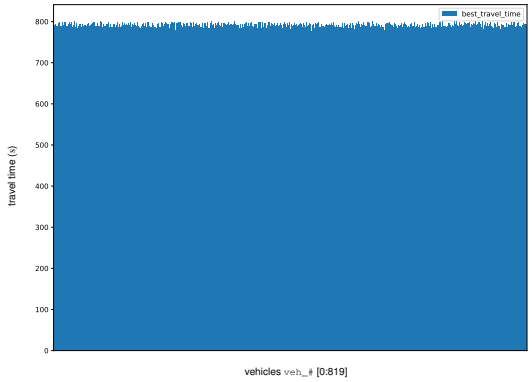


Fig. A.10-18. Best travel time for each vehicle, in seconds (s), during the simulation of a 24 h period.

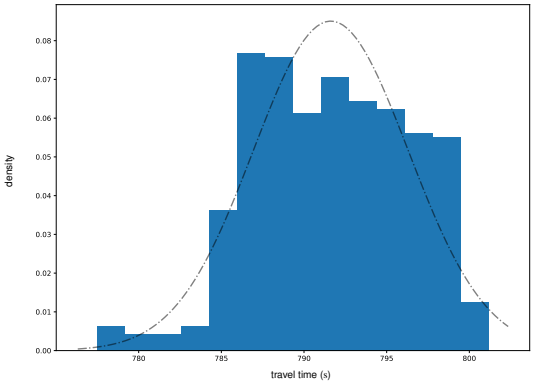


Fig. A.10-19. Density histogram of best travel time for vehicles, in seconds (s), during the simulation of a 24 h period, superimposing the normal density curve. The number of bins was calculated by the Freedman Diaconis rule.

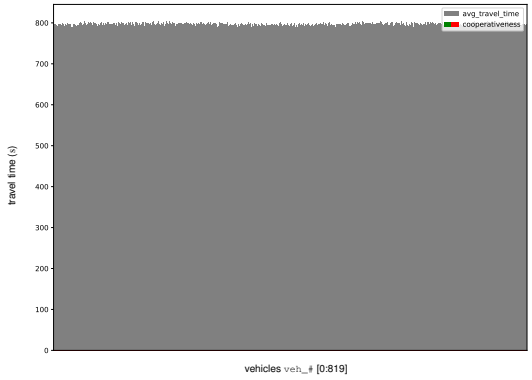


Fig. A.10-20. Average of the travel times, in seconds (s), of individual vehicles, during the simulation of a 24 h period. The bottom graph represents the *degree of cooperativeness**, downscaled by a normalization factor for the purpose of comparison with average times.

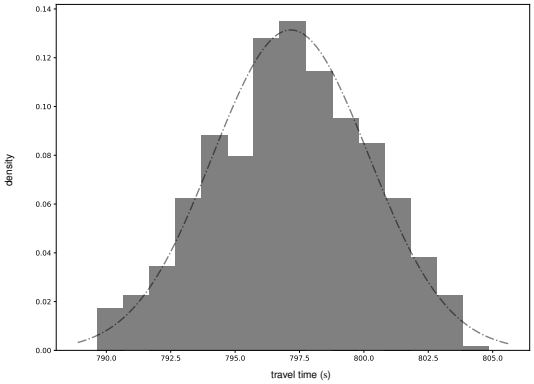


Fig. A.10-21. Density histogram of the average travel times, in seconds (s), of individual vehicles, during the simulation of a 24 h period, superimposing the normal density curve. The number of bins was calculated by the Freedman Diaconis rule.

* The *degree of cooperativeness* is a cumulative sum, calculated at each iteration, based on the complement of the ratio of cooperators, i.e., the higher the number of cooperators the less it increases, but the defectors are more penalized, and vice-versa. It varies inversely with the size of the group to which the player belongs.

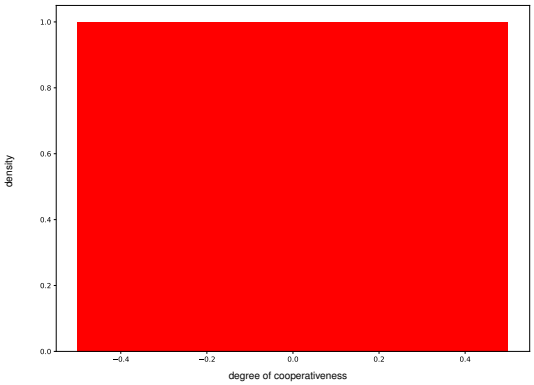


Fig. A.10-22. Density histogram of the *degree of cooperativeness** of individual vehicles, superimposing the normal density curve. The number of bins was calculated by the Freedman Diaconis rule. Generally, when strongly correlated with travel times, it presents a symmetric curve with respect to the *yy*-axis. All vehicles followed the preferred route and rejected the recommendation (all *Defectors*).

A.11 820veh-24h-00061111

```
Scenario: scenario-1
Timestamp: 20210521T164226Z
Number of vehicles: 820 vehs
Simulation time: 24.0 h
Warm up end time: 1866.6 s; step 18665
Vehicle selection strategy: stochastic
RSU turned off: False
RSU strategy: proportional_dynamic
Runner options:
   nogui: True
   step_length: 0.1
   seed: 19750808
   output_prefix: 820veh-24h-00061111
   sim_run_time: 24.0
   num_vehicles: 820
   warmup_speed: 13.96
   warmup_routes_weight: [473, 527]
   network_speed: 25.0
   change_behavior_probability: [100, 0]
   cooperation_probability: [100, 0]
   vehicle_selection_strategy: stochastic
   turn_rsu_off: False
   rsu_dynamic_dissemination: False
   rsu_dissemination_interval: 5
   rsu_probabilistic_dissemination: False
   rsu_suggestion_strategy: proportional_dynamic
   rsu_routes_weight: [460, 540]
   rsu_moving_avg_size: 5
   travel_times_ttl: 60
   rsu_dissemination_ttl: 0
   rsu_send_travel_time_info: False
   payoff_matrix: [360.0, 240.0, 0.0, -120.0]
   roth_erev_parameters: [0.1, 0.15]
Network Mean speed after warmup:
   Max: 9.61
   Min: 1.87
```

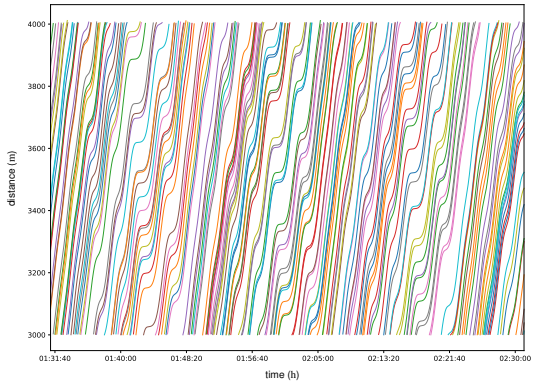


Fig. A.11-1. Time-Space diagram, for the one hour period after the end of the warmup, from 1:00:00 to 2:00:00 simulation time, plotted for the data from the sensor placed in the middle of the *direct* route (between 3000 m and 4000 m). In the case of an overloaded network, congestion shock waves can be observed.

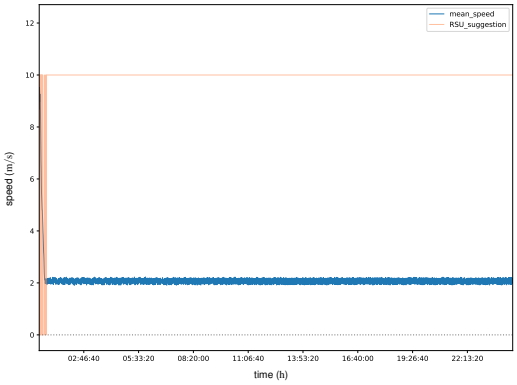


Fig. A.11-2. Mean speed in the network, in meters per second (m/s), over a 24 h period, superimposing (vertically, in orange) the time instants in which the RSU issued a recommendation to follow the *alternative* route.

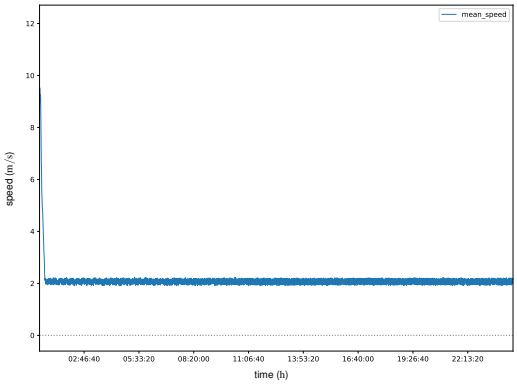


Fig. A.11-3. Mean speed in the network, in meters per second (m/s), over a 24 h period.

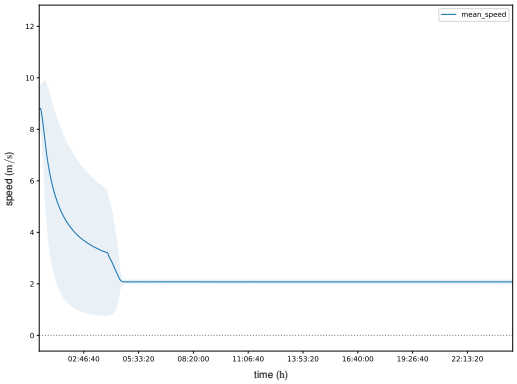


Fig. A.11-4. Mean speed in the network, in meters per second (m/s), over a 24 h period, 4 h Simple Moving Average, mean (line) and standard deviation (shaded).

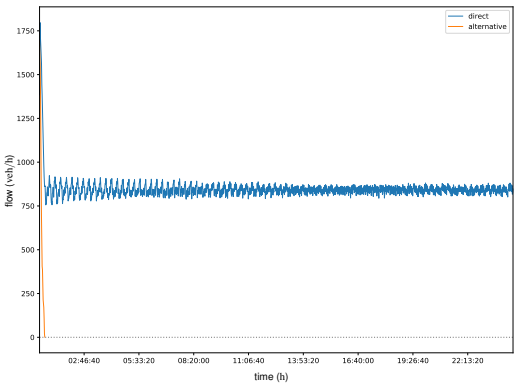


Fig. A.11-5. Traffic flow on each route, in vehicles per hour (veh/h), over a 24 h period.

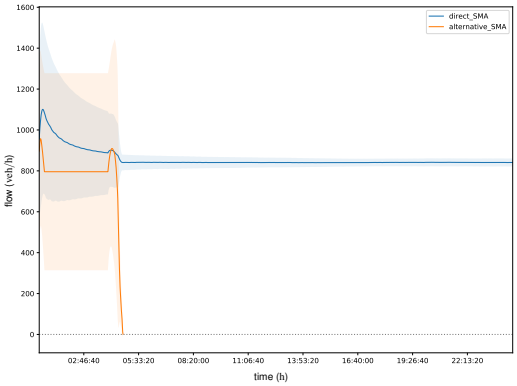


Fig. A.11-6. TrafficTraffic flow on each route, in vehicles per hour (veh/h), over a 24 h period, 4 h Simple Moving Average, mean (line) and standard deviation (shaded).

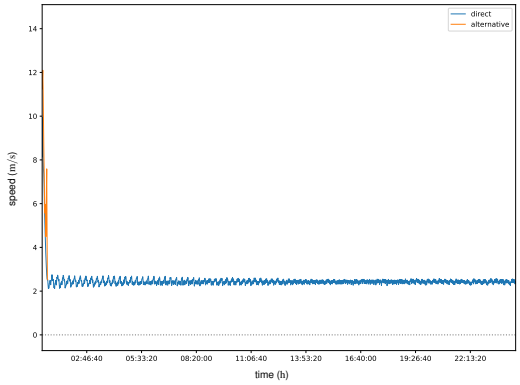


Fig. A.11-7. Mean speed on each route, in meters per second (m/s), aggregated to 1 min, over a 24 h period.

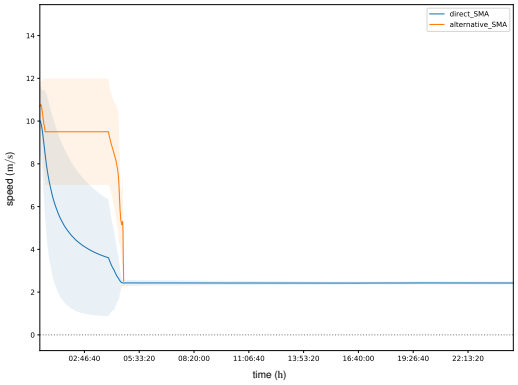


Fig. A.11-8. Mean speed on each route, in meters per second (m/s), aggregated to 1 min, over a 24 h period, 4 h Simple Moving Average, mean (line) and standard deviation (shaded).

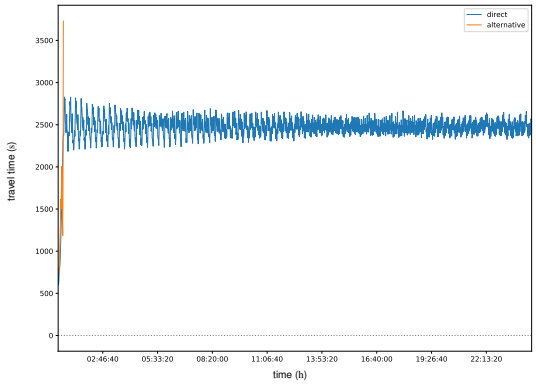


Fig. A.11-9. Travel times on each route, in seconds (s), aggregated to 1 min, over a 24 h period.

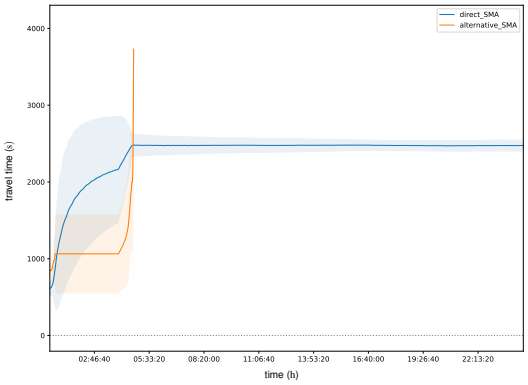


Fig. A.11-10. Travel times on each route, in seconds (s), aggregated to 1 min, over a 24 h period, 4 h Simple Moving Average, mean (line) and standard deviation (shaded).

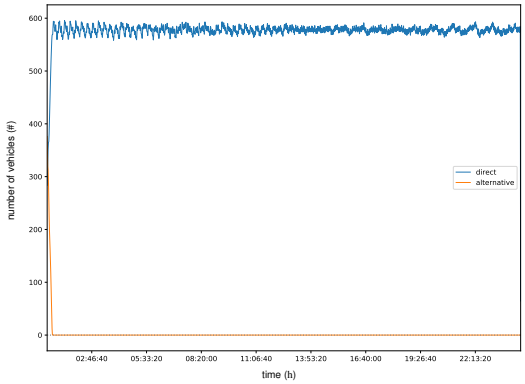


Fig. A.11-11. Average number of vehicles on each route, aggregated to 1 min, over a 24 h period.

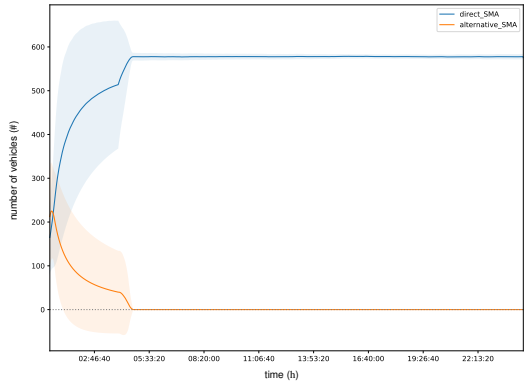


Fig. A.11-12. Average number of vehicles on each route, aggregated to 1 min, over a 24 h period, 4 h Simple Moving Average, mean (line) and standard deviation (shaded).

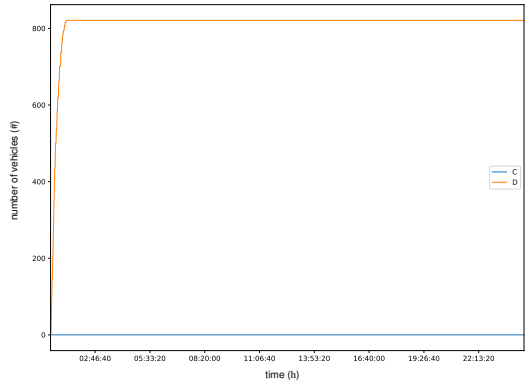


Fig. A.11-13. Evolution of the number of *Cooperators* and *Defectors* over a 24 h period.

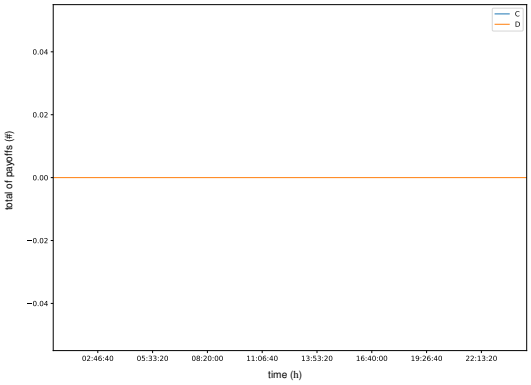


Fig. A.11-14. Evolution of total payoffs for *Cooperators* and *Defectors* (*individual payoff* times the *number of players receiving it*, $C(n) \times n$ and $D(n) \times (N-n)$, where n is the number of *Cooperators*), over a 24 h period.

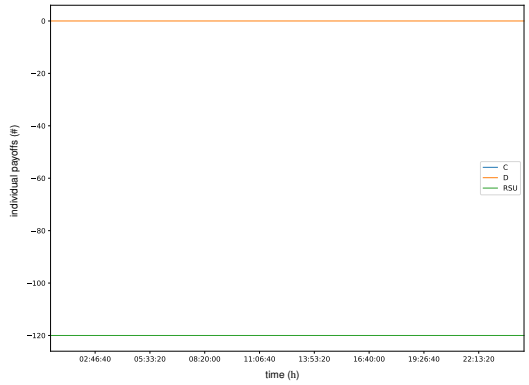


Fig. A.11-15. Evolution of the individual payoffs for *Cooperators, Defectors,* and *RSU* (always cooperating), over a 24 h period.

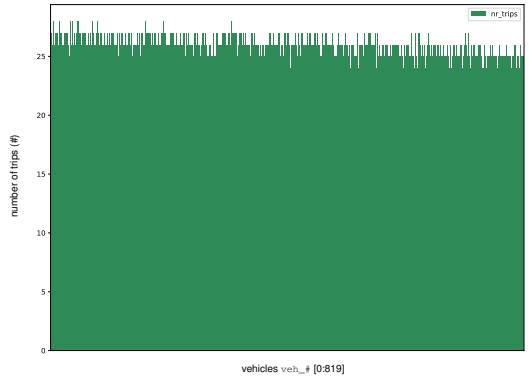


Fig. A.11-16. Number of trips made by each vehicle, during the simulation of a 24 h period.

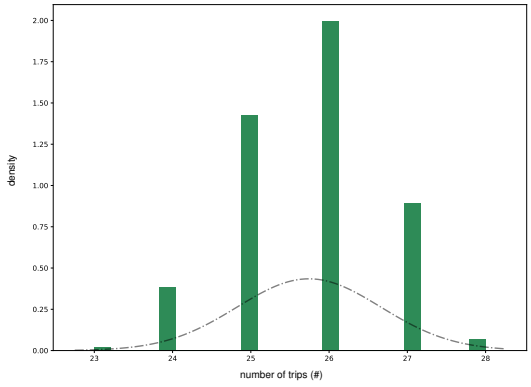


Fig. A.11-17. Density histogram of the number of trips made by each vehicle, during the simulation of a 24 h period, superimposing the normal density curve. The number of bins was calculated by the Freedman Diaconis rule.

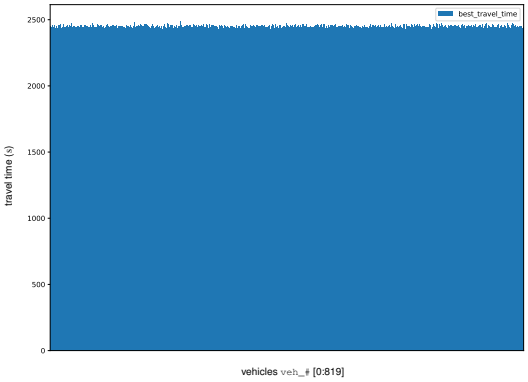


Fig. A.11-18. Best travel time for each vehicle, in seconds (s), during the simulation of a 24 h period.

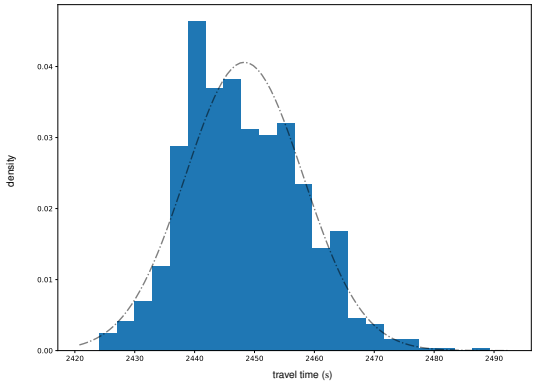


Fig. A.11-19. Density histogram of best travel time for vehicles, in seconds (s), during the simulation of a 24 h period, superimposing the normal density curve. The number of bins was calculated by the Freedman Diaconis rule.

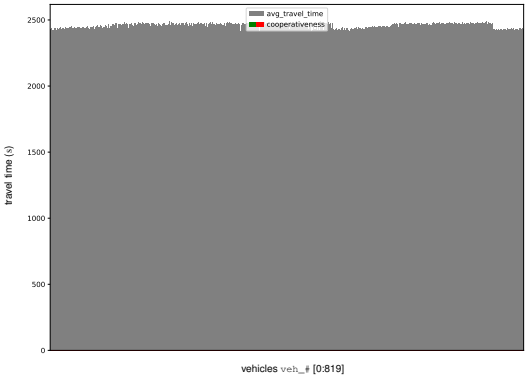


Fig. A.11-20. Average of the travel times, in seconds (s), of individual vehicles, during the simulation of a 24 h period. The bottom graph represents the *degree of cooperativeness**, downscaled by a normalization factor for the purpose of comparison with average times.

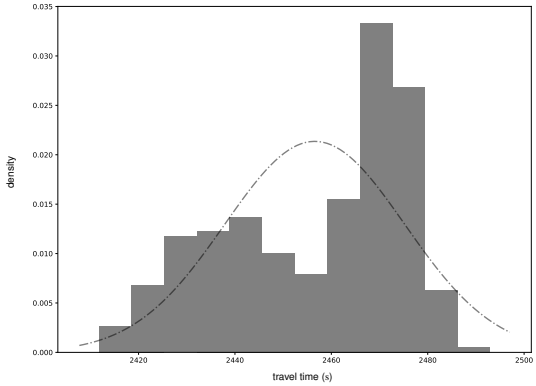


Fig. A.11-21. Density histogram of the average travel times, in seconds (s), of individual vehicles, during the simulation of a 24 h period, superimposing the normal density curve. The number of bins was calculated by the Freedman Diaconis rule.

* The *degree of cooperativeness* is a cumulative sum, calculated at each iteration, based on the complement of the ratio of cooperators, i.e., the higher the number of cooperators the less it increases, but the defectors are more penalized, and vice-versa. It varies inversely with the size of the group to which the player belongs.

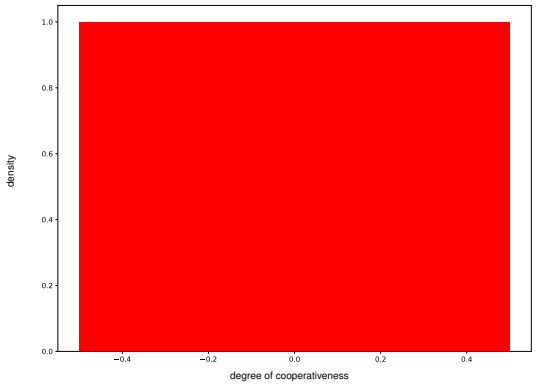


Fig. A.11-22. Density histogram of the *degree of cooperativeness** of individual vehicles, superimposing the normal density curve. The number of bins was calculated by the Freedman Diaconis rule. Generally, when strongly correlated with travel times, it presents a symmetric curve with respect to the *yy*-axis. All vehicles followed the preferred route and rejected the recommendation (all *Defectors*).

A.12 `930veh-24h-00061111`

```
Scenario: scenario-1
Timestamp: 20210613T070930Z
Number of vehicles: 930 vehs
Simulation time: 24.0 h
Warm up end time: 2110.2 s; step 21101
Vehicle selection strategy: stochastic
RSU turned off: False
RSU strategy: proportional
Runner options:
   nogui: True
   step_length: 0.1
   seed: 19750808
   output_prefix: 930veh-24h-00061111
   sim_run_time: 24.0
   num_vehicles: 930
   warmup_speed: 11.42
   warmup_routes_weight: [473, 527]
   network_speed: 25.0
   change_behavior_probability: [100, 0]
   cooperation_probability: [100, 0]
   vehicle_selection_strategy: stochastic
   turn_rsu_off: False
   rsu_dynamic_dissemination: False
   rsu_dissemination_interval: 5
   rsu_probabilistic_dissemination: False
   rsu_suggestion_strategy: proportional
   rsu_routes_weight: [455, 545]
   rsu_moving_avg_size: 5
   travel_times_ttl: 60
   rsu_dissemination_ttl: 0
   rsu_send_travel_time_info: False
   payoff_matrix: [360.0, 240.0, 0.0, -120.0]
   roth_erev_parameters: [0.1, 0.15]
   rsu_change_dissemination: False
   rsu_change_dissemination_steps: [14400, 28800, 43200, 57600, 72000]
   rsu_change_dissemination_intervals: [10, 20, 40, 80, 160]
Network Mean speed after warmup:
   Max: 9.29
   Min: 0.84
```

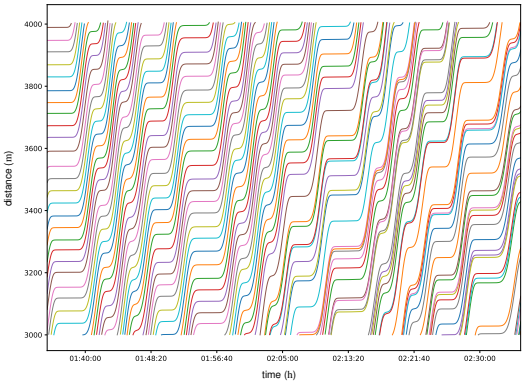


Fig. A.12-1. Time-Space diagram, for the one hour period after the end of the warmup, from 1:00:00 to 2:00:00 simulation time, plotted for the data from the sensor placed in the middle of the *direct* route (between 3000 m and 4000 m). In the case of an overloaded network, congestion shock waves can be observed.

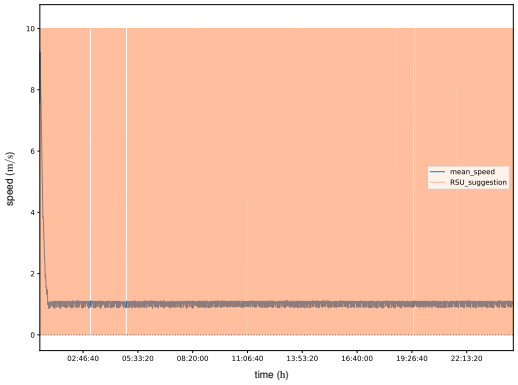


Fig. A.12-2. Mean speed in the network, in meters per second (m/s), over a 24 h period, superimposing (vertically, in orange) the time instants in which the RSU issued a recommendation to follow the *alternative* route.

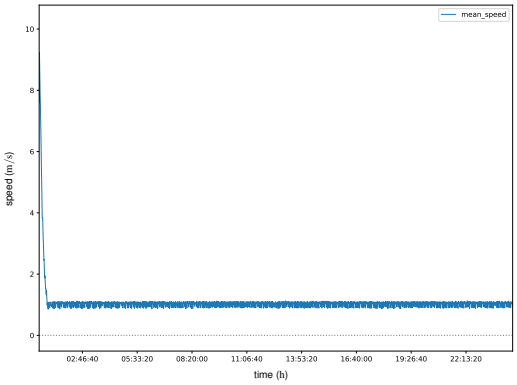


Fig. A.12-3. Mean speed in the network, in meters per second (m/s), over a 24 h period.

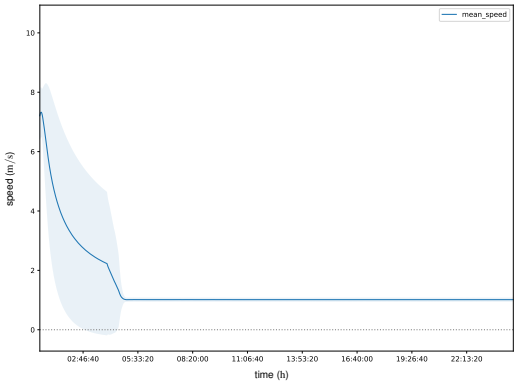


Fig. A.12-4. Mean speed in the network, in meters per second (m/s), over a 24 h period, 4 h Simple Moving Average, mean (line) and standard deviation (shaded).

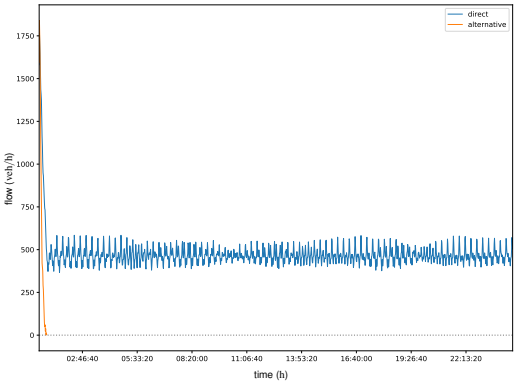


Fig. A.12-5. Traffic flow on each route, in vehicles per hour (veh/h), over a 24 h period.

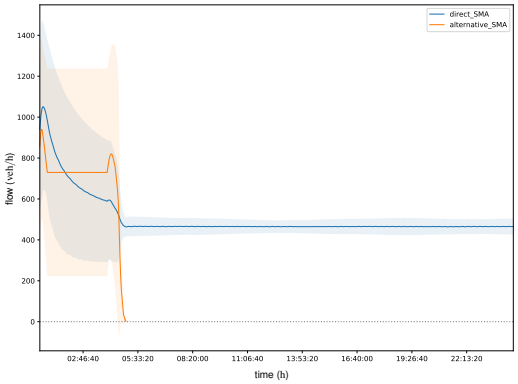


Fig. A.12-6. TrafficTraffic flow on each route, in vehicles per hour (veh/h), over a 24 h period, 4 h Simple Moving Average, mean (line) and standard deviation (shaded).

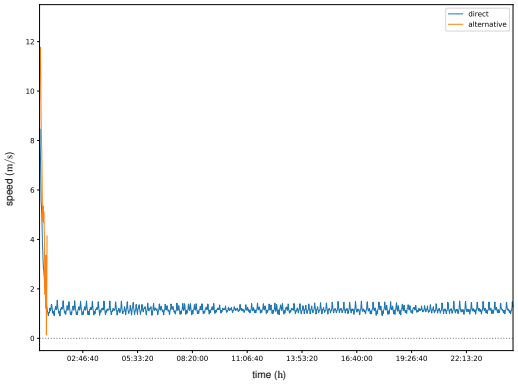


Fig. A.12-7. Mean speed on each route, in meters per second (m/s), aggregated to 1 min, over a 24 h period.

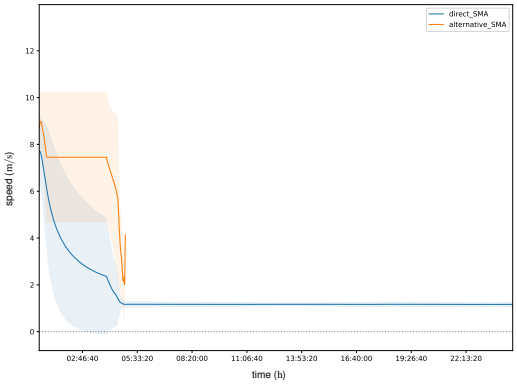


Fig. A.12-8. Mean speed on each route, in meters per second (m/s), aggregated to 1 min, over a 24 h period, 4 h Simple Moving Average, mean (line) and standard deviation (shaded).

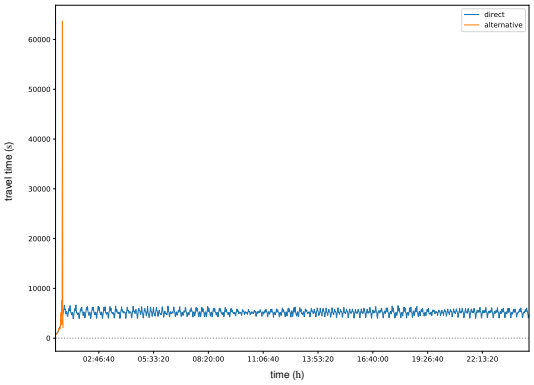


Fig. A.12-9. Travel times on each route, in seconds (s), aggregated to 1 min, over a 24 h period.

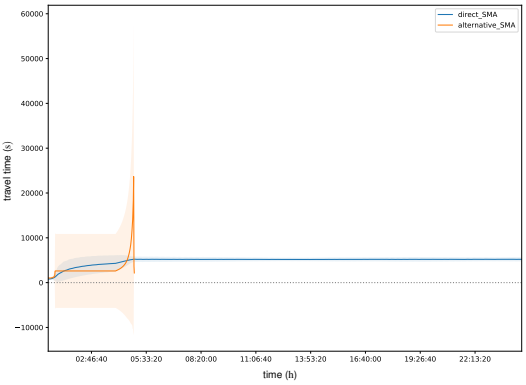


Fig. A.12-10. Travel times on each route, in seconds (s), aggregated to 1 min, over a 24 h period, 4 h Simple Moving Average, mean (line) and standard deviation (shaded).

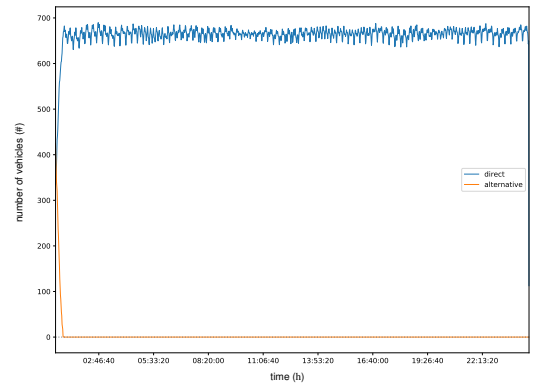


Fig. A.12-11. Average number of vehicles on each route, aggregated to 1 min, over a 24 h period.

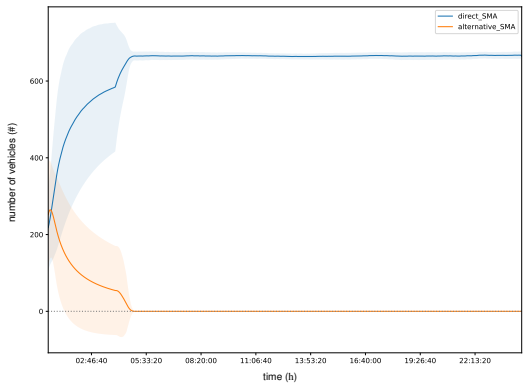


Fig. A.12-12. Average number of vehicles on each route, aggregated to 1 min, over a 24 h period, 4 h Simple Moving Average, mean (line) and standard deviation (shaded).

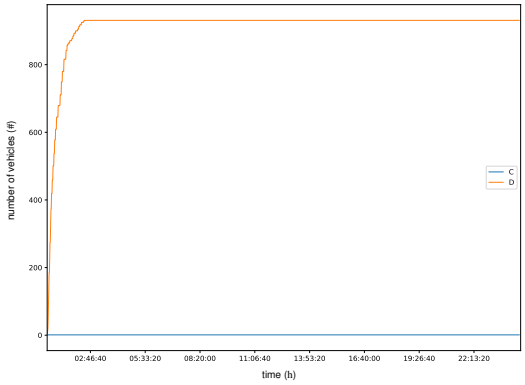


Fig. A.12-13. Evolution of the number of *Cooperators* and *Defectors* over a 24 h period.

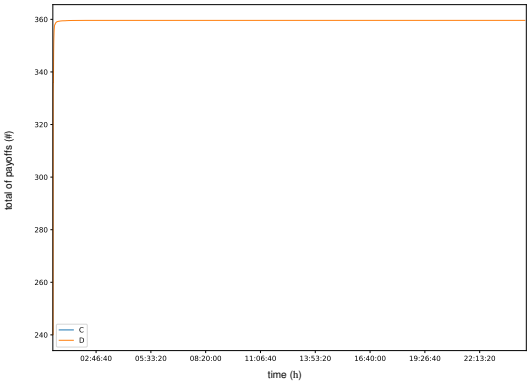


Fig. A.12-14. Evolution of total payoffs for *Cooperators* and *Defectors* (*individual payoff* times the *number of players receiving it*, $C(n) \times n$ and $D(n) \times (N-n)$, where n is the number of *Cooperators*), over a 24 h period.

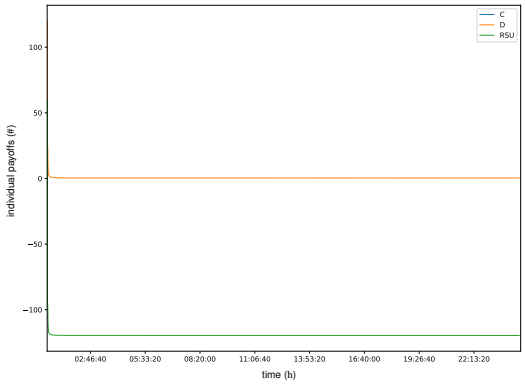


Fig. A.12-15. Evolution of the individual payoffs for *Cooperators, Defectors,* and *RSU* (always cooperating), over a 24 h period.

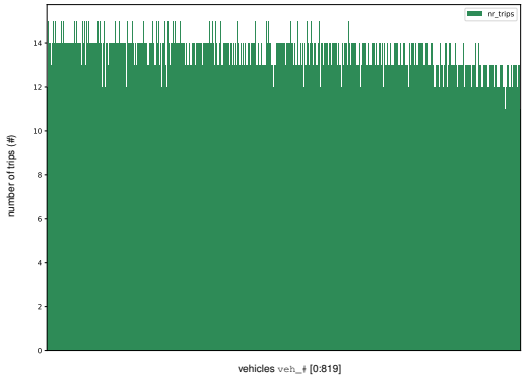


Fig. A.12-16. Number of trips made by each vehicle, during the simulation of a 24 h period.

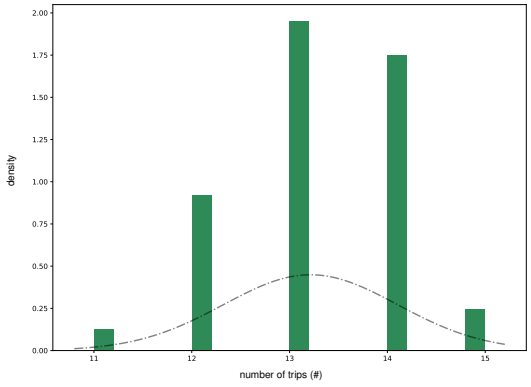


Fig. A.12-17. Density histogram of the number of trips made by each vehicle, during the simulation of a 24 h period, superimposing the normal density curve. The number of bins was calculated by the Freedman Diaconis rule.

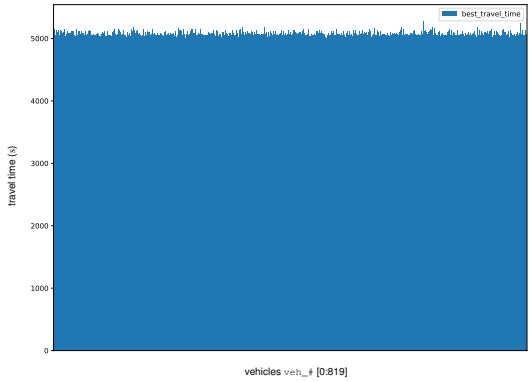


Fig. A.12-18. Best travel time for each vehicle, in seconds (s), during the simulation of a 24 h period.

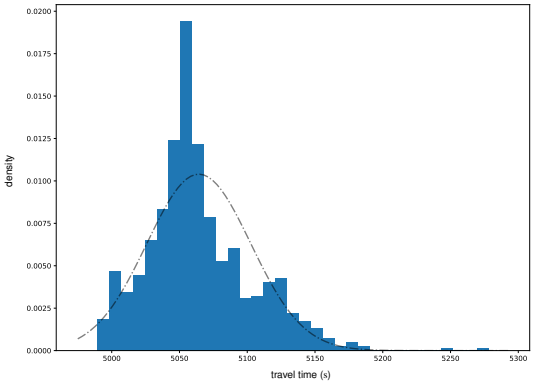


Fig. A.12-19. Density histogram of best travel time for vehicles, in seconds (s), during the simulation of a 24 h period, superimposing the normal density curve. The number of bins was calculated by the Freedman Diaconis rule.

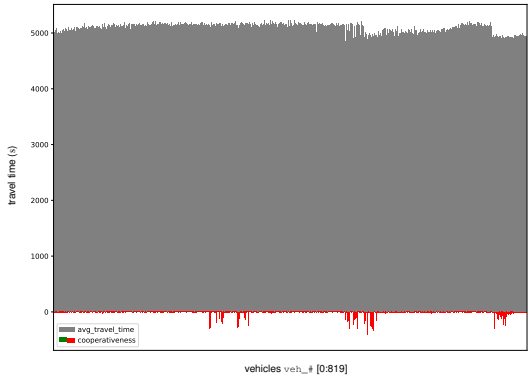


Fig. A.12-20. Average of the travel times, in seconds (s), of individual vehicles, during the simulation of a 24 h period. The bottom graph represents the *degree of cooperativeness**, downscaled by a normalization factor for the purpose of comparison with average times.

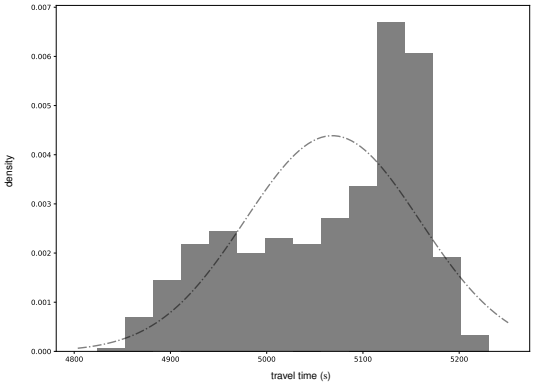


Fig. A.12-21. Density histogram of the average travel times, in seconds (s), of individual vehicles, during the simulation of a 24 h period, superimposing the normal density curve. The number of bins was calculated by the Freedman Diaconis rule.

* The *degree of cooperativeness* is a cumulative sum, calculated at each iteration, based on the complement of the ratio of cooperators, i.e., the higher the number of cooperators the less it increases, but the defectors are more penalized, and vice-versa. It varies inversely with the size of the group to which the player belongs.

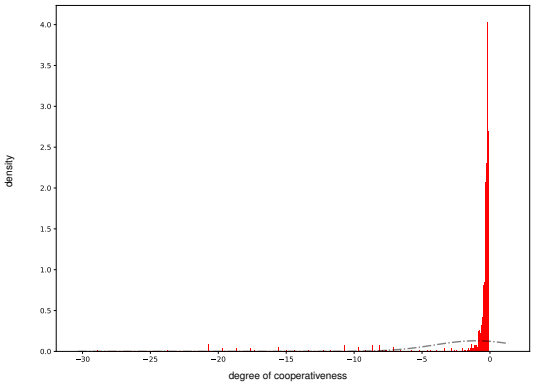


Fig. A.12-22. Density histogram of the *degree of cooperativeness** of individual vehicles, superimposing the normal density curve. The number of bins was calculated by the Freedman Diaconis rule. Generally, when strongly correlated with travel times, it presents a symmetric curve with respect to the *yy*-axis. All vehicles followed the preferred route and rejected the recommendation (all *Defectors*).

A.13 820veh-24h-01060000

```
Scenario: scenario-1
Timestamp: 20210521T190413Z
Number of vehicles: 820 vehs
Simulation time: 24.0 h
Warm up end time: 1866.6 s; step 18665
Vehicle selection strategy: stochastic
RSU turned off: False
RSU strategy: proportional_dynamic
Runner options:
   nogui: True
   step_length: 0.1
   seed: 19750808
   output_prefix: 820veh-24h-01060000
   sim_run_time: 24.0
   num_vehicles: 820
   warmup_speed: 13.96
   warmup_routes_weight: [473, 527]
   network_speed: 25.0
   change_behavior_probability: [0, 100]
   cooperation_probability: [0, 100]
   vehicle_selection_strategy: stochastic
   turn_rsu_off: False
   rsu_dynamic_dissemination: False
   rsu_dissemination_interval: 5
   rsu_probabilistic_dissemination: False
   rsu_suggestion_strategy: proportional_dynamic
   rsu_routes_weight: [471, 529]
   rsu_moving_avg_size: 5
   travel_times_ttl: 60
   rsu_dissemination_ttl: 0
   rsu_send_travel_time_info: False
   payoff_matrix: [360.0, 240.0, 0.0, -120.0]
   roth_erev_parameters: [0.1, 0.15]
Network Mean speed after warmup:
   Max: 11.05
   Min: 7.38
```

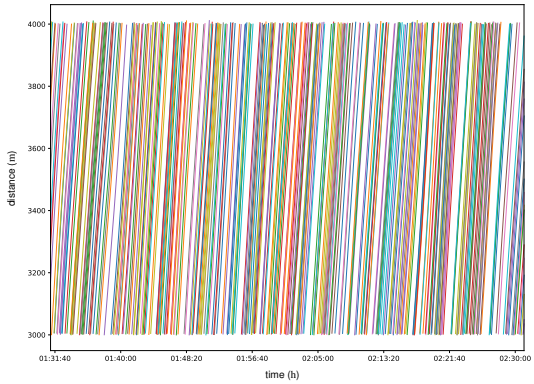


Fig. A.13-1. Time-Space diagram, for the one hour period after the end of the warmup, from 1:00:00 to 2:00:00 simulation time, plotted for the data from the sensor placed in the middle of the *direct* route (between 3000 m and 4000 m). In the case of an overloaded network, congestion shock waves can be observed.

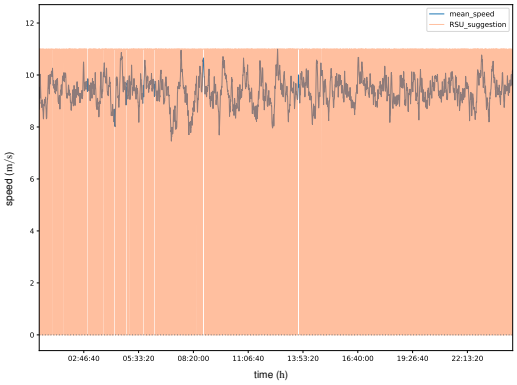


Fig. A.13-2. Mean speed in the network, in meters per second (m/s), over a 24 h period, superimposing (vertically, in orange) the time instants in which the RSU issued a recommendation to follow the *alternative* route.

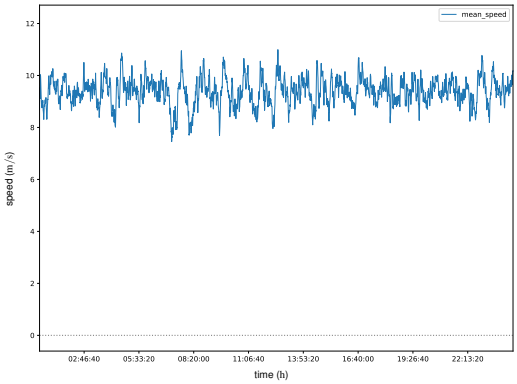


Fig. A.13-3. Mean speed in the network, in meters per second (m/s), over a 24 h period.

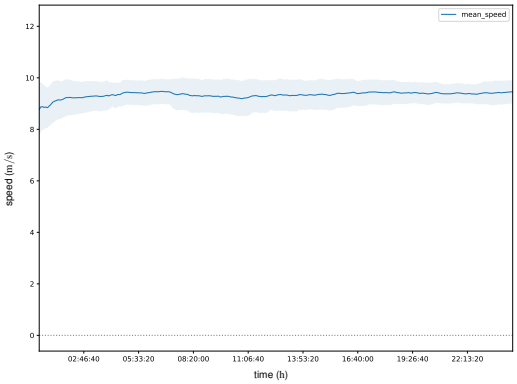


Fig. A.13-4. Mean speed in the network, in meters per second (m/s), over a 24 h period, 4 h Simple Moving Average, mean (line) and standard deviation (shaded).

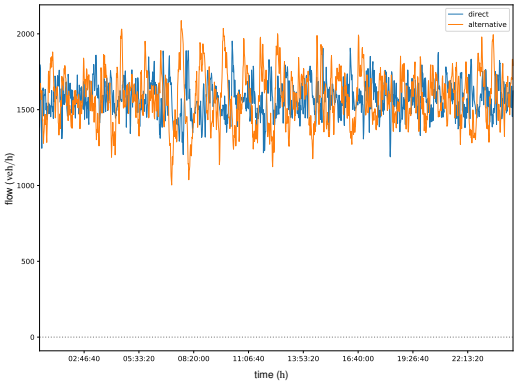


Fig. A.13-5. Traffic flow on each route, in vehicles per hour (veh/h), over a 24 h period.

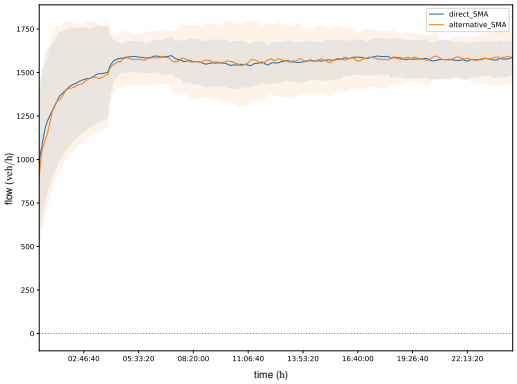


Fig. A.13-6. TrafficTraffic flow on each route, in vehicles per hour (veh/h), over a 24 h period, 4 h Simple Moving Average, mean (line) and standard deviation (shaded).

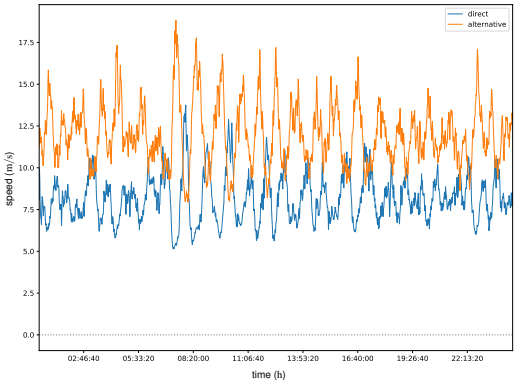


Fig. A.13-7. Mean speed on each route, in meters per second (m/s), aggregated to 1 min, over a 24 h period.

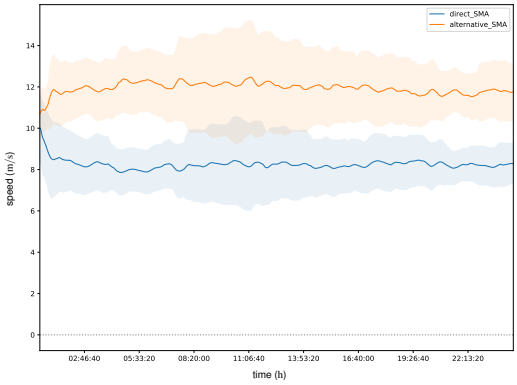


Fig. A.13-8. Mean speed on each route, in meters per second (m/s), aggregated to 1 min, over a 24 h period, 4 h Simple Moving Average, mean (line) and standard deviation (shaded).

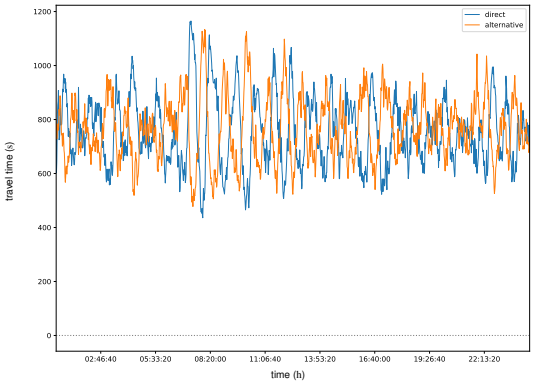


Fig. A.13-9. Travel times on each route, in seconds (s), aggregated to 1 min, over a 24 h period.

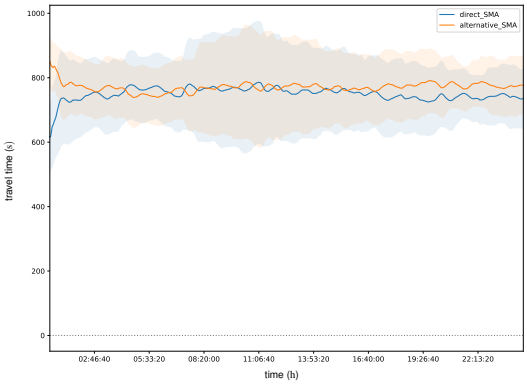


Fig. A.13-10. Travel times on each route, in seconds (s), aggregated to 1 min, over a 24 h period, 4 h Simple Moving Average, mean (line) and standard deviation (shaded).

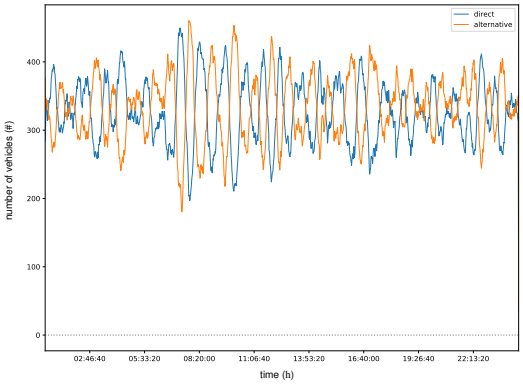


Fig. A.13-11. Average number of vehicles on each route, aggregated to 1 min, over a 24 h period.

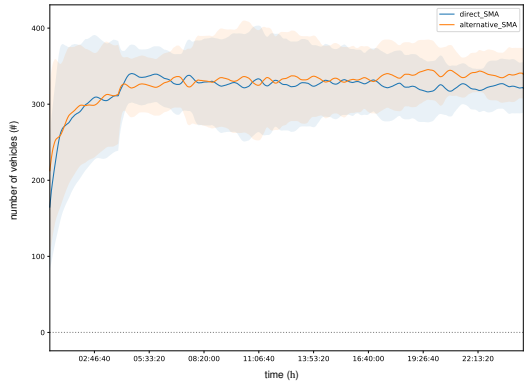


Fig. A.13-12. Average number of vehicles on each route, aggregated to 1 min, over a 24 h period, 4 h Simple Moving Average, mean (line) and standard deviation (shaded).

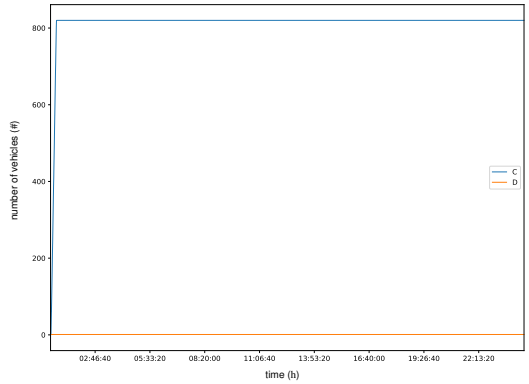


Fig. A.13-13. Evolution of the number of *Cooperators* and *Defectors* over a 24 h period.

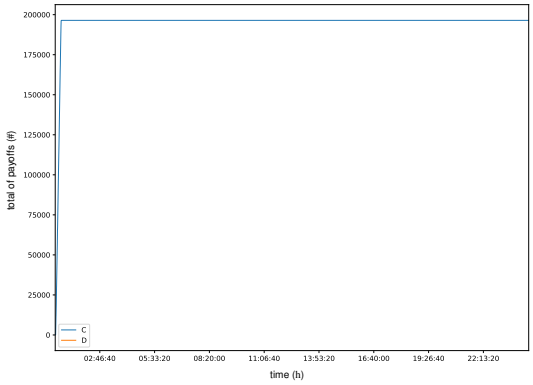


Fig. A.13-14. Evolution of total payoffs for *Cooperators* and *Defectors* (*individual payoff* times the *number of players receiving it*, $C(n) \times n$ and $D(n) \times (N-n)$, where n is the number of *Cooperators*), over a 24 h period.

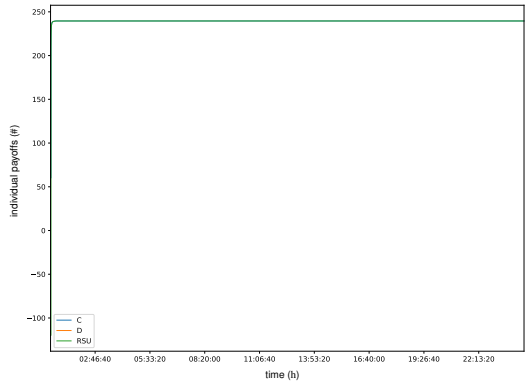


Fig. A.13-15. Evolution of the individual payoffs for *Cooperators, Defectors,* and *RSU* (always cooperating), over a 24 h period.

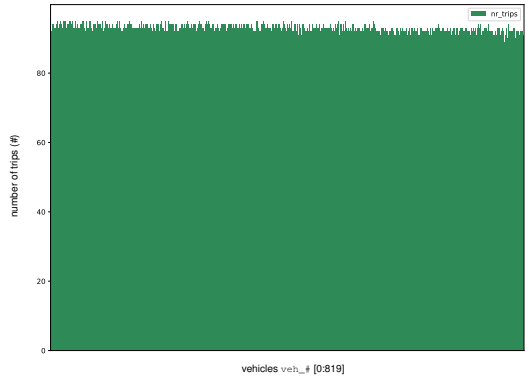


Fig. A.13-16. Number of trips made by each vehicle, during the simulation of a 24 h period.

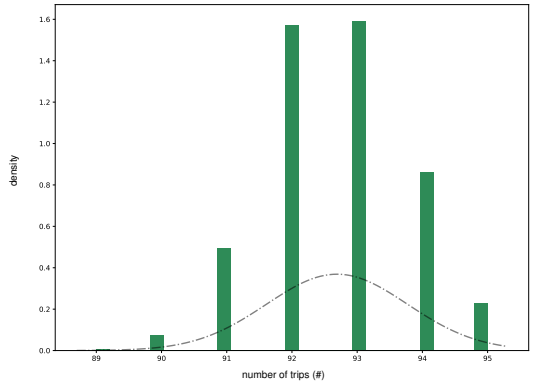


Fig. A.13-17. Density histogram of the number of trips made by each vehicle, during the simulation of a 24 h period, superimposing the normal density curve. The number of bins was calculated by the Freedman Diaconis rule.

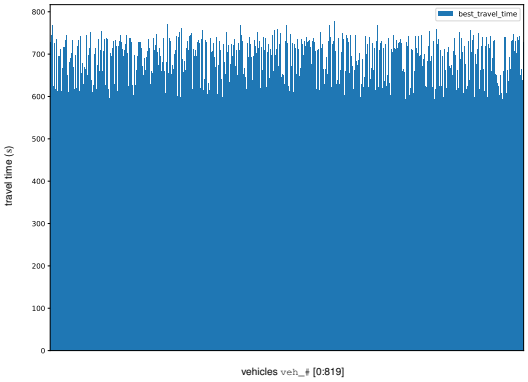


Fig. A.13-18. Best travel time for each vehicle, in seconds (s), during the simulation of a 24 h period.

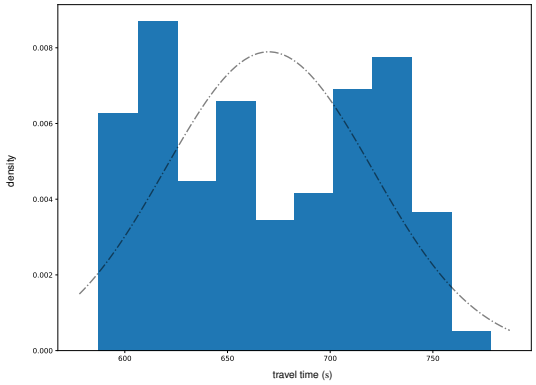


Fig. A.13-19. Density histogram of best travel time for vehicles, in seconds (s), during the simulation of a 24 h period, superimposing the normal density curve. The number of bins was calculated by the Freedman Diaconis rule.

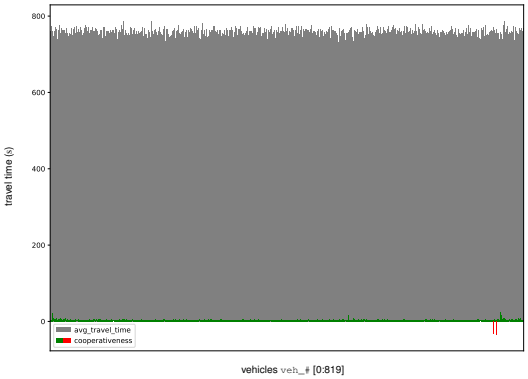


Fig. A.13-20. Average of the travel times, in seconds (s), of individual vehicles, during the simulation of a 24 h period. The bottom graph represents the *degree of cooperativeness**, downscaled by a normalization factor for the purpose of comparison with average times.

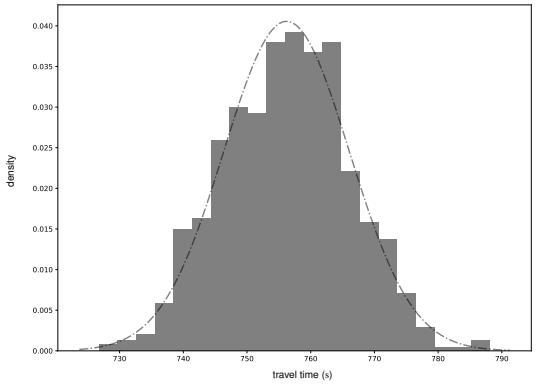


Fig. A.13-21. Density histogram of the average travel times, in seconds (s), of individual vehicles, during the simulation of a 24 h period, superimposing the normal density curve. The number of bins was calculated by the Freedman Diaconis rule.

* The *degree of cooperativeness* is a cumulative sum, calculated at each iteration, based on the complement of the ratio of cooperators, i.e., the higher the number of cooperators the less it increases, but the defectors are more penalized, and vice-versa. It varies inversely with the size of the group to which the player belongs.

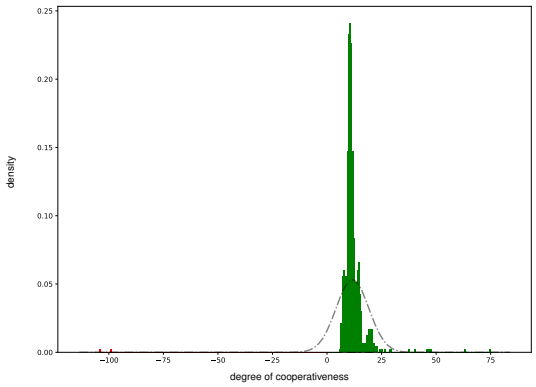


Fig. A.13-22. Density histogram of the *degree of cooperativeness** of individual vehicles, superimposing the normal density curve. The number of bins was calculated by the Freedman Diaconis rule. Generally, when strongly correlated with travel times, it presents a symmetric curve with respect to the *yy*-axis. Because some vehicles choose their preferred route immediately after the end of warmup, due to the gap between the RSU coverage and the route selection point, there may be some outliers.

A.14 `820veh-24h-02060000`

```
Scenario: scenario-1
Timestamp: 20210617T032712Z
Number of vehicles: 820 vehs
Simulation time: 24.0 h
Warm up end time: 1866.6 s; step 18665
Vehicle selection strategy: stochastic
RSU turned off: False
RSU strategy: occupancy_simple
Runner options:
   nogui: True
   step_length: 0.1
   seed: 19750808
   output_prefix: 820veh-24h-02060000
   sim_run_time: 24.0
   num_vehicles: 820
   warmup_speed: 13.96
   warmup_routes_weight: [473, 527]
   network_speed: 25.0
   change_behavior_probability: [0, 100]
   cooperation_probability: [0, 100]
   vehicle_selection_strategy: stochastic
   turn_rsu_off: False
   rsu_dynamic_dissemination: False
   rsu_dissemination_interval: 5
   rsu_probabilistic_dissemination: False
   rsu_suggestion_strategy: occupancy_simple
   rsu_routes_weight: [460, 540]
   rsu_moving_avg_size: 5
   travel_times_ttl: 60
   rsu_dissemination_ttl: 0
   rsu_send_travel_time_info: False
   payoff_matrix: [360.0, 240.0, 0.0, -120.0]
   roth_erev_parameters: [0.1, 0.15]
   rsu_change_dissemination: False
   rsu_change_dissemination_steps: [14400, 28800, 43200, 57600, 72000]
   rsu_change_dissemination_intervals: [10, 20, 40, 80, 160]
Network Mean speed after warmup:
   Max: 9.83
   Min: 5.16
```

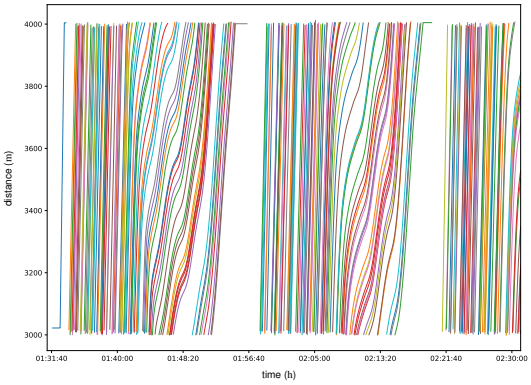


Fig. A.14-1. Time-Space diagram, for the one hour period after the end of the warmup, from 1:00:00 to 2:00:00 simulation time, plotted for the data from the sensor placed in the middle of the *direct* route (between 3000 m and 4000 m). In the case of an overloaded network, congestion shock waves can be observed.

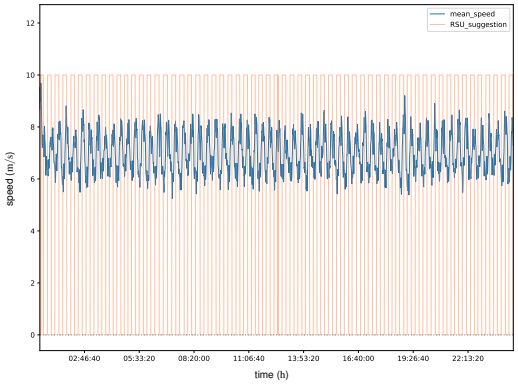


Fig. A.14-2. Mean speed in the network, in meters per second (m/s), over a 24 h period, superimposing (vertically, in orange) the time instants in which the RSU issued a recommendation to follow the *alternative* route.

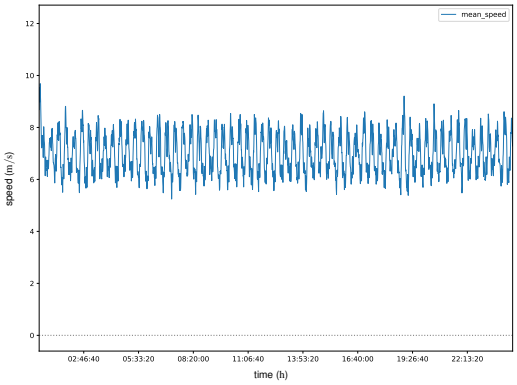


Fig. A.14-3. Mean speed in the network, in meters per second (m/s), over a 24 h period.

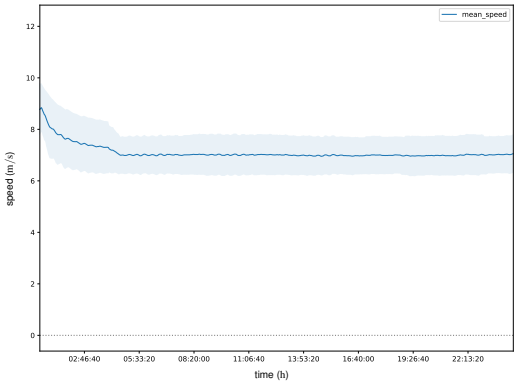


Fig. A.14-4. Mean speed in the network, in meters per second (m/s), over a 24 h period, 4 h Simple Moving Average, mean (line) and standard deviation (shaded).

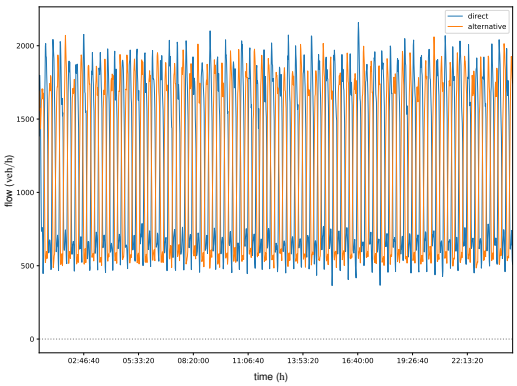


Fig. A.14-5. Traffic flow on each route, in vehicles per hour (veh/h), over a 24 h period.

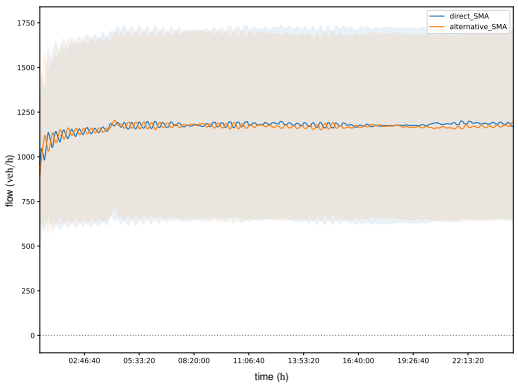


Fig. A.14-6. TrafficTraffic flow on each route, in vehicles per hour (veh/h), over a 24 h period, 4 h Simple Moving Average, mean (line) and standard deviation (shaded).

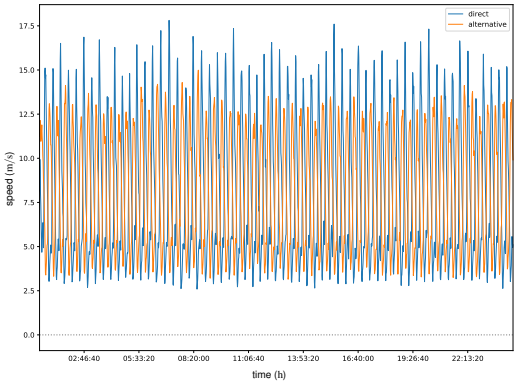


Fig. A.14-7. Mean speed on each route, in meters per second (m/s), aggregated to 1 min, over a 24 h period.

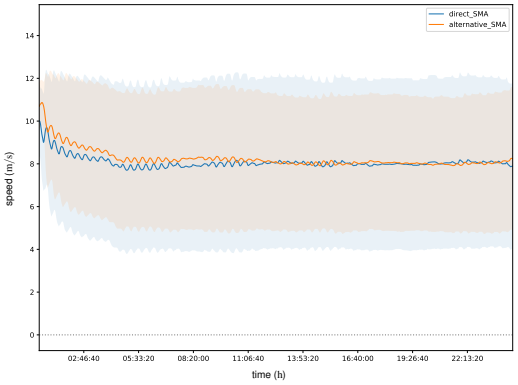


Fig. A.14-8. Mean speed on each route, in meters per second (m/s), aggregated to 1 min, over a 24 h period, 4 h Simple Moving Average, mean (line) and standard deviation (shaded).

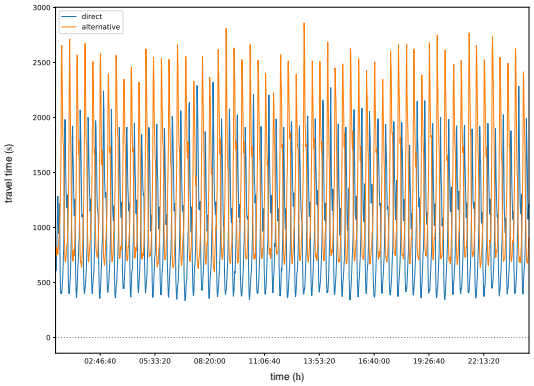


Fig. A.14-9. Travel times on each route, in seconds (s), aggregated to 1 min, over a 24 h period.

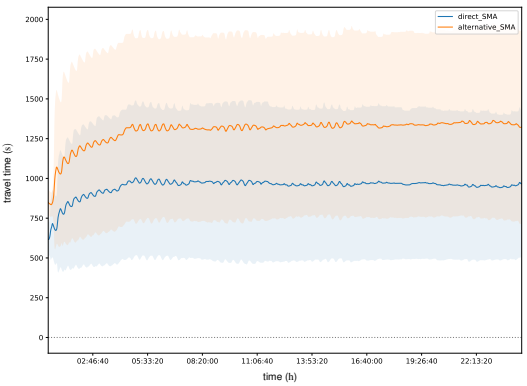


Fig. A.14-10. Travel times on each route, in seconds (s), aggregated to 1 min, over a 24 h period, 4 h Simple Moving Average, mean (line) and standard deviation (shaded).

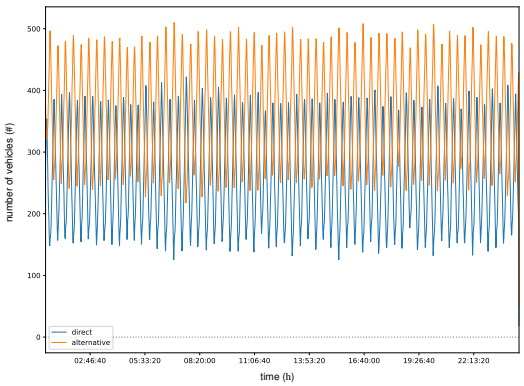


Fig. A.14-11. Average number of vehicles on each route, aggregated to 1 min, over a 24 h period.

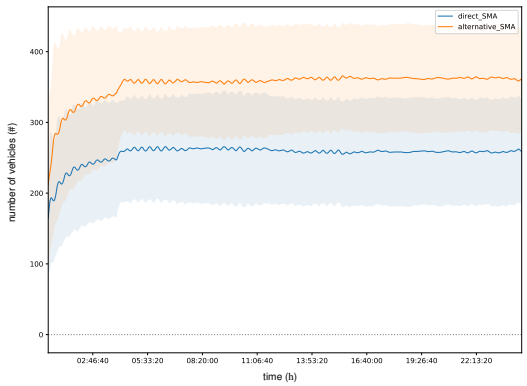


Fig. A.14-12. Average number of vehicles on each route, aggregated to 1 min, over a 24 h period, 4 h Simple Moving Average, mean (line) and standard deviation (shaded).

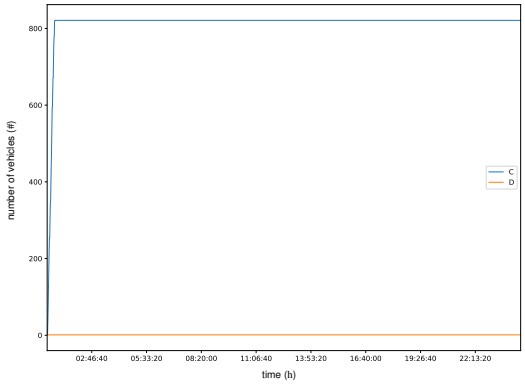


Fig. A.14-13. Evolution of the number of *Cooperators* and *Defectors* over a 24 h period.

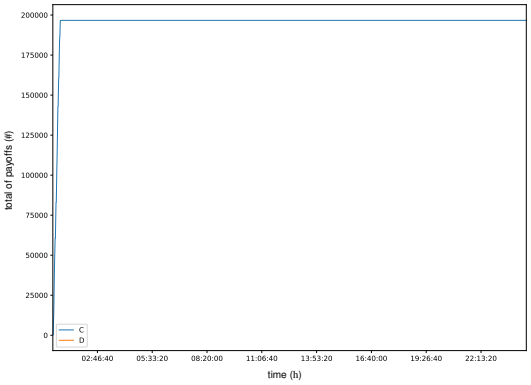


Fig. A.14-14. Evolution of total payoffs for *Cooperators* and *Defectors* (*individual payoff* times the *number of players receiving it*, $C(n) \times n$ and $D(n) \times (N-n)$, where n is the number of *Cooperators*), over a 24 h period.

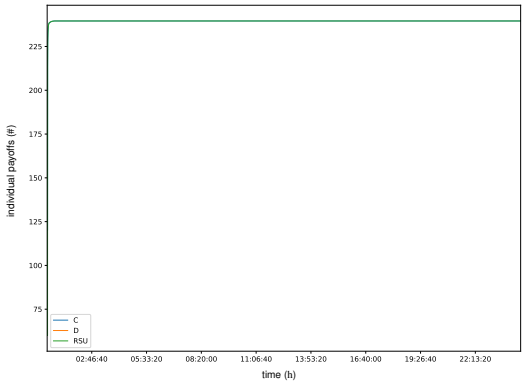


Fig. A.14-15. Evolution of the individual payoffs for *Cooperators, Defectors,* and *RSU* (always cooperating), over a 24 h period.

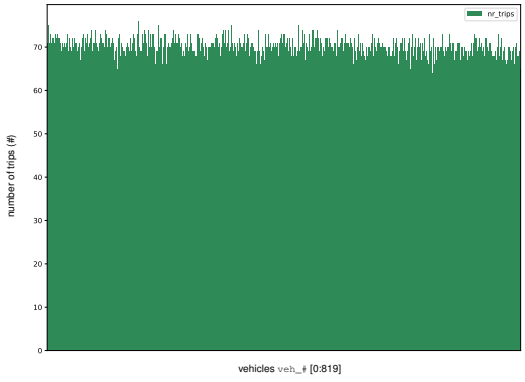


Fig. A.14-16. Number of trips made by each vehicle, during the simulation of a 24 h period.

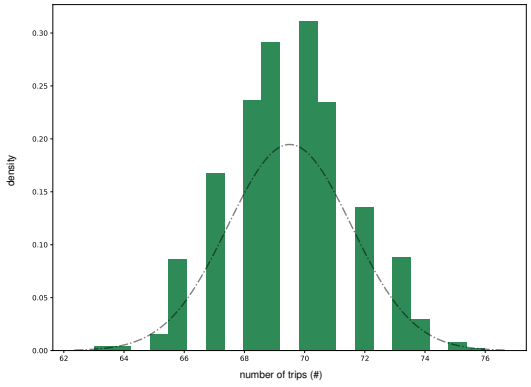


Fig. A.14-17. Density histogram of the number of trips made by each vehicle, during the simulation of a 24 h period, superimposing the normal density curve. The number of bins was calculated by the Freedman Diaconis rule.

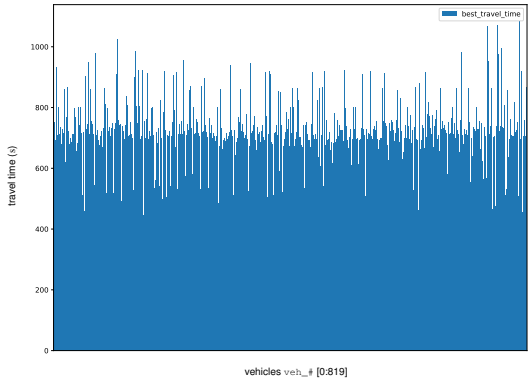


Fig. A.14-18. Best travel time for each vehicle, in seconds (s), during the simulation of a 24 h period.

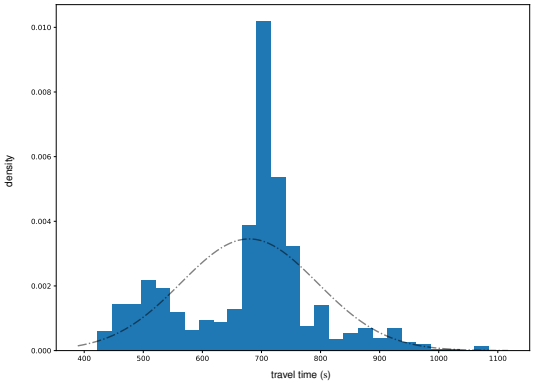


Fig. A.14-19. Density histogram of best travel time for vehicles, in seconds (s), during the simulation of a 24 h period, superimposing the normal density curve. The number of bins was calculated by the Freedman Diaconis rule.

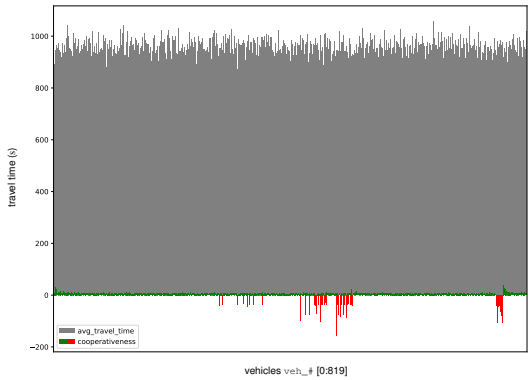


Fig. A.14-20. Average of the travel times, in seconds (s), of individual vehicles, during the simulation of a 24 h period. The bottom graph represents the *degree of cooperativeness**, downscaled by a normalization factor for the purpose of comparison with average times.

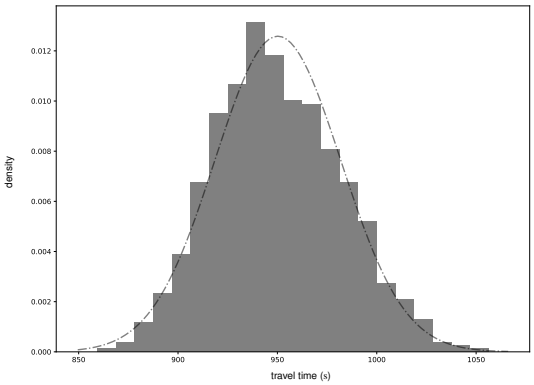


Fig. A.14-21. Density histogram of the average travel times, in seconds (s), of individual vehicles, during the simulation of a 24 h period, superimposing the normal density curve. The number of bins was calculated by the Freedman Diaconis rule.

* The *degree of cooperativeness* is a cumulative sum, calculated at each iteration, based on the complement of the ratio of cooperators, i.e., the higher the number of cooperators the less it increases, but the defectors are more penalized, and vice-versa. It varies inversely with the size of the group to which the player belongs.

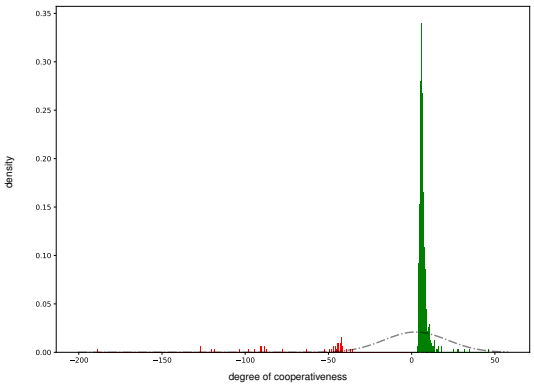


Fig. A.14-22. Density histogram of the *degree of cooperativeness** of individual vehicles, superimposing the normal density curve. The number of bins was calculated by the Freedman Diaconis rule. Generally, when strongly correlated with travel times, it presents a symmetric curve with respect to the *yy*-axis. Because some vehicles choose their preferred route immediately after the end of warmup, due to the gap between the RSU coverage and the route selection point, there may be some outliers.

A.15 820veh-24h-03060000

```
Scenario: scenario-1
Timestamp: 20210617T032716Z
Number of vehicles: 820 vehs
Simulation time: 24.0 h
Warm up end time: 1866.6 s; step 18665
Vehicle selection strategy: stochastic
RSU turned off: False
RSU strategy: occupancy_product
Runner options:
   nogui: True
   step_length: 0.1
   seed: 19750808
   output_prefix: 820veh-24h-03060000
   sim_run_time: 24.0
   num_vehicles: 820
   warmup_speed: 13.96
   warmup_routes_weight: [473, 527]
   network_speed: 25.0
   change_behavior_probability: [0, 100]
   cooperation_probability: [0, 100]
   vehicle_selection_strategy: stochastic
   turn_rsu_off: False
   rsu_dynamic_dissemination: False
   rsu_dissemination_interval: 5
   rsu_probabilistic_dissemination: False
   rsu_suggestion_strategy: occupancy_product
   rsu_routes_weight: [460, 540]
   rsu_moving_avg_size: 5
   travel_times_ttl: 60
   rsu_dissemination_ttl: 0
   rsu_send_travel_time_info: False
   payoff_matrix: [360.0, 240.0, 0.0, -120.0]
   roth_erev_parameters: [0.1, 0.15]
   rsu_change_dissemination: False
   rsu_change_dissemination_steps: [14400, 28800, 43200, 57600, 72000]
   rsu_change_dissemination_intervals: [10, 20, 40, 80, 160]
Network Mean speed after warmup:
   Max: 9.97
   Min: 5.4
```

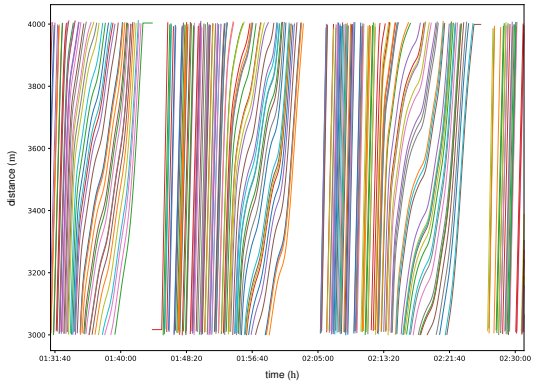


Fig. A.15-1. Time-Space diagram, for the one hour period after the end of the warmup, from 1:00:00 to 2:00:00 simulation time, plotted for the data from the sensor placed in the middle of the *direct* route (between 3000 m and 4000 m). In the case of an overloaded network, congestion shock waves can be observed.

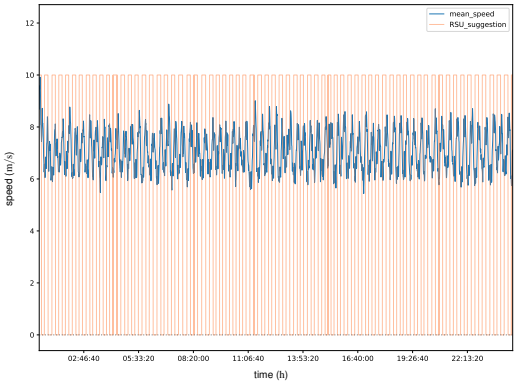


Fig. A.15-2. Mean speed in the network, in meters per second (m/s), over a 24 h period, superimposing (vertically, in orange) the time instants in which the RSU issued a recommendation to follow the *alternative* route.

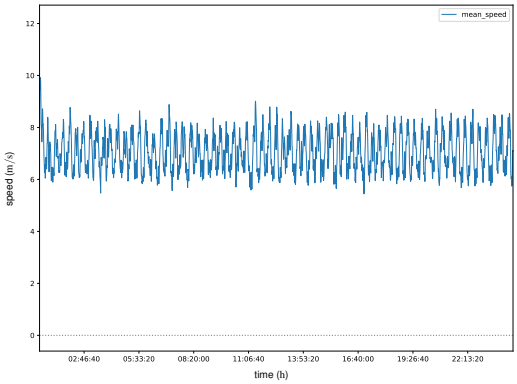


Fig. A.15-3. Mean speed in the network, in meters per second (m/s), over a 24 h period.

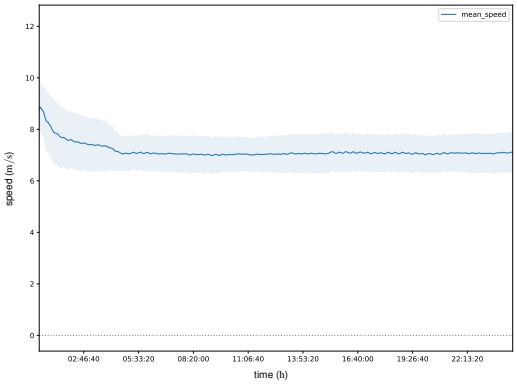


Fig. A.15-4. Mean speed in the network, in meters per second (m/s), over a 24 h period, 4 h Simple Moving Average, mean (line) and standard deviation (shaded).

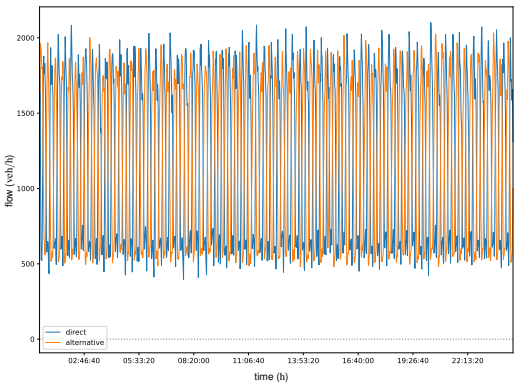


Fig. A.15-5. Traffic flow on each route, in vehicles per hour (veh/h), over a 24 h period.

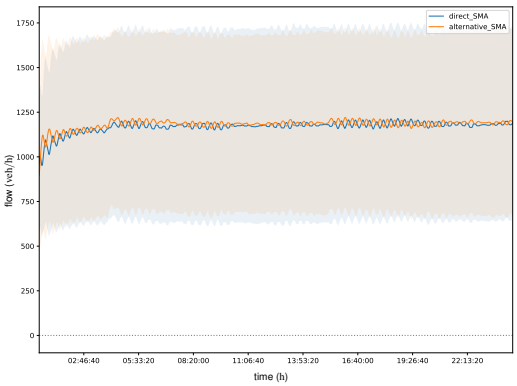


Fig. A.15-6. TrafficTraffic flow on each route, in vehicles per hour (veh/h), over a 24 h period, 4 h Simple Moving Average, mean (line) and standard deviation (shaded).

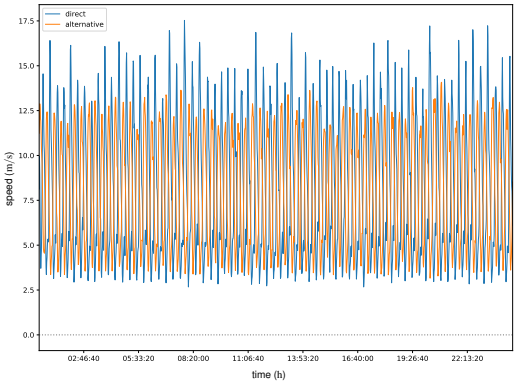


Fig. A.15-7. Mean speed on each route, in meters per second (m/s), aggregated to 1 min, over a 24 h period.

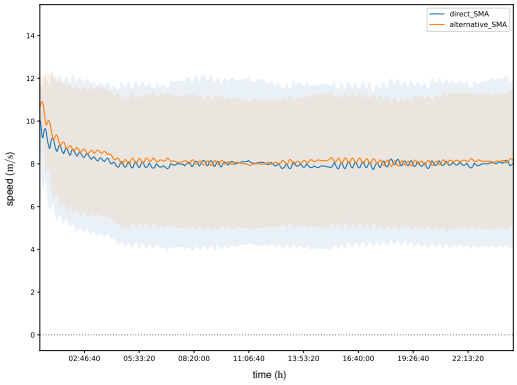


Fig. A.15-8. Mean speed on each route, in meters per second (m/s), aggregated to 1 min, over a 24 h period, 4 h Simple Moving Average, mean (line) and standard deviation (shaded).

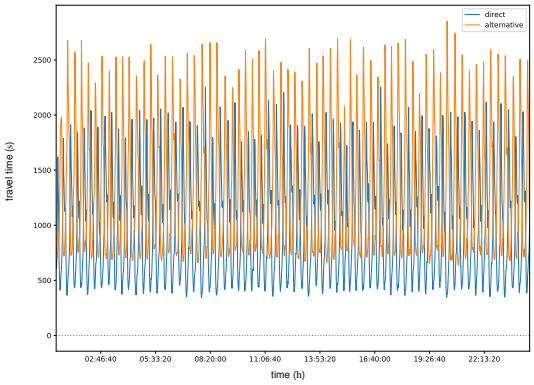


Fig. A.15-9. Travel times on each route, in seconds (s), aggregated to 1 min, over a 24 h period.

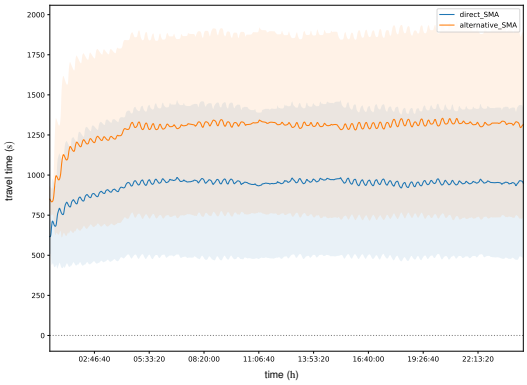


Fig. A.15-10. Travel times on each route, in seconds (s), aggregated to 1 min, over a 24 h period, 4 h Simple Moving Average, mean (line) and standard deviation (shaded).

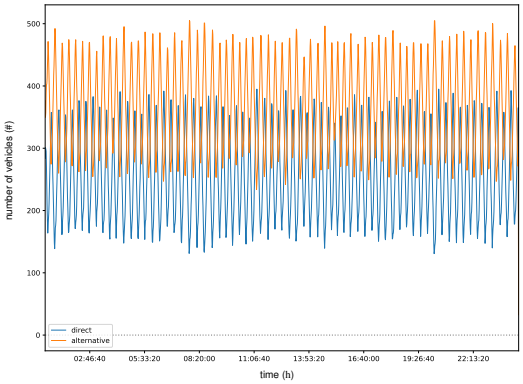


Fig. A.15-11. Average number of vehicles on each route, aggregated to 1 min, over a 24 h period.

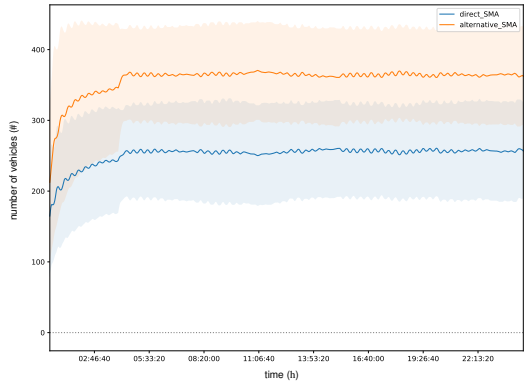


Fig. A.15-12. Average number of vehicles on each route, aggregated to 1 min, over a 24 h period, 4 h Simple Moving Average, mean (line) and standard deviation (shaded).

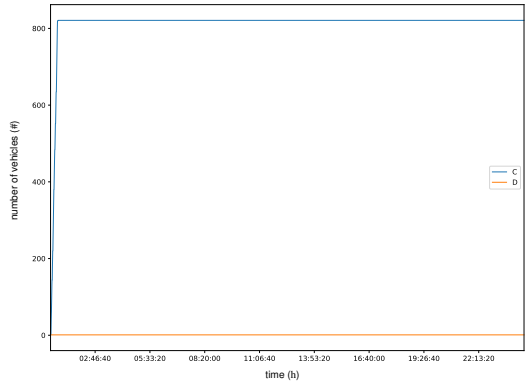


Fig. A.15-13. Evolution of the number of *Cooperators* and *Defectors* over a 24 h period.

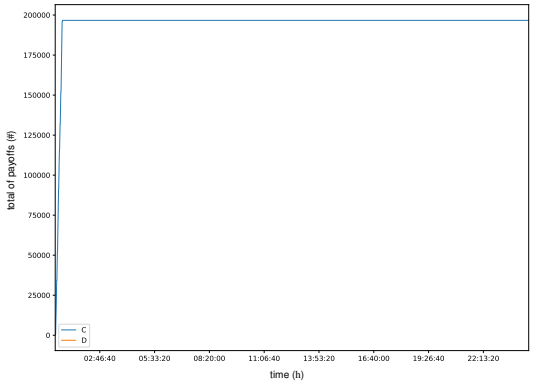


Fig. A.15-14. Evolution of total payoffs for *Cooperators* and *Defectors* (*individual payoff* times the *number of players receiving it*, $C(n) \times n$ and $D(n) \times (N-n)$, where n is the number of *Cooperators*), over a 24 h period.

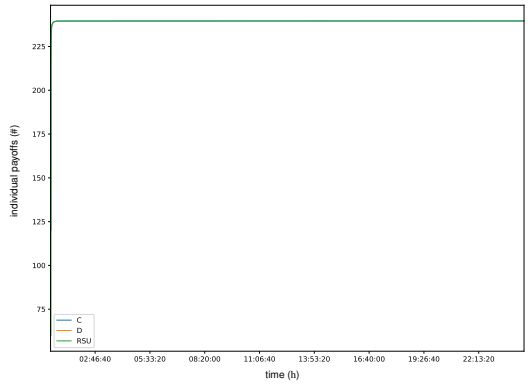


Fig. A.15-15. Evolution of the individual payoffs for *Cooperators, Defectors,* and *RSU* (always cooperating), over a 24 h period.

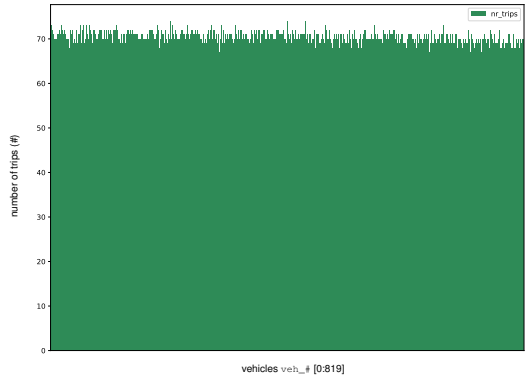


Fig. A.15-16. Number of trips made by each vehicle, during the simulation of a 24 h period.

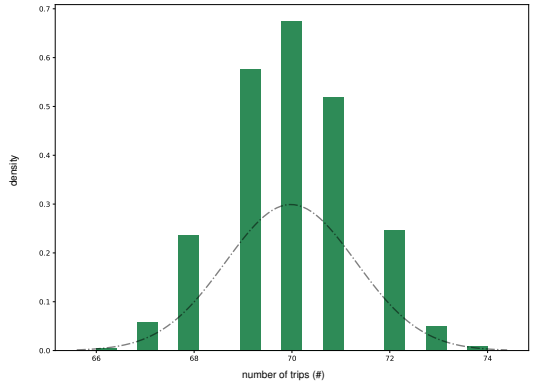


Fig. A.15-17. Density histogram of the number of trips made by each vehicle, during the simulation of a 24 h period, superimposing the normal density curve. The number of bins was calculated by the Freedman Diaconis rule.

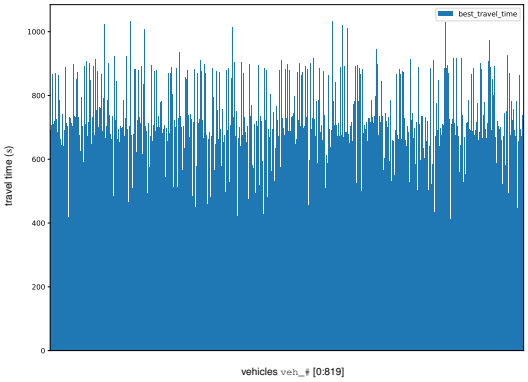


Fig. A.15-18. Best travel time for each vehicle, in seconds (s), during the simulation of a 24 h period.

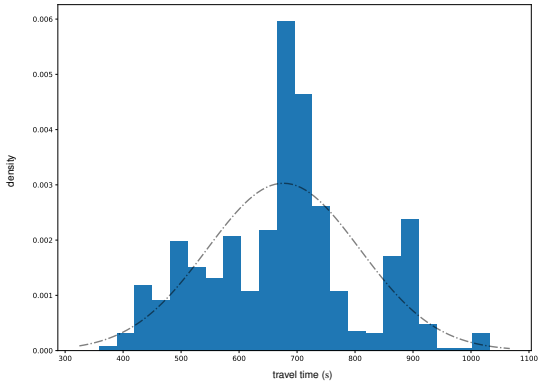


Fig. A.15-19. Density histogram of best travel time for vehicles, in seconds (s), during the simulation of a 24 h period, superimposing the normal density curve. The number of bins was calculated by the Freedman Diaconis rule.

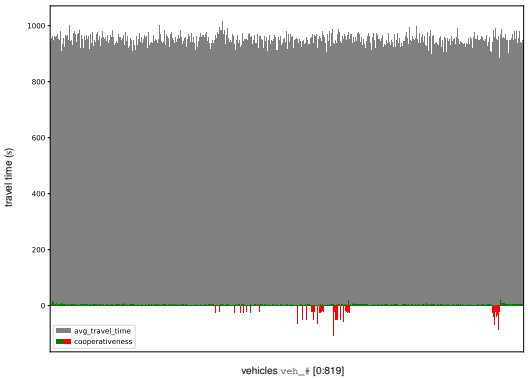


Fig. A.15-20. Average of the travel times, in seconds (s), of individual vehicles, during the simulation of a 24 h period. The bottom graph represents the *degree of cooperativeness**, downscaled by a normalization factor for the purpose of comparison with average times.

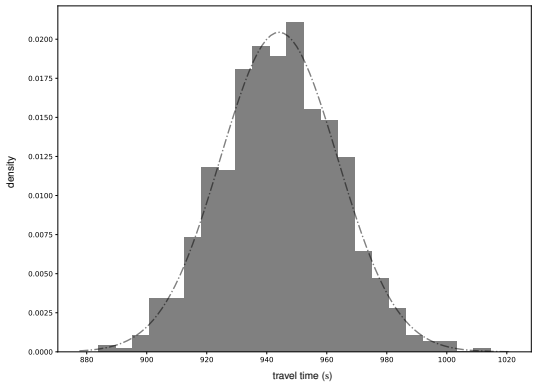


Fig. A.15-21. Density histogram of the average travel times, in seconds (s), of individual vehicles, during the simulation of a 24 h period, superimposing the normal density curve. The number of bins was calculated by the Freedman Diaconis rule.

* The *degree of cooperativeness* is a cumulative sum, calculated at each iteration, based on the complement of the ratio of cooperators, i.e., the higher the number of cooperators the less it increases, but the defectors are more penalized, and vice-versa. It varies inversely with the size of the group to which the player belongs.

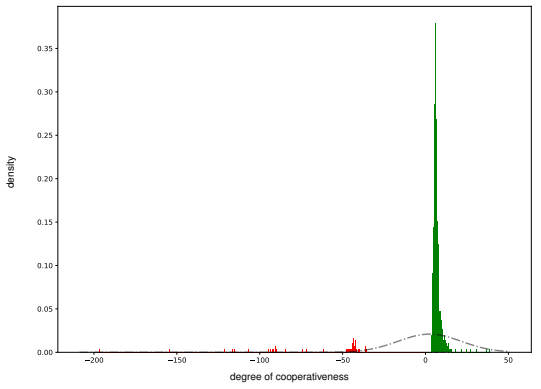


Fig. A.15-22. Density histogram of the *degree of cooperativeness** of individual vehicles, superimposing the normal density curve. The number of bins was calculated by the Freedman Diaconis rule. Generally, when strongly correlated with travel times, it presents a symmetric curve with respect to the *yy*-axis. Because some vehicles choose their preferred route immediately after the end of warmup, due to the gap between the RSU coverage and the route selection point, there may be some outliers.

A.16 `820veh-24h-04060000`

```
Scenario: scenario-1
Timestamp: 20210627T110342Z
Number of vehicles: 820 vehs
Simulation time: 24.0 h
Warm up end time: 1866.6 s; step 18665
Vehicle selection strategy: stochastic
RSU turned off: False
RSU strategy: end_of_queue_occupancy
Runner options:
   nogui: True
   step_length: 0.1
   seed: 19750808
   output_prefix: 820veh-24h-04060000
   sim_run_time: 24.0
   num_vehicles: 820
   warmup_speed: 13.96
   warmup_routes_weight: [473, 527]
   network_speed: 25.0
   change_behavior_probability: [0, 100]
   cooperation_probability: [0, 100]
   vehicle_selection_strategy: stochastic
   turn_rsu_off: False
   rsu_dynamic_dissemination: False
   rsu_dissemination_interval: 5
   rsu_probabilistic_dissemination: False
   rsu_suggestion_strategy: end_of_queue_occupancy
   rsu_routes_weight: [460, 540]
   rsu_moving_avg_size: 5
   travel_times_ttl: 60
   rsu_dissemination_ttl: 0
   rsu_send_travel_time_info: False
   payoff_matrix: [360.0, 240.0, 0.0, -120.0]
   roth_erev_parameters: [0.1, 0.15]
   rsu_change_dissemination: False
   rsu_change_dissemination_steps: [14400, 28800, 43200, 57600, 72000]
   rsu_change_dissemination_intervals: [10, 20, 40, 80, 160]
Network Mean speed after warmup:
   Max: 10.62
   Min: 4.34
```

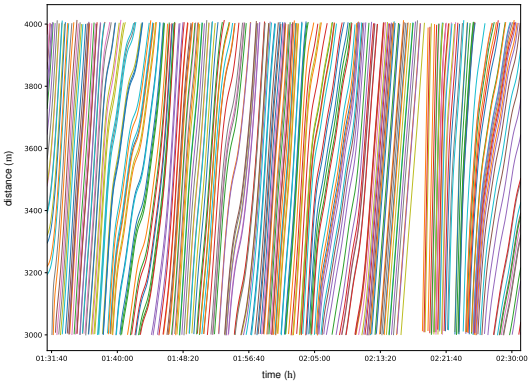


Fig. A.16-1. Time-Space diagram, for the one hour period after the end of the warmup, from 1:00:00 to 2:00:00 simulation time, plotted for the data from the sensor placed in the middle of the *direct* route (between 3000 m and 4000 m). In the case of an overloaded network, congestion shock waves can be observed.

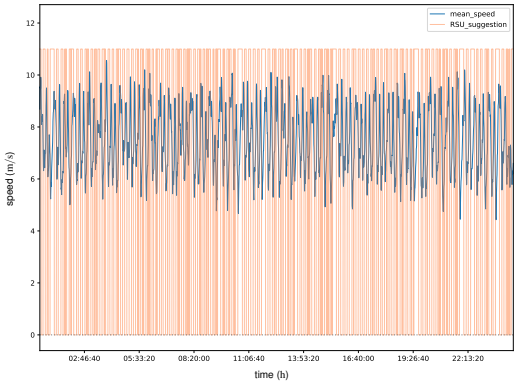


Fig. A.16-2. Mean speed in the network, in meters per second (m/s), over a 24 h period, superimposing (vertically, in orange) the time instants in which the RSU issued a recommendation to follow the *alternative* route.

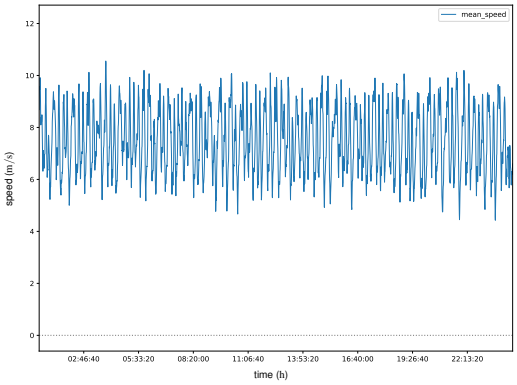


Fig. A.16-3. Mean speed in the network, in meters per second (m/s), over a 24 h period.

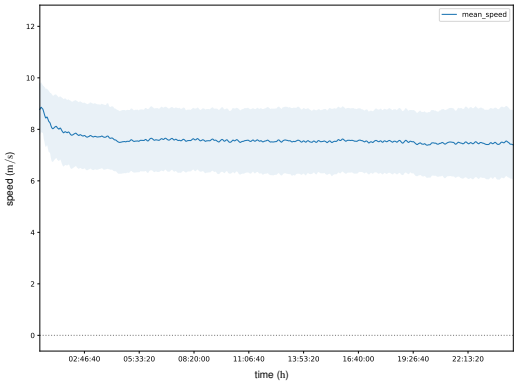


Fig. A.16-4. Mean speed in the network, in meters per second (m/s), over a 24 h period, 4 h Simple Moving Average, mean (line) and standard deviation (shaded).

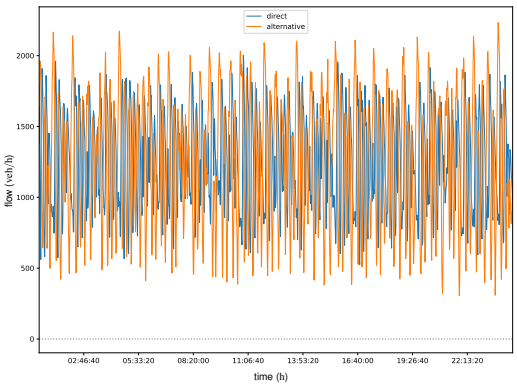


Fig. A.16-5. Traffic flow on each route, in vehicles per hour (veh/h), over a 24 h period.

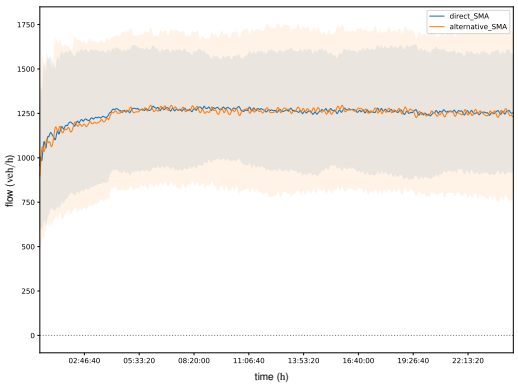


Fig. A.16-6. TrafficTraffic flow on each route, in vehicles per hour (veh/h), over a 24 h period, 4 h Simple Moving Average, mean (line) and standard deviation (shaded).

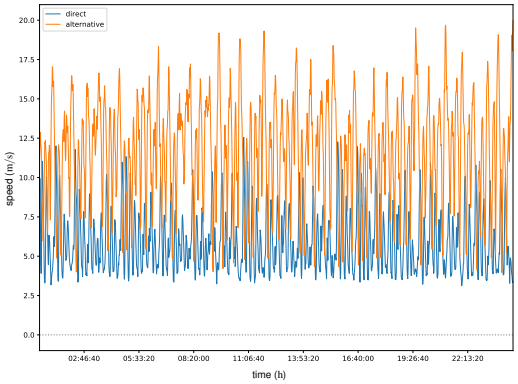


Fig. A.16-7. Mean speed on each route, in meters per second (m/s), aggregated to 1 min, over a 24 h period.

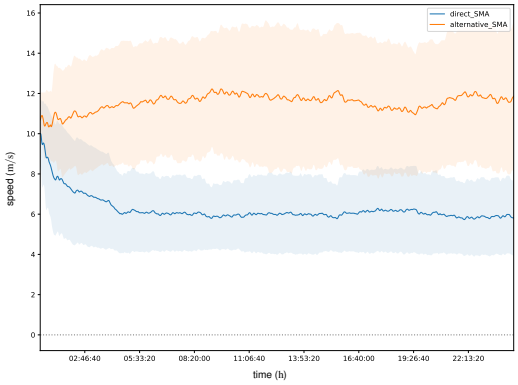


Fig. A.16-8. Mean speed on each route, in meters per second (m/s), aggregated to 1 min, over a 24 h period, 4 h Simple Moving Average, mean (line) and standard deviation (shaded).

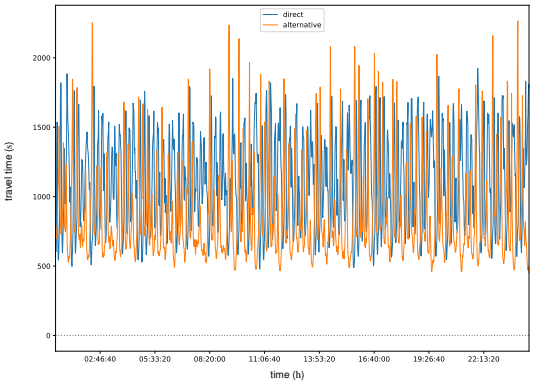


Fig. A.16-9. Travel times on each route, in seconds (s), aggregated to 1 min, over a 24 h period.

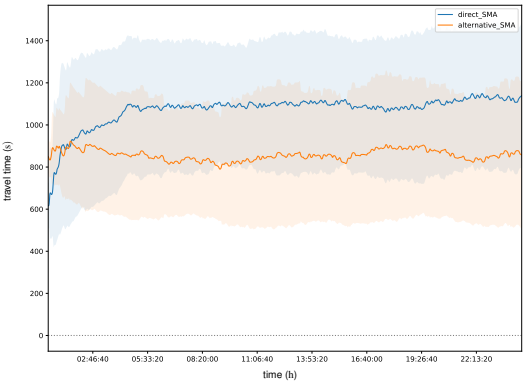


Fig. A.16-10. Travel times on each route, in seconds (s), aggregated to 1 min, over a 24 h period, 4 h Simple Moving Average, mean (line) and standard deviation (shaded).

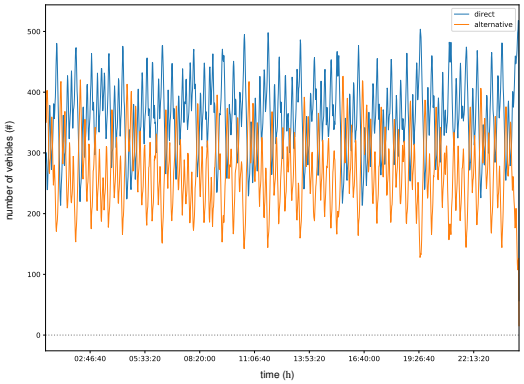


Fig. A.16-11. Average number of vehicles on each route, aggregated to 1 min, over a 24 h period.

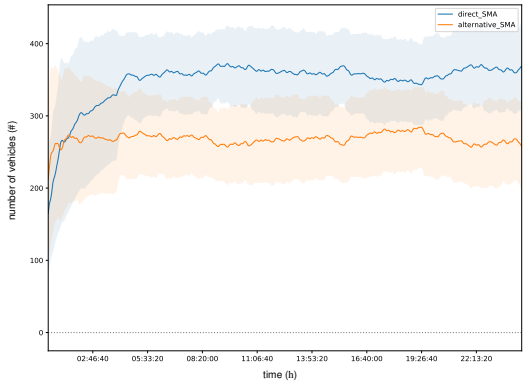


Fig. A.16-12. Average number of vehicles on each route, aggregated to 1 min, over a 24 h period, 4 h Simple Moving Average, mean (line) and standard deviation (shaded).

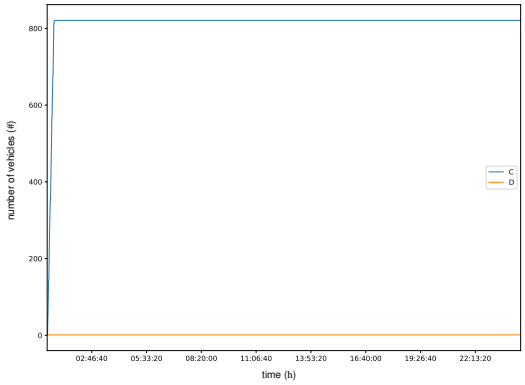


Fig. A.16-13. Evolution of the number of *Cooperators* and *Defectors* over a 24 h period.

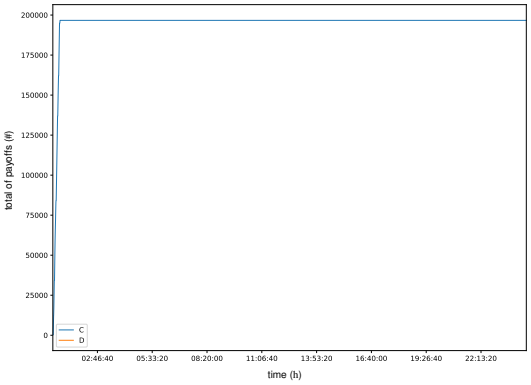


Fig. A.16-14. Evolution of total payoffs for *Cooperators* and *Defectors* (*individual payoff* times the *number of players receiving it*, $C(n) \times n$ and $D(n) \times (N-n)$, where n is the number of *Cooperators*), over a 24 h period.

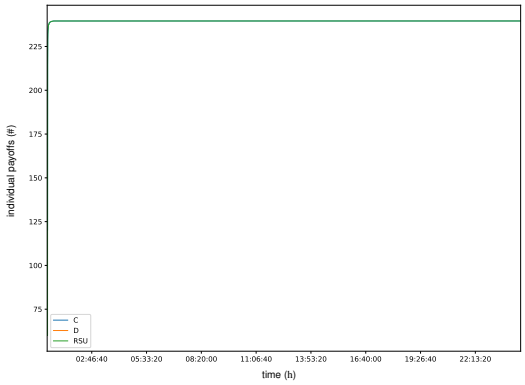


Fig. A.16-15. Evolution of the individual payoffs for *Cooperators, Defectors,* and *RSU* (always cooperating), over a 24 h period.

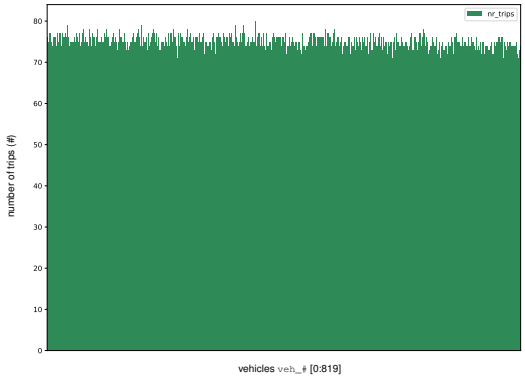


Fig. A.16-16. Number of trips made by each vehicle, during the simulation of a 24 h period.

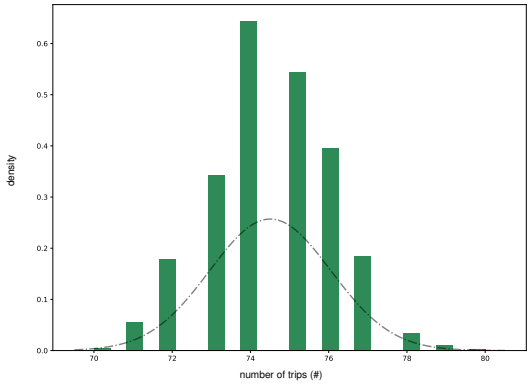


Fig. A.16-17. Density histogram of the number of trips made by each vehicle, during the simulation of a 24 h period, superimposing the normal density curve. The number of bins was calculated by the Freedman Diaconis rule.

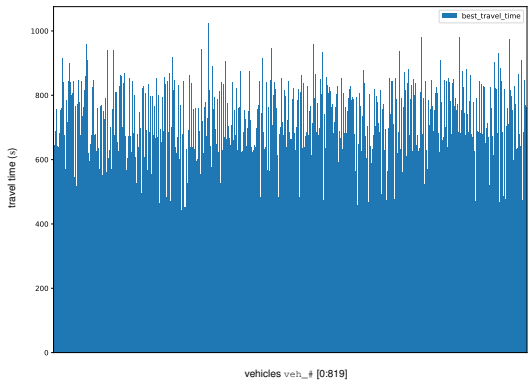


Fig. A.16-18. Best travel time for each vehicle, in seconds (s), during the simulation of a 24 h period.

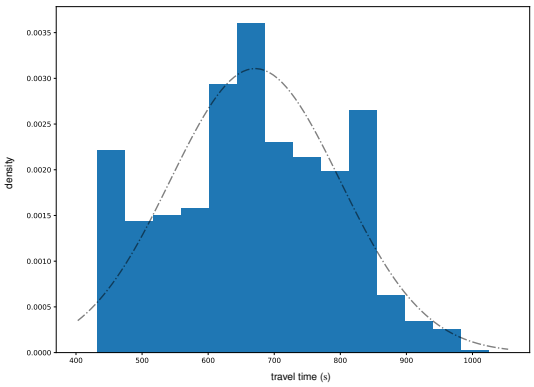


Fig. A.16-19. Density histogram of best travel time for vehicles, in seconds (s), during the simulation of a 24 h period, superimposing the normal density curve. The number of bins was calculated by the Freedman Diaconis rule.

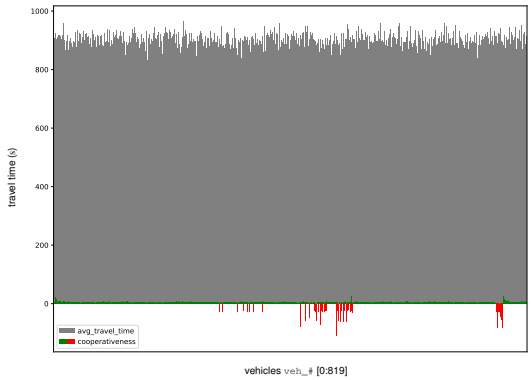


Fig. A.16-20. Average of the travel times, in seconds (s), of individual vehicles, during the simulation of a 24 h period. The bottom graph represents the *degree of cooperativeness**, downscaled by a normalization factor for the purpose of comparison with average times.

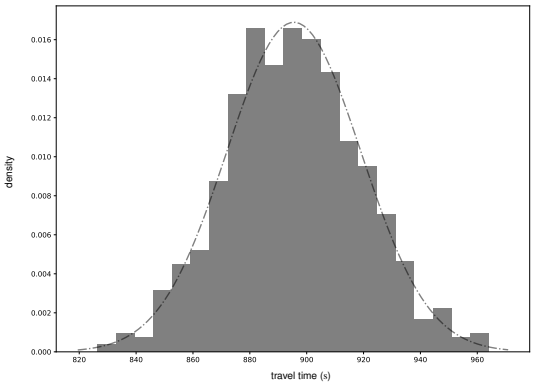


Fig. A.16-21. Density histogram of the average travel times, in seconds (s), of individual vehicles, during the simulation of a 24 h period, superimposing the normal density curve. The number of bins was calculated by the Freedman Diaconis rule.

* The *degree of cooperativeness* is a cumulative sum, calculated at each iteration, based on the complement of the ratio of cooperators, i.e., the higher the number of cooperators the less it increases, but the defectors are more penalized, and vice-versa. It varies inversely with the size of the group to which the player belongs.

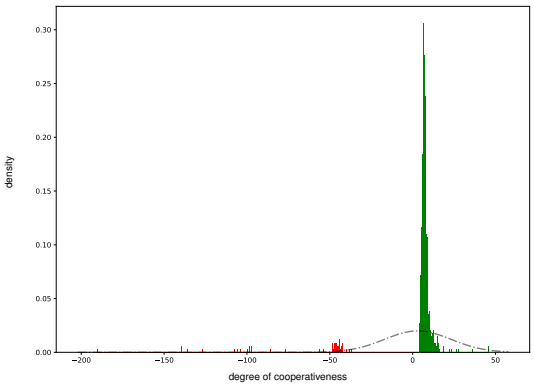


Fig. A.16-22. Density histogram of the *degree of cooperativeness** of individual vehicles, superimposing the normal density curve. The number of bins was calculated by the Freedman Diaconis rule. Generally, when strongly correlated with travel times, it presents a symmetric curve with respect to the *yy*-axis. Because some vehicles choose their preferred route immediately after the end of warmup, due to the gap between the RSU coverage and the route selection point, there may be some outliers.

A.17 820veh-24h-05060000

```
Scenario: scenario-1
Timestamp: 20210522T085901Z
Number of vehicles: 820 vehs
Simulation time: 24.0 h
Warm up end time: 1866.6 s; step 18665
Vehicle selection strategy: stochastic
RSU turned off: False
RSU strategy: travel_time_simple
Runner options:
   nogui: True
   step_length: 0.1
   seed: 19750808
   output_prefix: 820veh-24h-05060000
   sim_run_time: 24.0
   num_vehicles: 820
   warmup_speed: 13.96
   warmup_routes_weight: [473, 527]
   network_speed: 25.0
   change_behavior_probability: [0, 100]
   cooperation_probability: [0, 100]
   vehicle_selection_strategy: stochastic
   turn_rsu_off: False
   rsu_dynamic_dissemination: False
   rsu_dissemination_interval: 5
   rsu_probabilistic_dissemination: False
   rsu_suggestion_strategy: travel_time_simple
   rsu_routes_weight: [460, 540]
   rsu_moving_avg_size: 5
   travel_times_ttl: 60
   rsu_dissemination_ttl: 0
   rsu_send_travel_time_info: False
   payoff_matrix: [360.0, 240.0, 0.0, -120.0]
   roth_erev_parameters: [0.1, 0.15]
Network Mean speed after warmup:
   Max: 10.77
   Min: 1.87
```

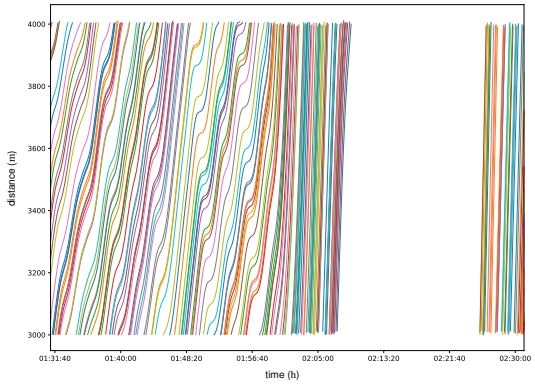


Fig. A.17-1. Time-Space diagram, for the one hour period after the end of the warmup, from 1:00:00 to 2:00:00 simulation time, plotted for the data from the sensor placed in the middle of the *direct* route (between 3000 m and 4000 m). In the case of an overloaded network, congestion shock waves can be observed.

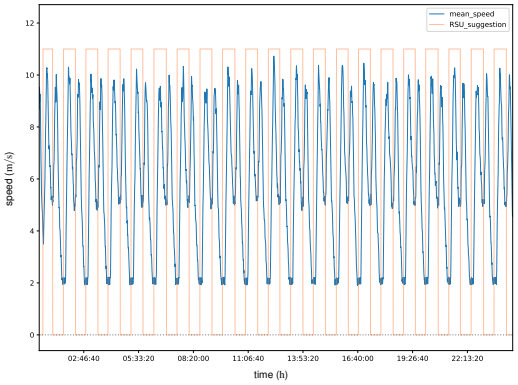


Fig. A.17-2. Mean speed in the network, in meters per second (m/s), over a 24 h period, superimposing (vertically, in orange) the time instants in which the RSU issued a recommendation to follow the *alternative* route.

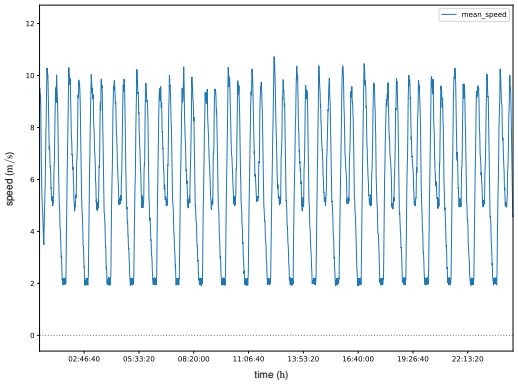


Fig. A.17-3. Mean speed in the network, in meters per second (m/s), over a 24 h period.

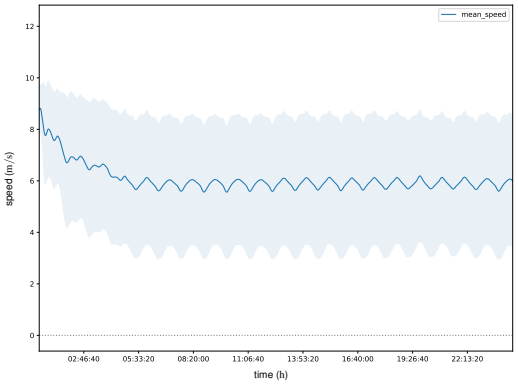


Fig. A.17-4. Mean speed in the network, in meters per second (m/s), over a 24 h period, 4 h Simple Moving Average, mean (line) and standard deviation (shaded).

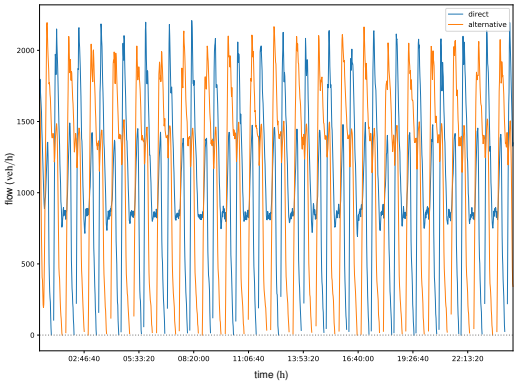


Fig. A.17-5. Traffic flow on each route, in vehicles per hour (veh/h), over a 24 h period.

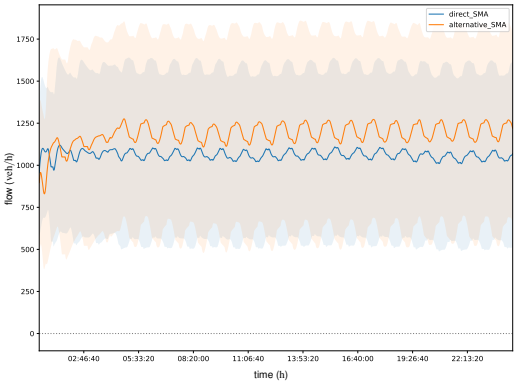


Fig. A.17-6. TrafficTraffic flow on each route, in vehicles per hour (veh/h), over a 24 h period, 4 h Simple Moving Average, mean (line) and standard deviation (shaded).

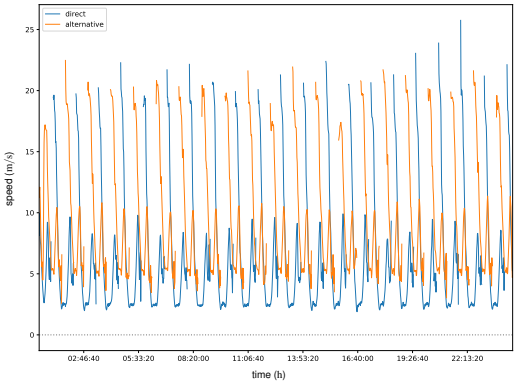


Fig. A.17-7. Mean speed on each route, in meters per second (m/s), aggregated to 1 min, over a 24 h period.

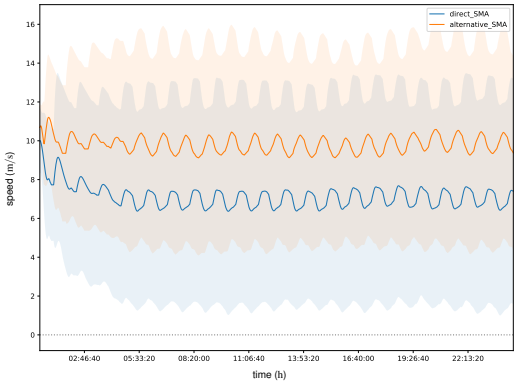


Fig. A.17-8. Mean speed on each route, in meters per second (m/s), aggregated to 1 min, over a 24 h period, 4 h Simple Moving Average, mean (line) and standard deviation (shaded).

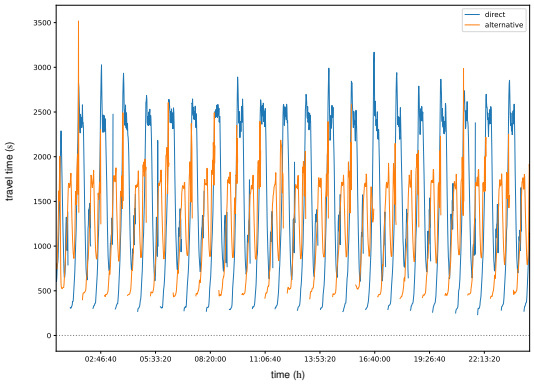


Fig. A.17-9. Travel times on each route, in seconds (s), aggregated to 1 min, over a 24 h period.

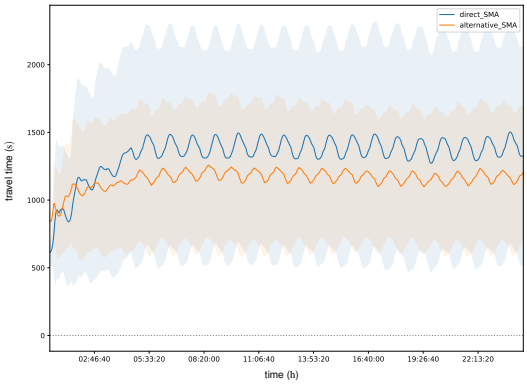


Fig. A.17-10. Travel times on each route, in seconds (s), aggregated to 1 min, over a 24 h period, 4 h Simple Moving Average, mean (line) and standard deviation (shaded).

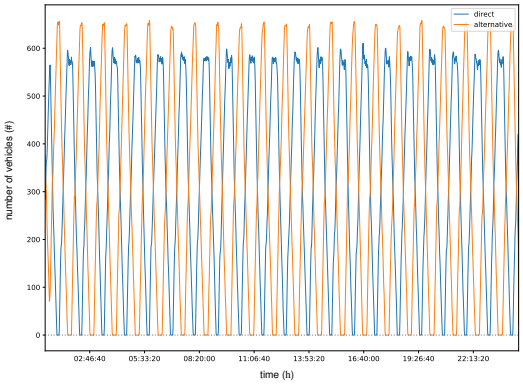


Fig. A.17-11. Average number of vehicles on each route, aggregated to 1 min, over a 24 h period.

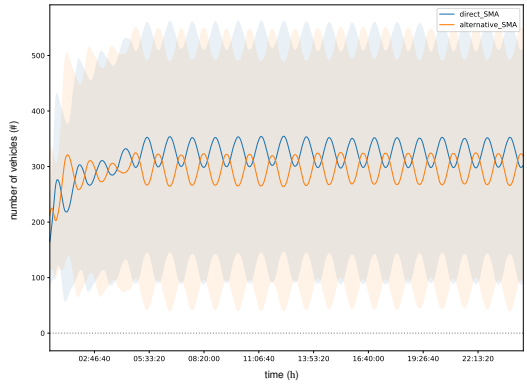


Fig. A.17-12. Average number of vehicles on each route, aggregated to 1 min, over a 24 h period, 4 h Simple Moving Average, mean (line) and standard deviation (shaded).

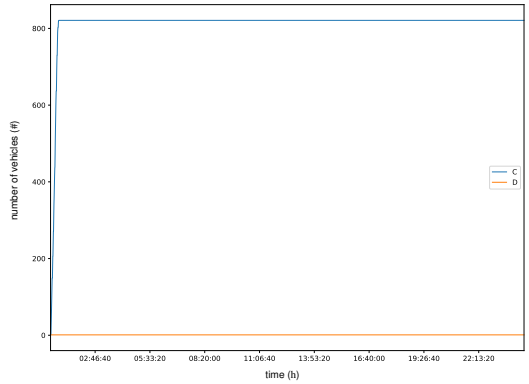


Fig. A.17-13. Evolution of the number of *Cooperators* and *Defectors* over a 24 h period.

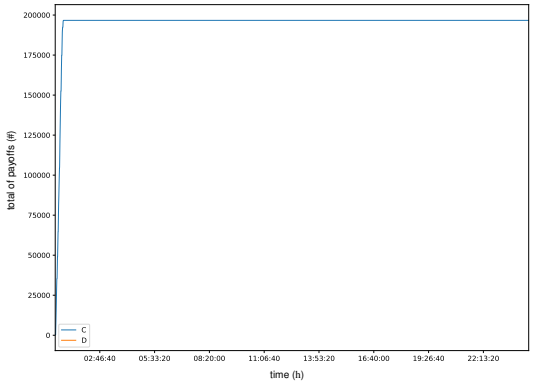


Fig. A.17-14. Evolution of total payoffs for *Cooperators* and *Defectors* (*individual payoff* times the *number of players receiving it*, $C(n) \times n$ and $D(n) \times (N-n)$, where n is the number of *Cooperators*), over a 24 h period.

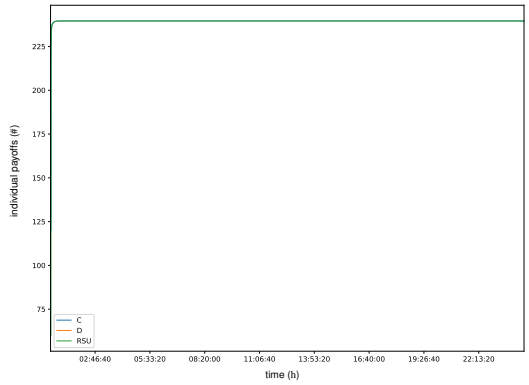


Fig. A.17-15. Evolution of the individual payoffs for *Cooperators, Defectors,* and *RSU* (always cooperating), over a 24 h period.

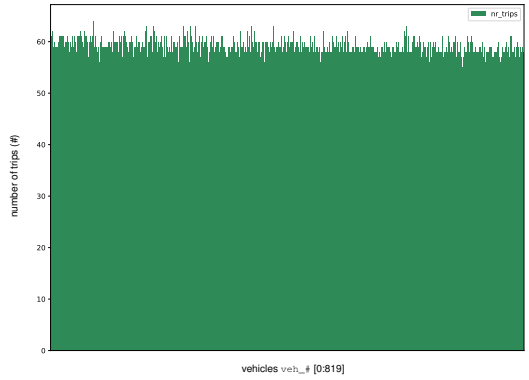


Fig. A.17-16. Number of trips made by each vehicle, during the simulation of a 24 h period.

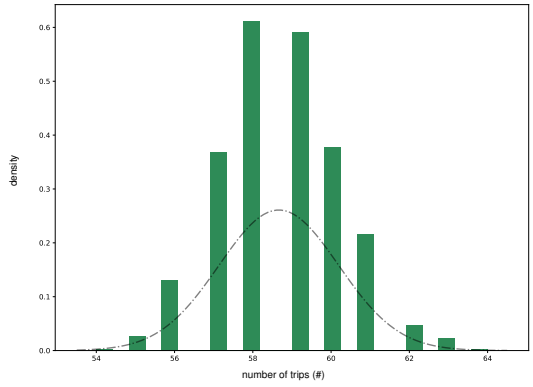


Fig. A.17-17. Density histogram of the number of trips made by each vehicle, during the simulation of a 24 h period, superimposing the normal density curve. The number of bins was calculated by the Freedman Diaconis rule.

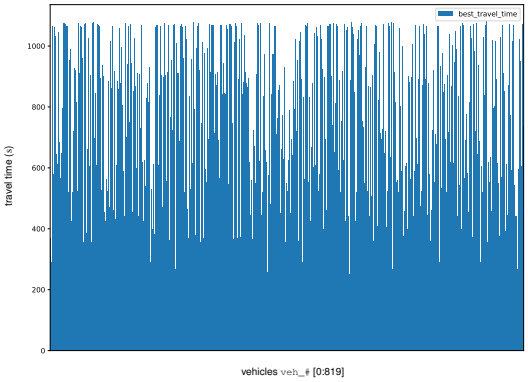


Fig. A.17-18. Best travel time for each vehicle, in seconds (s), during the simulation of a 24 h period.

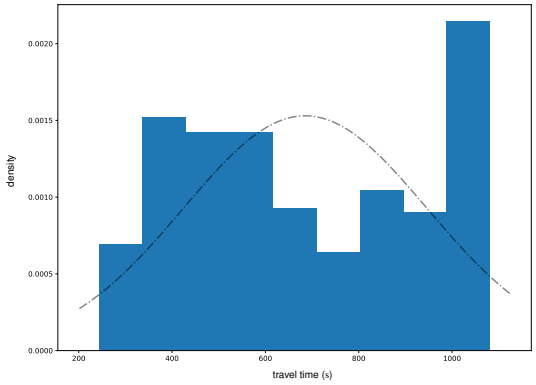


Fig. A.17-19. Density histogram of best travel time for vehicles, in seconds (s), during the simulation of a 24 h period, superimposing the normal density curve. The number of bins was calculated by the Freedman Diaconis rule.

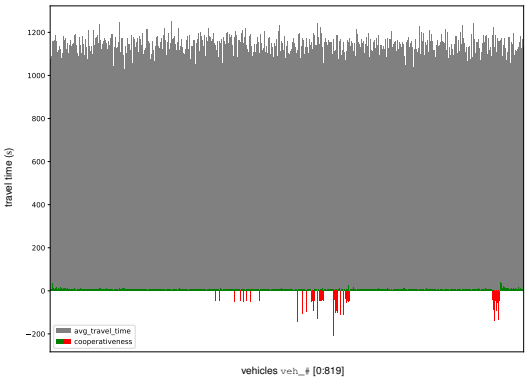


Fig. A.17-20. Average of the travel times, in seconds (s), of individual vehicles, during the simulation of a 24 h period. The bottom graph represents the *degree of cooperativeness**, downscaled by a normalization factor for the purpose of comparison with average times.

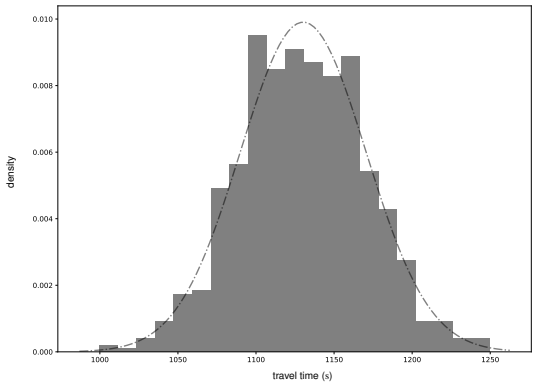


Fig. A.17-21. Density histogram of the average travel times, in seconds (s), of individual vehicles, during the simulation of a 24 h period, superimposing the normal density curve. The number of bins was calculated by the Freedman Diaconis rule.

* The *degree of cooperativeness* is a cumulative sum, calculated at each iteration, based on the complement of the ratio of cooperators, i.e., the higher the number of cooperators the less it increases, but the defectors are more penalized, and vice-versa. It varies inversely with the size of the group to which the player belongs.

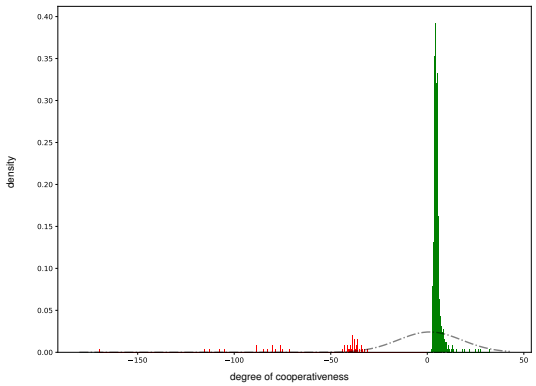


Fig. A.17-22. Density histogram of the *degree of cooperativeness** of individual vehicles, superimposing the normal density curve. The number of bins was calculated by the Freedman Diaconis rule. Generally, when strongly correlated with travel times, it presents a symmetric curve with respect to the *yy*-axis. Because some vehicles choose their preferred route immediately after the end of warmup, due to the gap between the RSU coverage and the route selection point, there may be some outliers.

A.18 `820veh-24h-06060000`

```
Scenario: scenario-1
Timestamp: 20210522T092542Z
Number of vehicles: 820 vehs
Simulation time: 24.0 h
Warm up end time: 1866.6 s; step 18665
Vehicle selection strategy: stochastic
RSU turned off: False
RSU strategy: travel_time_product
Runner options:
   nogui: True
   step_length: 0.1
   seed: 19750808
   output_prefix: 820veh-24h-06060000
   sim_run_time: 24.0
   num_vehicles: 820
   warmup_speed: 13.96
   warmup_routes_weight: [473, 527]
   network_speed: 25.0
   change_behavior_probability: [0, 100]
   cooperation_probability: [0, 100]
   vehicle_selection_strategy: stochastic
   turn_rsu_off: False
   rsu_dynamic_dissemination: False
   rsu_dissemination_interval: 5
   rsu_probabilistic_dissemination: False
   rsu_suggestion_strategy: travel_time_product
   rsu_routes_weight: [460, 540]
   rsu_moving_avg_size: 5
   travel_times_ttl: 60
   rsu_dissemination_ttl: 0
   rsu_send_travel_time_info: False
   payoff_matrix: [360.0, 240.0, 0.0, -120.0]
   roth_erev_parameters: [0.1, 0.15]
Network Mean speed after warmup:
   Max: 9.82
   Min: 3.75
```

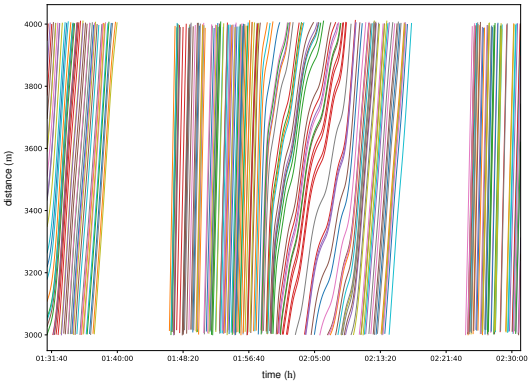


Fig. A.18-1. Time-Space diagram, for the one hour period after the end of the warmup, from 1:00:00 to 2:00:00 simulation time, plotted for the data from the sensor placed in the middle of the *direct* route (between 3000 m and 4000 m). In the case of an overloaded network, congestion shock waves can be observed.

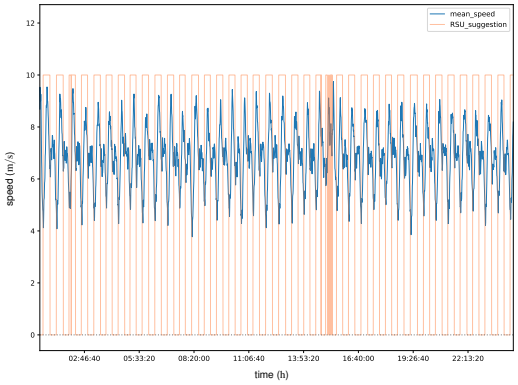


Fig. A.18-2. Mean speed in the network, in meters per second (m/s), over a 24 h period, superimposing (vertically, in orange) the time instants in which the RSU issued a recommendation to follow the *alternative* route.

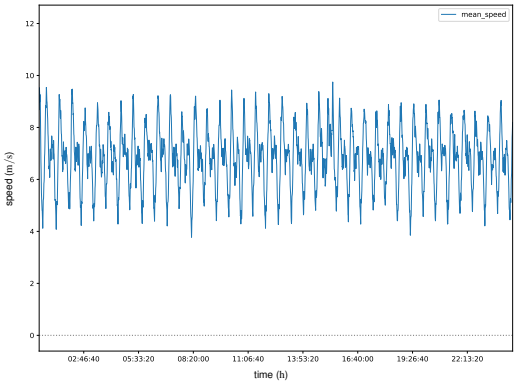


Fig. A.18-3. Mean speed in the network, in meters per second (m/s), over a 24 h period.

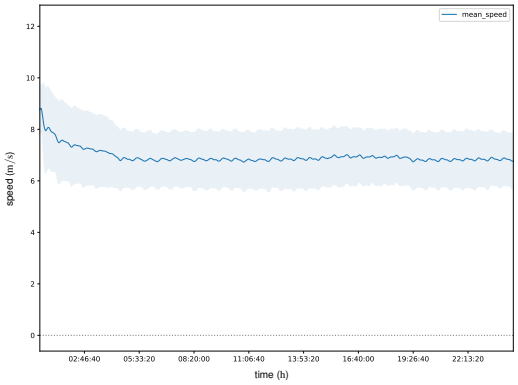


Fig. A.18-4. Mean speed in the network, in meters per second (m/s), over a 24 h period, 4 h Simple Moving Average, mean (line) and standard deviation (shaded).

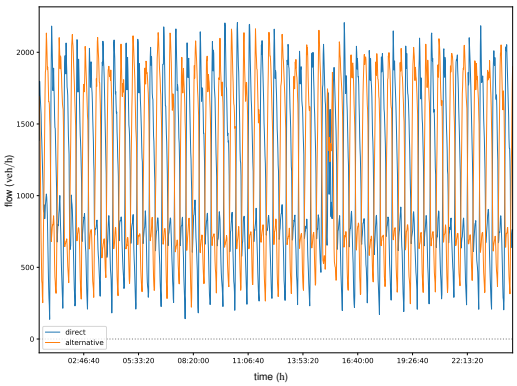


Fig. A.18-5. Traffic flow on each route, in vehicles per hour (veh/h), over a 24 h period.

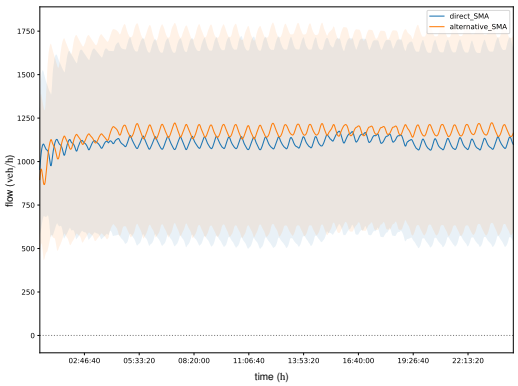


Fig. A.18-6. TrafficTraffic flow on each route, in vehicles per hour (veh/h), over a 24 h period, 4 h Simple Moving Average, mean (line) and standard deviation (shaded).

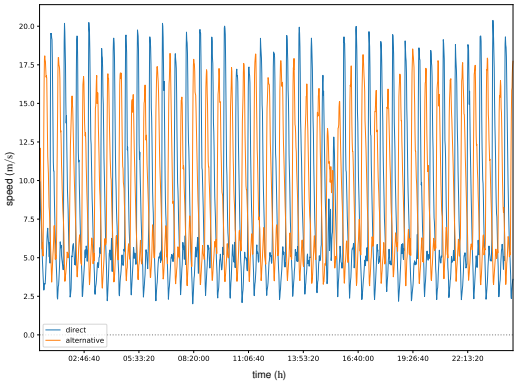


Fig. A.18-7. Mean speed on each route, in meters per second (m/s), aggregated to 1 min, over a 24 h period.

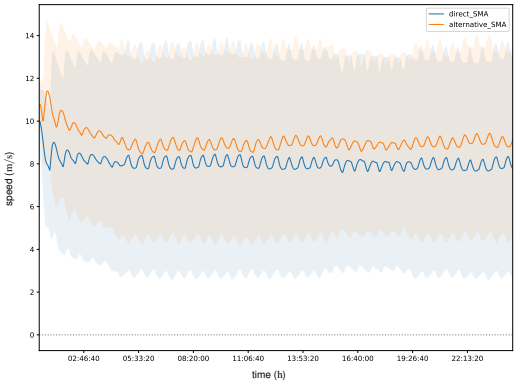


Fig. A.18-8. Mean speed on each route, in meters per second (m/s), aggregated to 1 min, over a 24 h period, 4 h Simple Moving Average, mean (line) and standard deviation (shaded).

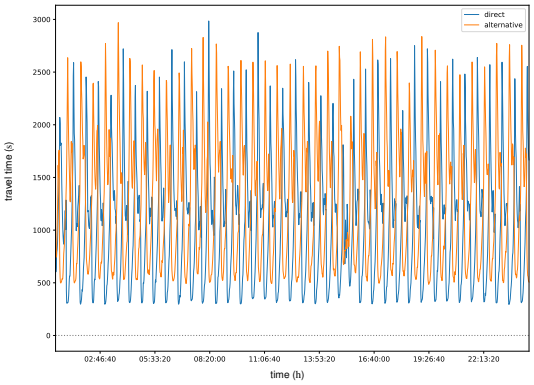


Fig. A.18-9. Travel times on each route, in seconds (s), aggregated to 1 min, over a 24 h period.

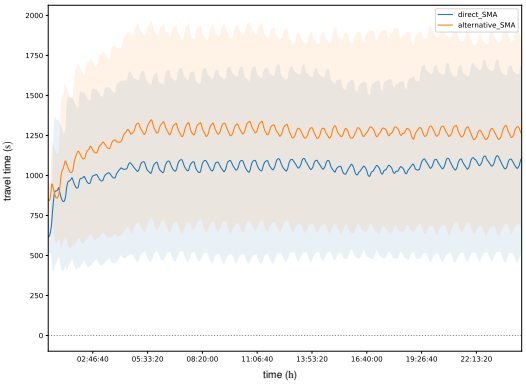


Fig. A.18-10. Travel times on each route, in seconds (s), aggregated to 1 min, over a 24 h period, 4 h Simple Moving Average, mean (line) and standard deviation (shaded).

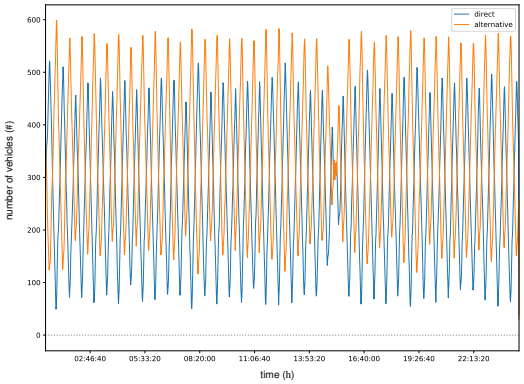


Fig. A.18-11. Average number of vehicles on each route, aggregated to 1 min, over a 24 h period.

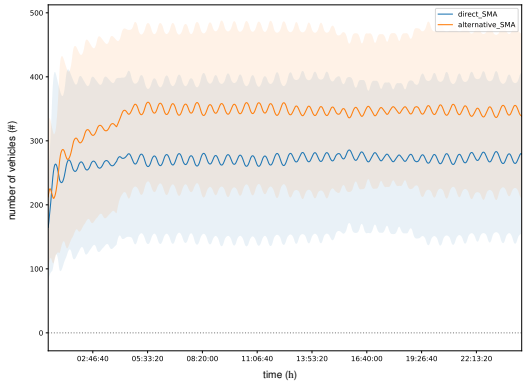


Fig. A.18-12. Average number of vehicles on each route, aggregated to 1 min, over a 24 h period, 4 h Simple Moving Average, mean (line) and standard deviation (shaded).

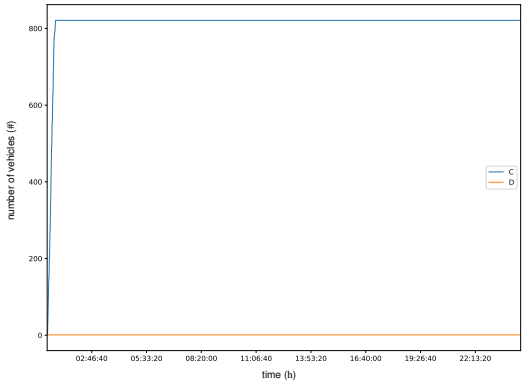


Fig. A.18-13. Evolution of the number of *Cooperators* and *Defectors* over a 24 h period.

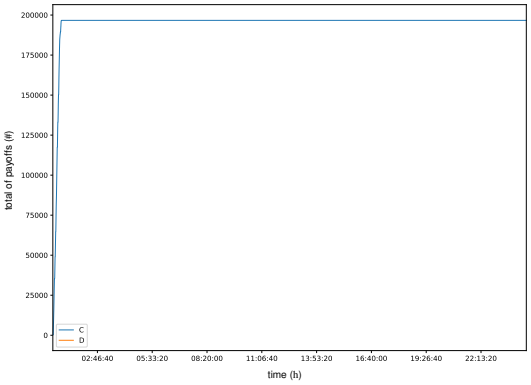


Fig. A.18-14. Evolution of total payoffs for *Cooperators* and *Defectors* (*individual payoff* times the *number of players receiving it*, $C(n) \times n$ and $D(n) \times (N-n)$, where n is the number of *Cooperators*), over a 24 h period.

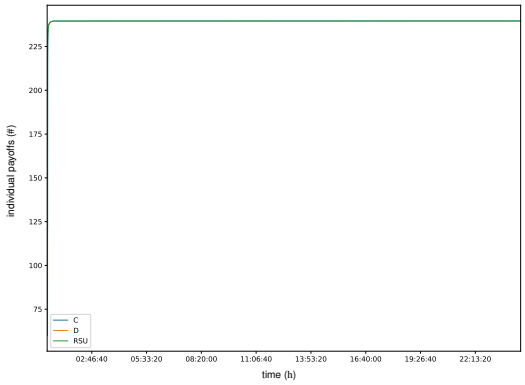


Fig. A.18-15. Evolution of the individual payoffs for *Cooperators, Defectors,* and *RSU* (always cooperating), over a 24 h period.

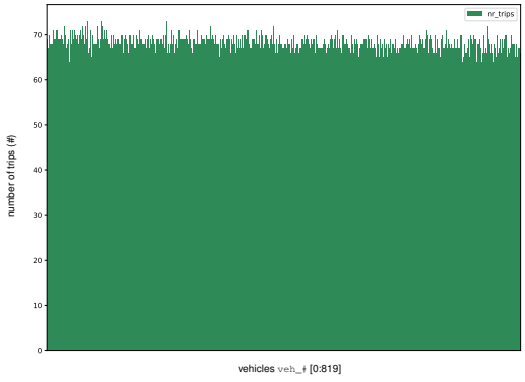


Fig. A.18-16. Number of trips made by each vehicle, during the simulation of a 24 h period.

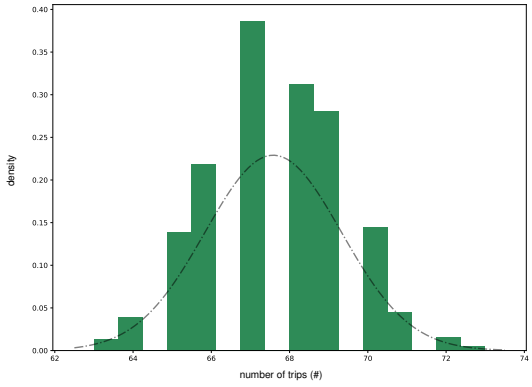


Fig. A.18-17. Density histogram of the number of trips made by each vehicle, during the simulation of a 24 h period, superimposing the normal density curve. The number of bins was calculated by the Freedman Diaconis rule.

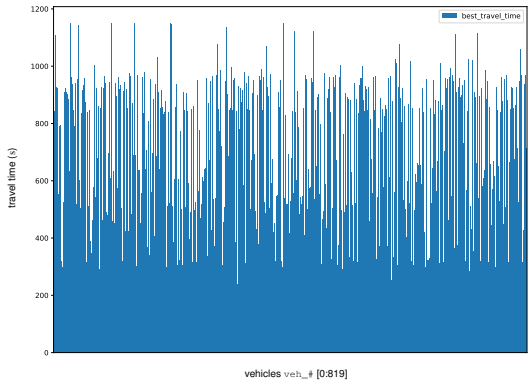


Fig. A.18-18. Best travel time for each vehicle, in seconds (s), during the simulation of a 24 h period.

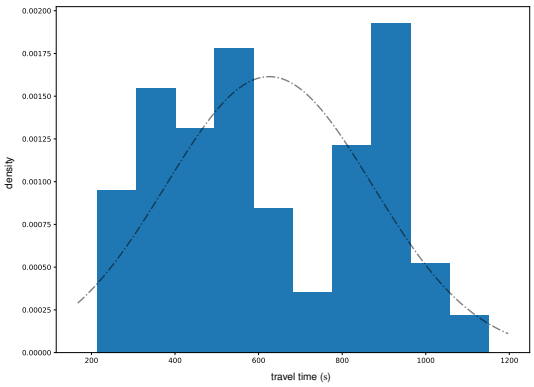


Fig. A.18-19. Density histogram of best travel time for vehicles, in seconds (s), during the simulation of a 24 h period, superimposing the normal density curve. The number of bins was calculated by the Freedman Diaconis rule.

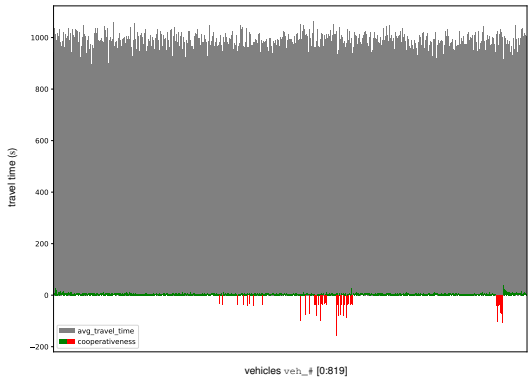


Fig. A.18-20. Average of the travel times, in seconds (s), of individual vehicles, during the simulation of a 24 h period. The bottom graph represents the *degree of cooperativeness**, downscaled by a normalization factor for the purpose of comparison with average times.

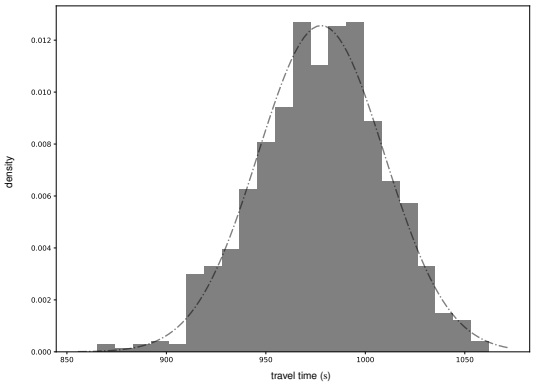


Fig. A.18-21. Density histogram of the average travel times, in seconds (s), of individual vehicles, during the simulation of a 24 h period, superimposing the normal density curve. The number of bins was calculated by the Freedman Diaconis rule.

* The *degree of cooperativeness* is a cumulative sum, calculated at each iteration, based on the complement of the ratio of cooperators, i.e., the higher the number of cooperators the less it increases, but the defectors are more penalized, and vice-versa. It varies inversely with the size of the group to which the player belongs.

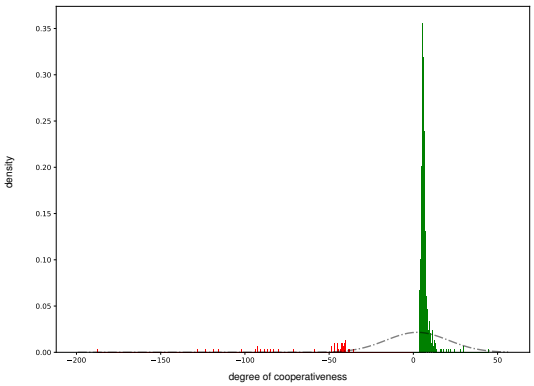


Fig. A.18-22. Density histogram of the *degree of cooperativeness** of individual vehicles, superimposing the normal density curve. The number of bins was calculated by the Freedman Diaconis rule. Generally, when strongly correlated with travel times, it presents a symmetric curve with respect to the *yy*-axis. Because some vehicles choose their preferred route immediately after the end of warmup, due to the gap between the RSU coverage and the route selection point, there may be some outliers.

A.19 820veh-24h-07060000

```
Scenario: scenario-1
Timestamp: 20210522T113645Z
Number of vehicles: 820 vehs
Simulation time: 24.0 h
Warm up end time: 1866.6 s; step 18665
Vehicle selection strategy: stochastic
RSU turned off: False
RSU strategy: travel_time_moving_average_simple
Runner options:
   nogui: True
   step_length: 0.1
   seed: 19750808
   output_prefix: 820veh-24h-07060000
   sim_run_time: 24.0
   num_vehicles: 820
   warmup_speed: 13.96
   warmup_routes_weight: [473, 527]
   network_speed: 25.0
   change_behavior_probability: [0, 100]
   cooperation_probability: [0, 100]
   vehicle_selection_strategy: stochastic
   turn_rsu_off: False
   rsu_dynamic_dissemination: False
   rsu_dissemination_interval: 5
   rsu_probabilistic_dissemination: False
   rsu_suggestion_strategy: travel_time_moving_average_simple
   rsu_routes_weight: [460, 540]
   rsu_moving_avg_size: 5
   travel_times_ttl: 60
   rsu_dissemination_ttl: 0
   rsu_send_travel_time_info: False
   payoff_matrix: [360.0, 240.0, 0.0, -120.0]
   roth_erev_parameters: [0.1, 0.15]
Network Mean speed after warmup:
   Max: 10.67
   Min: 1.87
```

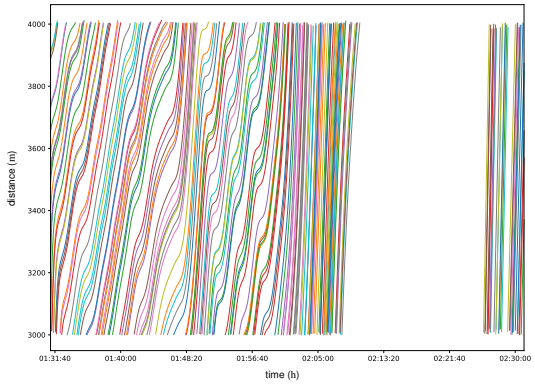


Fig. A.19-1. Time-Space diagram, for the one hour period after the end of the warmup, from 1:00:00 to 2:00:00 simulation time, plotted for the data from the sensor placed in the middle of the *direct* route (between 3000 m and 4000 m). In the case of an overloaded network, congestion shock waves can be observed.

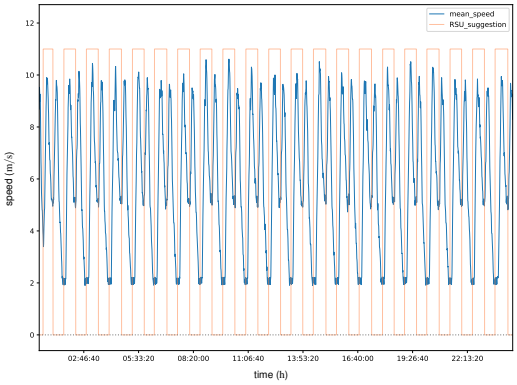


Fig. A.19-2. Mean speed in the network, in meters per second (m/s), over a 24 h period, superimposing (vertically, in orange) the time instants in which the RSU issued a recommendation to follow the *alternative* route.

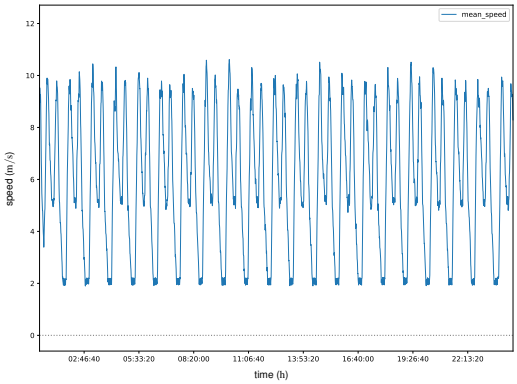


Fig. A.19-3. Mean speed in the network, in meters per second (m/s), over a 24 h period.

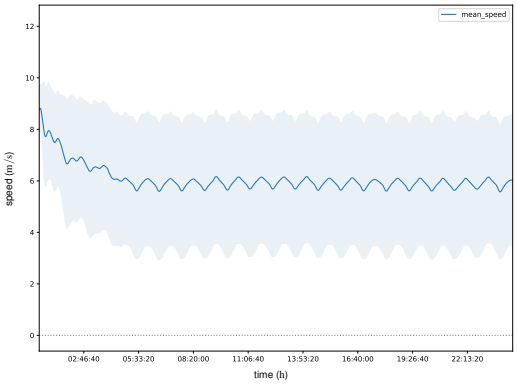


Fig. A.19-4. Mean speed in the network, in meters per second (m/s), over a 24 h period, 4 h Simple Moving Average, mean (line) and standard deviation (shaded).

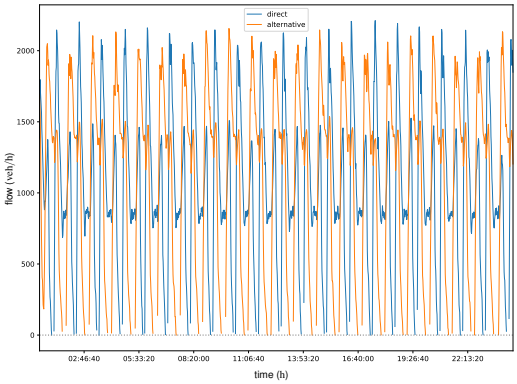


Fig. A.19-5. Traffic flow on each route, in vehicles per hour (veh/h), over a 24 h period.

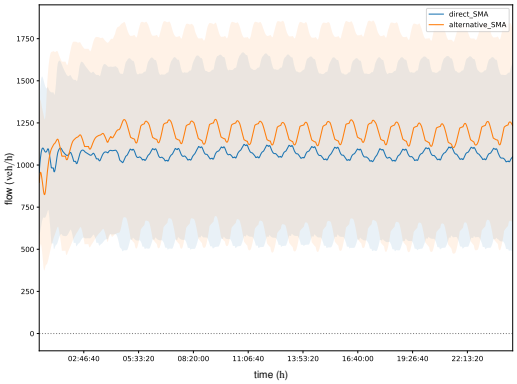


Fig. A.19-6. TrafficTraffic flow on each route, in vehicles per hour (veh/h), over a 24 h period, 4 h Simple Moving Average, mean (line) and standard deviation (shaded).

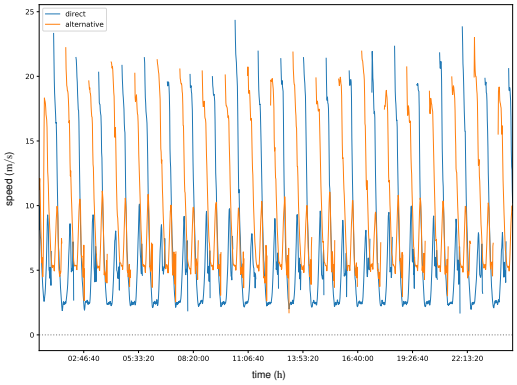


Fig. A.19-7. Mean speed on each route, in meters per second (m/s), aggregated to 1 min, over a 24 h period.

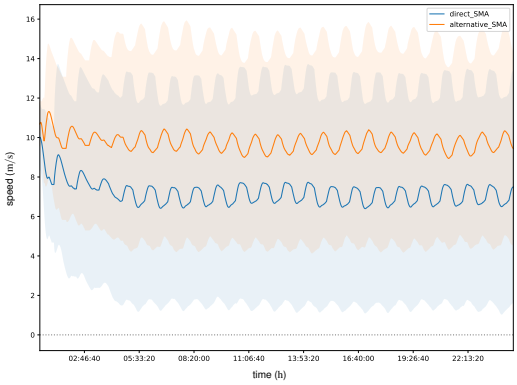


Fig. A.19-8. Mean speed on each route, in meters per second (m/s), aggregated to 1 min, over a 24 h period, 4 h Simple Moving Average, mean (line) and standard deviation (shaded).

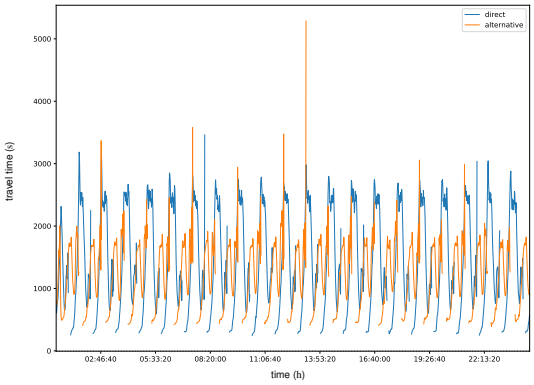


Fig. A.19-9. Travel times on each route, in seconds (s), aggregated to 1 min, over a 24 h period.

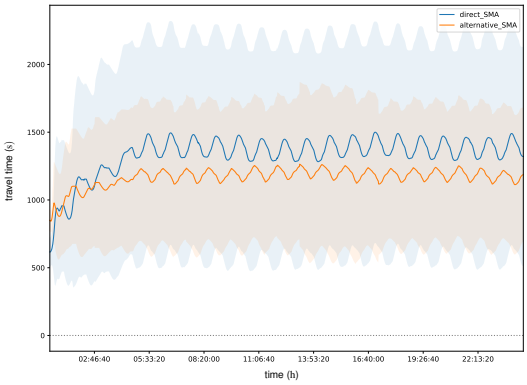


Fig. A.19-10. Travel times on each route, in seconds (s), aggregated to 1 min, over a 24 h period, 4 h Simple Moving Average, mean (line) and standard deviation (shaded).

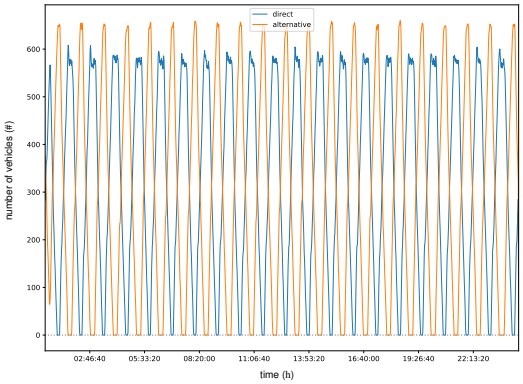


Fig. A.19-11. Average number of vehicles on each route, aggregated to 1 min, over a 24 h period.

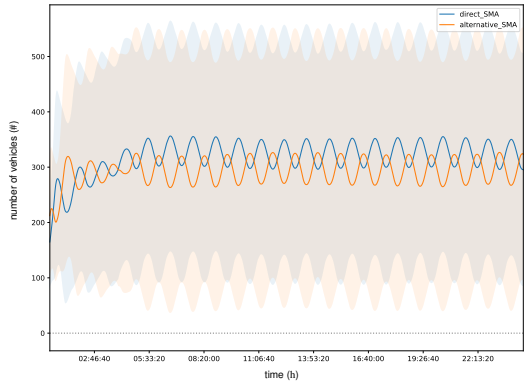


Fig. A.19-12. Average number of vehicles on each route, aggregated to 1 min, over a 24 h period, 4 h Simple Moving Average, mean (line) and standard deviation (shaded).

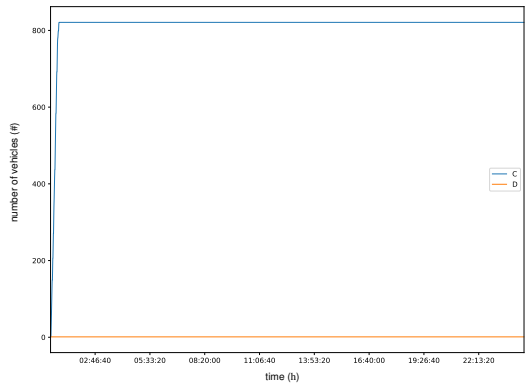


Fig. A.19-13. Evolution of the number of *Cooperators* and *Defectors* over a 24 h period.

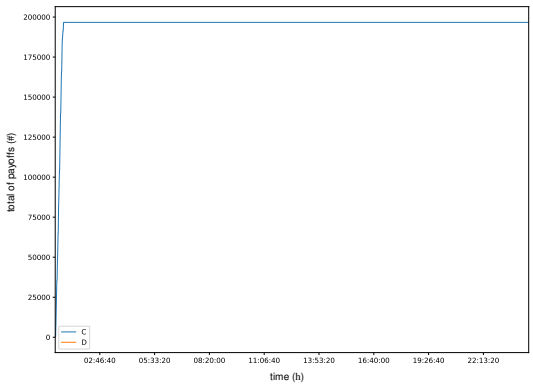


Fig. A.19-14. Evolution of total payoffs for *Cooperators* and *Defectors* (*individual payoff* times the *number of players receiving it*, $C(n) \times n$ and $D(n) \times (N-n)$, where n is the number of *Cooperators*), over a 24 h period.

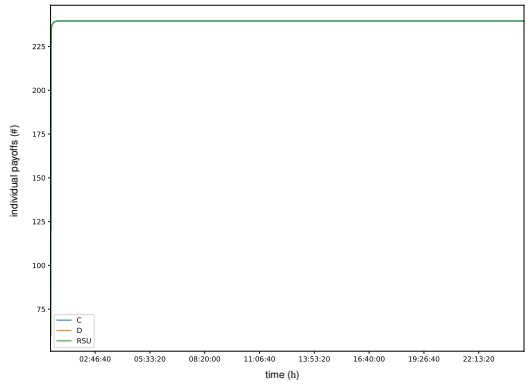


Fig. A.19-15. Evolution of the individual payoffs for *Cooperators, Defectors,* and *RSU* (always cooperating), over a 24 h period.

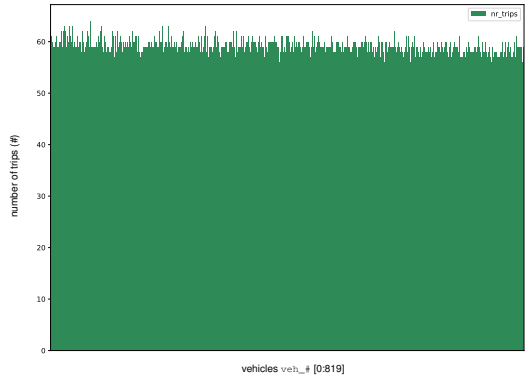


Fig. A.19-16. Number of trips made by each vehicle, during the simulation of a 24 h period.

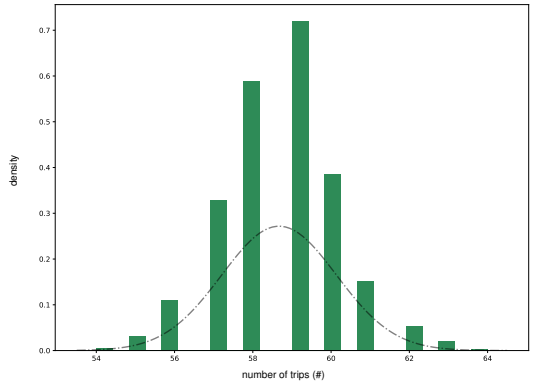


Fig. A.19-17. Density histogram of the number of trips made by each vehicle, during the simulation of a 24 h period, superimposing the normal density curve. The number of bins was calculated by the Freedman Diaconis rule.

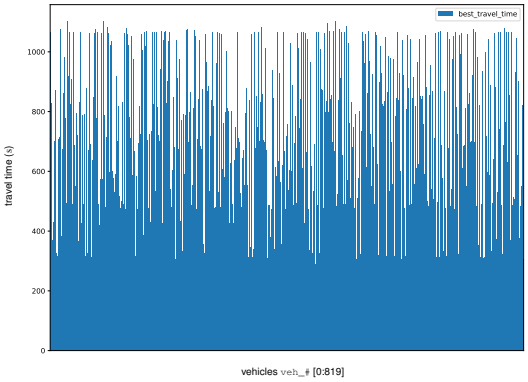


Fig. A.19-18. Best travel time for each vehicle, in seconds (s), during the simulation of a 24 h period.

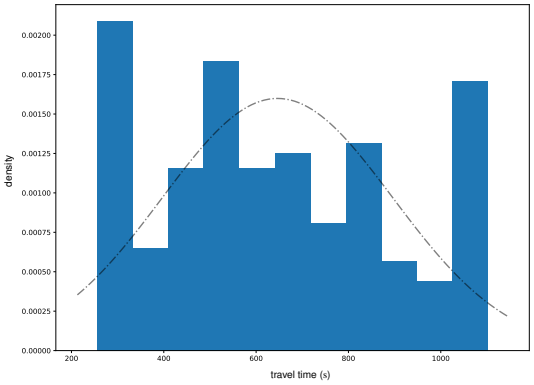


Fig. A.19-19. Density histogram of best travel time for vehicles, in seconds (s), during the simulation of a 24 h period, superimposing the normal density curve. The number of bins was calculated by the Freedman Diaconis rule.

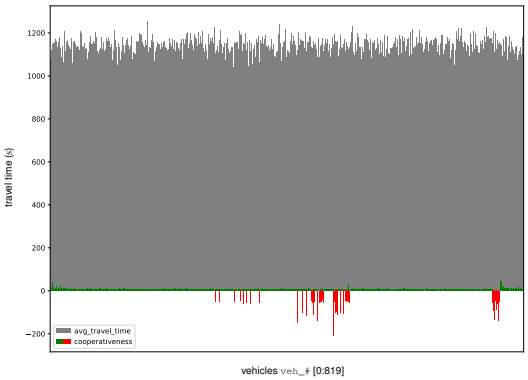


Fig. A.19-20. Average of the travel times, in seconds (s), of individual vehicles, during the simulation of a 24 h period. The bottom graph represents the *degree of cooperativeness**, downscaled by a normalization factor for the purpose of comparison with average times.

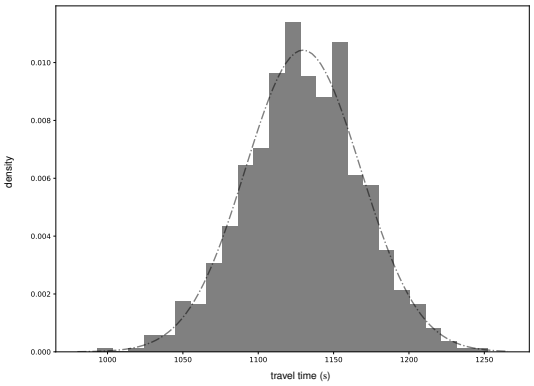


Fig. A.19-21. Density histogram of the average travel times, in seconds (s), of individual vehicles, during the simulation of a 24 h period, superimposing the normal density curve. The number of bins was calculated by the Freedman Diaconis rule.

* The *degree of cooperativeness* is a cumulative sum, calculated at each iteration, based on the complement of the ratio of cooperators, i.e., the higher the number of cooperators the less it increases, but the defectors are more penalized, and vice-versa. It varies inversely with the size of the group to which the player belongs.

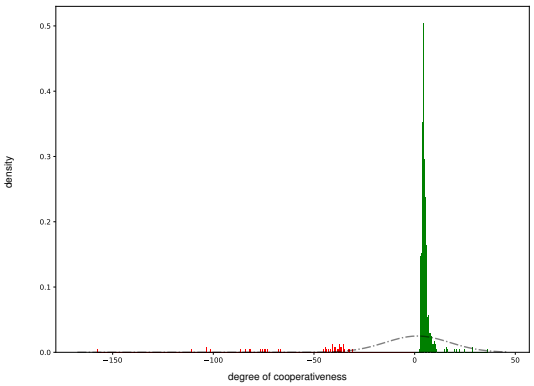


Fig. A.19-22. Density histogram of the *degree of cooperativeness** of individual vehicles, superimposing the normal density curve. The number of bins was calculated by the Freedman Diaconis rule. Generally, when strongly correlated with travel times, it presents a symmetric curve with respect to the *yy*-axis. Because some vehicles choose their preferred route immediately after the end of warmup, due to the gap between the RSU coverage and the route selection point, there may be some outliers.

A.20 `820veh-24h-08060000`

```
Scenario: scenario-1
Timestamp: 20210522T113659Z
Number of vehicles: 820 vehs
Simulation time: 24.0 h
Warm up end time: 1866.6 s; step 18665
Vehicle selection strategy: stochastic
RSU turned off: False
RSU strategy: travel_time_moving_average_product
Runner options:
   nogui: True
   step_length: 0.1
   seed: 19750808
   output_prefix: 820veh-24h-08060000
   sim_run_time: 24.0
   num_vehicles: 820
   warmup_speed: 13.96
   warmup_routes_weight: [473, 527]
   network_speed: 25.0
   change_behavior_probability: [0, 100]
   cooperation_probability: [0, 100]
   vehicle_selection_strategy: stochastic
   turn_rsu_off: False
   rsu_dynamic_dissemination: False
   rsu_dissemination_interval: 5
   rsu_probabilistic_dissemination: False
   rsu_suggestion_strategy: travel_time_moving_average_product
   rsu_routes_weight: [460, 540]
   rsu_moving_avg_size: 5
   travel_times_ttl: 60
   rsu_dissemination_ttl: 0
   rsu_send_travel_time_info: False
   payoff_matrix: [360.0, 240.0, 0.0, -120.0]
   roth_erev_parameters: [0.1, 0.15]
Network Mean speed after warmup:
   Max: 9.89
   Min: 3.87
```

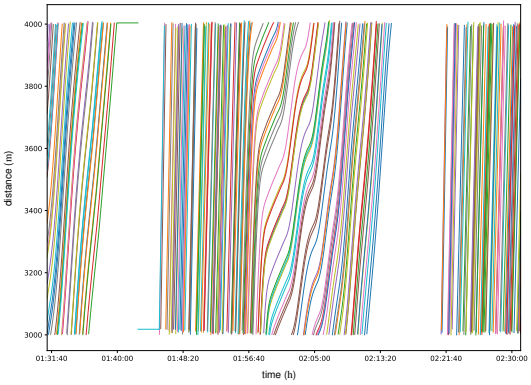


Fig. A.20-1. Time-Space diagram, for the one hour period after the end of the warmup, from 1:00:00 to 2:00:00 simulation time, plotted for the data from the sensor placed in the middle of the *direct* route (between 3000 m and 4000 m). In the case of an overloaded network, congestion shock waves can be observed.

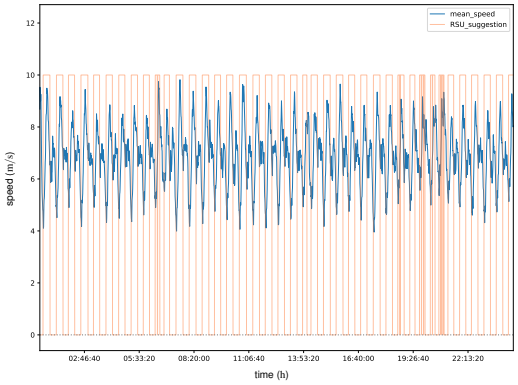


Fig. A.20-2. Mean speed in the network, in meters per second (m/s), over a 24 h period, superimposing (vertically, in orange) the time instants in which the RSU issued a recommendation to follow the *alternative* route.

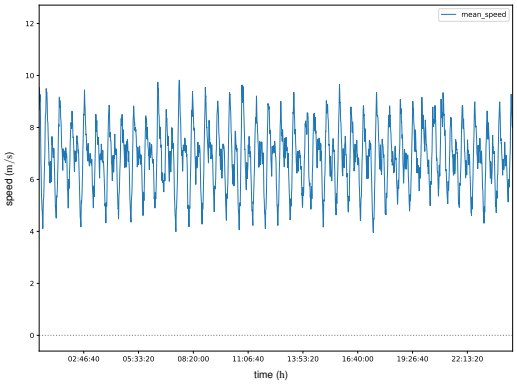


Fig. A.20-3. Mean speed in the network, in meters per second (m/s), over a 24 h period.

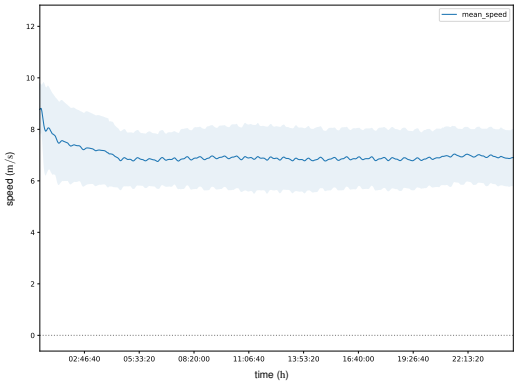


Fig. A.20-4. Mean speed in the network, in meters per second (m/s), over a 24 h period, 4 h Simple Moving Average, mean (line) and standard deviation (shaded).

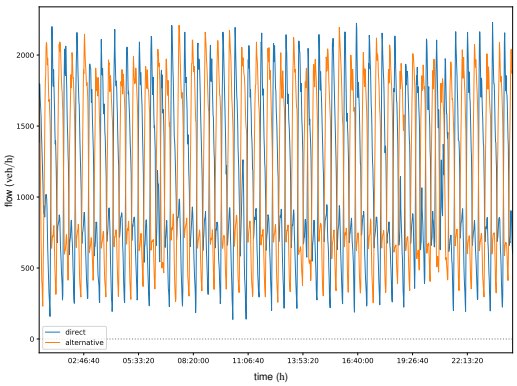


Fig. A.20-5. Traffic flow on each route, in vehicles per hour (veh/h), over a 24 h period.

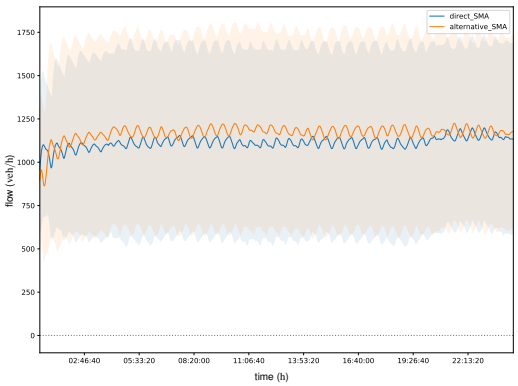


Fig. A.20-6. TrafficTraffic flow on each route, in vehicles per hour (veh/h), over a 24 h period, 4 h Simple Moving Average, mean (line) and standard deviation (shaded).

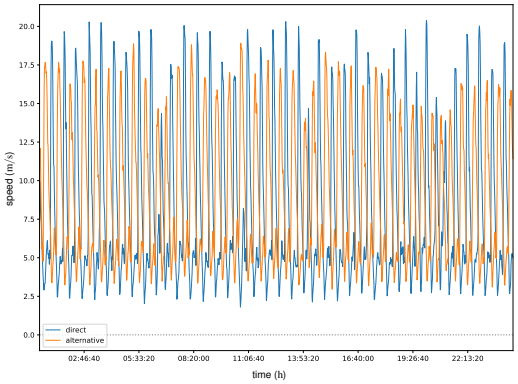


Fig. A.20-7. Mean speed on each route, in meters per second (m/s), aggregated to 1 min, over a 24 h period.

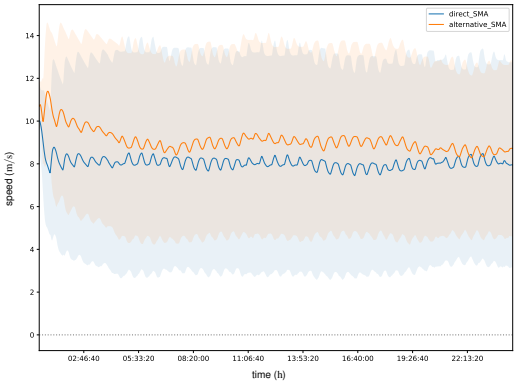


Fig. A.20-8. Mean speed on each route, in meters per second (m/s), aggregated to 1 min, over a 24 h period, 4 h Simple Moving Average, mean (line) and standard deviation (shaded).

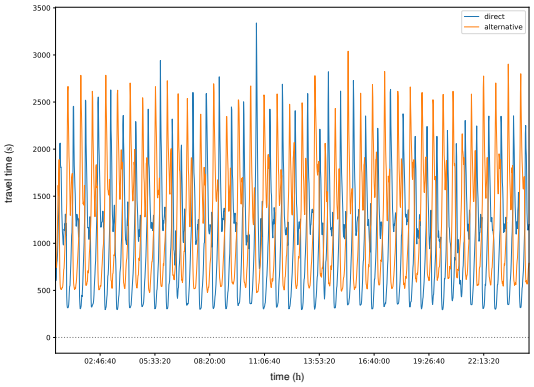


Fig. A.20-9. Travel times on each route, in seconds (s), aggregated to 1 min, over a 24 h period.

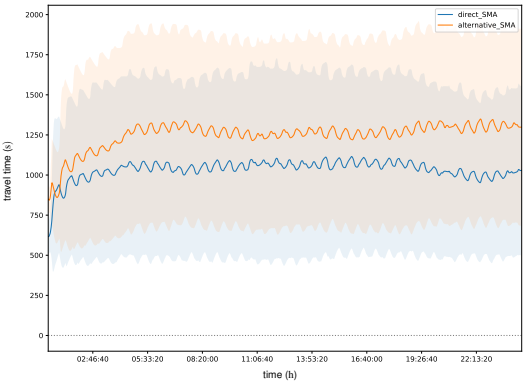


Fig. A.20-10. Travel times on each route, in seconds (s), aggregated to 1 min, over a 24 h period, 4 h Simple Moving Average, mean (line) and standard deviation (shaded).

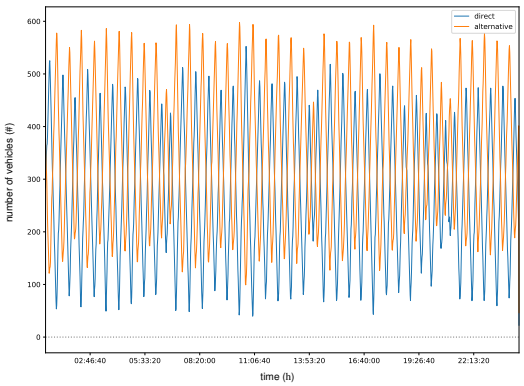


Fig. A.20-11. Average number of vehicles on each route, aggregated to 1 min, over a 24 h period.

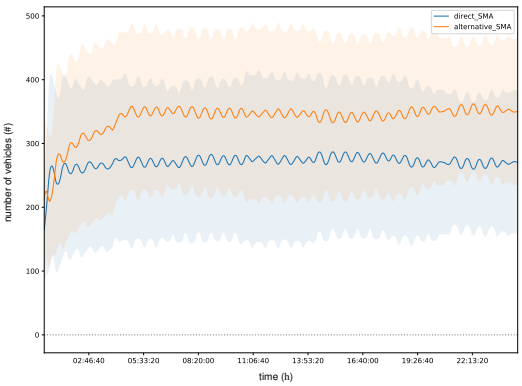


Fig. A.20-12. Average number of vehicles on each route, aggregated to 1 min, over a 24 h period, 4 h Simple Moving Average, mean (line) and standard deviation (shaded).

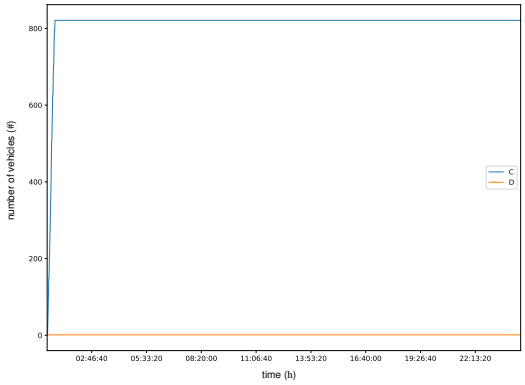


Fig. A.20-13. Evolution of the number of *Cooperators* and *Defectors* over a 24 h period.

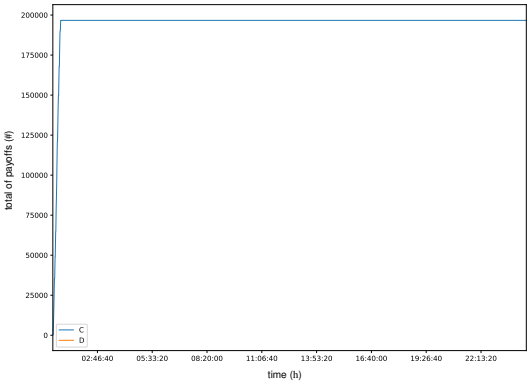


Fig. A.20-14. Evolution of total payoffs for *Cooperators* and *Defectors* (*individual payoff* times the *number of players receiving it*, $C(n) \times n$ and $D(n) \times (N-n)$, where n is the number of *Cooperators*), over a 24 h period.

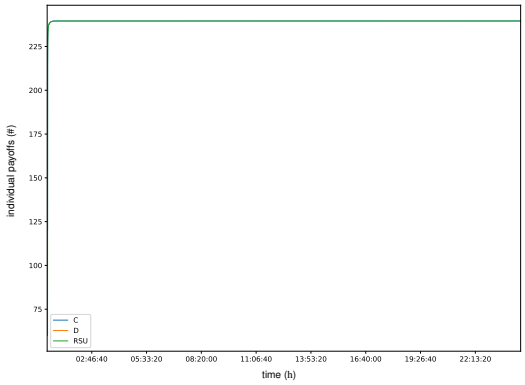


Fig. A.20-15. Evolution of the individual payoffs for *Cooperators, Defectors,* and *RSU* (always cooperating), over a 24 h period.

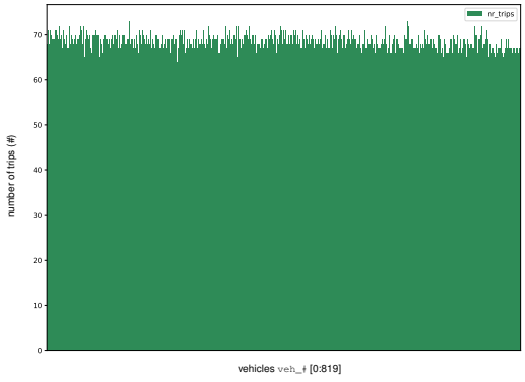


Fig. A.20-16. Number of trips made by each vehicle, during the simulation of a 24 h period.

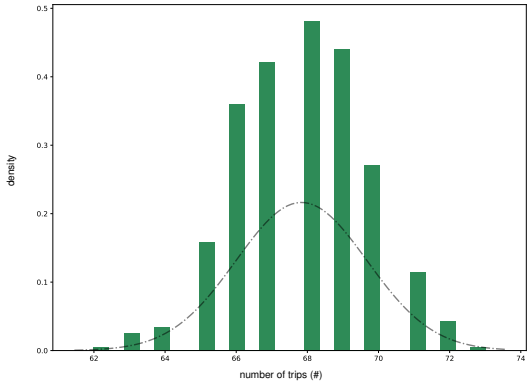


Fig. A.20-17. Density histogram of the number of trips made by each vehicle, during the simulation of a 24 h period, superimposing the normal density curve. The number of bins was calculated by the Freedman Diaconis rule.

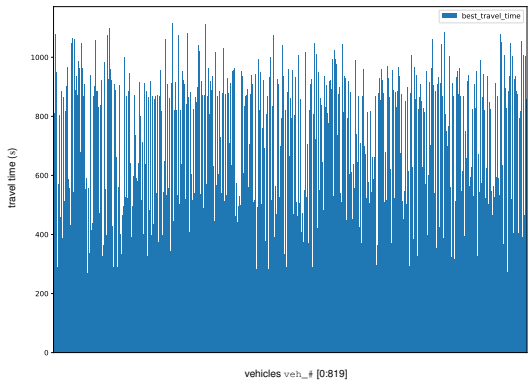


Fig. A.20-18. Best travel time for each vehicle, in seconds (s), during the simulation of a 24 h period.

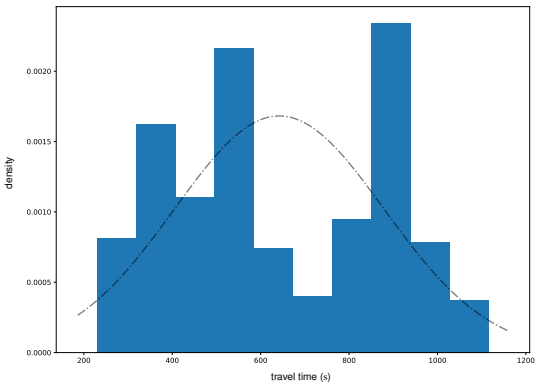


Fig. A.20-19. Density histogram of best travel time for vehicles, in seconds (s), during the simulation of a 24 h period, superimposing the normal density curve. The number of bins was calculated by the Freedman Diaconis rule.

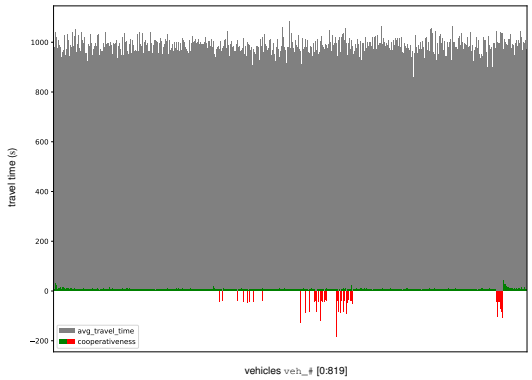


Fig. A.20-20. Average of the travel times, in seconds (s), of individual vehicles, during the simulation of a 24 h period. The bottom graph represents the *degree of cooperativeness**, downscaled by a normalization factor for the purpose of comparison with average times.

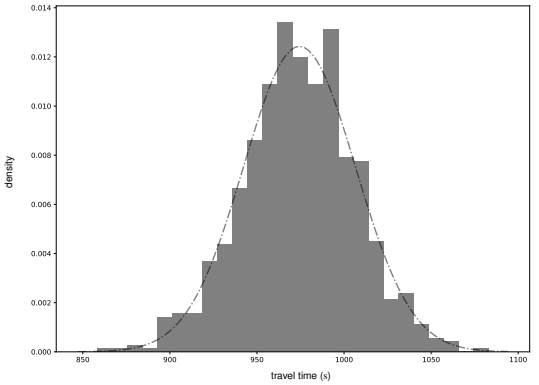


Fig. A.20-21. Density histogram of the average travel times, in seconds (s), of individual vehicles, during the simulation of a 24 h period, superimposing the normal density curve. The number of bins was calculated by the Freedman Diaconis rule.

* The *degree of cooperativeness* is a cumulative sum, calculated at each iteration, based on the complement of the ratio of cooperators, i.e., the higher the number of cooperators the less it increases, but the defectors are more penalized, and vice-versa. It varies inversely with the size of the group to which the player belongs.

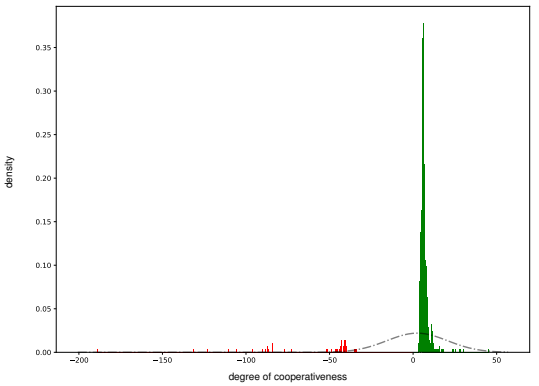


Fig. A.20-22. Density histogram of the *degree of cooperativeness** of individual vehicles, superimposing the normal density curve. The number of bins was calculated by the Freedman Diaconis rule. Generally, when strongly correlated with travel times, it presents a symmetric curve with respect to the *yy*-axis. Because some vehicles choose their preferred route immediately after the end of warmup, due to the gap between the RSU coverage and the route selection point, there may be some outliers.

A.21 820veh-24h-09060000

```
Scenario: scenario-1
Timestamp: 20210617T055530Z
Number of vehicles: 820 vehs
Simulation time: 24.0 h
Warm up end time: 1866.6 s; step 18665
Vehicle selection strategy: stochastic
RSU turned off: False
RSU strategy: travel_time_occupancy
Runner options:
   nogui: True
   step_length: 0.1
   seed: 19750808
   output_prefix: 820veh-24h-09060000
   sim_run_time: 24.0
   num_vehicles: 820
   warmup_speed: 13.96
   warmup_routes_weight: [473, 527]
   network_speed: 25.0
   change_behavior_probability: [0, 100]
   cooperation_probability: [0, 100]
   vehicle_selection_strategy: stochastic
   turn_rsu_off: False
   rsu_dynamic_dissemination: False
   rsu_dissemination_interval: 5
   rsu_probabilistic_dissemination: False
   rsu_suggestion_strategy: travel_time_occupancy
   rsu_routes_weight: [460, 540]
   rsu_moving_avg_size: 5
   travel_times_ttl: 60
   rsu_dissemination_ttl: 0
   rsu_send_travel_time_info: False
   payoff_matrix: [360.0, 240.0, 0.0, -120.0]
   roth_erev_parameters: [0.1, 0.15]
   rsu_change_dissemination: False
   rsu_change_dissemination_steps: [14400, 28800, 43200, 57600, 72000]
   rsu_change_dissemination_intervals: [10, 20, 40, 80, 160]
Network Mean speed after warmup:
   Max: 9.61
   Min: 5.19
```

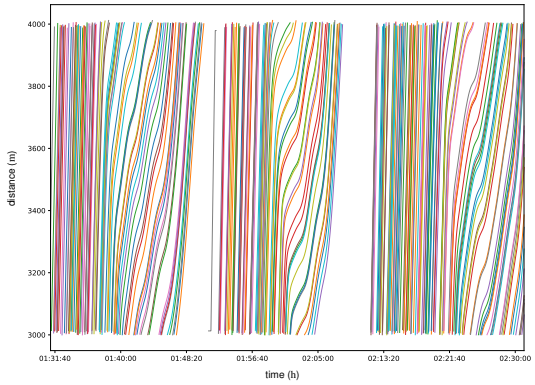


Fig. A.21-1. Time-Space diagram, for the one hour period after the end of the warmup, from 1:00:00 to 2:00:00 simulation time, plotted for the data from the sensor placed in the middle of the *direct* route (between 3000 m and 4000 m). In the case of an overloaded network, congestion shock waves can be observed.

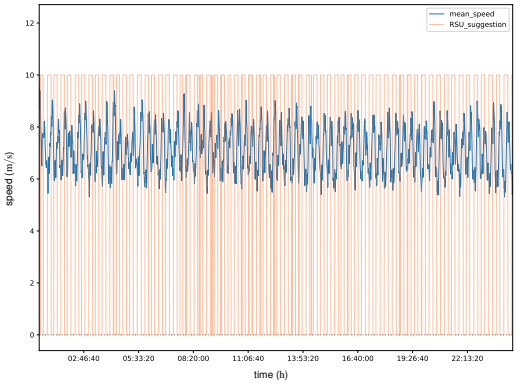


Fig. A.21-2. Mean speed in the network, in meters per second (m/s), over a 24 h period, superimposing (vertically, in orange) the time instants in which the RSU issued a recommendation to follow the *alternative* route.

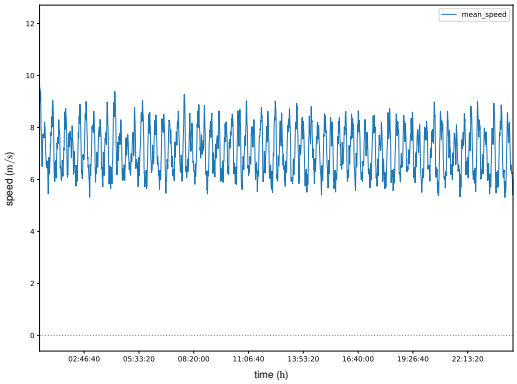


Fig. A.21-3. Mean speed in the network, in meters per second (m/s), over a 24 h period.

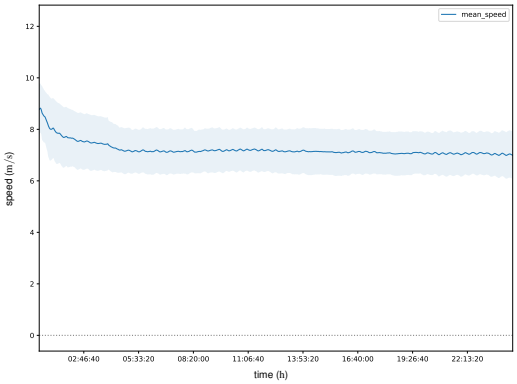


Fig. A.21-4. Mean speed in the network, in meters per second (m/s), over a 24 h period, 4 h Simple Moving Average, mean (line) and standard deviation (shaded).

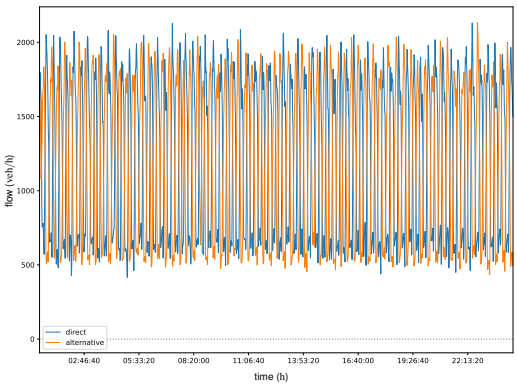


Fig. A.21-5. Traffic flow on each route, in vehicles per hour (veh/h), over a 24 h period.

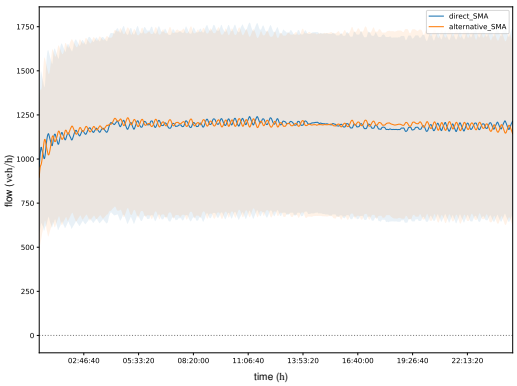


Fig. A.21-6. TrafficTraffic flow on each route, in vehicles per hour (veh/h), over a 24 h period, 4 h Simple Moving Average, mean (line) and standard deviation (shaded).

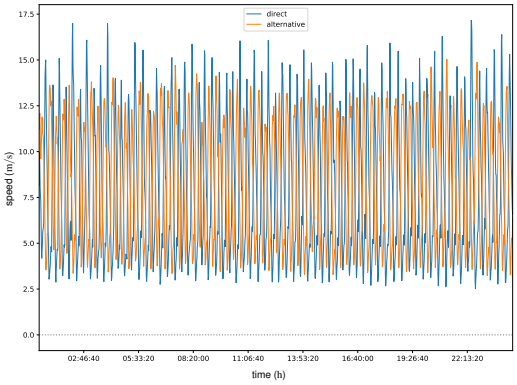


Fig. A.21-7. Mean speed on each route, in meters per second (m/s), aggregated to 1 min, over a 24 h period.

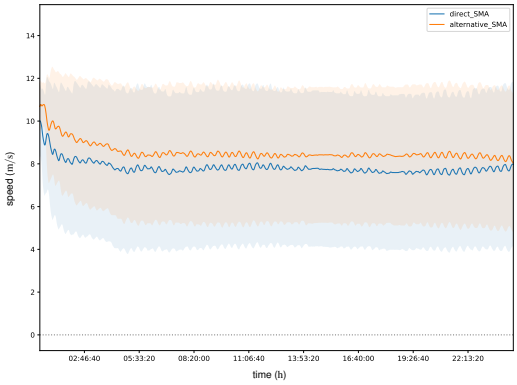


Fig. A.21-8. Mean speed on each route, in meters per second (m/s), aggregated to 1 min, over a 24 h period, 4 h Simple Moving Average, mean (line) and standard deviation (shaded).

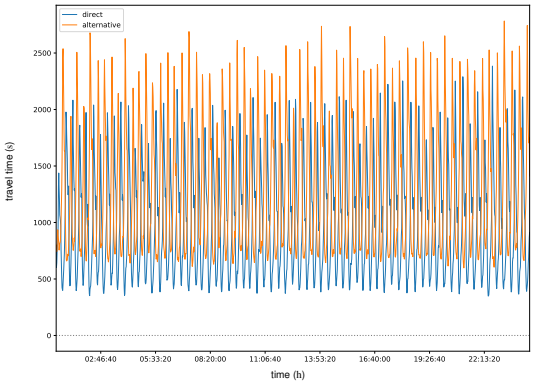


Fig. A.21-9. Travel times on each route, in seconds (s), aggregated to 1 min, over a 24 h period.

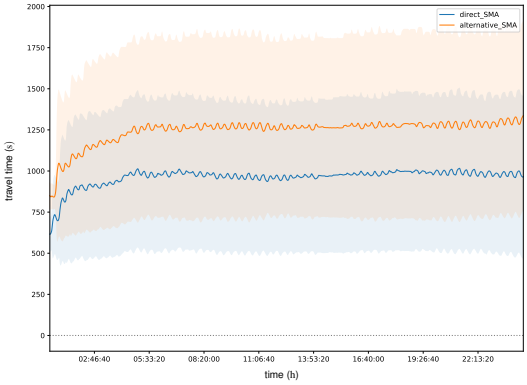


Fig. A.21-10. Travel times on each route, in seconds (s), aggregated to 1 min, over a 24 h period, 4 h Simple Moving Average, mean (line) and standard deviation (shaded).

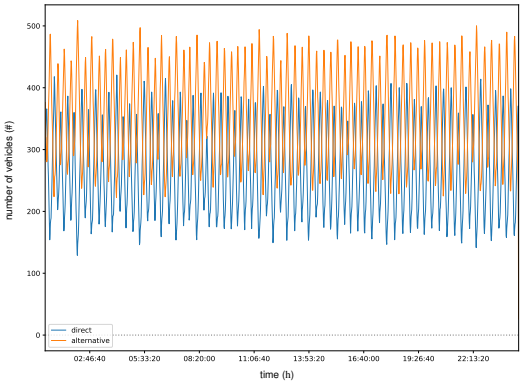


Fig. A.21-11. Average number of vehicles on each route, aggregated to 1 min, over a 24 h period.

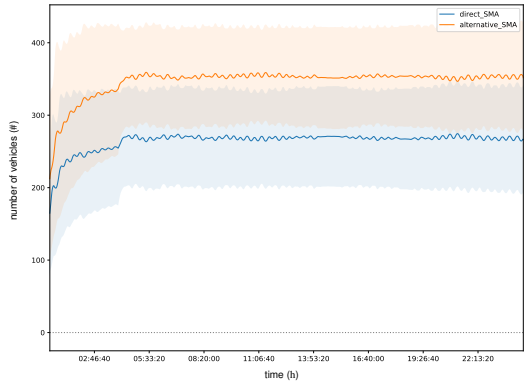


Fig. A.21-12. Average number of vehicles on each route, aggregated to 1 min, over a 24 h period, 4 h Simple Moving Average, mean (line) and standard deviation (shaded).

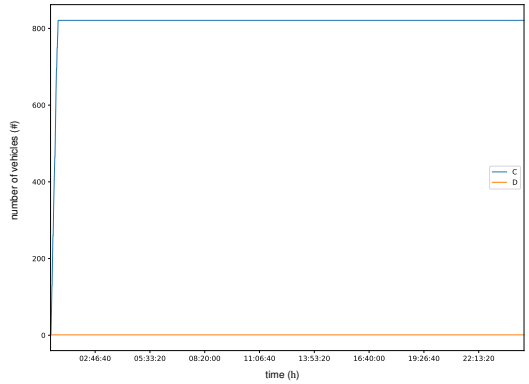


Fig. A.21-13. Evolution of the number of *Cooperators* and *Defectors* over a 24 h period.

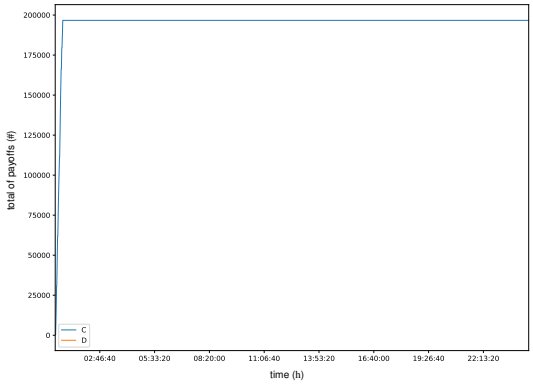


Fig. A.21-14. Evolution of total payoffs for *Cooperators* and *Defectors* (*individual payoff* times the *number of players receiving it*, $C(n) \times n$ and $D(n) \times (N-n)$, where n is the number of *Cooperators*), over a 24 h period.

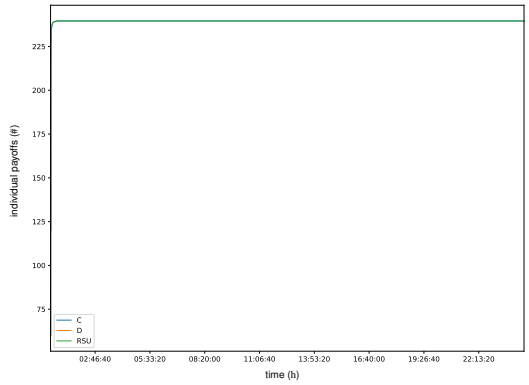


Fig. A.21-15. Evolution of the individual payoffs for *Cooperators, Defectors,* and *RSU* (always cooperating), over a 24 h period.

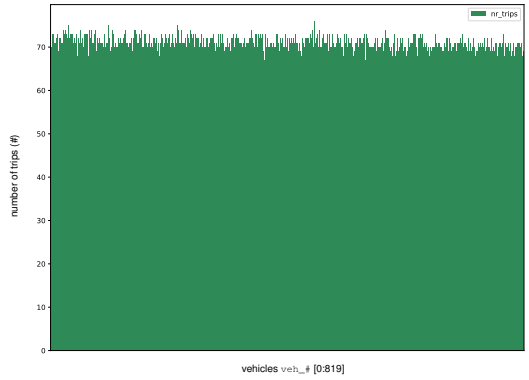


Fig. A.21-16. Number of trips made by each vehicle, during the simulation of a 24 h period.

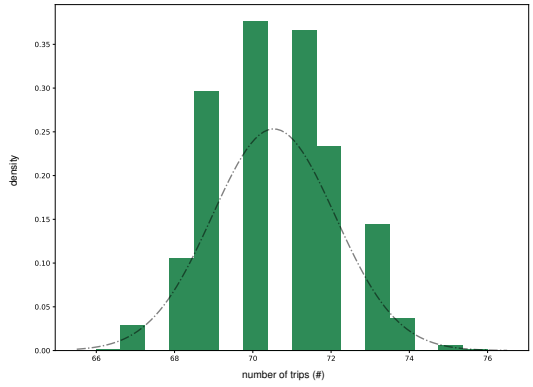


Fig. A.21-17. Density histogram of the number of trips made by each vehicle, during the simulation of a 24 h period, superimposing the normal density curve. The number of bins was calculated by the Freedman Diaconis rule.

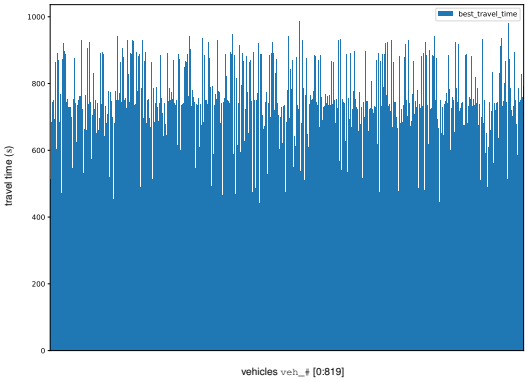


Fig. A.21-18. Best travel time for each vehicle, in seconds (s), during the simulation of a 24 h period.

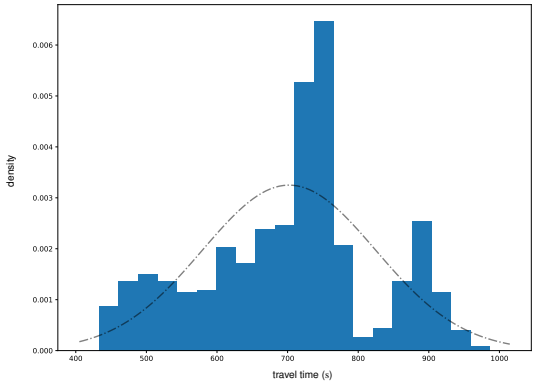


Fig. A.21-19. Density histogram of best travel time for vehicles, in seconds (s), during the simulation of a 24 h period, superimposing the normal density curve. The number of bins was calculated by the Freedman Diaconis rule.

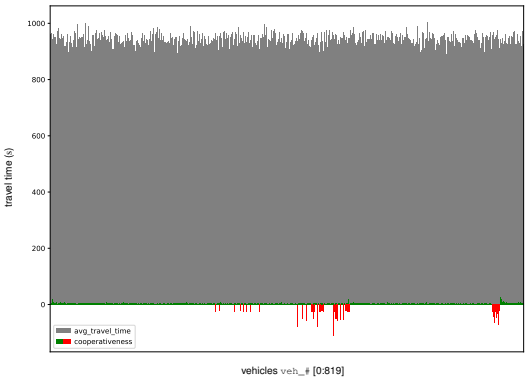


Fig. A.21-20. Average of the travel times, in seconds (s), of individual vehicles, during the simulation of a 24 h period. The bottom graph represents the *degree of cooperativeness**, downscaled by a normalization factor for the purpose of comparison with average times.

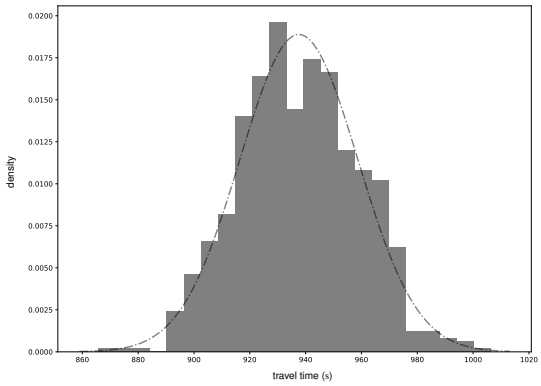


Fig. A.21-21. Density histogram of the average travel times, in seconds (s), of individual vehicles, during the simulation of a 24 h period, superimposing the normal density curve. The number of bins was calculated by the Freedman Diaconis rule.

* The *degree of cooperativeness* is a cumulative sum, calculated at each iteration, based on the complement of the ratio of cooperators, i.e., the higher the number of cooperators the less it increases, but the defectors are more penalized, and vice-versa. It varies inversely with the size of the group to which the player belongs.

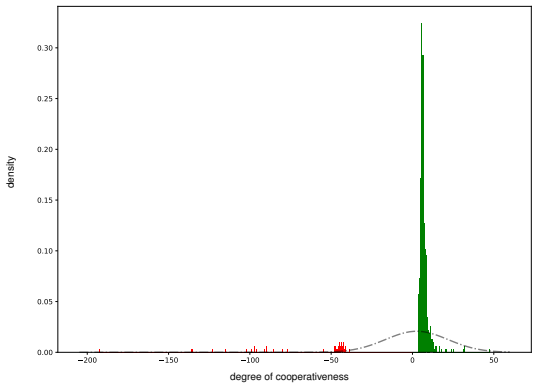


Fig. A.21-22. Density histogram of the *degree of cooperativeness** of individual vehicles, superimposing the normal density curve. The number of bins was calculated by the Freedman Diaconis rule. Generally, when strongly correlated with travel times, it presents a symmetric curve with respect to the *yy*-axis. Because some vehicles choose their preferred route immediately after the end of warmup, due to the gap between the RSU coverage and the route selection point, there may be some outliers.

A.22 `820veh-24h-10060000`

```
Scenario: scenario-1
Timestamp: 20210522T142026Z
Number of vehicles: 820 vehs
Simulation time: 24.0 h
Warm up end time: 1866.6 s; step 18665
Vehicle selection strategy: stochastic
RSU turned off: False
RSU strategy: travel_time_free_flow_tt
Runner options:
   nogui: True
   step_length: 0.1
   seed: 19750808
   output_prefix: 820veh-24h-10060000
   sim_run_time: 24.0
   num_vehicles: 820
   warmup_speed: 13.96
   warmup_routes_weight: [473, 527]
   network_speed: 25.0
   change_behavior_probability: [0, 100]
   cooperation_probability: [0, 100]
   vehicle_selection_strategy: stochastic
   turn_rsu_off: False
   rsu_dynamic_dissemination: False
   rsu_dissemination_interval: 5
   rsu_probabilistic_dissemination: False
   rsu_suggestion_strategy: travel_time_free_flow_tt
   rsu_routes_weight: [460, 540]
   rsu_moving_avg_size: 5
   travel_times_ttl: 60
   rsu_dissemination_ttl: 0
   rsu_send_travel_time_info: False
   payoff_matrix: [360.0, 240.0, 0.0, -120.0]
   roth_erev_parameters: [0.1, 0.15]
Network Mean speed after warmup:
   Max: 10.77
   Min: 1.87
```

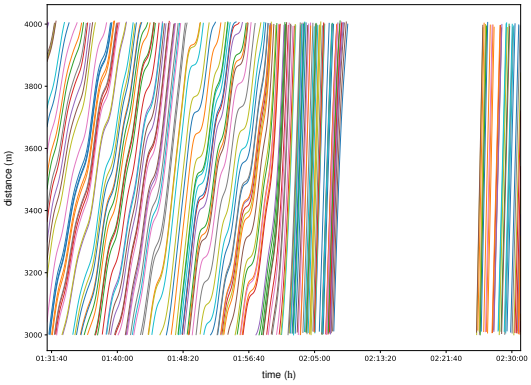


Fig. A.22-1. Time-Space diagram, for the one hour period after the end of the warmup, from 1:00:00 to 2:00:00 simulation time, plotted for the data from the sensor placed in the middle of the *direct* route (between 3000 m and 4000 m). In the case of an overloaded network, congestion shock waves can be observed.

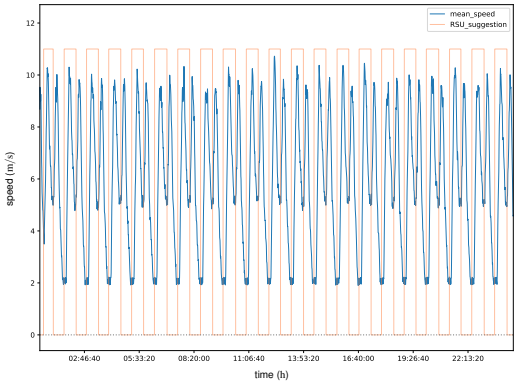


Fig. A.22-2. Mean speed in the network, in meters per second (m/s), over a 24 h period, superimposing (vertically, in orange) the time instants in which the RSU issued a recommendation to follow the *alternative* route.

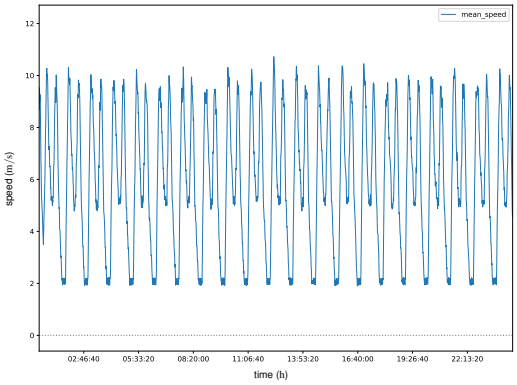


Fig. A.22-3. Mean speed in the network, in meters per second (m/s), over a 24 h period.

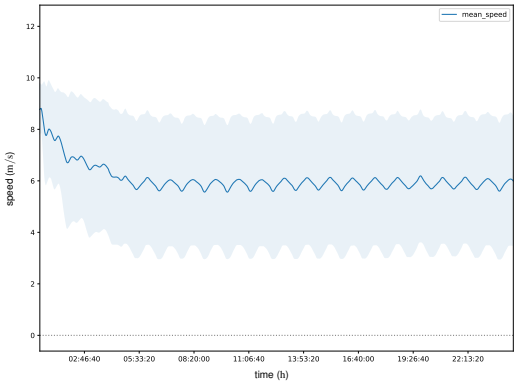


Fig. A.22-4. Mean speed in the network, in meters per second (m/s), over a 24 h period, 4 h Simple Moving Average, mean (line) and standard deviation (shaded).

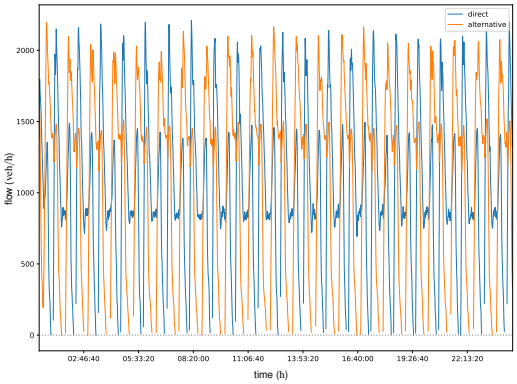


Fig. A.22-5. Traffic flow on each route, in vehicles per hour (veh/h), over a 24 h period.

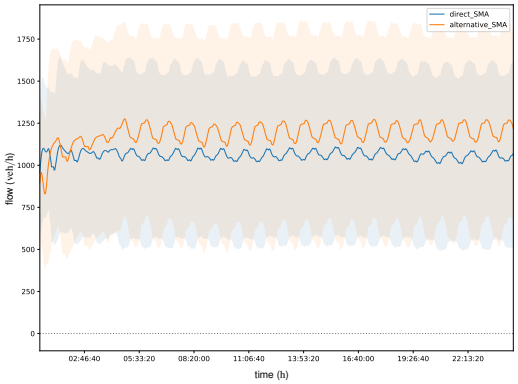


Fig. A.22-6. TrafficTraffic flow on each route, in vehicles per hour (veh/h), over a 24 h period, 4 h Simple Moving Average, mean (line) and standard deviation (shaded).

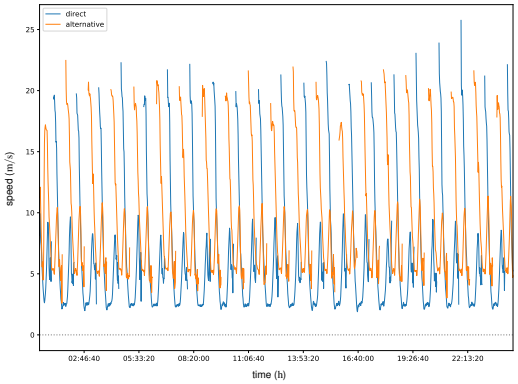


Fig. A.22-7. Mean speed on each route, in meters per second (m/s), aggregated to 1 min, over a 24 h period.

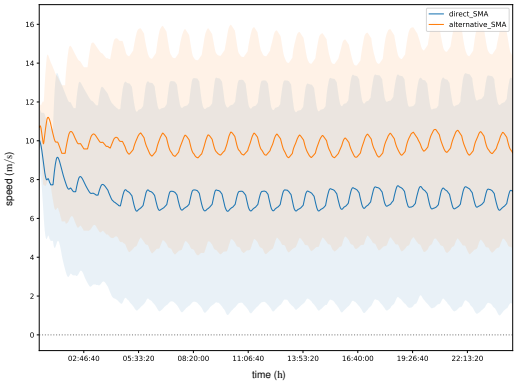


Fig. A.22-8. Mean speed on each route, in meters per second (m/s), aggregated to 1 min, over a 24 h period, 4 h Simple Moving Average, mean (line) and standard deviation (shaded).

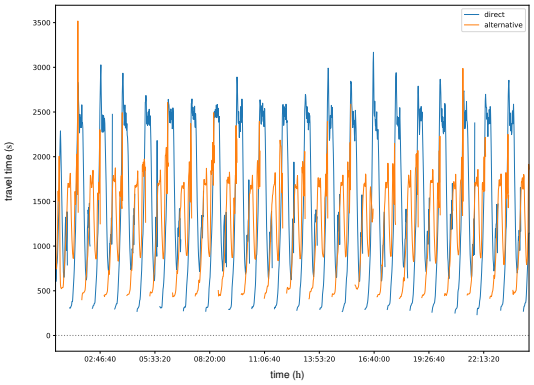


Fig. A.22-9. Travel times on each route, in seconds (s), aggregated to 1 min, over a 24 h period.

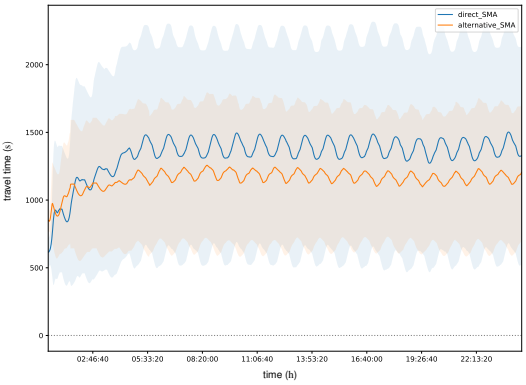


Fig. A.22-10. Travel times on each route, in seconds (s), aggregated to 1 min, over a 24 h period, 4 h Simple Moving Average, mean (line) and standard deviation (shaded).

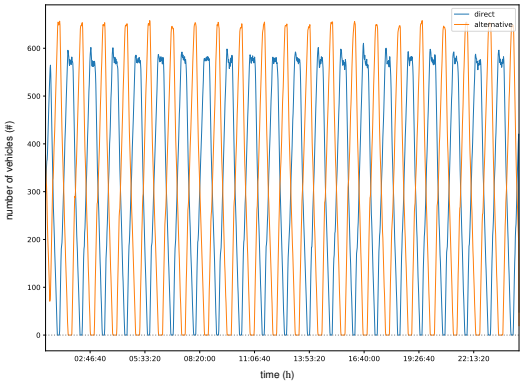


Fig. A.22-11. Average number of vehicles on each route, aggregated to 1 min, over a 24 h period.

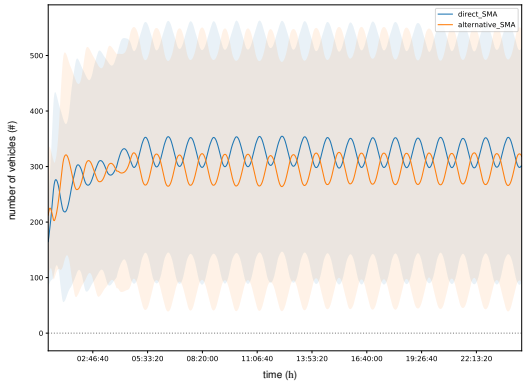


Fig. A.22-12. Average number of vehicles on each route, aggregated to 1 min, over a 24 h period, 4 h Simple Moving Average, mean (line) and standard deviation (shaded).

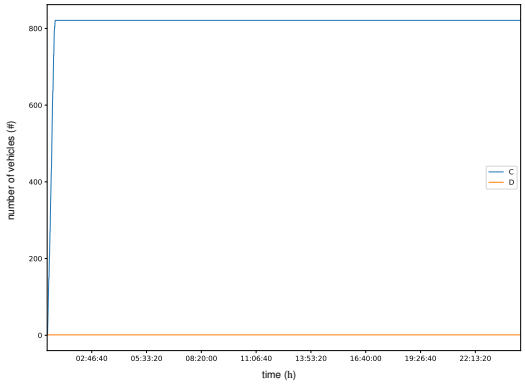


Fig. A.22-13. Evolution of the number of *Cooperators* and *Defectors* over a 24 h period.

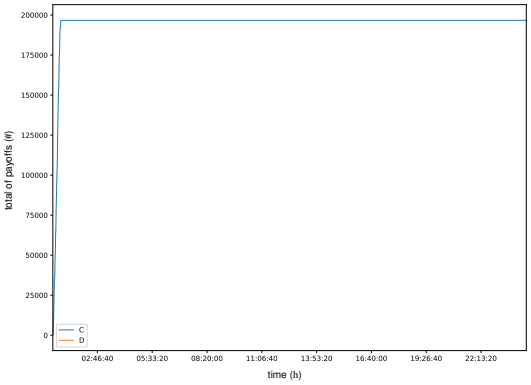


Fig. A.22-14. Evolution of total payoffs for *Cooperators* and *Defectors* (*individual payoff* times the *number of players receiving it*, $C(n) \times n$ and $D(n) \times (N-n)$, where n is the number of *Cooperators*), over a 24 h period.

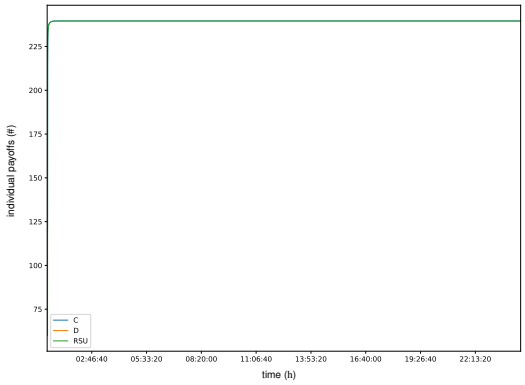


Fig. A.22-15. Evolution of the individual payoffs for *Cooperators, Defectors,* and *RSU* (always cooperating), over a 24 h period.

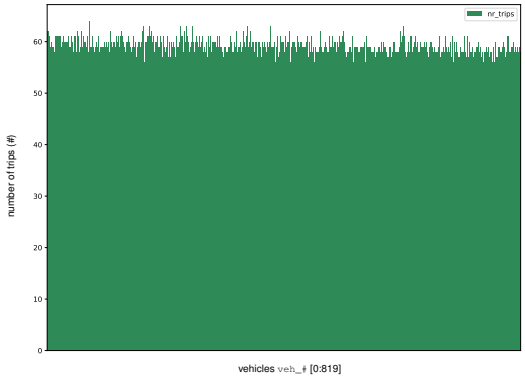


Fig. A.22-16. Number of trips made by each vehicle, during the simulation of a 24 h period.

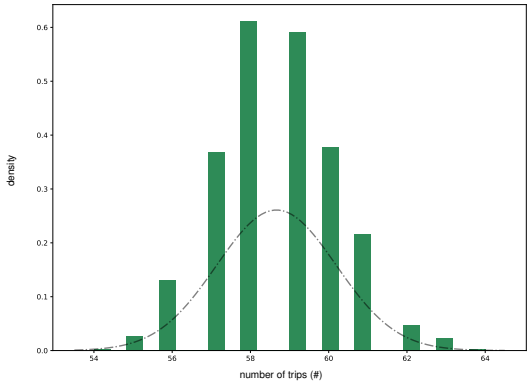


Fig. A.22-17. Density histogram of the number of trips made by each vehicle, during the simulation of a 24 h period, superimposing the normal density curve. The number of bins was calculated by the Freedman Diaconis rule.

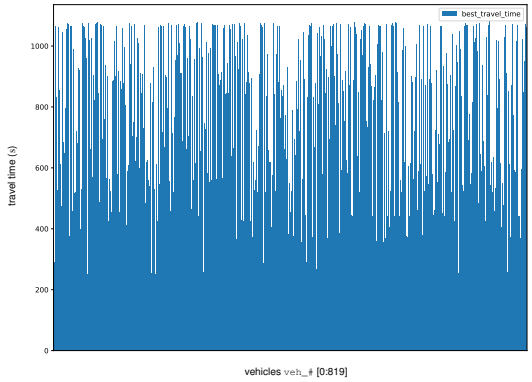


Fig. A.22-18. Best travel time for each vehicle, in seconds (s), during the simulation of a 24 h period.

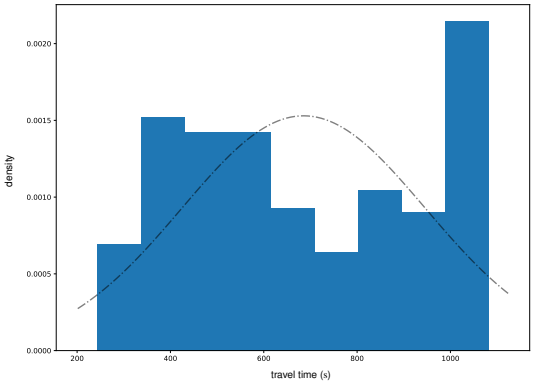


Fig. A.22-19. Density histogram of best travel time for vehicles, in seconds (s), during the simulation of a 24 h period, superimposing the normal density curve. The number of bins was calculated by the Freedman Diaconis rule.

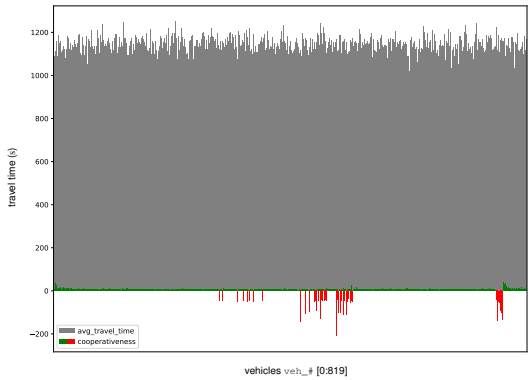


Fig. A.22-20. Average of the travel times, in seconds (s), of individual vehicles, during the simulation of a 24 h period. The bottom graph represents the *degree of cooperativeness**, downscaled by a normalization factor for the purpose of comparison with average times.

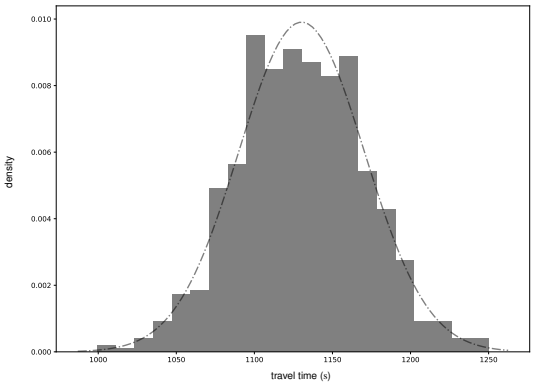


Fig. A.22-21. Density histogram of the average travel times, in seconds (s), of individual vehicles, during the simulation of a 24 h period, superimposing the normal density curve. The number of bins was calculated by the Freedman Diaconis rule.

* The *degree of cooperativeness* is a cumulative sum, calculated at each iteration, based on the complement of the ratio of cooperators, i.e., the higher the number of cooperators the less it increases, but the defectors are more penalized, and vice-versa. It varies inversely with the size of the group to which the player belongs.

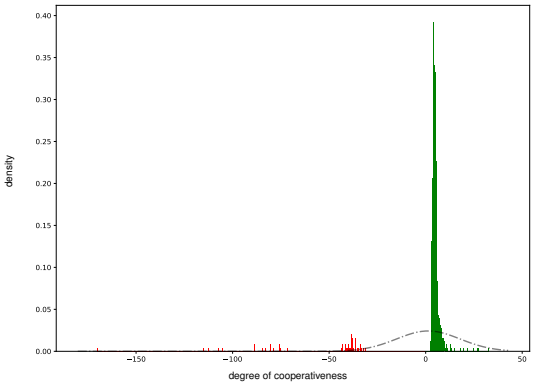


Fig. A.22-22. Density histogram of the *degree of cooperativeness** of individual vehicles, superimposing the normal density curve. The number of bins was calculated by the Freedman Diaconis rule. Generally, when strongly correlated with travel times, it presents a symmetric curve with respect to the *yy*-axis. Because some vehicles choose their preferred route immediately after the end of warmup, due to the gap between the RSU coverage and the route selection point, there may be some outliers.

A.23 820veh-24h-11060000

```
Scenario: scenario-1
Timestamp: 20210522T142037Z
Number of vehicles: 820 vehs
Simulation time: 24.0 h
Warm up end time: 1866.6 s; step 18665
Vehicle selection strategy: stochastic
RSU turned off: False
RSU strategy: intermediate_travel_time_free_flow_tt
Runner options:
   nogui: True
   step_length: 0.1
   seed: 19750808
   output_prefix: 820veh-24h-11060000
   sim_run_time: 24.0
   num_vehicles: 820
   warmup_speed: 13.96
   warmup_routes_weight: [473, 527]
   network_speed: 25.0
   change_behavior_probability: [0, 100]
   cooperation_probability: [0, 100]
   vehicle_selection_strategy: stochastic
   turn_rsu_off: False
   rsu_dynamic_dissemination: False
   rsu_dissemination_interval: 5
   rsu_probabilistic_dissemination: False
   rsu_suggestion_strategy: intermediate_travel_time_free_flow_tt
   rsu_routes_weight: [460, 540]
   rsu_moving_avg_size: 5
   travel_times_ttl: 60
   rsu_dissemination_ttl: 0
   rsu_send_travel_time_info: False
   payoff_matrix: [360.0, 240.0, 0.0, -120.0]
   roth_erev_parameters: [0.1, 0.15]
Network Mean speed after warmup:
   Max: 9.88
   Min: 3.53
```

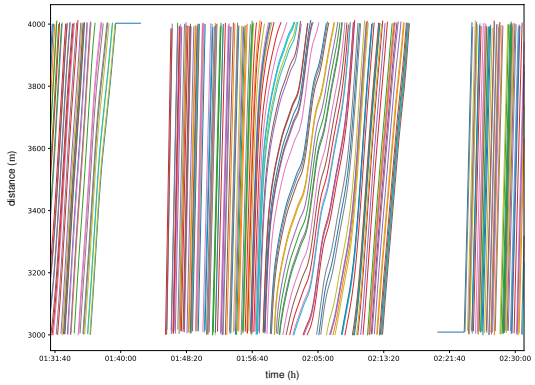


Fig. A.23-1. Time-Space diagram, for the one hour period after the end of the warmup, from 1:00:00 to 2:00:00 simulation time, plotted for the data from the sensor placed in the middle of the *direct* route (between 3000 m and 4000 m). In the case of an overloaded network, congestion shock waves can be observed.

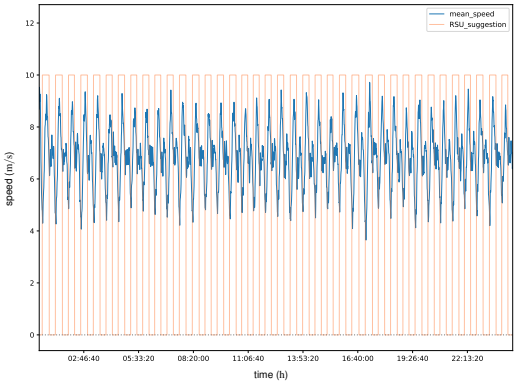


Fig. A.23-2. Mean speed in the network, in meters per second (m/s), over a 24 h period, superimposing (vertically, in orange) the time instants in which the RSU issued a recommendation to follow the *alternative* route.

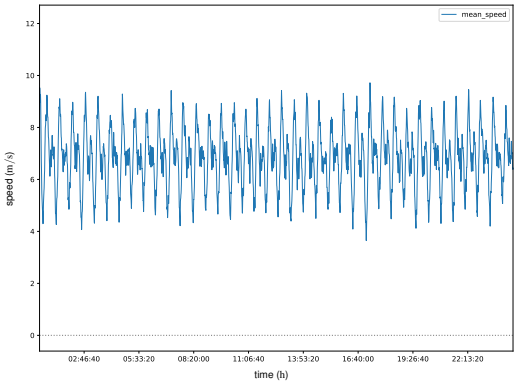


Fig. A.23-3. Mean speed in the network, in meters per second (m/s), over a 24 h period.

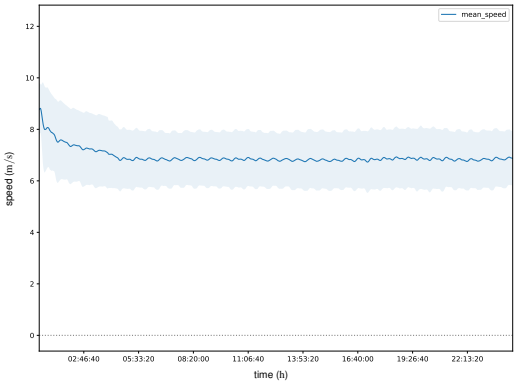


Fig. A.23-4. Mean speed in the network, in meters per second (m/s), over a 24 h period, 4 h Simple Moving Average, mean (line) and standard deviation (shaded).

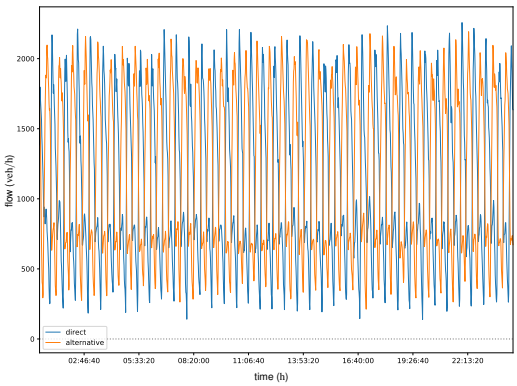


Fig. A.23-5. Traffic flow on each route, in vehicles per hour (veh/h), over a 24 h period.

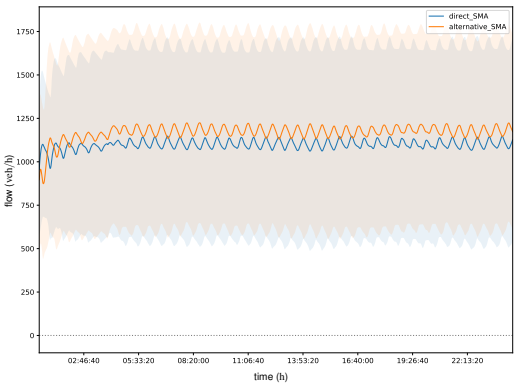


Fig. A.23-6. TrafficTraffic flow on each route, in vehicles per hour (veh/h), over a 24 h period, 4 h Simple Moving Average, mean (line) and standard deviation (shaded).

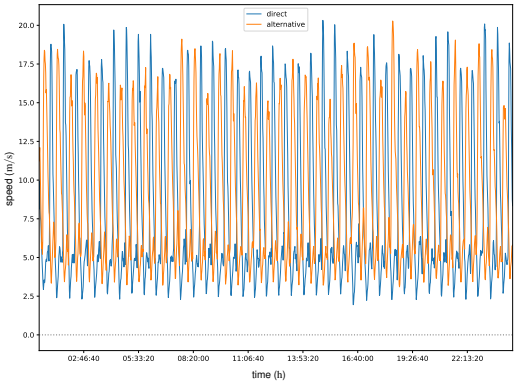


Fig. A.23-7. Mean speed on each route, in meters per second (m/s), aggregated to 1 min, over a 24 h period.

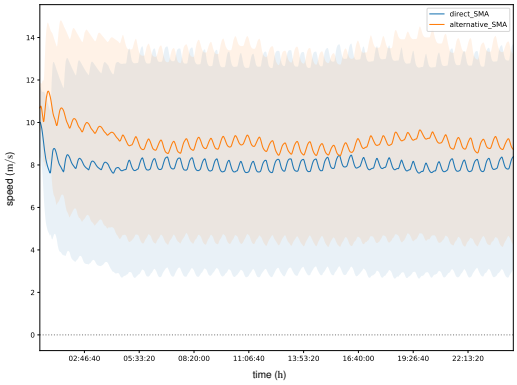


Fig. A.23-8. Mean speed on each route, in meters per second (m/s), aggregated to 1 min, over a 24 h period, 4 h Simple Moving Average, mean (line) and standard deviation (shaded).

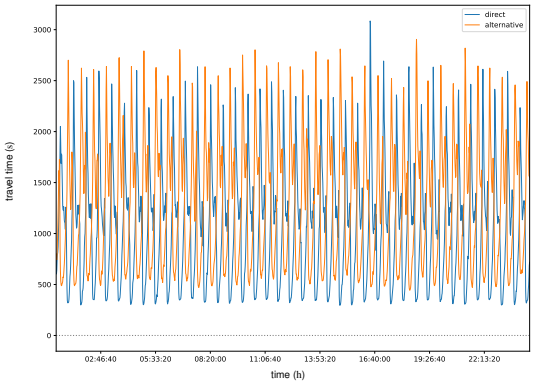


Fig. A.23-9. Travel times on each route, in seconds (s), aggregated to 1 min, over a 24 h period.

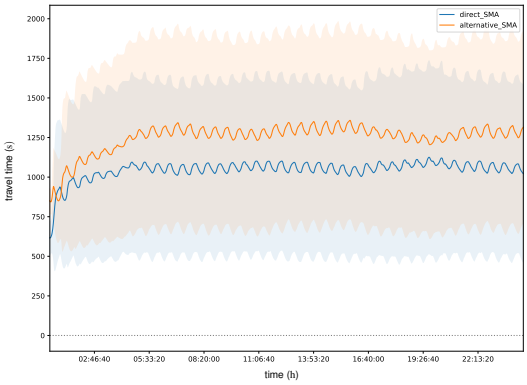


Fig. A.23-10. Travel times on each route, in seconds (s), aggregated to 1 min, over a 24 h period, 4 h Simple Moving Average, mean (line) and standard deviation (shaded).

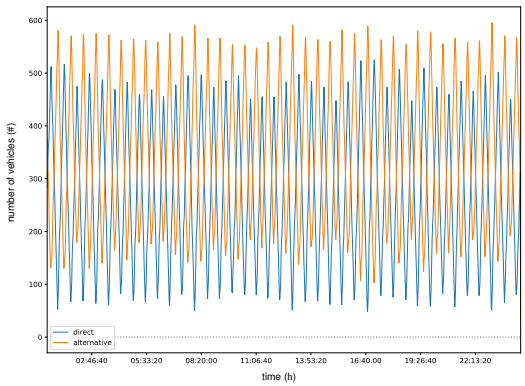


Fig. A.23-11. Average number of vehicles on each route, aggregated to 1 min, over a 24 h period.

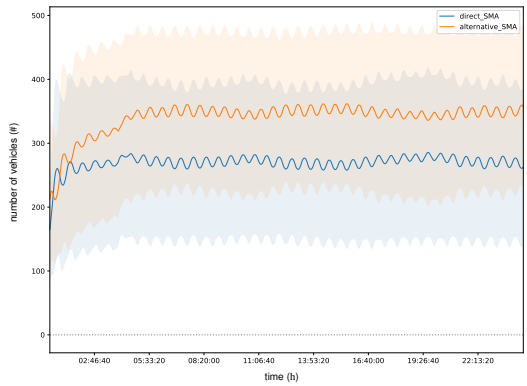


Fig. A.23-12. Average number of vehicles on each route, aggregated to 1 min, over a 24 h period, 4 h Simple Moving Average, mean (line) and standard deviation (shaded).

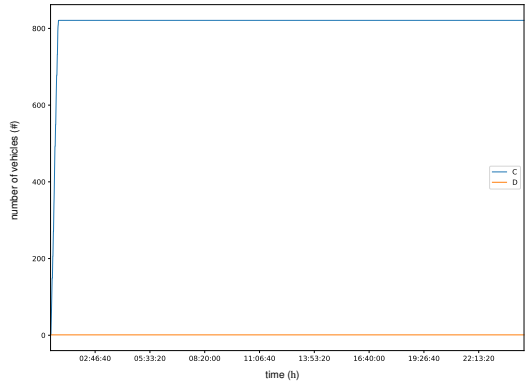


Fig. A.23-13. Evolution of the number of *Cooperators* and *Defectors* over a 24 h period.

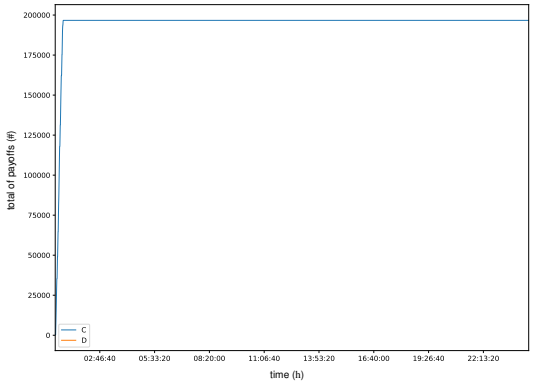


Fig. A.23-14. Evolution of total payoffs for *Cooperators* and *Defectors* (*individual payoff* times the *number of players receiving it*, $C(n) \times n$ and $D(n) \times (N-n)$, where n is the number of *Cooperators*), over a 24 h period.

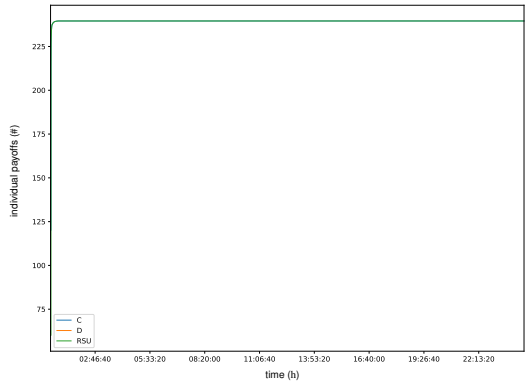


Fig. A.23-15. Evolution of the individual payoffs for *Cooperators, Defectors,* and *RSU* (always cooperating), over a 24 h period.

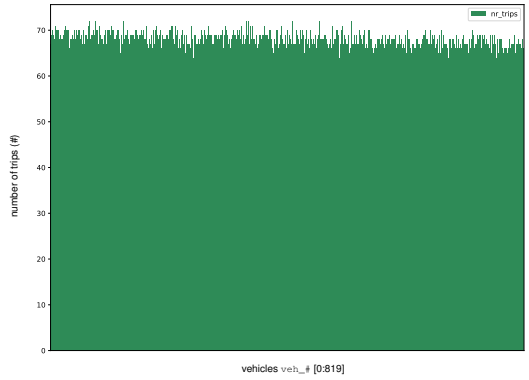


Fig. A.23-16. Number of trips made by each vehicle, during the simulation of a 24 h period.

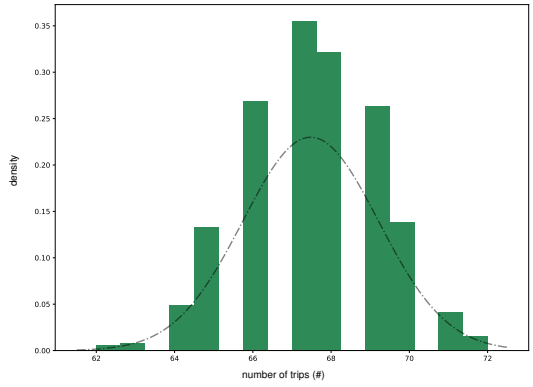


Fig. A.23-17. Density histogram of the number of trips made by each vehicle, during the simulation of a 24 h period, superimposing the normal density curve. The number of bins was calculated by the Freedman Diaconis rule.

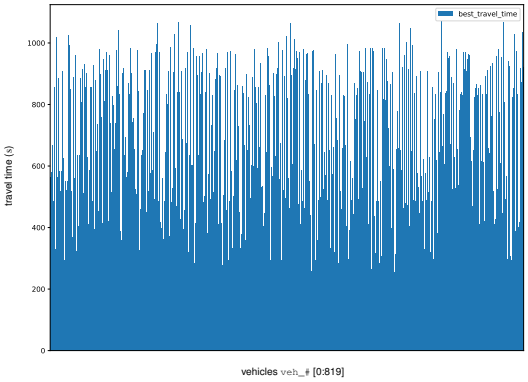


Fig. A.23-18. Best travel time for each vehicle, in seconds (s), during the simulation of a 24 h period.

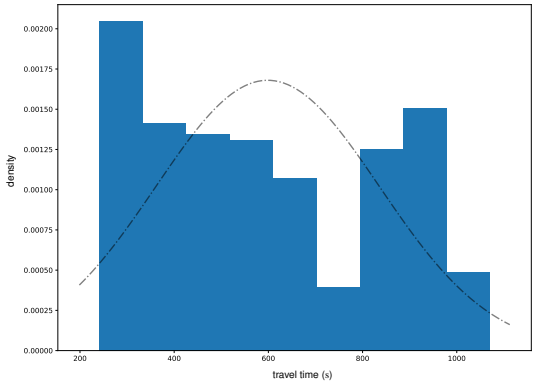


Fig. A.23-19. Density histogram of best travel time for vehicles, in seconds (s), during the simulation of a 24 h period, superimposing the normal density curve. The number of bins was calculated by the Freedman Diaconis rule.

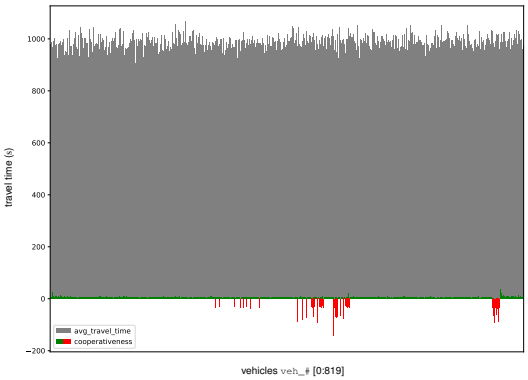


Fig. A.23-20. Average of the travel times, in seconds (s), of individual vehicles, during the simulation of a 24 h period. The bottom graph represents the *degree of cooperativeness**, downscaled by a normalization factor for the purpose of comparison with average times.

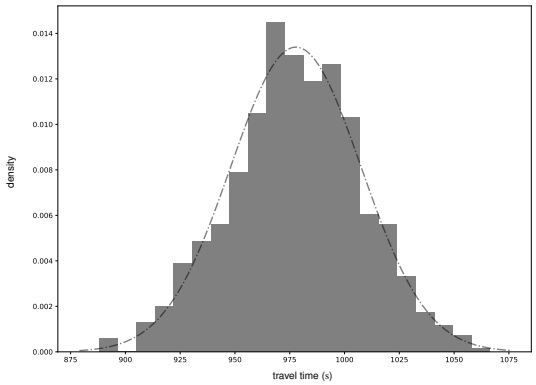


Fig. A.23-21. Density histogram of the average travel times, in seconds (s), of individual vehicles, during the simulation of a 24 h period, superimposing the normal density curve. The number of bins was calculated by the Freedman Diaconis rule.

* The *degree of cooperativeness* is a cumulative sum, calculated at each iteration, based on the complement of the ratio of cooperators, i.e., the higher the number of cooperators the less it increases, but the defectors are more penalized, and vice-versa. It varies inversely with the size of the group to which the player belongs.

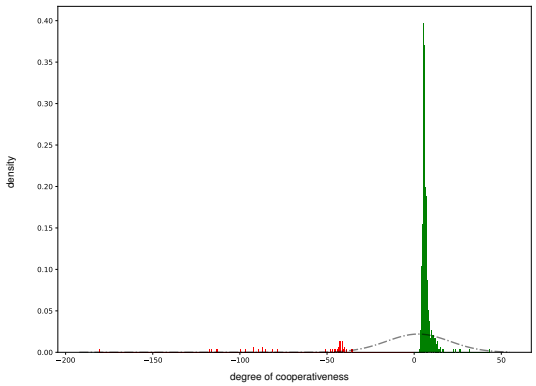


Fig. A.23-22. Density histogram of the *degree of cooperativeness** of individual vehicles, superimposing the normal density curve. The number of bins was calculated by the Freedman Diaconis rule. Generally, when strongly correlated with travel times, it presents a symmetric curve with respect to the *yy*-axis. Because some vehicles choose their preferred route immediately after the end of warmup, due to the gap between the RSU coverage and the route selection point, there may be some outliers.

A.24 `820veh-24h-12060000`

```
Scenario: scenario-1
Timestamp: 20210522T145712Z
Number of vehicles: 820 vehs
Simulation time: 24.0 h
Warm up end time: 1866.6 s; step 18665
Vehicle selection strategy: stochastic
RSU turned off: False
RSU strategy: mean_speed
Runner options:
   nogui: True
   step_length: 0.1
   seed: 19750808
   output_prefix: 820veh-24h-12060000
   sim_run_time: 24.0
   num_vehicles: 820
   warmup_speed: 13.96
   warmup_routes_weight: [473, 527]
   network_speed: 25.0
   change_behavior_probability: [0, 100]
   cooperation_probability: [0, 100]
   vehicle_selection_strategy: stochastic
   turn_rsu_off: False
   rsu_dynamic_dissemination: False
   rsu_dissemination_interval: 5
   rsu_probabilistic_dissemination: False
   rsu_suggestion_strategy: mean_speed
   rsu_routes_weight: [460, 540]
   rsu_moving_avg_size: 5
   travel_times_ttl: 60
   rsu_dissemination_ttl: 0
   rsu_send_travel_time_info: False
   payoff_matrix: [360.0, 240.0, 0.0, -120.0]
   roth_erev_parameters: [0.1, 0.15]
Network Mean speed after warmup:
   Max: 9.97
   Min: 4.66
```

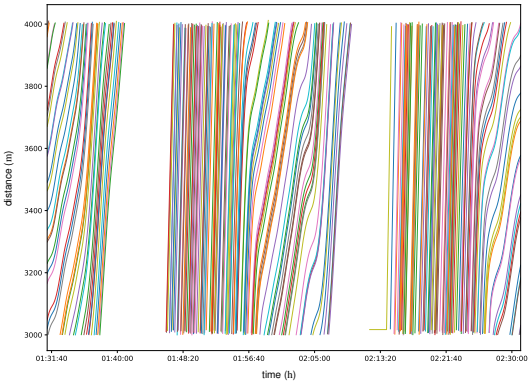


Fig. A.24-1. Time-Space diagram, for the one hour period after the end of the warmup, from 1:00:00 to 2:00:00 simulation time, plotted for the data from the sensor placed in the middle of the *direct* route (between 3000 m and 4000 m). In the case of an overloaded network, congestion shock waves can be observed.

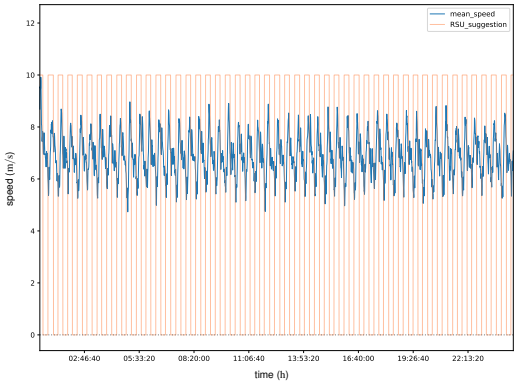


Fig. A.24-2. Mean speed in the network, in meters per second (m/s), over a 24 h period, superimposing (vertically, in orange) the time instants in which the RSU issued a recommendation to follow the *alternative* route.

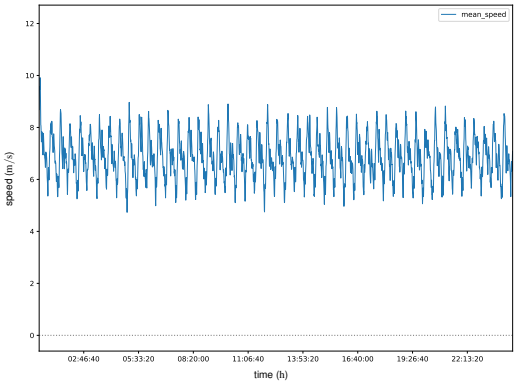


Fig. A.24-3. Mean speed in the network, in meters per second (m/s), over a 24 h period.

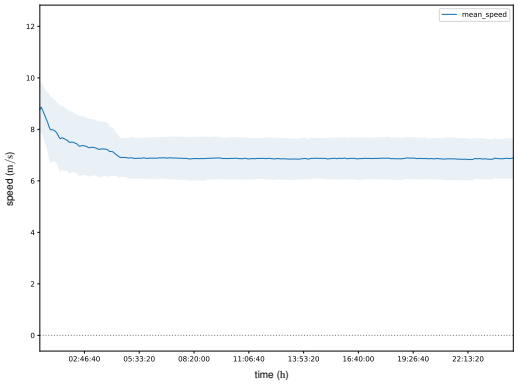


Fig. A.24-4. Mean speed in the network, in meters per second (m/s), over a 24 h period, 4 h Simple Moving Average, mean (line) and standard deviation (shaded).

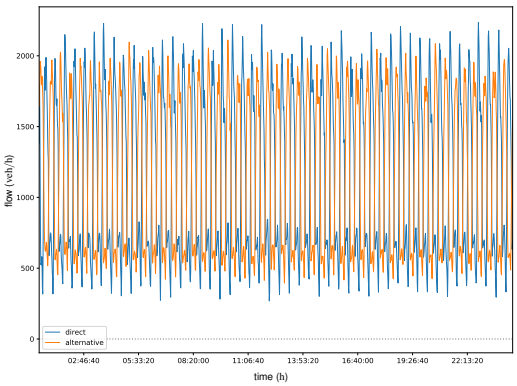


Fig. A.24-5. Traffic flow on each route, in vehicles per hour (veh/h), over a 24 h period.

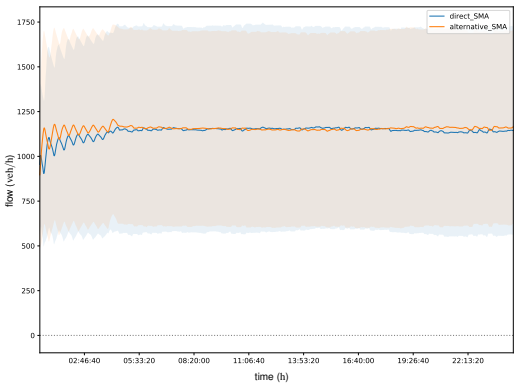


Fig. A.24-6. TrafficTraffic flow on each route, in vehicles per hour (veh/h), over a 24 h period, 4 h Simple Moving Average, mean (line) and standard deviation (shaded).

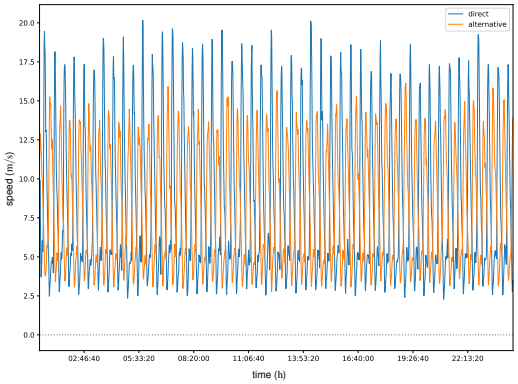


Fig. A.24-7. Mean speed on each route, in meters per second (m/s), aggregated to 1 min, over a 24 h period.

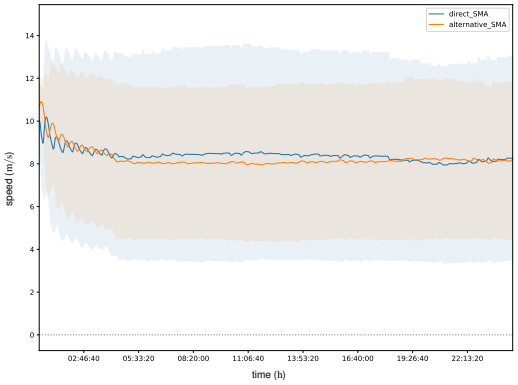


Fig. A.24-8. Mean speed on each route, in meters per second (m/s), aggregated to 1 min, over a 24 h period, 4 h Simple Moving Average, mean (line) and standard deviation (shaded).

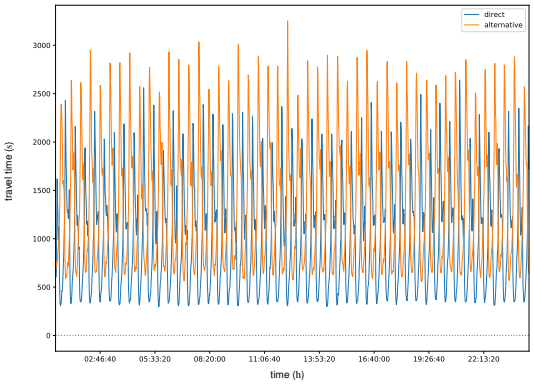


Fig. A.24-9. Travel times on each route, in seconds (s), aggregated to 1 min, over a 24 h period.

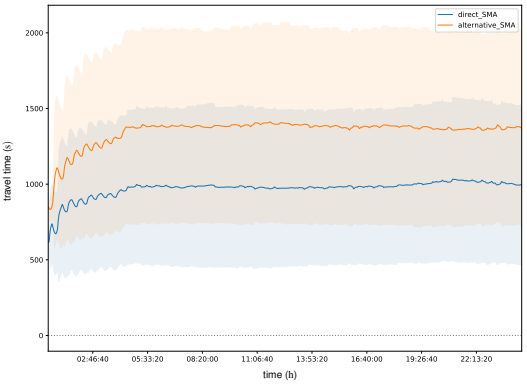


Fig. A.24-10. Travel times on each route, in seconds (s), aggregated to 1 min, over a 24 h period, 4 h Simple Moving Average, mean (line) and standard deviation (shaded).

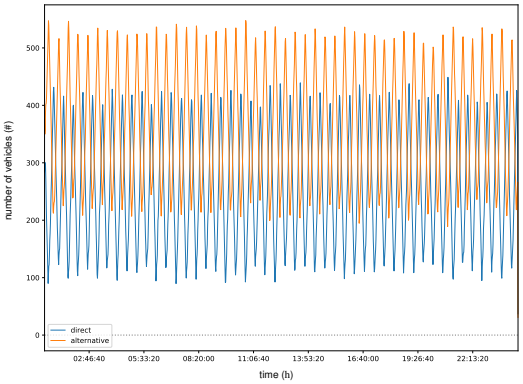


Fig. A.24-11. Average number of vehicles on each route, aggregated to 1 min, over a 24 h period.

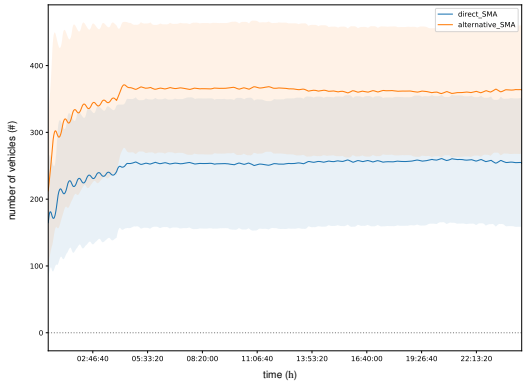


Fig. A.24-12. Average number of vehicles on each route, aggregated to 1 min, over a 24 h period, 4 h Simple Moving Average, mean (line) and standard deviation (shaded).

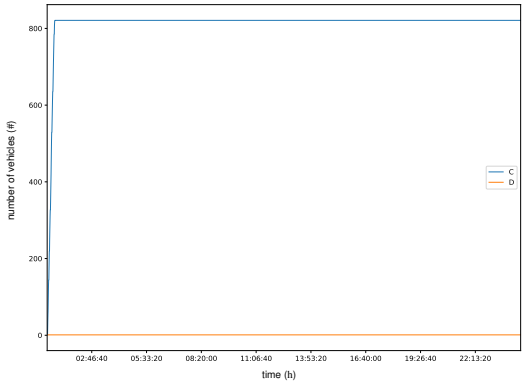


Fig. A.24-13. Evolution of the number of *Cooperators* and *Defectors* over a 24 h period.

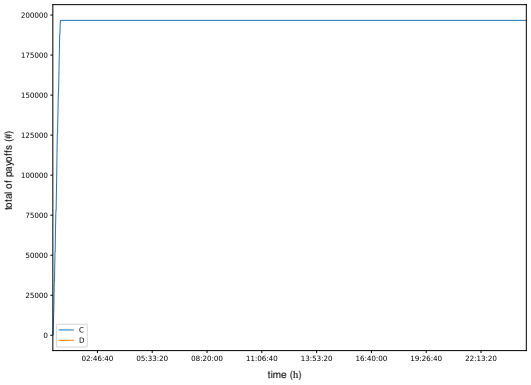


Fig. A.24-14. Evolution of total payoffs for *Cooperators* and *Defectors* (*individual payoff* times the *number of players receiving it*, $C(n) \times n$ and $D(n) \times (N-n)$, where n is the number of *Cooperators*), over a 24 h period.

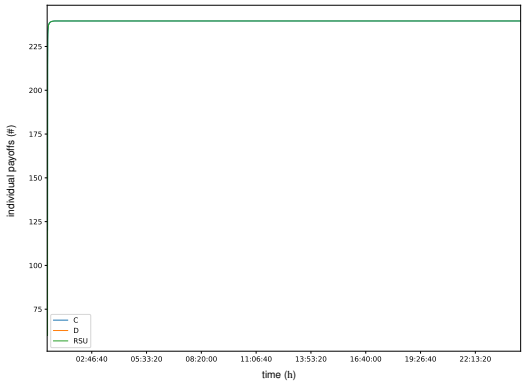


Fig. A.24-15. Evolution of the individual payoffs for *Cooperators, Defectors,* and *RSU* (always cooperating), over a 24 h period.

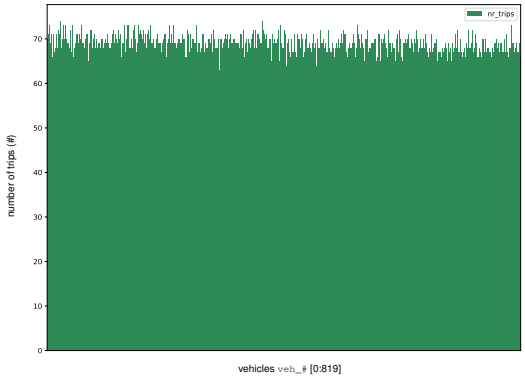


Fig. A.24-16. Number of trips made by each vehicle, during the simulation of a 24 h period.

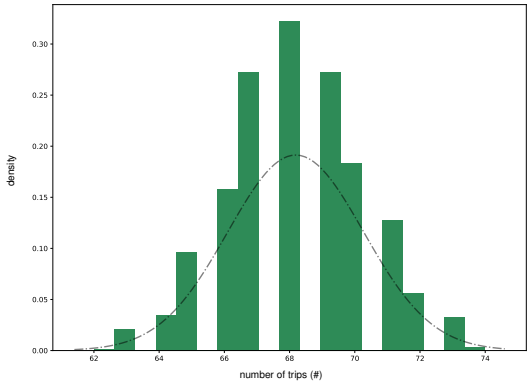


Fig. A.24-17. Density histogram of the number of trips made by each vehicle, during the simulation of a 24 h period, superimposing the normal density curve. The number of bins was calculated by the Freedman Diaconis rule.

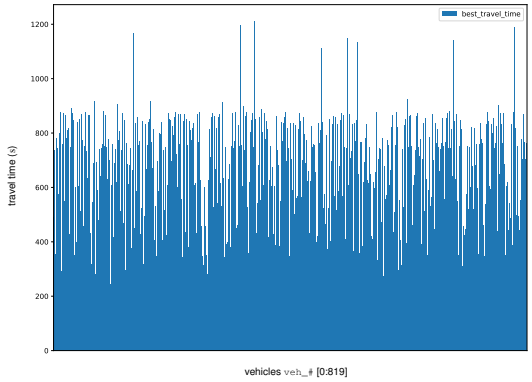


Fig. A.24-18. Best travel time for each vehicle, in seconds (s), during the simulation of a 24 h period.

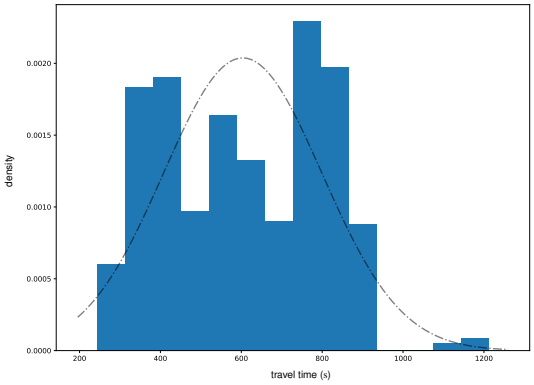


Fig. A.24-19. Density histogram of best travel time for vehicles, in seconds (s), during the simulation of a 24 h period, superimposing the normal density curve. The number of bins was calculated by the Freedman Diaconis rule.

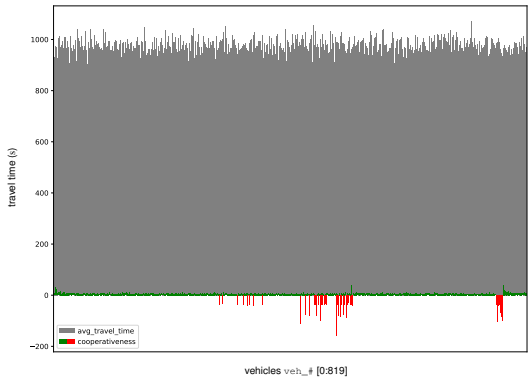


Fig. A.24-20. Average of the travel times, in seconds (s), of individual vehicles, during the simulation of a 24 h period. The bottom graph represents the *degree of cooperativeness**, downscaled by a normalization factor for the purpose of comparison with average times.

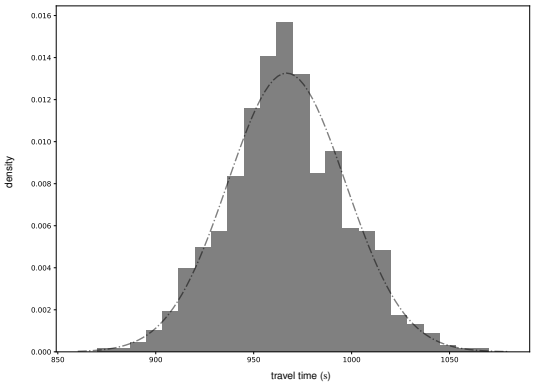


Fig. A.24-21. Density histogram of the average travel times, in seconds (s), of individual vehicles, during the simulation of a 24 h period, superimposing the normal density curve. The number of bins was calculated by the Freedman Diaconis rule.

* The *degree of cooperativeness* is a cumulative sum, calculated at each iteration, based on the complement of the ratio of cooperators, i.e., the higher the number of cooperators the less it increases, but the defectors are more penalized, and vice-versa. It varies inversely with the size of the group to which the player belongs.

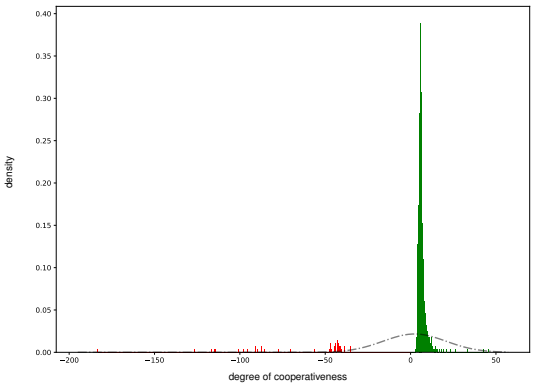


Fig. A.24-22. Density histogram of the *degree of cooperativeness** of individual vehicles, superimposing the normal density curve. The number of bins was calculated by the Freedman Diaconis rule. Generally, when strongly correlated with travel times, it presents a symmetric curve with respect to the *yy*-axis. Because some vehicles choose their preferred route immediately after the end of warmup, due to the gap between the RSU coverage and the route selection point, there may be some outliers.

A.25 820veh-24h-13060000

```
Scenario: scenario-1
Timestamp: 20210522T173448Z
Number of vehicles: 820 vehs
Simulation time: 24.0 h
Warm up end time: 1866.6 s; step 18665
Vehicle selection strategy: stochastic
RSU turned off: False
RSU strategy: lane_estimated_travel_time
Runner options:
   nogui: True
   step_length: 0.1
   seed: 19750808
   output_prefix: 820veh-24h-13060000
   sim_run_time: 24.0
   num_vehicles: 820
   warmup_speed: 13.96
   warmup_routes_weight: [473, 527]
   network_speed: 25.0
   change_behavior_probability: [0, 100]
   cooperation_probability: [0, 100]
   vehicle_selection_strategy: stochastic
   turn_rsu_off: False
   rsu_dynamic_dissemination: False
   rsu_dissemination_interval: 5
   rsu_probabilistic_dissemination: False
   rsu_suggestion_strategy: lane_estimated_travel_time
   rsu_routes_weight: [460, 540]
   rsu_moving_avg_size: 5
   travel_times_ttl: 60
   rsu_dissemination_ttl: 0
   rsu_send_travel_time_info: False
   payoff_matrix: [360.0, 240.0, 0.0, -120.0]
   roth_erev_parameters: [0.1, 0.15]
Network Mean speed after warmup:
   Max: 9.97
   Min: 3.83
```

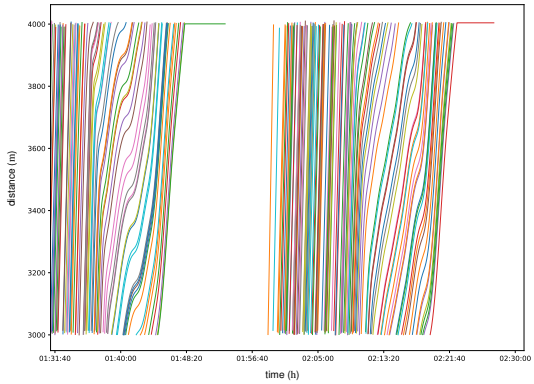


Fig. A.25-1. Time-Space diagram, for the one hour period after the end of the warmup, from 1:00:00 to 2:00:00 simulation time, plotted for the data from the sensor placed in the middle of the *direct* route (between 3000 m and 4000 m). In the case of an overloaded network, congestion shock waves can be observed.

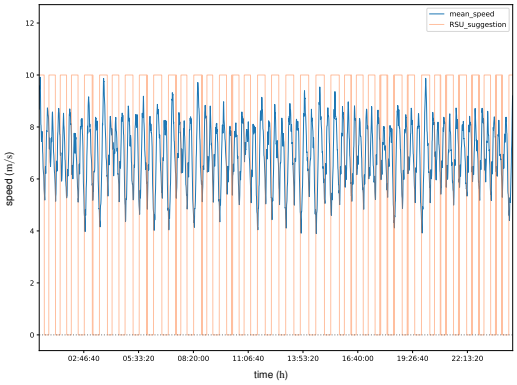


Fig. A.25-2. Mean speed in the network, in meters per second (m/s), over a 24 h period, superimposing (vertically, in orange) the time instants in which the RSU issued a recommendation to follow the *alternative* route.

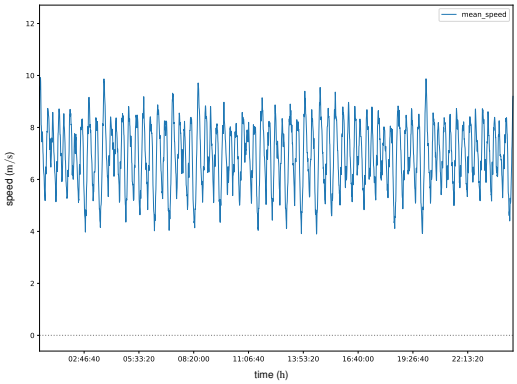


Fig. A.25-3. Mean speed in the network, in meters per second (m/s), over a 24 h period.

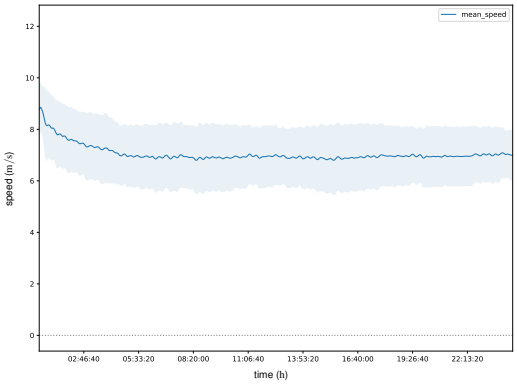


Fig. A.25-4. Mean speed in the network, in meters per second (m/s), over a 24 h period, 4 h Simple Moving Average, mean (line) and standard deviation (shaded).

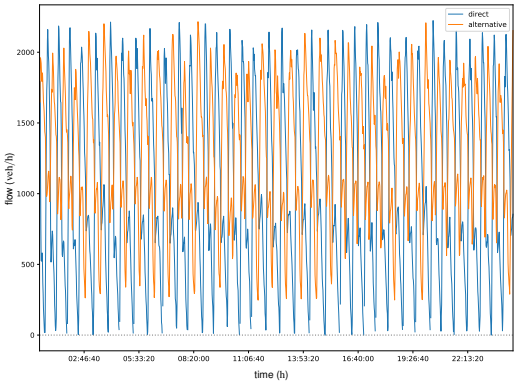


Fig. A.25-5. Traffic flow on each route, in vehicles per hour (veh/h), over a 24 h period.

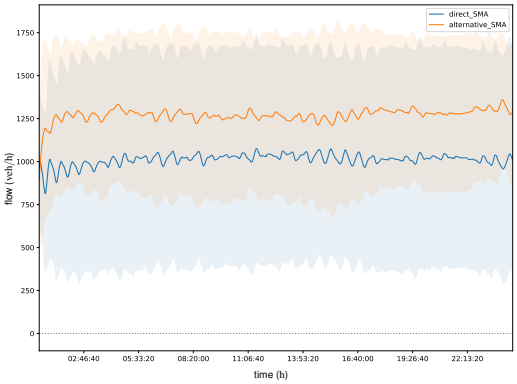


Fig. A.25-6. TrafficTraffic flow on each route, in vehicles per hour (veh/h), over a 24 h period, 4 h Simple Moving Average, mean (line) and standard deviation (shaded).

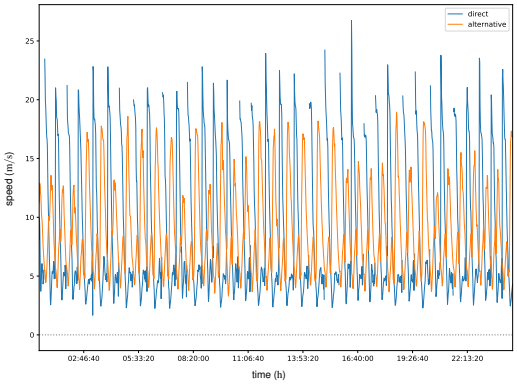


Fig. A.25-7. Mean speed on each route, in meters per second (m/s), aggregated to 1 min, over a 24 h period.

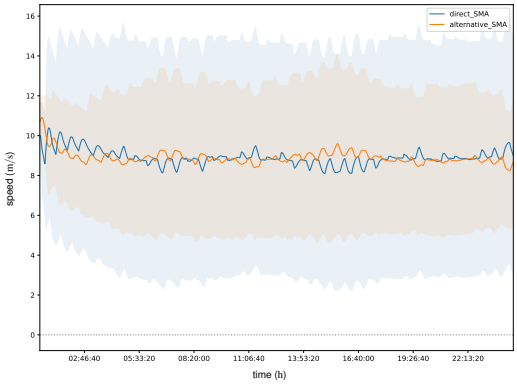


Fig. A.25-8. Mean speed on each route, in meters per second (m/s), aggregated to 1 min, over a 24 h period, 4 h Simple Moving Average, mean (line) and standard deviation (shaded).

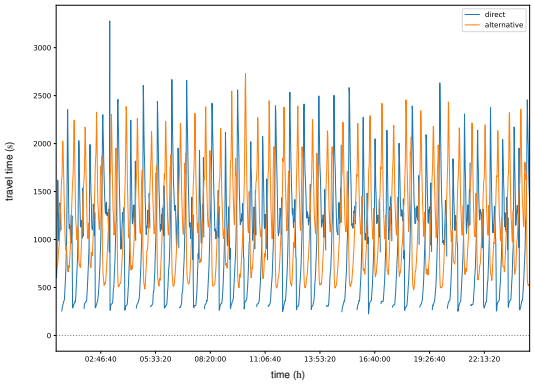


Fig. A.25-9. Travel times on each route, in seconds (s), aggregated to 1 min, over a 24 h period.

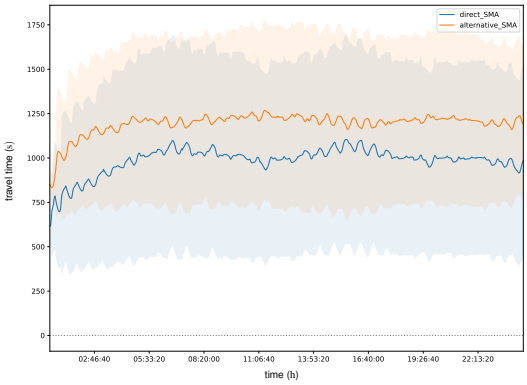


Fig. A.25-10. Travel times on each route, in seconds (s), aggregated to 1 min, over a 24 h period, 4 h Simple Moving Average, mean (line) and standard deviation (shaded).

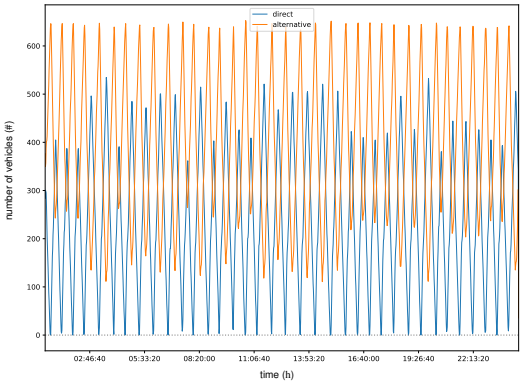


Fig. A.25-11. Average number of vehicles on each route, aggregated to 1 min, over a 24 h period.

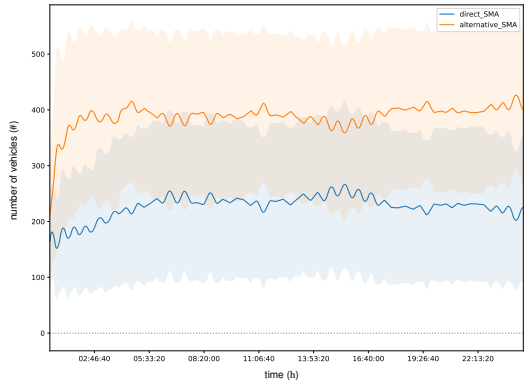


Fig. A.25-12. Average number of vehicles on each route, aggregated to 1 min, over a 24 h period, 4 h Simple Moving Average, mean (line) and standard deviation (shaded).

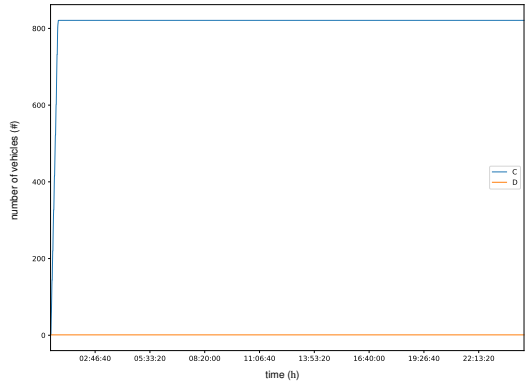


Fig. A.25-13. Evolution of the number of *Cooperators* and *Defectors* over a 24 h period.

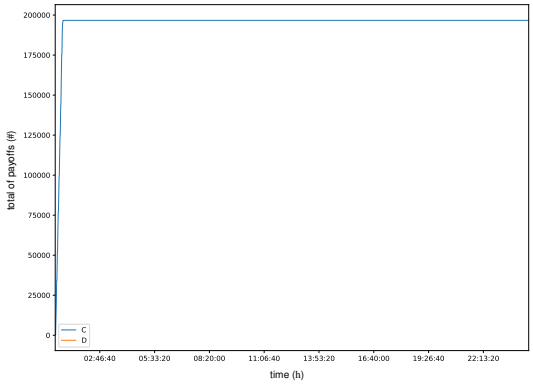


Fig. A.25-14. Evolution of total payoffs for *Cooperators* and *Defectors* (*individual payoff* times the *number of players receiving it*, $C(n) \times n$ and $D(n) \times (N-n)$, where n is the number of *Cooperators*), over a 24 h period.

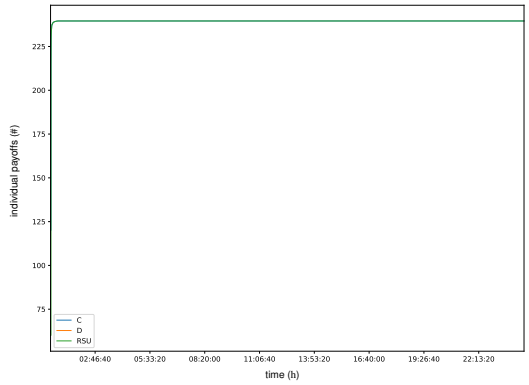


Fig. A.25-15. Evolution of the individual payoffs for *Cooperators, Defectors,* and *RSU* (always cooperating), over a 24 h period.

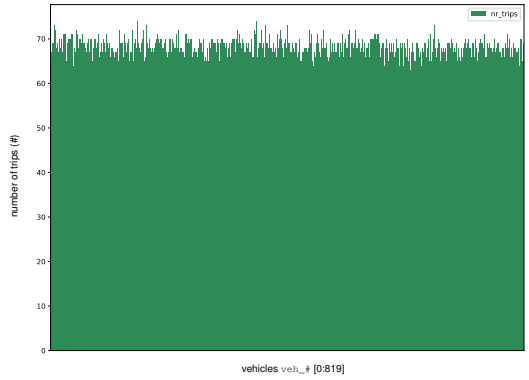


Fig. A.25-16. Number of trips made by each vehicle, during the simulation of a 24 h period.

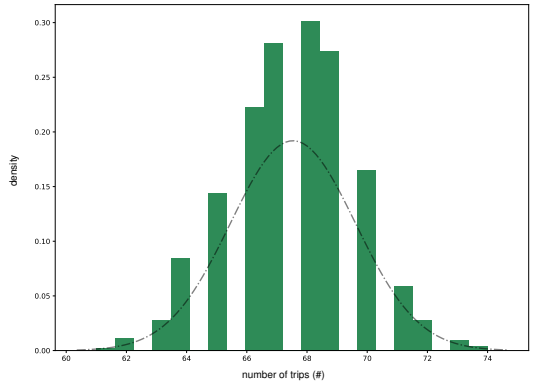


Fig. A.25-17. Density histogram of the number of trips made by each vehicle, during the simulation of a 24 h period, superimposing the normal density curve. The number of bins was calculated by the Freedman Diaconis rule.

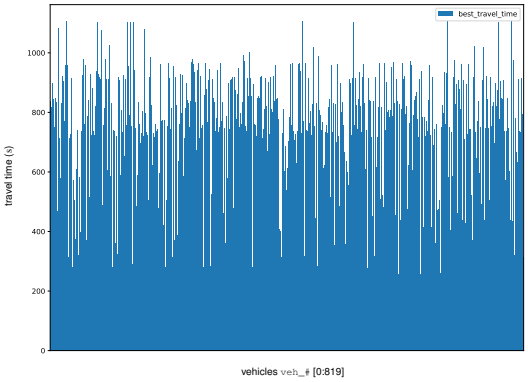


Fig. A.25-18. Best travel time for each vehicle, in seconds (s), during the simulation of a 24 h period.

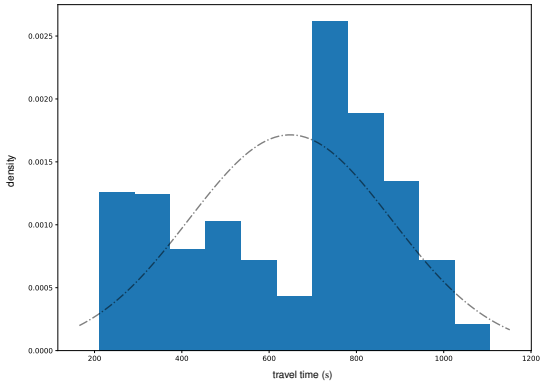


Fig. A.25-19. Density histogram of best travel time for vehicles, in seconds (s), during the simulation of a 24 h period, superimposing the normal density curve. The number of bins was calculated by the Freedman Diaconis rule.

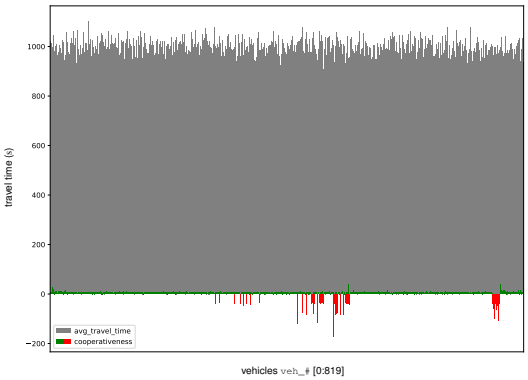


Fig. A.25-20. Average of the travel times, in seconds (s), of individual vehicles, during the simulation of a 24 h period. The bottom graph represents the *degree of cooperativeness**, downscaled by a normalization factor for the purpose of comparison with average times.

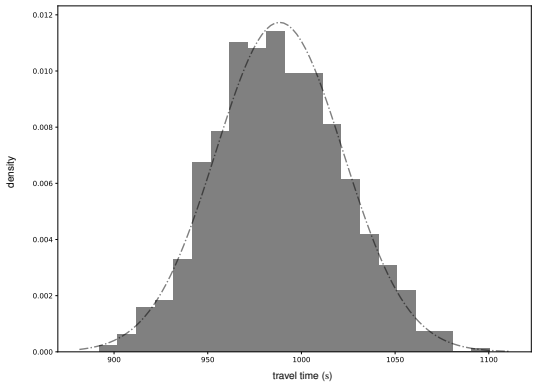


Fig. A.25-21. Density histogram of the average travel times, in seconds (s), of individual vehicles, during the simulation of a 24 h period, superimposing the normal density curve. The number of bins was calculated by the Freedman Diaconis rule.

* The *degree of cooperativeness* is a cumulative sum, calculated at each iteration, based on the complement of the ratio of cooperators, i.e., the higher the number of cooperators the less it increases, but the defectors are more penalized, and vice-versa. It varies inversely with the size of the group to which the player belongs.

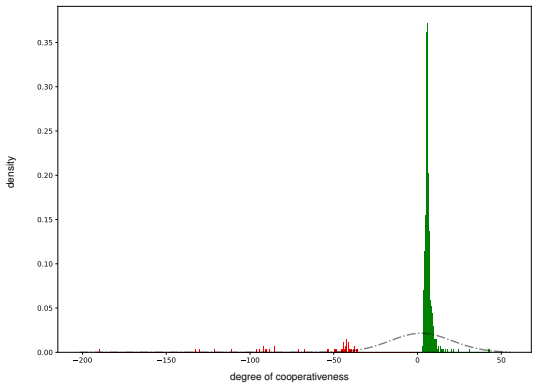


Fig. A.25-22. Density histogram of the *degree of cooperativeness** of individual vehicles, superimposing the normal density curve. The number of bins was calculated by the Freedman Diaconis rule. Generally, when strongly correlated with travel times, it presents a symmetric curve with respect to the *yy*-axis. Because some vehicles choose their preferred route immediately after the end of warmup, due to the gap between the RSU coverage and the route selection point, there may be some outliers.

A.26 820veh-24h-14060000

```
Scenario: scenario-1
Timestamp: 20210522T173508Z
Number of vehicles: 820 vehs
Simulation time: 24.0 h
Warm up end time: 1866.6 s; step 18665
Vehicle selection strategy: stochastic
RSU turned off: False
RSU strategy: proportional_dynamic_v2
Runner options:
   nogui: True
   step_length: 0.1
   seed: 19750808
   output_prefix: 820veh-24h-14060000
   sim_run_time: 24.0
   num_vehicles: 820
   warmup_speed: 13.96
   warmup_routes_weight: [473, 527]
   network_speed: 25.0
   change_behavior_probability: [0, 100]
   cooperation_probability: [0, 100]
   vehicle_selection_strategy: stochastic
   turn_rsu_off: False
   rsu_dynamic_dissemination: False
   rsu_dissemination_interval: 5
   rsu_probabilistic_dissemination: False
   rsu_suggestion_strategy: proportional_dynamic_v2
   rsu_routes_weight: [460, 540]
   rsu_moving_avg_size: 5
   travel_times_ttl: 60
   rsu_dissemination_ttl: 0
   rsu_send_travel_time_info: False
   payoff_matrix: [360.0, 240.0, 0.0, -120.0]
   roth_erev_parameters: [0.1, 0.15]
Network Mean speed after warmup:
   Max: 11.05
   Min: 7.38
```

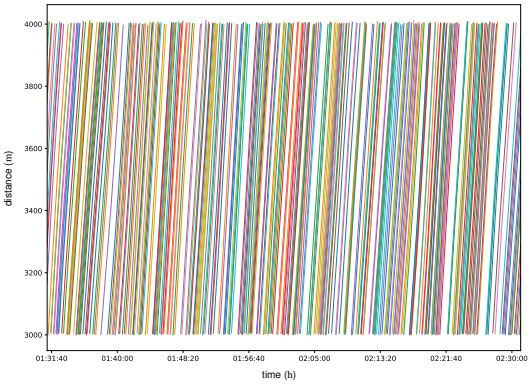


Fig. A.26-1. Time-Space diagram, for the one hour period after the end of the warmup, from 1:00:00 to 2:00:00 simulation time, plotted for the data from the sensor placed in the middle of the *direct* route (between 3000 m and 4000 m). In the case of an overloaded network, congestion shock waves can be observed.

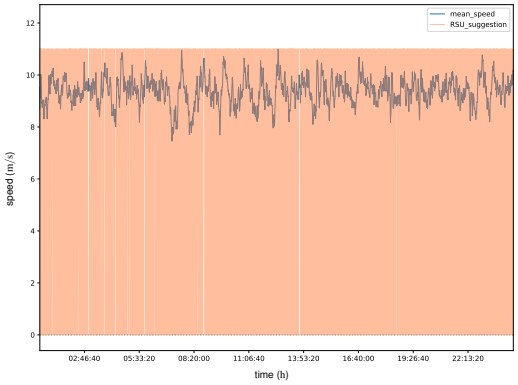


Fig. A.26-2. Mean speed in the network, in meters per second (m/s), over a 24 h period, superimposing (vertically, in orange) the time instants in which the RSU issued a recommendation to follow the *alternative* route.

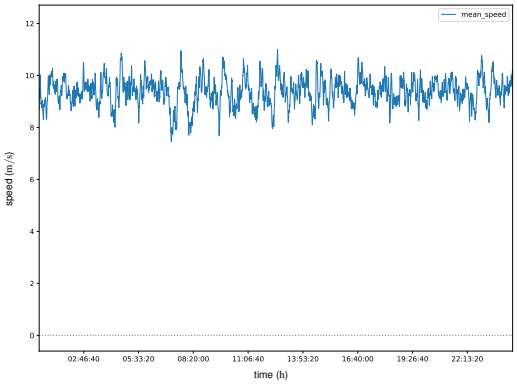


Fig. A.26-3. Mean speed in the network, in meters per second (m/s), over a 24 h period.

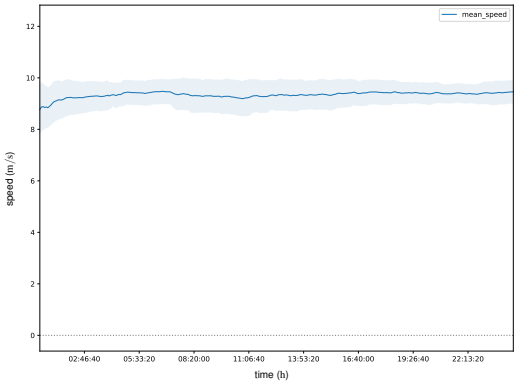


Fig. A.26-4. Mean speed in the network, in meters per second (m/s), over a 24 h period, 4 h Simple Moving Average, mean (line) and standard deviation (shaded).

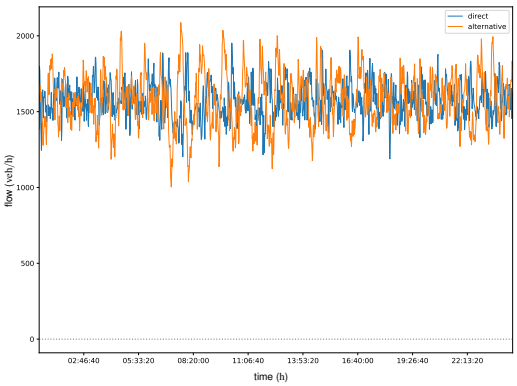


Fig. A.26-5. Traffic flow on each route, in vehicles per hour (veh/h), over a 24 h period.

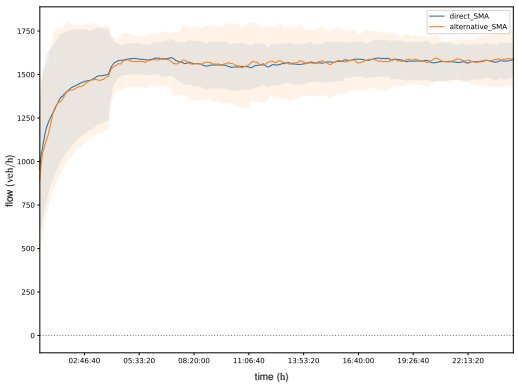


Fig. A.26-6. TrafficTraffic flow on each route, in vehicles per hour (veh/h), over a 24 h period, 4 h Simple Moving Average, mean (line) and standard deviation (shaded).

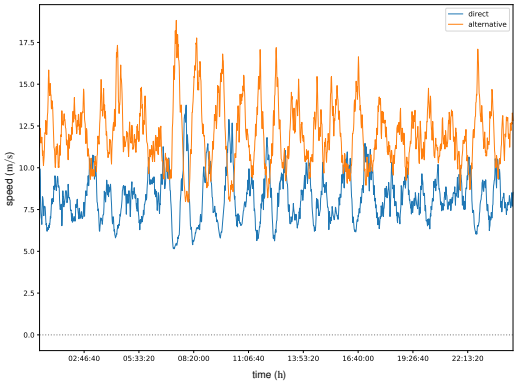


Fig. A.26-7. Mean speed on each route, in meters per second (m/s), aggregated to 1 min, over a 24 h period.

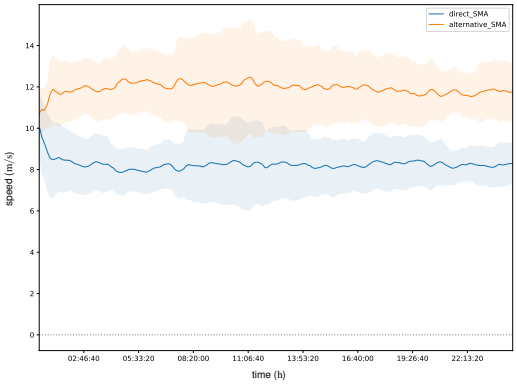


Fig. A.26-8. Mean speed on each route, in meters per second (m/s), aggregated to 1 min, over a 24 h period, 4 h Simple Moving Average, mean (line) and standard deviation (shaded).

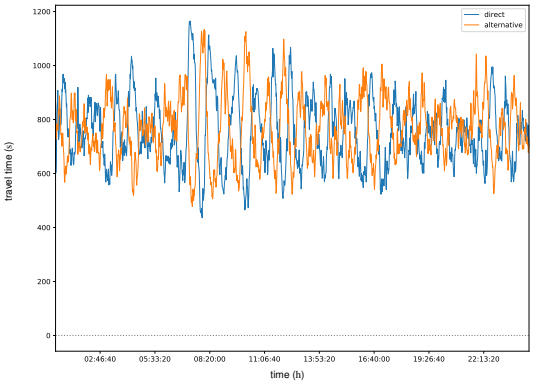


Fig. A.26-9. Travel times on each route, in seconds (s), aggregated to 1 min, over a 24 h period.

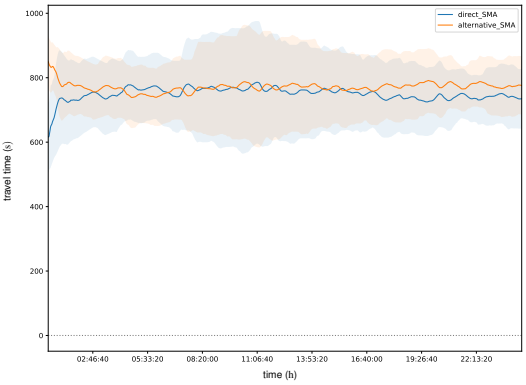


Fig. A.26-10. Travel times on each route, in seconds (s), aggregated to 1 min, over a 24 h period, 4 h Simple Moving Average, mean (line) and standard deviation (shaded).

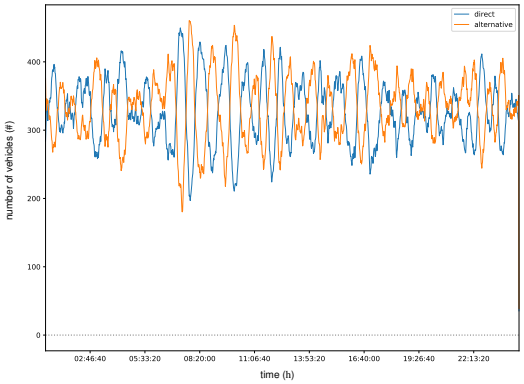


Fig. A.26-11. Average number of vehicles on each route, aggregated to 1 min, over a 24 h period.

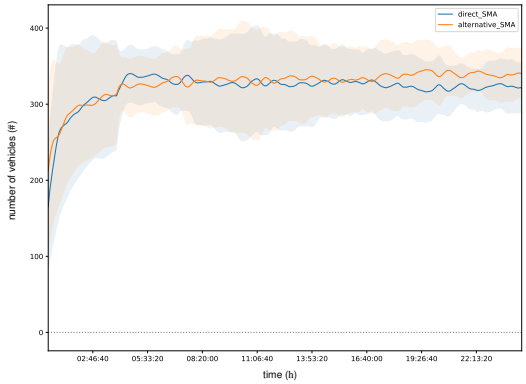


Fig. A.26-12. Average number of vehicles on each route, aggregated to 1 min, over a 24 h period, 4 h Simple Moving Average, mean (line) and standard deviation (shaded).

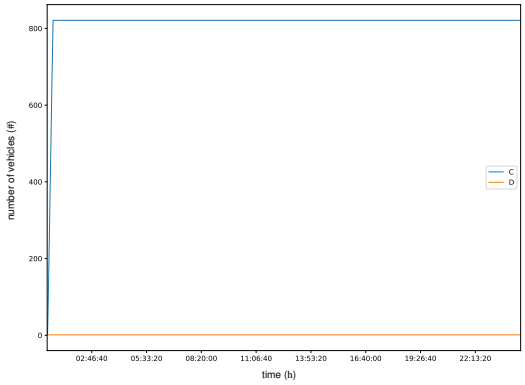


Fig. A.26-13. Evolution of the number of *Cooperators* and *Defectors* over a 24 h period.

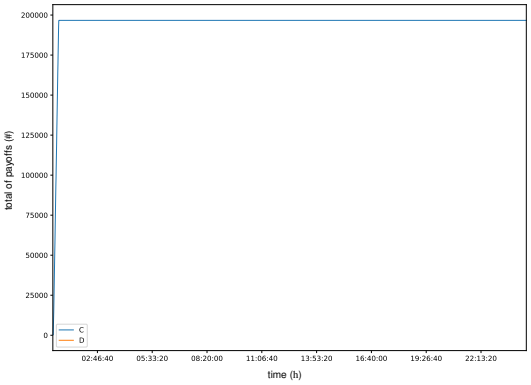


Fig. A.26-14. Evolution of total payoffs for *Cooperators* and *Defectors* (*individual payoff* times the *number of players receiving it*, $C(n) \times n$ and $D(n) \times (N-n)$, where n is the number of *Cooperators*), over a 24 h period.

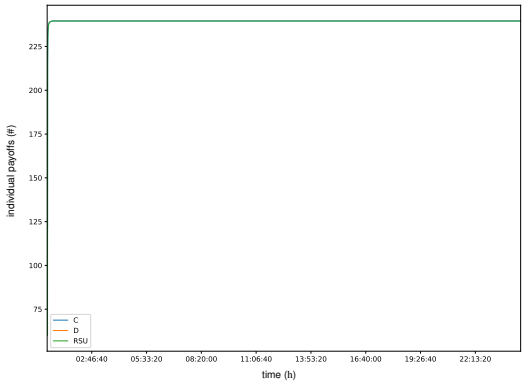


Fig. A.26-15. Evolution of the individual payoffs for *Cooperators, Defectors,* and *RSU* (always cooperating), over a 24 h period.

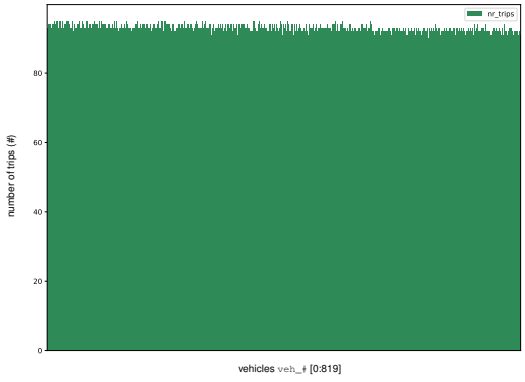


Fig. A.26-16. Number of trips made by each vehicle, during the simulation of a 24 h period.

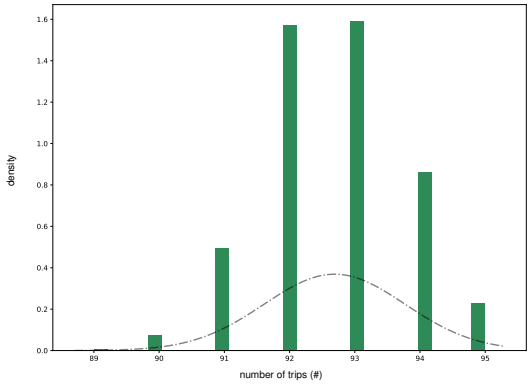


Fig. A.26-17. Density histogram of the number of trips made by each vehicle, during the simulation of a 24 h period, superimposing the normal density curve. The number of bins was calculated by the Freedman Diaconis rule.

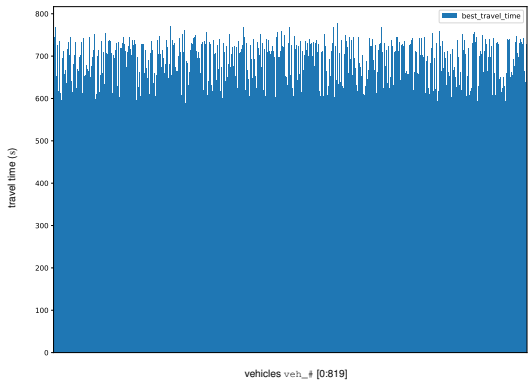


Fig. A.26-18. Best travel time for each vehicle, in seconds (s), during the simulation of a 24 h period.

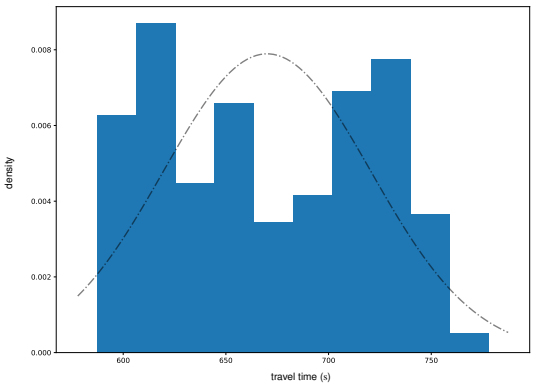


Fig. A.26-19. Density histogram of best travel time for vehicles, in seconds (s), during the simulation of a 24 h period, superimposing the normal density curve. The number of bins was calculated by the Freedman Diaconis rule.

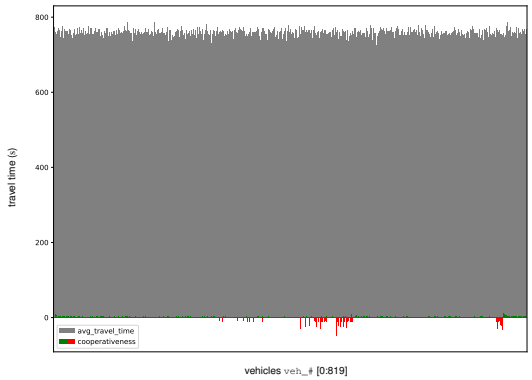


Fig. A.26-20. Average of the travel times, in seconds (s), of individual vehicles, during the simulation of a 24 h period. The bottom graph represents the *degree of cooperativeness**, downscaled by a normalization factor for the purpose of comparison with average times.

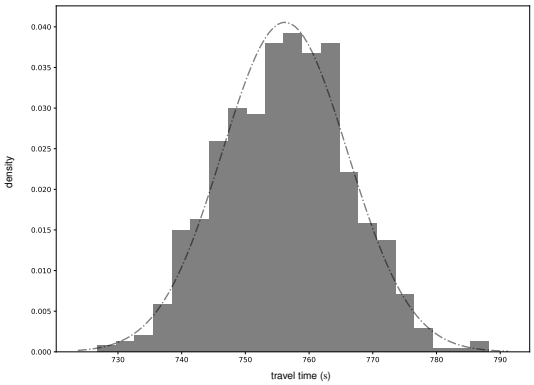


Fig. A.26-21. Density histogram of the average travel times, in seconds (s), of individual vehicles, during the simulation of a 24 h period, superimposing the normal density curve. The number of bins was calculated by the Freedman Diaconis rule.

* The *degree of cooperativeness* is a cumulative sum, calculated at each iteration, based on the complement of the ratio of cooperators, i.e., the higher the number of cooperators the less it increases, but the defectors are more penalized, and vice-versa. It varies inversely with the size of the group to which the player belongs.

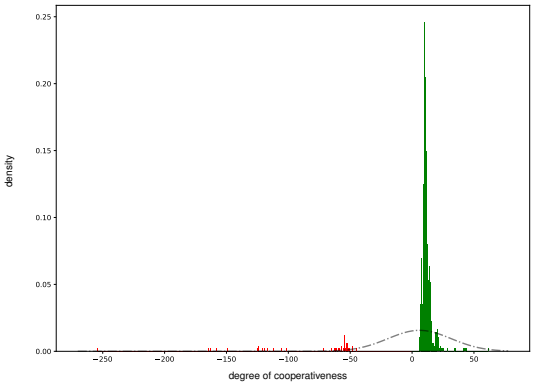


Fig. A.26-22. Density histogram of the *degree of cooperativeness** of individual vehicles, superimposing the normal density curve. The number of bins was calculated by the Freedman Diaconis rule. Generally, when strongly correlated with travel times, it presents a symmetric curve with respect to the *yy*-axis. Because some vehicles choose their preferred route immediately after the end of warmup, due to the gap between the RSU coverage and the route selection point, there may be some outliers.

A.27 820veh-24h-15060000

```
Scenario: scenario-1
Timestamp: 20210521T142355Z
Number of vehicles: 820 vehs
Simulation time: 24.0 h
Warm up end time: 1866.6 s; step 18665
Vehicle selection strategy: stochastic
RSU turned off: False
RSU strategy: proportional_dynamic_v3
Runner options:
   nogui: True
   step_length: 0.1
   seed: 19750808
   output_prefix: 820veh-24h-15060000
   sim_run_time: 24.0
   num_vehicles: 820
   warmup_speed: 13.96
   warmup_routes_weight: [473, 527]
   network_speed: 25.0
   change_behavior_probability: [0, 100]
   cooperation_probability: [0, 100]
   vehicle_selection_strategy: stochastic
   turn_rsu_off: False
   rsu_dynamic_dissemination: False
   rsu_dissemination_interval: 5
   rsu_probabilistic_dissemination: False
   rsu_suggestion_strategy: proportional_dynamic_v3
   rsu_routes_weight: [460, 540]
   rsu_moving_avg_size: 5
   travel_times_ttl: 60
   rsu_dissemination_ttl: 0
   rsu_send_travel_time_info: False
   payoff_matrix: [360.0, 240.0, 0.0, -120.0]
   roth_erev_parameters: [0.1, 0.15]
Network Mean speed after warmup:
   Max: 10.91
   Min: 7.1
```

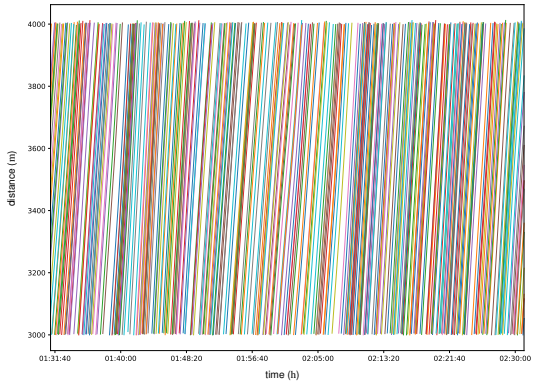


Fig. A.27-1. Time-Space diagram, for the one hour period after the end of the warmup, from 1:00:00 to 2:00:00 simulation time, plotted for the data from the sensor placed in the middle of the *direct* route (between 3000 m and 4000 m). In the case of an overloaded network, congestion shock waves can be observed.

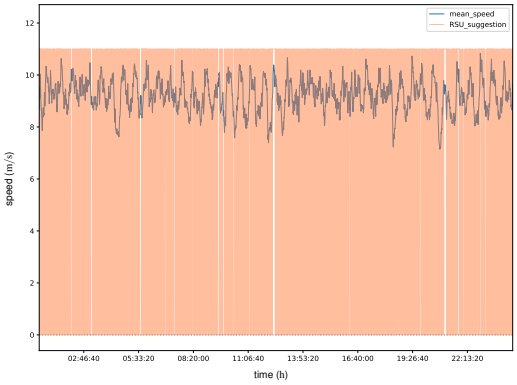


Fig. A.27-2. Mean speed in the network, in meters per second (m/s), over a 24 h period, superimposing (vertically, in orange) the time instants in which the RSU issued a recommendation to follow the *alternative* route.

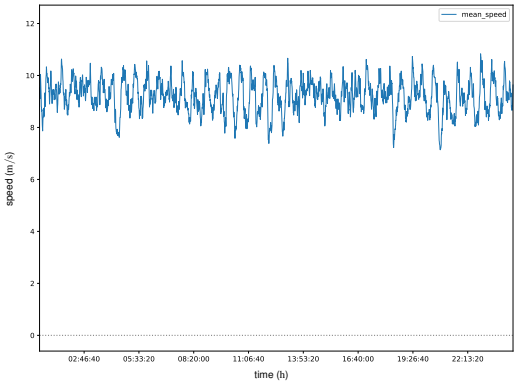


Fig. A.27-3. Mean speed in the network, in meters per second (m/s), over a 24 h period.

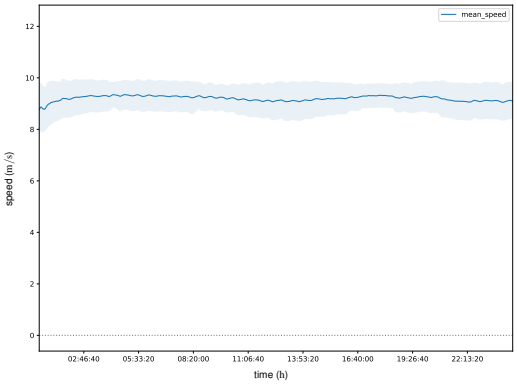


Fig. A.27-4. Mean speed in the network, in meters per second (m/s), over a 24 h period, 4 h Simple Moving Average, mean (line) and standard deviation (shaded).

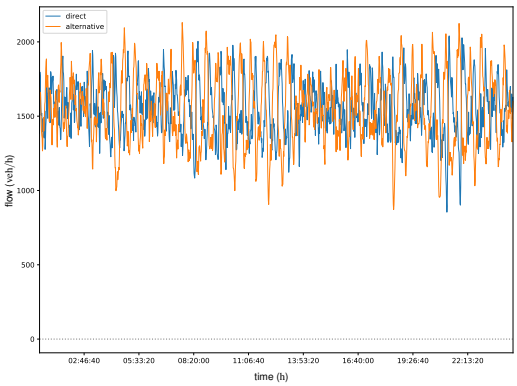


Fig. A.27-5. Traffic flow on each route, in vehicles per hour (veh/h), over a 24 h period.

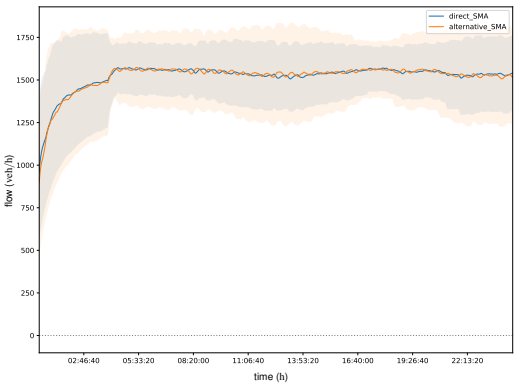


Fig. A.27-6. TrafficTraffic flow on each route, in vehicles per hour (veh/h), over a 24 h period, 4 h Simple Moving Average, mean (line) and standard deviation (shaded).

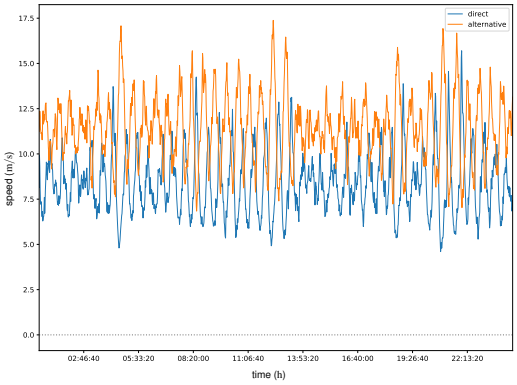


Fig. A.27-7. Mean speed on each route, in meters per second (m/s), aggregated to 1 min, over a 24 h period.

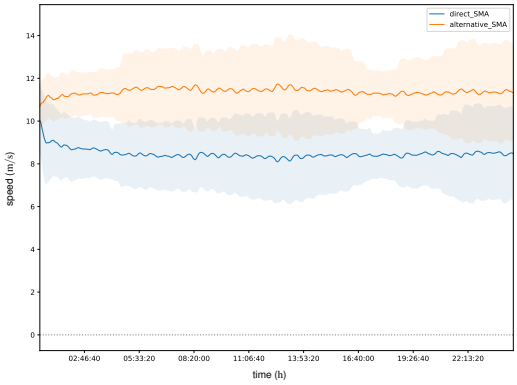


Fig. A.27-8. Mean speed on each route, in meters per second (m/s), aggregated to 1 min, over a 24 h period, 4 h Simple Moving Average, mean (line) and standard deviation (shaded).

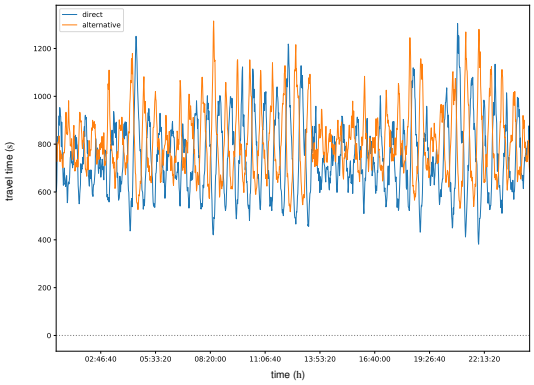


Fig. A.27-9. Travel times on each route, in seconds (s), aggregated to 1 min, over a 24 h period.

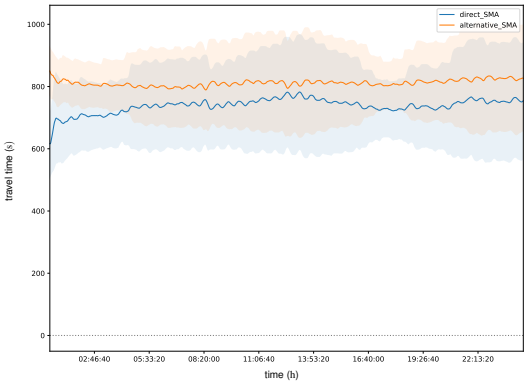


Fig. A.27-10. Travel times on each route, in seconds (s), aggregated to 1 min, over a 24 h period, 4 h Simple Moving Average, mean (line) and standard deviation (shaded).

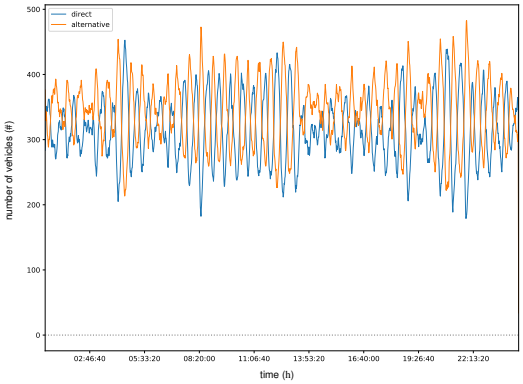


Fig. A.27-11. Average number of vehicles on each route, aggregated to 1 min, over a 24 h period.

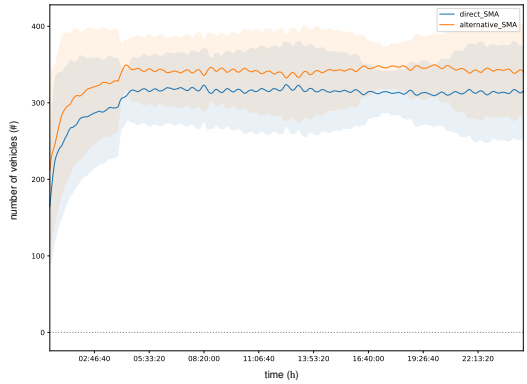


Fig. A.27-12. Average number of vehicles on each route, aggregated to 1 min, over a 24 h period, 4 h Simple Moving Average, mean (line) and standard deviation (shaded).

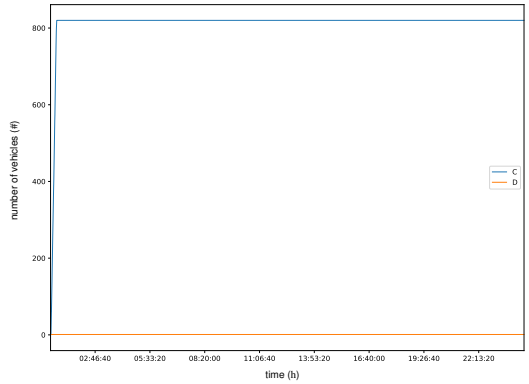


Fig. A.27-13. Evolution of the number of *Cooperators* and *Defectors* over a 24 h period.

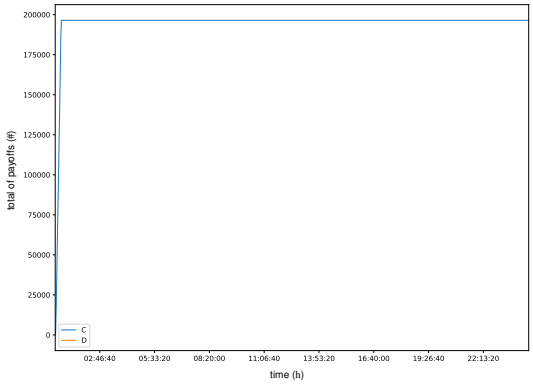


Fig. A.27-14. Evolution of total payoffs for *Cooperators* and *Defectors* (*individual payoff* times the *number of players receiving it*, $C(n) \times n$ and $D(n) \times (N-n)$, where n is the number of *Cooperators*), over a 24 h period.

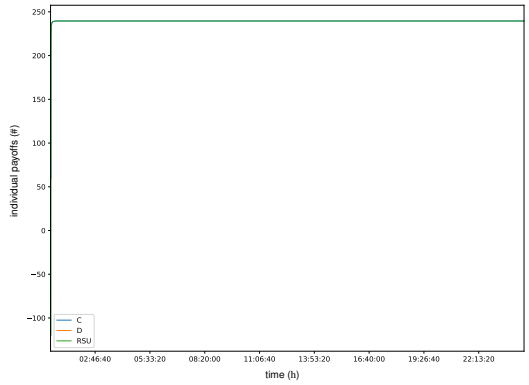


Fig. A.27-15. Evolution of the individual payoffs for *Cooperators, Defectors,* and *RSU* (always cooperating), over a 24 h period.

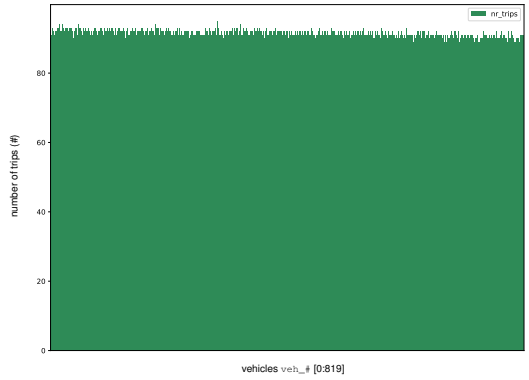


Fig. A.27-16. Number of trips made by each vehicle, during the simulation of a 24 h period.

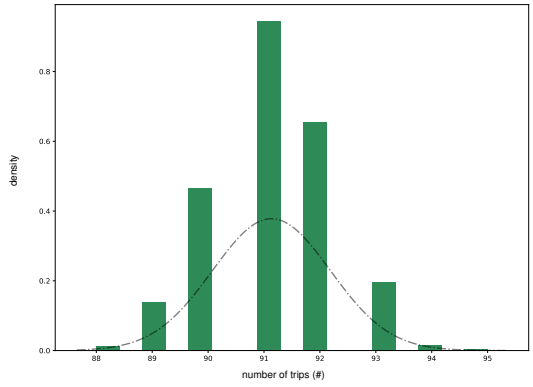


Fig. A.27-17. Density histogram of the number of trips made by each vehicle, during the simulation of a 24 h period, superimposing the normal density curve. The number of bins was calculated by the Freedman Diaconis rule.

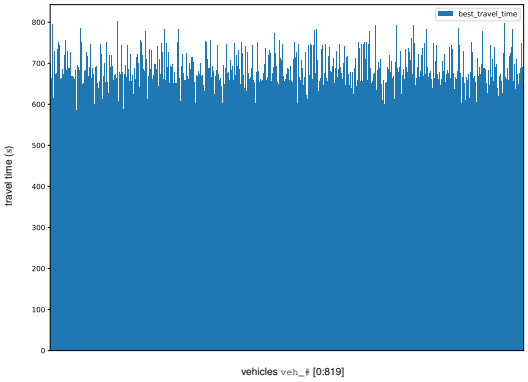


Fig. A.27-18. Best travel time for each vehicle, in seconds (s), during the simulation of a 24 h period.

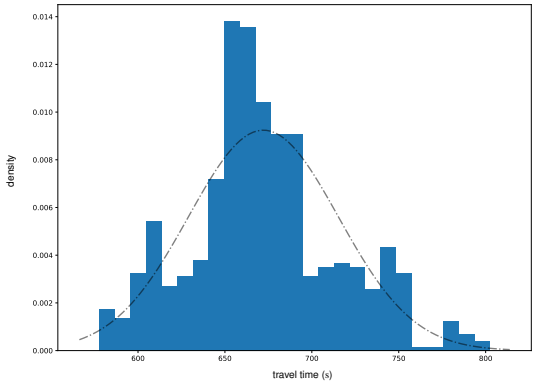


Fig. A.27-19. Density histogram of best travel time for vehicles, in seconds (s), during the simulation of a 24 h period, superimposing the normal density curve. The number of bins was calculated by the Freedman Diaconis rule.

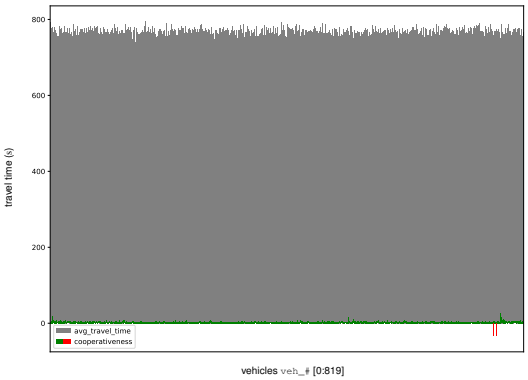


Fig. A.27-20. Average of the travel times, in seconds (s), of individual vehicles, during the simulation of a 24 h period. The bottom graph represents the *degree of cooperativeness**, downscaled by a normalization factor for the purpose of comparison with average times.

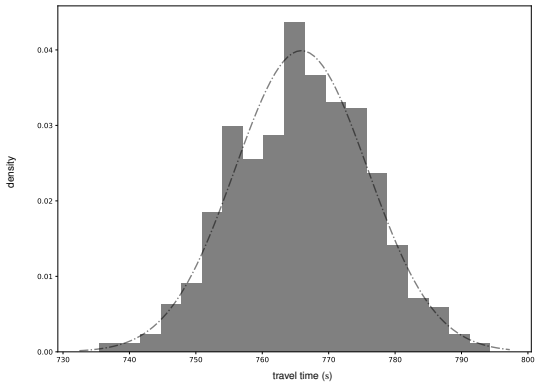


Fig. A.27-21. Density histogram of the average travel times, in seconds (s), of individual vehicles, during the simulation of a 24 h period, superimposing the normal density curve. The number of bins was calculated by the Freedman Diaconis rule.

* The *degree of cooperativeness* is a cumulative sum, calculated at each iteration, based on the complement of the ratio of cooperators, i.e., the higher the number of cooperators the less it increases, but the defectors are more penalized, and vice-versa. It varies inversely with the size of the group to which the player belongs.

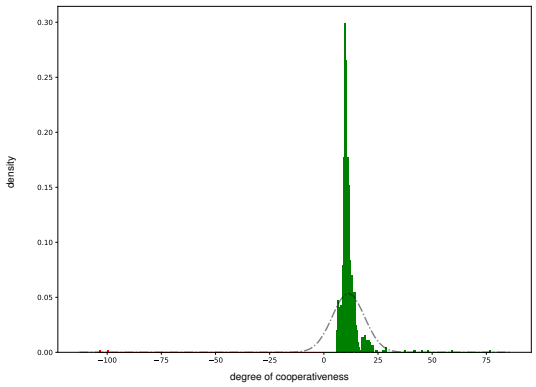


Fig. A.27-22. Density histogram of the *degree of cooperativeness** of individual vehicles, superimposing the normal density curve. The number of bins was calculated by the Freedman Diaconis rule. Generally, when strongly correlated with travel times, it presents a symmetric curve with respect to the *yy*-axis. Because some vehicles choose their preferred route immediately after the end of warmup, due to the gap between the RSU coverage and the route selection point, there may be some outliers.

A.28 820veh-24h-16060000

```
Scenario: scenario-1
Timestamp: 20210521T142409Z
Number of vehicles: 820 vehs
Simulation time: 24.0 h
Warm up end time: 1866.6 s; step 18665
Vehicle selection strategy: stochastic
RSU turned off: False
RSU strategy: pigous_example
Runner options:
   nogui: True
   step_length: 0.1
   seed: 19750808
   output_prefix: 820veh-24h-16060000
   sim_run_time: 24.0
   num_vehicles: 820
   warmup_speed: 13.96
   warmup_routes_weight: [473, 527]
   network_speed: 25.0
   change_behavior_probability: [0, 100]
   cooperation_probability: [0, 100]
   vehicle_selection_strategy: stochastic
   turn_rsu_off: False
   rsu_dynamic_dissemination: False
   rsu_dissemination_interval: 5
   rsu_probabilistic_dissemination: False
   rsu_suggestion_strategy: pigous_example
   rsu_routes_weight: [460, 540]
   rsu_moving_avg_size: 5
   travel_times_ttl: 60
   rsu_dissemination_ttl: 0
   rsu_send_travel_time_info: False
   payoff_matrix: [360.0, 240.0, 0.0, -120.0]
   roth_erev_parameters: [0.1, 0.15]
Network Mean speed after warmup:
   Max: 10.8
   Min: 8.0
```

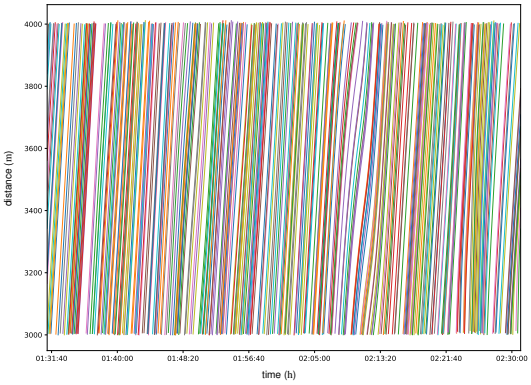


Fig. A.28-1. Time-Space diagram, for the one hour period after the end of the warmup, from 1:00:00 to 2:00:00 simulation time, plotted for the data from the sensor placed in the middle of the *direct* route (between 3000 m and 4000 m). In the case of an overloaded network, congestion shock waves can be observed.

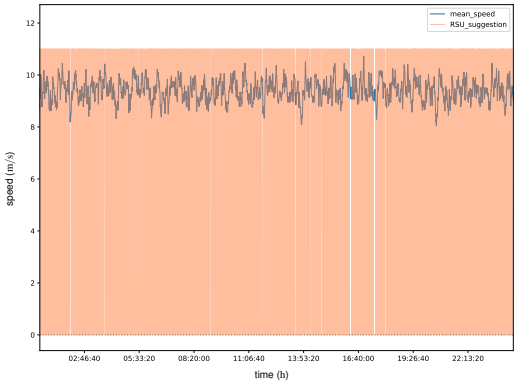


Fig. A.28-2. Mean speed in the network, in meters per second (m/s), over a 24 h period, superimposing (vertically, in orange) the time instants in which the RSU issued a recommendation to follow the *alternative* route.

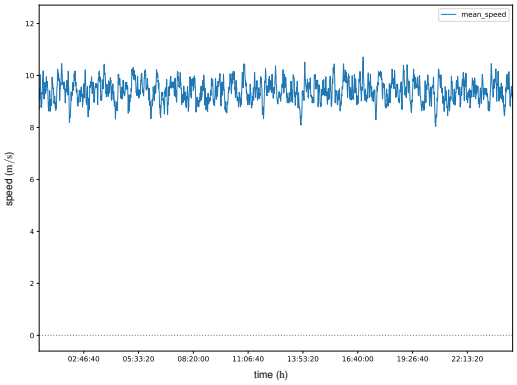


Fig. A.28-3. Mean speed in the network, in meters per second (m/s), over a 24 h period.

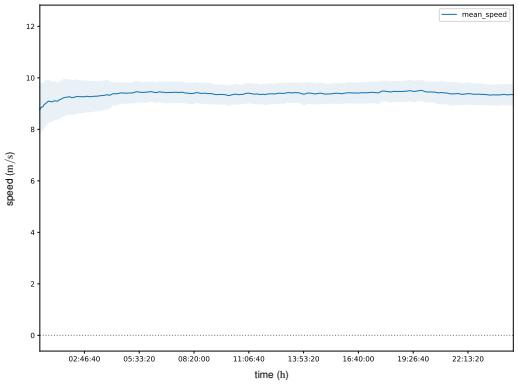


Fig. A.28-4. Mean speed in the network, in meters per second (m/s), over a 24 h period, 4 h Simple Moving Average, mean (line) and standard deviation (shaded).

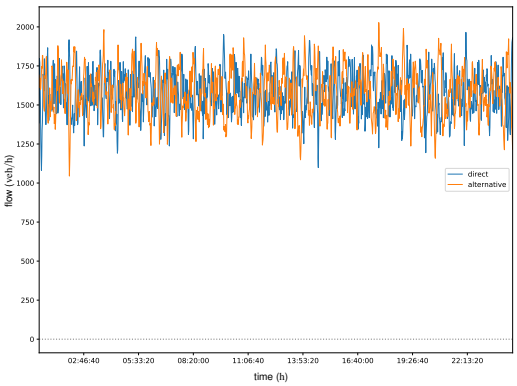


Fig. A.28-5. Traffic flow on each route, in vehicles per hour (veh/h), over a 24 h period.

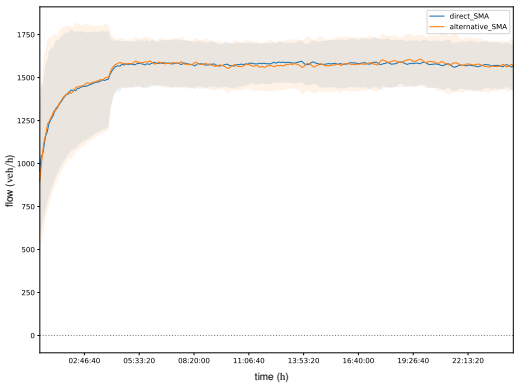


Fig. A.28-6. TrafficTraffic flow on each route, in vehicles per hour (veh/h), over a 24 h period, 4 h Simple Moving Average, mean (line) and standard deviation (shaded).

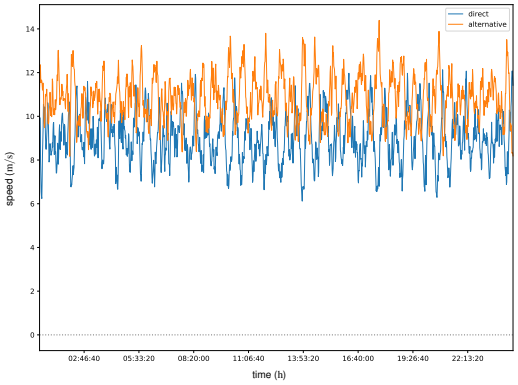


Fig. A.28-7. Mean speed on each route, in meters per second (m/s), aggregated to 1 min, over a 24 h period.

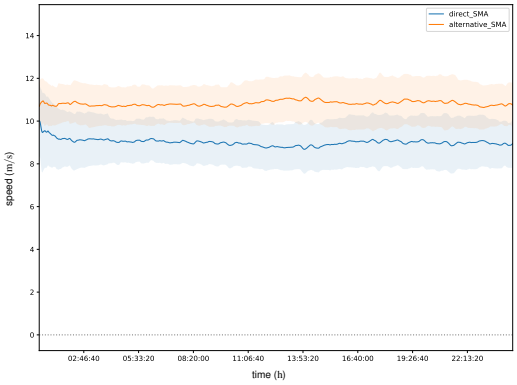


Fig. A.28-8. Mean speed on each route, in meters per second (m/s), aggregated to 1 min, over a 24 h period, 4 h Simple Moving Average, mean (line) and standard deviation (shaded).

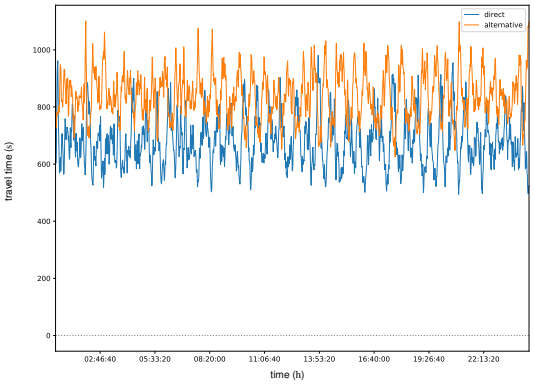


Fig. A.28-9. Travel times on each route, in seconds (s), aggregated to 1 min, over a 24 h period.

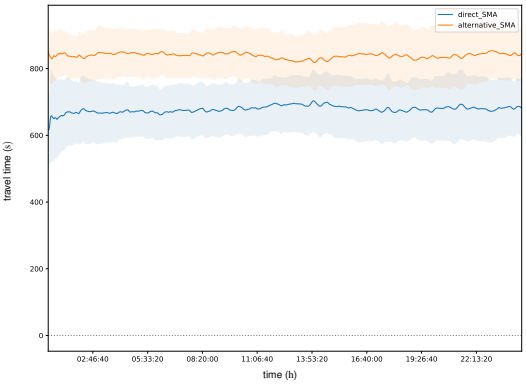


Fig. A.28-10. Travel times on each route, in seconds (s), aggregated to 1 min, over a 24 h period, 4 h Simple Moving Average, mean (line) and standard deviation (shaded).

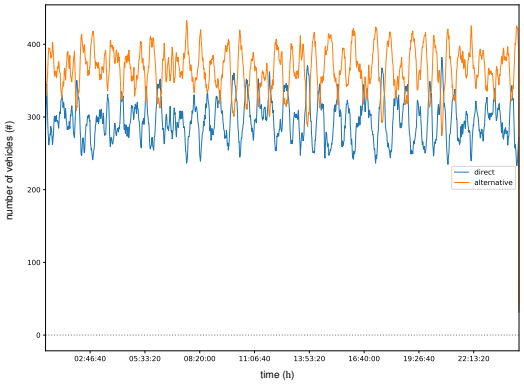


Fig. A.28-11. Average number of vehicles on each route, aggregated to 1 min, over a 24 h period.

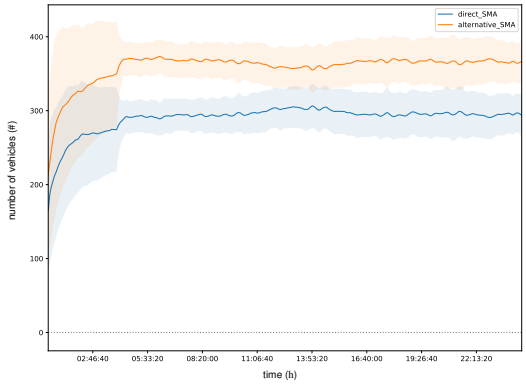


Fig. A.28-12. Average number of vehicles on each route, aggregated to 1 min, over a 24 h period, 4 h Simple Moving Average, mean (line) and standard deviation (shaded).

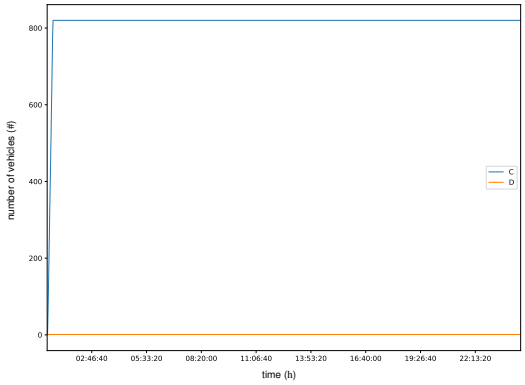


Fig. A.28-13. Evolution of the number of *Cooperators* and *Defectors* over a 24 h period.

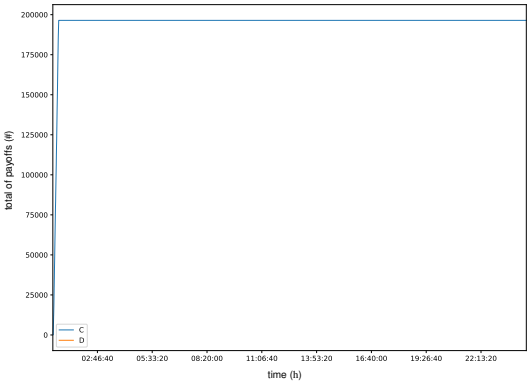


Fig. A.28-14. Evolution of total payoffs for *Cooperators* and *Defectors* (*individual payoff* times the *number of players receiving it*, $C(n) \times n$ and $D(n) \times (N-n)$, where n is the number of *Cooperators*), over a 24 h period.

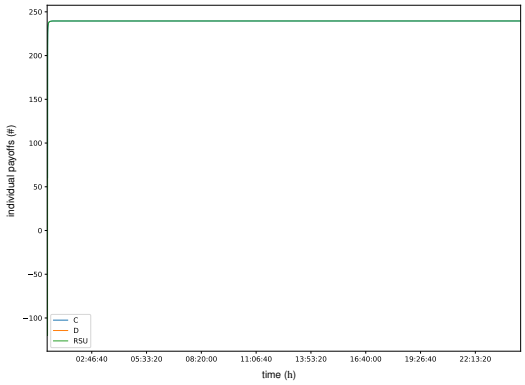


Fig. A.28-15. Evolution of the individual payoffs for *Cooperators, Defectors,* and *RSU* (always cooperating), over a 24 h period.

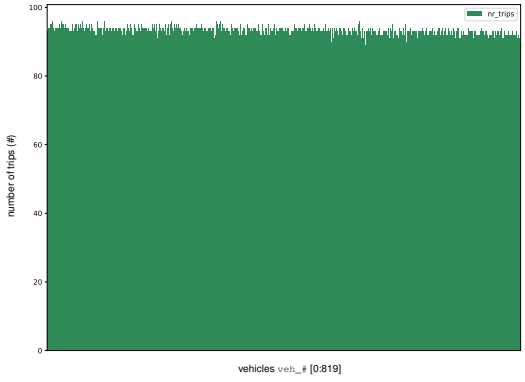


Fig. A.28-16. Number of trips made by each vehicle, during the simulation of a 24 h period.

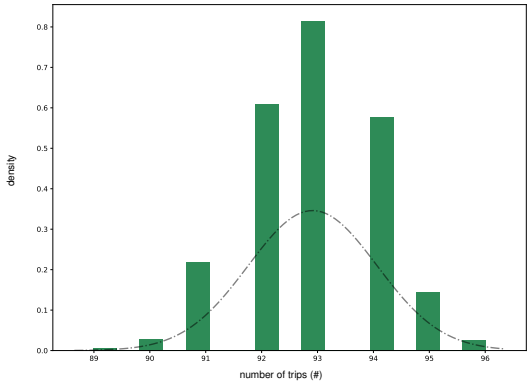


Fig. A.28-17. Density histogram of the number of trips made by each vehicle, during the simulation of a 24 h period, superimposing the normal density curve. The number of bins was calculated by the Freedman Diaconis rule.

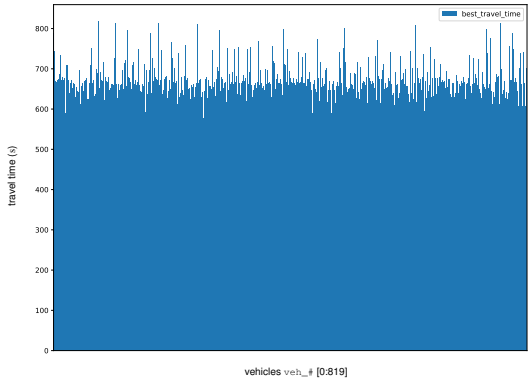


Fig. A.28-18. Best travel time for each vehicle, in seconds (s), during the simulation of a 24 h period.

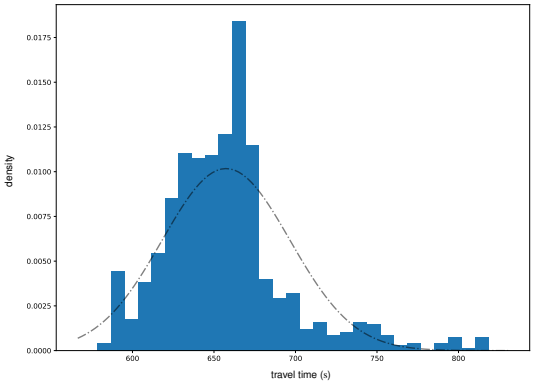


Fig. A.28-19. Density histogram of best travel time for vehicles, in seconds (s), during the simulation of a 24 h period, superimposing the normal density curve. The number of bins was calculated by the Freedman Diaconis rule.

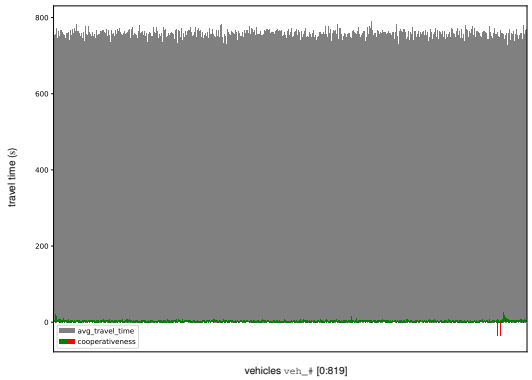


Fig. A.28-20. Average of the travel times, in seconds (s), of individual vehicles, during the simulation of a 24 h period. The bottom graph represents the *degree of cooperativeness**, downscaled by a normalization factor for the purpose of comparison with average times.

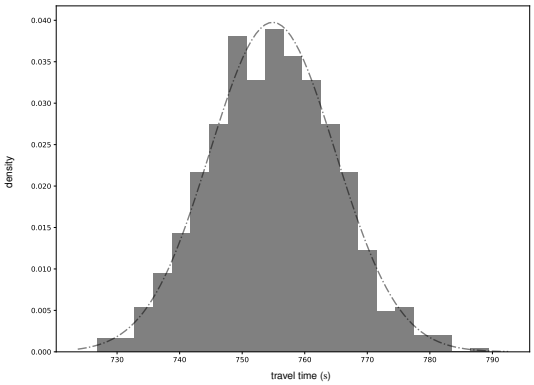


Fig. A.28-21. Density histogram of the average travel times, in seconds (s), of individual vehicles, during the simulation of a 24 h period, superimposing the normal density curve. The number of bins was calculated by the Freedman Diaconis rule.

* The *degree of cooperativeness* is a cumulative sum, calculated at each iteration, based on the complement of the ratio of cooperators, i.e., the higher the number of cooperators the less it increases, but the defectors are more penalized, and vice-versa. It varies inversely with the size of the group to which the player belongs.

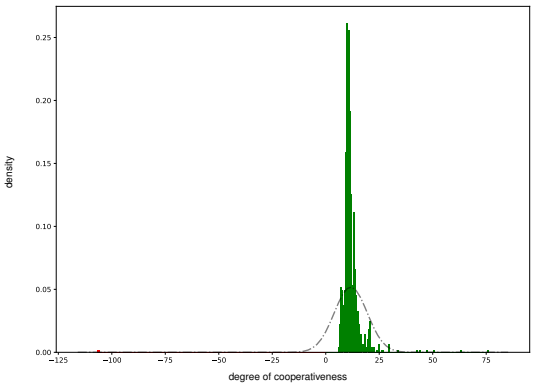


Fig. A.28-22. Density histogram of the *degree of cooperativeness** of individual vehicles, superimposing the normal density curve. The number of bins was calculated by the Freedman Diaconis rule. Generally, when strongly correlated with travel times, it presents a symmetric curve with respect to the *yy*-axis. Because some vehicles choose their preferred route immediately after the end of warmup, due to the gap between the RSU coverage and the route selection point, there may be some outliers.

A.29 820veh-24h-17060000

```
Scenario: scenario-1
Timestamp: 20210617T032708Z
Number of vehicles: 820 vehs
Simulation time: 24.0 h
Warm up end time: 1866.6 s; step 18665
Vehicle selection strategy: stochastic
RSU turned off: False
RSU strategy: proportional_dynamic_v4
Runner options:
   nogui: True
   step_length: 0.1
   seed: 19750808
   output_prefix: 820veh-24h-17060000
   sim_run_time: 24.0
   num_vehicles: 820
   warmup_speed: 13.96
   warmup_routes_weight: [473, 527]
   network_speed: 25.0
   change_behavior_probability: [0, 100]
   cooperation_probability: [0, 100]
   vehicle_selection_strategy: stochastic
   turn_rsu_off: False
   rsu_dynamic_dissemination: False
   rsu_dissemination_interval: 5
   rsu_probabilistic_dissemination: False
   rsu_suggestion_strategy: proportional_dynamic_v4
   rsu_routes_weight: [460, 540]
   rsu_moving_avg_size: 5
   travel_times_ttl: 60
   rsu_dissemination_ttl: 0
   rsu_send_travel_time_info: False
   payoff_matrix: [360.0, 240.0, 0.0, -120.0]
   roth_erev_parameters: [0.1, 0.15]
   rsu_change_dissemination: False
   rsu_change_dissemination_steps: [14400, 28800, 43200, 57600, 72000]
   rsu_change_dissemination_intervals: [10, 20, 40, 80, 160]
Network Mean speed after warmup:
   Max: 10.52
   Min: 6.79
```

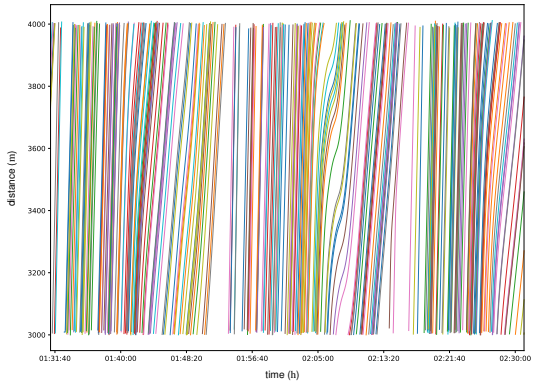


Fig. A.29-1. Time-Space diagram, for the one hour period after the end of the warmup, from 1:00:00 to 2:00:00 simulation time, plotted for the data from the sensor placed in the middle of the *direct* route (between 3000 m and 4000 m). In the case of an overloaded network, congestion shock waves can be observed.

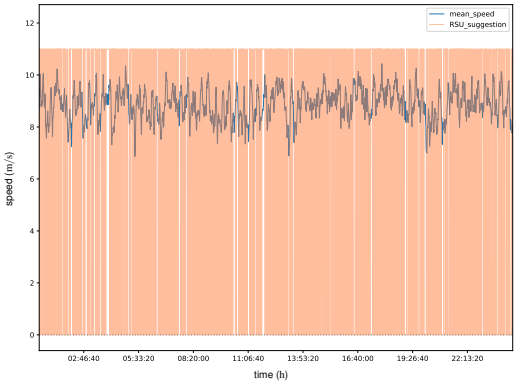


Fig. A.29-2. Mean speed in the network, in meters per second (m/s), over a 24 h period, superimposing (vertically, in orange) the time instants in which the RSU issued a recommendation to follow the *alternative* route.

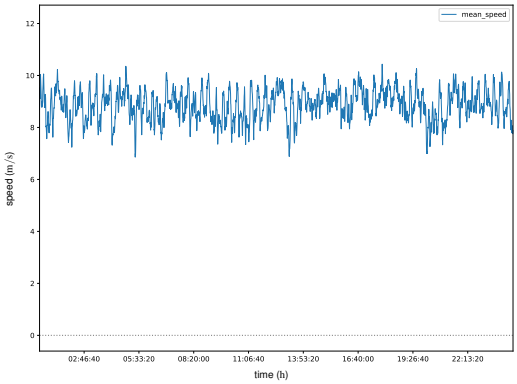


Fig. A.29-3. Mean speed in the network, in meters per second (m/s), over a 24 h period.

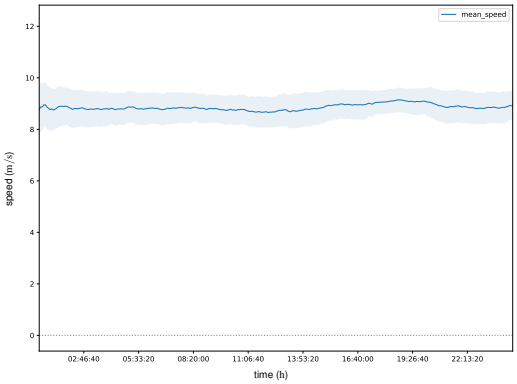


Fig. A.29-4. Mean speed in the network, in meters per second (m/s), over a 24 h period, 4 h Simple Moving Average, mean (line) and standard deviation (shaded).

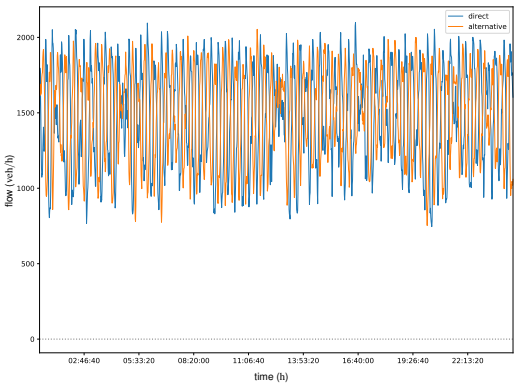


Fig. A.29-5. Traffic flow on each route, in vehicles per hour (veh/h), over a 24 h period.

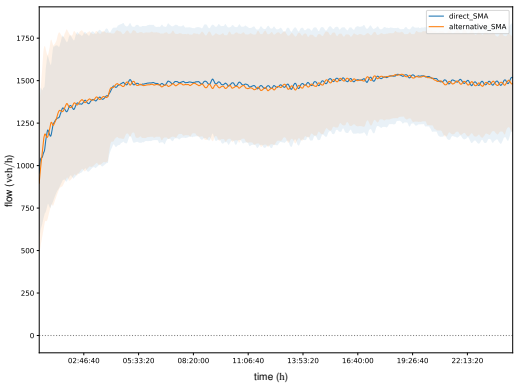


Fig. A.29-6. TrafficTraffic flow on each route, in vehicles per hour (veh/h), over a 24 h period, 4 h Simple Moving Average, mean (line) and standard deviation (shaded).

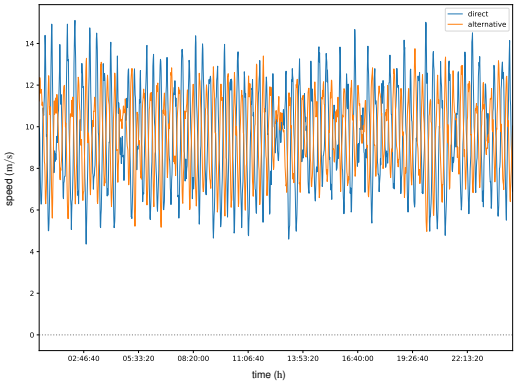


Fig. A.29-7. Mean speed on each route, in meters per second (m/s), aggregated to 1 min, over a 24 h period.

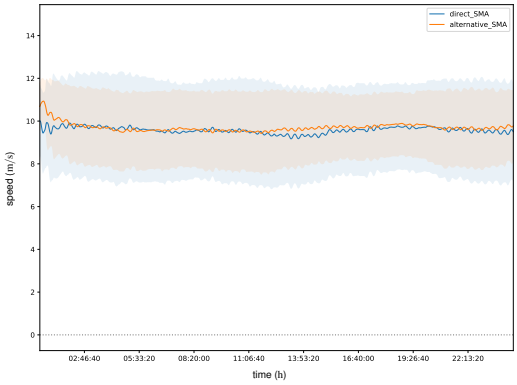


Fig. A.29-8. Mean speed on each route, in meters per second (m/s), aggregated to 1 min, over a 24 h period, 4 h Simple Moving Average, mean (line) and standard deviation (shaded).

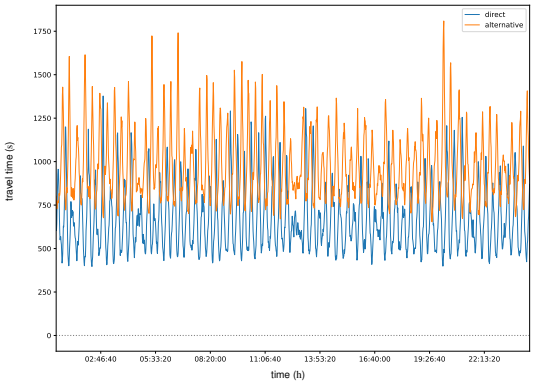


Fig. A.29-9. Travel times on each route, in seconds (s), aggregated to 1 min, over a 24 h period.

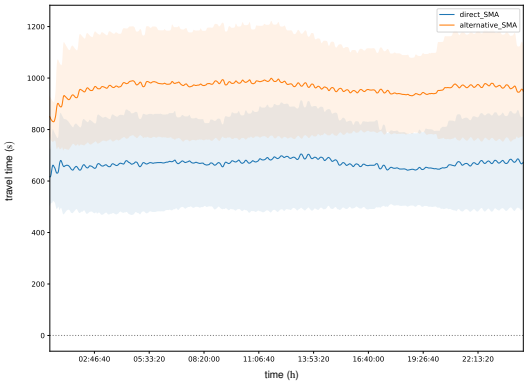


Fig. A.29-10. Travel times on each route, in seconds (s), aggregated to 1 min, over a 24 h period, 4 h Simple Moving Average, mean (line) and standard deviation (shaded).

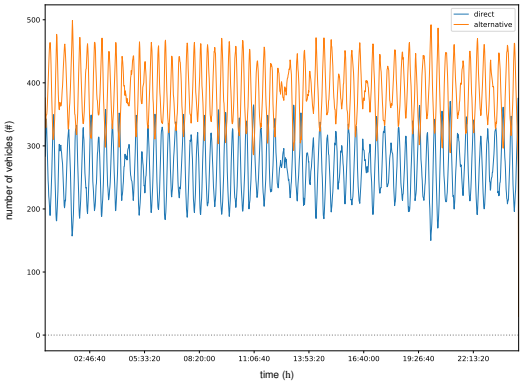


Fig. A.29-11. Average number of vehicles on each route, aggregated to 1 min, over a 24 h period.

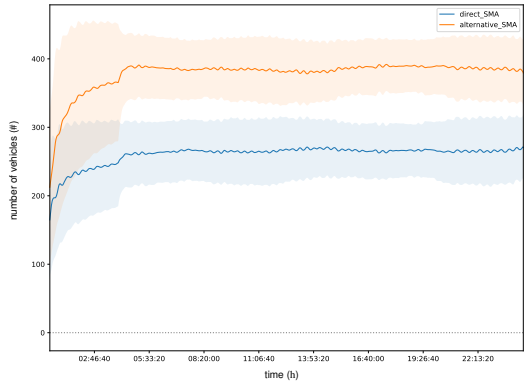


Fig. A.29-12. Average number of vehicles on each route, aggregated to 1 min, over a 24 h period, 4 h Simple Moving Average, mean (line) and standard deviation (shaded).

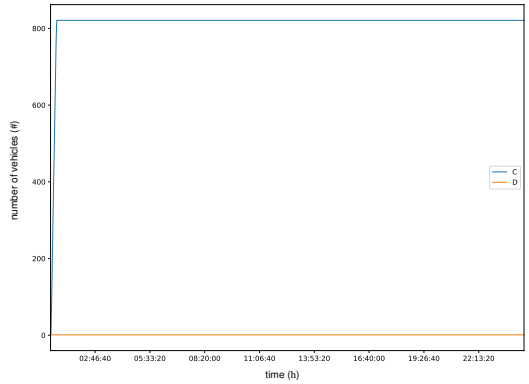


Fig. A.29-13. Evolution of the number of *Cooperators* and *Defectors* over a 24 h period.

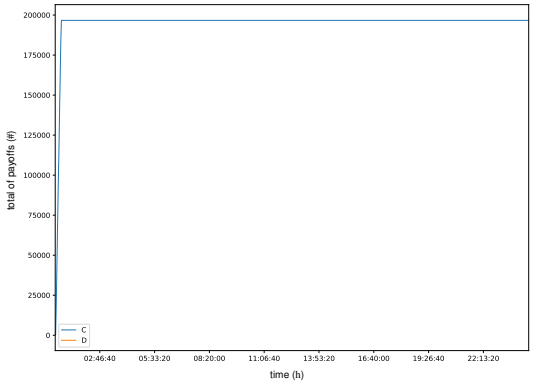


Fig. A.29-14. Evolution of total payoffs for *Cooperators* and *Defectors* (*individual payoff* times the *number of players receiving it*, $C(n) \times n$ and $D(n) \times (N-n)$, where n is the number of *Cooperators*), over a 24 h period.

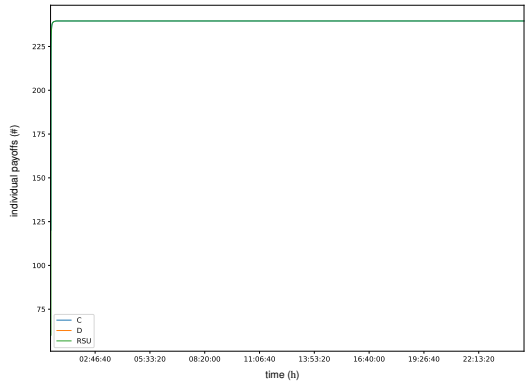


Fig. A.29-15. Evolution of the individual payoffs for *Cooperators, Defectors,* and *RSU* (always cooperating), over a 24 h period.

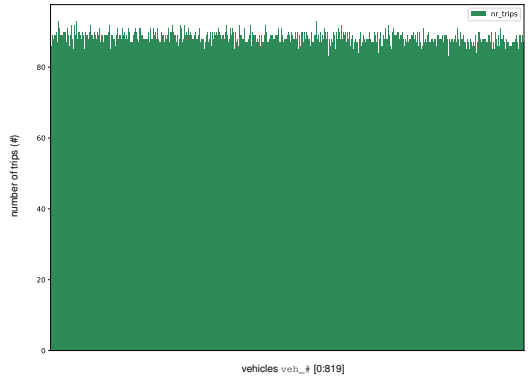


Fig. A.29-16. Number of trips made by each vehicle, during the simulation of a 24 h period.

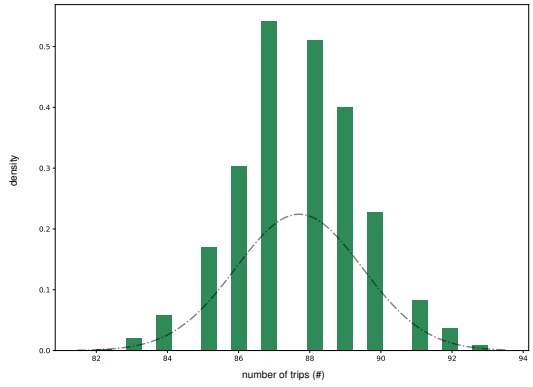


Fig. A.29-17. Density histogram of the number of trips made by each vehicle, during the simulation of a 24 h period, superimposing the normal density curve. The number of bins was calculated by the Freedman Diaconis rule.

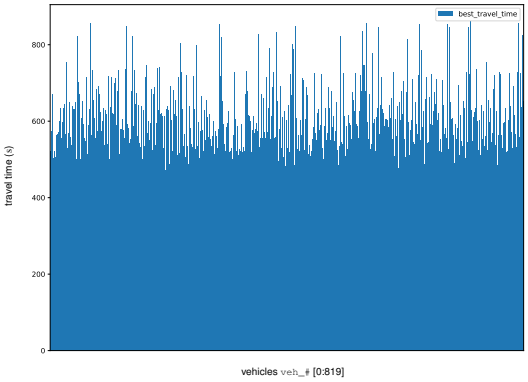


Fig. A.29-18. Best travel time for each vehicle, in seconds (s), during the simulation of a 24 h period.

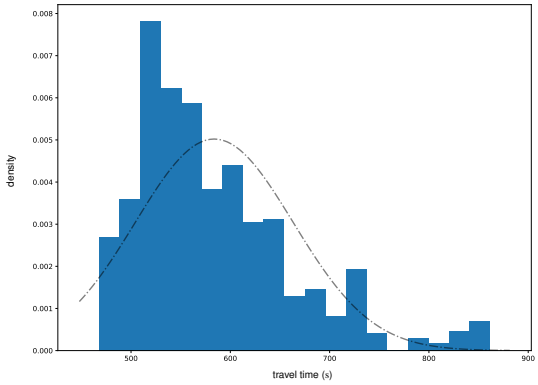


Fig. A.29-19. Density histogram of best travel time for vehicles, in seconds (s), during the simulation of a 24 h period, superimposing the normal density curve. The number of bins was calculated by the Freedman Diaconis rule.

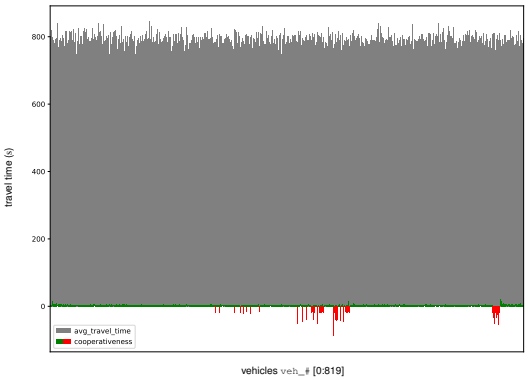


Fig. A.29-20. Average of the travel times, in seconds (s), of individual vehicles, during the simulation of a 24 h period. The bottom graph represents the *degree of cooperativeness**, downscaled by a normalization factor for the purpose of comparison with average times.

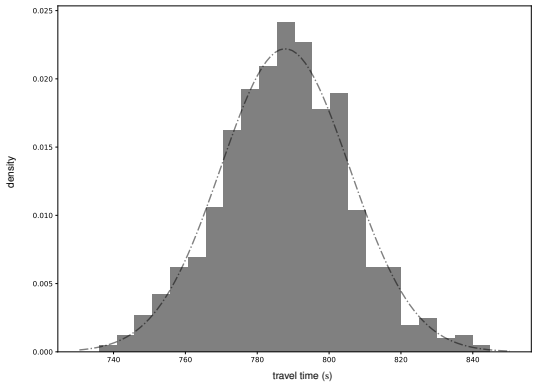


Fig. A.29-21. Density histogram of the average travel times, in seconds (s), of individual vehicles, during the simulation of a 24 h period, superimposing the normal density curve. The number of bins was calculated by the Freedman Diaconis rule.

* The *degree of cooperativeness* is a cumulative sum, calculated at each iteration, based on the complement of the ratio of cooperators, i.e., the higher the number of cooperators the less it increases, but the defectors are more penalized, and vice-versa. It varies inversely with the size of the group to which the player belongs.

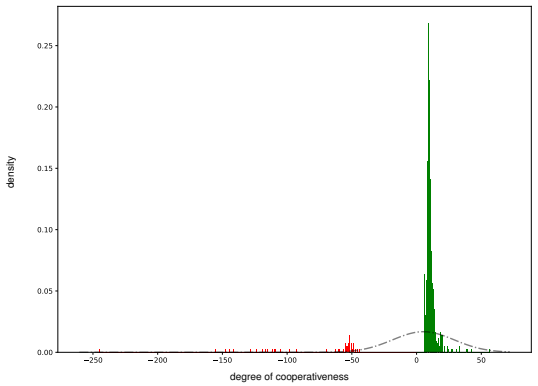


Fig. A.29-22. Density histogram of the *degree of cooperativeness** of individual vehicles, superimposing the normal density curve. The number of bins was calculated by the Freedman Diaconis rule. Generally, when strongly correlated with travel times, it presents a symmetric curve with respect to the *yy*-axis. Because some vehicles choose their preferred route immediately after the end of warmup, due to the gap between the RSU coverage and the route selection point, there may be some outliers.

A.30 820veh-24h-18060000

```
Scenario: scenario-1
Timestamp: 20210526T112326Z
Number of vehicles: 820 vehs
Simulation time: 24.0 h
Warm up end time: 1866.6 s; step 18665
Vehicle selection strategy: stochastic
RSU turned off: False
RSU strategy: proportional_dynamic_v5
Runner options:
   nogui: True
   step_length: 0.1
   seed: 19750808
   output_prefix: 820veh-24h-18060000
   sim_run_time: 24.0
   num_vehicles: 820
   warmup_speed: 13.96
   warmup_routes_weight: [473, 527]
   network_speed: 25.0
   change_behavior_probability: [0, 100]
   cooperation_probability: [0, 100]
   vehicle_selection_strategy: stochastic
   turn_rsu_off: False
   rsu_dynamic_dissemination: False
   rsu_dissemination_interval: 5
   rsu_probabilistic_dissemination: False
   rsu_suggestion_strategy: proportional_dynamic_v5
   rsu_routes_weight: [460, 540]
   rsu_moving_avg_size: 5
   travel_times_ttl: 60
   rsu_dissemination_ttl: 0
   rsu_send_travel_time_info: False
   payoff_matrix: [360.0, 240.0, 0.0, -120.0]
   roth_erev_parameters: [0.1, 0.15]
Network Mean speed after warmup:
   Max: 9.97
   Min: 6.02
```

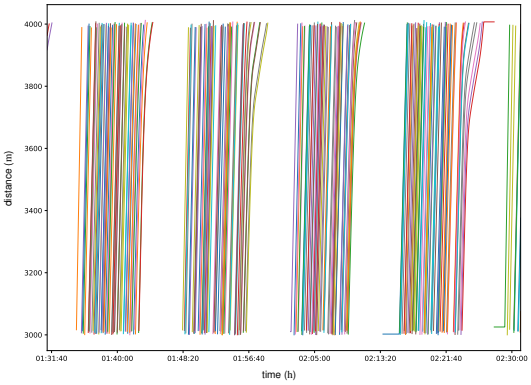


Fig. A.30-1. Time-Space diagram, for the one hour period after the end of the warmup, from 1:00:00 to 2:00:00 simulation time, plotted for the data from the sensor placed in the middle of the *direct* route (between 3000 m and 4000 m). In the case of an overloaded network, congestion shock waves can be observed.

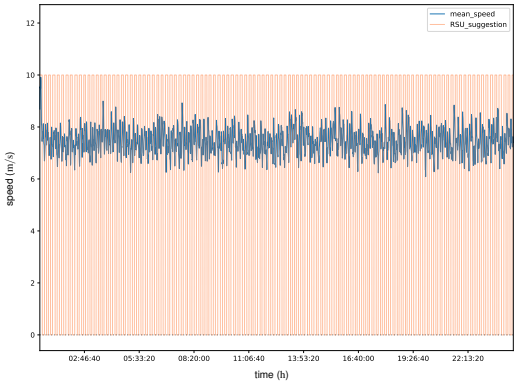


Fig. A.30-2. Mean speed in the network, in meters per second (m/s), over a 24 h period, superimposing (vertically, in orange) the time instants in which the RSU issued a recommendation to follow the *alternative* route.

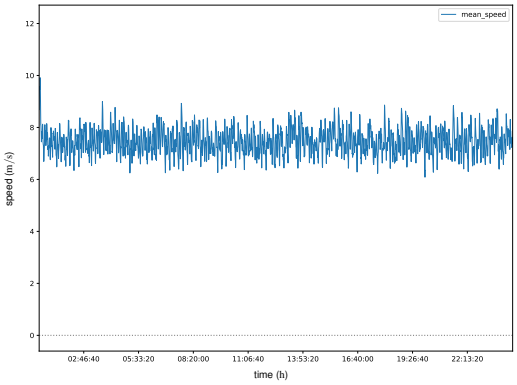


Fig. A.30-3. Mean speed in the network, in meters per second (m/s), over a 24 h period.

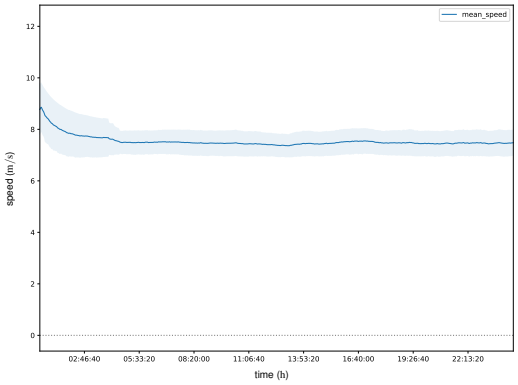


Fig. A.30-4. Mean speed in the network, in meters per second (m/s), over a 24 h period, 4 h Simple Moving Average, mean (line) and standard deviation (shaded).

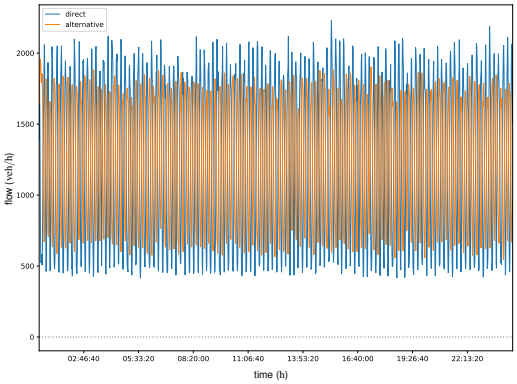


Fig. A.30-5. Traffic flow on each route, in vehicles per hour (veh/h), over a 24 h period.

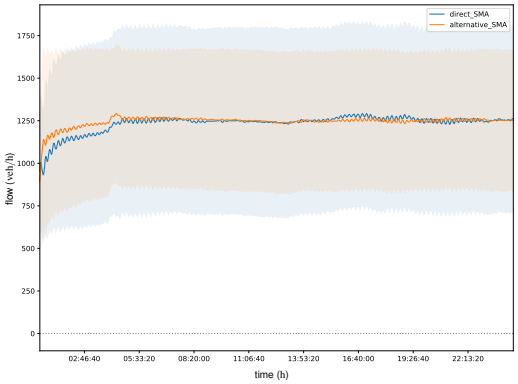


Fig. A.30-6. TrafficTraffic flow on each route, in vehicles per hour (veh/h), over a 24 h period, 4 h Simple Moving Average, mean (line) and standard deviation (shaded).

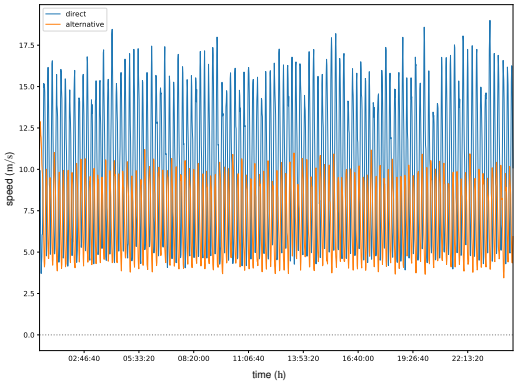


Fig. A.30-7. Mean speed on each route, in meters per second (m/s), aggregated to 1 min, over a 24 h period.

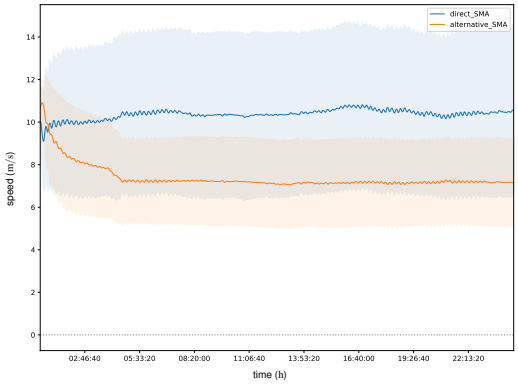


Fig. A.30-8. Mean speed on each route, in meters per second (m/s), aggregated to 1 min, over a 24 h period, 4 h Simple Moving Average, mean (line) and standard deviation (shaded).

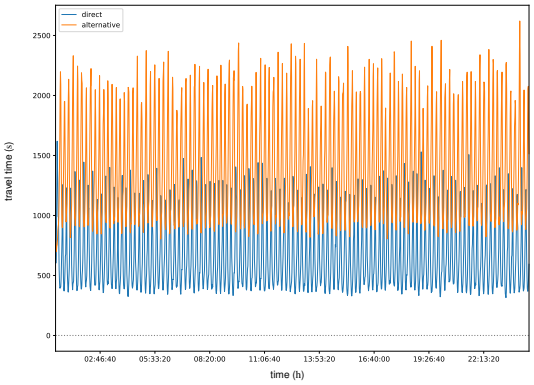


Fig. A.30-9. Travel times on each route, in seconds (s), aggregated to 1 min, over a 24 h period.

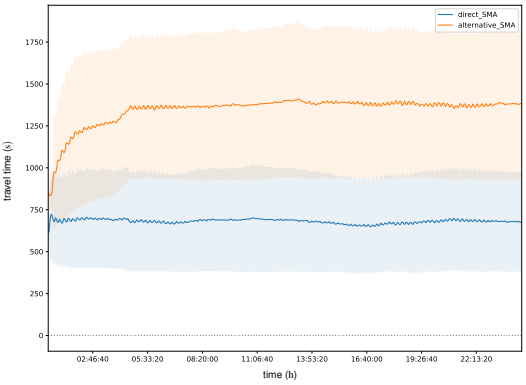


Fig. A.30-10. Travel times on each route, in seconds (s), aggregated to 1 min, over a 24 h period, 4 h Simple Moving Average, mean (line) and standard deviation (shaded).

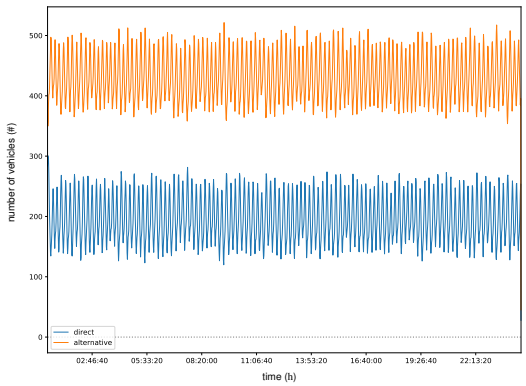


Fig. A.30-11. Average number of vehicles on each route, aggregated to 1 min, over a 24 h period.

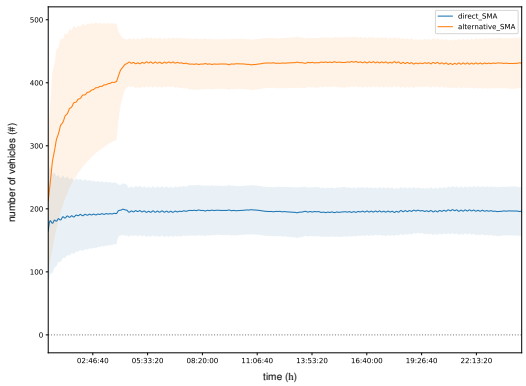


Fig. A.30-12. Average number of vehicles on each route, aggregated to 1 min, over a 24 h period, 4 h Simple Moving Average, mean (line) and standard deviation (shaded).

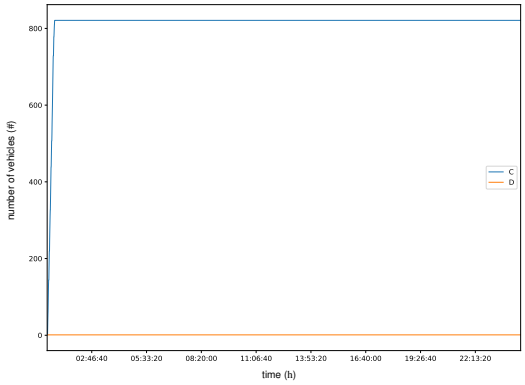


Fig. A.30-13. Evolution of the number of *Cooperators* and *Defectors* over a 24 h period.

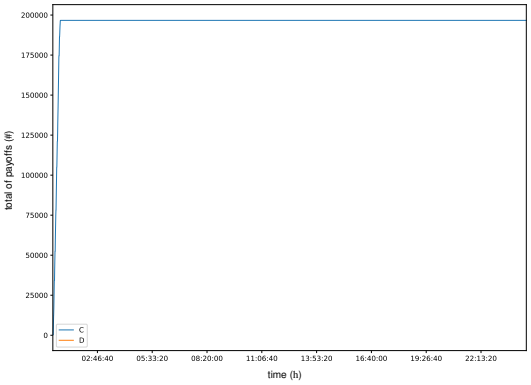


Fig. A.30-14. Evolution of total payoffs for *Cooperators* and *Defectors* (*individual payoff* times the *number of players receiving it*, $C(n) \times n$ and $D(n) \times (N-n)$, where n is the number of *Cooperators*), over a 24 h period.

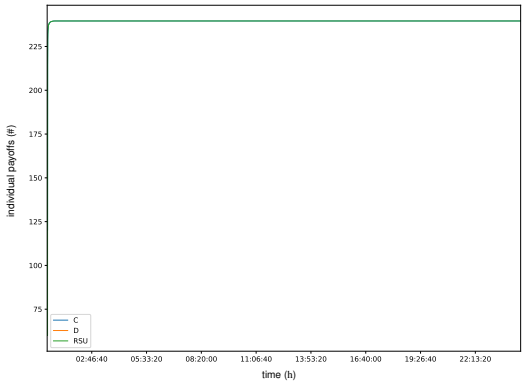


Fig. A.30-15. Evolution of the individual payoffs for *Cooperators, Defectors,* and *RSU* (always cooperating), over a 24 h period.

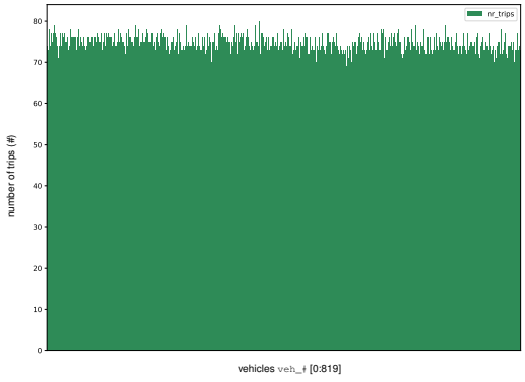


Fig. A.30-16. Number of trips made by each vehicle, during the simulation of a 24 h period.

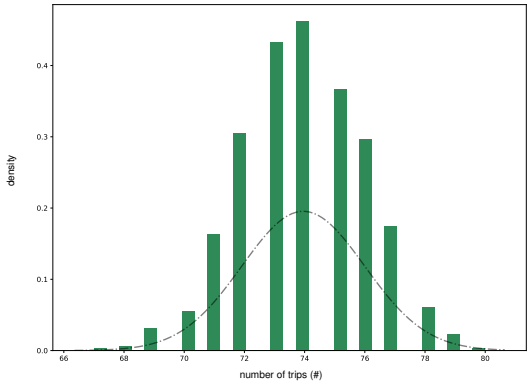


Fig. A.30-17. Density histogram of the number of trips made by each vehicle, during the simulation of a 24 h period, superimposing the normal density curve. The number of bins was calculated by the Freedman Diaconis rule.

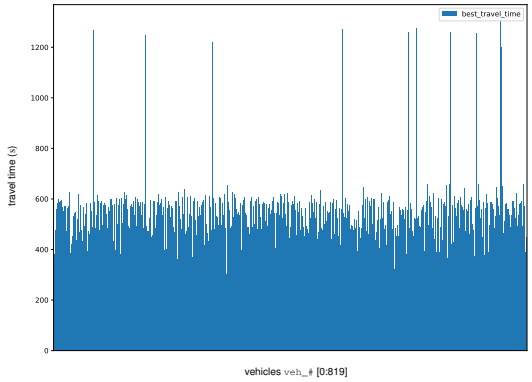


Fig. A.30-18. Best travel time for each vehicle, in seconds (s), during the simulation of a 24 h period.

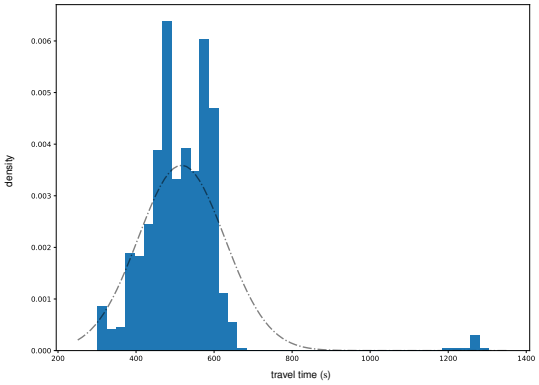


Fig. A.30-19. Density histogram of best travel time for vehicles, in seconds (s), during the simulation of a 24 h period, superimposing the normal density curve. The number of bins was calculated by the Freedman Diaconis rule.

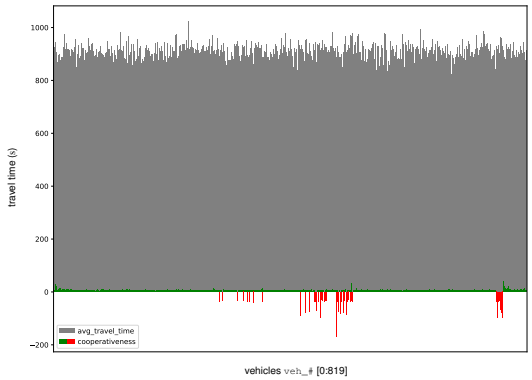


Fig. A.30-20. Average of the travel times, in seconds (s), of individual vehicles, during the simulation of a 24 h period. The bottom graph represents the *degree of cooperativeness**, downscaled by a normalization factor for the purpose of comparison with average times.

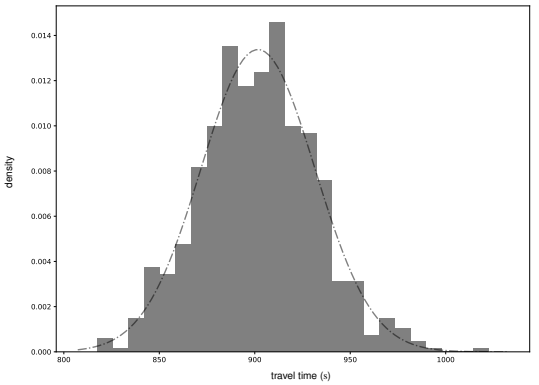


Fig. A.30-21. Density histogram of the average travel times, in seconds (s), of individual vehicles, during the simulation of a 24 h period, superimposing the normal density curve. The number of bins was calculated by the Freedman Diaconis rule.

* The *degree of cooperativeness* is a cumulative sum, calculated at each iteration, based on the complement of the ratio of cooperators, i.e., the higher the number of cooperators the less it increases, but the defectors are more penalized, and vice-versa. It varies inversely with the size of the group to which the player belongs.

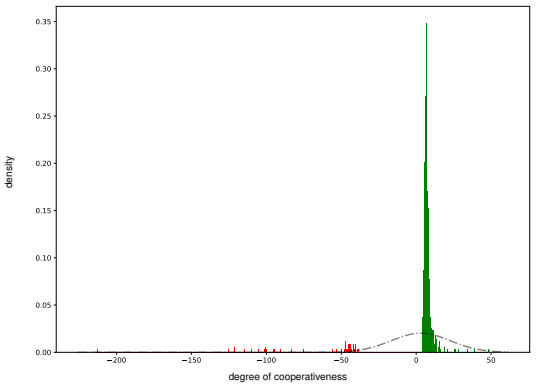


Fig. A.30-22. Density histogram of the *degree of cooperativeness** of individual vehicles, superimposing the normal density curve. The number of bins was calculated by the Freedman Diaconis rule. Generally, when strongly correlated with travel times, it presents a symmetric curve with respect to the *yy*-axis. Because some vehicles choose their preferred route immediately after the end of warmup, due to the gap between the RSU coverage and the route selection point, there may be some outliers.

A.31 820veh-24h-19060000

```
Scenario: scenario-1
Timestamp: 20210610T200813Z
Number of vehicles: 820 vehs
Simulation time: 24.0 h
Warm up end time: 1866.6 s; step 18665
Vehicle selection strategy: stochastic
RSU turned off: False
RSU strategy: pigous_example_cooperation_weighted
Runner options:
   nogui: True
   step_length: 0.1
   seed: 19750808
   output_prefix: 820veh-24h-19060000
   sim_run_time: 24.0
   num_vehicles: 820
   warmup_speed: 13.96
   warmup_routes_weight: [473, 527]
   network_speed: 25.0
   change_behavior_probability: [0, 100]
   cooperation_probability: [0, 100]
   vehicle_selection_strategy: stochastic
   turn_rsu_off: False
   rsu_dynamic_dissemination: False
   rsu_dissemination_interval: 5
   rsu_probabilistic_dissemination: False
   rsu_suggestion_strategy: pigous_example_cooperation_weighted
   rsu_routes_weight: [460, 540]
   rsu_moving_avg_size: 5
   travel_times_ttl: 60
   rsu_dissemination_ttl: 0
   rsu_send_travel_time_info: False
   payoff_matrix: [360.0, 240.0, 0.0, -120.0]
   roth_erev_parameters: [0.1, 0.15]
   rsu_change_dissemination: False
   rsu_change_dissemination_steps: [14400, 28800, 43200, 57600, 72000]
   rsu_change_dissemination_intervals: [10, 20, 40, 80, 160]
Network Mean speed after warmup:
   Max: 10.8
   Min: 8.0
```

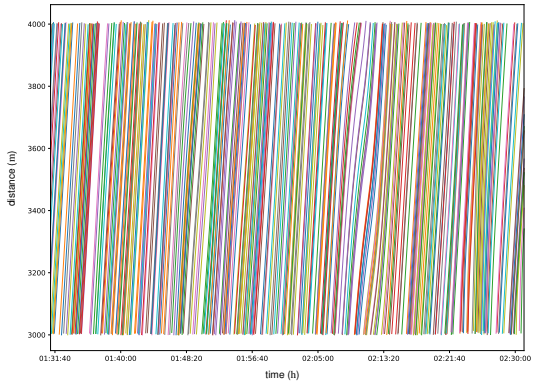


Fig. A.31-1. Time-Space diagram, for the one hour period after the end of the warmup, from 1:00:00 to 2:00:00 simulation time, plotted for the data from the sensor placed in the middle of the *direct* route (between 3000 m and 4000 m). In the case of an overloaded network, congestion shock waves can be observed.

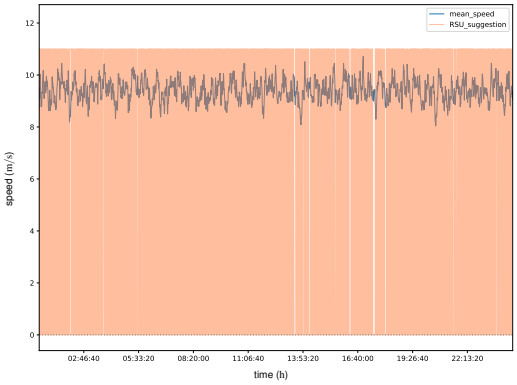


Fig. A.31-2. Mean speed in the network, in meters per second (m/s), over a 24 h period, superimposing (vertically, in orange) the time instants in which the RSU issued a recommendation to follow the *alternative* route.

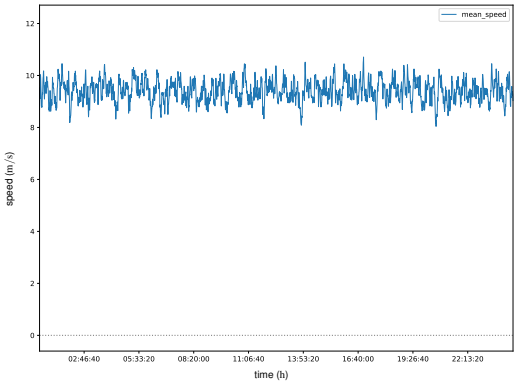


Fig. A.31-3. Mean speed in the network, in meters per second (m/s), over a 24 h period.

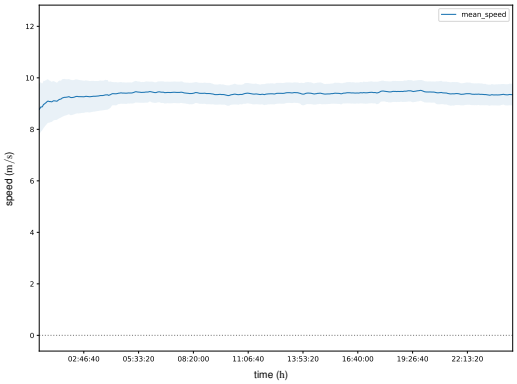


Fig. A.31-4. Mean speed in the network, in meters per second (m/s), over a 24 h period, 4 h Simple Moving Average, mean (line) and standard deviation (shaded).

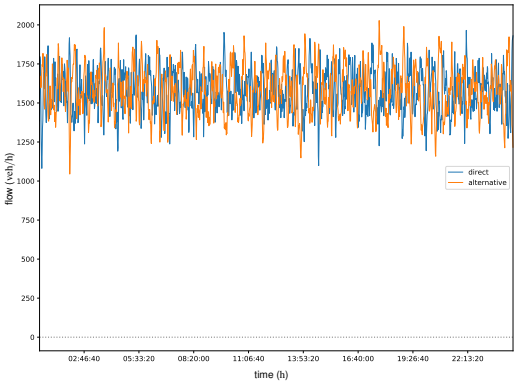


Fig. A.31-5. Traffic flow on each route, in vehicles per hour (veh/h), over a 24 h period.

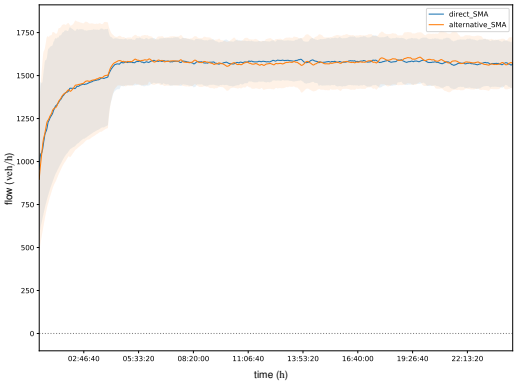


Fig. A.31-6. TrafficTraffic flow on each route, in vehicles per hour (veh/h), over a 24 h period, 4 h Simple Moving Average, mean (line) and standard deviation (shaded).

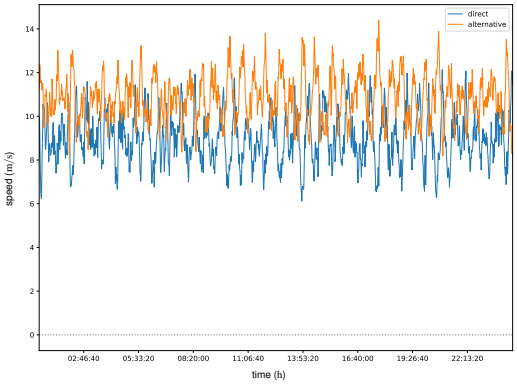


Fig. A.31-7. Mean speed on each route, in meters per second (m/s), aggregated to 1 min, over a 24 h period.

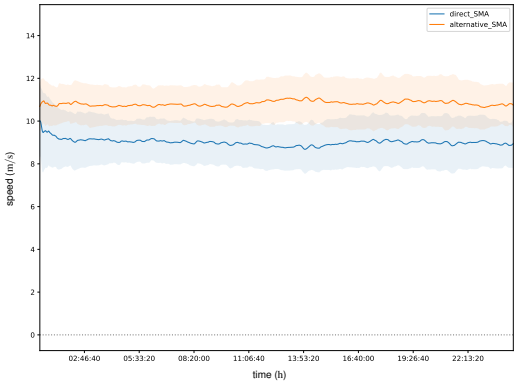


Fig. A.31-8. Mean speed on each route, in meters per second (m/s), aggregated to 1 min, over a 24 h period, 4 h Simple Moving Average, mean (line) and standard deviation (shaded).

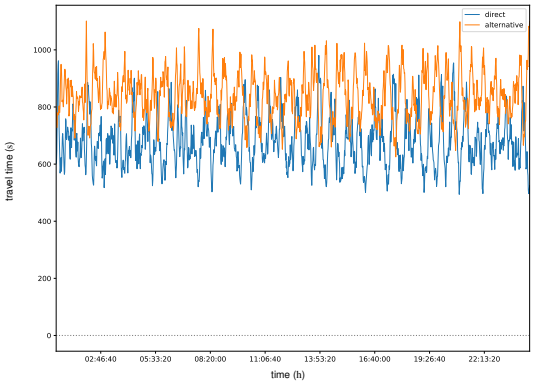


Fig. A.31-9. Travel times on each route, in seconds (s), aggregated to 1 min, over a 24 h period.

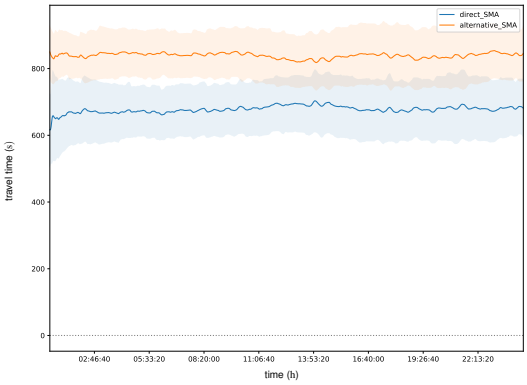


Fig. A.31-10. Travel times on each route, in seconds (s), aggregated to 1 min, over a 24 h period, 4 h Simple Moving Average, mean (line) and standard deviation (shaded).

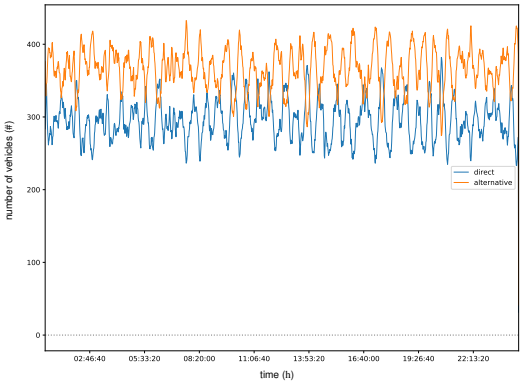


Fig. A.31-11. Average number of vehicles on each route, aggregated to 1 min, over a 24 h period.

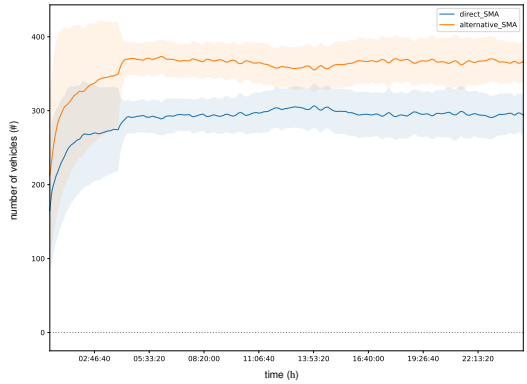


Fig. A.31-12. Average number of vehicles on each route, aggregated to 1 min, over a 24 h period, 4 h Simple Moving Average, mean (line) and standard deviation (shaded).

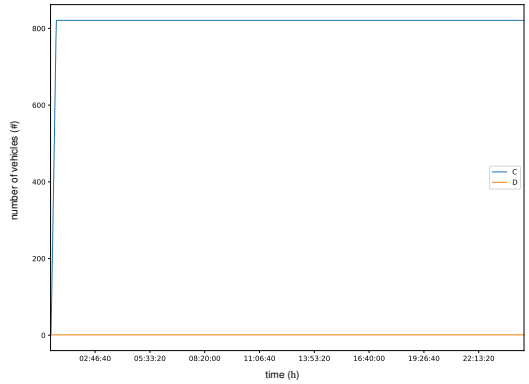


Fig. A.31-13. Evolution of the number of *Cooperators* and *Defectors* over a 24 h period.

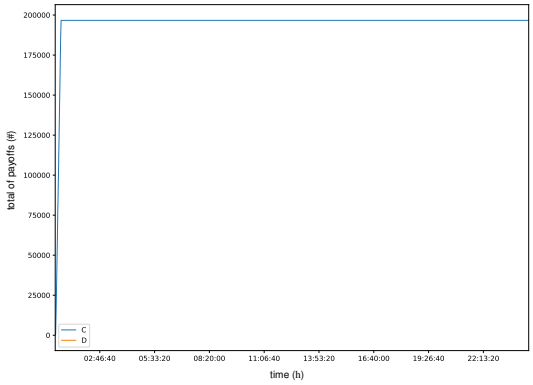


Fig. A.31-14. Evolution of total payoffs for *Cooperators* and *Defectors* (*individual payoff* times the *number of players receiving it*, $C(n) \times n$ and $D(n) \times (N-n)$, where n is the number of *Cooperators*), over a 24 h period.

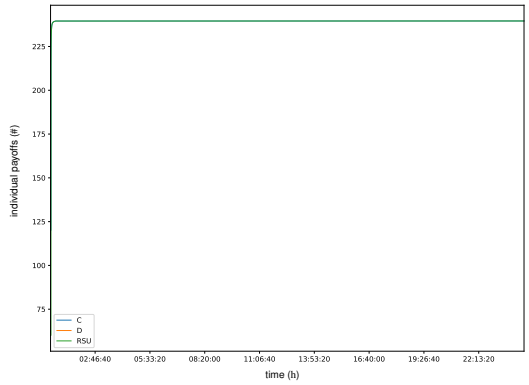


Fig. A.31-15. Evolution of the individual payoffs for *Cooperators, Defectors,* and *RSU* (always cooperating), over a 24 h period.

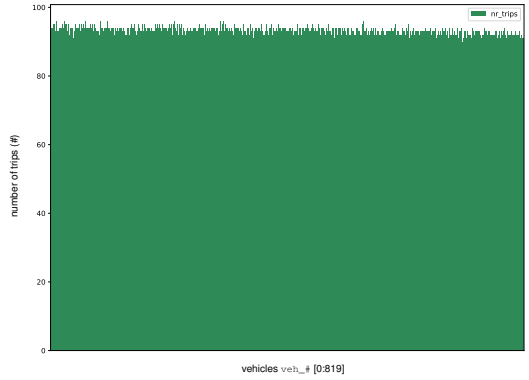


Fig. A.31-16. Number of trips made by each vehicle, during the simulation of a 24 h period.

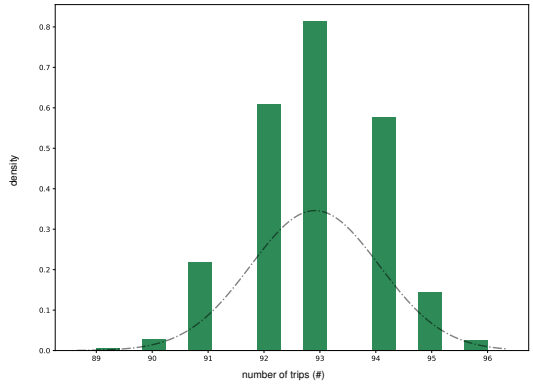


Fig. A.31-17. Density histogram of the number of trips made by each vehicle, during the simulation of a 24 h period, superimposing the normal density curve. The number of bins was calculated by the Freedman Diaconis rule.

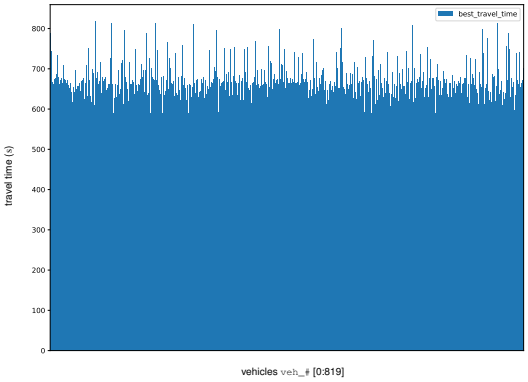


Fig. A.31-18. Best travel time for each vehicle, in seconds (s), during the simulation of a 24 h period.

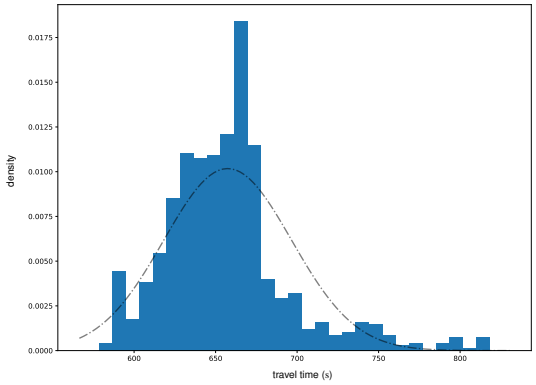


Fig. A.31-19. Density histogram of best travel time for vehicles, in seconds (s), during the simulation of a 24 h period, superimposing the normal density curve. The number of bins was calculated by the Freedman Diaconis rule.

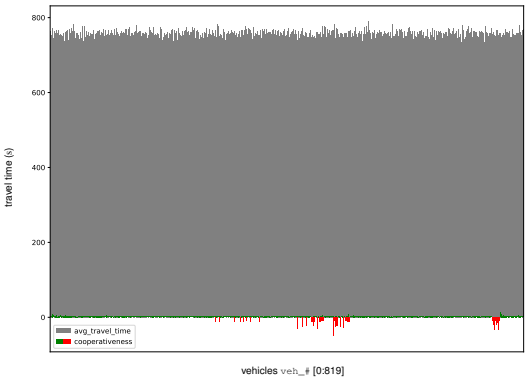


Fig. A.31-20. Average of the travel times, in seconds (s), of individual vehicles, during the simulation of a 24 h period. The bottom graph represents the *degree of cooperativeness**, downscaled by a normalization factor for the purpose of comparison with average times.

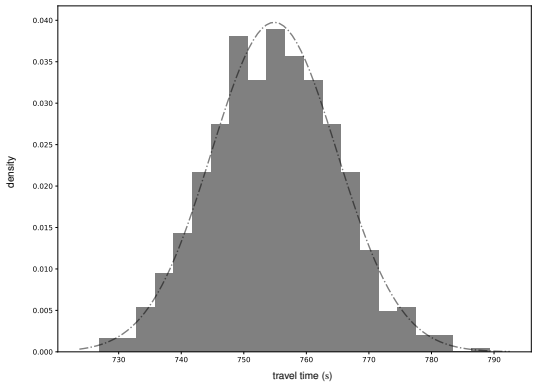


Fig. A.31-21. Density histogram of the average travel times, in seconds (s), of individual vehicles, during the simulation of a 24 h period, superimposing the normal density curve. The number of bins was calculated by the Freedman Diaconis rule.

* The *degree of cooperativeness* is a cumulative sum, calculated at each iteration, based on the complement of the ratio of cooperators, i.e., the higher the number of cooperators the less it increases, but the defectors are more penalized, and vice-versa. It varies inversely with the size of the group to which the player belongs.

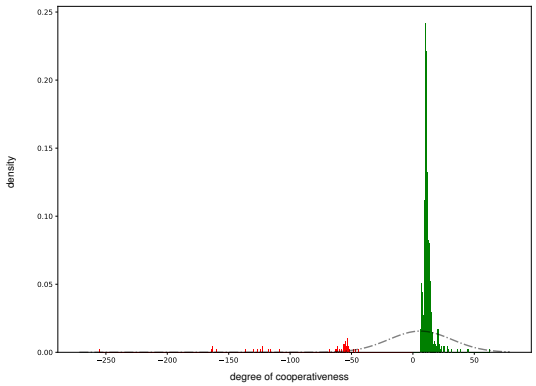


Fig. A.31-22. Density histogram of the *degree of cooperativeness** of individual vehicles, superimposing the normal density curve. The number of bins was calculated by the Freedman Diaconis rule. Generally, when strongly correlated with travel times, it presents a symmetric curve with respect to the *yy*-axis. Because some vehicles choose their preferred route immediately after the end of warmup, due to the gap between the RSU coverage and the route selection point, there may be some outliers.

A.32 `820veh-24h-00060001`

```
Scenario: scenario-1
Timestamp: 20210616T102845Z
Number of vehicles: 820 vehs
Simulation time: 24.0 h
Warm up end time: 1866.6 s; step 18665
Vehicle selection strategy: stochastic
RSU turned off: False
RSU strategy: proportional
Runner options:
   nogui: True
   step_length: 0.1
   seed: 19750808
   output_prefix: 820veh-24h-00060001
   sim_run_time: 24.0
   num_vehicles: 820
   warmup_speed: 13.96
   warmup_routes_weight: [473, 527]
   network_speed: 25.0
   change_behavior_probability: [100, 0]
   cooperation_probability: [50, 50]
   vehicle_selection_strategy: stochastic
   turn_rsu_off: False
   rsu_dynamic_dissemination: False
   rsu_dissemination_interval: 5
   rsu_probabilistic_dissemination: False
   rsu_suggestion_strategy: proportional
   rsu_routes_weight: [460, 540]
   rsu_moving_avg_size: 5
   travel_times_ttl: 60
   rsu_dissemination_ttl: 0
   rsu_send_travel_time_info: False
   payoff_matrix: [360.0, 240.0, 0.0, -120.0]
   roth_erev_parameters: [0.1, 0.15]
   rsu_change_dissemination: False
   rsu_change_dissemination_steps: [14400, 28800, 43200, 57600, 72000]
   rsu_change_dissemination_intervals: [10, 20, 40, 80, 160]
Network Mean speed after warmup:
   Max: 9.67
   Min: 2.32
```

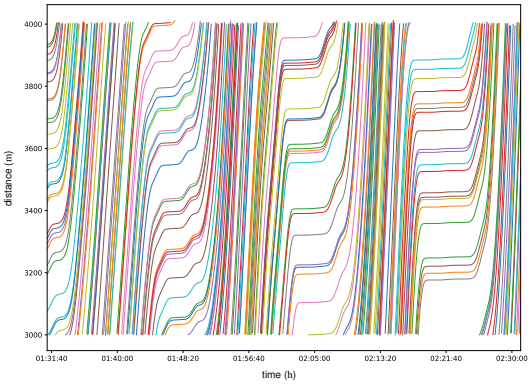


Fig. A.32-1. Time-Space diagram, for the one hour period after the end of the warmup, from 1:00:00 to 2:00:00 simulation time, plotted for the data from the sensor placed in the middle of the *direct* route (between 3000 m and 4000 m). In the case of an overloaded network, congestion shock waves can be observed.

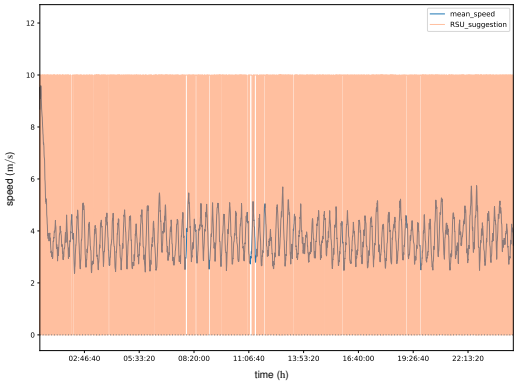


Fig. A.32-2. Mean speed in the network, in meters per second (m/s), over a 24 h period, superimposing (vertically, in orange) the time instants in which the RSU issued a recommendation to follow the *alternative* route.

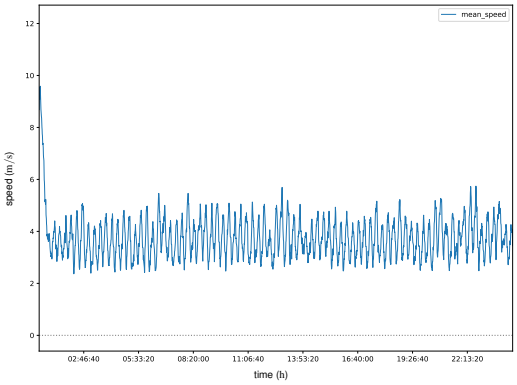


Fig. A.32-3. Mean speed in the network, in meters per second (m/s), over a 24 h period.

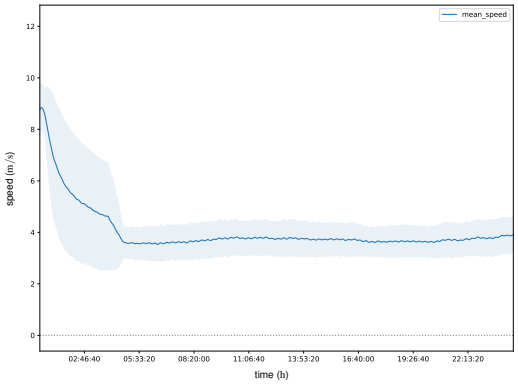


Fig. A.32-4. Mean speed in the network, in meters per second (m/s), over a 24 h period, 4 h Simple Moving Average, mean (line) and standard deviation (shaded).

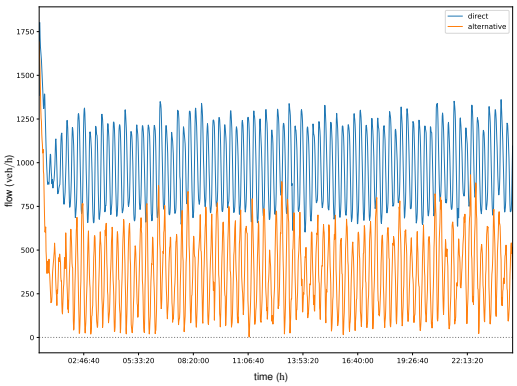


Fig. A.32-5. Traffic flow on each route, in vehicles per hour (veh/h), over a 24 h period.

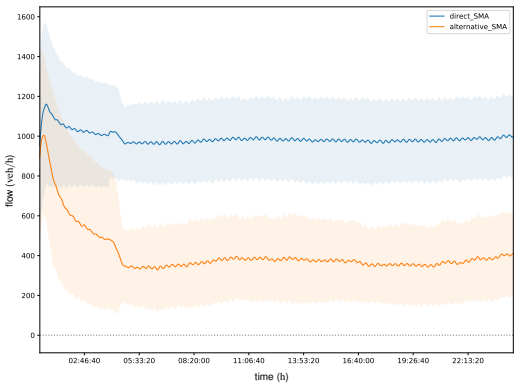


Fig. A.32-6. TrafficTraffic flow on each route, in vehicles per hour (veh/h), over a 24 h period, 4 h Simple Moving Average, mean (line) and standard deviation (shaded).

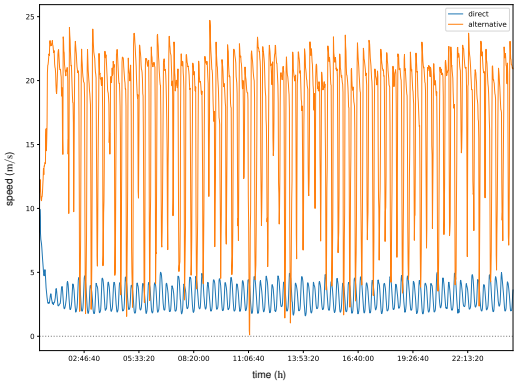


Fig. A.32-7. Mean speed on each route, in meters per second (m/s), aggregated to 1 min, over a 24 h period.

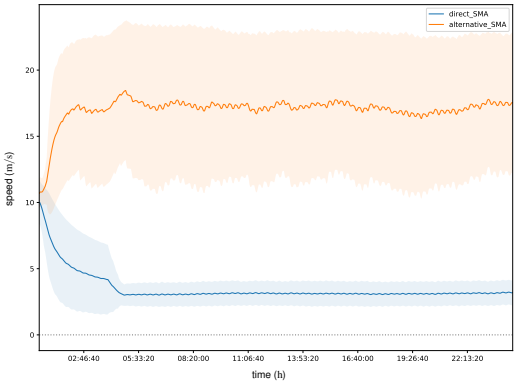


Fig. A.32-8. Mean speed on each route, in meters per second (m/s), aggregated to 1 min, over a 24 h period, 4 h Simple Moving Average, mean (line) and standard deviation (shaded).

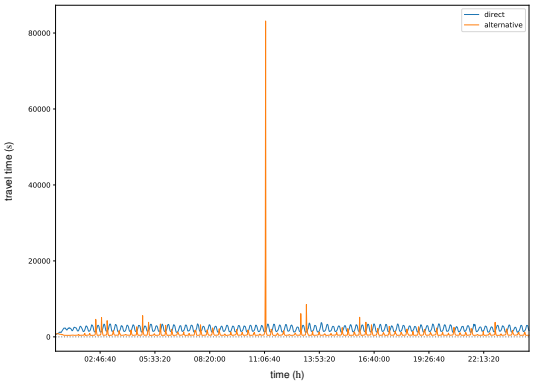


Fig. A.32-9. Travel times on each route, in seconds (s), aggregated to 1 min, over a 24 h period.

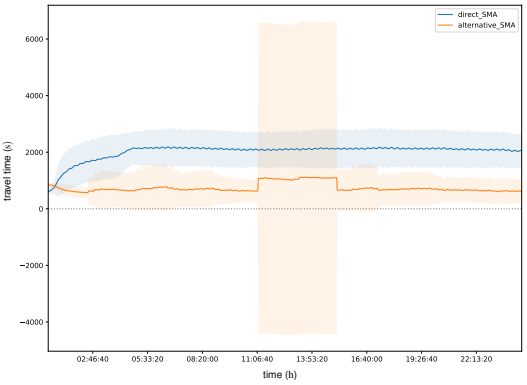


Fig. A.32-10. Travel times on each route, in seconds (s), aggregated to 1 min, over a 24 h period, 4 h Simple Moving Average, mean (line) and standard deviation (shaded).

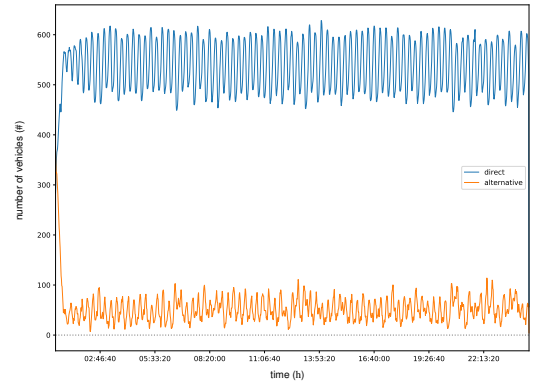


Fig. A.32-11. Average number of vehicles on each route, aggregated to 1 min, over a 24 h period.

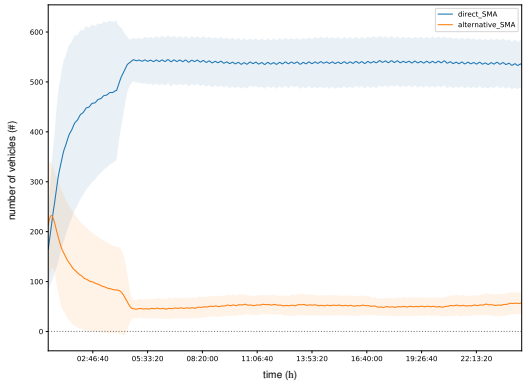


Fig. A.32-12. Average number of vehicles on each route, aggregated to 1 min, over a 24 h period, 4 h Simple Moving Average, mean (line) and standard deviation (shaded).

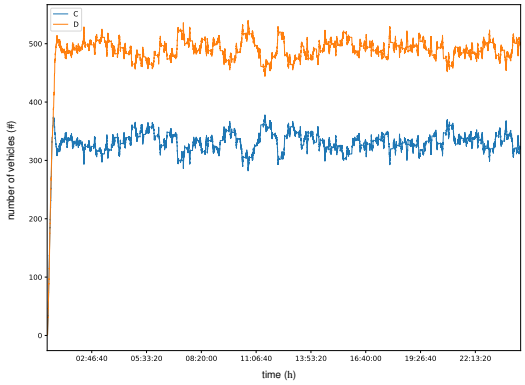


Fig. A.32-13. Evolution of the number of *Cooperators* and *Defectors* over a 24 h period.

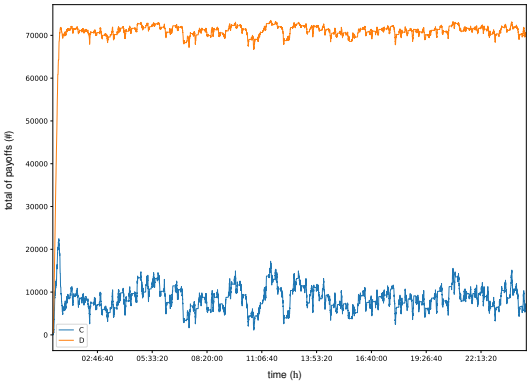


Fig. A.32-14. Evolution of total payoffs for *Cooperators* and *Defectors* (*individual payoff* times the *number of players receiving it*, $C(n) \times n$ and $D(n) \times (N-n)$, where n is the number of *Cooperators*), over a 24 h period.

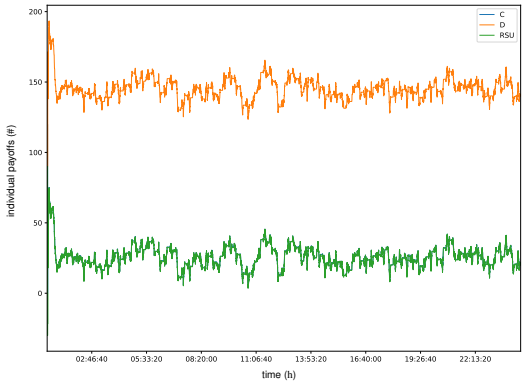


Fig. A.32-15. Evolution of the individual payoffs for *Cooperators, Defectors,* and *RSU* (always cooperating), over a 24 h period.

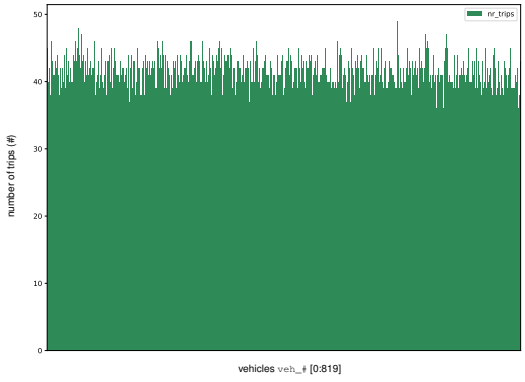


Fig. A.32-16. Number of trips made by each vehicle, during the simulation of a 24 h period.

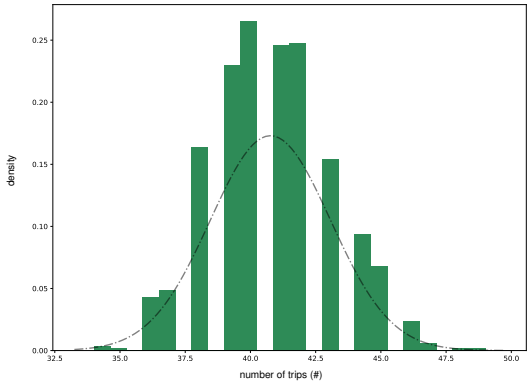


Fig. A.32-17. Density histogram of the number of trips made by each vehicle, during the simulation of a 24 h period, superimposing the normal density curve. The number of bins was calculated by the Freedman Diaconis rule.

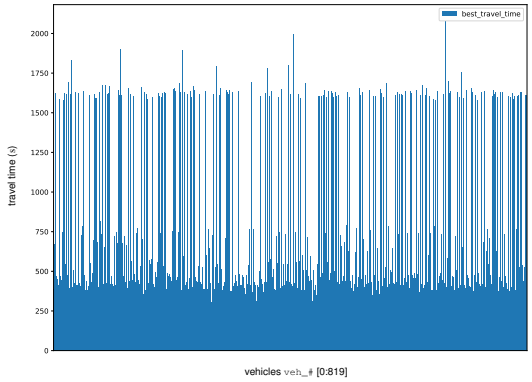


Fig. A.32-18. Best travel time for each vehicle, in seconds (s), during the simulation of a 24 h period.

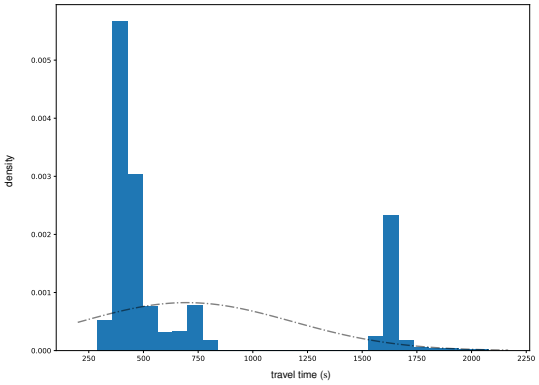


Fig. A.32-19. Density histogram of best travel time for vehicles, in seconds (s), during the simulation of a 24 h period, superimposing the normal density curve. The number of bins was calculated by the Freedman Diaconis rule.

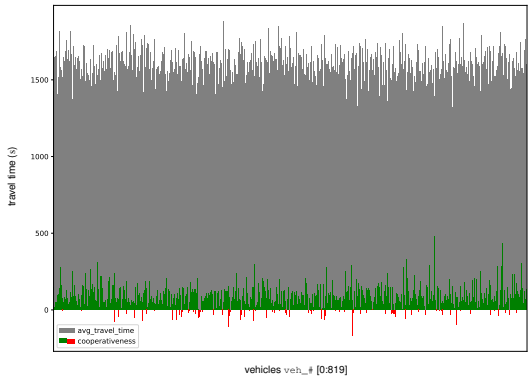


Fig. A.32-20. Average of the travel times, in seconds (s), of individual vehicles, during the simulation of a 24 h period. The bottom graph represents the *degree of cooperativeness**, downscaled by a normalization factor for the purpose of comparison with average times.

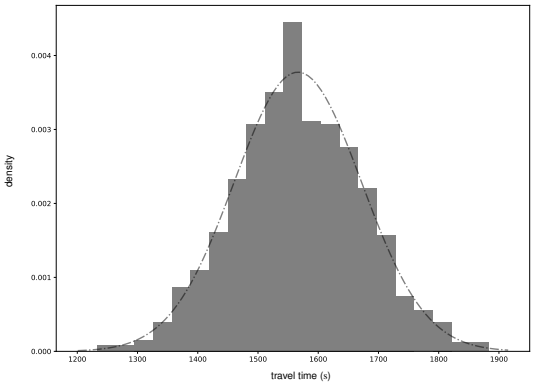


Fig. A.32-21. Density histogram of the average travel times, in seconds (s), of individual vehicles, during the simulation of a 24 h period, superimposing the normal density curve. The number of bins was calculated by the Freedman Diaconis rule.

* The *degree of cooperativeness* is a cumulative sum, calculated at each iteration, based on the complement of the ratio of cooperators, i.e., the higher the number of cooperators the less it increases, but the defectors are more penalized, and vice-versa. It varies inversely with the size of the group to which the player belongs.

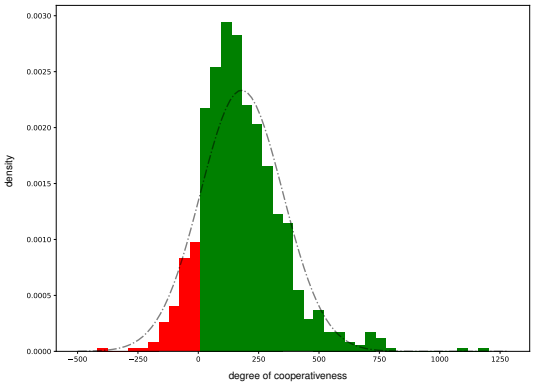


Fig. A.32-22. Density histogram of the *degree of cooperativeness** of individual vehicles, superimposing the normal density curve. The number of bins was calculated by the Freedman Diaconis rule. Generally, when strongly correlated with travel times, it presents a symmetric curve with respect to the *yy*-axis.

A.33 820veh-24h-01060001

```
Scenario: scenario-1
Timestamp: 20210616T125627Z
Number of vehicles: 820 vehs
Simulation time: 24.0 h
Warm up end time: 1866.6 s; step 18665
Vehicle selection strategy: stochastic
RSU turned off: False
RSU strategy: proportional_dynamic
Runner options:
   nogui: True
   step_length: 0.1
   seed: 19750808
   output_prefix: 820veh-24h-01060001
   sim_run_time: 24.0
   num_vehicles: 820
   warmup_speed: 13.96
   warmup_routes_weight: [473, 527]
   network_speed: 25.0
   change_behavior_probability: [100, 0]
   cooperation_probability: [50, 50]
   vehicle_selection_strategy: stochastic
   turn_rsu_off: False
   rsu_dynamic_dissemination: False
   rsu_dissemination_interval: 5
   rsu_probabilistic_dissemination: False
   rsu_suggestion_strategy: proportional_dynamic
   rsu_routes_weight: [460, 540]
   rsu_moving_avg_size: 5
   travel_times_ttl: 60
   rsu_dissemination_ttl: 0
   rsu_send_travel_time_info: False
   payoff_matrix: [360.0, 240.0, 0.0, -120.0]
   roth_erev_parameters: [0.1, 0.15]
   rsu_change_dissemination: False
   rsu_change_dissemination_steps: [14400, 28800, 43200, 57600, 72000]
   rsu_change_dissemination_intervals: [10, 20, 40, 80, 160]
Network Mean speed after warmup:
   Max: 9.61
   Min: 2.65
```

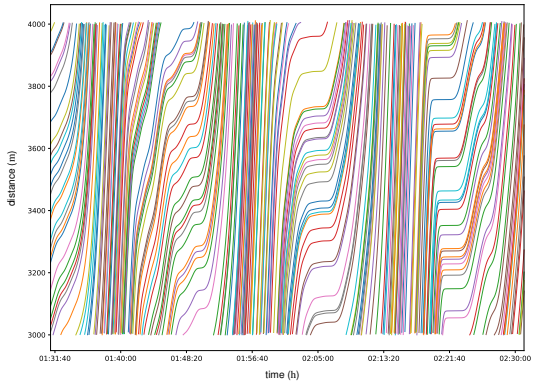


Fig. A.33-1. Time-Space diagram, for the one hour period after the end of the warmup, from 1:00:00 to 2:00:00 simulation time, plotted for the data from the sensor placed in the middle of the *direct* route (between 3000 m and 4000 m). In the case of an overloaded network, congestion shock waves can be observed.

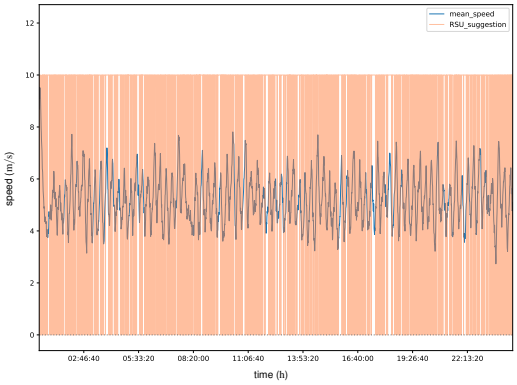


Fig. A.33-2. Mean speed in the network, in meters per second (m/s), over a 24 h period, superimposing (vertically, in orange) the time instants in which the RSU issued a recommendation to follow the *alternative* route.

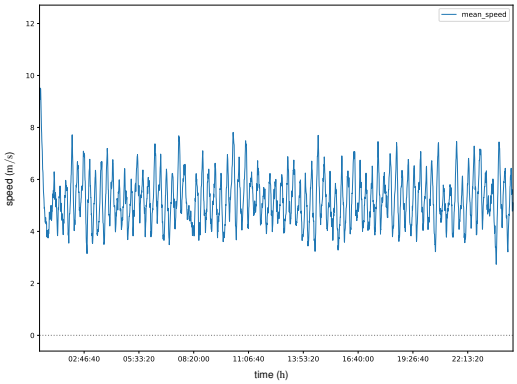


Fig. A.33-3. Mean speed in the network, in meters per second (m/s), over a 24 h period.

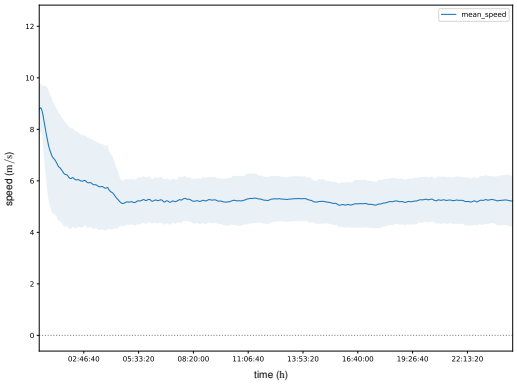


Fig. A.33-4. Mean speed in the network, in meters per second (m/s), over a 24 h period, 4 h Simple Moving Average, mean (line) and standard deviation (shaded).

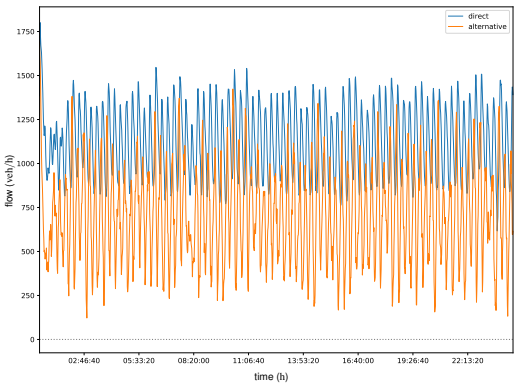


Fig. A.33-5. Traffic flow on each route, in vehicles per hour (veh/h), over a 24 h period.

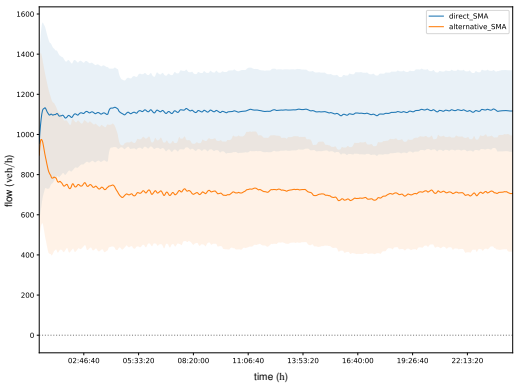


Fig. A.33-6. TrafficTraffic flow on each route, in vehicles per hour (veh/h), over a 24 h period, 4 h Simple Moving Average, mean (line) and standard deviation (shaded).

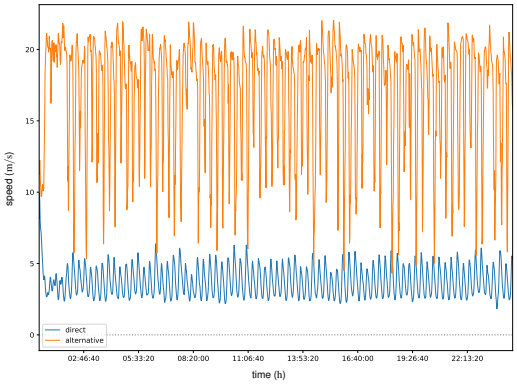


Fig. A.33-7. Mean speed on each route, in meters per second (m/s), aggregated to 1 min, over a 24 h period.

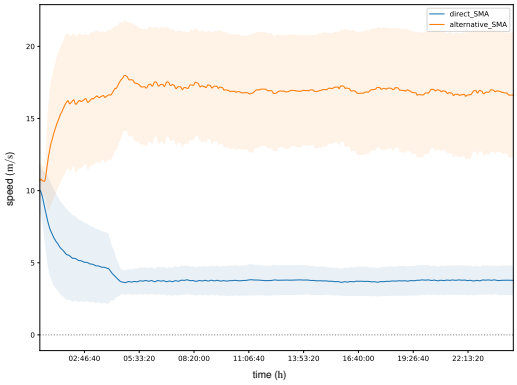


Fig. A.33-8. Mean speed on each route, in meters per second (m/s), aggregated to 1 min, over a 24 h period, 4 h Simple Moving Average, mean (line) and standard deviation (shaded).

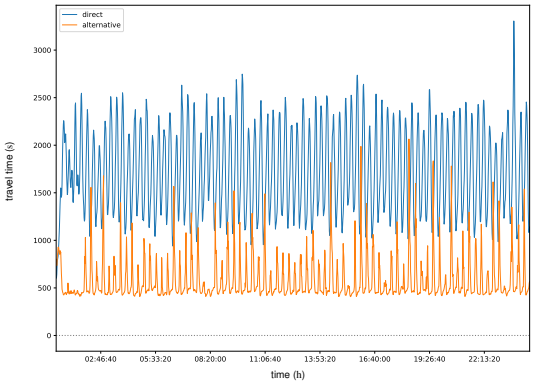


Fig. A.33-9. Travel times on each route, in seconds (s), aggregated to 1 min, over a 24 h period.

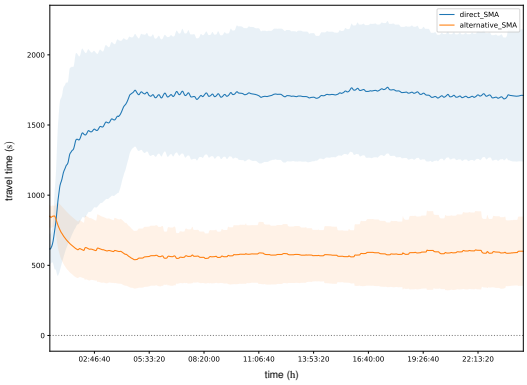


Fig. A.33-10. Travel times on each route, in seconds (s), aggregated to 1 min, over a 24 h period, 4 h Simple Moving Average, mean (line) and standard deviation (shaded).

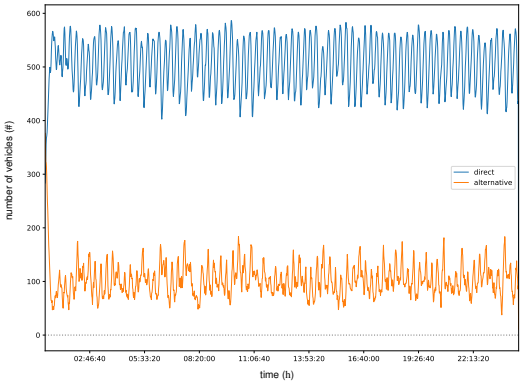


Fig. A.33-11. Average number of vehicles on each route, aggregated to 1 min, over a 24 h period.

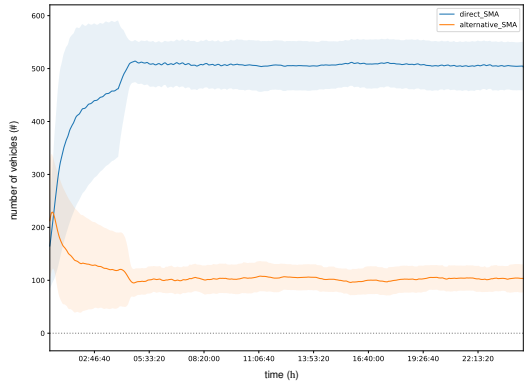


Fig. A.33-12. Average number of vehicles on each route, aggregated to 1 min, over a 24 h period, 4 h Simple Moving Average, mean (line) and standard deviation (shaded).

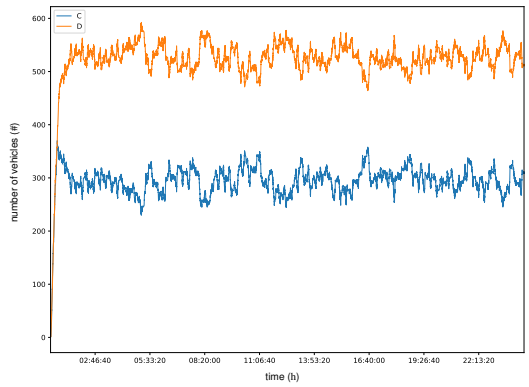


Fig. A.33-13. Evolution of the number of *Cooperators* and *Defectors* over a 24 h period.

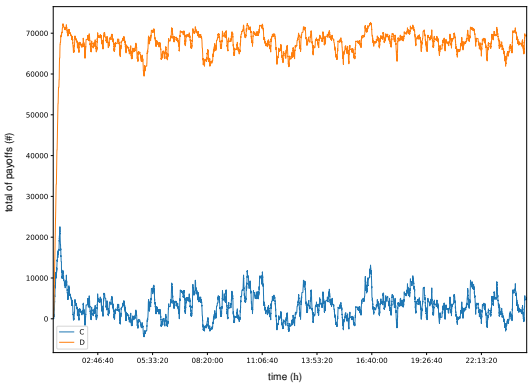


Fig. A.33-14. Evolution of total payoffs for *Cooperators* and *Defectors* (*individual payoff* times the *number of players receiving it*, $C(n) \times n$ and $D(n) \times (N-n)$, where n is the number of *Cooperators*), over a 24 h period.

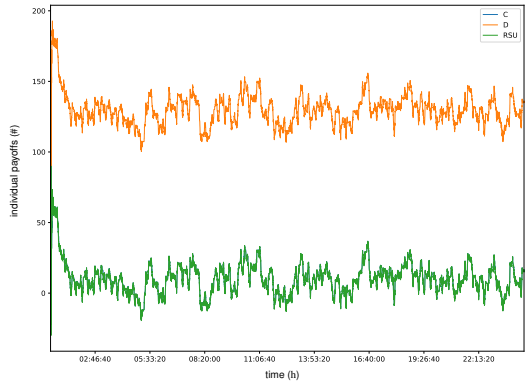


Fig. A.33-15. Evolution of the individual payoffs for *Cooperators, Defectors,* and *RSU* (always cooperating), over a 24 h period.

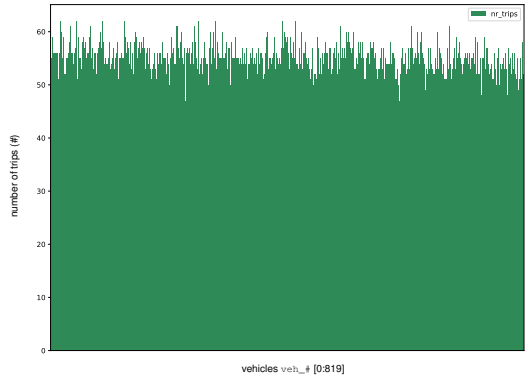


Fig. A.33-16. Number of trips made by each vehicle, during the simulation of a 24 h period.

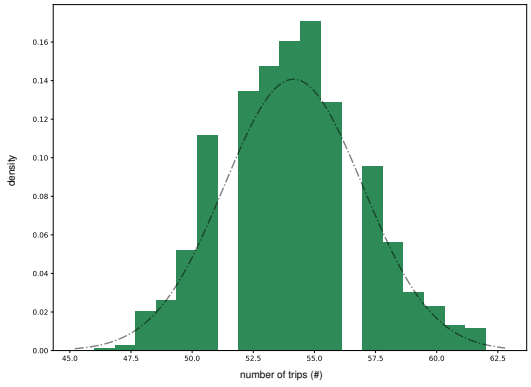


Fig. A.33-17. Density histogram of the number of trips made by each vehicle, during the simulation of a 24 h period, superimposing the normal density curve. The number of bins was calculated by the Freedman Diaconis rule.

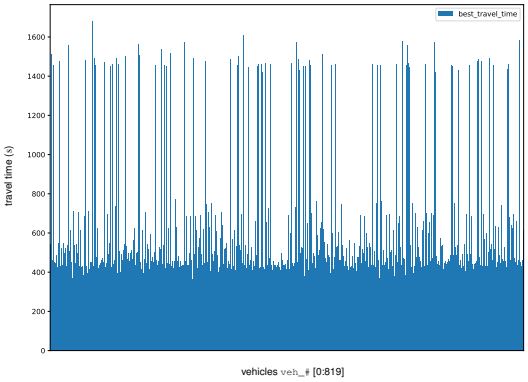


Fig. A.33-18. Best travel time for each vehicle, in seconds (s), during the simulation of a 24 h period.

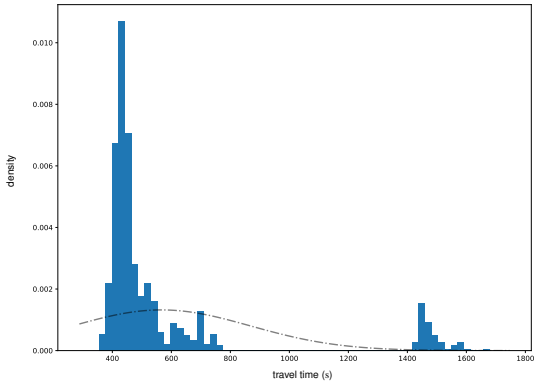


Fig. A.33-19. Density histogram of best travel time for vehicles, in seconds (s), during the simulation of a 24 h period, superimposing the normal density curve. The number of bins was calculated by the Freedman Diaconis rule.

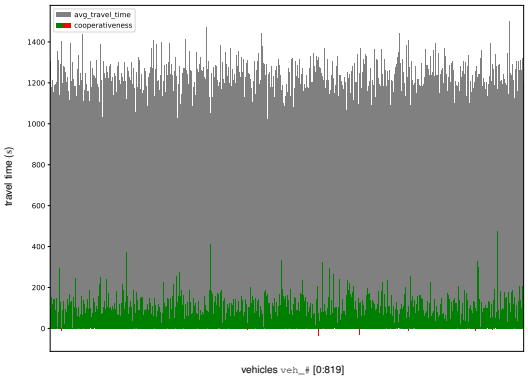


Fig. A.33-20. Average of the travel times, in seconds (s), of individual vehicles, during the simulation of a 24 h period. The bottom graph represents the *degree of cooperativeness**, downscaled by a normalization factor for the purpose of comparison with average times.

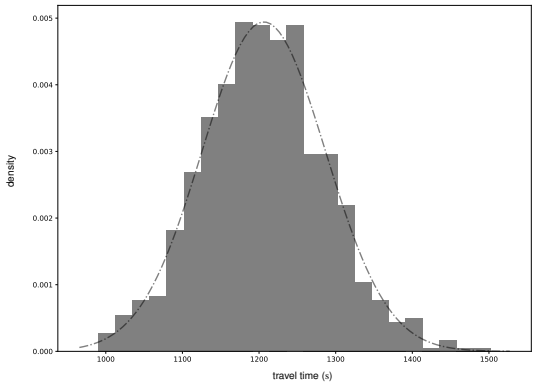


Fig. A.33-21. Density histogram of the average travel times, in seconds (s), of individual vehicles, during the simulation of a 24 h period, superimposing the normal density curve. The number of bins was calculated by the Freedman Diaconis rule.

* The *degree of cooperativeness* is a cumulative sum, calculated at each iteration, based on the complement of the ratio of cooperators, i.e., the higher the number of cooperators the less it increases, but the defectors are more penalized, and vice-versa. It varies inversely with the size of the group to which the player belongs.

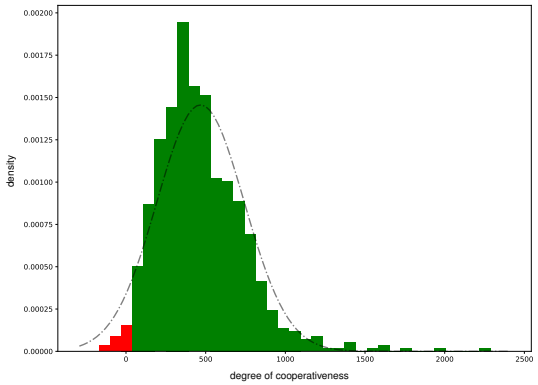


Fig. A.33-22. Density histogram of the *degree of cooperativeness** of individual vehicles, superimposing the normal density curve. The number of bins was calculated by the Freedman Diaconis rule. Generally, when strongly correlated with travel times, it presents a symmetric curve with respect to the *yy*-axis.

A.34 `820veh-24h-17060001`

```
Scenario: scenario-1
Timestamp: 20210617T055443Z
Number of vehicles: 820 vehs
Simulation time: 24.0 h
Warm up end time: 1866.6 s; step 18665
Vehicle selection strategy: stochastic
RSU turned off: False
RSU strategy: proportional_dynamic_v4
Runner options:
   nogui: True
   step_length: 0.1
   seed: 19750808
   output_prefix: 820veh-24h-17060001
   sim_run_time: 24.0
   num_vehicles: 820
   warmup_speed: 13.96
   warmup_routes_weight: [473, 527]
   network_speed: 25.0
   change_behavior_probability: [100, 0]
   cooperation_probability: [50, 50]
   vehicle_selection_strategy: stochastic
   turn_rsu_off: False
   rsu_dynamic_dissemination: False
   rsu_dissemination_interval: 5
   rsu_probabilistic_dissemination: False
   rsu_suggestion_strategy: proportional_dynamic_v4
   rsu_routes_weight: [460, 540]
   rsu_moving_avg_size: 5
   travel_times_ttl: 60
   rsu_dissemination_ttl: 0
   rsu_send_travel_time_info: False
   payoff_matrix: [360.0, 240.0, 0.0, -120.0]
   roth_erev_parameters: [0.1, 0.15]
   rsu_change_dissemination: False
   rsu_change_dissemination_steps: [14400, 28800, 43200, 57600, 72000]
   rsu_change_dissemination_intervals: [10, 20, 40, 80, 160]
Network Mean speed after warmup:
   Max: 9.81
   Min: 3.7
```

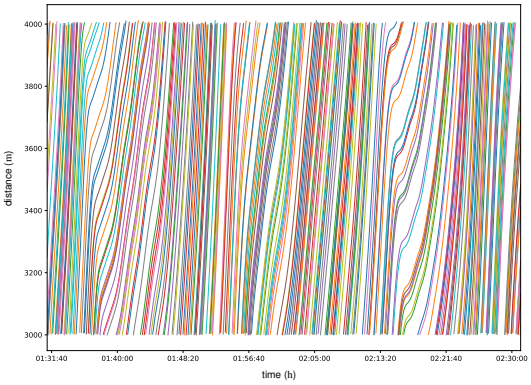


Fig. A.34-1. Time-Space diagram, for the one hour period after the end of the warmup, from 1:00:00 to 2:00:00 simulation time, plotted for the data from the sensor placed in the middle of the *direct* route (between 3000 m and 4000 m). In the case of an overloaded network, congestion shock waves can be observed.

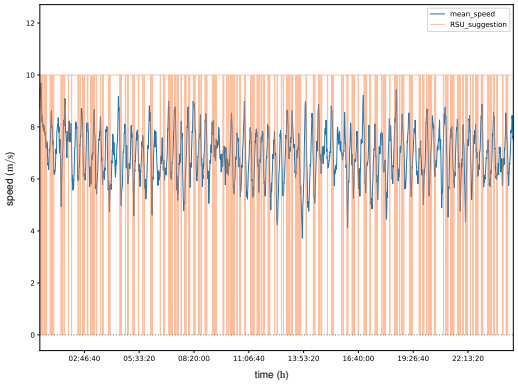


Fig. A.34-2. Mean speed in the network, in meters per second (m/s), over a 24 h period, superimposing (vertically, in orange) the time instants in which the RSU issued a recommendation to follow the *alternative* route.

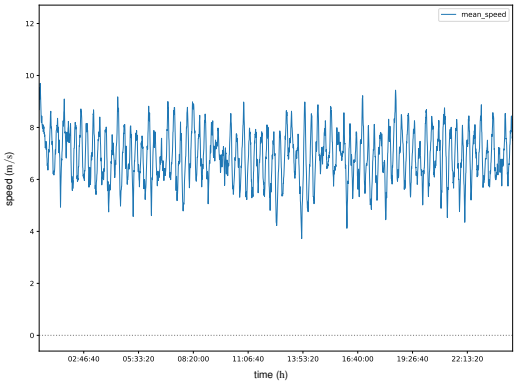


Fig. A.34-3. Mean speed in the network, in meters per second (m/s), over a 24 h period.

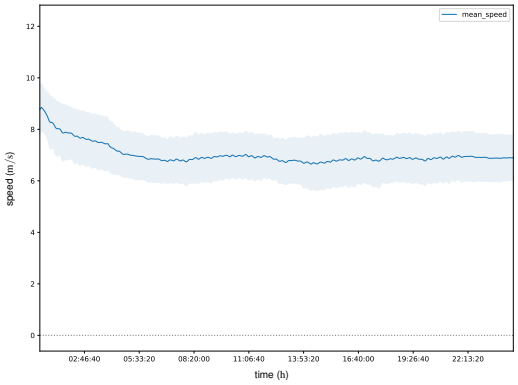


Fig. A.34-4. Mean speed in the network, in meters per second (m/s), over a 24 h period, 4 h Simple Moving Average, mean (line) and standard deviation (shaded).

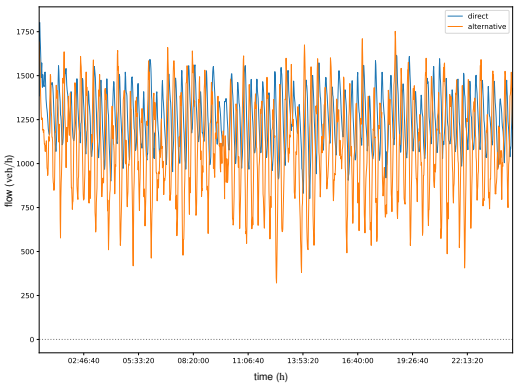


Fig. A.34-5. Traffic flow on each route, in vehicles per hour (veh/h), over a 24 h period.

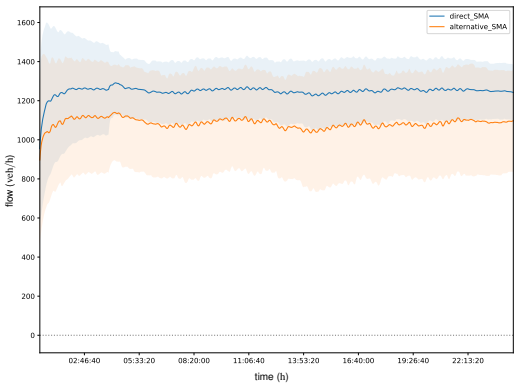


Fig. A.34-6. TrafficTraffic flow on each route, in vehicles per hour (veh/h), over a 24 h period, 4 h Simple Moving Average, mean (line) and standard deviation (shaded).

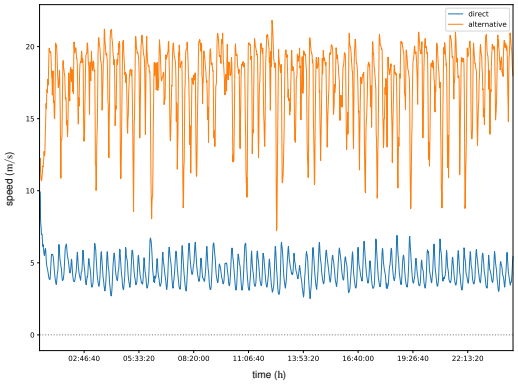


Fig. A.34-7. Mean speed on each route, in meters per second (m/s), aggregated to 1 min, over a 24 h period.

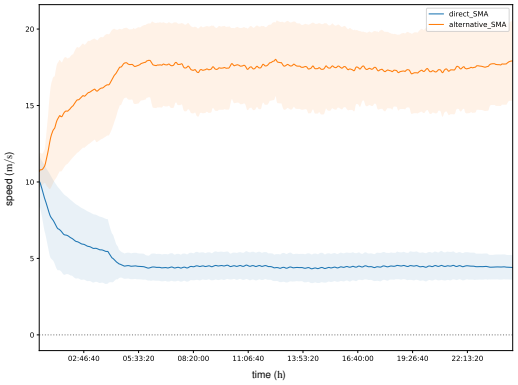


Fig. A.34-8. Mean speed on each route, in meters per second (m/s), aggregated to 1 min, over a 24 h period, 4 h Simple Moving Average, mean (line) and standard deviation (shaded).

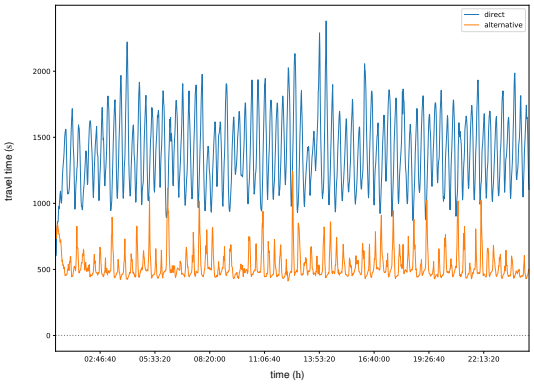


Fig. A.34-9. Travel times on each route, in seconds (s), aggregated to 1 min, over a 24 h period.

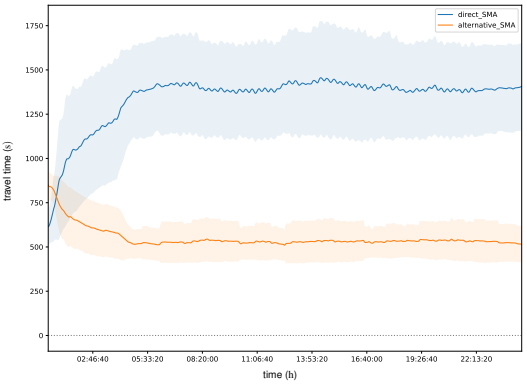


Fig. A.34-10. Travel times on each route, in seconds (s), aggregated to 1 min, over a 24 h period, 4 h Simple Moving Average, mean (line) and standard deviation (shaded).

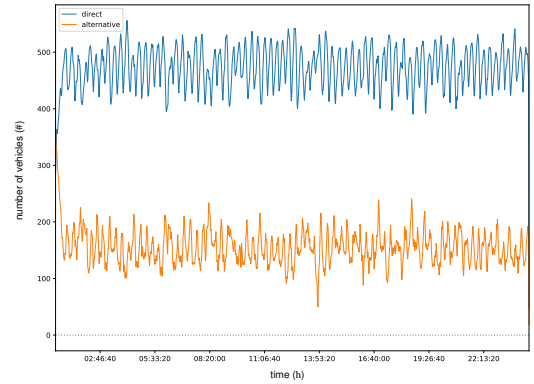


Fig. A.34-11. Average number of vehicles on each route, aggregated to 1 min, over a 24 h period.

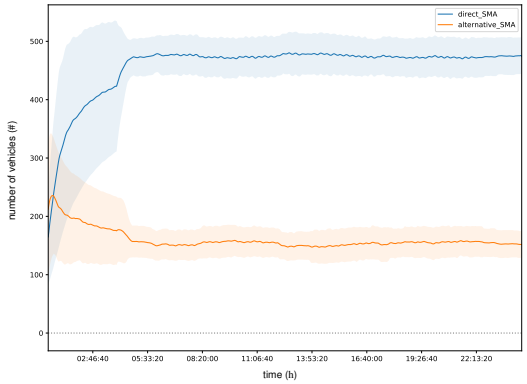


Fig. A.34-12. Average number of vehicles on each route, aggregated to 1 min, over a 24 h period, 4 h Simple Moving Average, mean (line) and standard deviation (shaded).

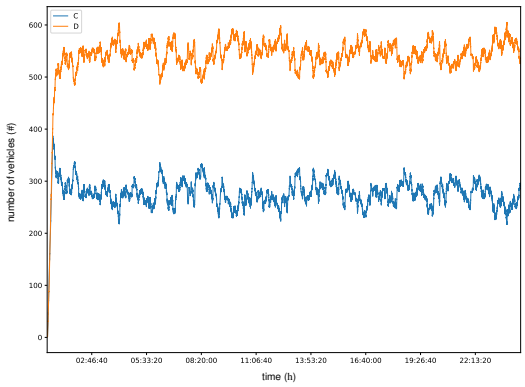


Fig. A.34-13. Evolution of the number of *Cooperators* and *Defectors* over a 24 h period.

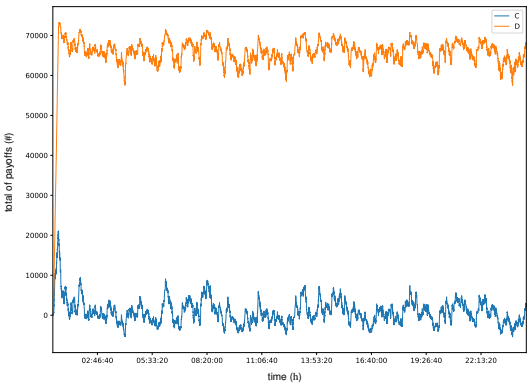


Fig. A.34-14. Evolution of total payoffs for *Cooperators* and *Defectors* (*individual payoff* times the *number of players receiving it*, $C(n) \times n$ and $D(n) \times (N-n)$, where n is the number of *Cooperators*), over a 24 h period.

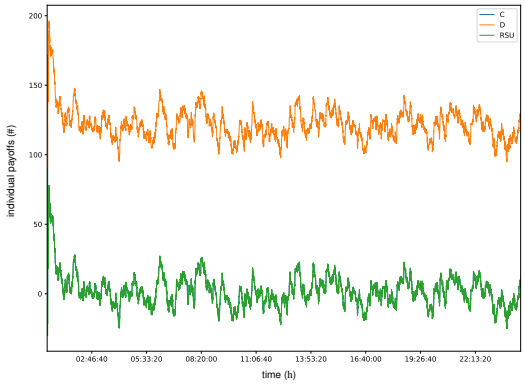


Fig. A.34-15. Evolution of the individual payoffs for *Cooperators, Defectors,* and *RSU* (always cooperating), over a 24 h period.

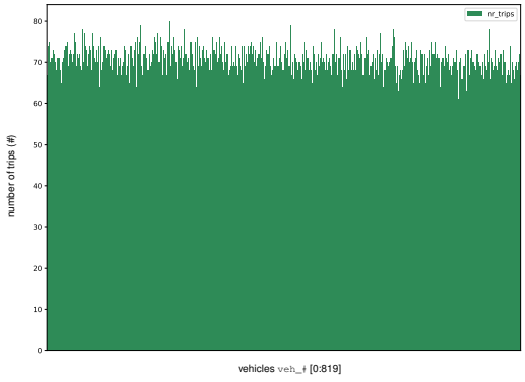


Fig. A.34-16. Number of trips made by each vehicle, during the simulation of a 24 h period.

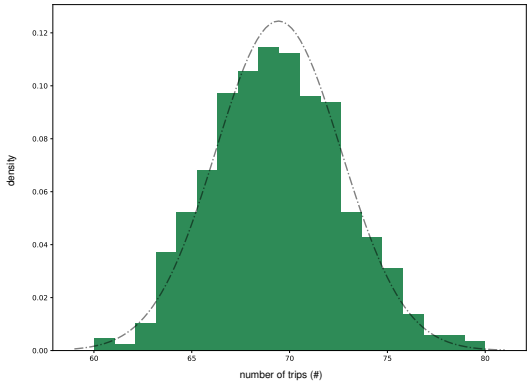


Fig. A.34-17. Density histogram of the number of trips made by each vehicle, during the simulation of a 24 h period, superimposing the normal density curve. The number of bins was calculated by the Freedman Diaconis rule.

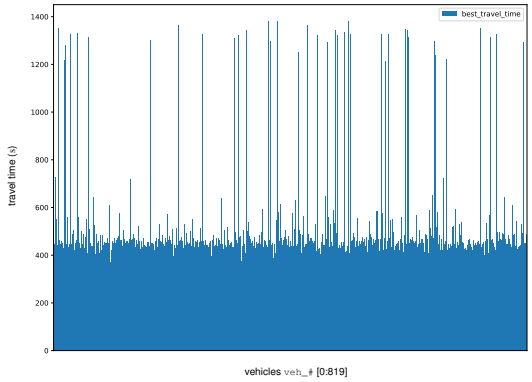


Fig. A.34-18. Best travel time for each vehicle, in seconds (s), during the simulation of a 24 h period.

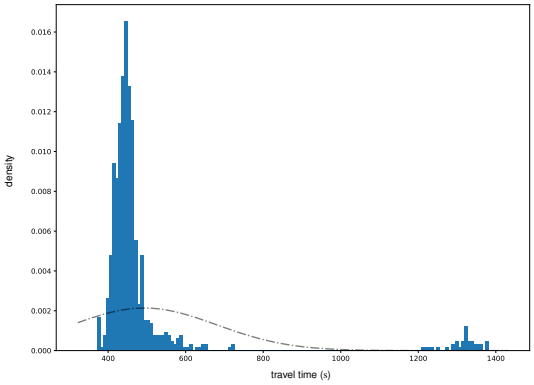


Fig. A.34-19. Density histogram of best travel time for vehicles, in seconds (s), during the simulation of a 24 h period, superimposing the normal density curve. The number of bins was calculated by the Freedman Diaconis rule.

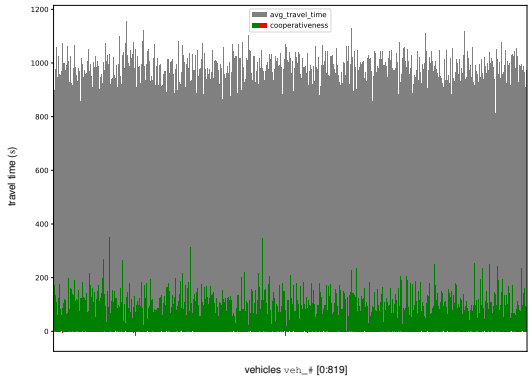


Fig. A.34-20. Average of the travel times, in seconds (s), of individual vehicles, during the simulation of a 24 h period. The bottom graph represents the *degree of cooperativeness**, downscaled by a normalization factor for the purpose of comparison with average times.

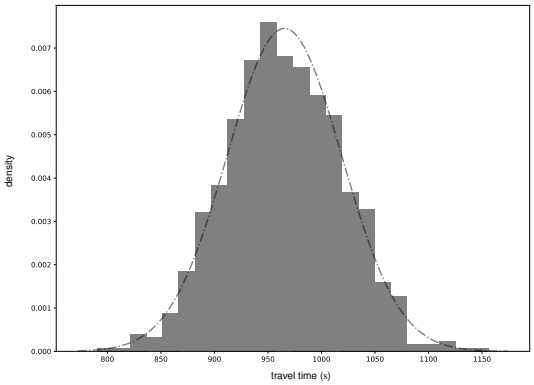


Fig. A.34-21. Density histogram of the average travel times, in seconds (s), of individual vehicles, during the simulation of a 24 h period, superimposing the normal density curve. The number of bins was calculated by the Freedman Diaconis rule.

* The *degree of cooperativeness* is a cumulative sum, calculated at each iteration, based on the complement of the ratio of cooperators, i.e., the higher the number of cooperators the less it increases, but the defectors are more penalized, and vice-versa. It varies inversely with the size of the group to which the player belongs.

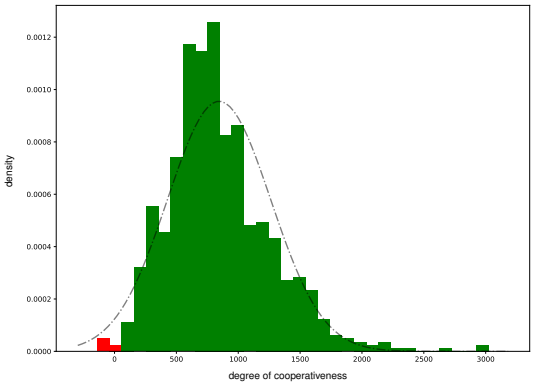


Fig. A.34-22. Density histogram of the *degree of cooperativeness** of individual vehicles, superimposing the normal density curve. The number of bins was calculated by the Freedman Diaconis rule. Generally, when strongly correlated with travel times, it presents a symmetric curve with respect to the *yy*-axis.

A.35 820veh-24h-19060001

```
Scenario: scenario-1
Timestamp: 20210616T102908Z
Number of vehicles: 820 vehs
Simulation time: 24.0 h
Warm up end time: 1866.6 s; step 18665
Vehicle selection strategy: stochastic
RSU turned off: False
RSU strategy: pigous_example_cooperation_weighted
Runner options:
   nogui: True
   step_length: 0.1
   seed: 19750808
   output_prefix: 820veh-24h-19060001
   sim_run_time: 24.0
   num_vehicles: 820
   warmup_speed: 13.96
   warmup_routes_weight: [473, 527]
   network_speed: 25.0
   change_behavior_probability: [100, 0]
   cooperation_probability: [50, 50]
   vehicle_selection_strategy: stochastic
   turn_rsu_off: False
   rsu_dynamic_dissemination: False
   rsu_dissemination_interval: 5
   rsu_probabilistic_dissemination: False
   rsu_suggestion_strategy: pigous_example_cooperation_weighted
   rsu_routes_weight: [460, 540]
   rsu_moving_avg_size: 5
   travel_times_ttl: 60
   rsu_dissemination_ttl: 0
   rsu_send_travel_time_info: False
   payoff_matrix: [360.0, 240.0, 0.0, -120.0]
   roth_erev_parameters: [0.1, 0.15]
   rsu_change_dissemination: False
   rsu_change_dissemination_steps: [14400, 28800, 43200, 57600, 72000]
   rsu_change_dissemination_intervals: [10, 20, 40, 80, 160]
Network Mean speed after warmup:
   Max: 9.96
   Min: 5.16
```

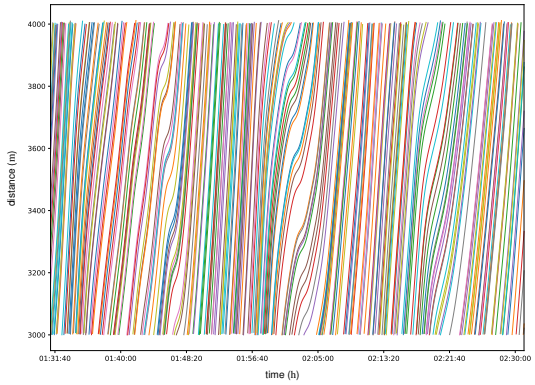


Fig. A.35-1. Time-Space diagram, for the one hour period after the end of the warmup, from 1:00:00 to 2:00:00 simulation time, plotted for the data from the sensor placed in the middle of the *direct* route (between 3000 m and 4000 m). In the case of an overloaded network, congestion shock waves can be observed.

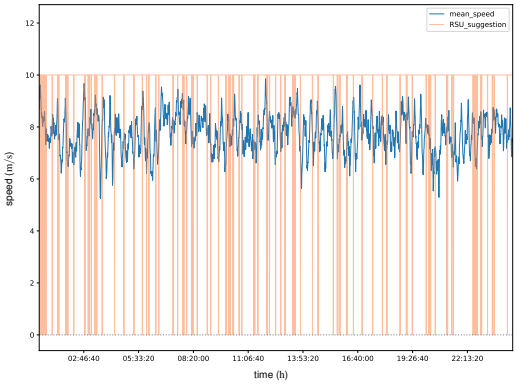


Fig. A.35-2. Mean speed in the network, in meters per second (m/s), over a 24 h period, superimposing (vertically, in orange) the time instants in which the RSU issued a recommendation to follow the *alternative* route.

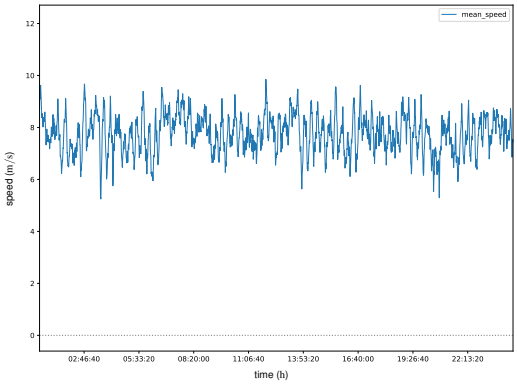


Fig. A.35-3. Mean speed in the network, in meters per second (m/s), over a 24 h period.

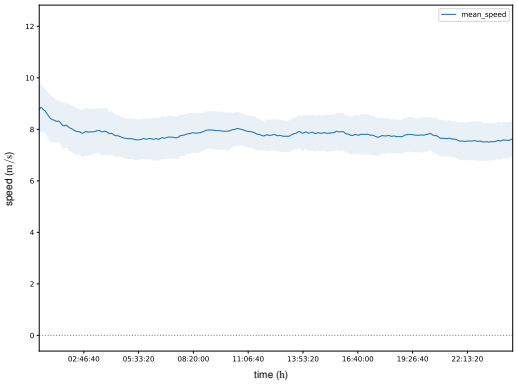


Fig. A.35-4. Mean speed in the network, in meters per second (m/s), over a 24 h period, 4 h Simple Moving Average, mean (line) and standard deviation (shaded).

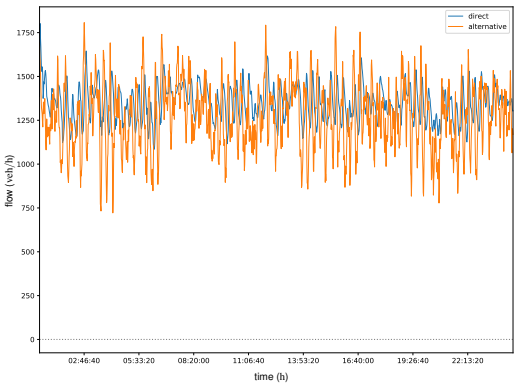


Fig. A.35-5. Traffic flow on each route, in vehicles per hour (veh/h), over a 24 h period.

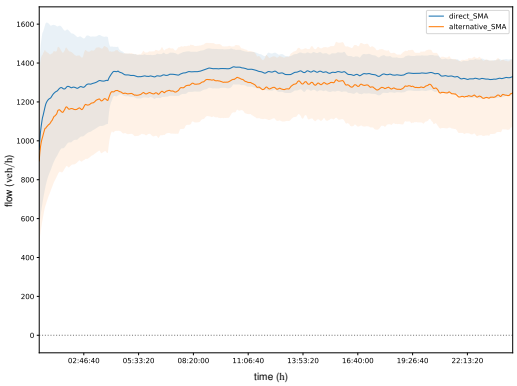


Fig. A.35-6. TrafficTraffic flow on each route, in vehicles per hour (veh/h), over a 24 h period, 4 h Simple Moving Average, mean (line) and standard deviation (shaded).

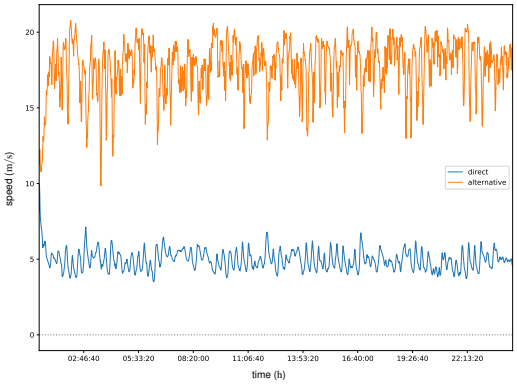


Fig. A.35-7. Mean speed on each route, in meters per second (m/s), aggregated to 1 min, over a 24 h period.

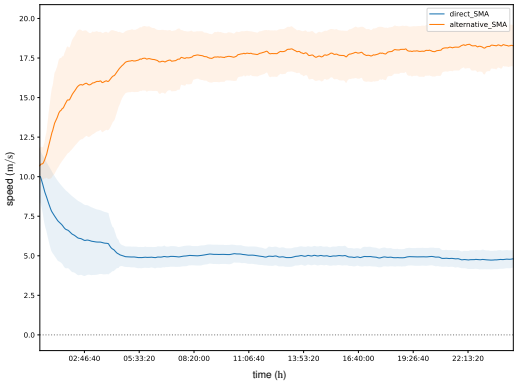


Fig. A.35-8. Mean speed on each route, in meters per second (m/s), aggregated to 1 min, over a 24 h period, 4 h Simple Moving Average, mean (line) and standard deviation (shaded).

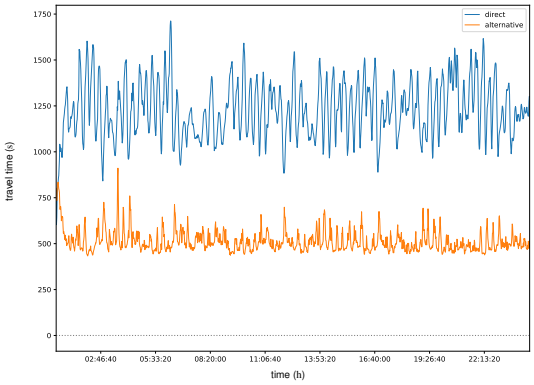


Fig. A.35-9. Travel times on each route, in seconds (s), aggregated to 1 min, over a 24 h period.

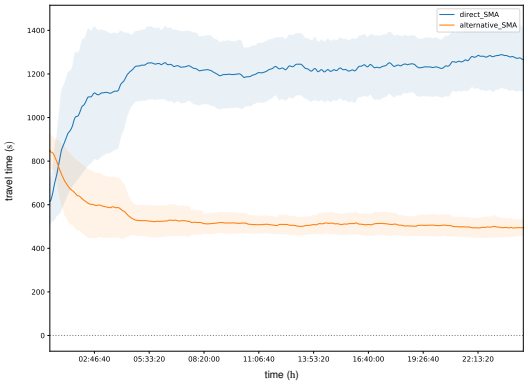


Fig. A.35-10. Travel times on each route, in seconds (s), aggregated to 1 min, over a 24 h period, 4 h Simple Moving Average, mean (line) and standard deviation (shaded).

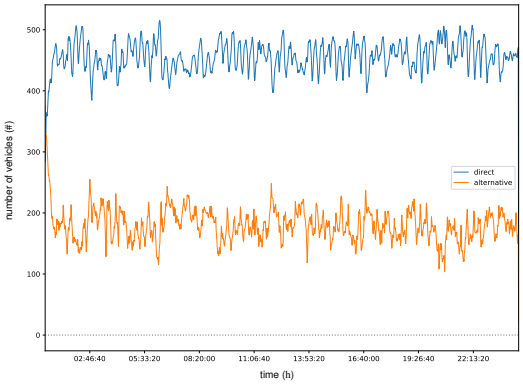


Fig. A.35-11. Average number of vehicles on each route, aggregated to 1 min, over a 24 h period.

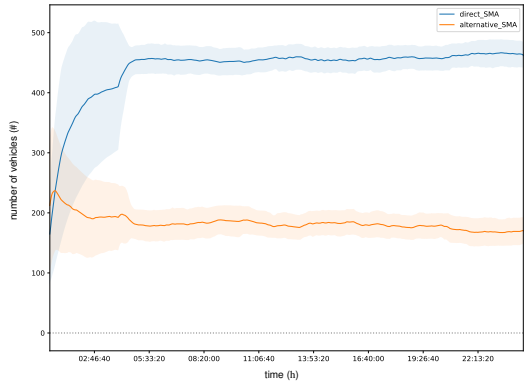


Fig. A.35-12. Average number of vehicles on each route, aggregated to 1 min, over a 24 h period, 4 h Simple Moving Average, mean (line) and standard deviation (shaded).

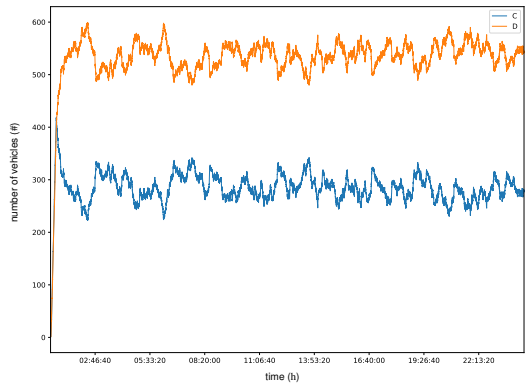


Fig. A.35-13. Evolution of the number of *Cooperators* and *Defectors* over a 24 h period.

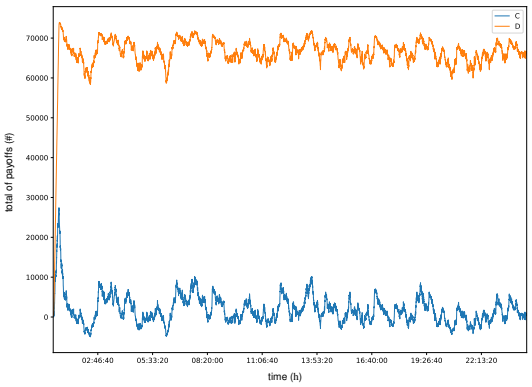


Fig. A.35-14. Evolution of total payoffs for *Cooperators* and *Defectors* (*individual payoff* times the *number of players receiving it*, $C(n) \times n$ and $D(n) \times (N-n)$, where n is the number of *Cooperators*), over a 24 h period.

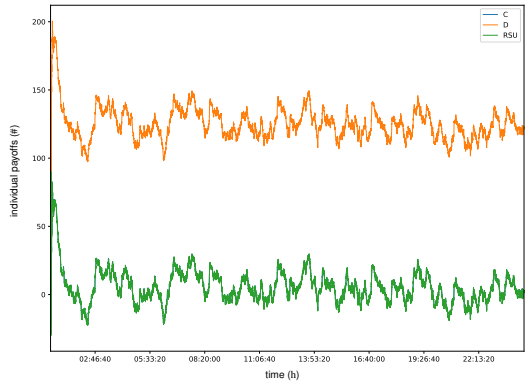


Fig. A.35-15. Evolution of the individual payoffs for *Cooperators, Defectors,* and *RSU* (always cooperating), over a 24 h period.

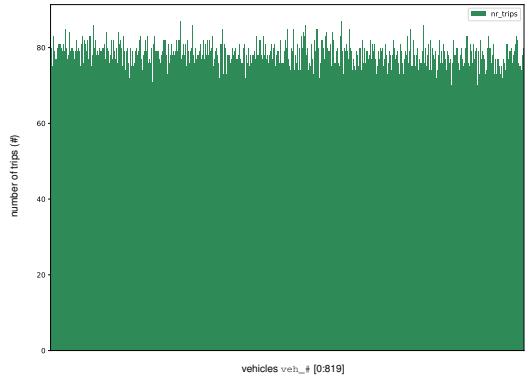


Fig. A.35-16. Number of trips made by each vehicle, during the simulation of a 24 h period.

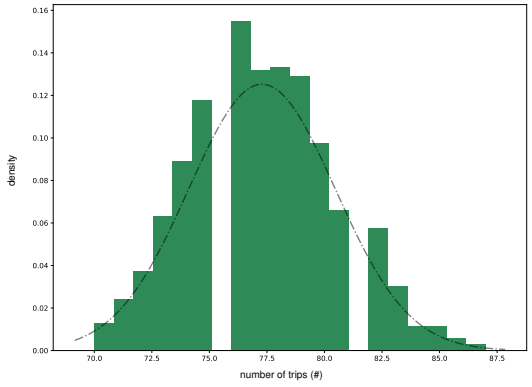


Fig. A.35-17. Density histogram of the number of trips made by each vehicle, during the simulation of a 24 h period, superimposing the normal density curve. The number of bins was calculated by the Freedman Diaconis rule.

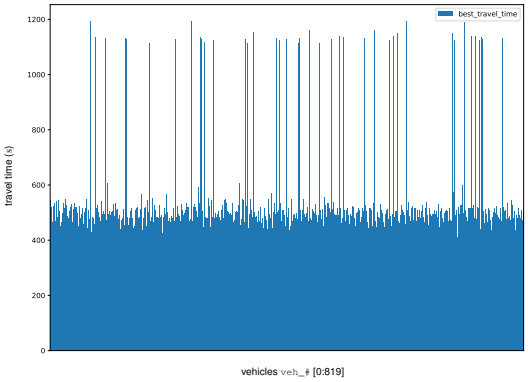


Fig. A.35-18. Best travel time for each vehicle, in seconds (s), during the simulation of a 24 h period.

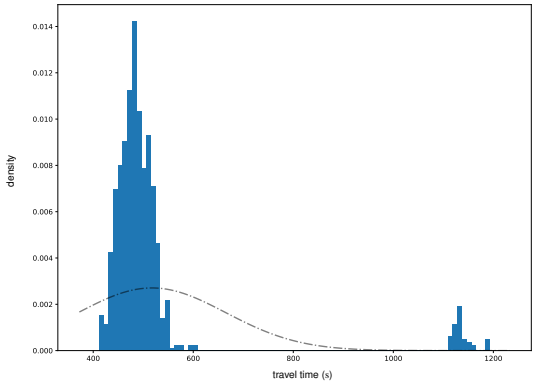


Fig. A.35-19. Density histogram of best travel time for vehicles, in seconds (s), during the simulation of a 24 h period, superimposing the normal density curve. The number of bins was calculated by the Freedman Diaconis rule.

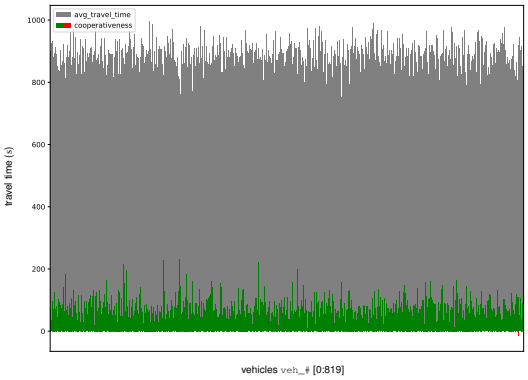


Fig. A.35-20. Average of the travel times, in seconds (s), of individual vehicles, during the simulation of a 24 h period. The bottom graph represents the *degree of cooperativeness**, downscaled by a normalization factor for the purpose of comparison with average times.

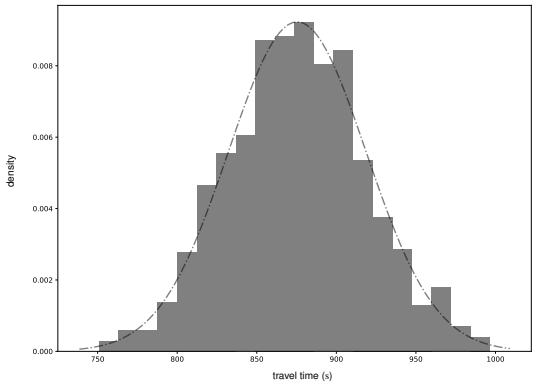


Fig. A.35-21. Density histogram of the average travel times, in seconds (s), of individual vehicles, during the simulation of a 24 h period, superimposing the normal density curve. The number of bins was calculated by the Freedman Diaconis rule.

* The *degree of cooperativeness* is a cumulative sum, calculated at each iteration, based on the complement of the ratio of cooperators, i.e., the higher the number of cooperators the less it increases, but the defectors are more penalized, and vice-versa. It varies inversely with the size of the group to which the player belongs.

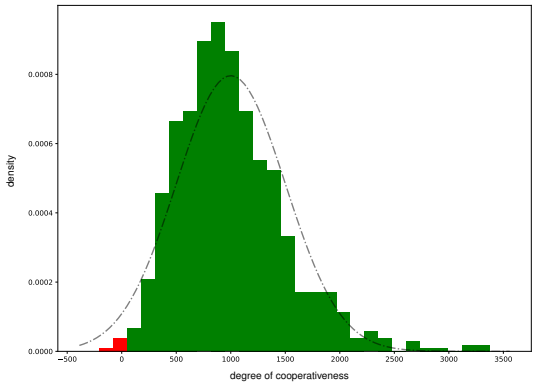


Fig. A.35-22. Density histogram of the *degree of cooperativeness** of individual vehicles, superimposing the normal density curve. The number of bins was calculated by the Freedman Diaconis rule. Generally, when strongly correlated with travel times, it presents a symmetric curve with respect to the *yy*-axis.

A.36 `820veh-24h-15060001`

```
Scenario: scenario-1
Timestamp: 20210523T003745Z
Number of vehicles: 820 vehs
Simulation time: 24.0 h
Warm up end time: 1866.6 s; step 18665
Vehicle selection strategy: stochastic
RSU turned off: False
RSU strategy: proportional_dynamic_v3
Runner options:
   nogui: True
   step_length: 0.1
   seed: 19750808
   output_prefix: 820veh-24h-15060001
   sim_run_time: 24.0
   num_vehicles: 820
   warmup_speed: 13.96
   warmup_routes_weight: [473, 527]
   network_speed: 25.0
   change_behavior_probability: [100, 0]
   cooperation_probability: [50, 50]
   vehicle_selection_strategy: stochastic
   turn_rsu_off: False
   rsu_dynamic_dissemination: False
   rsu_dissemination_interval: 5
   rsu_probabilistic_dissemination: False
   rsu_suggestion_strategy: proportional_dynamic_v3
   rsu_routes_weight: [460, 540]
   rsu_moving_avg_size: 5
   travel_times_ttl: 60
   rsu_dissemination_ttl: 0
   rsu_send_travel_time_info: False
   payoff_matrix: [360.0, 240.0, 0.0, -120.0]
   roth_erev_parameters: [0.1, 0.15]
Network Mean speed after warmup:
   Max: 9.61
   Min: 3.6
```

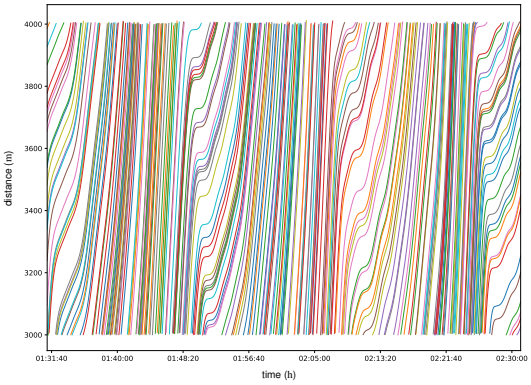


Fig. A.36-1. Time-Space diagram, for the one hour period after the end of the warmup, from 1:00:00 to 2:00:00 simulation time, plotted for the data from the sensor placed in the middle of the *direct* route (between 3000 m and 4000 m). In the case of an overloaded network, congestion shock waves can be observed.

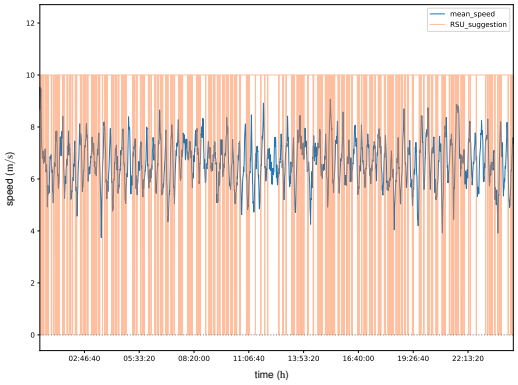


Fig. A.36-2. Mean speed in the network, in meters per second (m/s), over a 24 h period, superimposing (vertically, in orange) the time instants in which the RSU issued a recommendation to follow the *alternative* route.

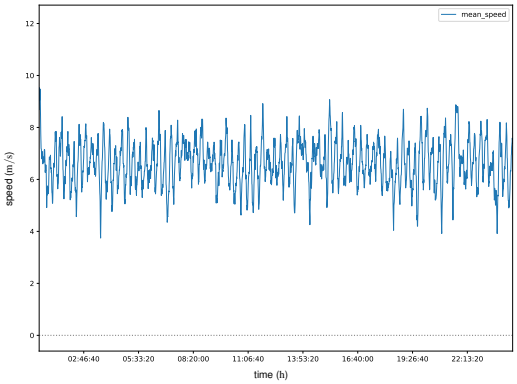


Fig. A.36-3. Mean speed in the network, in meters per second (m/s), over a 24 h period.

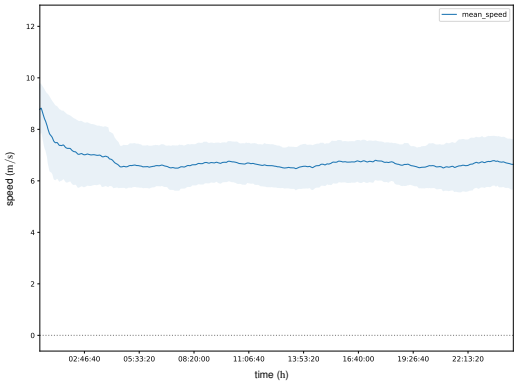


Fig. A.36-4. Mean speed in the network, in meters per second (m/s), over a 24 h period, 4 h Simple Moving Average, mean (line) and standard deviation (shaded).

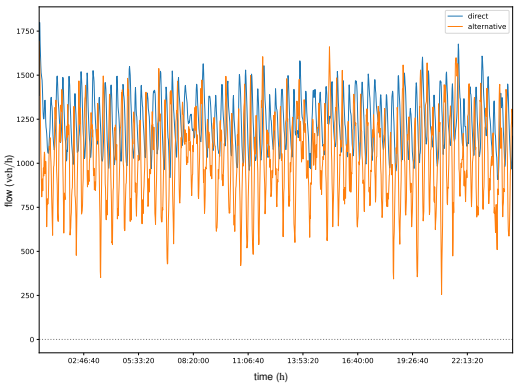


Fig. A.36-5. Traffic flow on each route, in vehicles per hour (veh/h), over a 24 h period.

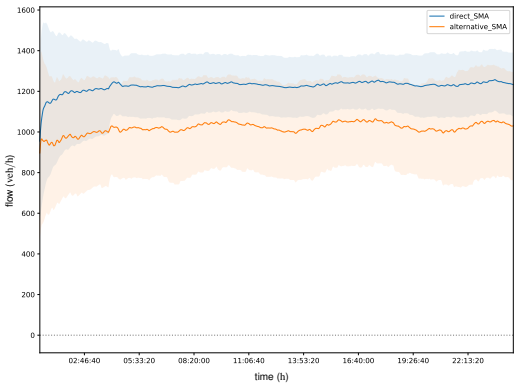


Fig. A.36-6. TrafficTraffic flow on each route, in vehicles per hour (veh/h), over a 24 h period, 4 h Simple Moving Average, mean (line) and standard deviation (shaded).

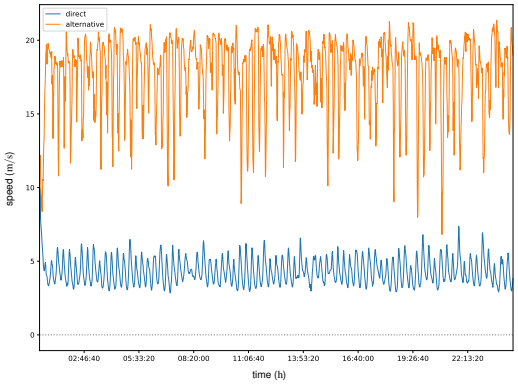


Fig. A.36-7. Mean speed on each route, in meters per second (m/s), aggregated to 1 min, over a 24 h period.

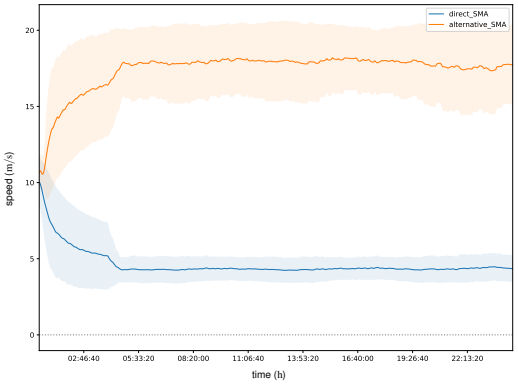


Fig. A.36-8. Mean speed on each route, in meters per second (m/s), aggregated to 1 min, over a 24 h period, 4 h Simple Moving Average, mean (line) and standard deviation (shaded).

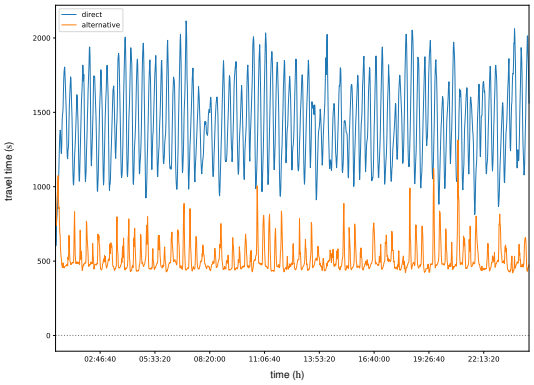


Fig. A.36-9. Travel times on each route, in seconds (s), aggregated to 1 min, over a 24 h period.

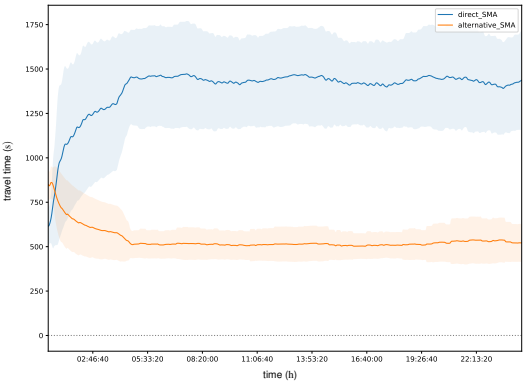


Fig. A.36-10. Travel times on each route, in seconds (s), aggregated to 1 min, over a 24 h period, 4 h Simple Moving Average, mean (line) and standard deviation (shaded).

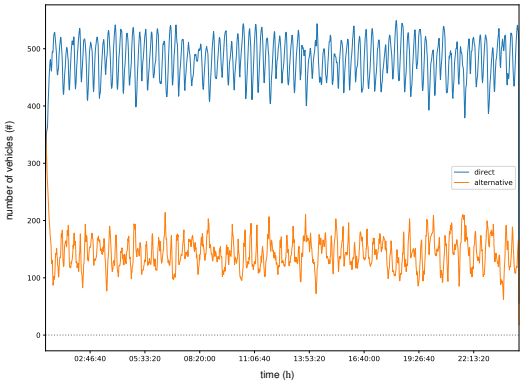


Fig. A.36-11. Average number of vehicles on each route, aggregated to 1 min, over a 24 h period.

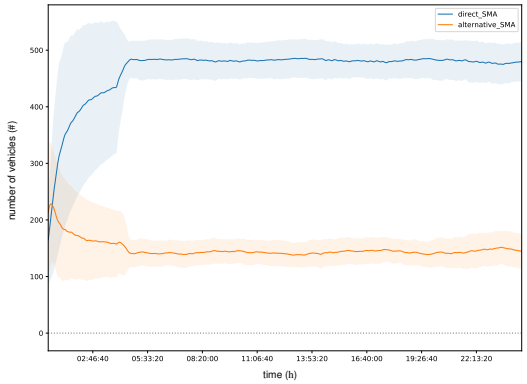


Fig. A.36-12. Average number of vehicles on each route, aggregated to 1 min, over a 24 h period, 4 h Simple Moving Average, mean (line) and standard deviation (shaded).

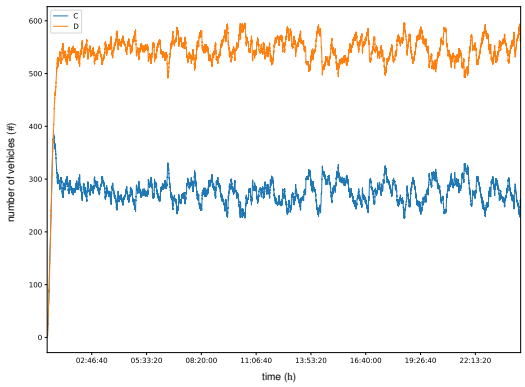


Fig. A.36-13. Evolution of the number of *Cooperators* and *Defectors* over a 24 h period.

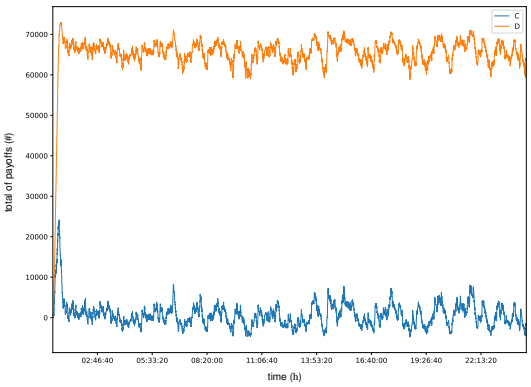


Fig. A.36-14. Evolution of total payoffs for *Cooperators* and *Defectors* (*individual payoff* times the *number of players receiving it*, $C(n) \times n$ and $D(n) \times (N-n)$, where n is the number of *Cooperators*), over a 24 h period.

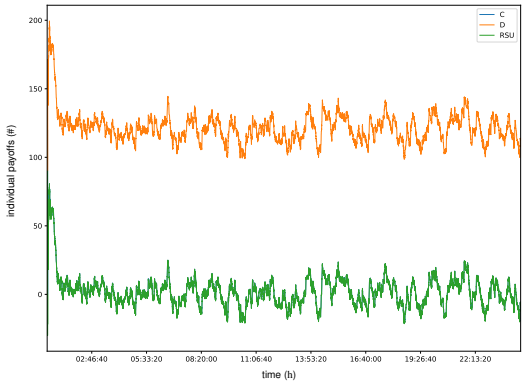


Fig. A.36-15. Evolution of the individual payoffs for *Cooperators, Defectors,* and *RSU* (always cooperating), over a 24 h period.

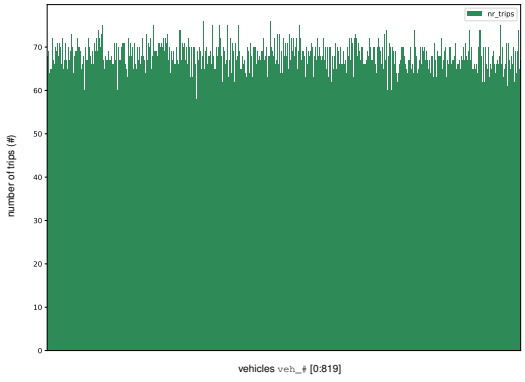


Fig. A.36-16. Number of trips made by each vehicle, during the simulation of a 24 h period.

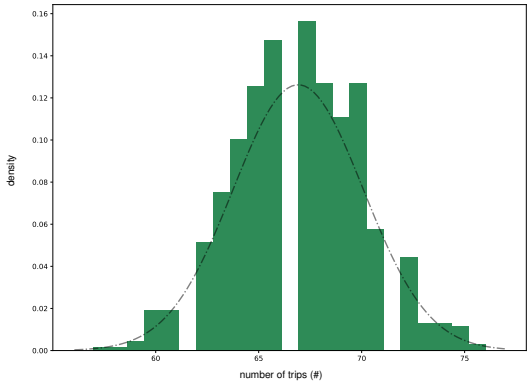


Fig. A.36-17. Density histogram of the number of trips made by each vehicle, during the simulation of a 24 h period, superimposing the normal density curve. The number of bins was calculated by the Freedman Diaconis rule.

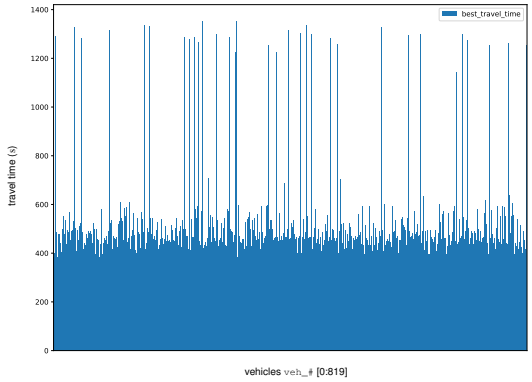


Fig. A.36-18. Best travel time for each vehicle, in seconds (s), during the simulation of a 24 h period.

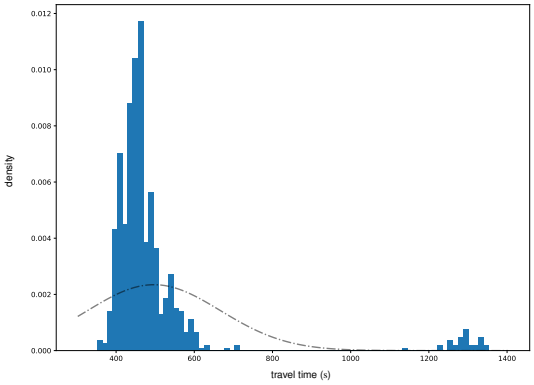


Fig. A.36-19. Density histogram of best travel time for vehicles, in seconds (s), during the simulation of a 24 h period, superimposing the normal density curve. The number of bins was calculated by the Freedman Diaconis rule.

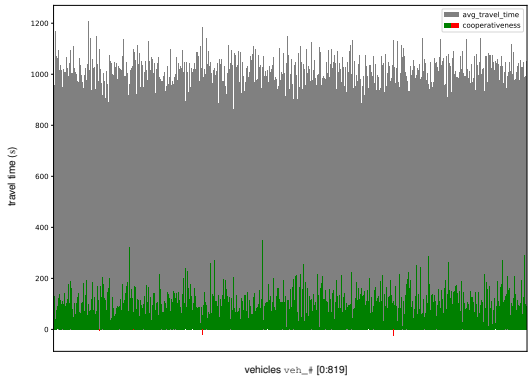


Fig. A.36-20. Average of the travel times, in seconds (s), of individual vehicles, during the simulation of a 24 h period. The bottom graph represents the *degree of cooperativeness**, downscaled by a normalization factor for the purpose of comparison with average times.

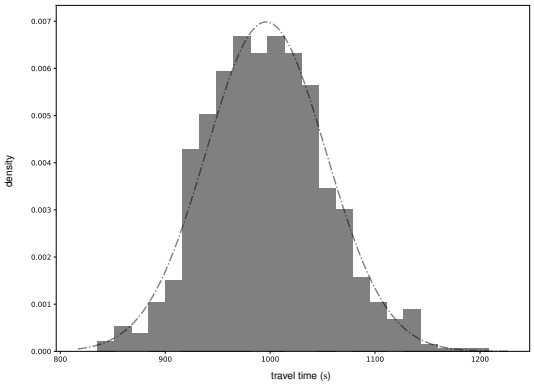


Fig. A.36-21. Density histogram of the average travel times, in seconds (s), of individual vehicles, during the simulation of a 24 h period, superimposing the normal density curve. The number of bins was calculated by the Freedman Diaconis rule.

* The *degree of cooperativeness* is a cumulative sum, calculated at each iteration, based on the complement of the ratio of cooperators, i.e., the higher the number of cooperators the less it increases, but the defectors are more penalized, and vice-versa. It varies inversely with the size of the group to which the player belongs.

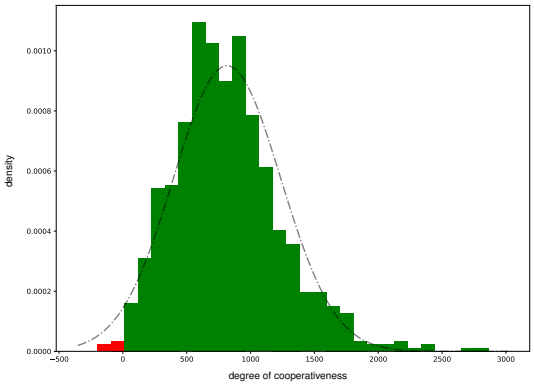


Fig. A.36-22. Density histogram of the *degree of cooperativeness** of individual vehicles, superimposing the normal density curve. The number of bins was calculated by the Freedman Diaconis rule. Generally, when strongly correlated with travel times, it presents a symmetric curve with respect to the *yy*-axis.

A.37 820veh-24h-16000001

```
Scenario: scenario-1
Timestamp: 20210607T190843Z
Number of vehicles: 820 vehs
Simulation time: 24.0 h
Warm up end time: 1866.6 s; step 18665
Vehicle selection strategy: best_travel_time
RSU turned off: False
RSU strategy: pigous_example
Runner options:
   nogui: True
   step_length: 0.1
   seed: 19750808
   output_prefix: 820veh-24h-16000001
   sim_run_time: 24.0
   num_vehicles: 820
   warmup_speed: 13.96
   warmup_routes_weight: [473, 527]
   network_speed: 25.0
   change_behavior_probability: [100, 0]
   cooperation_probability: [50, 50]
   vehicle_selection_strategy: best_travel_time
   turn_rsu_off: False
   rsu_dynamic_dissemination: False
   rsu_dissemination_interval: 5
   rsu_probabilistic_dissemination: False
   rsu_suggestion_strategy: pigous_example
   rsu_routes_weight: [460, 540]
   rsu_moving_avg_size: 5
   travel_times_ttl: 60
   rsu_dissemination_ttl: 0
   rsu_send_travel_time_info: False
   payoff_matrix: [360.0, 240.0, 0.0, -120.0]
   roth_erev_parameters: [0.1, 0.15]
Network Mean speed after warmup:
   Max: 11.22
   Min: 5.03
```

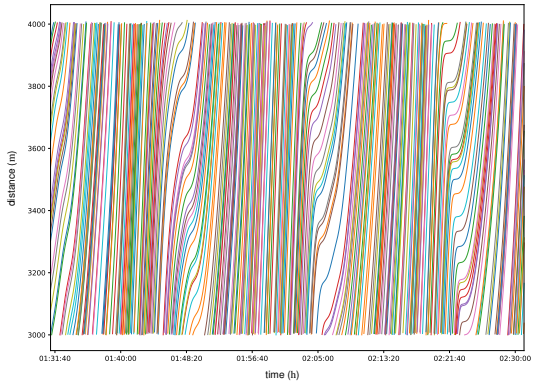


Fig. A.37-1. Time-Space diagram, for the one hour period after the end of the warmup, from 1:00:00 to 2:00:00 simulation time, plotted for the data from the sensor placed in the middle of the *direct* route (between 3000 m and 4000 m). In the case of an overloaded network, congestion shock waves can be observed.

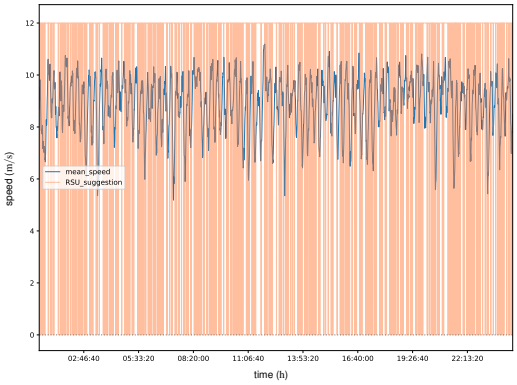


Fig. A.37-2. Mean speed in the network, in meters per second (m/s), over a 24 h period, superimposing (vertically, in orange) the time instants in which the RSU issued a recommendation to follow the *alternative* route.

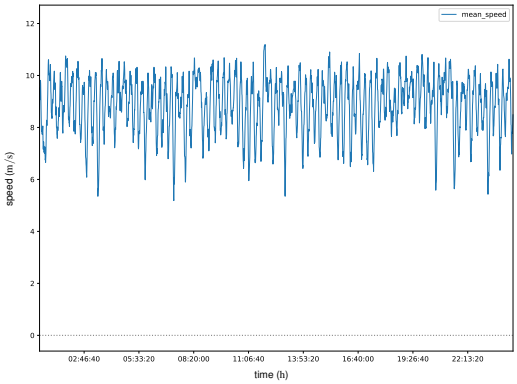


Fig. A.37-3. Mean speed in the network, in meters per second (m/s), over a 24 h period.

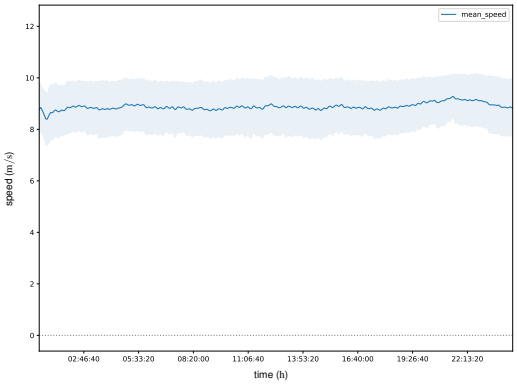


Fig. A.37-4. Mean speed in the network, in meters per second (m/s), over a 24 h period, 4 h Simple Moving Average, mean (line) and standard deviation (shaded).

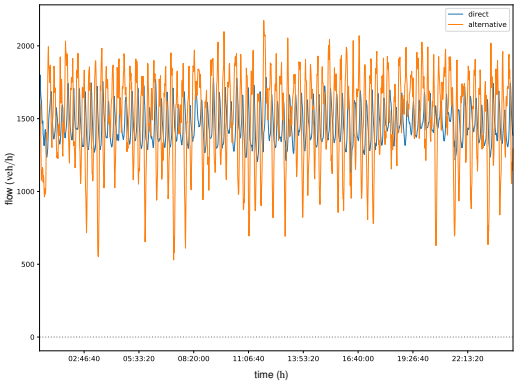


Fig. A.37-5. Traffic flow on each route, in vehicles per hour (veh/h), over a 24 h period.

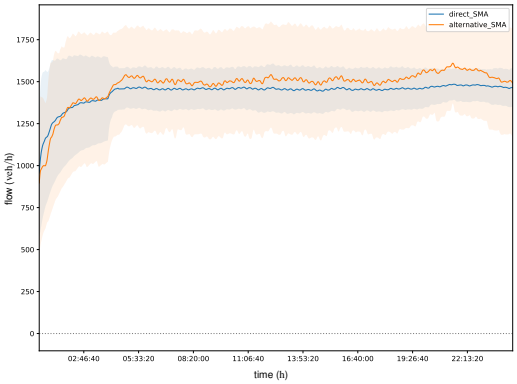


Fig. A.37-6. TrafficTraffic flow on each route, in vehicles per hour (veh/h), over a 24 h period, 4 h Simple Moving Average, mean (line) and standard deviation (shaded).

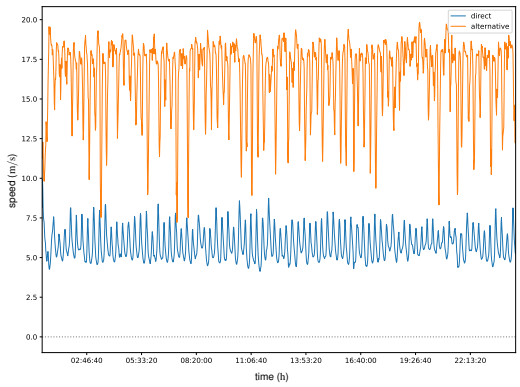


Fig. A.37-7. Mean speed on each route, in meters per second (m/s), aggregated to 1 min, over a 24 h period.

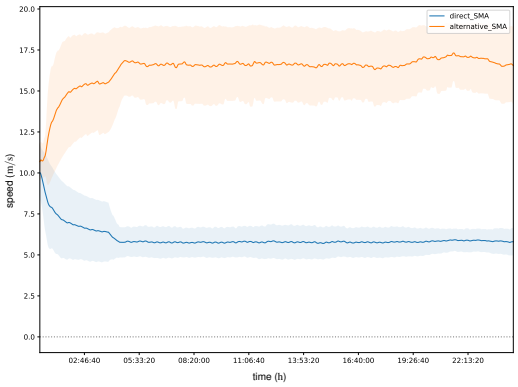


Fig. A.37-8. Mean speed on each route, in meters per second (m/s), aggregated to 1 min, over a 24 h period, 4 h Simple Moving Average, mean (line) and standard deviation (shaded).

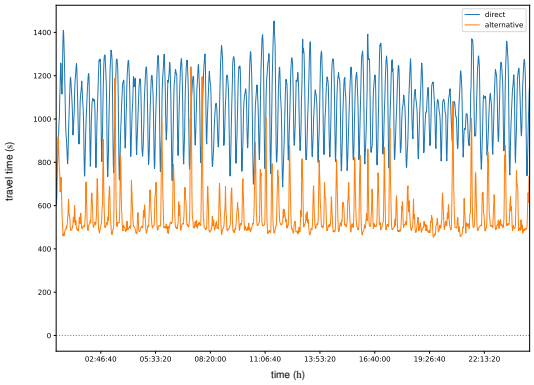


Fig. A.37-9. Travel times on each route, in seconds (s), aggregated to 1 min, over a 24 h period.

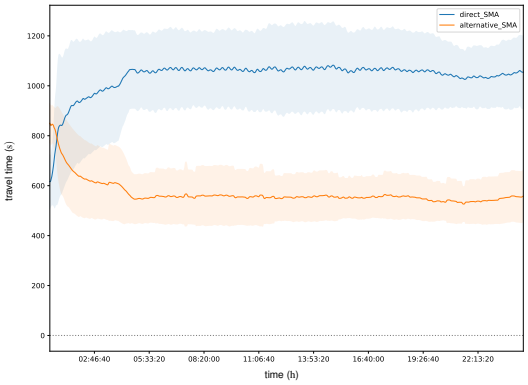


Fig. A.37-10. Travel times on each route, in seconds (s), aggregated to 1 min, over a 24 h period, 4 h Simple Moving Average, mean (line) and standard deviation (shaded).

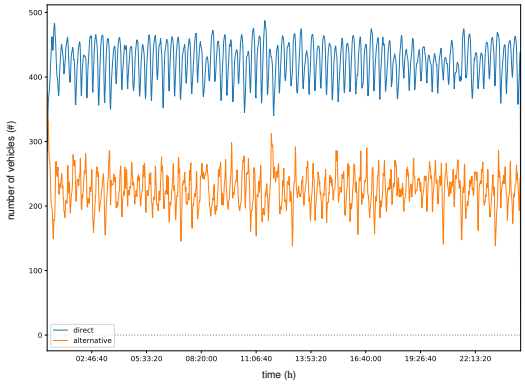


Fig. A.37-11. Average number of vehicles on each route, aggregated to 1 min, over a 24 h period.

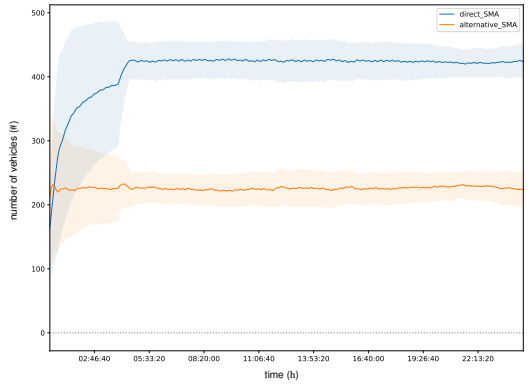


Fig. A.37-12. Average number of vehicles on each route, aggregated to 1 min, over a 24 h period, 4 h Simple Moving Average, mean (line) and standard deviation (shaded).

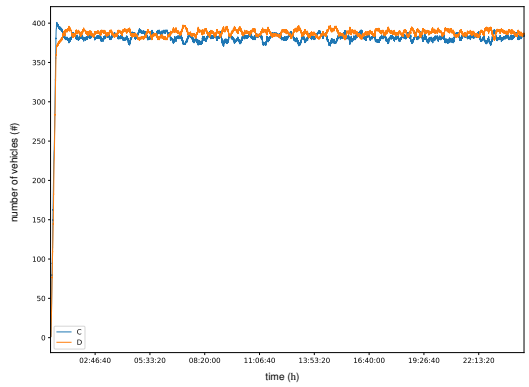


Fig. A.37-13. Evolution of the number of *Cooperators* and *Defectors* over a 24 h period.

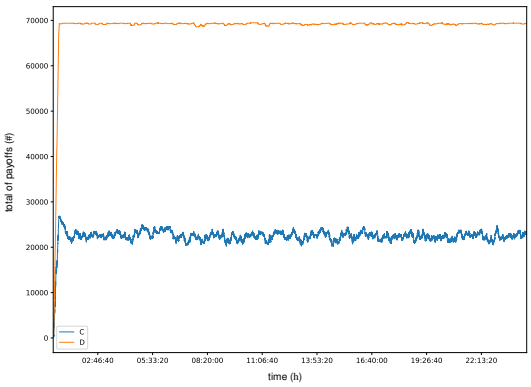


Fig. A.37-14. Evolution of total payoffs for *Cooperators* and *Defectors* (*individual payoff* times the *number of players receiving it*, $C(n) \times n$ and $D(n) \times (N-n)$, where n is the number of *Cooperators*), over a 24 h period.

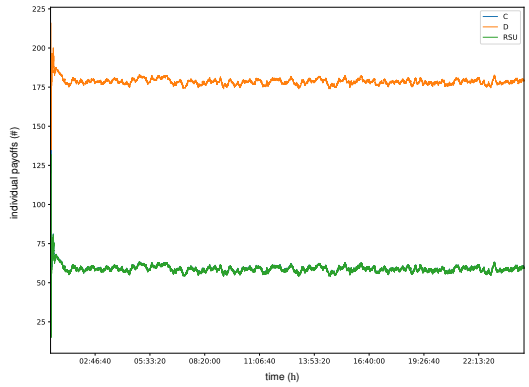


Fig. A.37-15. Evolution of the individual payoffs for *Cooperators, Defectors,* and *RSU* (always cooperating), over a 24 h period.

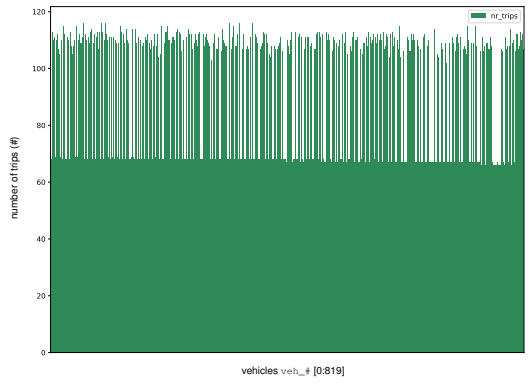


Fig. A.37-16. Number of trips made by each vehicle, during the simulation of a 24 h period.

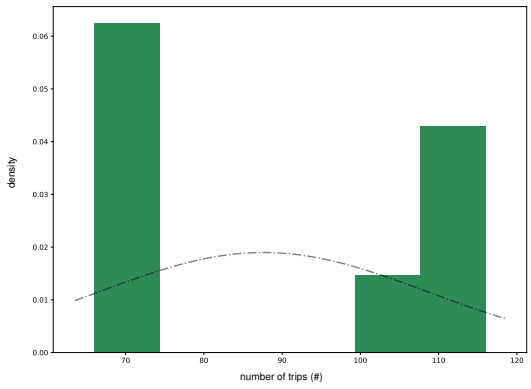


Fig. A.37-17. Density histogram of the number of trips made by each vehicle, during the simulation of a 24 h period, superimposing the normal density curve. The number of bins was calculated by the Freedman Diaconis rule.

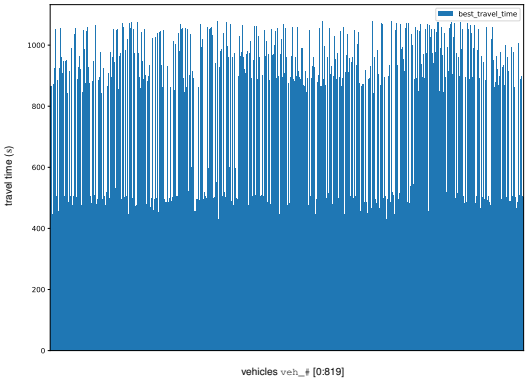


Fig. A.37-18. Best travel time for each vehicle, in seconds (s), during the simulation of a 24 h period.

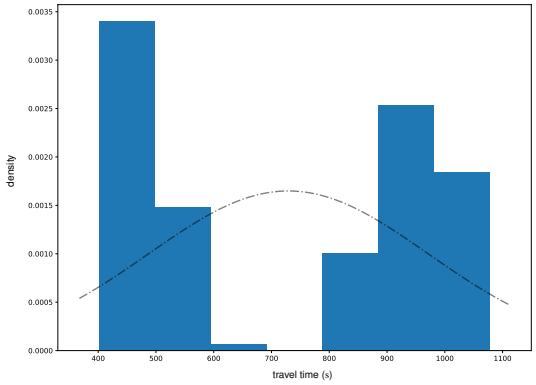


Fig. A.37-19. Density histogram of best travel time for vehicles, in seconds (s), during the simulation of a 24 h period, superimposing the normal density curve. The number of bins was calculated by the Freedman Diaconis rule.

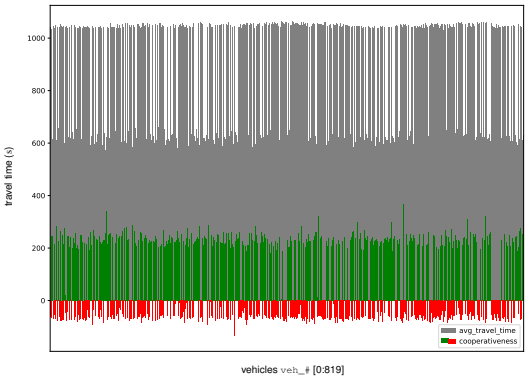


Fig. A.37-20. Average of the travel times, in seconds (s), of individual vehicles, during the simulation of a 24 h period. The bottom graph represents the *degree of cooperativeness**, downscaled by a normalization factor for the purpose of comparison with average times.

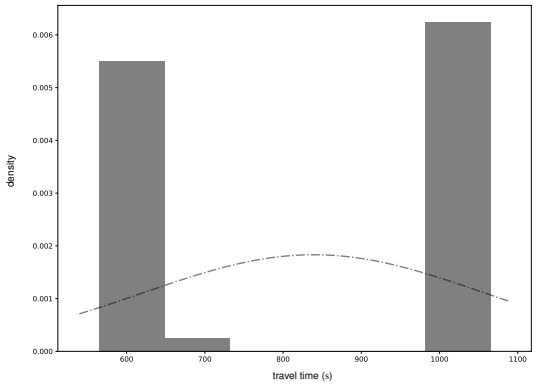


Fig. A.37-21. Density histogram of the average travel times, in seconds (s), of individual vehicles, during the simulation of a 24 h period, superimposing the normal density curve. The number of bins was calculated by the Freedman Diaconis rule.

* The *degree of cooperativeness* is a cumulative sum, calculated at each iteration, based on the complement of the ratio of cooperators, i.e., the higher the number of cooperators the less it increases, but the defectors are more penalized, and vice-versa. It varies inversely with the size of the group to which the player belongs.

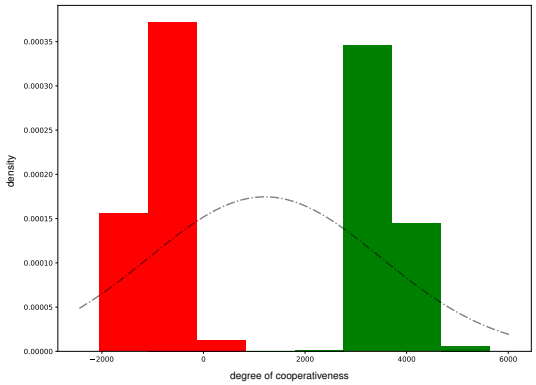


Fig. A.37-22. Density histogram of the *degree of cooperativeness** of individual vehicles, superimposing the normal density curve. The number of bins was calculated by the Freedman Diaconis rule. Generally, when strongly correlated with travel times, it presents a symmetric curve with respect to the *yy*-axis.

A.38 820veh-24h-16060001

```
Scenario: scenario-1
Timestamp: 20210607T212612Z
Number of vehicles: 820 vehs
Simulation time: 24.0 h
Warm up end time: 1866.6 s; step 18665
Vehicle selection strategy: stochastic
RSU turned off: False
RSU strategy: pigous_example
Runner options:
   nogui: True
   step_length: 0.1
   seed: 19750808
   output_prefix: 820veh-24h-16060001
   sim_run_time: 24.0
   num_vehicles: 820
   warmup_speed: 13.96
   warmup_routes_weight: [473, 527]
   network_speed: 25.0
   change_behavior_probability: [100, 0]
   cooperation_probability: [50, 50]
   vehicle_selection_strategy: stochastic
   turn_rsu_off: False
   rsu_dynamic_dissemination: False
   rsu_dissemination_interval: 5
   rsu_probabilistic_dissemination: False
   rsu_suggestion_strategy: pigous_example
   rsu_routes_weight: [460, 540]
   rsu_moving_avg_size: 5
   travel_times_ttl: 60
   rsu_dissemination_ttl: 0
   rsu_send_travel_time_info: False
   payoff_matrix: [360.0, 240.0, 0.0, -120.0]
   roth_erev_parameters: [0.1, 0.15]
Network Mean speed after warmup:
   Max: 10.19
   Min: 3.89
```

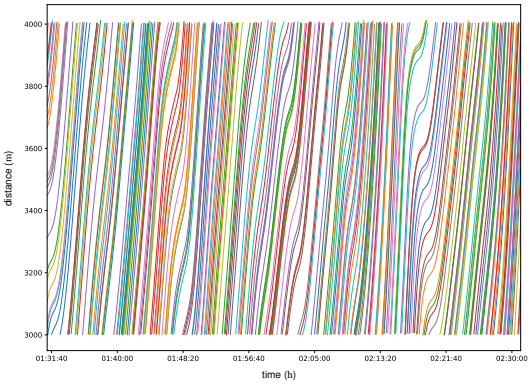


Fig. A.38-1. Time-Space diagram, for the one hour period after the end of the warmup, from 1:00:00 to 2:00:00 simulation time, plotted for the data from the sensor placed in the middle of the *direct* route (between 3000 m and 4000 m). In the case of an overloaded network, congestion shock waves can be observed.

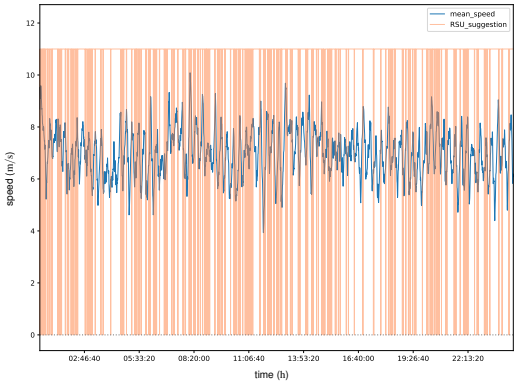


Fig. A.38-2. Mean speed in the network, in meters per second (m/s), over a 24 h period, superimposing (vertically, in orange) the time instants in which the RSU issued a recommendation to follow the *alternative* route.

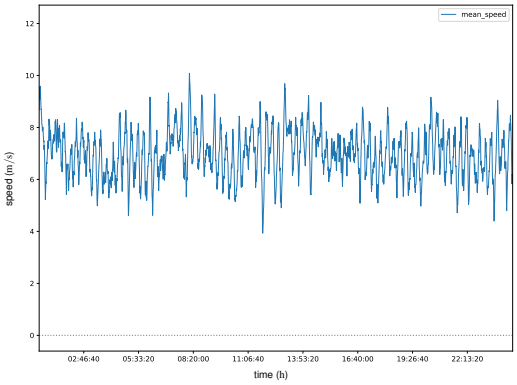


Fig. A.38-3. Mean speed in the network, in meters per second (m/s), over a 24 h period.

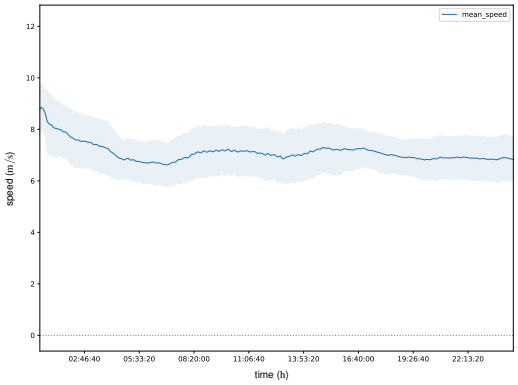


Fig. A.38-4. Mean speed in the network, in meters per second (m/s), over a 24 h period, 4 h Simple Moving Average, mean (line) and standard deviation (shaded).

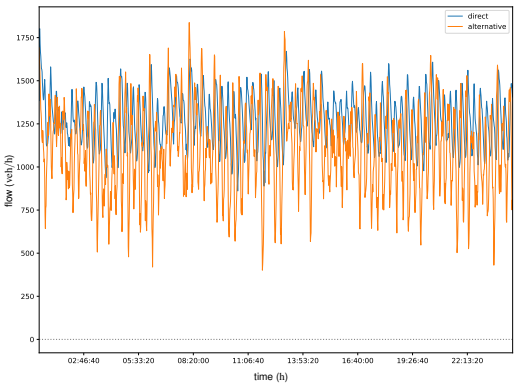


Fig. A.38-5. Traffic flow on each route, in vehicles per hour (veh/h), over a 24 h period.

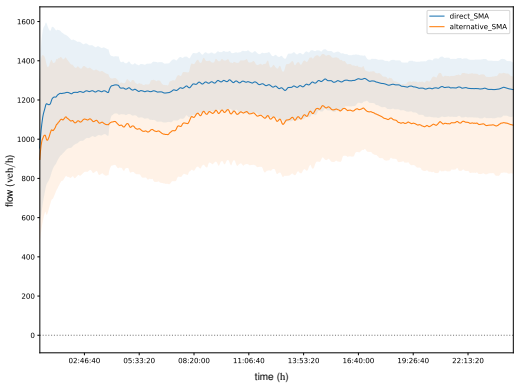


Fig. A.38-6. TrafficTraffic flow on each route, in vehicles per hour (veh/h), over a 24 h period, 4 h Simple Moving Average, mean (line) and standard deviation (shaded).

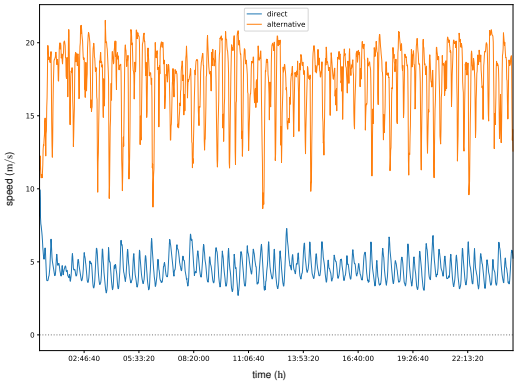


Fig. A.38-7. Mean speed on each route, in meters per second (m/s), aggregated to 1 min, over a 24 h period.

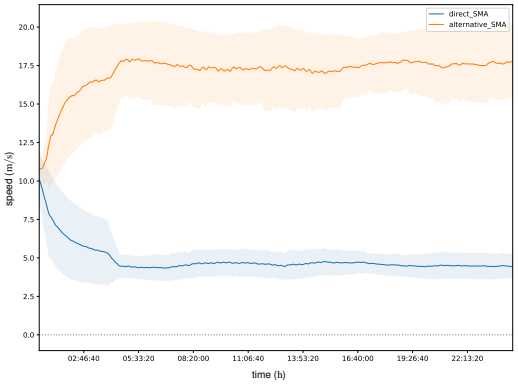


Fig. A.38-8. Mean speed on each route, in meters per second (m/s), aggregated to 1 min, over a 24 h period, 4 h Simple Moving Average, mean (line) and standard deviation (shaded).

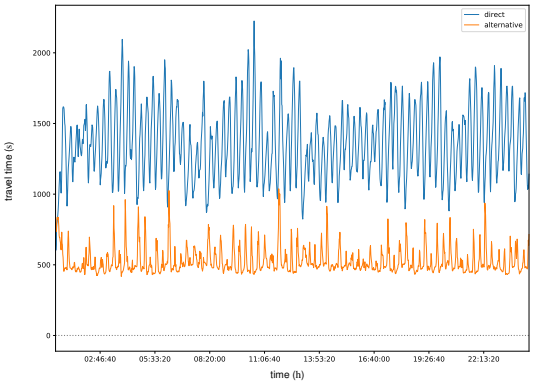


Fig. A.38-9. Travel times on each route, in seconds (s), aggregated to 1 min, over a 24 h period.

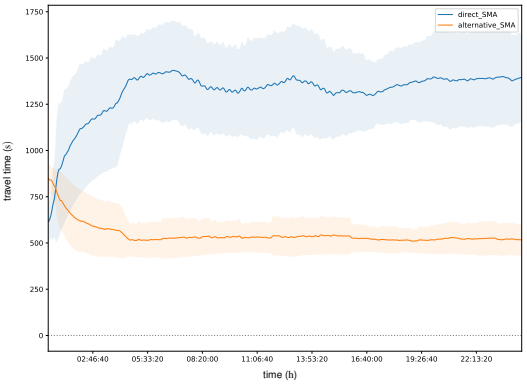


Fig. A.38-10. Travel times on each route, in seconds (s), aggregated to 1 min, over a 24 h period, 4 h Simple Moving Average, mean (line) and standard deviation (shaded).

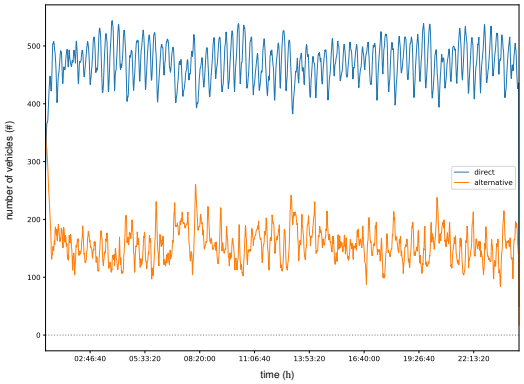


Fig. A.38-11. Average number of vehicles on each route, aggregated to 1 min, over a 24 h period.

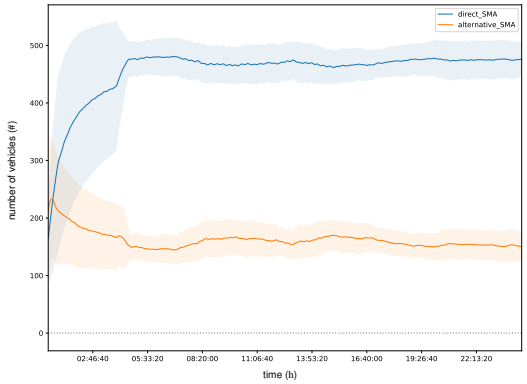


Fig. A.38-12. Average number of vehicles on each route, aggregated to 1 min, over a 24 h period, 4 h Simple Moving Average, mean (line) and standard deviation (shaded).

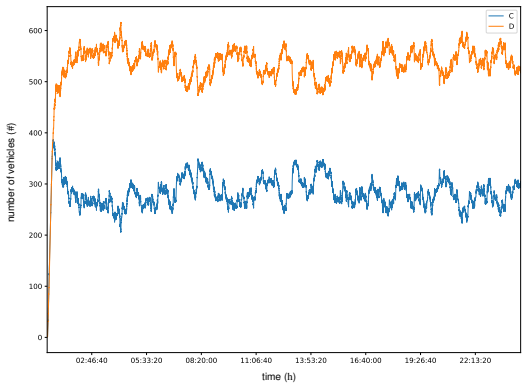


Fig. A.38-13. Evolution of the number of *Cooperators* and *Defectors* over a 24 h period.

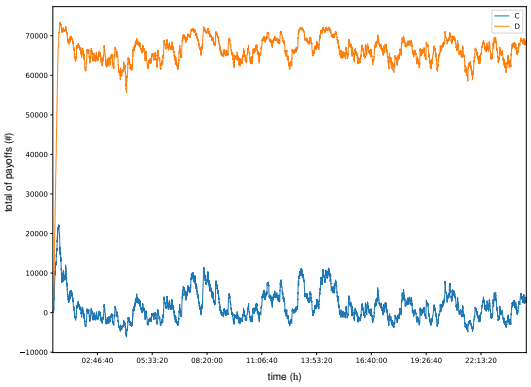


Fig. A.38-14. Evolution of total payoffs for *Cooperators* and *Defectors* (*individual payoff* times the *number of players receiving it*, $C(n) \times n$ and $D(n) \times (N-n)$, where n is the number of *Cooperators*), over a 24 h period.

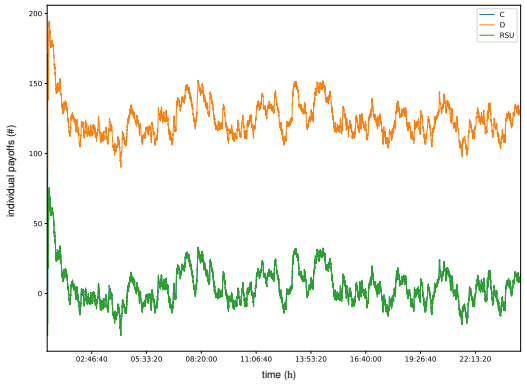


Fig. A.38-15. Evolution of the individual payoffs for *Cooperators, Defectors,* and *RSU* (always cooperating), over a 24 h period.

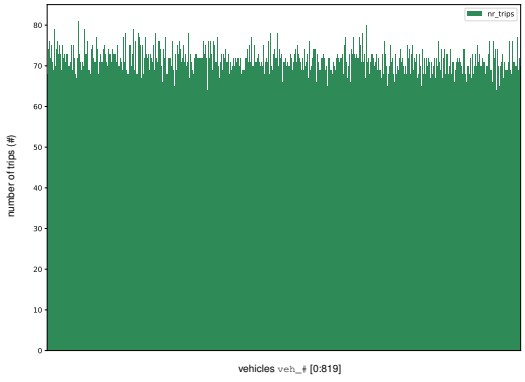


Fig. A.38-16. Number of trips made by each vehicle, during the simulation of a 24 h period.

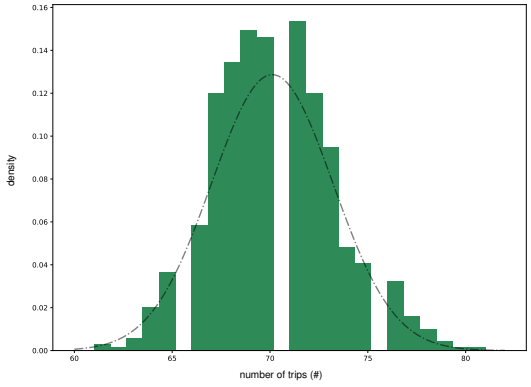


Fig. A.38-17. Density histogram of the number of trips made by each vehicle, during the simulation of a 24 h period, superimposing the normal density curve. The number of bins was calculated by the Freedman Diaconis rule.

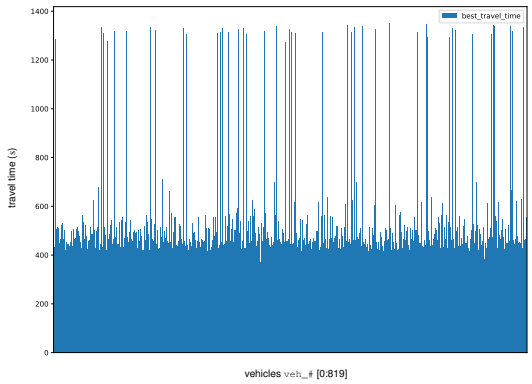


Fig. A.38-18. Best travel time for each vehicle, in seconds (s), during the simulation of a 24 h period.

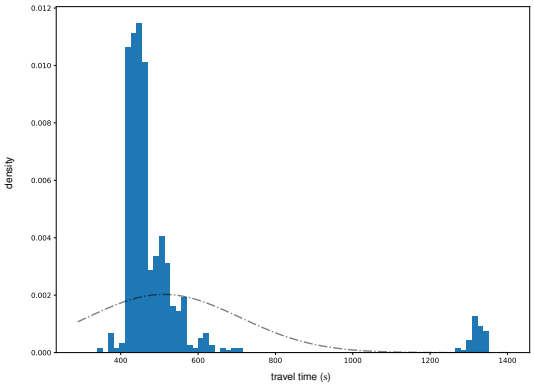


Fig. A.38-19. Density histogram of best travel time for vehicles, in seconds (s), during the simulation of a 24 h period, superimposing the normal density curve. The number of bins was calculated by the Freedman Diaconis rule.

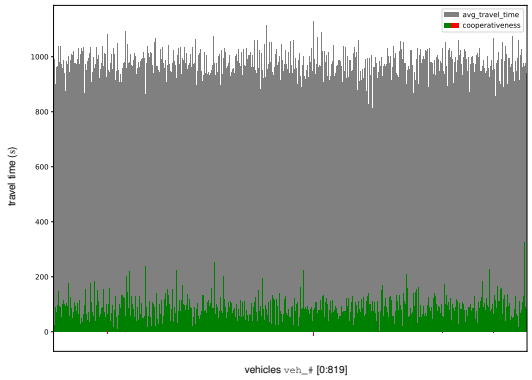


Fig. A.38-20. Average of the travel times, in seconds (s), of individual vehicles, during the simulation of a 24 h period. The bottom graph represents the *degree of cooperativeness**, downscaled by a normalization factor for the purpose of comparison with average times.

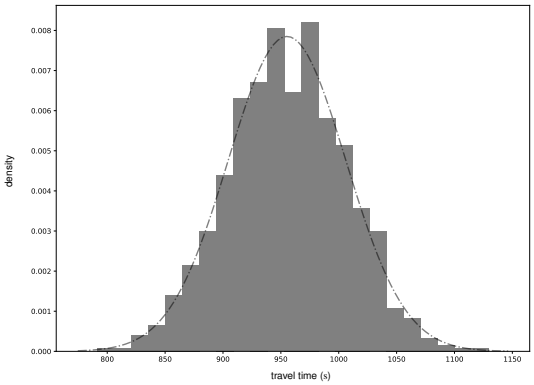


Fig. A.38-21. Density histogram of the average travel times, in seconds (s), of individual vehicles, during the simulation of a 24 h period, superimposing the normal density curve. The number of bins was calculated by the Freedman Diaconis rule.

* The *degree of cooperativeness* is a cumulative sum, calculated at each iteration, based on the complement of the ratio of cooperators, i.e., the higher the number of cooperators the less it increases, but the defectors are more penalized, and vice-versa. It varies inversely with the size of the group to which the player belongs.

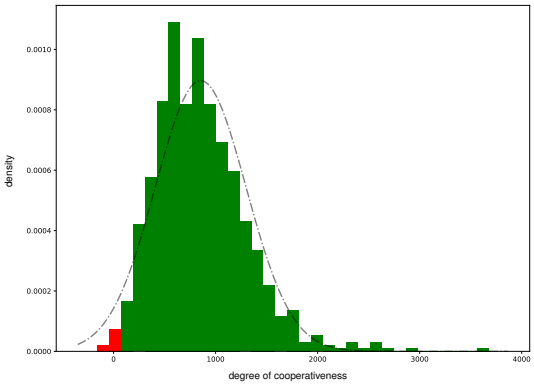


Fig. A.38-22. Density histogram of the *degree of cooperativeness** of individual vehicles, superimposing the normal density curve. The number of bins was calculated by the Freedman Diaconis rule. Generally, when strongly correlated with travel times, it presents a symmetric curve with respect to the *yy*-axis.

A.39 820veh-24h-19000001

```
Scenario: scenario-1
Timestamp: 20210617T133941Z
Number of vehicles: 820 vehs
Simulation time: 24.0 h
Warm up end time: 1866.6 s; step 18665
Vehicle selection strategy: best_travel_time
RSU turned off: False
RSU strategy: pigous_example_cooperation_weighted
Runner options:
   nogui: True
   step_length: 0.1
   seed: 19750808
   output_prefix: 820veh-24h-19000001
   sim_run_time: 24.0
   num_vehicles: 820
   warmup_speed: 13.96
   warmup_routes_weight: [473, 527]
   network_speed: 25.0
   change_behavior_probability: [100, 0]
   cooperation_probability: [50, 50]
   vehicle_selection_strategy: best_travel_time
   turn_rsu_off: False
   rsu_dynamic_dissemination: False
   rsu_dissemination_interval: 5
   rsu_probabilistic_dissemination: False
   rsu_suggestion_strategy: pigous_example_cooperation_weighted
   rsu_routes_weight: [460, 540]
   rsu_moving_avg_size: 5
   travel_times_ttl: 60
   rsu_dissemination_ttl: 0
   rsu_send_travel_time_info: False
   payoff_matrix: [360.0, 240.0, 0.0, -120.0]
   roth_erev_parameters: [0.1, 0.15]
   rsu_change_dissemination: False
   rsu_change_dissemination_steps: [14400, 28800, 43200, 57600, 72000]
   rsu_change_dissemination_intervals: [10, 20, 40, 80, 160]
Network Mean speed after warmup:
   Max: 11.74
   Min: 6.84
```

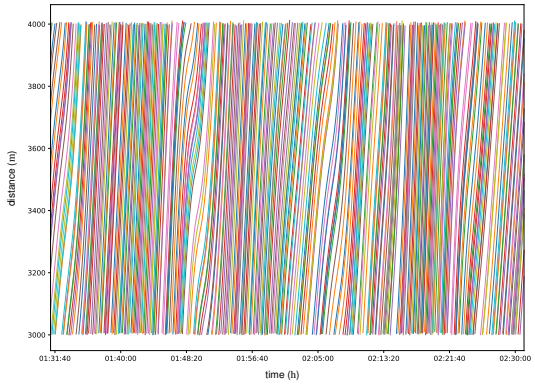


Fig. A.39-1. Time-Space diagram, for the one hour period after the end of the warmup, from 1:00:00 to 2:00:00 simulation time, plotted for the data from the sensor placed in the middle of the *direct* route (between 3000 m and 4000 m). In the case of an overloaded network, congestion shock waves can be observed.

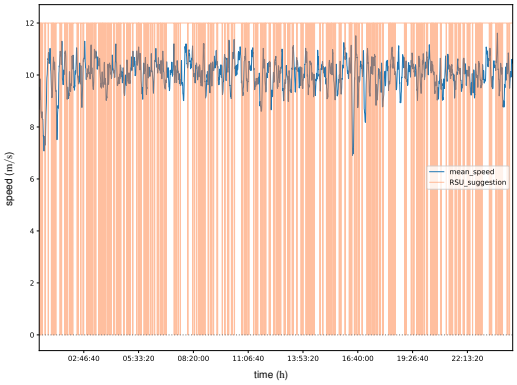


Fig. A.39-2. Mean speed in the network, in meters per second (m/s), over a 24 h period, superimposing (vertically, in orange) the time instants in which the RSU issued a recommendation to follow the *alternative* route.

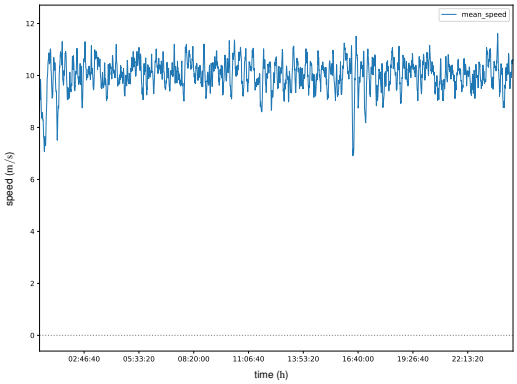


Fig. A.39-3. Mean speed in the network, in meters per second (m/s), over a 24 h period.

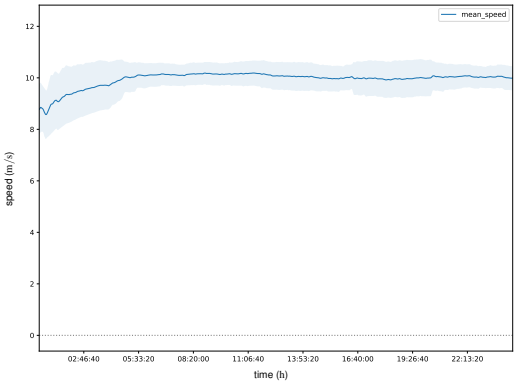


Fig. A.39-4. Mean speed in the network, in meters per second (m/s), over a 24 h period, 4 h Simple Moving Average, mean (line) and standard deviation (shaded).

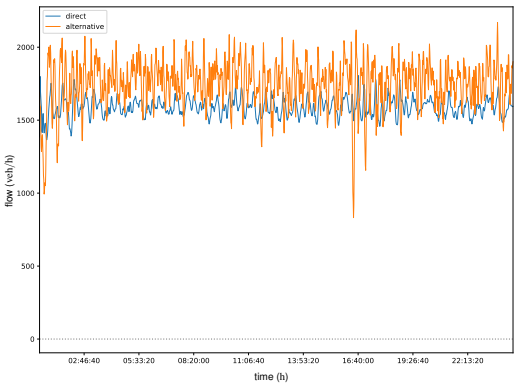


Fig. A.39-5. Traffic flow on each route, in vehicles per hour (veh/h), over a 24 h period.

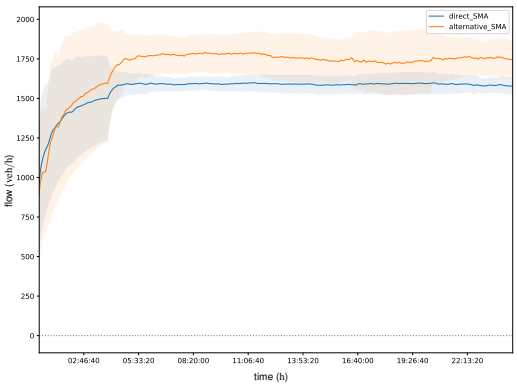


Fig. A.39-6. TrafficTraffic flow on each route, in vehicles per hour (veh/h), over a 24 h period, 4 h Simple Moving Average, mean (line) and standard deviation (shaded).

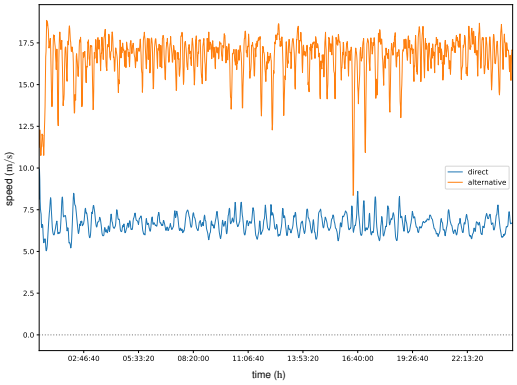


Fig. A.39-7. Mean speed on each route, in meters per second (m/s), aggregated to 1 min, over a 24 h period.

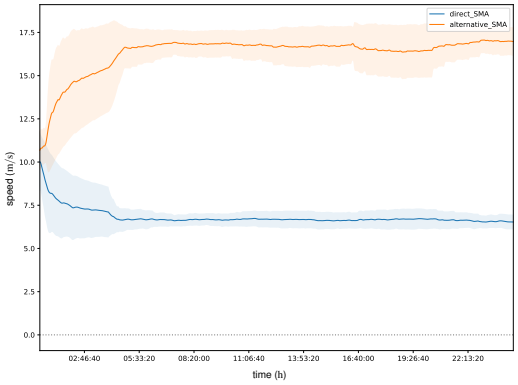


Fig. A.39-8. Mean speed on each route, in meters per second (m/s), aggregated to 1 min, over a 24 h period, 4 h Simple Moving Average, mean (line) and standard deviation (shaded).

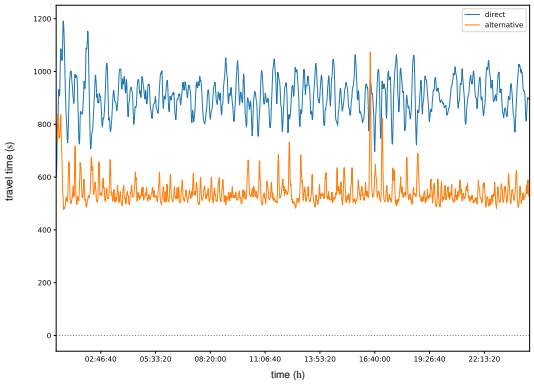


Fig. A.39-9. Travel times on each route, in seconds (s), aggregated to 1 min, over a 24 h period.

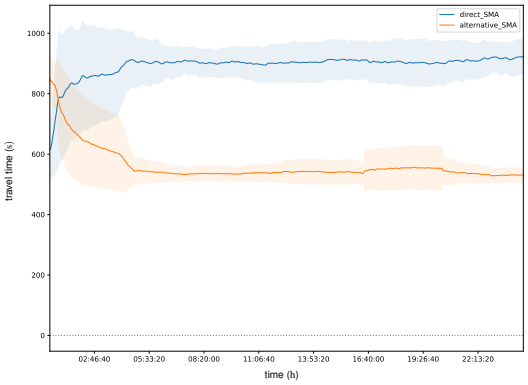


Fig. A.39-10. Travel times on each route, in seconds (s), aggregated to 1 min, over a 24 h period, 4 h Simple Moving Average, mean (line) and standard deviation (shaded).

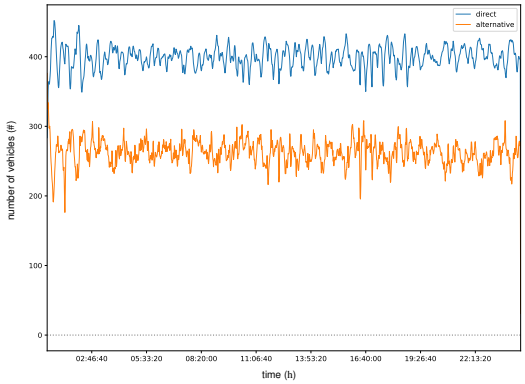


Fig. A.39-11. Average number of vehicles on each route, aggregated to 1 min, over a 24 h period.

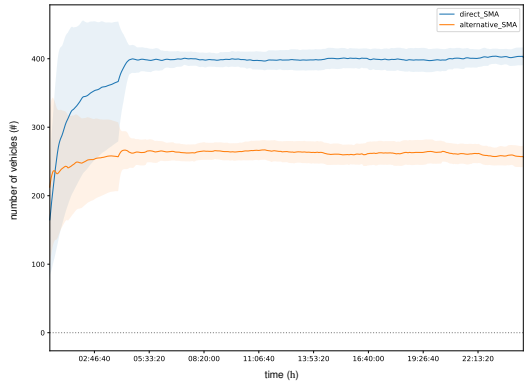


Fig. A.39-12. Average number of vehicles on each route, aggregated to 1 min, over a 24 h period, 4 h Simple Moving Average, mean (line) and standard deviation (shaded).

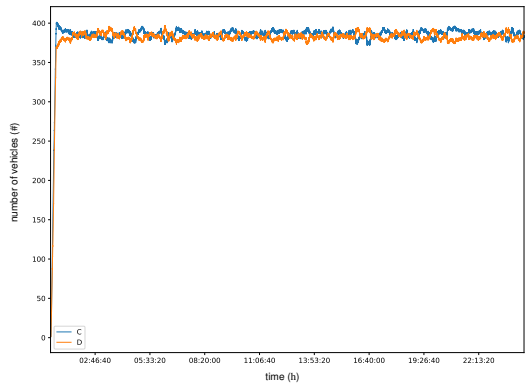


Fig. A.39-13. Evolution of the number of *Cooperators* and *Defectors* over a 24 h period.

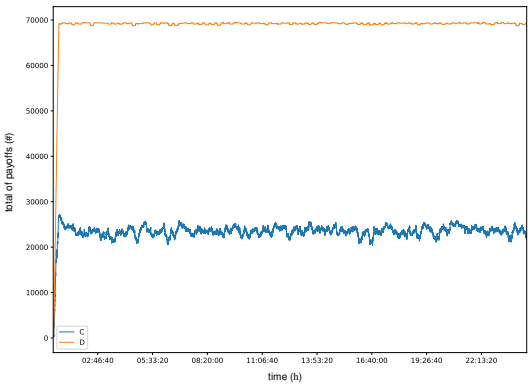


Fig. A.39-14. Evolution of total payoffs for *Cooperators* and *Defectors* (*individual payoff* times the *number of players receiving it*, $C(n) \times n$ and $D(n) \times (N-n)$, where n is the number of *Cooperators*), over a 24 h period.

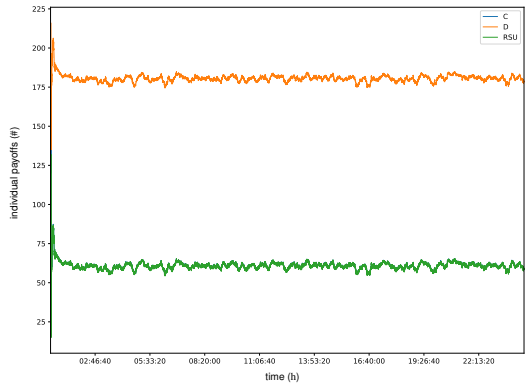


Fig. A.39-15. Evolution of the individual payoffs for *Cooperators, Defectors,* and *RSU* (always cooperating), over a 24 h period.

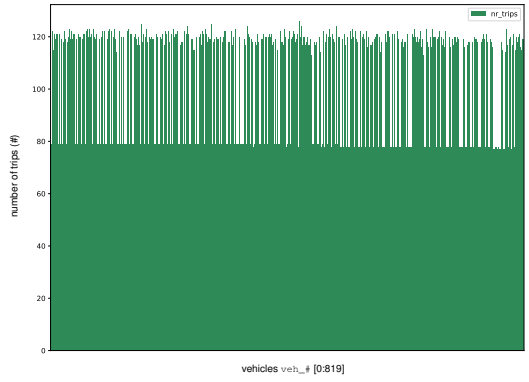


Fig. A.39-16. Number of trips made by each vehicle, during the simulation of a 24 h period.

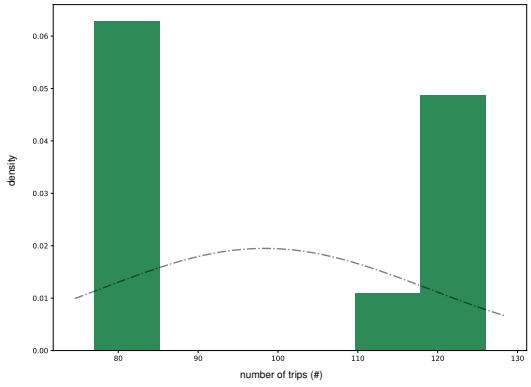


Fig. A.39-17. Density histogram of the number of trips made by each vehicle, during the simulation of a 24 h period, superimposing the normal density curve. The number of bins was calculated by the Freedman Diaconis rule.

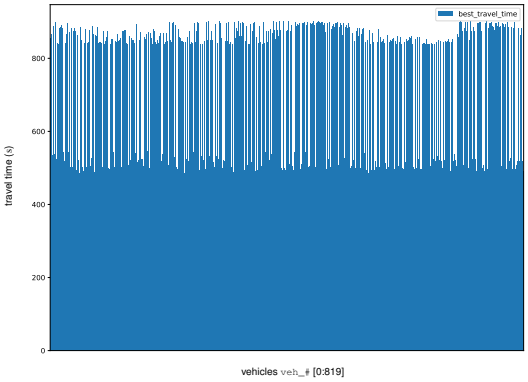


Fig. A.39-18. Best travel time for each vehicle, in seconds (s), during the simulation of a 24 h period.

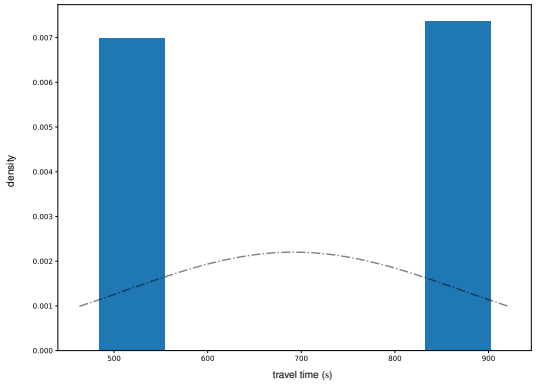


Fig. A.39-19. Density histogram of best travel time for vehicles, in seconds (s), during the simulation of a 24 h period, superimposing the normal density curve. The number of bins was calculated by the Freedman Diaconis rule.

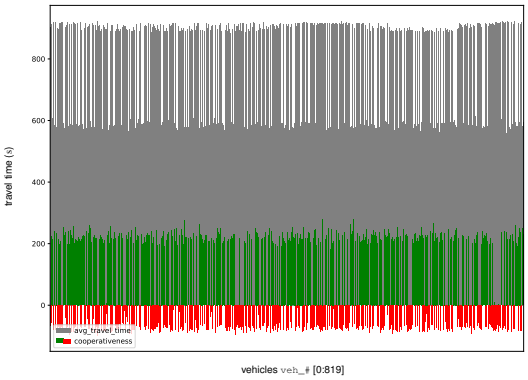


Fig. A.39-20. Average of the travel times, in seconds (s), of individual vehicles, during the simulation of a 24 h period. The bottom graph represents the *degree of cooperativeness**, downscaled by a normalization factor for the purpose of comparison with average times.

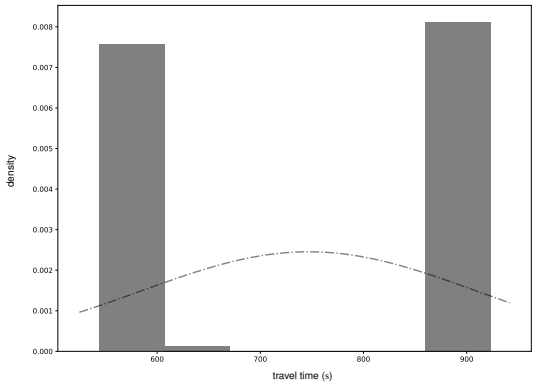


Fig. A.39-21. Density histogram of the average travel times, in seconds (s), of individual vehicles, during the simulation of a 24 h period, superimposing the normal density curve. The number of bins was calculated by the Freedman Diaconis rule.

* The *degree of cooperativeness* is a cumulative sum, calculated at each iteration, based on the complement of the ratio of cooperators, i.e., the higher the number of cooperators the less it increases, but the defectors are more penalized, and vice-versa. It varies inversely with the size of the group to which the player belongs.

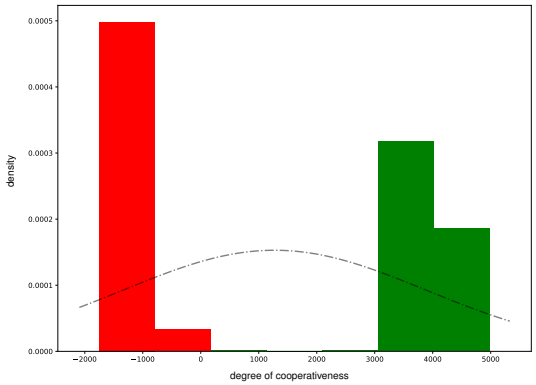


Fig. A.39-22. Density histogram of the *degree of cooperativeness** of individual vehicles, superimposing the normal density curve. The number of bins was calculated by the Freedman Diaconis rule. Generally, when strongly correlated with travel times, it presents a symmetric curve with respect to the *yy*-axis.

A.40 820veh-24h-19010001

```
Scenario: scenario-1
Timestamp: 20210617T161132Z
Number of vehicles: 820 vehs
Simulation time: 24.0 h
Warm up end time: 1866.6 s; step 18665
Vehicle selection strategy: best_payoff
RSU turned off: False
RSU strategy: pigous_example_cooperation_weighted
Runner options:
   nogui: True
   step_length: 0.1
   seed: 19750808
   output_prefix: 820veh-24h-19010001
   sim_run_time: 24.0
   num_vehicles: 820
   warmup_speed: 13.96
   warmup_routes_weight: [473, 527]
   network_speed: 25.0
   change_behavior_probability: [100, 0]
   cooperation_probability: [50, 50]
   vehicle_selection_strategy: best_payoff
   turn_rsu_off: False
   rsu_dynamic_dissemination: False
   rsu_dissemination_interval: 5
   rsu_probabilistic_dissemination: False
   rsu_suggestion_strategy: pigous_example_cooperation_weighted
   rsu_routes_weight: [460, 540]
   rsu_moving_avg_size: 5
   travel_times_ttl: 60
   rsu_dissemination_ttl: 0
   rsu_send_travel_time_info: False
   payoff_matrix: [360.0, 240.0, 0.0, -120.0]
   roth_erev_parameters: [0.1, 0.15]
   rsu_change_dissemination: False
   rsu_change_dissemination_steps: [14400, 28800, 43200, 57600, 72000]
   rsu_change_dissemination_intervals: [10, 20, 40, 80, 160]
Network Mean speed after warmup:
   Max: 9.88
   Min: 1.86
```

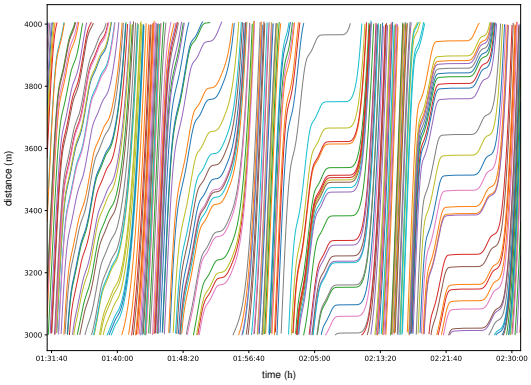


Fig. A.40-1. Time-Space diagram, for the one hour period after the end of the warmup, from 1:00:00 to 2:00:00 simulation time, plotted for the data from the sensor placed in the middle of the *direct* route (between 3000 m and 4000 m). In the case of an overloaded network, congestion shock waves can be observed.

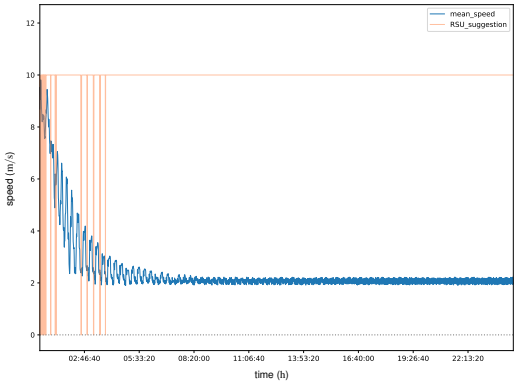


Fig. A.40-2. Mean speed in the network, in meters per second (m/s), over a 24 h period, superimposing (vertically, in orange) the time instants in which the RSU issued a recommendation to follow the *alternative* route.

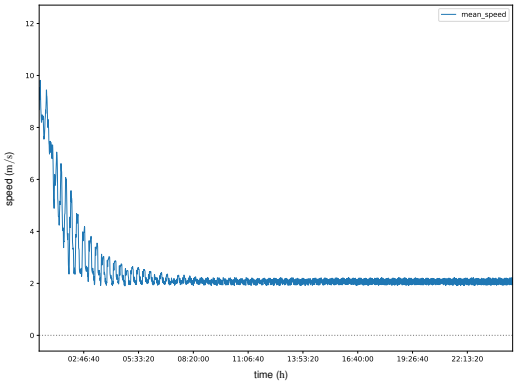


Fig. A.40-3. Mean speed in the network, in meters per second (m/s), over a 24 h period.

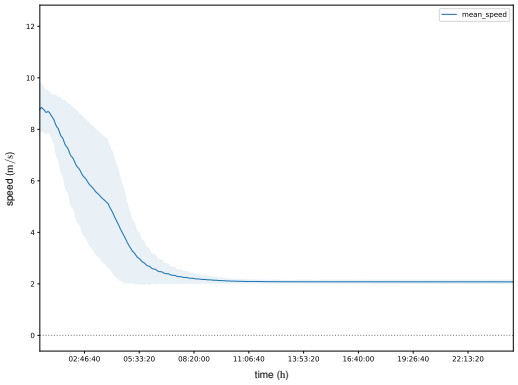


Fig. A.40-4. Mean speed in the network, in meters per second (m/s), over a 24 h period, 4 h Simple Moving Average, mean (line) and standard deviation (shaded).

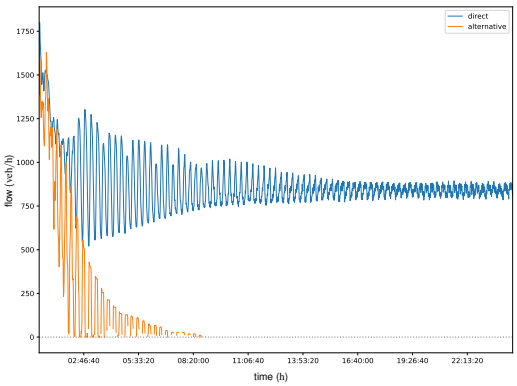


Fig. A.40-5. Traffic flow on each route, in vehicles per hour (veh/h), over a 24 h period.

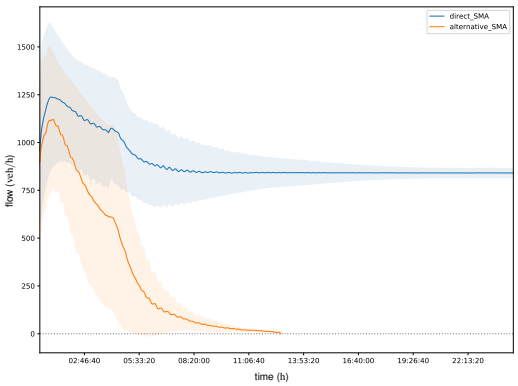


Fig. A.40-6. TrafficTraffic flow on each route, in vehicles per hour (veh/h), over a 24 h period, 4 h Simple Moving Average, mean (line) and standard deviation (shaded).

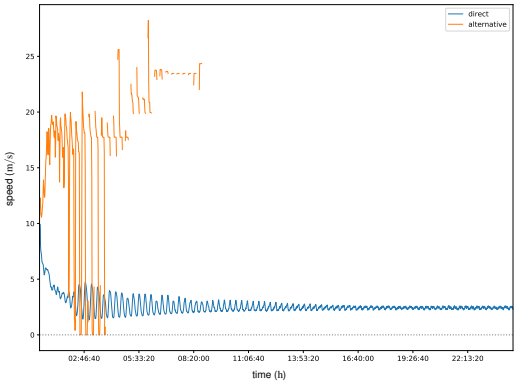


Fig. A.40-7. Mean speed on each route, in meters per second (m/s), aggregated to 1 min, over a 24 h period.

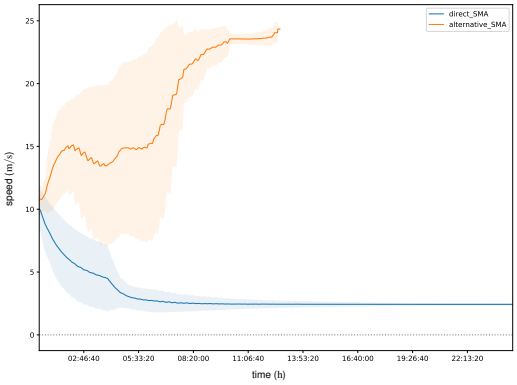


Fig. A.40-8. Mean speed on each route, in meters per second (m/s), aggregated to 1 min, over a 24 h period, 4 h Simple Moving Average, mean (line) and standard deviation (shaded).

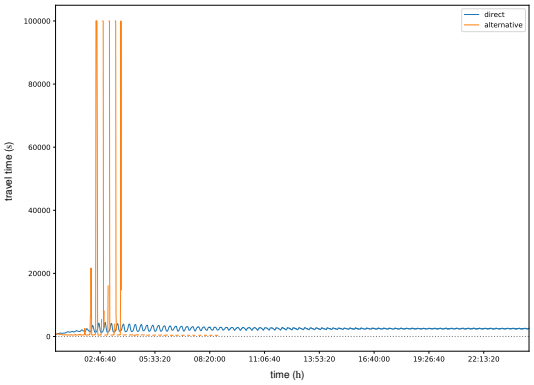


Fig. A.40-9. Travel times on each route, in seconds (s), aggregated to 1 min, over a 24 h period.

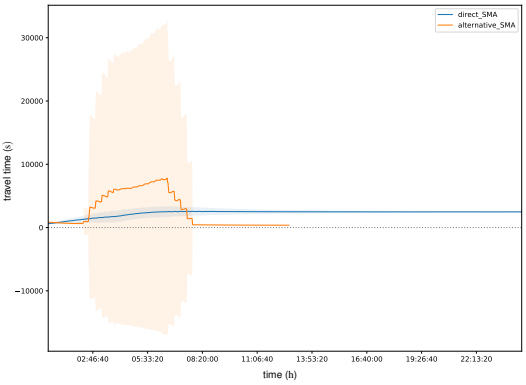


Fig. A.40-10. Travel times on each route, in seconds (s), aggregated to 1 min, over a 24 h period, 4 h Simple Moving Average, mean (line) and standard deviation (shaded).

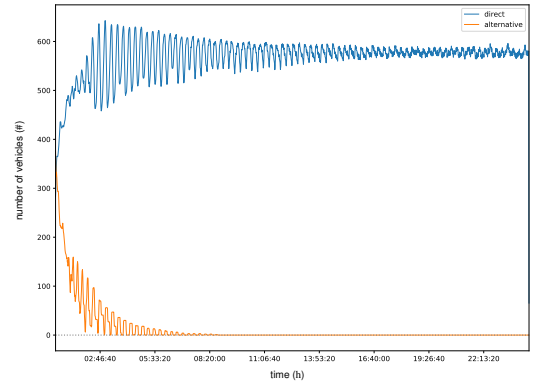


Fig. A.40-11. Average number of vehicles on each route, aggregated to 1 min, over a 24 h period.

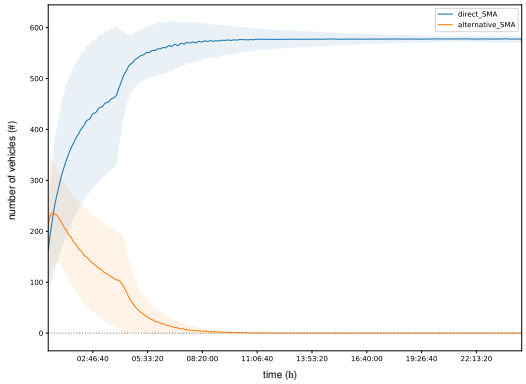


Fig. A.40-12. Average number of vehicles on each route, aggregated to 1 min, over a 24 h period, 4 h Simple Moving Average, mean (line) and standard deviation (shaded).

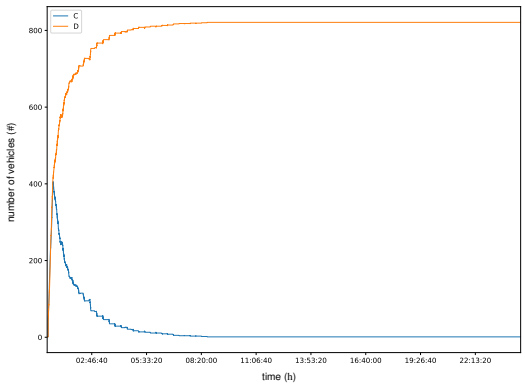


Fig. A.40-13. Evolution of the number of *Cooperators* and *Defectors* over a 24 h period.

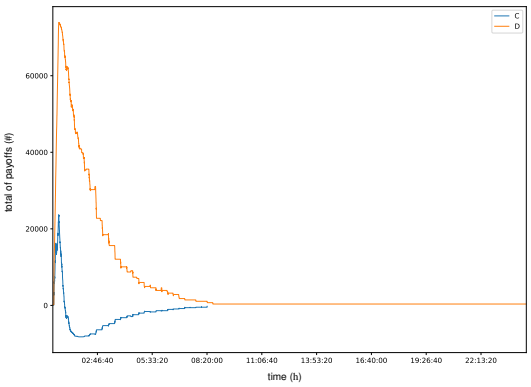


Fig. A.40-14. Evolution of total payoffs for *Cooperators* and *Defectors* (*individual payoff* times the *number of players receiving it*, $C(n) \times n$ and $D(n) \times (N-n)$, where n is the number of *Cooperators*), over a 24 h period.

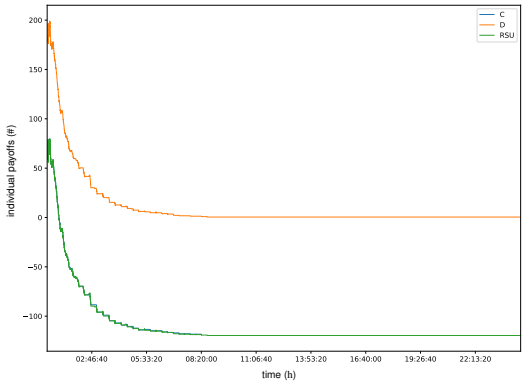


Fig. A.40-15. Evolution of the individual payoffs for *Cooperators, Defectors,* and *RSU* (always cooperating), over a 24 h period.

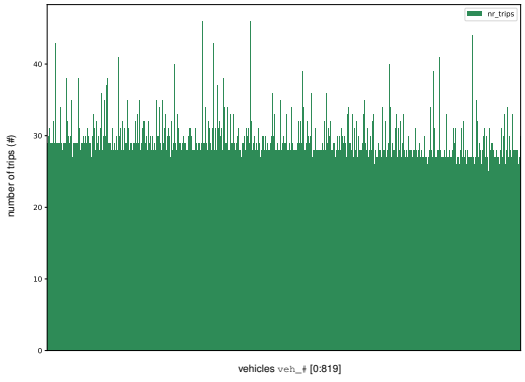


Fig. A.40-16. Number of trips made by each vehicle, during the simulation of a 24 h period.

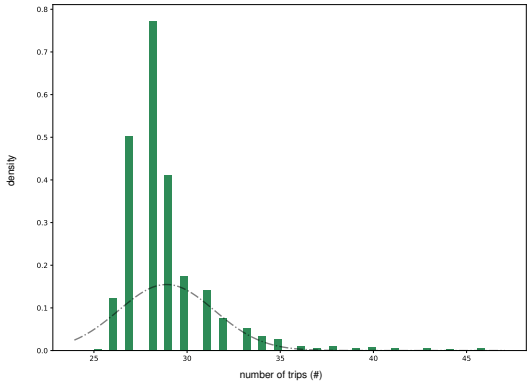


Fig. A.40-17. Density histogram of the number of trips made by each vehicle, during the simulation of a 24 h period, superimposing the normal density curve. The number of bins was calculated by the Freedman Diaconis rule.

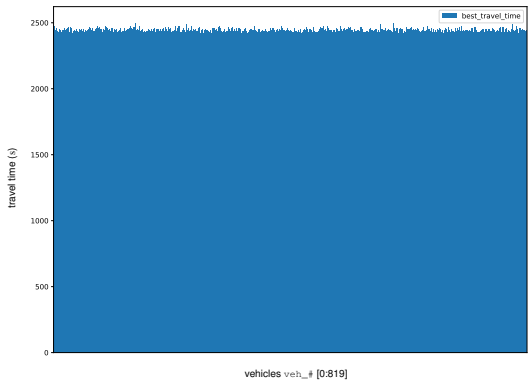


Fig. A.40-18. Best travel time for each vehicle, in seconds (s), during the simulation of a 24 h period.

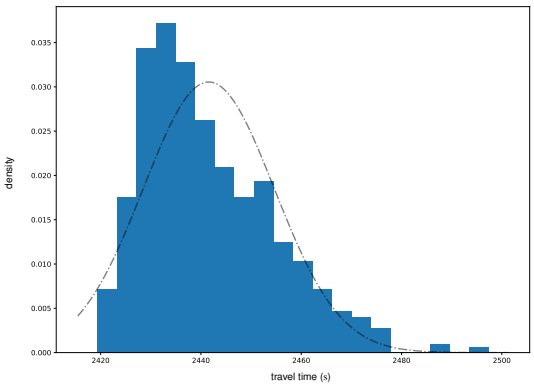


Fig. A.40-19. Density histogram of best travel time for vehicles, in seconds (s), during the simulation of a 24 h period, superimposing the normal density curve. The number of bins was calculated by the Freedman Diaconis rule.

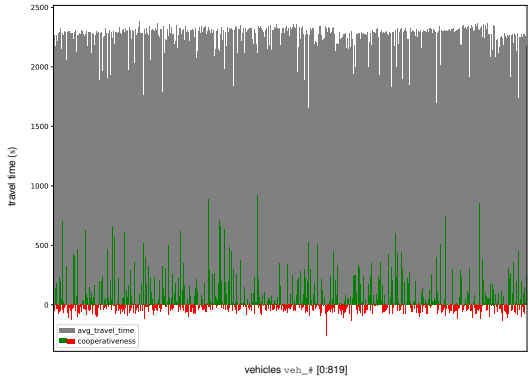


Fig. A.40-20. Average of the travel times, in seconds (s), of individual vehicles, during the simulation of a 24 h period. The bottom graph represents the *degree of cooperativeness**, downscaled by a normalization factor for the purpose of comparison with average times.

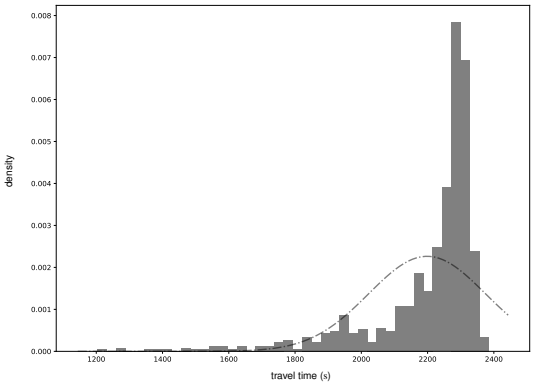


Fig. A.40-21. Density histogram of the average travel times, in seconds (s), of individual vehicles, during the simulation of a 24 h period, superimposing the normal density curve. The number of bins was calculated by the Freedman Diaconis rule.

* The *degree of cooperativeness* is a cumulative sum, calculated at each iteration, based on the complement of the ratio of cooperators, i.e., the higher the number of cooperators the less it increases, but the defectors are more penalized, and vice-versa. It varies inversely with the size of the group to which the player belongs.

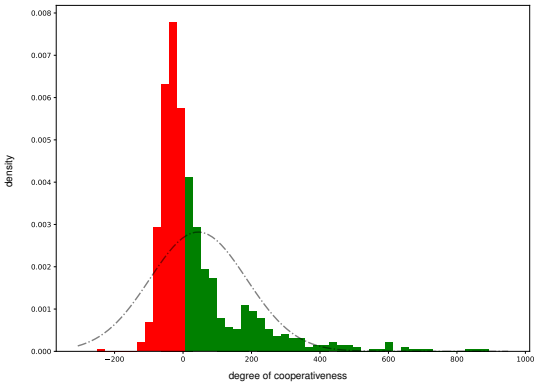


Fig. A.40-22. Density histogram of the *degree of cooperativeness** of individual vehicles, superimposing the normal density curve. The number of bins was calculated by the Freedman Diaconis rule. Generally, when strongly correlated with travel times, it presents a symmetric curve with respect to the *yy*-axis.

A.41 820veh-24h-19020001

```
Scenario: scenario-1
Timestamp: 20210617T160948Z
Number of vehicles: 820 vehs
Simulation time: 24.0 h
Warm up end time: 1866.6 s; step 18665
Vehicle selection strategy: best_payoff_utility
RSU turned off: False
RSU strategy: pigous_example_cooperation_weighted
Runner options:
   nogui: True
   step_length: 0.1
   seed: 19750808
   output_prefix: 820veh-24h-19020001
   sim_run_time: 24.0
   num_vehicles: 820
   warmup_speed: 13.96
   warmup_routes_weight: [473, 527]
   network_speed: 25.0
   change_behavior_probability: [100, 0]
   cooperation_probability: [50, 50]
   vehicle_selection_strategy: best_payoff_utility
   turn_rsu_off: False
   rsu_dynamic_dissemination: False
   rsu_dissemination_interval: 5
   rsu_probabilistic_dissemination: False
   rsu_suggestion_strategy: pigous_example_cooperation_weighted
   rsu_routes_weight: [460, 540]
   rsu_moving_avg_size: 5
   travel_times_ttl: 60
   rsu_dissemination_ttl: 0
   rsu_send_travel_time_info: False
   payoff_matrix: [360.0, 240.0, 0.0, -120.0]
   roth_erev_parameters: [0.1, 0.15]
   rsu_change_dissemination: False
   rsu_change_dissemination_steps: [14400, 28800, 43200, 57600, 72000]
   rsu_change_dissemination_intervals: [10, 20, 40, 80, 160]
Network Mean speed after warmup:
   Max: 9.88
   Min: 1.11
```

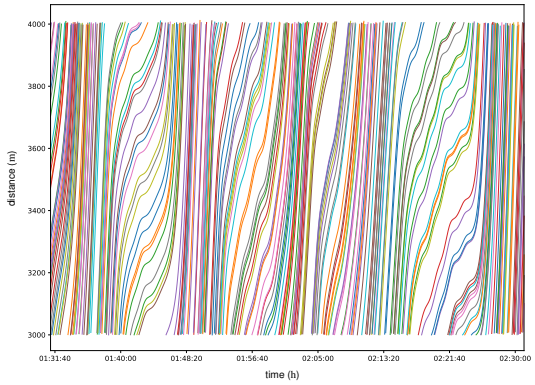


Fig. A.41-1. Time-Space diagram, for the one hour period after the end of the warmup, from 1:00:00 to 2:00:00 simulation time, plotted for the data from the sensor placed in the middle of the *direct* route (between 3000 m and 4000 m). In the case of an overloaded network, congestion shock waves can be observed.

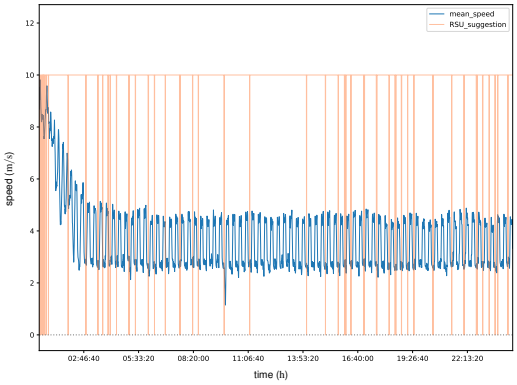


Fig. A.41-2. Mean speed in the network, in meters per second (m/s), over a 24 h period, superimposing (vertically, in orange) the time instants in which the RSU issued a recommendation to follow the *alternative* route.

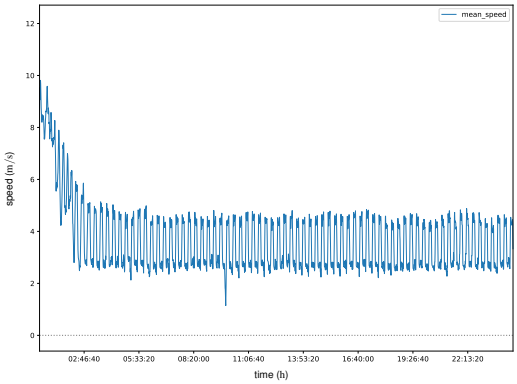


Fig. A.41-3. Mean speed in the network, in meters per second (m/s), over a 24 h period.

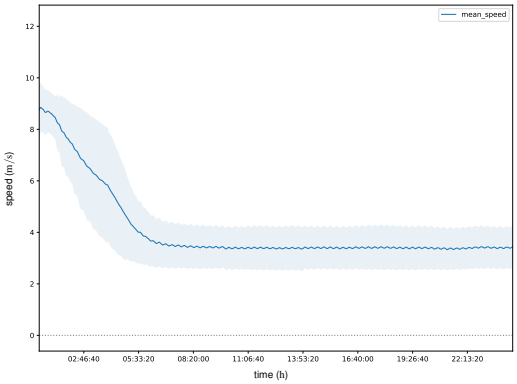


Fig. A.41-4. Mean speed in the network, in meters per second (m/s), over a 24 h period, 4 h Simple Moving Average, mean (line) and standard deviation (shaded).

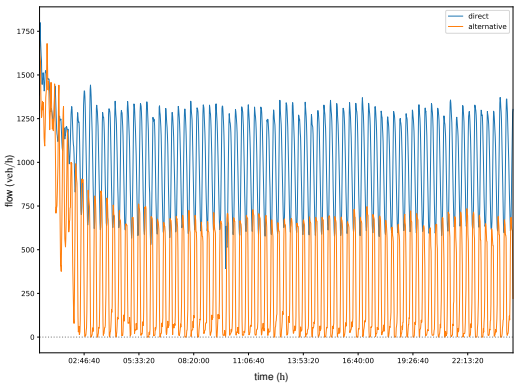


Fig. A.41-5. Traffic flow on each route, in vehicles per hour (veh/h), over a 24 h period.

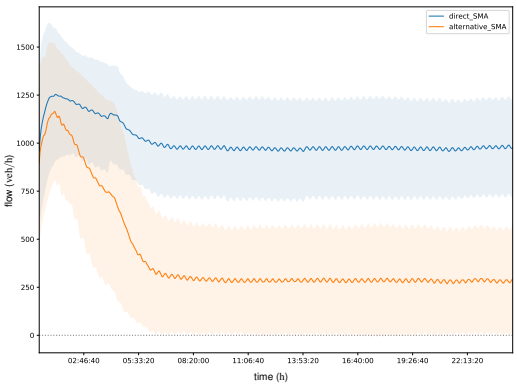


Fig. A.41-6. TrafficTraffic flow on each route, in vehicles per hour (veh/h), over a 24 h period, 4 h Simple Moving Average, mean (line) and standard deviation (shaded).

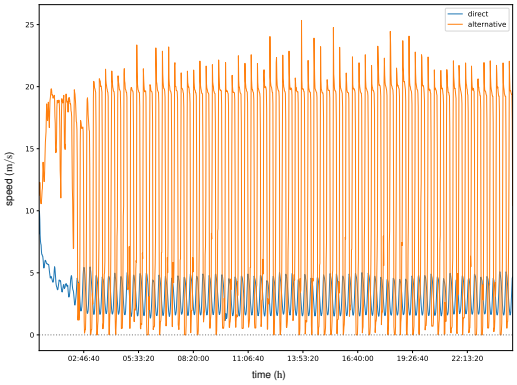


Fig. A.41-7. Mean speed on each route, in meters per second (m/s), aggregated to 1 min, over a 24 h period.

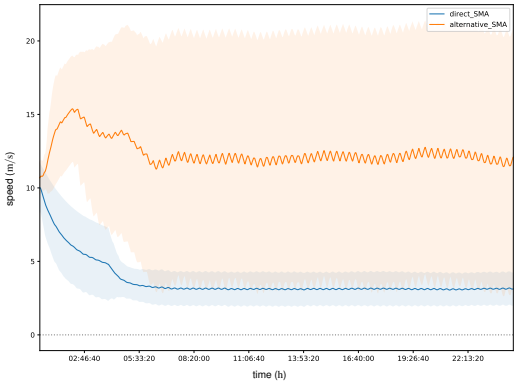


Fig. A.41-8. Mean speed on each route, in meters per second (m/s), aggregated to 1 min, over a 24 h period, 4 h Simple Moving Average, mean (line) and standard deviation (shaded).

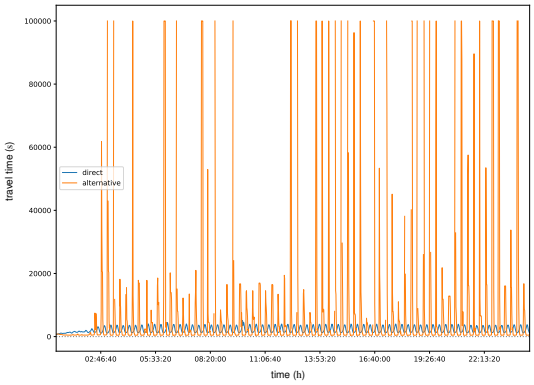


Fig. A.41-9. Travel times on each route, in seconds (s), aggregated to 1 min, over a 24 h period.

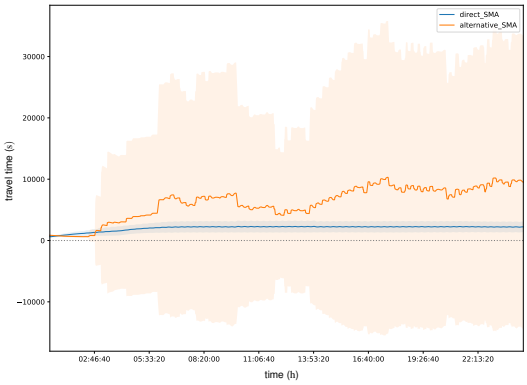


Fig. A.41-10. Travel times on each route, in seconds (s), aggregated to 1 min, over a 24 h period, 4 h Simple Moving Average, mean (line) and standard deviation (shaded).

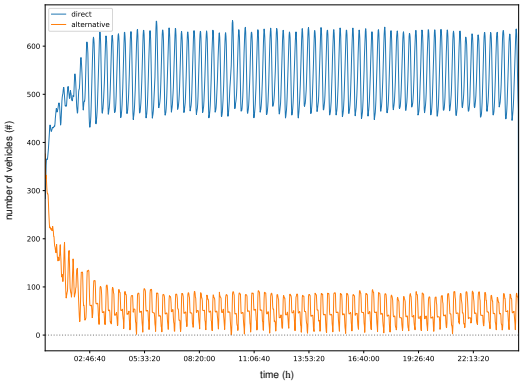


Fig. A.41-11. Average number of vehicles on each route, aggregated to 1 min, over a 24 h period.

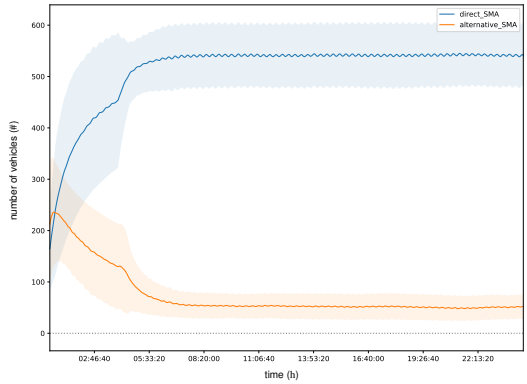


Fig. A.41-12. Average number of vehicles on each route, aggregated to 1 min, over a 24 h period, 4 h Simple Moving Average, mean (line) and standard deviation (shaded).

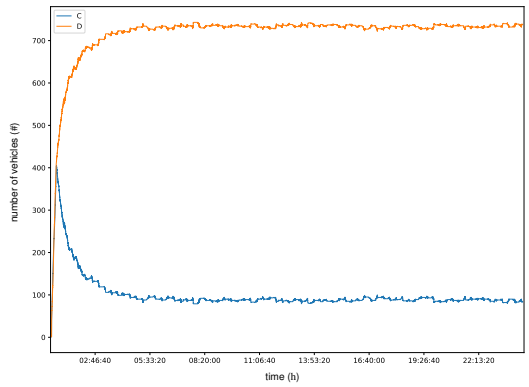


Fig. A.41-13. Evolution of the number of *Cooperators* and *Defectors* over a 24 h period.

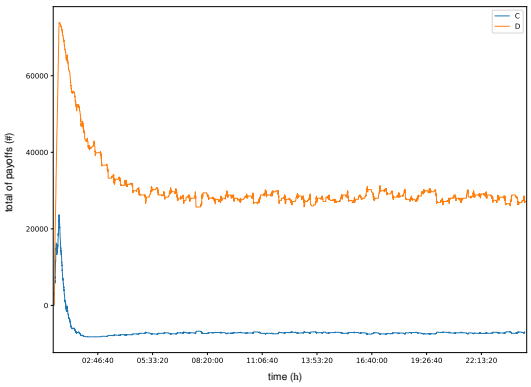


Fig. A.41-14. Evolution of total payoffs for *Cooperators* and *Defectors* (*individual payoff* times the *number of players receiving it*, $C(n) \times n$ and $D(n) \times (N-n)$, where n is the number of *Cooperators*), over a 24 h period.

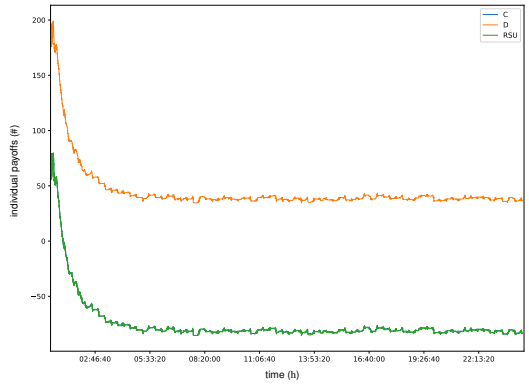


Fig. A.41-15. Evolution of the individual payoffs for *Cooperators, Defectors,* and *RSU* (always cooperating), over a 24 h period.

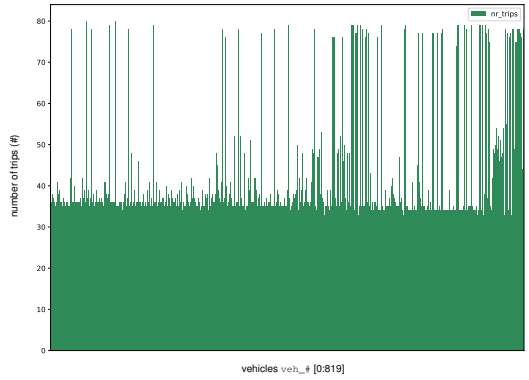


Fig. A.41-16. Number of trips made by each vehicle, during the simulation of a 24 h period.

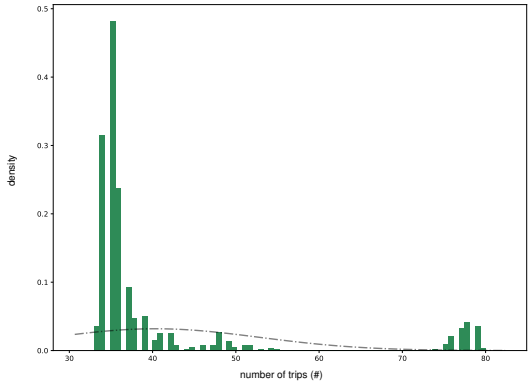


Fig. A.41-17. Density histogram of the number of trips made by each vehicle, during the simulation of a 24 h period, superimposing the normal density curve. The number of bins was calculated by the Freedman Diaconis rule.

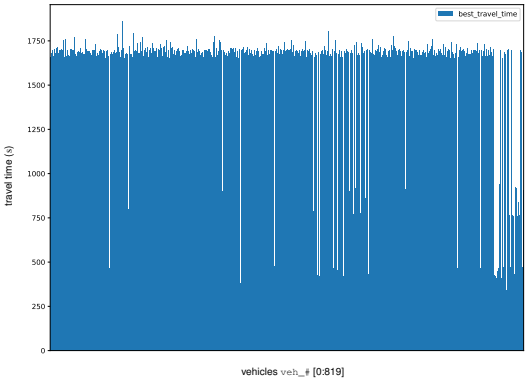


Fig. A.41-18. Best travel time for each vehicle, in seconds (s), during the simulation of a 24 h period.

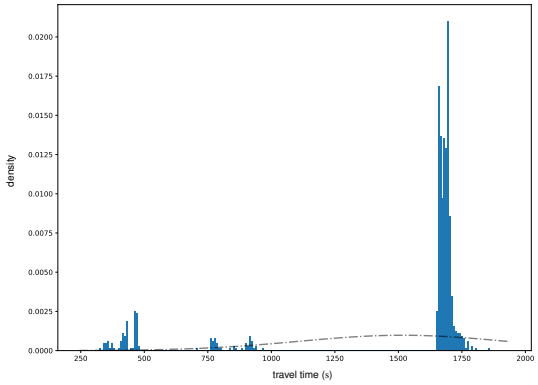


Fig. A.41-19. Density histogram of best travel time for vehicles, in seconds (s), during the simulation of a 24 h period, superimposing the normal density curve. The number of bins was calculated by the Freedman Diaconis rule.

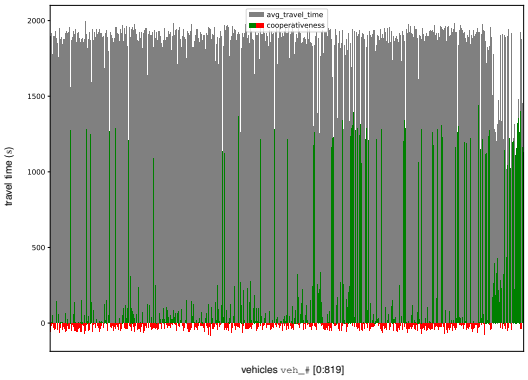


Fig. A.41-20. Average of the travel times, in seconds (s), of individual vehicles, during the simulation of a 24 h period. The bottom graph represents the *degree of cooperativeness**, downscaled by a normalization factor for the purpose of comparison with average times.

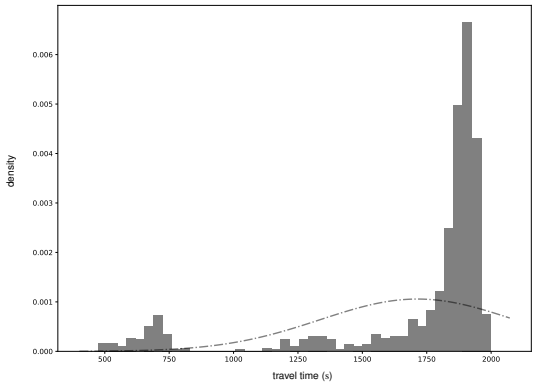


Fig. A.41-21. Density histogram of the average travel times, in seconds (s), of individual vehicles, during the simulation of a 24 h period, superimposing the normal density curve. The number of bins was calculated by the Freedman Diaconis rule.

* The *degree of cooperativeness* is a cumulative sum, calculated at each iteration, based on the complement of the ratio of cooperators, i.e., the higher the number of cooperators the less it increases, but the defectors are more penalized, and vice-versa. It varies inversely with the size of the group to which the player belongs.

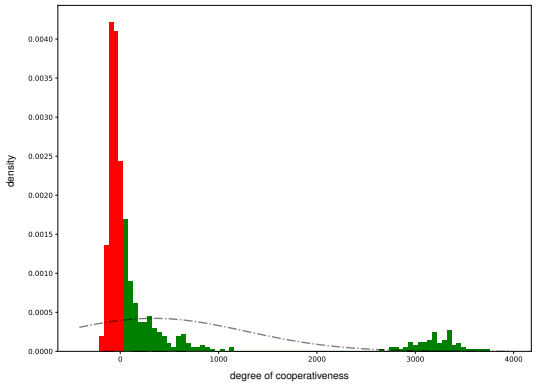


Fig. A.41-22. Density histogram of the *degree of cooperativeness** of individual vehicles, superimposing the normal density curve. The number of bins was calculated by the Freedman Diaconis rule. Generally, when strongly correlated with travel times, it presents a symmetric curve with respect to the *yy*-axis.

A.42 820veh-24h-19030001

```
Scenario: scenario-1
Timestamp: 20210617T133934Z
Number of vehicles: 820 vehs
Simulation time: 24.0 h
Warm up end time: 1866.6 s; step 18665
Vehicle selection strategy: mean_payoff
RSU turned off: False
RSU strategy: pigous_example_cooperation_weighted
Runner options:
   nogui: True
   step_length: 0.1
   seed: 19750808
   output_prefix: 820veh-24h-19030001
   sim_run_time: 24.0
   num_vehicles: 820
   warmup_speed: 13.96
   warmup_routes_weight: [473, 527]
   network_speed: 25.0
   change_behavior_probability: [100, 0]
   cooperation_probability: [50, 50]
   vehicle_selection_strategy: mean_payoff
   turn_rsu_off: False
   rsu_dynamic_dissemination: False
   rsu_dissemination_interval: 5
   rsu_probabilistic_dissemination: False
   rsu_suggestion_strategy: pigous_example_cooperation_weighted
   rsu_routes_weight: [460, 540]
   rsu_moving_avg_size: 5
   travel_times_ttl: 60
   rsu_dissemination_ttl: 0
   rsu_send_travel_time_info: False
   payoff_matrix: [360.0, 240.0, 0.0, -120.0]
   roth_erev_parameters: [0.1, 0.15]
   rsu_change_dissemination: False
   rsu_change_dissemination_steps: [14400, 28800, 43200, 57600, 72000]
   rsu_change_dissemination_intervals: [10, 20, 40, 80, 160]
Network Mean speed after warmup:
   Max: 10.71
   Min: 1.85
```

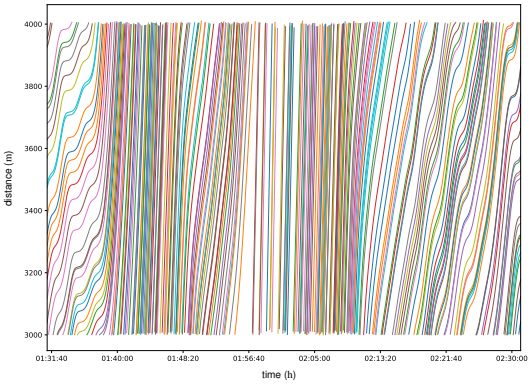


Fig. A.42-1. Time-Space diagram, for the one hour period after the end of the warmup, from 1:00:00 to 2:00:00 simulation time, plotted for the data from the sensor placed in the middle of the *direct* route (between 3000 m and 4000 m). In the case of an overloaded network, congestion shock waves can be observed.

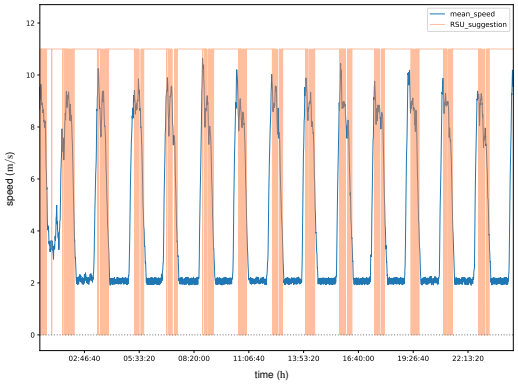


Fig. A.42-2. Mean speed in the network, in meters per second (m/s), over a 24 h period, superimposing (vertically, in orange) the time instants in which the RSU issued a recommendation to follow the *alternative* route.

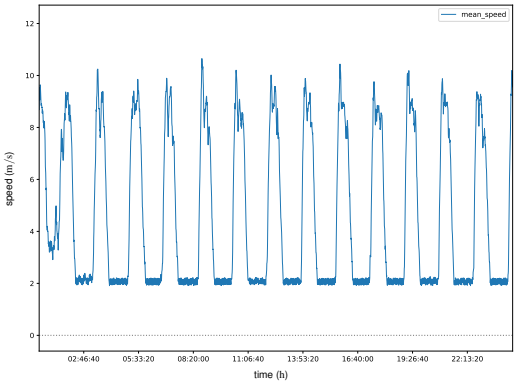


Fig. A.42-3. Mean speed in the network, in meters per second (m/s), over a 24 h period.

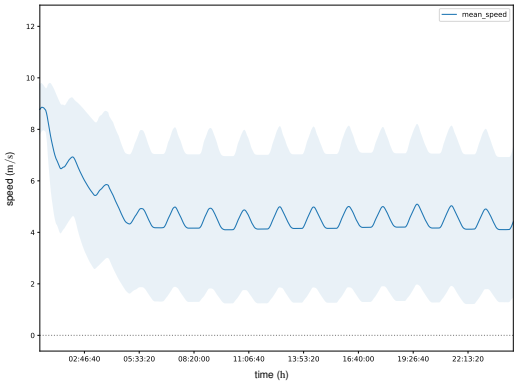


Fig. A.42-4. Mean speed in the network, in meters per second (m/s), over a 24 h period, 4 h Simple Moving Average, mean (line) and standard deviation (shaded).

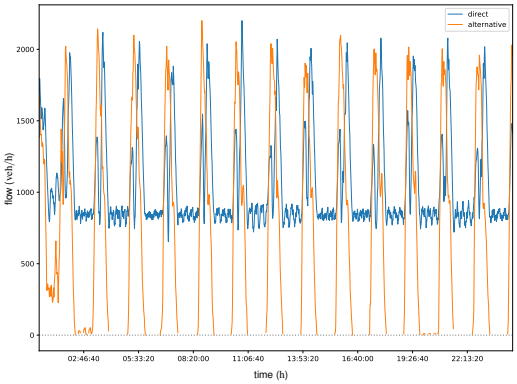


Fig. A.42-5. Traffic flow on each route, in vehicles per hour (veh/h), over a 24 h period.

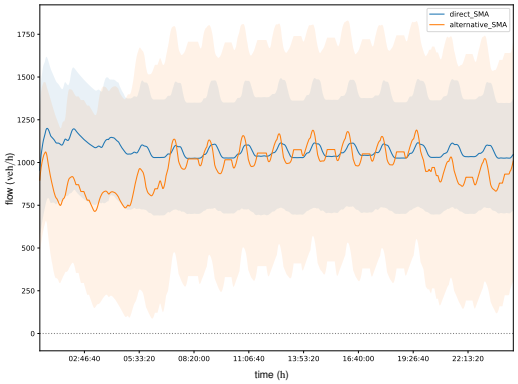


Fig. A.42-6. TrafficTraffic flow on each route, in vehicles per hour (veh/h), over a 24 h period, 4 h Simple Moving Average, mean (line) and standard deviation (shaded).

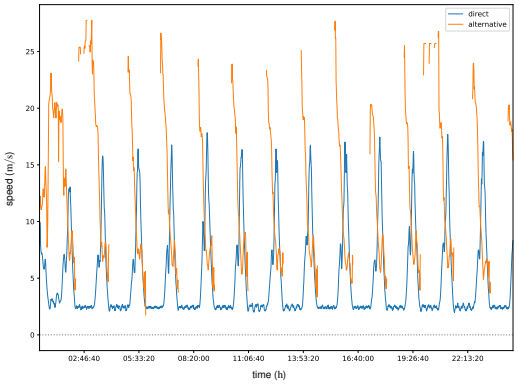


Fig. A.42-7. Mean speed on each route, in meters per second (m/s), aggregated to 1 min, over a 24 h period.

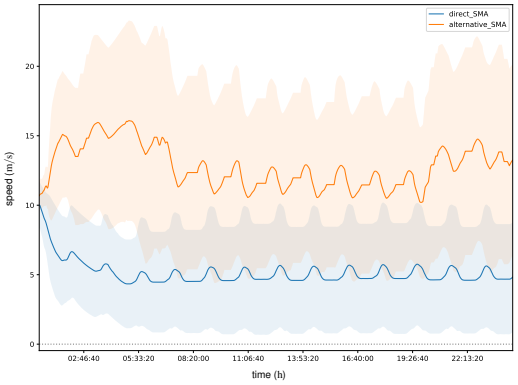


Fig. A.42-8. Mean speed on each route, in meters per second (m/s), aggregated to 1 min, over a 24 h period, 4 h Simple Moving Average, mean (line) and standard deviation (shaded).

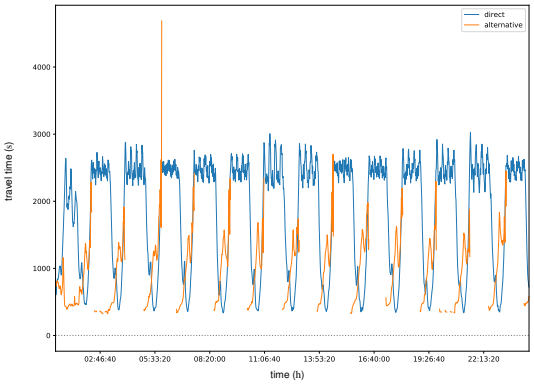


Fig. A.42-9. Travel times on each route, in seconds (s), aggregated to 1 min, over a 24 h period.

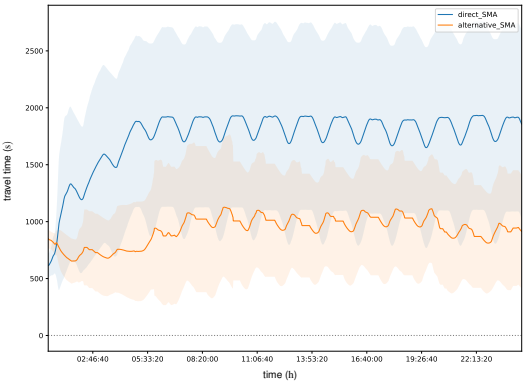


Fig. A.42-10. Travel times on each route, in seconds (s), aggregated to 1 min, over a 24 h period, 4 h Simple Moving Average, mean (line) and standard deviation (shaded).

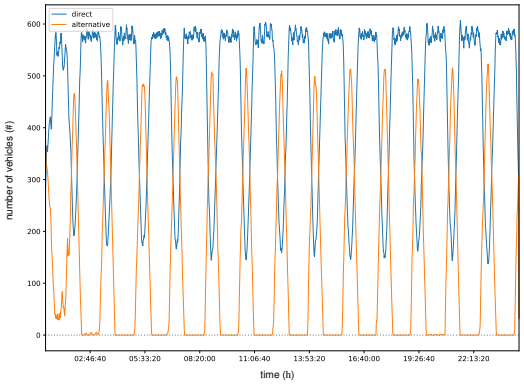


Fig. A.42-11. Average number of vehicles on each route, aggregated to 1 min, over a 24 h period.

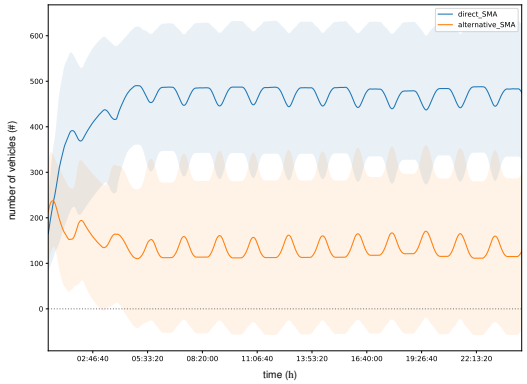


Fig. A.42-12. Average number of vehicles on each route, aggregated to 1 min, over a 24 h period, 4 h Simple Moving Average, mean (line) and standard deviation (shaded).

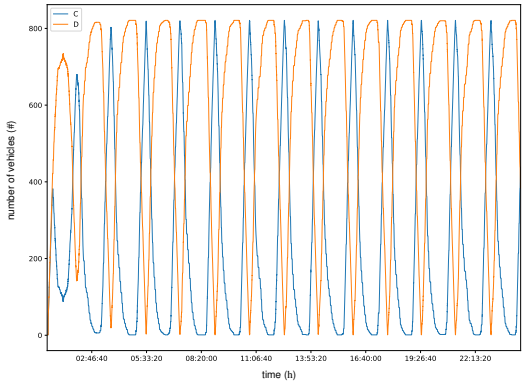


Fig. A.42-13. Evolution of the number of *Cooperators* and *Defectors* over a 24 h period.

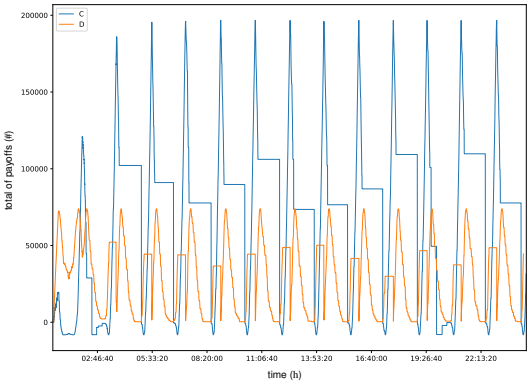


Fig. A.42-14. Evolution of total payoffs for *Cooperators* and *Defectors* (*individual payoff* times the *number of players receiving it*, $C(n) \times n$ and $D(n) \times (N-n)$, where n is the number of *Cooperators*), over a 24 h period.

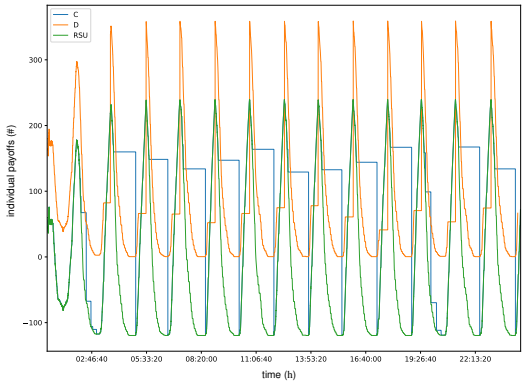


Fig. A.42-15. Evolution of the individual payoffs for *Cooperators, Defectors,* and *RSU* (always cooperating), over a 24 h period.

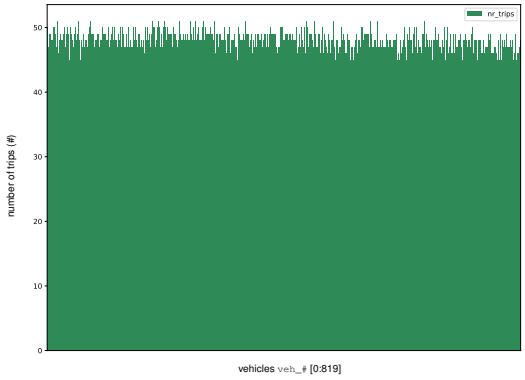


Fig. A.42-16. Number of trips made by each vehicle, during the simulation of a 24 h period.

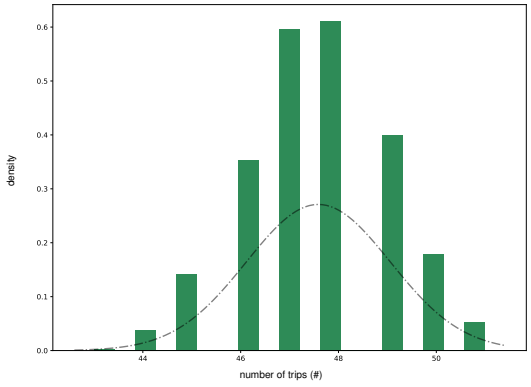


Fig. A.42-17. Density histogram of the number of trips made by each vehicle, during the simulation of a 24 h period, superimposing the normal density curve. The number of bins was calculated by the Freedman Diaconis rule.

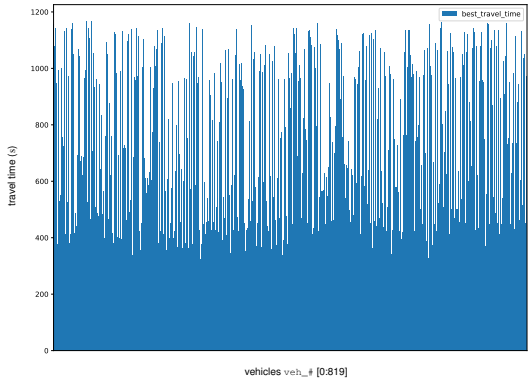


Fig. A.42-18. Best travel time for each vehicle, in seconds (s), during the simulation of a 24 h period.

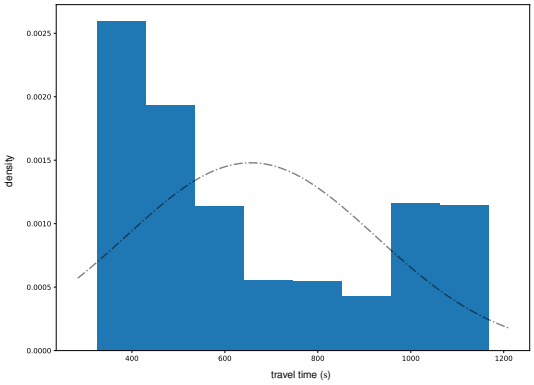


Fig. A.42-19. Density histogram of best travel time for vehicles, in seconds (s), during the simulation of a 24 h period, superimposing the normal density curve. The number of bins was calculated by the Freedman Diaconis rule.

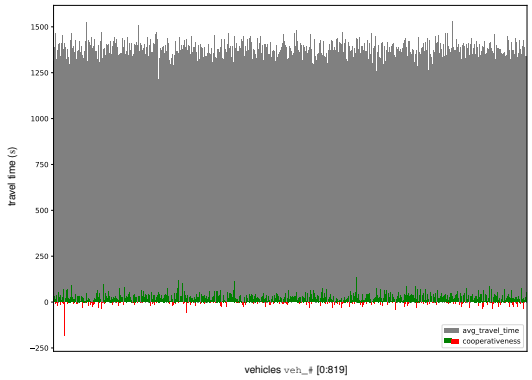


Fig. A.42-20. Average of the travel times, in seconds (s), of individual vehicles, during the simulation of a 24 h period. The bottom graph represents the *degree of cooperativeness**, downscaled by a normalization factor for the purpose of comparison with average times.

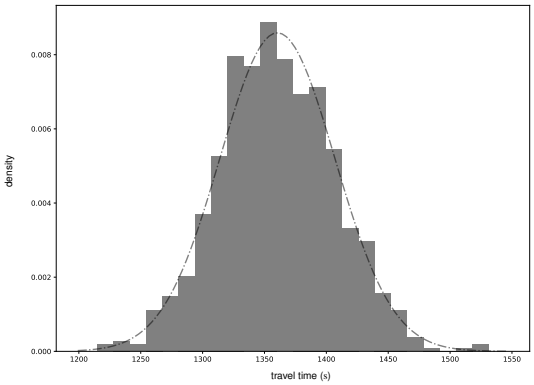


Fig. A.42-21. Density histogram of the average travel times, in seconds (s), of individual vehicles, during the simulation of a 24 h period, superimposing the normal density curve. The number of bins was calculated by the Freedman Diaconis rule.

* The *degree of cooperativeness* is a cumulative sum, calculated at each iteration, based on the complement of the ratio of cooperators, i.e., the higher the number of cooperators the less it increases, but the defectors are more penalized, and vice-versa. It varies inversely with the size of the group to which the player belongs.

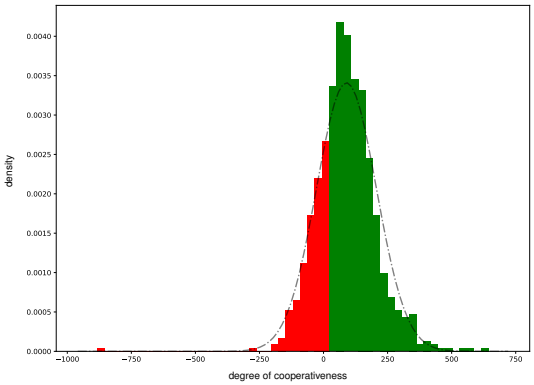


Fig. A.42-22. Density histogram of the *degree of cooperativeness** of individual vehicles, superimposing the normal density curve. The number of bins was calculated by the Freedman Diaconis rule. Generally, when strongly correlated with travel times, it presents a symmetric curve with respect to the *yy*-axis.

A.43 820veh-24h-19060001

```
Scenario: scenario-1
Timestamp: 20210616T102908Z
Number of vehicles: 820 vehs
Simulation time: 24.0 h
Warm up end time: 1866.6 s; step 18665
Vehicle selection strategy: stochastic
RSU turned off: False
RSU strategy: pigous_example_cooperation_weighted
Runner options:
   nogui: True
   step_length: 0.1
   seed: 19750808
   output_prefix: 820veh-24h-19060001
   sim_run_time: 24.0
   num_vehicles: 820
   warmup_speed: 13.96
   warmup_routes_weight: [473, 527]
   network_speed: 25.0
   change_behavior_probability: [100, 0]
   cooperation_probability: [50, 50]
   vehicle_selection_strategy: stochastic
   turn_rsu_off: False
   rsu_dynamic_dissemination: False
   rsu_dissemination_interval: 5
   rsu_probabilistic_dissemination: False
   rsu_suggestion_strategy: pigous_example_cooperation_weighted
   rsu_routes_weight: [460, 540]
   rsu_moving_avg_size: 5
   travel_times_ttl: 60
   rsu_dissemination_ttl: 0
   rsu_send_travel_time_info: False
   payoff_matrix: [360.0, 240.0, 0.0, -120.0]
   roth_erev_parameters: [0.1, 0.15]
   rsu_change_dissemination: False
   rsu_change_dissemination_steps: [14400, 28800, 43200, 57600, 72000]
   rsu_change_dissemination_intervals: [10, 20, 40, 80, 160]
Network Mean speed after warmup:
   Max: 9.96
   Min: 5.16
```

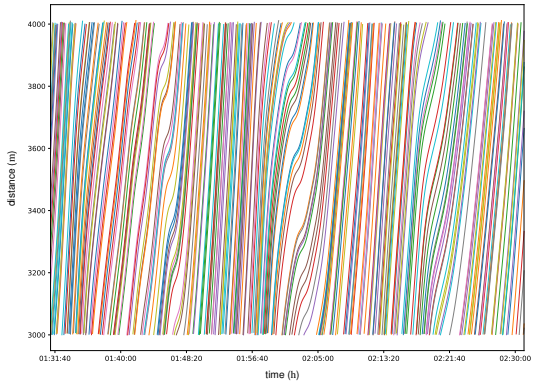


Fig. A.43-1. Time-Space diagram, for the one hour period after the end of the warmup, from 1:00:00 to 2:00:00 simulation time, plotted for the data from the sensor placed in the middle of the *direct* route (between 3000 m and 4000 m). In the case of an overloaded network, congestion shock waves can be observed.

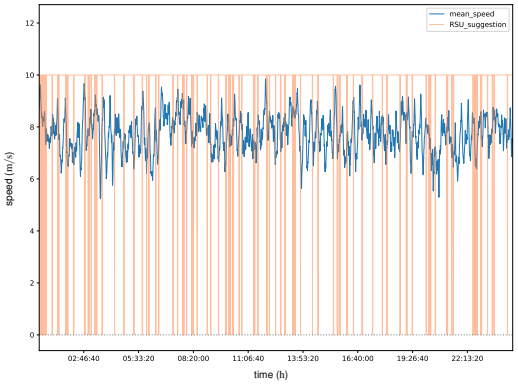


Fig. A.43-2. Mean speed in the network, in meters per second (m/s), over a 24 h period, superimposing (vertically, in orange) the time instants in which the RSU issued a recommendation to follow the *alternative* route.

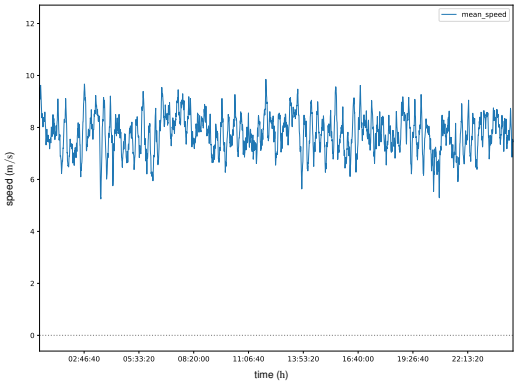


Fig. A.43-3. Mean speed in the network, in meters per second (m/s), over a 24 h period.

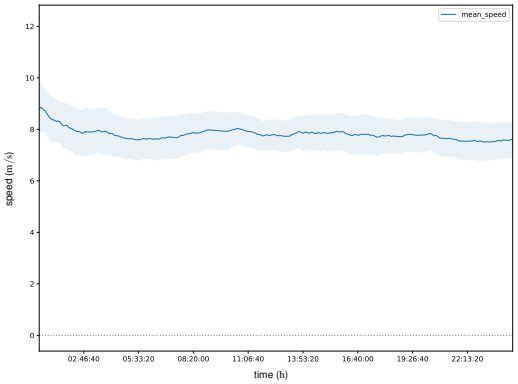


Fig. A.43-4. Mean speed in the network, in meters per second (m/s), over a 24 h period, 4 h Simple Moving Average, mean (line) and standard deviation (shaded).

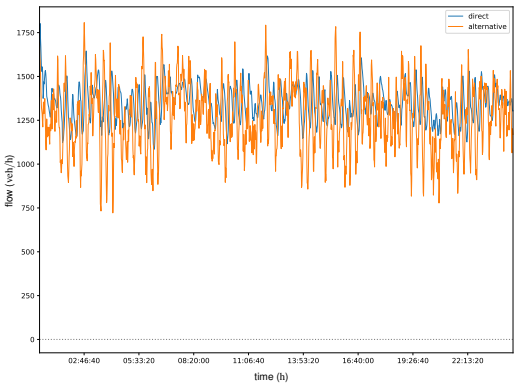


Fig. A.43-5. Traffic flow on each route, in vehicles per hour (veh/h), over a 24 h period.

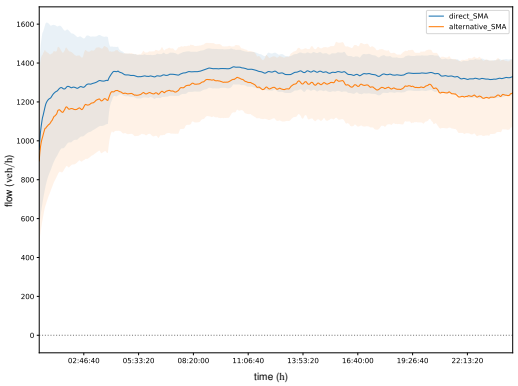


Fig. A.43-6. TrafficTraffic flow on each route, in vehicles per hour (veh/h), over a 24 h period, 4 h Simple Moving Average, mean (line) and standard deviation (shaded).

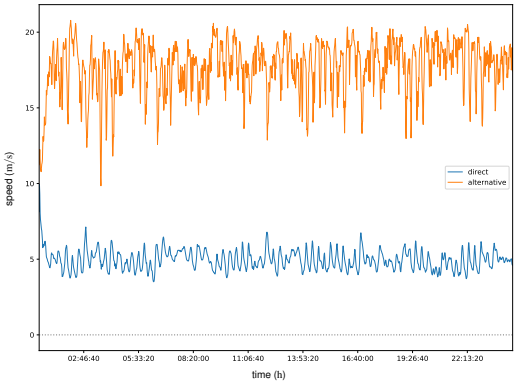


Fig. A.43-7. Mean speed on each route, in meters per second (m/s), aggregated to 1 min, over a 24 h period.

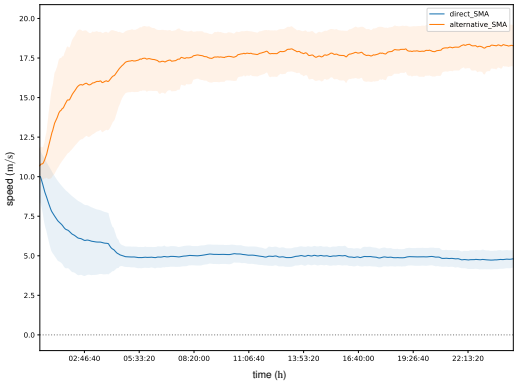


Fig. A.43-8. Mean speed on each route, in meters per second (m/s), aggregated to 1 min, over a 24 h period, 4 h Simple Moving Average, mean (line) and standard deviation (shaded).

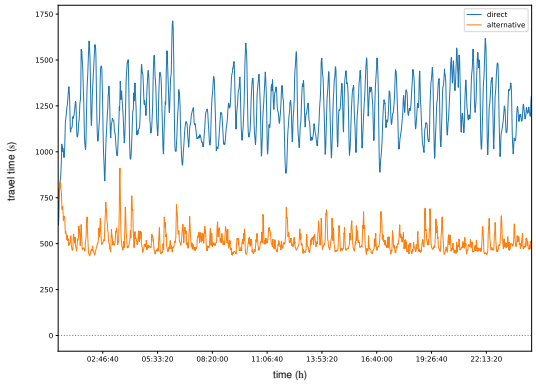


Fig. A.43-9. Travel times on each route, in seconds (s), aggregated to 1 min, over a 24 h period.

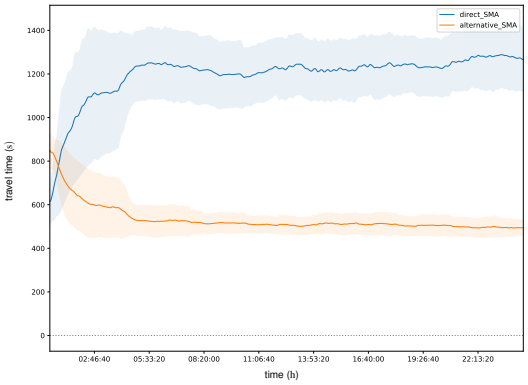


Fig. A.43-10. Travel times on each route, in seconds (s), aggregated to 1 min, over a 24 h period, 4 h Simple Moving Average, mean (line) and standard deviation (shaded).

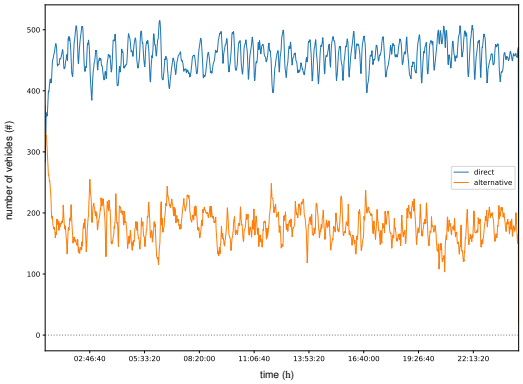


Fig. A.43-11. Average number of vehicles on each route, aggregated to 1 min, over a 24 h period.

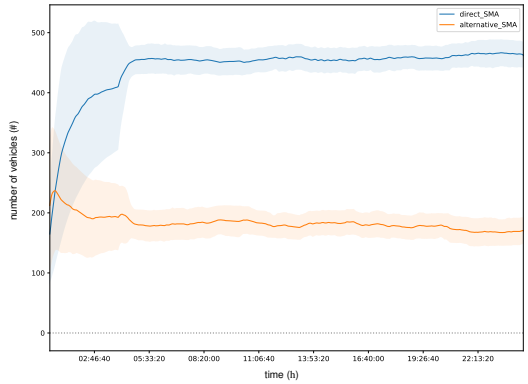


Fig. A.43-12. Average number of vehicles on each route, aggregated to 1 min, over a 24 h period, 4 h Simple Moving Average, mean (line) and standard deviation (shaded).

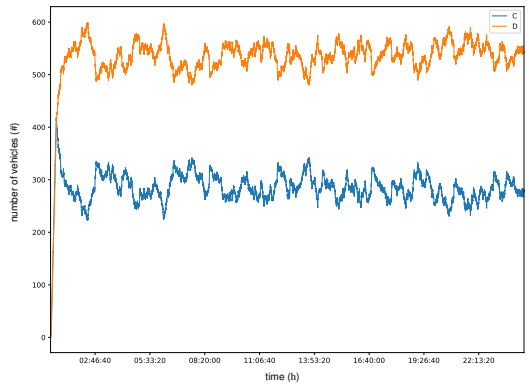


Fig. A.43-13. Evolution of the number of *Cooperators* and *Defectors* over a 24 h period.

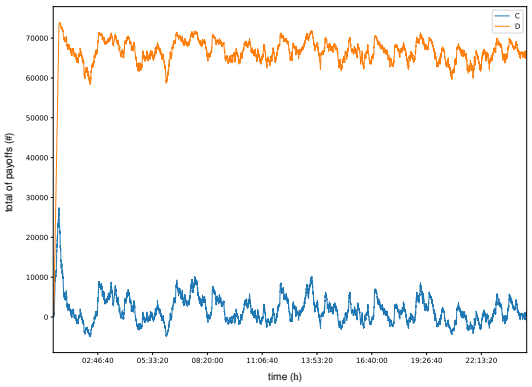


Fig. A.43-14. Evolution of total payoffs for *Cooperators* and *Defectors* (*individual payoff* times the *number of players receiving it*, $C(n) \times n$ and $D(n) \times (N-n)$, where n is the number of *Cooperators*), over a 24 h period.

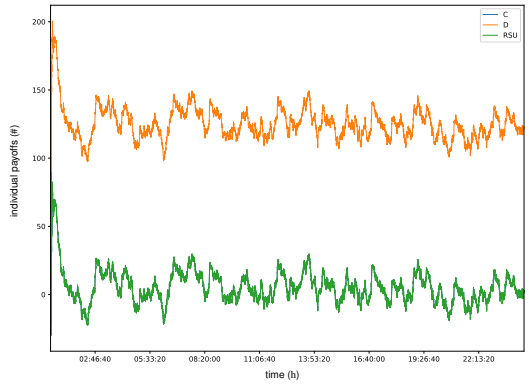


Fig. A.43-15. Evolution of the individual payoffs for *Cooperators, Defectors,* and *RSU* (always cooperating), over a 24 h period.

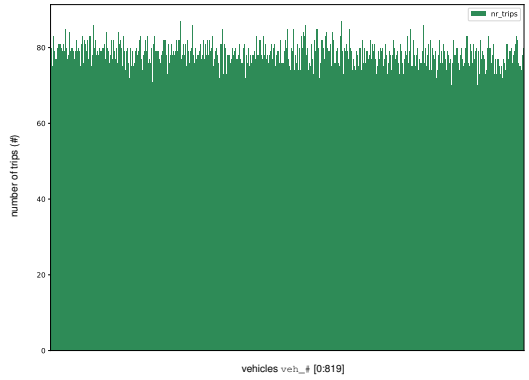


Fig. A.43-16. Number of trips made by each vehicle, during the simulation of a 24 h period.

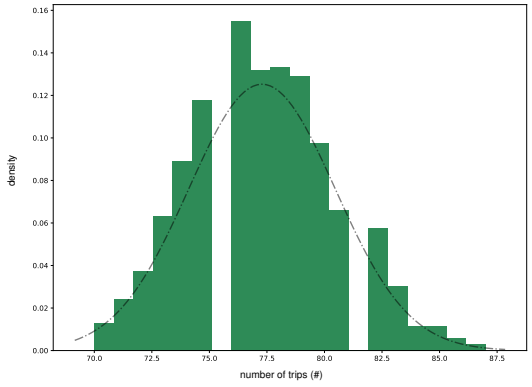


Fig. A.43-17. Density histogram of the number of trips made by each vehicle, during the simulation of a 24 h period, superimposing the normal density curve. The number of bins was calculated by the Freedman Diaconis rule.

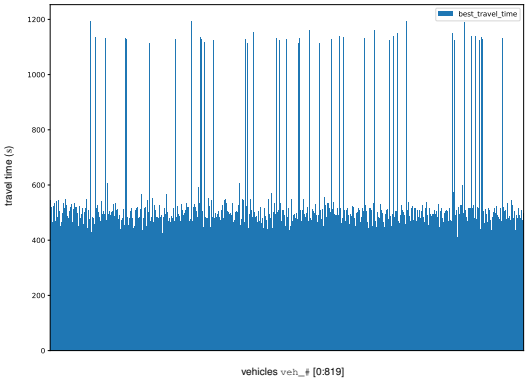


Fig. A.43-18. Best travel time for each vehicle, in seconds (s), during the simulation of a 24 h period.

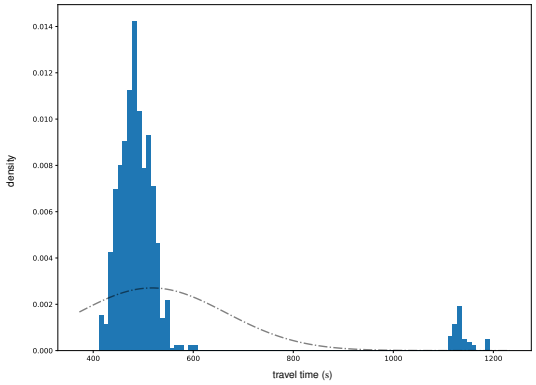


Fig. A.43-19. Density histogram of best travel time for vehicles, in seconds (s), during the simulation of a 24 h period, superimposing the normal density curve. The number of bins was calculated by the Freedman Diaconis rule.

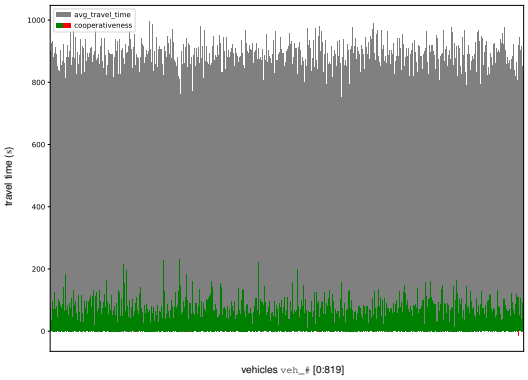


Fig. A.43-20. Average of the travel times, in seconds (s), of individual vehicles, during the simulation of a 24 h period. The bottom graph represents the *degree of cooperativeness**, downscaled by a normalization factor for the purpose of comparison with average times.

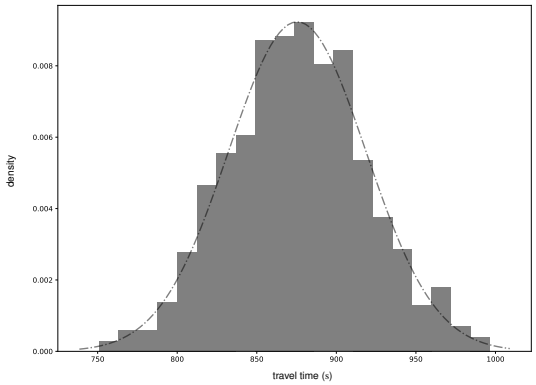


Fig. A.43-21. Density histogram of the average travel times, in seconds (s), of individual vehicles, during the simulation of a 24 h period, superimposing the normal density curve. The number of bins was calculated by the Freedman Diaconis rule.

* The *degree of cooperativeness* is a cumulative sum, calculated at each iteration, based on the complement of the ratio of cooperators, i.e., the higher the number of cooperators the less it increases, but the defectors are more penalized, and vice-versa. It varies inversely with the size of the group to which the player belongs.

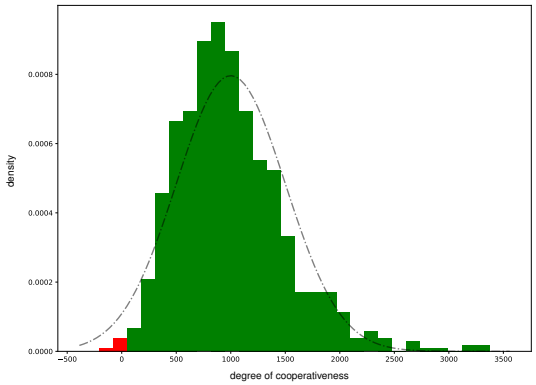


Fig. A.43-22. Density histogram of the *degree of cooperativeness** of individual vehicles, superimposing the normal density curve. The number of bins was calculated by the Freedman Diaconis rule. Generally, when strongly correlated with travel times, it presents a symmetric curve with respect to the *yy*-axis.

A.44 820veh-24h-19070001

```
Scenario: scenario-1
Timestamp: 20210617T133938Z
Number of vehicles: 820 vehs
Simulation time: 24.0 h
Warm up end time: 1866.6 s; step 18665
Vehicle selection strategy: mean_payoff_v2
RSU turned off: False
RSU strategy: pigous_example_cooperation_weighted
Runner options:
   nogui: True
   step_length: 0.1
   seed: 19750808
   output_prefix: 820veh-24h-19070001
   sim_run_time: 24.0
   num_vehicles: 820
   warmup_speed: 13.96
   warmup_routes_weight: [473, 527]
   network_speed: 25.0
   change_behavior_probability: [100, 0]
   cooperation_probability: [50, 50]
   vehicle_selection_strategy: mean_payoff_v2
   turn_rsu_off: False
   rsu_dynamic_dissemination: False
   rsu_dissemination_interval: 5
   rsu_probabilistic_dissemination: False
   rsu_suggestion_strategy: pigous_example_cooperation_weighted
   rsu_routes_weight: [460, 540]
   rsu_moving_avg_size: 5
   travel_times_ttl: 60
   rsu_dissemination_ttl: 0
   rsu_send_travel_time_info: False
   payoff_matrix: [360.0, 240.0, 0.0, -120.0]
   roth_erev_parameters: [0.1, 0.15]
   rsu_change_dissemination: False
   rsu_change_dissemination_steps: [14400, 28800, 43200, 57600, 72000]
   rsu_change_dissemination_intervals: [10, 20, 40, 80, 160]
Network Mean speed after warmup:
   Max: 11.07
   Min: 1.69
```

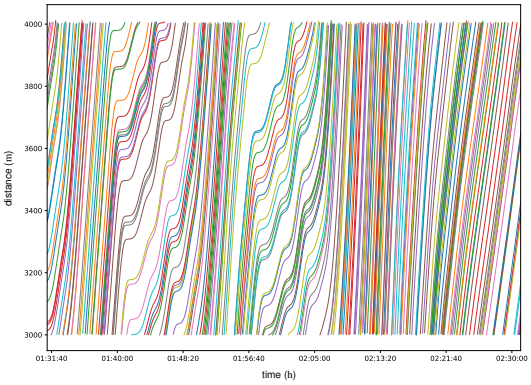


Fig. A.44-1. Time-Space diagram, for the one hour period after the end of the warmup, from 1:00:00 to 2:00:00 simulation time, plotted for the data from the sensor placed in the middle of the *direct* route (between 3000 m and 4000 m). In the case of an overloaded network, congestion shock waves can be observed.

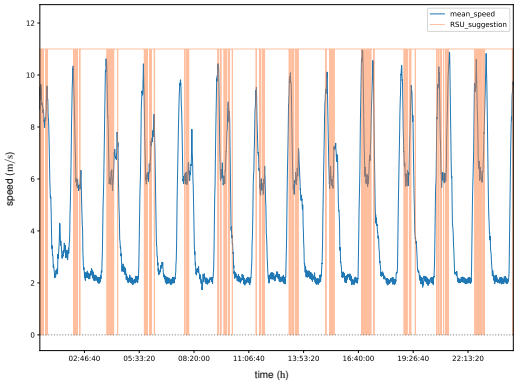


Fig. A.44-2. Mean speed in the network, in meters per second (m/s), over a 24 h period, superimposing (vertically, in orange) the time instants in which the RSU issued a recommendation to follow the *alternative* route.

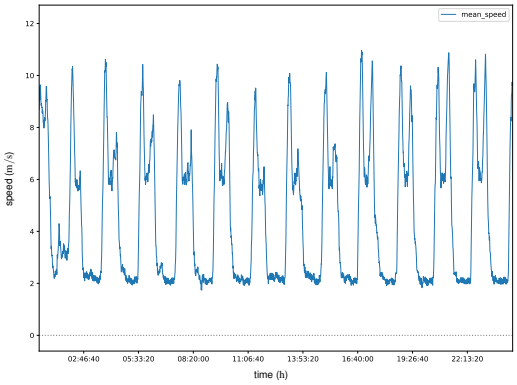


Fig. A.44-3. Mean speed in the network, in meters per second (m/s), over a 24 h period.

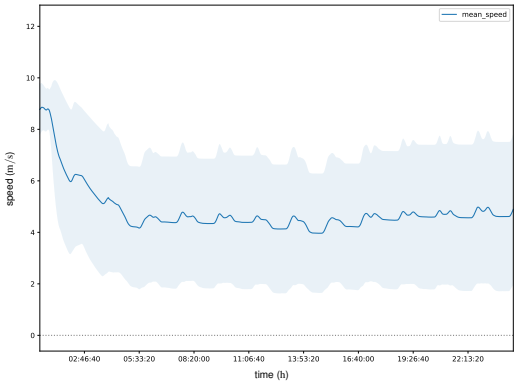


Fig. A.44-4. Mean speed in the network, in meters per second (m/s), over a 24 h period, 4 h Simple Moving Average, mean (line) and standard deviation (shaded).

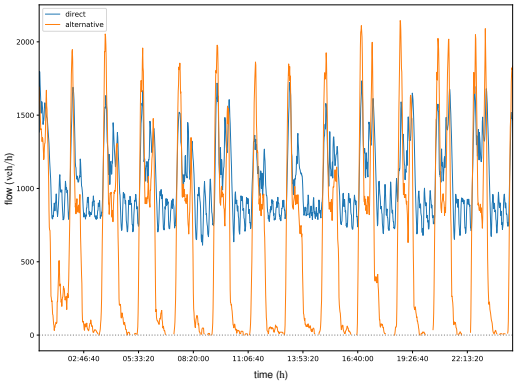


Fig. A.44-5. Traffic flow on each route, in vehicles per hour (veh/h), over a 24 h period.

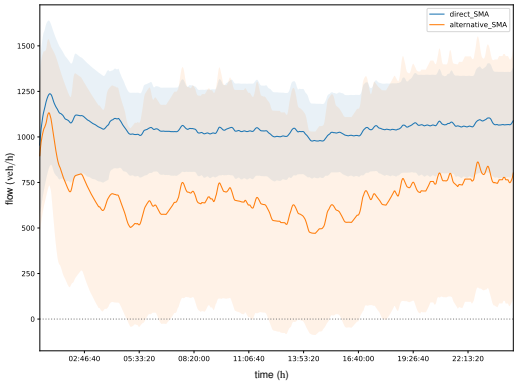


Fig. A.44-6. TrafficTraffic flow on each route, in vehicles per hour (veh/h), over a 24 h period, 4 h Simple Moving Average, mean (line) and standard deviation (shaded).

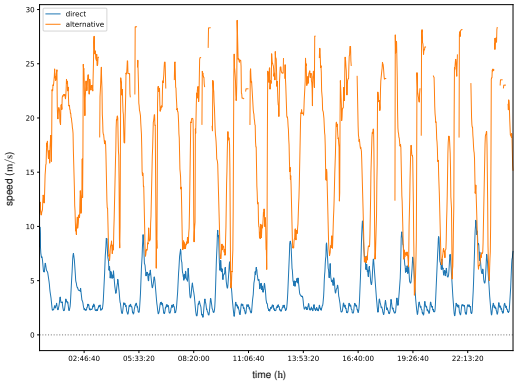


Fig. A.44-7. Mean speed on each route, in meters per second (m/s), aggregated to 1 min, over a 24 h period.

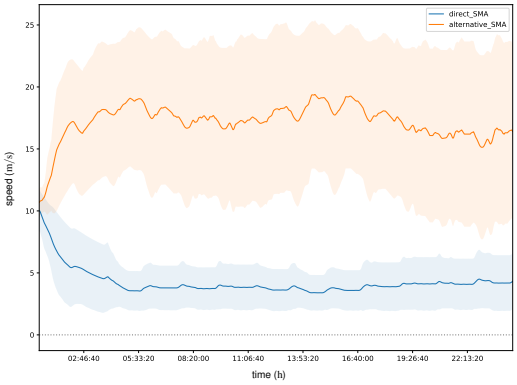


Fig. A.44-8. Mean speed on each route, in meters per second (m/s), aggregated to 1 min, over a 24 h period, 4 h Simple Moving Average, mean (line) and standard deviation (shaded).

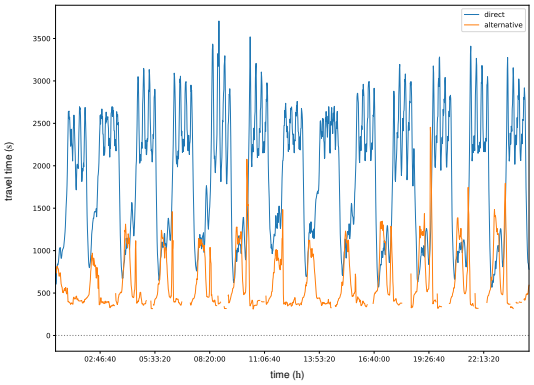


Fig. A.44-9. Travel times on each route, in seconds (s), aggregated to 1 min, over a 24 h period.

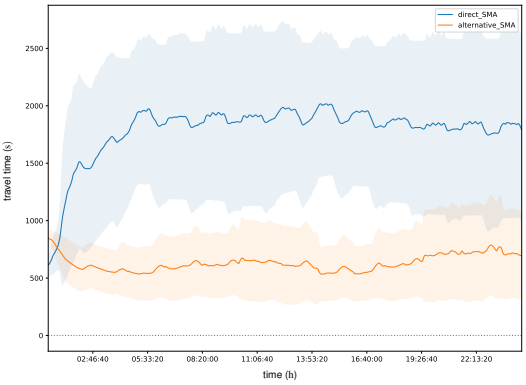


Fig. A.44-10. Travel times on each route, in seconds (s), aggregated to 1 min, over a 24 h period, 4 h Simple Moving Average, mean (line) and standard deviation (shaded).

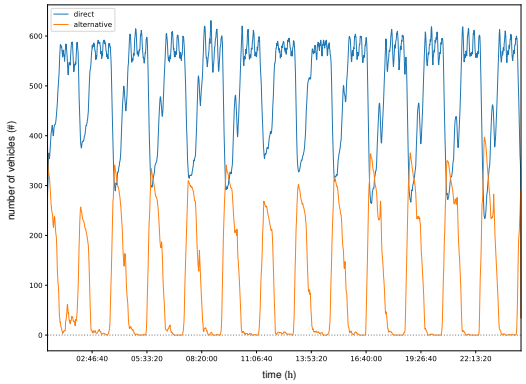


Fig. A.44-11. Average number of vehicles on each route, aggregated to 1 min, over a 24 h period.

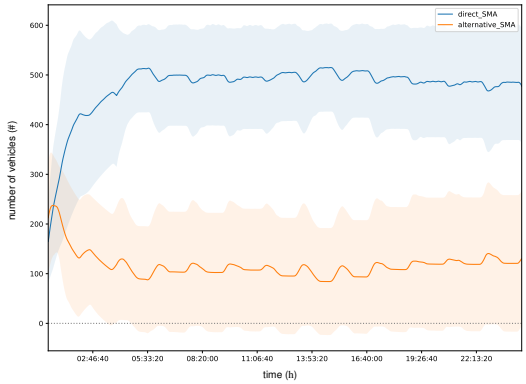


Fig. A.44-12. Average number of vehicles on each route, aggregated to 1 min, over a 24 h period, 4 h Simple Moving Average, mean (line) and standard deviation (shaded).

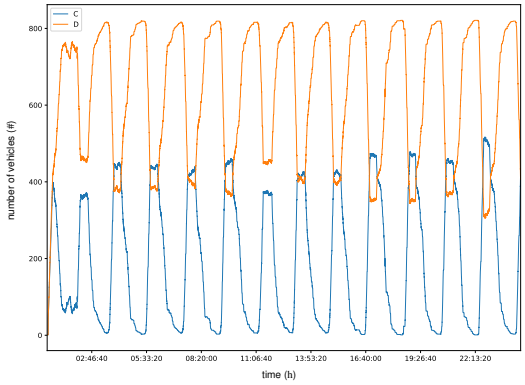


Fig. A.44-13. Evolution of the number of *Cooperators* and *Defectors* over a 24 h period.

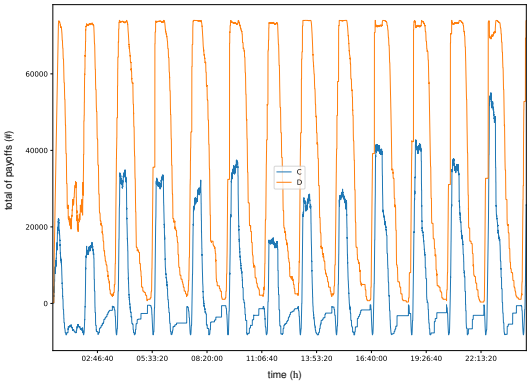


Fig. A.44-14. Evolution of total payoffs for *Cooperators* and *Defectors* (*individual payoff* times the *number of players receiving it*, $C(n) \times n$ and $D(n) \times (N-n)$, where n is the number of *Cooperators*), over a 24 h period.

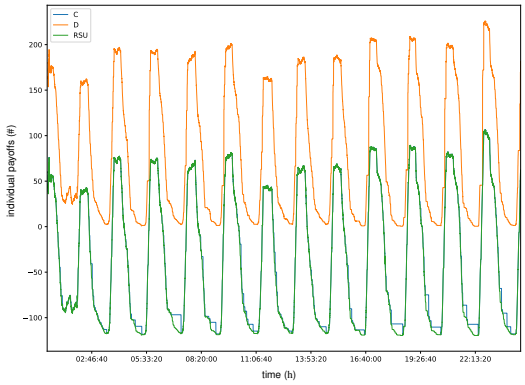


Fig. A.44-15. Evolution of the individual payoffs for *Cooperators, Defectors,* and *RSU* (always cooperating), over a 24 h period.

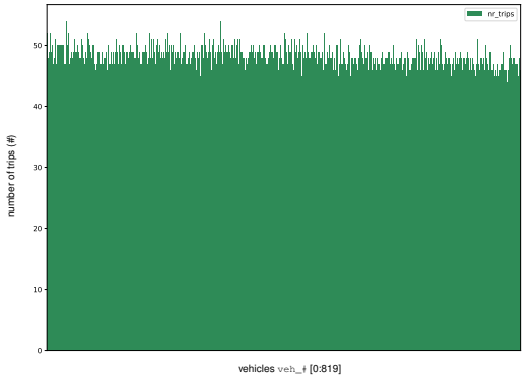


Fig. A.44-16. Number of trips made by each vehicle, during the simulation of a 24 h period.

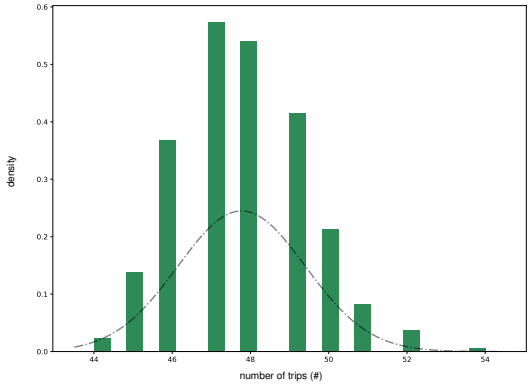


Fig. A.44-17. Density histogram of the number of trips made by each vehicle, during the simulation of a 24 h period, superimposing the normal density curve. The number of bins was calculated by the Freedman Diaconis rule.

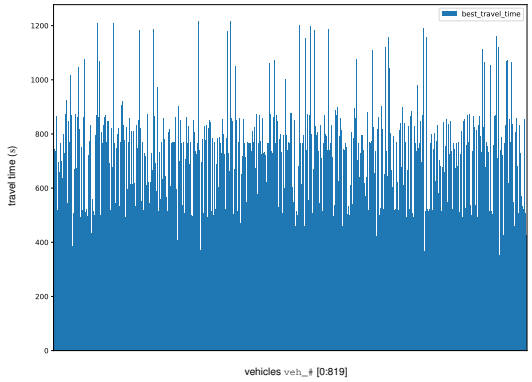


Fig. A.44-18. Best travel time for each vehicle, in seconds (s), during the simulation of a 24 h period.

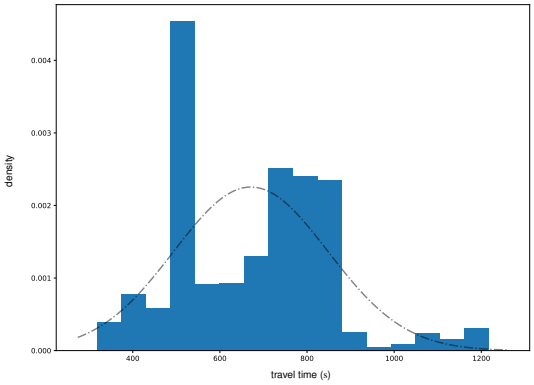


Fig. A.44-19. Density histogram of best travel time for vehicles, in seconds (s), during the simulation of a 24 h period, superimposing the normal density curve. The number of bins was calculated by the Freedman Diaconis rule.

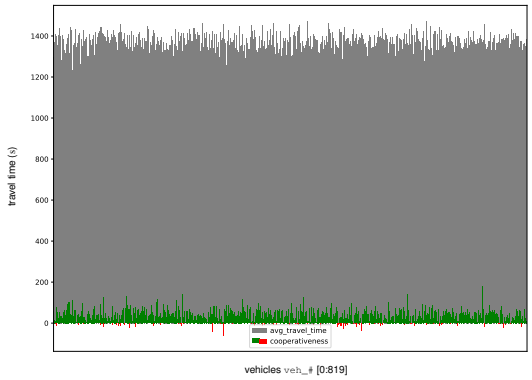


Fig. A.44-20. Average of the travel times, in seconds (s), of individual vehicles, during the simulation of a 24 h period. The bottom graph represents the *degree of cooperativeness**, downscaled by a normalization factor for the purpose of comparison with average times.

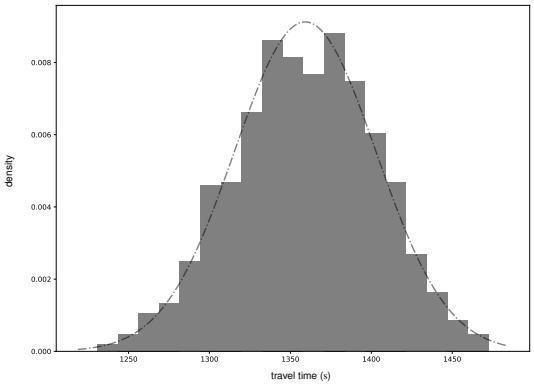


Fig. A.44-21. Density histogram of the average travel times, in seconds (s), of individual vehicles, during the simulation of a 24 h period, superimposing the normal density curve. The number of bins was calculated by the Freedman Diaconis rule.

* The *degree of cooperativeness* is a cumulative sum, calculated at each iteration, based on the complement of the ratio of cooperators, i.e., the higher the number of cooperators the less it increases, but the defectors are more penalized, and vice-versa. It varies inversely with the size of the group to which the player belongs.

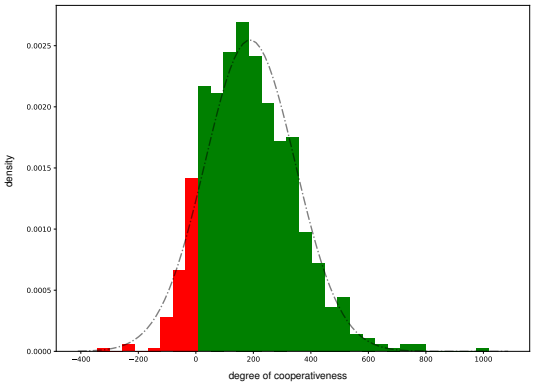


Fig. A.44-22. Density histogram of the *degree of cooperativeness** of individual vehicles, superimposing the normal density curve. The number of bins was calculated by the Freedman Diaconis rule. Generally, when strongly correlated with travel times, it presents a symmetric curve with respect to the *yy*-axis.

A.45 820veh-24h-19040001

```
Scenario: scenario-1
Timestamp: 20210610T200823Z
Number of vehicles: 820 vehs
Simulation time: 24.0 h
Warm up end time: 1866.6 s; step 18665
Vehicle selection strategy: roth_erev
RSU turned off: False
RSU strategy: pigous_example_cooperation_weighted
Runner options:
   nogui: True
   step_length: 0.1
   seed: 19750808
   output_prefix: 820veh-24h-19040001
   sim_run_time: 24.0
   num_vehicles: 820
   warmup_speed: 13.96
   warmup_routes_weight: [473, 527]
   network_speed: 25.0
   change_behavior_probability: [100, 0]
   cooperation_probability: [50, 50]
   vehicle_selection_strategy: roth_erev
   turn_rsu_off: False
   rsu_dynamic_dissemination: False
   rsu_dissemination_interval: 5
   rsu_probabilistic_dissemination: False
   rsu_suggestion_strategy: pigous_example_cooperation_weighted
   rsu_routes_weight: [460, 540]
   rsu_moving_avg_size: 5
   travel_times_ttl: 60
   rsu_dissemination_ttl: 0
   rsu_send_travel_time_info: False
   payoff_matrix: [360.0, 240.0, 0.0, -120.0]
   roth_erev_parameters: [0.1, 0.2]
   rsu_change_dissemination: False
   rsu_change_dissemination_steps: [14400, 28800, 43200, 57600, 72000]
   rsu_change_dissemination_intervals: [10, 20, 40, 80, 160]
Network Mean speed after warmup:
   Max: 11.96
   Min: 4.06
```

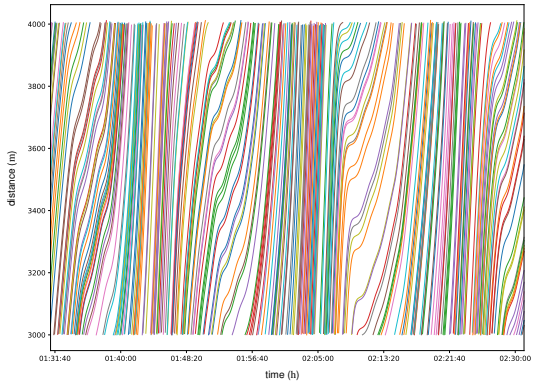


Fig. A.45-1. Time-Space diagram, for the one hour period after the end of the warmup, from 1:00:00 to 2:00:00 simulation time, plotted for the data from the sensor placed in the middle of the *direct* route (between 3000 m and 4000 m). In the case of an overloaded network, congestion shock waves can be observed.

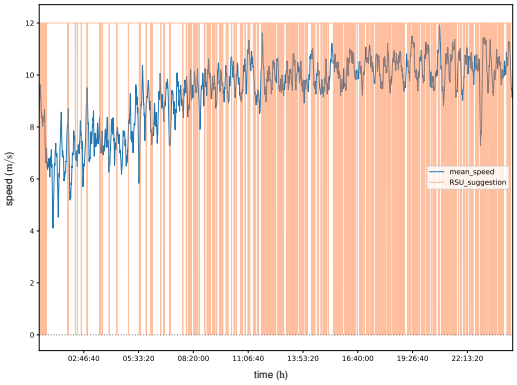


Fig. A.45-2. Mean speed in the network, in meters per second (m/s), over a 24 h period, superimposing (vertically, in orange) the time instants in which the RSU issued a recommendation to follow the *alternative* route.

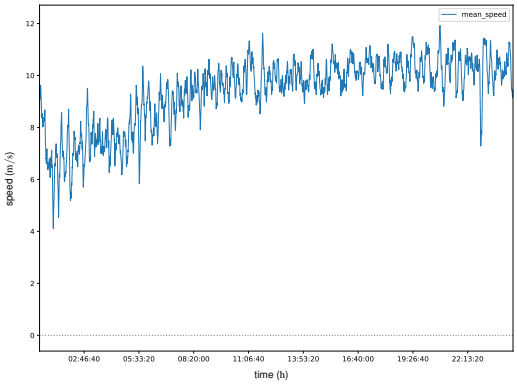


Fig. A.45-3. Mean speed in the network, in meters per second (m/s), over a 24 h period.

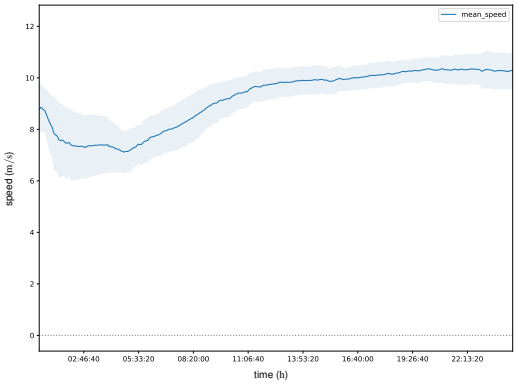


Fig. A.45-4. Mean speed in the network, in meters per second (m/s), over a 24 h period, 4 h Simple Moving Average, mean (line) and standard deviation (shaded).

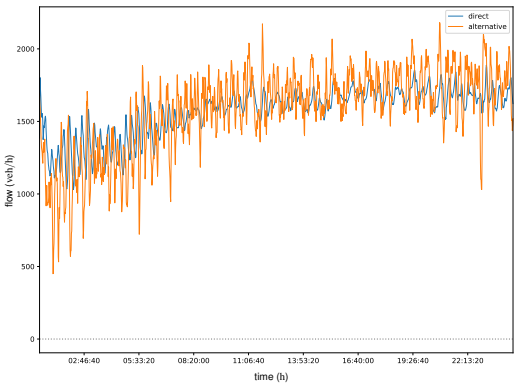


Fig. A.45-5. Traffic flow on each route, in vehicles per hour (veh/h), over a 24 h period.

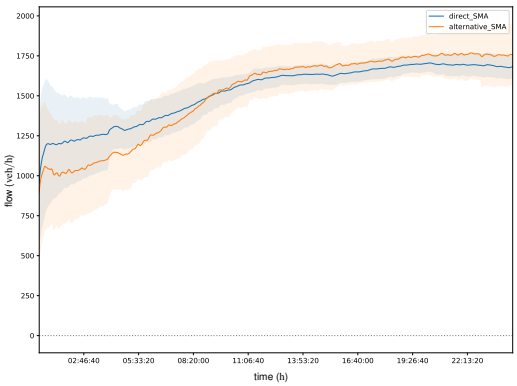


Fig. A.45-6. TrafficTraffic flow on each route, in vehicles per hour (veh/h), over a 24 h period, 4 h Simple Moving Average, mean (line) and standard deviation (shaded).

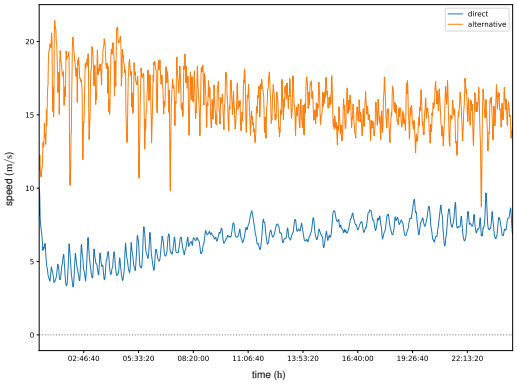


Fig. A.45-7. Mean speed on each route, in meters per second (m/s), aggregated to 1 min, over a 24 h period.

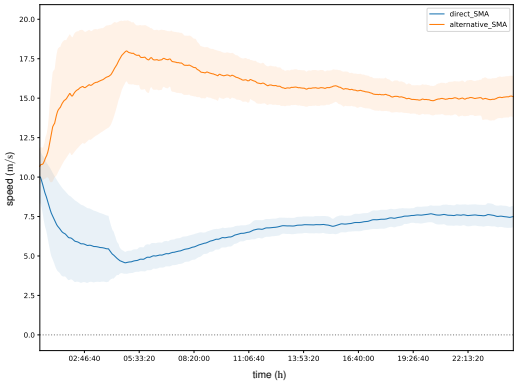


Fig. A.45-8. Mean speed on each route, in meters per second (m/s), aggregated to 1 min, over a 24 h period, 4 h Simple Moving Average, mean (line) and standard deviation (shaded).

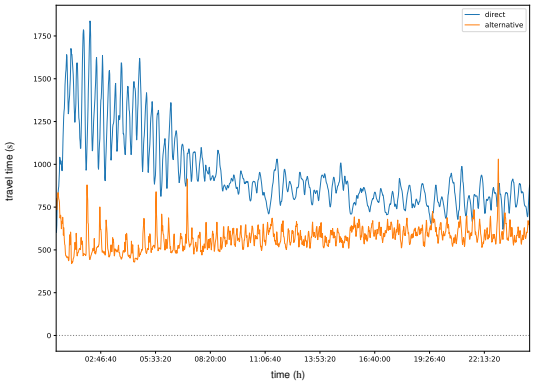


Fig. A.45-9. Travel times on each route, in seconds (s), aggregated to 1 min, over a 24 h period.

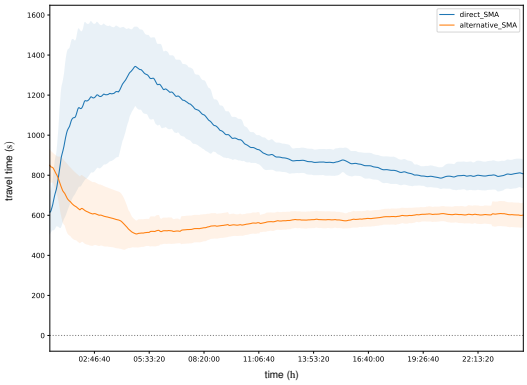


Fig. A.45-10. Travel times on each route, in seconds (s), aggregated to 1 min, over a 24 h period, 4 h Simple Moving Average, mean (line) and standard deviation (shaded).

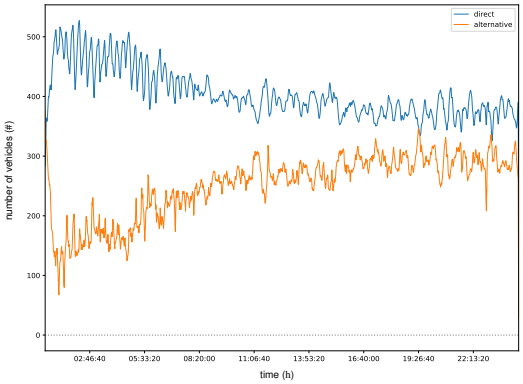


Fig. A.45-11. Average number of vehicles on each route, aggregated to 1 min, over a 24 h period.

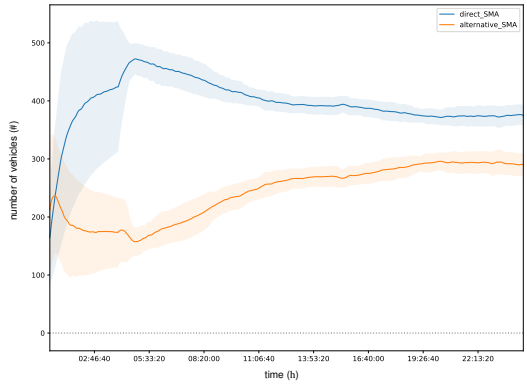


Fig. A.45-12. Average number of vehicles on each route, aggregated to 1 min, over a 24 h period, 4 h Simple Moving Average, mean (line) and standard deviation (shaded).

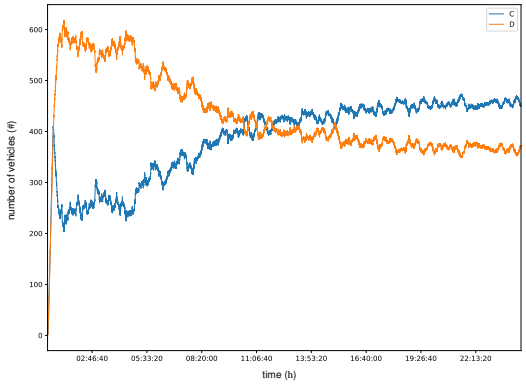


Fig. A.45-13. Evolution of the number of *Cooperators* and *Defectors* over a 24 h period.

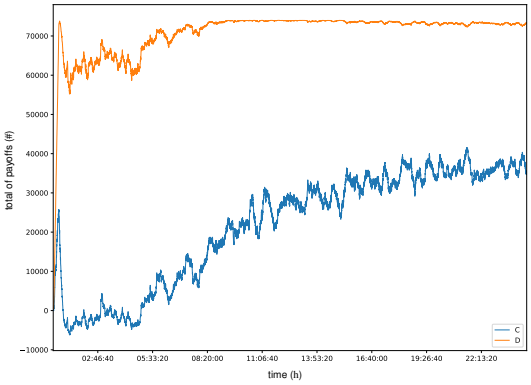


Fig. A.45-14. Evolution of total payoffs for *Cooperators* and *Defectors* (*individual payoff* times the *number of players receiving it*, $C(n) \times n$ and $D(n) \times (N-n)$, where n is the number of *Cooperators*), over a 24 h period.

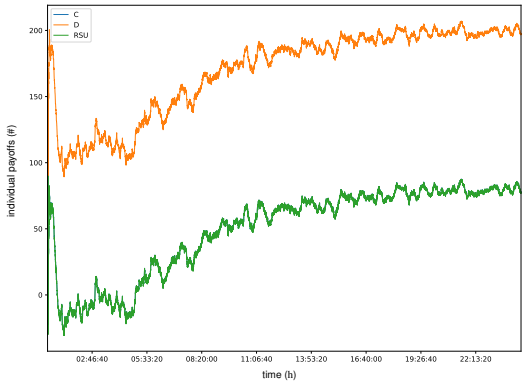


Fig. A.45-15. Evolution of the individual payoffs for *Cooperators, Defectors,* and *RSU* (always cooperating), over a 24 h period.

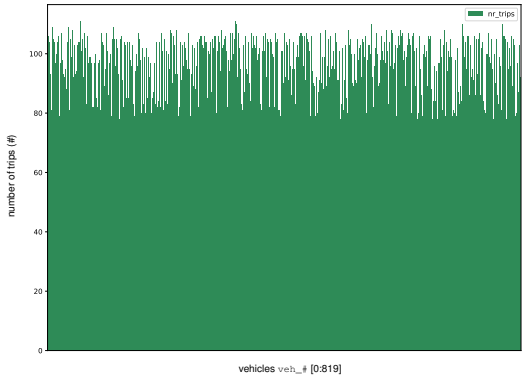


Fig. A.45-16. Number of trips made by each vehicle, during the simulation of a 24 h period.

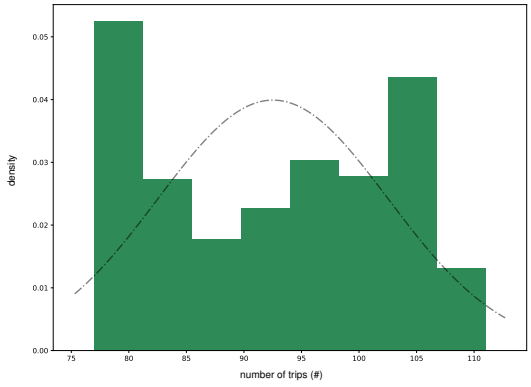


Fig. A.45-17. Density histogram of the number of trips made by each vehicle, during the simulation of a 24 h period, superimposing the normal density curve. The number of bins was calculated by the Freedman Diaconis rule.

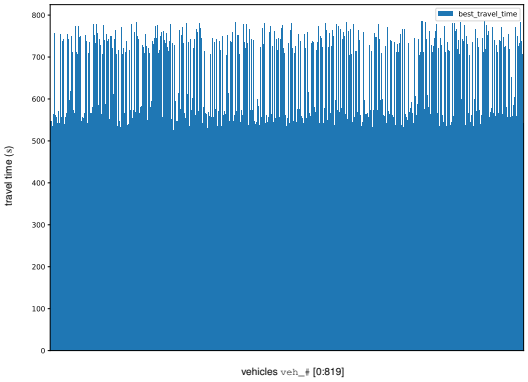


Fig. A.45-18. Best travel time for each vehicle, in seconds (s), during the simulation of a 24 h period.

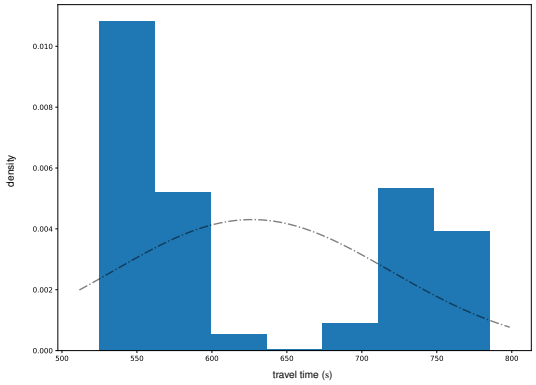


Fig. A.45-19. Density histogram of best travel time for vehicles, in seconds (s), during the simulation of a 24 h period, superimposing the normal density curve. The number of bins was calculated by the Freedman Diaconis rule.

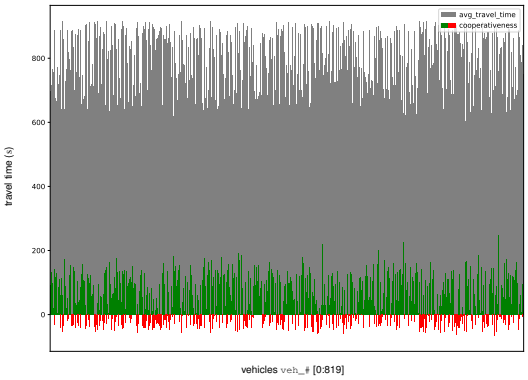


Fig. A.45-20. Average of the travel times, in seconds (s), of individual vehicles, during the simulation of a 24 h period. The bottom graph represents the *degree of cooperativeness**, downscaled by a normalization factor for the purpose of comparison with average times.

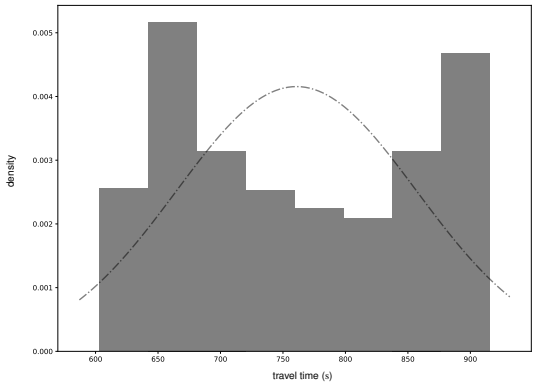


Fig. A.45-21. Density histogram of the average travel times, in seconds (s), of individual vehicles, during the simulation of a 24 h period, superimposing the normal density curve. The number of bins was calculated by the Freedman Diaconis rule.

* The *degree of cooperativeness* is a cumulative sum, calculated at each iteration, based on the complement of the ratio of cooperators, i.e., the higher the number of cooperators the less it increases, but the defectors are more penalized, and vice-versa. It varies inversely with the size of the group to which the player belongs.

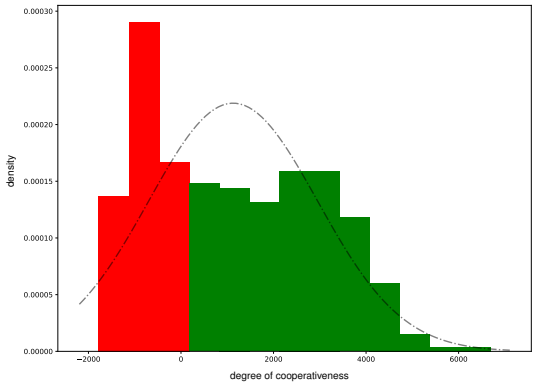


Fig. A.45-22. Density histogram of the *degree of cooperativeness** of individual vehicles, superimposing the normal density curve. The number of bins was calculated by the Freedman Diaconis rule. Generally, when strongly correlated with travel times, it presents a symmetric curve with respect to the *yy*-axis.

A.46 820veh-24h-19050001

```
Scenario: scenario-1
Timestamp: 20210610T224024Z
Number of vehicles: 820 vehs
Simulation time: 24.0 h
Warm up end time: 1866.6 s; step 18665
Vehicle selection strategy: roth_erev_utility
RSU turned off: False
RSU strategy: pigous_example_cooperation_weighted
Runner options:
   nogui: True
   step_length: 0.1
   seed: 19750808
   output_prefix: 820veh-24h-19050001
   sim_run_time: 24.0
   num_vehicles: 820
   warmup_speed: 13.96
   warmup_routes_weight: [473, 527]
   network_speed: 25.0
   change_behavior_probability: [100, 0]
   cooperation_probability: [50, 50]
   vehicle_selection_strategy: roth_erev_utility
   turn_rsu_off: False
   rsu_dynamic_dissemination: False
   rsu_dissemination_interval: 5
   rsu_probabilistic_dissemination: False
   rsu_suggestion_strategy: pigous_example_cooperation_weighted
   rsu_routes_weight: [460, 540]
   rsu_moving_avg_size: 5
   travel_times_ttl: 60
   rsu_dissemination_ttl: 0
   rsu_send_travel_time_info: False
   payoff_matrix: [360.0, 240.0, 0.0, -120.0]
   roth_erev_parameters: [0.1, 0.2]
   rsu_change_dissemination: False
   rsu_change_dissemination_steps: [14400, 28800, 43200, 57600, 72000]
   rsu_change_dissemination_intervals: [10, 20, 40, 80, 160]
Network Mean speed after warmup:
   Max: 11.55
   Min: 4.06
```

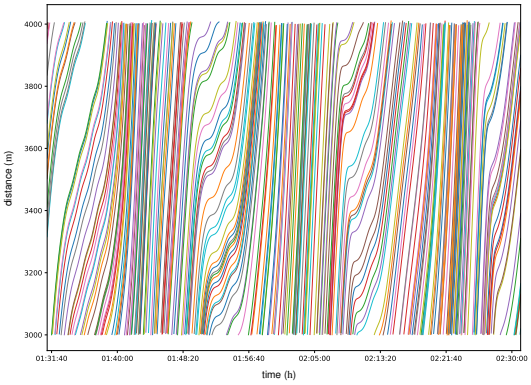


Fig. A.46-1. Time-Space diagram, for the one hour period after the end of the warmup, from 1:00:00 to 2:00:00 simulation time, plotted for the data from the sensor placed in the middle of the *direct* route (between 3000 m and 4000 m). In the case of an overloaded network, congestion shock waves can be observed.

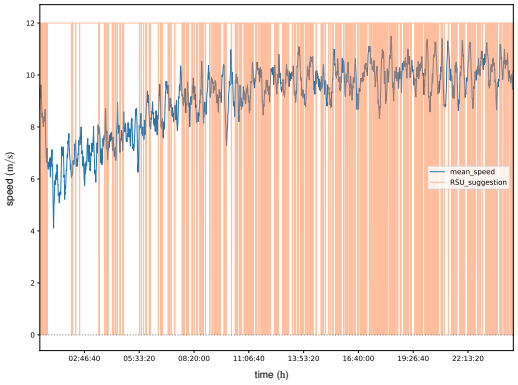


Fig. A.46-2. Mean speed in the network, in meters per second (m/s), over a 24 h period, superimposing (vertically, in orange) the time instants in which the RSU issued a recommendation to follow the *alternative* route.

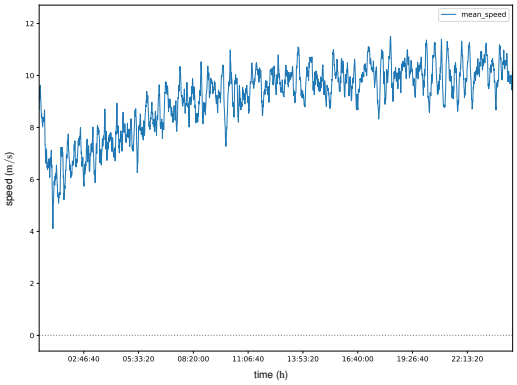


Fig. A.46-3. Mean speed in the network, in meters per second (m/s), over a 24 h period.

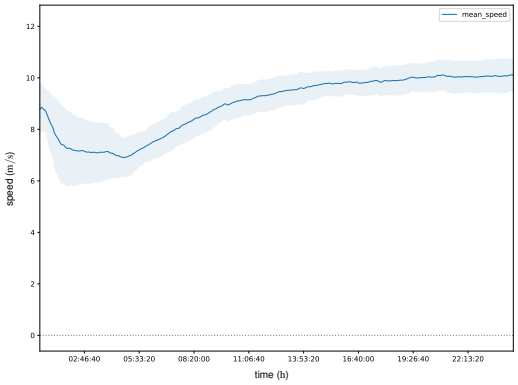


Fig. A.46-4. Mean speed in the network, in meters per second (m/s), over a 24 h period, 4 h Simple Moving Average, mean (line) and standard deviation (shaded).

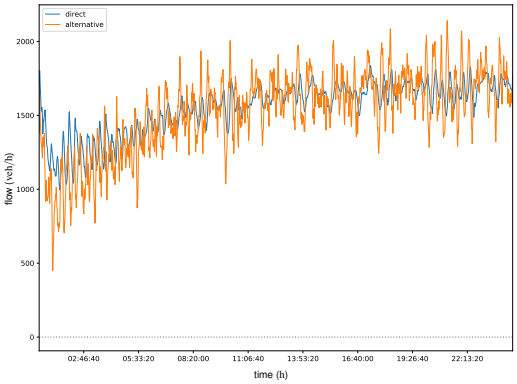


Fig. A.46-5. Traffic flow on each route, in vehicles per hour (veh/h), over a 24 h period.

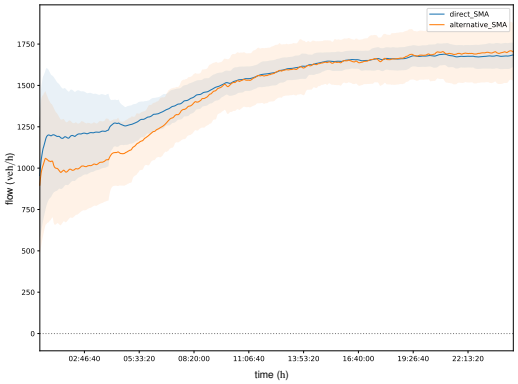


Fig. A.46-6. TrafficTraffic flow on each route, in vehicles per hour (veh/h), over a 24 h period, 4 h Simple Moving Average, mean (line) and standard deviation (shaded).

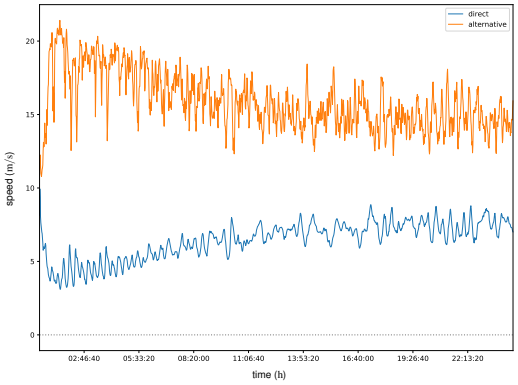


Fig. A.46-7. Mean speed on each route, in meters per second (m/s), aggregated to 1 min, over a 24 h period.

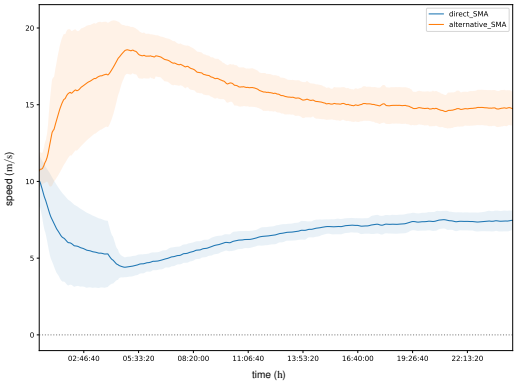


Fig. A.46-8. Mean speed on each route, in meters per second (m/s), aggregated to 1 min, over a 24 h period, 4 h Simple Moving Average, mean (line) and standard deviation (shaded).

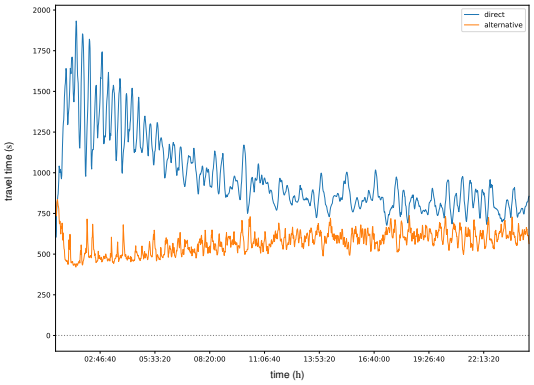


Fig. A.46-9. Travel times on each route, in seconds (s), aggregated to 1 min, over a 24 h period.

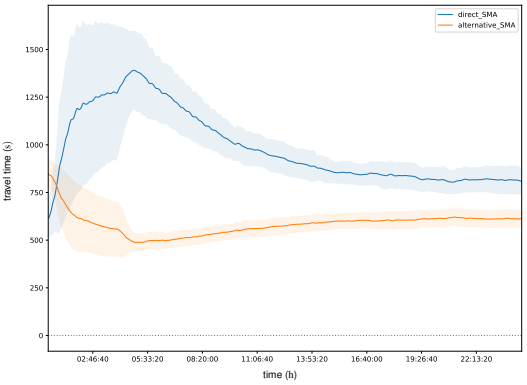


Fig. A.46-10. Travel times on each route, in seconds (s), aggregated to 1 min, over a 24 h period, 4 h Simple Moving Average, mean (line) and standard deviation (shaded).

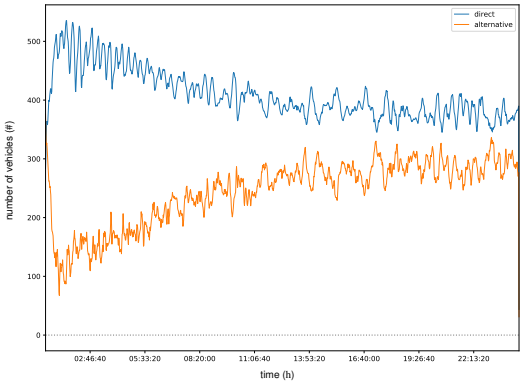


Fig. A.46-11. Average number of vehicles on each route, aggregated to 1 min, over a 24 h period.

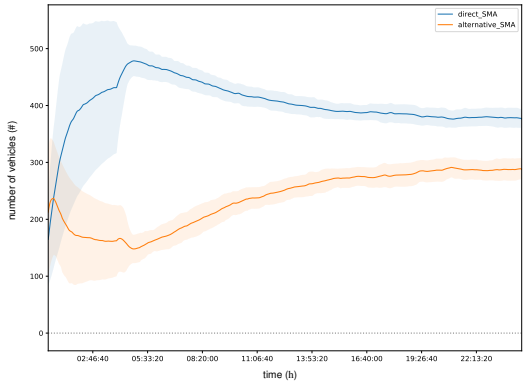


Fig. A.46-12. Average number of vehicles on each route, aggregated to 1 min, over a 24 h period, 4 h Simple Moving Average, mean (line) and standard deviation (shaded).

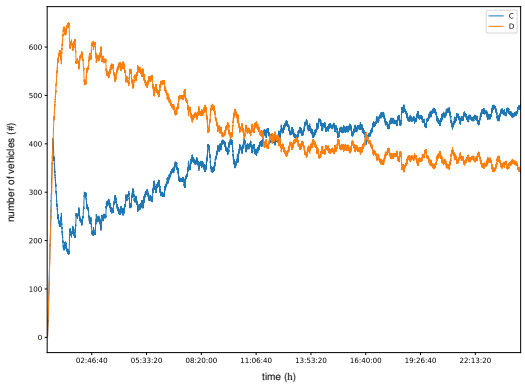


Fig. A.46-13. Evolution of the number of *Cooperators* and *Defectors* over a 24 h period.

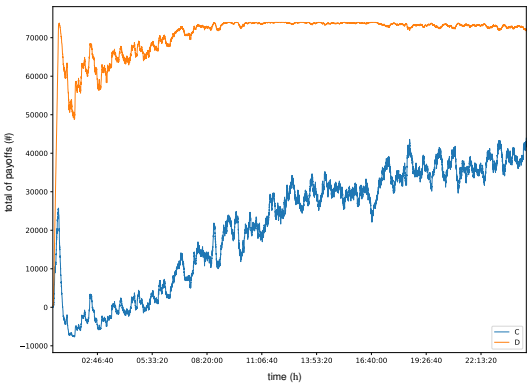


Fig. A.46-14. Evolution of total payoffs for *Cooperators* and *Defectors* (*individual payoff* times the *number of players receiving it*, $C(n) \times n$ and $D(n) \times (N-n)$, where n is the number of *Cooperators*), over a 24 h period.

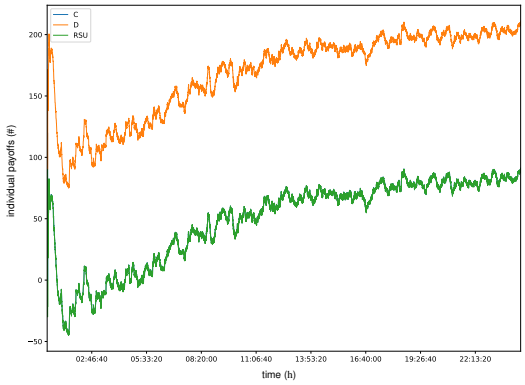


Fig. A.46-15. Evolution of the individual payoffs for *Cooperators, Defectors,* and *RSU* (always cooperating), over a 24 h period.

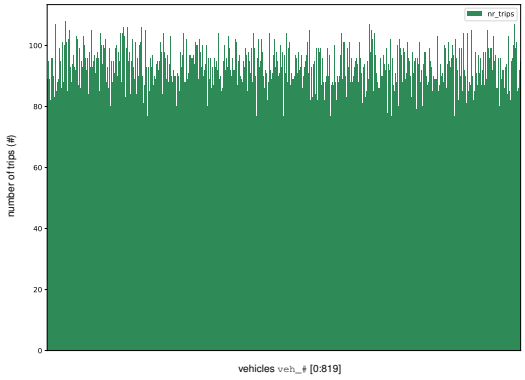


Fig. A.46-16. Number of trips made by each vehicle, during the simulation of a 24 h period.

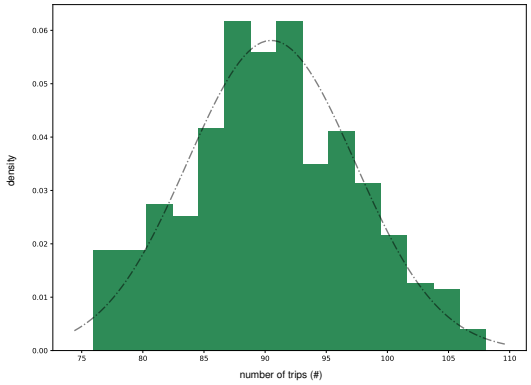


Fig. A.46-17. Density histogram of the number of trips made by each vehicle, during the simulation of a 24 h period, superimposing the normal density curve. The number of bins was calculated by the Freedman Diaconis rule.

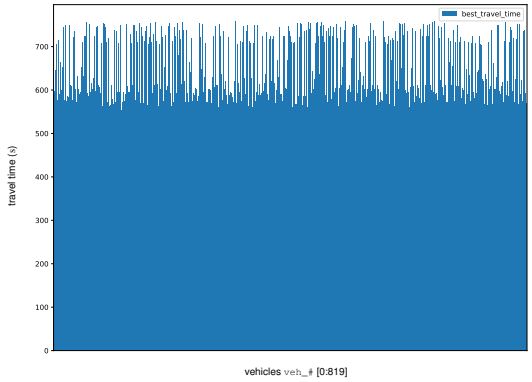


Fig. A.46-18. Best travel time for each vehicle, in seconds (s), during the simulation of a 24 h period.

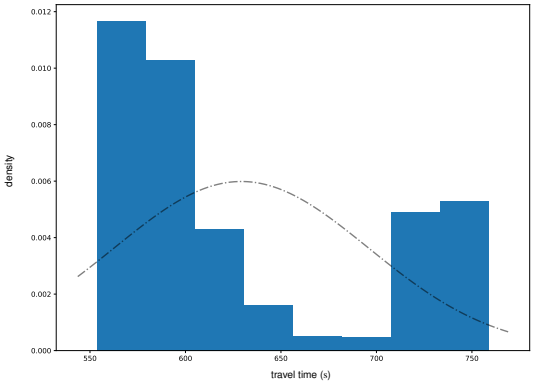


Fig. A.46-19. Density histogram of best travel time for vehicles, in seconds (s), during the simulation of a 24 h period, superimposing the normal density curve. The number of bins was calculated by the Freedman Diaconis rule.

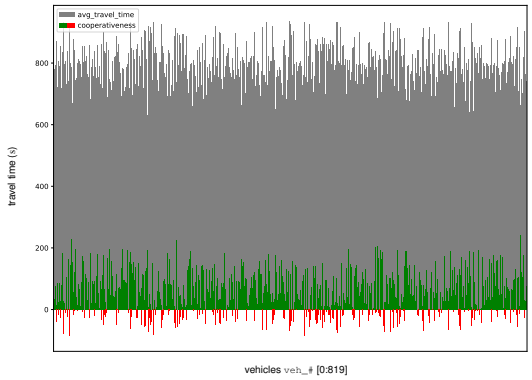


Fig. A.46-20. Average of the travel times, in seconds (s), of individual vehicles, during the simulation of a 24 h period. The bottom graph represents the *degree of cooperativeness**, downscaled by a normalization factor for the purpose of comparison with average times.

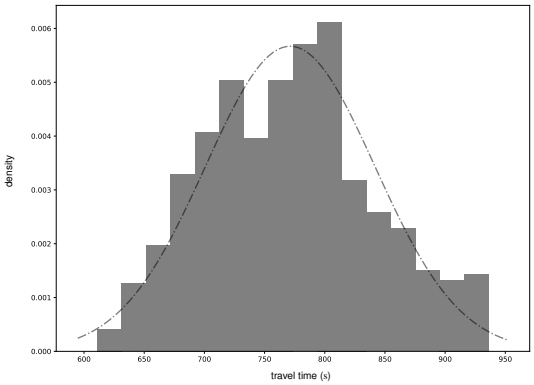


Fig. A.46-21. Density histogram of the average travel times, in seconds (s), of individual vehicles, during the simulation of a 24 h period, superimposing the normal density curve. The number of bins was calculated by the Freedman Diaconis rule.

* The *degree of cooperativeness* is a cumulative sum, calculated at each iteration, based on the complement of the ratio of cooperators, i.e., the higher the number of cooperators the less it increases, but the defectors are more penalized, and vice-versa. It varies inversely with the size of the group to which the player belongs.

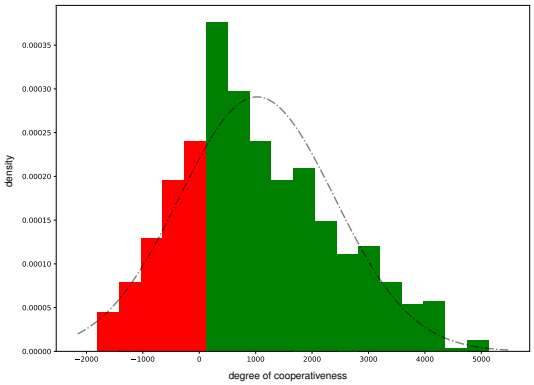


Fig. A.46-22. Density histogram of the *degree of cooperativeness** of individual vehicles, superimposing the normal density curve. The number of bins was calculated by the Freedman Diaconis rule. Generally, when strongly correlated with travel times, it presents a symmetric curve with respect to the *yy*-axis.

A.47 820veh-24h-19040003

```
Scenario: scenario-1
Timestamp: 20210611T061035Z
Number of vehicles: 820 vehs
Simulation time: 24.0 h
Warm up end time: 1866.6 s; step 18665
Vehicle selection strategy: roth_erev
RSU turned off: False
RSU strategy: pigous_example_cooperation_weighted
Runner options:
   nogui: True
   step_length: 0.1
   seed: 19750808
   output_prefix: 820veh-24h-19040003
   sim_run_time: 24.0
   num_vehicles: 820
   warmup_speed: 13.96
   warmup_routes_weight: [473, 527]
   network_speed: 25.0
   change_behavior_probability: [80, 20]
   cooperation_probability: [50, 50]
   vehicle_selection_strategy: roth_erev
   turn_rsu_off: False
   rsu_dynamic_dissemination: False
   rsu_dissemination_interval: 5
   rsu_probabilistic_dissemination: False
   rsu_suggestion_strategy: pigous_example_cooperation_weighted
   rsu_routes_weight: [460, 540]
   rsu_moving_avg_size: 5
   travel_times_ttl: 60
   rsu_dissemination_ttl: 0
   rsu_send_travel_time_info: True
   payoff_matrix: [180.0, 60.0, 0.0, -120.0]
   roth_erev_parameters: [0.1, 0.5]
   rsu_change_dissemination: False
   rsu_change_dissemination_steps: [14400, 28800, 43200, 57600, 72000]
   rsu_change_dissemination_intervals: [10, 20, 40, 80, 160]
Network Mean speed after warmup:
   Max: 11.03
   Min: 8.12
```

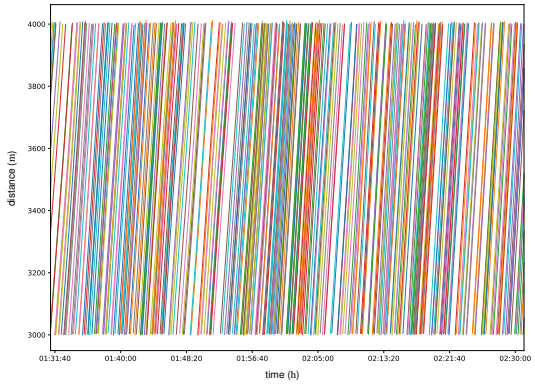


Fig. A.47-1. Time-Space diagram, for the one hour period after the end of the warmup, from 1:00:00 to 2:00:00 simulation time, plotted for the data from the sensor placed in the middle of the *direct* route (between 3000 m and 4000 m). In the case of an overloaded network, congestion shock waves can be observed.

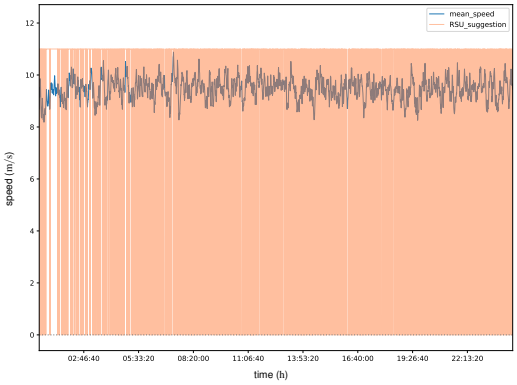


Fig. A.47-2. Mean speed in the network, in meters per second (m/s), over a 24 h period, superimposing (vertically, in orange) the time instants in which the RSU issued a recommendation to follow the *alternative* route.

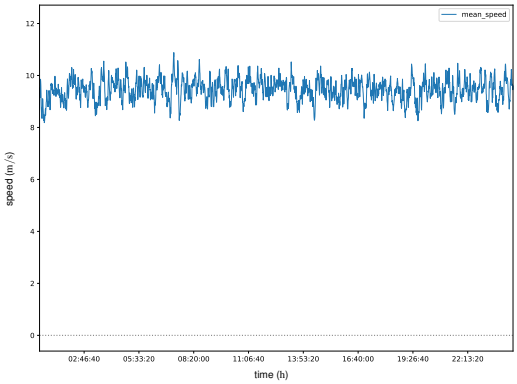


Fig. A.47-3. Mean speed in the network, in meters per second (m/s), over a 24 h period.

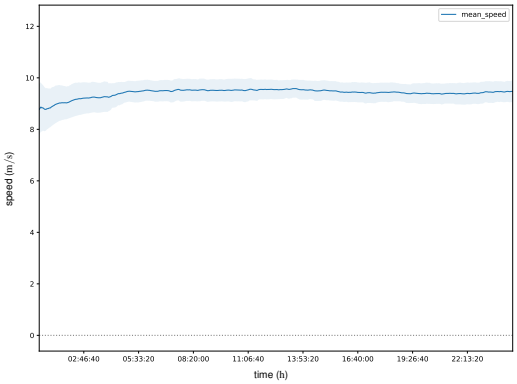


Fig. A.47-4. Mean speed in the network, in meters per second (m/s), over a 24 h period, 4 h Simple Moving Average, mean (line) and standard deviation (shaded).

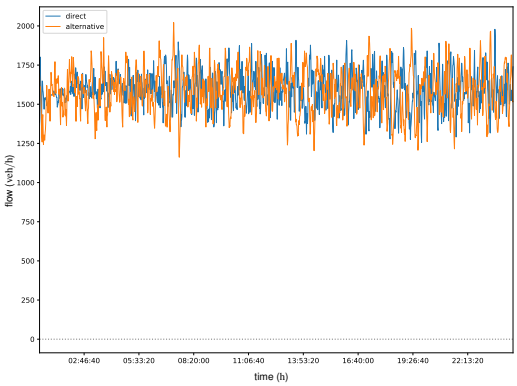


Fig. A.47-5. Traffic flow on each route, in vehicles per hour (veh/h), over a 24 h period.

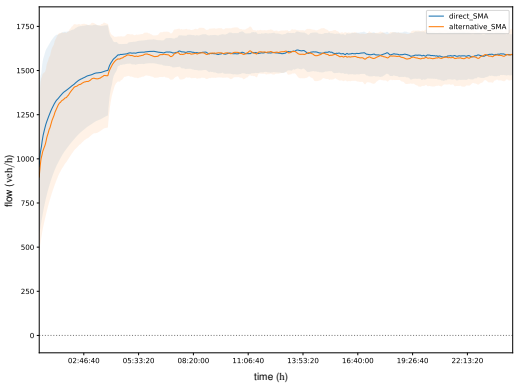


Fig. A.47-6. TrafficTraffic flow on each route, in vehicles per hour (veh/h), over a 24 h period, 4 h Simple Moving Average, mean (line) and standard deviation (shaded).

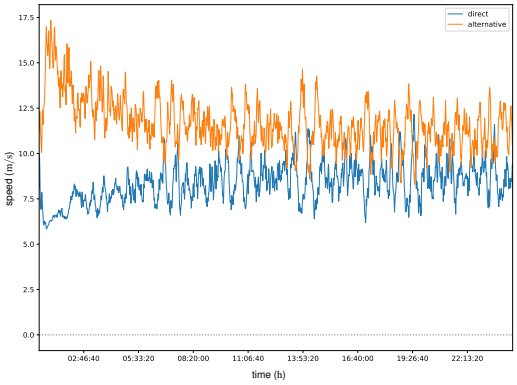


Fig. A.47-7. Mean speed on each route, in meters per second (m/s), aggregated to 1 min, over a 24 h period.

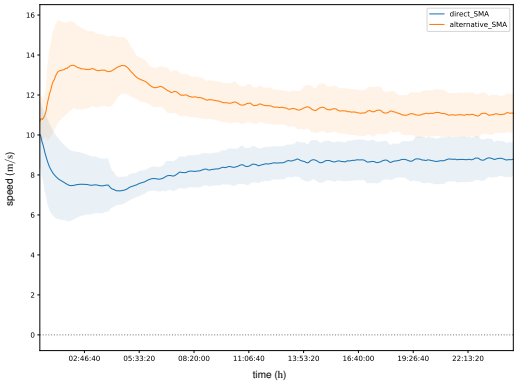


Fig. A.47-8. Mean speed on each route, in meters per second (m/s), aggregated to 1 min, over a 24 h period, 4 h Simple Moving Average, mean (line) and standard deviation (shaded).

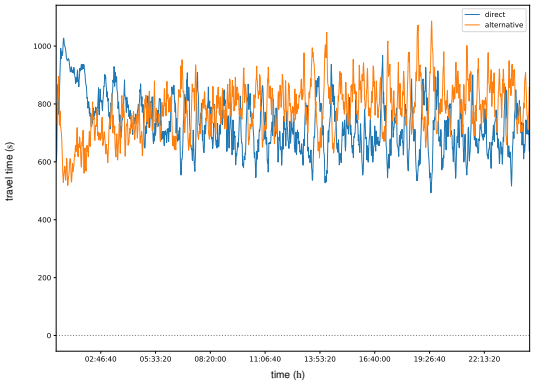


Fig. A.47-9. Travel times on each route, in seconds (s), aggregated to 1 min, over a 24 h period.

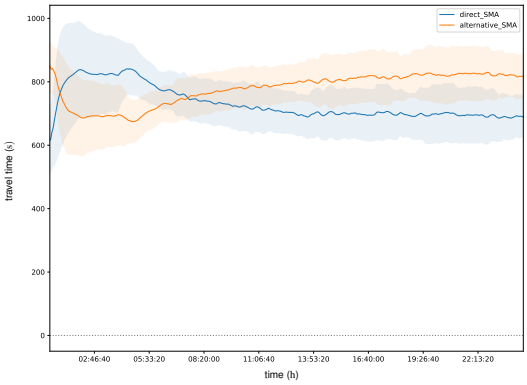


Fig. A.47-10. Travel times on each route, in seconds (s), aggregated to 1 min, over a 24 h period, 4 h Simple Moving Average, mean (line) and standard deviation (shaded).

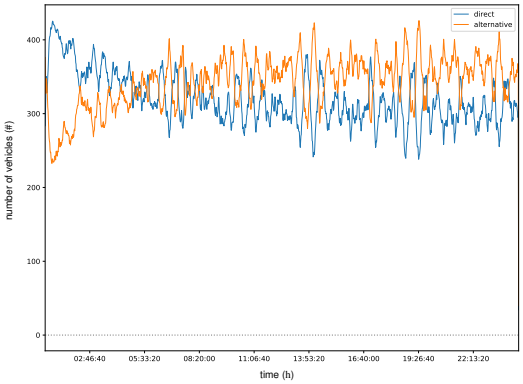


Fig. A.47-11. Average number of vehicles on each route, aggregated to 1 min, over a 24 h period.

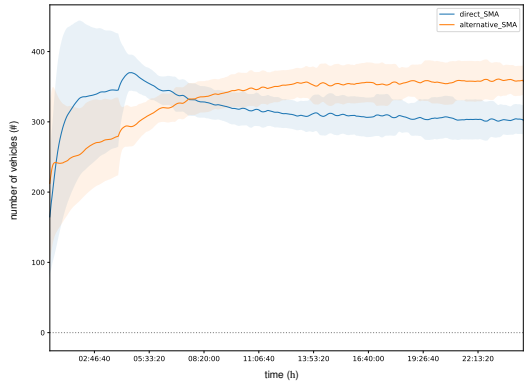


Fig. A.47-12. Average number of vehicles on each route, aggregated to 1 min, over a 24 h period, 4 h Simple Moving Average, mean (line) and standard deviation (shaded).

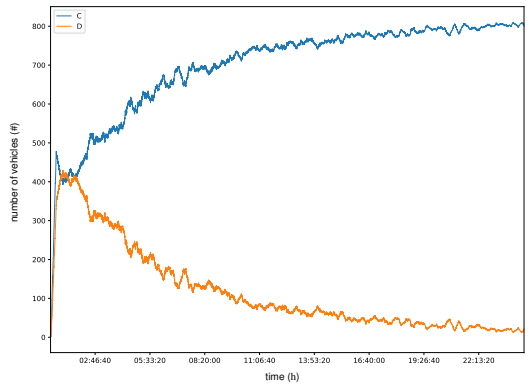


Fig. A.47-13. Evolution of the number of *Cooperators* and *Defectors* over a 24 h period.

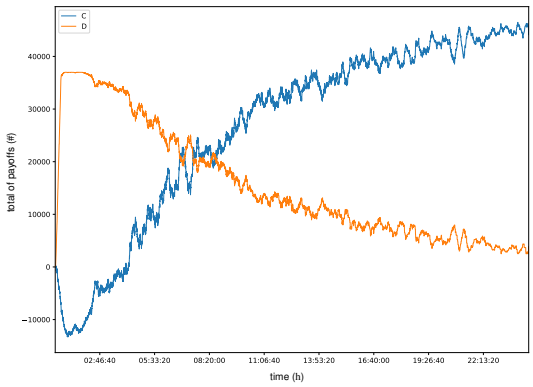


Fig. A.47-14. Evolution of total payoffs for *Cooperators* and *Defectors* (*individual payoff* times the *number of players receiving it*, $C(n) \times n$ and $D(n) \times (N-n)$, where n is the number of *Cooperators*), over a 24 h period.

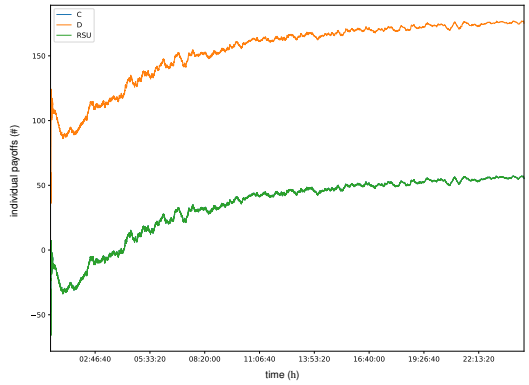


Fig. A.47-15. Evolution of the individual payoffs for *Cooperators, Defectors,* and *RSU* (always cooperating), over a 24 h period.

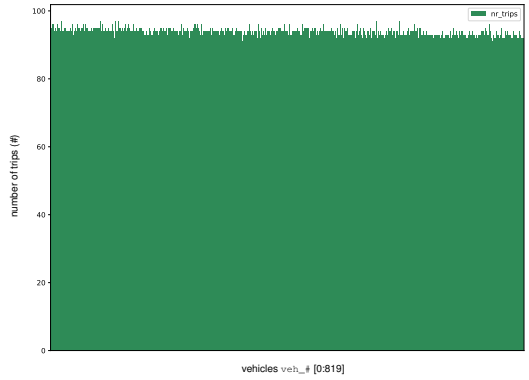


Fig. A.47-16. Number of trips made by each vehicle, during the simulation of a 24 h period.

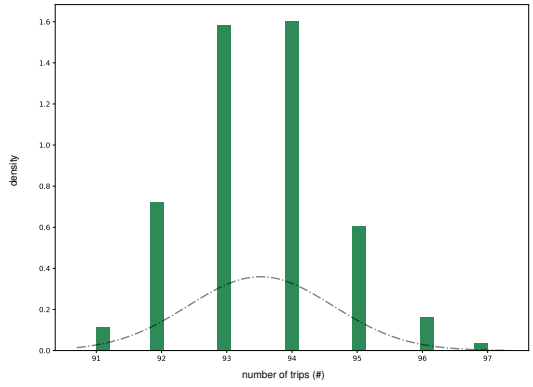


Fig. A.47-17. Density histogram of the number of trips made by each vehicle, during the simulation of a 24 h period, superimposing the normal density curve. The number of bins was calculated by the Freedman Diaconis rule.

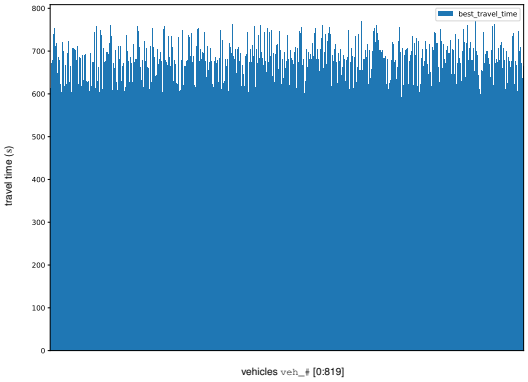


Fig. A.47-18. Best travel time for each vehicle, in seconds (s), during the simulation of a 24 h period.

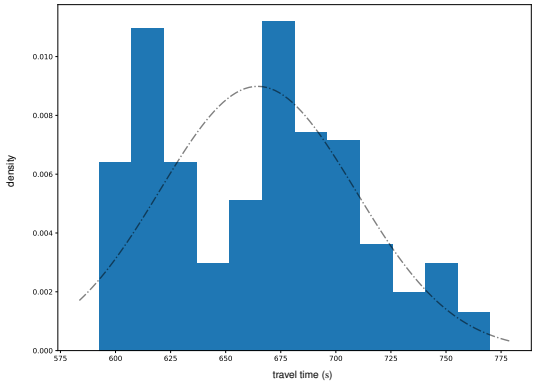


Fig. A.47-19. Density histogram of best travel time for vehicles, in seconds (s), during the simulation of a 24 h period, superimposing the normal density curve. The number of bins was calculated by the Freedman Diaconis rule.

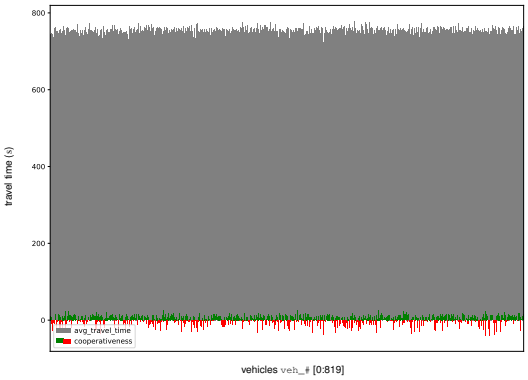


Fig. A.47-20. Average of the travel times, in seconds (s), of individual vehicles, during the simulation of a 24 h period. The bottom graph represents the *degree of cooperativeness**, downscaled by a normalization factor for the purpose of comparison with average times.

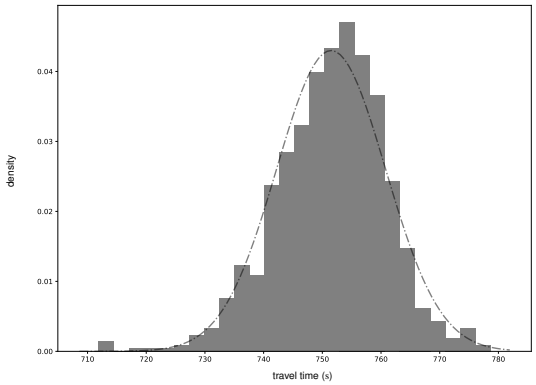


Fig. A.47-21. Density histogram of the average travel times, in seconds (s), of individual vehicles, during the simulation of a 24 h period, superimposing the normal density curve. The number of bins was calculated by the Freedman Diaconis rule.

* The *degree of cooperativeness* is a cumulative sum, calculated at each iteration, based on the complement of the ratio of cooperators, i.e., the higher the number of cooperators the less it increases, but the defectors are more penalized, and vice-versa. It varies inversely with the size of the group to which the player belongs.

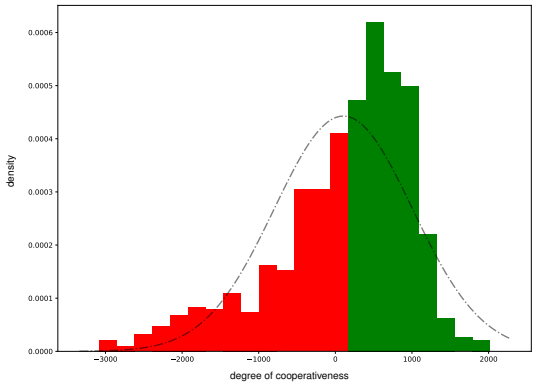


Fig. A.47-22. Density histogram of the *degree of cooperativeness** of individual vehicles, superimposing the normal density curve. The number of bins was calculated by the Freedman Diaconis rule. Generally, when strongly correlated with travel times, it presents a symmetric curve with respect to the *yy*-axis.

A.48 `820veh-24h-19040008`

```
Scenario: scenario-1
Timestamp: 20210611T034245Z
Number of vehicles: 820 vehs
Simulation time: 24.0 h
Warm up end time: 1866.6 s; step 18665
Vehicle selection strategy: roth_erev
RSU turned off: False
RSU strategy: pigous_example_cooperation_weighted
Runner options:
   nogui: True
   step_length: 0.1
   seed: 19750808
   output_prefix: 820veh-24h-19040008
   sim_run_time: 24.0
   num_vehicles: 820
   warmup_speed: 13.96
   warmup_routes_weight: [473, 527]
   network_speed: 25.0
   change_behavior_probability: [100, 0]
   cooperation_probability: [50, 50]
   vehicle_selection_strategy: roth_erev
   turn_rsu_off: False
   rsu_dynamic_dissemination: False
   rsu_dissemination_interval: 5
   rsu_probabilistic_dissemination: False
   rsu_suggestion_strategy: pigous_example_cooperation_weighted
   rsu_routes_weight: [460, 540]
   rsu_moving_avg_size: 5
   travel_times_ttl: 60
   rsu_dissemination_ttl: 0
   rsu_send_travel_time_info: False
   payoff_matrix: [180.0, 60.0, 0.0, -120.0]
   roth_erev_parameters: [0.1, 0.2]
   rsu_change_dissemination: False
   rsu_change_dissemination_steps: [14400, 28800, 43200, 57600, 72000]
   rsu_change_dissemination_intervals: [10, 20, 40, 80, 160]
Network Mean speed after warmup:
   Max: 11.95
   Min: 4.51
```

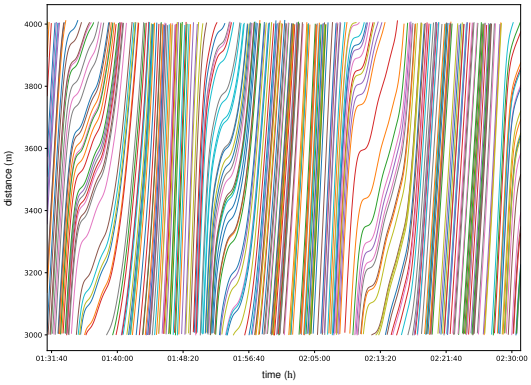


Fig. A.48-1. Time-Space diagram, for the one hour period after the end of the warmup, from 1:00:00 to 2:00:00 simulation time, plotted for the data from the sensor placed in the middle of the *direct* route (between 3000 m and 4000 m). In the case of an overloaded network, congestion shock waves can be observed.

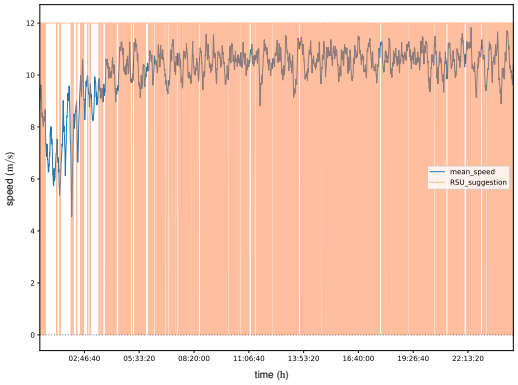


Fig. A.48-2. Mean speed in the network, in meters per second (m/s), over a 24 h period, superimposing (vertically, in orange) the time instants in which the RSU issued a recommendation to follow the *alternative* route.

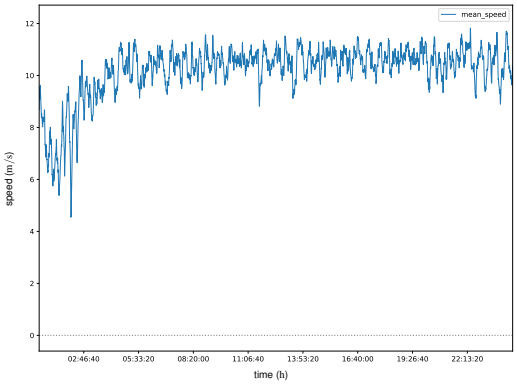


Fig. A.48-3. Mean speed in the network, in meters per second (m/s), over a 24 h period.

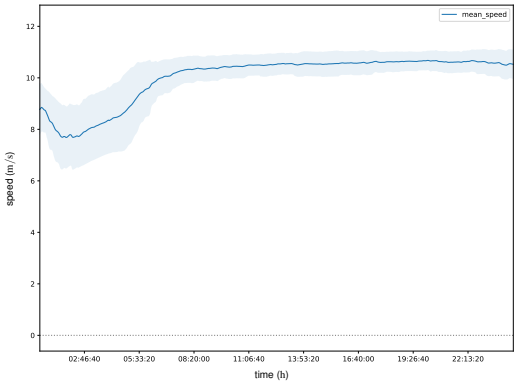


Fig. A.48-4. Mean speed in the network, in meters per second (m/s), over a 24 h period, 4 h Simple Moving Average, mean (line) and standard deviation (shaded).

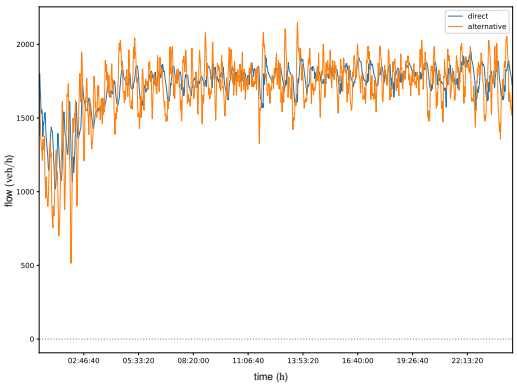


Fig. A.48-5. Traffic flow on each route, in vehicles per hour (veh/h), over a 24 h period.

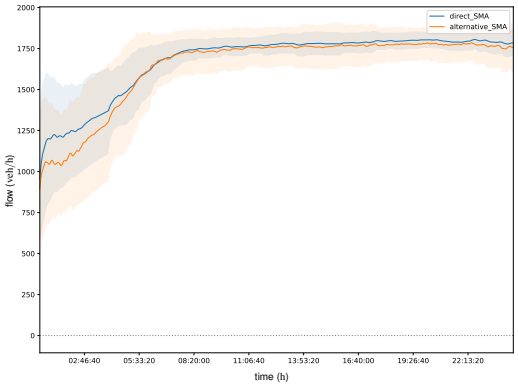


Fig. A.48-6. TrafficTraffic flow on each route, in vehicles per hour (veh/h), over a 24 h period, 4 h Simple Moving Average, mean (line) and standard deviation (shaded).

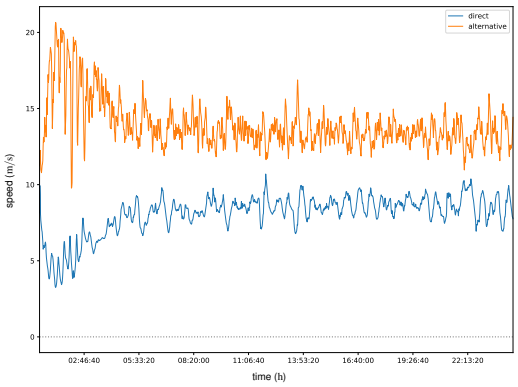


Fig. A.48-7. Mean speed on each route, in meters per second (m/s), aggregated to 1 min, over a 24 h period.

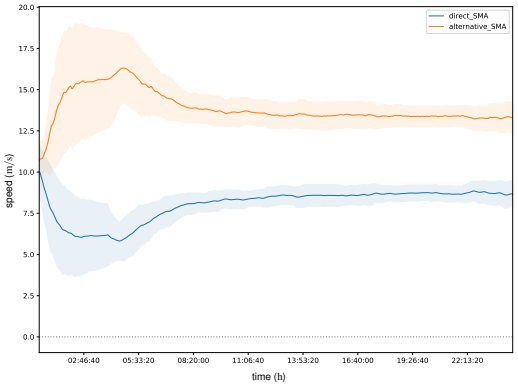


Fig. A.48-8. Mean speed on each route, in meters per second (m/s), aggregated to 1 min, over a 24 h period, 4 h Simple Moving Average, mean (line) and standard deviation (shaded).

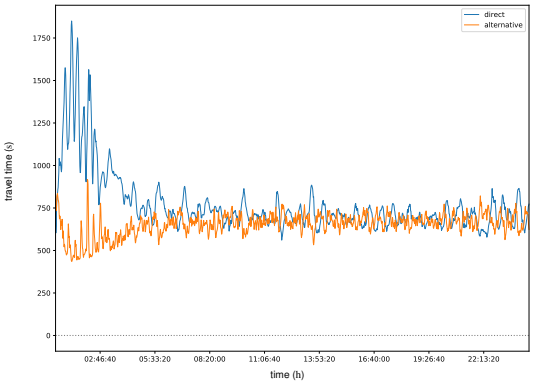


Fig. A.48-9. Travel times on each route, in seconds (s), aggregated to 1 min, over a 24 h period.

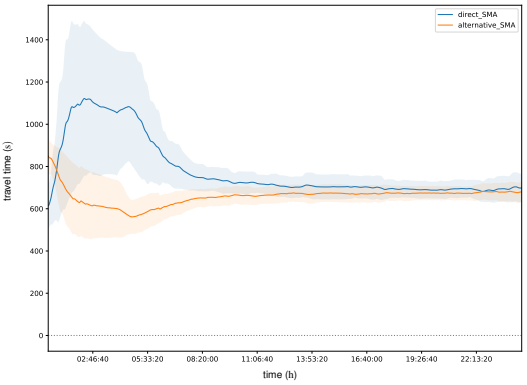


Fig. A.48-10. Travel times on each route, in seconds (s), aggregated to 1 min, over a 24 h period, 4 h Simple Moving Average, mean (line) and standard deviation (shaded).

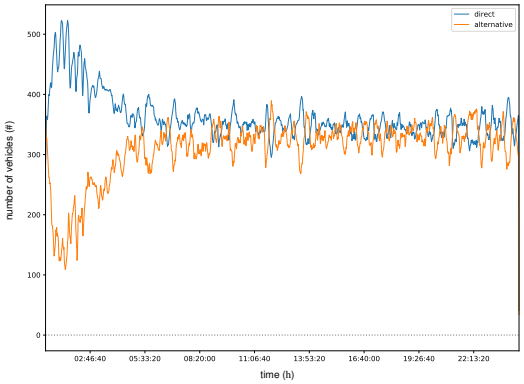


Fig. A.48-11. Average number of vehicles on each route, aggregated to 1 min, over a 24 h period.

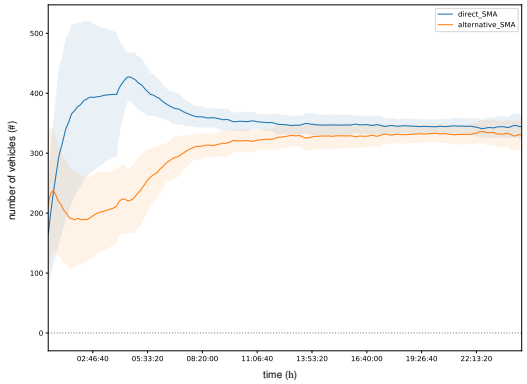


Fig. A.48-12. Average number of vehicles on each route, aggregated to 1 min, over a 24 h period, 4 h Simple Moving Average, mean (line) and standard deviation (shaded).

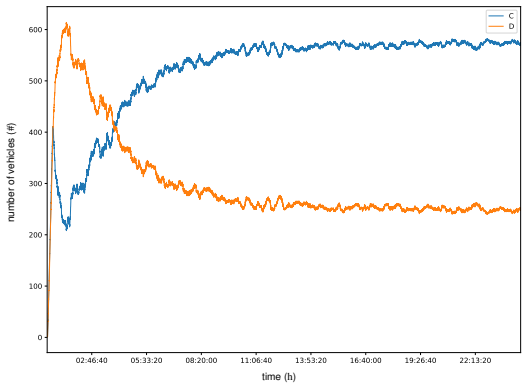


Fig. A.48-13. Evolution of the number of *Cooperators* and *Defectors* over a 24 h period.

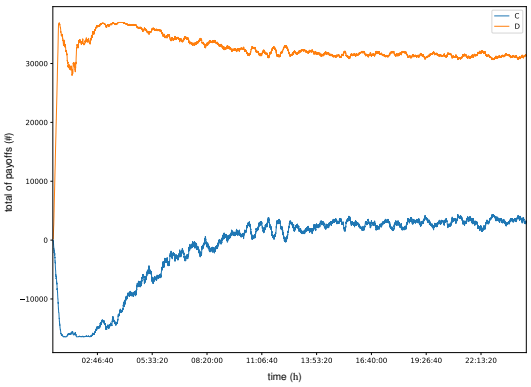


Fig. A.48-14. Evolution of total payoffs for *Cooperators* and *Defectors* (*individual payoff* times the *number of players receiving it*, $C(n) \times n$ and $D(n) \times (N-n)$, where n is the number of *Cooperators*), over a 24 h period.

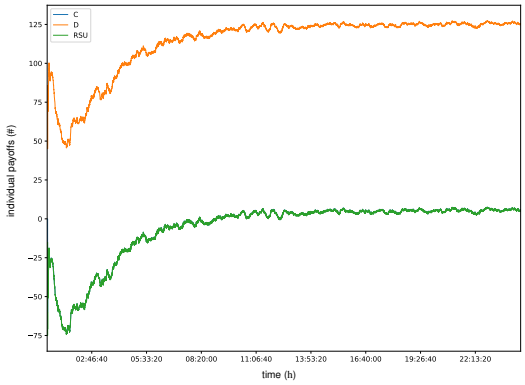


Fig. A.48-15. Evolution of the individual payoffs for *Cooperators, Defectors,* and *RSU* (always cooperating), over a 24 h period.

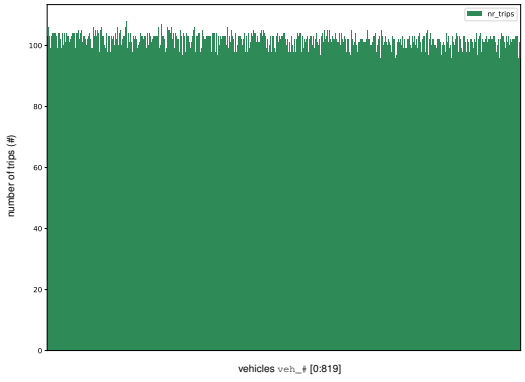


Fig. A.48-16. Number of trips made by each vehicle, during the simulation of a 24 h period.

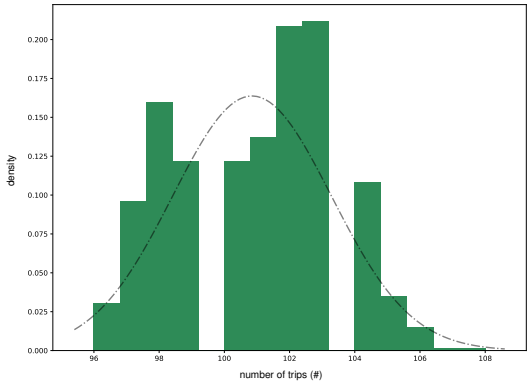


Fig. A.48-17. Density histogram of the number of trips made by each vehicle, during the simulation of a 24 h period, superimposing the normal density curve. The number of bins was calculated by the Freedman Diaconis rule.

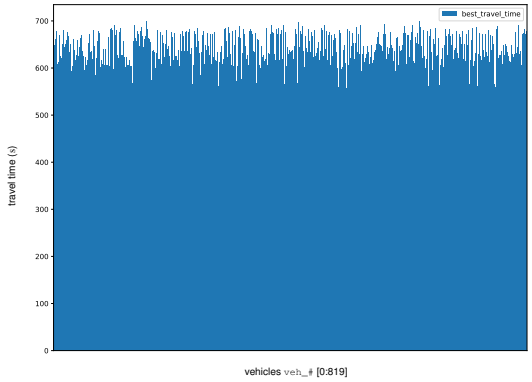


Fig. A.48-18. Best travel time for each vehicle, in seconds (s), during the simulation of a 24 h period.

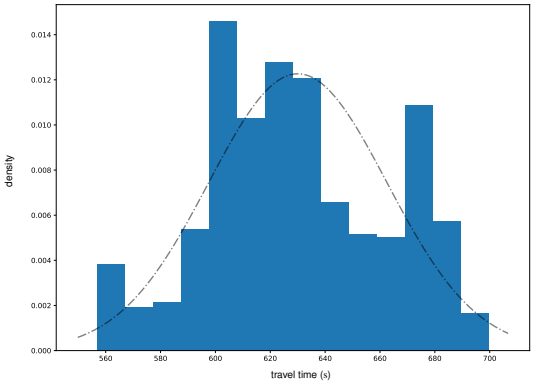


Fig. A.48-19. Density histogram of best travel time for vehicles, in seconds (s), during the simulation of a 24 h period, superimposing the normal density curve. The number of bins was calculated by the Freedman Diaconis rule.

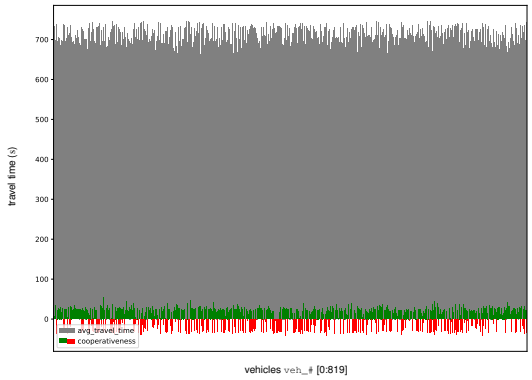


Fig. A.48-20. Average of the travel times, in seconds (s), of individual vehicles, during the simulation of a 24 h period. The bottom graph represents the *degree of cooperativeness**, downscaled by a normalization factor for the purpose of comparison with average times.

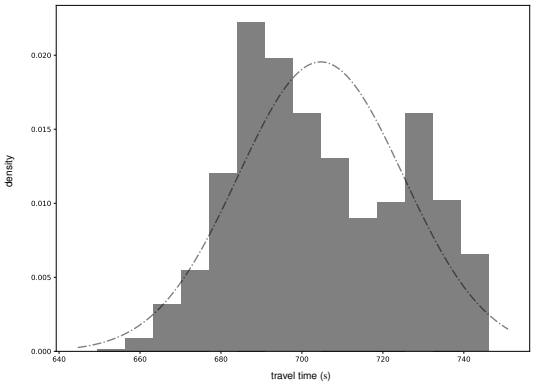


Fig. A.48-21. Density histogram of the average travel times, in seconds (s), of individual vehicles, during the simulation of a 24 h period, superimposing the normal density curve. The number of bins was calculated by the Freedman Diaconis rule.

* The *degree of cooperativeness* is a cumulative sum, calculated at each iteration, based on the complement of the ratio of cooperators, i.e., the higher the number of cooperators the less it increases, but the defectors are more penalized, and vice-versa. It varies inversely with the size of the group to which the player belongs.

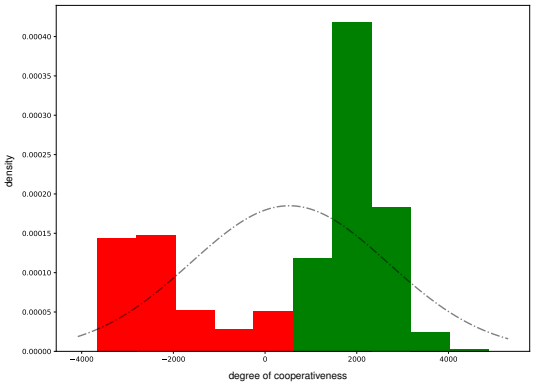


Fig. A.48-22. Density histogram of the *degree of cooperativeness** of individual vehicles, superimposing the normal density curve. The number of bins was calculated by the Freedman Diaconis rule. Generally, when strongly correlated with travel times, it presents a symmetric curve with respect to the *yy*-axis.

A.49 820veh-24h-19040010

```
Scenario: scenario-1
Timestamp: 20210610T223959Z
Number of vehicles: 820 vehs
Simulation time: 24.0 h
Warm up end time: 1866.6 s; step 18665
Vehicle selection strategy: roth_erev
RSU turned off: False
RSU strategy: pigous_example_cooperation_weighted
Runner options:
   nogui: True
   step_length: 0.1
   seed: 19750808
   output_prefix: 820veh-24h-19040010
   sim_run_time: 24.0
   num_vehicles: 820
   warmup_speed: 13.96
   warmup_routes_weight: [473, 527]
   network_speed: 25.0
   change_behavior_probability: [100, 0]
   cooperation_probability: [50, 50]
   vehicle_selection_strategy: roth_erev
   turn_rsu_off: False
   rsu_dynamic_dissemination: False
   rsu_dissemination_interval: 5
   rsu_probabilistic_dissemination: False
   rsu_suggestion_strategy: pigous_example_cooperation_weighted
   rsu_routes_weight: [460, 540]
   rsu_moving_avg_size: 5
   travel_times_ttl: 60
   rsu_dissemination_ttl: 0
   rsu_send_travel_time_info: False
   payoff_matrix: [180.0, 60.0, 0.0, -120.0]
   roth_erev_parameters: [0.1, 0.5]
   rsu_change_dissemination: False
   rsu_change_dissemination_steps: [14400, 28800, 43200, 57600, 72000]
   rsu_change_dissemination_intervals: [10, 20, 40, 80, 160]
Network Mean speed after warmup:
   Max: 11.83
   Min: 4.86
```

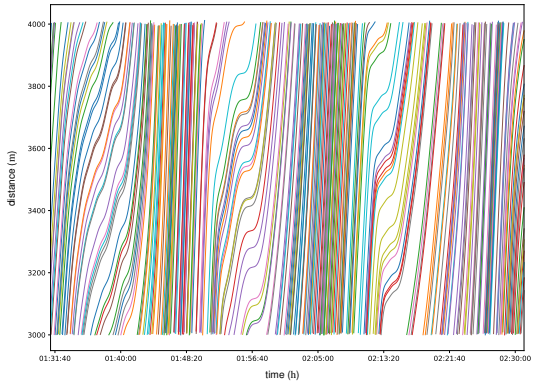


Fig. A.49-1. Time-Space diagram, for the one hour period after the end of the warmup, from 1:00:00 to 2:00:00 simulation time, plotted for the data from the sensor placed in the middle of the *direct* route (between 3000 m and 4000 m). In the case of an overloaded network, congestion shock waves can be observed.

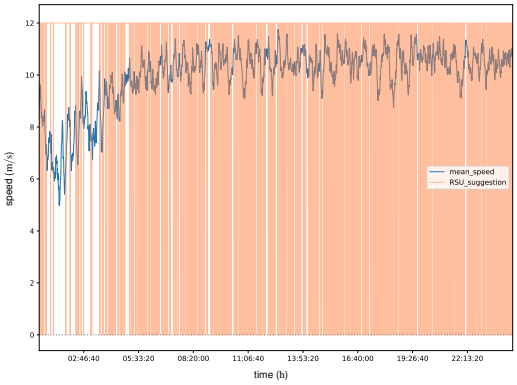


Fig. A.49-2. Mean speed in the network, in meters per second (m/s), over a 24 h period, superimposing (vertically, in orange) the time instants in which the RSU issued a recommendation to follow the *alternative* route.

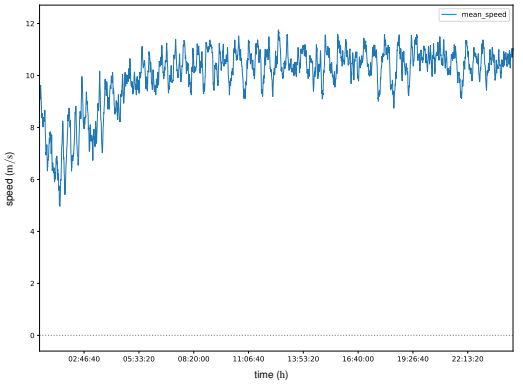


Fig. A.49-3. Mean speed in the network, in meters per second (m/s), over a 24 h period.

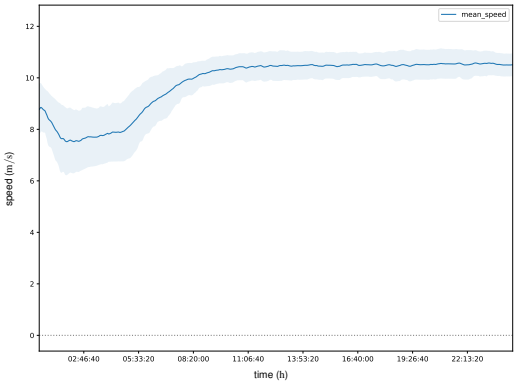


Fig. A.49-4. Mean speed in the network, in meters per second (m/s), over a 24 h period, 4 h Simple Moving Average, mean (line) and standard deviation (shaded).

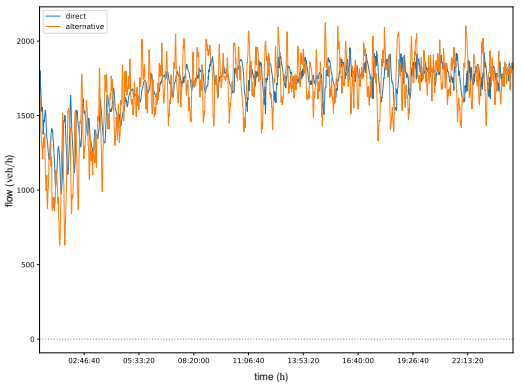


Fig. A.49-5. Traffic flow on each route, in vehicles per hour (veh/h), over a 24 h period.

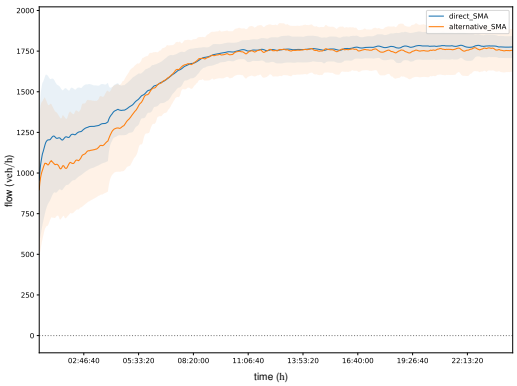


Fig. A.49-6. TrafficTraffic flow on each route, in vehicles per hour (veh/h), over a 24 h period, 4 h Simple Moving Average, mean (line) and standard deviation (shaded).

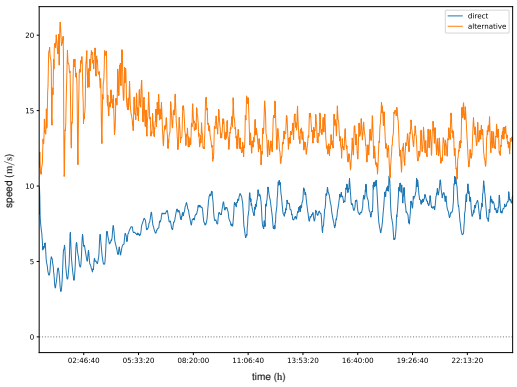


Fig. A.49-7. Mean speed on each route, in meters per second (m/s), aggregated to 1 min, over a 24 h period.

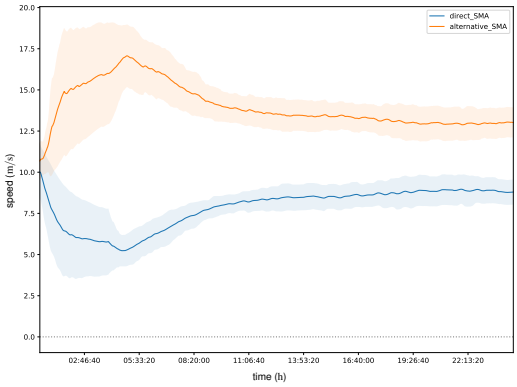


Fig. A.49-8. Mean speed on each route, in meters per second (m/s), aggregated to 1 min, over a 24 h period, 4 h Simple Moving Average, mean (line) and standard deviation (shaded).

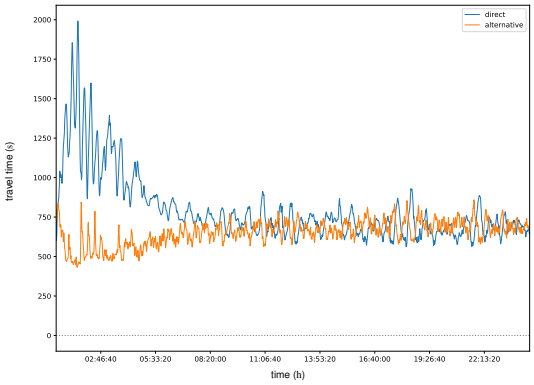


Fig. A.49-9. Travel times on each route, in seconds (s), aggregated to 1 min, over a 24 h period.

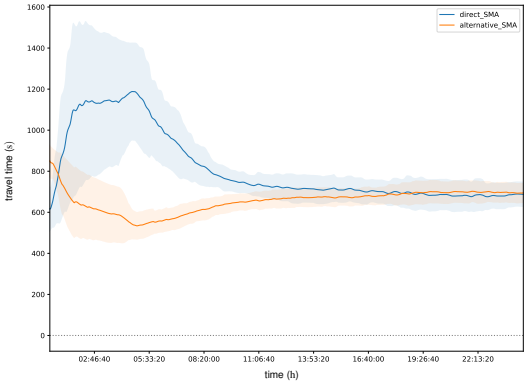


Fig. A.49-10. Travel times on each route, in seconds (s), aggregated to 1 min, over a 24 h period, 4 h Simple Moving Average, mean (line) and standard deviation (shaded).

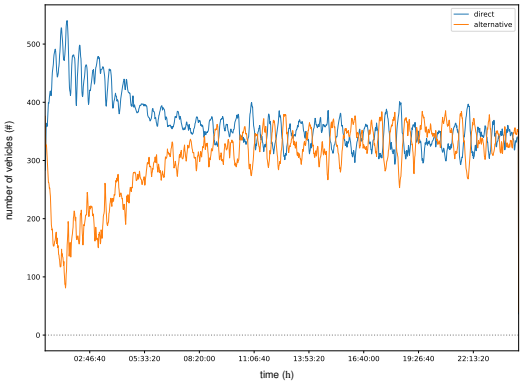


Fig. A.49-11. Average number of vehicles on each route, aggregated to 1 min, over a 24 h period.

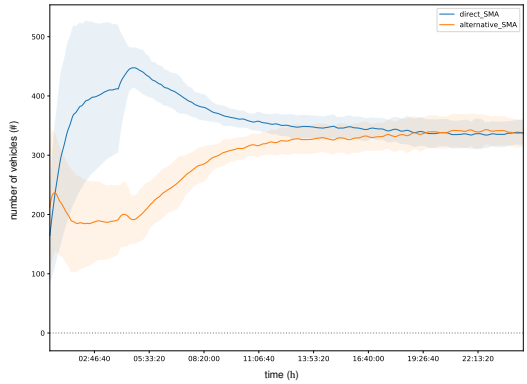


Fig. A.49-12. Average number of vehicles on each route, aggregated to 1 min, over a 24 h period, 4 h Simple Moving Average, mean (line) and standard deviation (shaded).

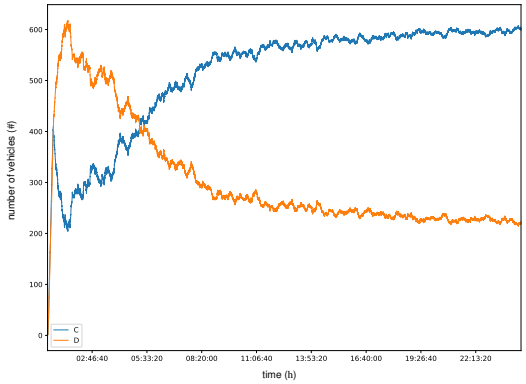


Fig. A.49-13. Evolution of the number of *Cooperators* and *Defectors* over a 24 h period.

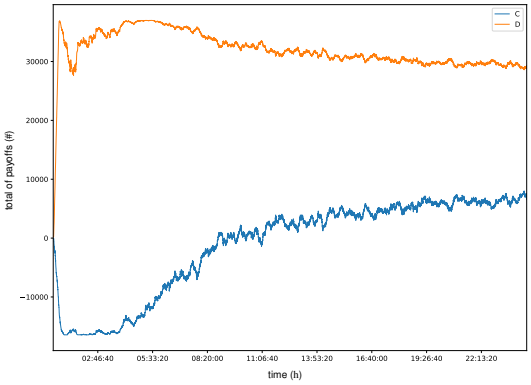


Fig. A.49-14. Evolution of total payoffs for *Cooperators* and *Defectors* (*individual payoff* times the *number of players receiving it*, $C(n) \times n$ and $D(n) \times (N-n)$, where n is the number of *Cooperators*), over a 24 h period.

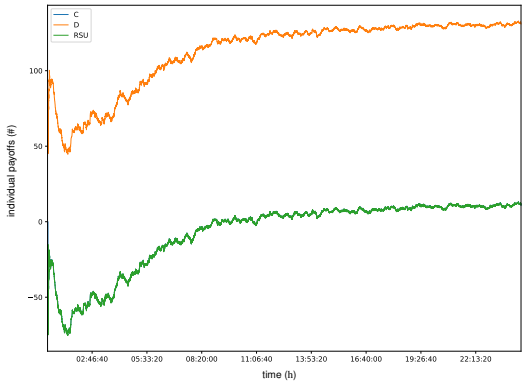


Fig. A.49-15. Evolution of the individual payoffs for *Cooperators, Defectors,* and *RSU* (always cooperating), over a 24 h period.

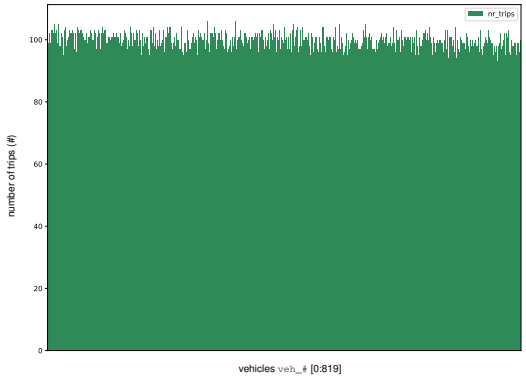


Fig. A.49-16. Number of trips made by each vehicle, during the simulation of a 24 h period.

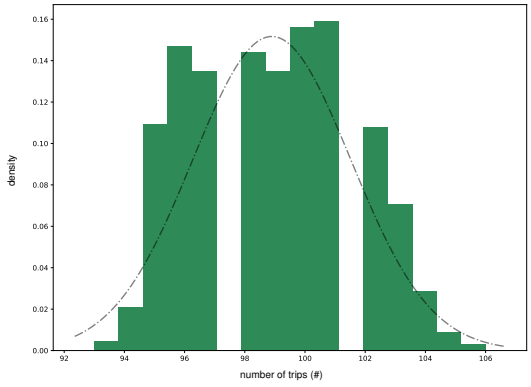


Fig. A.49-17. Density histogram of the number of trips made by each vehicle, during the simulation of a 24 h period, superimposing the normal density curve. The number of bins was calculated by the Freedman Diaconis rule.

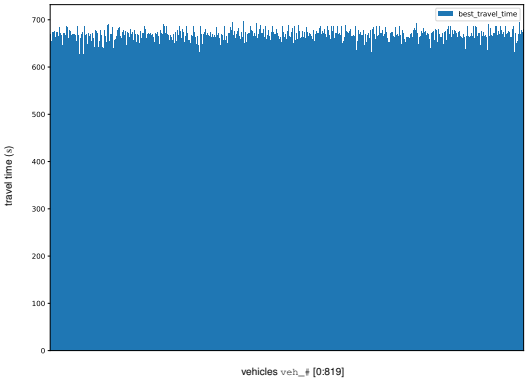


Fig. A.49-18. Best travel time for each vehicle, in seconds (s), during the simulation of a 24 h period.

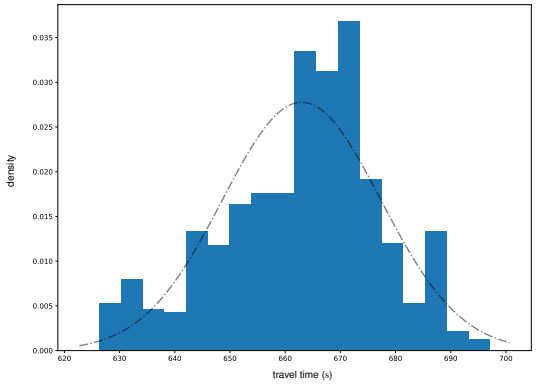


Fig. A.49-19. Density histogram of best travel time for vehicles, in seconds (s), during the simulation of a 24 h period, superimposing the normal density curve. The number of bins was calculated by the Freedman Diaconis rule.

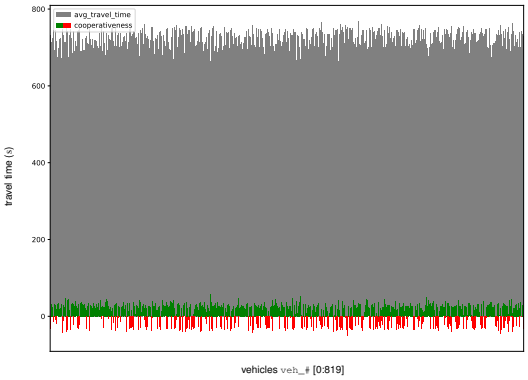


Fig. A.49-20. Average of the travel times, in seconds (s), of individual vehicles, during the simulation of a 24 h period. The bottom graph represents the *degree of cooperativeness**, downscaled by a normalization factor for the purpose of comparison with average times.

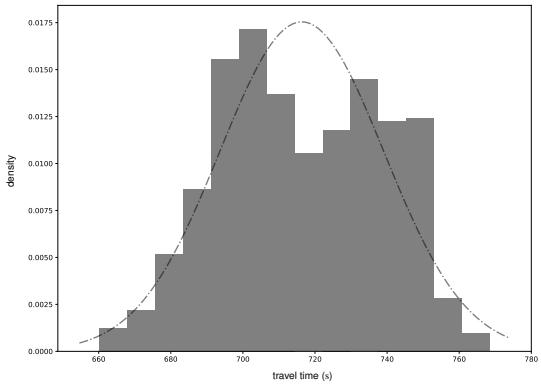


Fig. A.49-21. Density histogram of the average travel times, in seconds (s), of individual vehicles, during the simulation of a 24 h period, superimposing the normal density curve. The number of bins was calculated by the Freedman Diaconis rule.

* The *degree of cooperativeness* is a cumulative sum, calculated at each iteration, based on the complement of the ratio of cooperators, i.e., the higher the number of cooperators the less it increases, but the defectors are more penalized, and vice-versa. It varies inversely with the size of the group to which the player belongs.

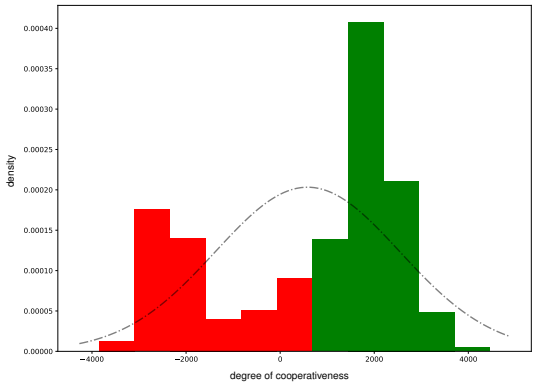


Fig. A.49-22. Density histogram of the *degree of cooperativeness** of individual vehicles, superimposing the normal density curve. The number of bins was calculated by the Freedman Diaconis rule. Generally, when strongly correlated with travel times, it presents a symmetric curve with respect to the *yy*-axis.

A.50 820veh-24h-19040011

```
Scenario: scenario-1
Timestamp: 20210611T010855Z
Number of vehicles: 820 vehs
Simulation time: 24.0 h
Warm up end time: 1866.6 s; step 18665
Vehicle selection strategy: roth_erev
RSU turned off: False
RSU strategy: pigous_example_cooperation_weighted
Runner options:
   nogui: True
   step_length: 0.1
   seed: 19750808
   output_prefix: 820veh-24h-19040011
   sim_run_time: 24.0
   num_vehicles: 820
   warmup_speed: 13.96
   warmup_routes_weight: [473, 527]
   network_speed: 25.0
   change_behavior_probability: [100, 0]
   cooperation_probability: [50, 50]
   vehicle_selection_strategy: roth_erev
   turn_rsu_off: False
   rsu_dynamic_dissemination: False
   rsu_dissemination_interval: 5
   rsu_probabilistic_dissemination: False
   rsu_suggestion_strategy: pigous_example_cooperation_weighted
   rsu_routes_weight: [460, 540]
   rsu_moving_avg_size: 5
   travel_times_ttl: 60
   rsu_dissemination_ttl: 0
   rsu_send_travel_time_info: False
   payoff_matrix: [180.0, 60.0, 0.0, -120.0]
   roth_erev_parameters: [0.5, 0.5]
   rsu_change_dissemination: False
   rsu_change_dissemination_steps: [14400, 28800, 43200, 57600, 72000]
   rsu_change_dissemination_intervals: [10, 20, 40, 80, 160]
Network Mean speed after warmup:
   Max: 11.95
   Min: 6.01
```

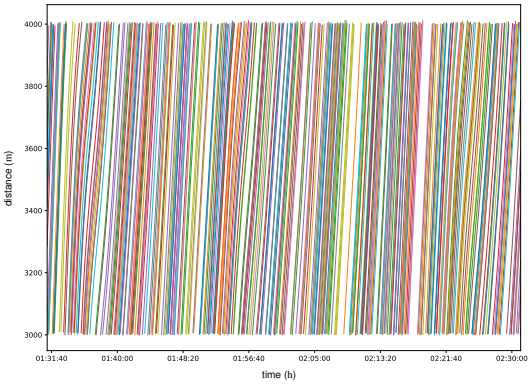


Fig. A.50-1. Time-Space diagram, for the one hour period after the end of the warmup, from 1:00:00 to 2:00:00 simulation time, plotted for the data from the sensor placed in the middle of the *direct* route (between 3000 m and 4000 m). In the case of an overloaded network, congestion shock waves can be observed.

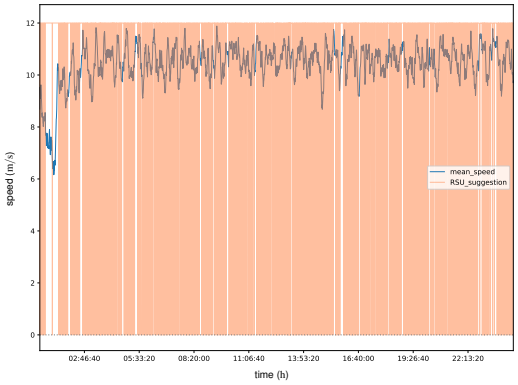


Fig. A.50-2. Mean speed in the network, in meters per second (m/s), over a 24 h period, superimposing (vertically, in orange) the time instants in which the RSU issued a recommendation to follow the *alternative* route.

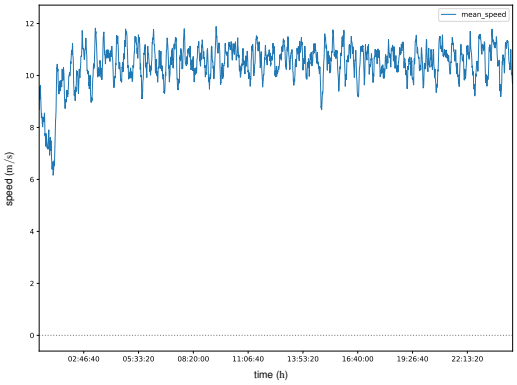


Fig. A.50-3. Mean speed in the network, in meters per second (m/s), over a 24 h period.

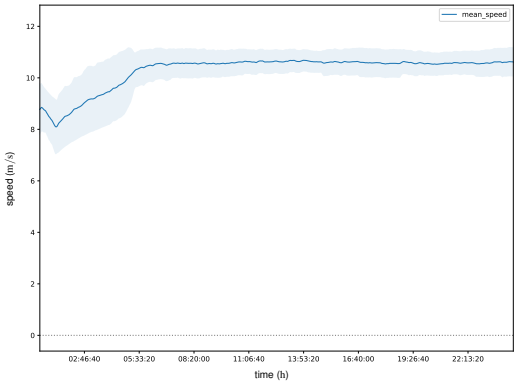


Fig. A.50-4. Mean speed in the network, in meters per second (m/s), over a 24 h period, 4 h Simple Moving Average, mean (line) and standard deviation (shaded).

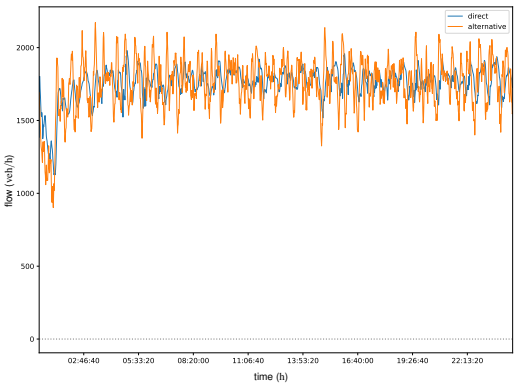


Fig. A.50-5. Traffic flow on each route, in vehicles per hour (veh/h), over a 24 h period.

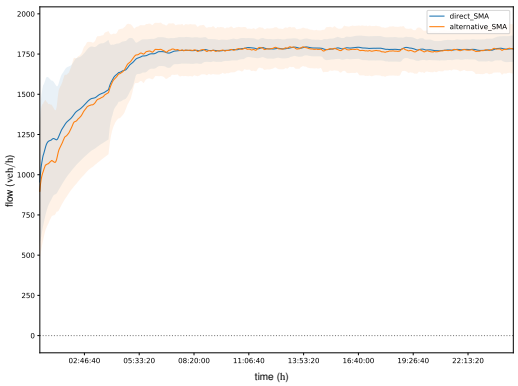


Fig. A.50-6. TrafficTraffic flow on each route, in vehicles per hour (veh/h), over a 24 h period, 4 h Simple Moving Average, mean (line) and standard deviation (shaded).

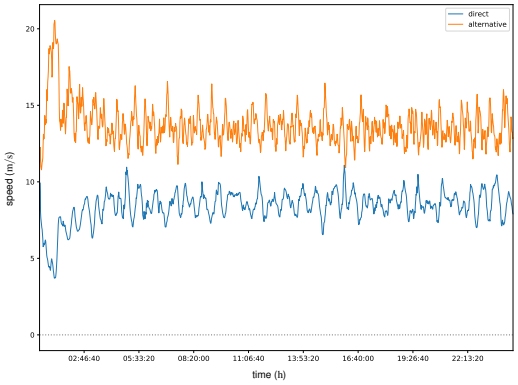


Fig. A.50-7. Mean speed on each route, in meters per second (m/s), aggregated to 1 min, over a 24 h period.

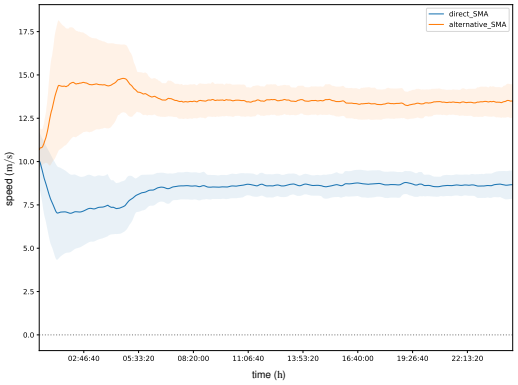


Fig. A.50-8. Mean speed on each route, in meters per second (m/s), aggregated to 1 min, over a 24 h period, 4 h Simple Moving Average, mean (line) and standard deviation (shaded).

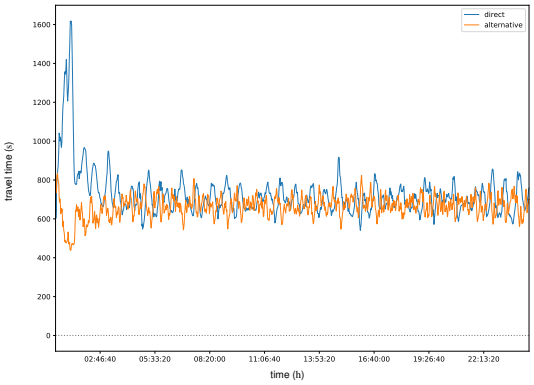


Fig. A.50-9. Travel times on each route, in seconds (s), aggregated to 1 min, over a 24 h period.

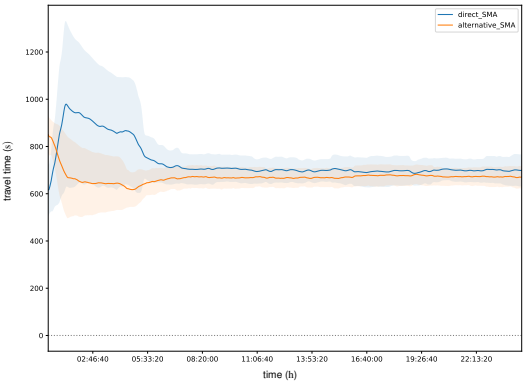


Fig. A.50-10. Travel times on each route, in seconds (s), aggregated to 1 min, over a 24 h period, 4 h Simple Moving Average, mean (line) and standard deviation (shaded).

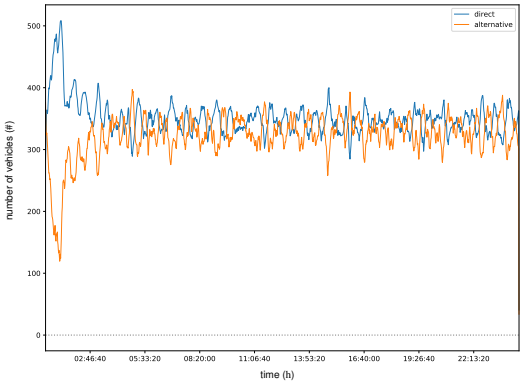


Fig. A.50-11. Average number of vehicles on each route, aggregated to 1 min, over a 24 h period.

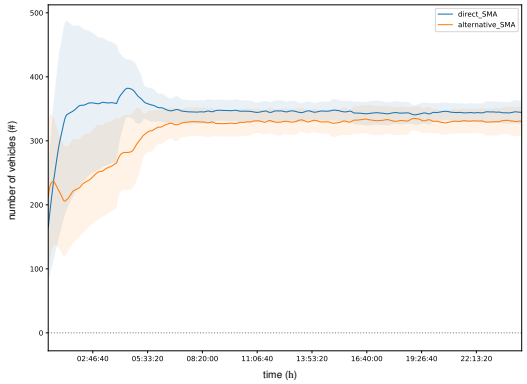


Fig. A.50-12. Average number of vehicles on each route, aggregated to 1 min, over a 24 h period, 4 h Simple Moving Average, mean (line) and standard deviation (shaded).

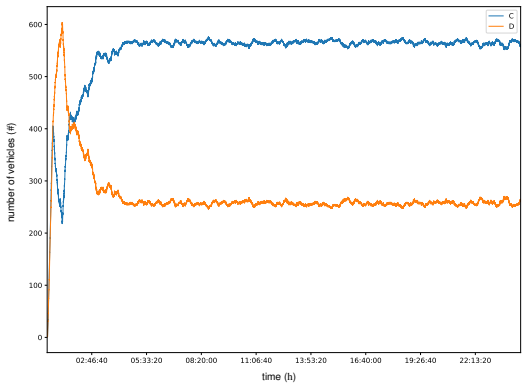


Fig. A.50-13. Evolution of the number of *Cooperators* and *Defectors* over a 24 h period.

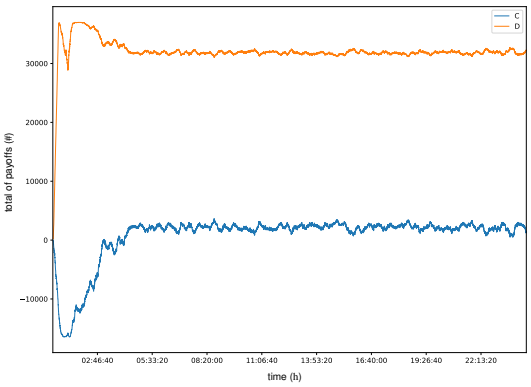


Fig. A.50-14. Evolution of total payoffs for *Cooperators* and *Defectors* (*individual payoff* times the *number of players receiving it*, $C(n) \times n$ and $D(n) \times (N-n)$, where n is the number of *Cooperators*), over a 24 h period.

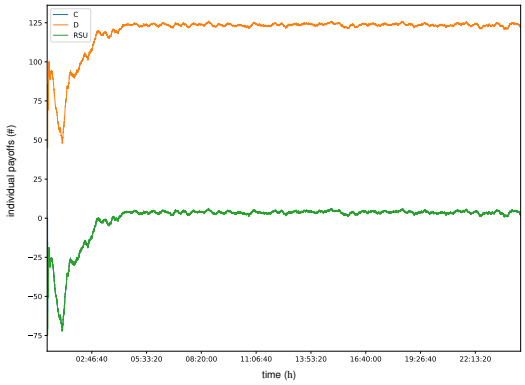


Fig. A.50-15. Evolution of the individual payoffs for *Cooperators, Defectors,* and *RSU* (always cooperating), over a 24 h period.

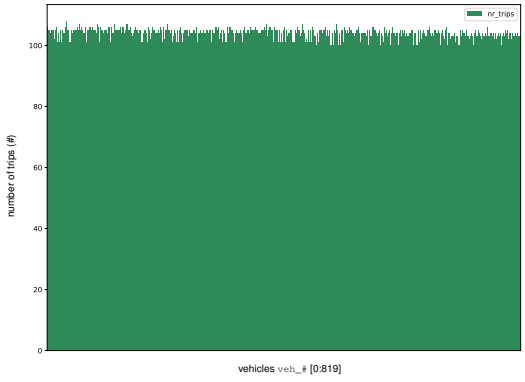


Fig. A.50-16. Number of trips made by each vehicle, during the simulation of a 24 h period.

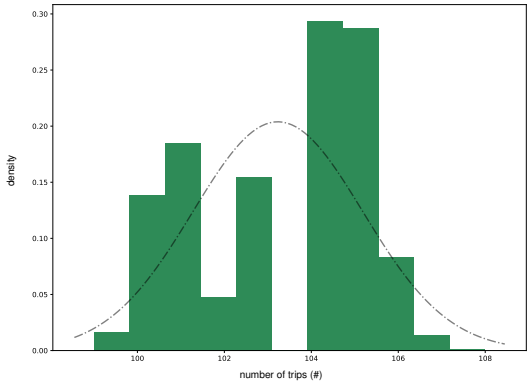


Fig. A.50-17. Density histogram of the number of trips made by each vehicle, during the simulation of a 24 h period, superimposing the normal density curve. The number of bins was calculated by the Freedman Diaconis rule.

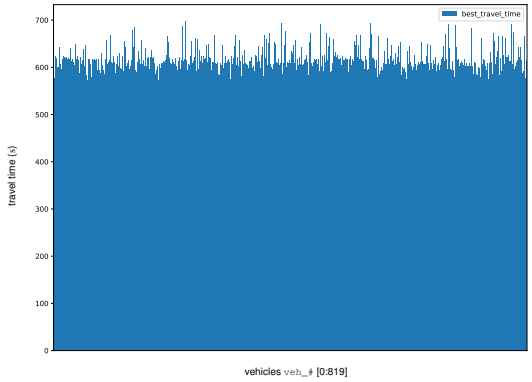


Fig. A.50-18. Best travel time for each vehicle, in seconds (s), during the simulation of a 24 h period.

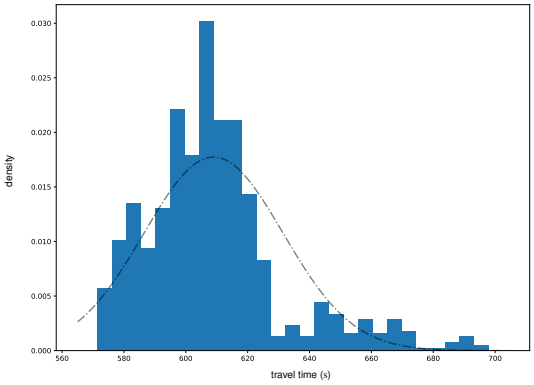


Fig. A.50-19. Density histogram of best travel time for vehicles, in seconds (s), during the simulation of a 24 h period, superimposing the normal density curve. The number of bins was calculated by the Freedman Diaconis rule.

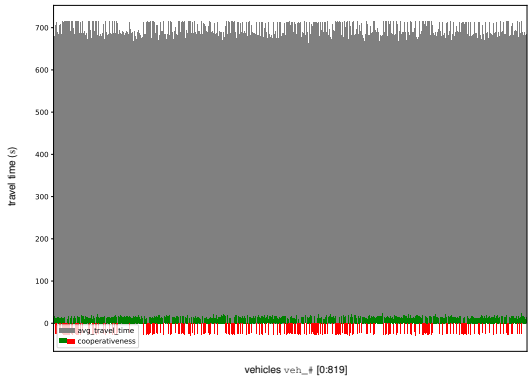


Fig. A.50-20. Average of the travel times, in seconds (s), of individual vehicles, during the simulation of a 24 h period. The bottom graph represents the *degree of cooperativeness**, downscaled by a normalization factor for the purpose of comparison with average times.

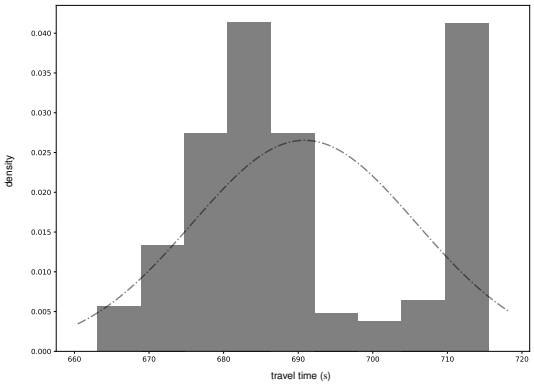


Fig. A.50-21. Density histogram of the average travel times, in seconds (s), of individual vehicles, during the simulation of a 24 h period, superimposing the normal density curve. The number of bins was calculated by the Freedman Diaconis rule.

* The *degree of cooperativeness* is a cumulative sum, calculated at each iteration, based on the complement of the ratio of cooperators, i.e., the higher the number of cooperators the less it increases, but the defectors are more penalized, and vice-versa. It varies inversely with the size of the group to which the player belongs.

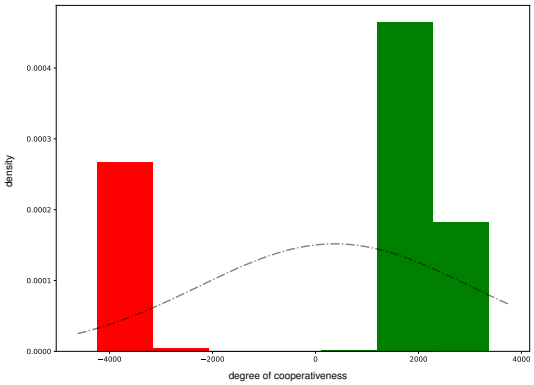


Fig. A.50-22. Density histogram of the *degree of cooperativeness** of individual vehicles, superimposing the normal density curve. The number of bins was calculated by the Freedman Diaconis rule. Generally, when strongly correlated with travel times, it presents a symmetric curve with respect to the *yy*-axis.

A.51 820veh-24h-19040012

```
Scenario: scenario-1
Timestamp: 20210611T033704Z
Number of vehicles: 820 vehs
Simulation time: 24.0 h
Warm up end time: 1866.6 s; step 18665
Vehicle selection strategy: roth_erev
RSU turned off: False
RSU strategy: pigous_example_cooperation_weighted
Runner options:
   nogui: True
   step_length: 0.1
   seed: 19750808
   output_prefix: 820veh-24h-19040012
   sim_run_time: 24.0
   num_vehicles: 820
   warmup_speed: 13.96
   warmup_routes_weight: [473, 527]
   network_speed: 25.0
   change_behavior_probability: [100, 0]
   cooperation_probability: [50, 50]
   vehicle_selection_strategy: roth_erev
   turn_rsu_off: False
   rsu_dynamic_dissemination: False
   rsu_dissemination_interval: 5
   rsu_probabilistic_dissemination: False
   rsu_suggestion_strategy: pigous_example_cooperation_weighted
   rsu_routes_weight: [460, 540]
   rsu_moving_avg_size: 5
   travel_times_ttl: 60
   rsu_dissemination_ttl: 0
   rsu_send_travel_time_info: False
   payoff_matrix: [180.0, 60.0, 0.0, -120.0]
   roth_erev_parameters: [0.2, 0.5]
   rsu_change_dissemination: False
   rsu_change_dissemination_steps: [14400, 28800, 43200, 57600, 72000]
   rsu_change_dissemination_intervals: [10, 20, 40, 80, 160]
Network Mean speed after warmup:
   Max: 11.97
   Min: 4.61
```

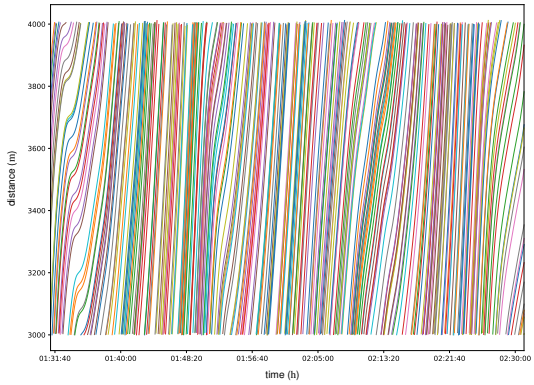


Fig. A.51-1. Time-Space diagram, for the one hour period after the end of the warmup, from 1:00:00 to 2:00:00 simulation time, plotted for the data from the sensor placed in the middle of the *direct* route (between 3000 m and 4000 m). In the case of an overloaded network, congestion shock waves can be observed.

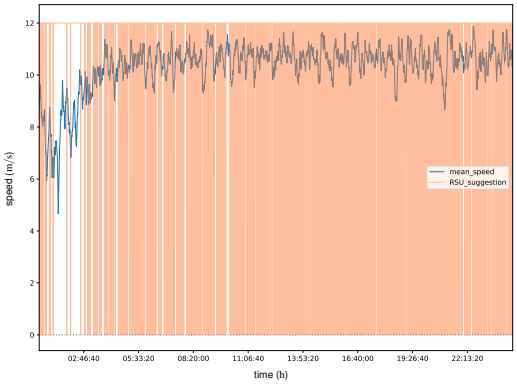


Fig. A.51-2. Mean speed in the network, in meters per second (m/s), over a 24 h period, superimposing (vertically, in orange) the time instants in which the RSU issued a recommendation to follow the *alternative* route.

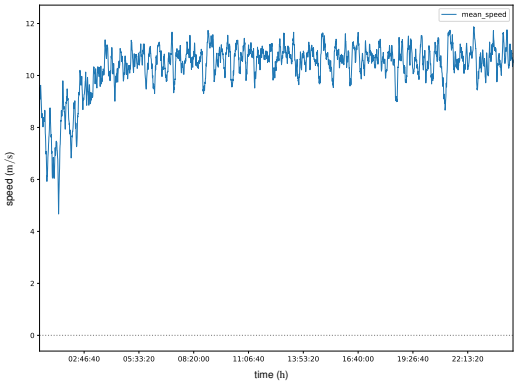


Fig. A.51-3. Mean speed in the network, in meters per second (m/s), over a 24 h period.

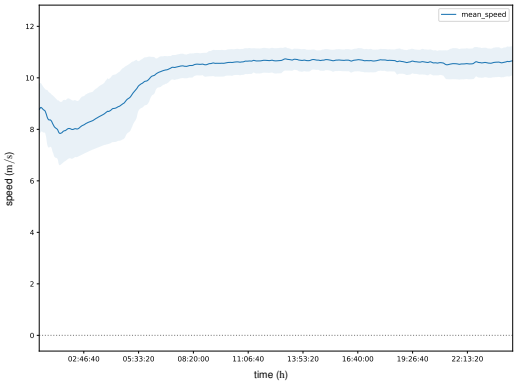


Fig. A.51-4. Mean speed in the network, in meters per second (m/s), over a 24 h period, 4 h Simple Moving Average, mean (line) and standard deviation (shaded).

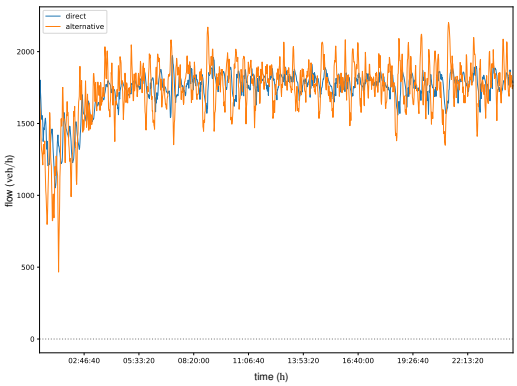


Fig. A.51-5. Traffic flow on each route, in vehicles per hour (veh/h), over a 24 h period.

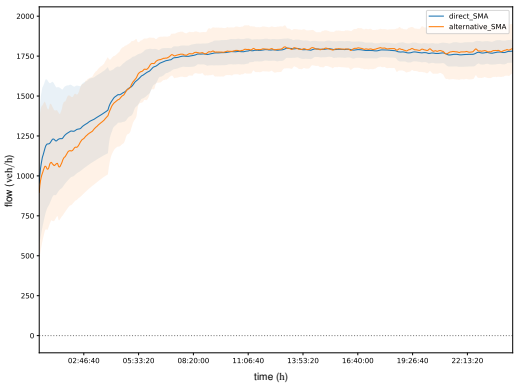


Fig. A.51-6. TrafficTraffic flow on each route, in vehicles per hour (veh/h), over a 24 h period, 4 h Simple Moving Average, mean (line) and standard deviation (shaded).

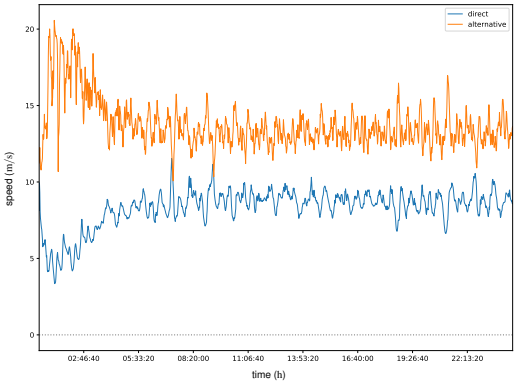


Fig. A.51-7. Mean speed on each route, in meters per second (m/s), aggregated to 1 min, over a 24 h period.

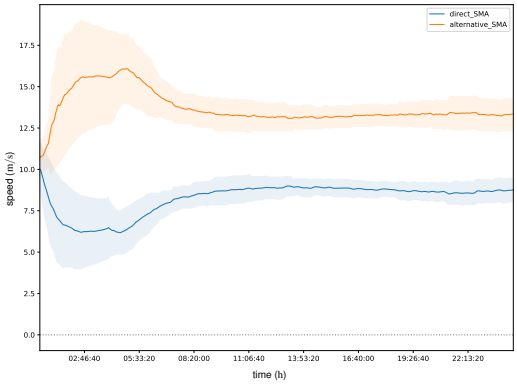


Fig. A.51-8. Mean speed on each route, in meters per second (m/s), aggregated to 1 min, over a 24 h period, 4 h Simple Moving Average, mean (line) and standard deviation (shaded).

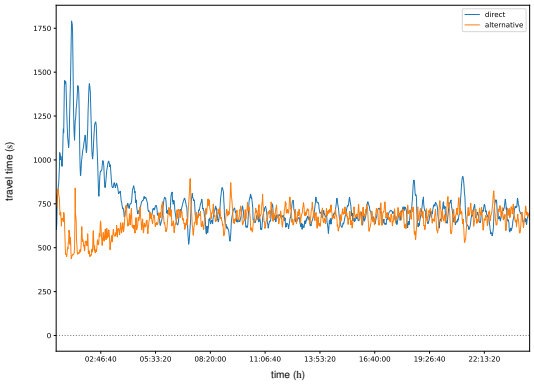


Fig. A.51-9. Travel times on each route, in seconds (s), aggregated to 1 min, over a 24 h period.

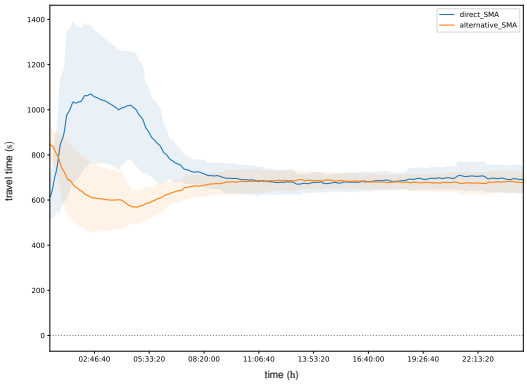


Fig. A.51-10. Travel times on each route, in seconds (s), aggregated to 1 min, over a 24 h period, 4 h Simple Moving Average, mean (line) and standard deviation (shaded).

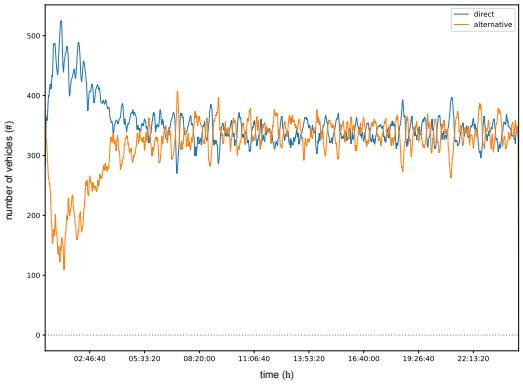


Fig. A.51-11. Average number of vehicles on each route, aggregated to 1 min, over a 24 h period.

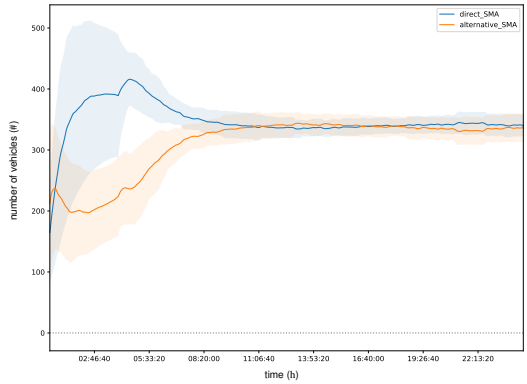


Fig. A.51-12. Average number of vehicles on each route, aggregated to 1 min, over a 24 h period, 4 h Simple Moving Average, mean (line) and standard deviation (shaded).

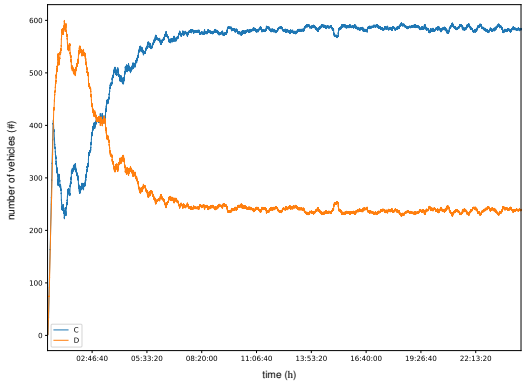


Fig. A.51-13. Evolution of the number of *Cooperators* and *Defectors* over a 24 h period.

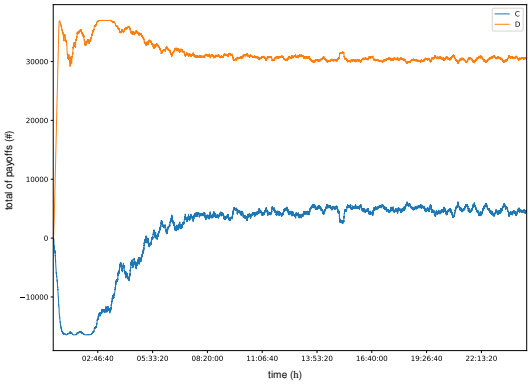


Fig. A.51-14. Evolution of total payoffs for *Cooperators* and *Defectors* (*individual payoff* times the *number of players receiving it*, $C(n) \times n$ and $D(n) \times (N-n)$, where n is the number of *Cooperators*), over a 24 h period.

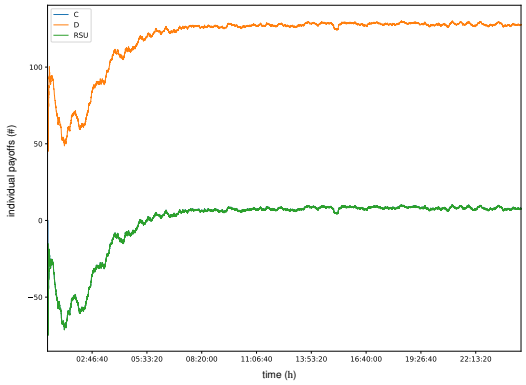


Fig. A.51-15. Evolution of the individual payoffs for *Cooperators, Defectors,* and *RSU* (always cooperating), over a 24 h period.

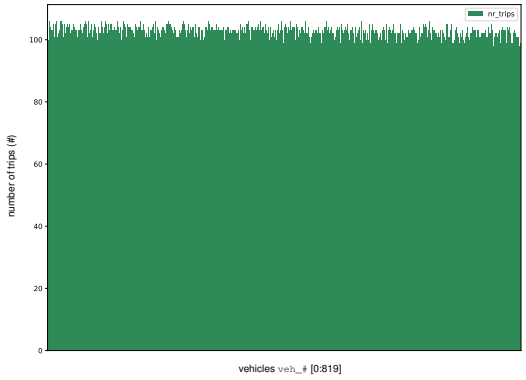


Fig. A.51-16. Number of trips made by each vehicle, during the simulation of a 24 h period.

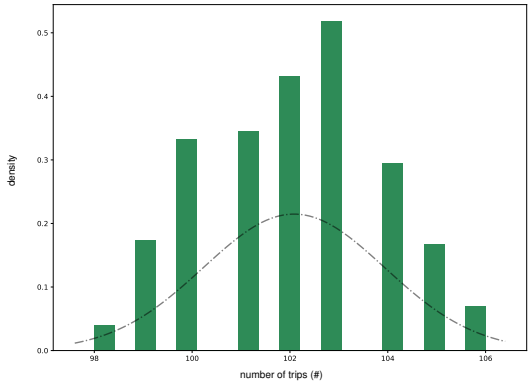


Fig. A.51-17. Density histogram of the number of trips made by each vehicle, during the simulation of a 24 h period, superimposing the normal density curve. The number of bins was calculated by the Freedman Diaconis rule.

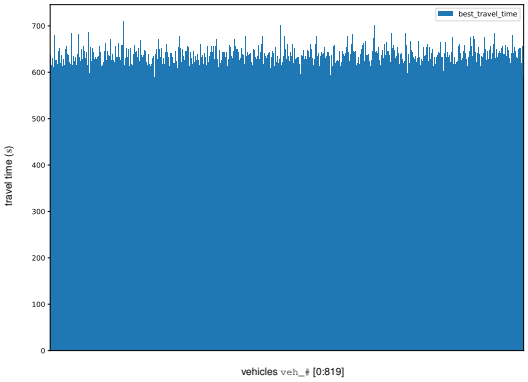


Fig. A.51-18. Best travel time for each vehicle, in seconds (s), during the simulation of a 24 h period.

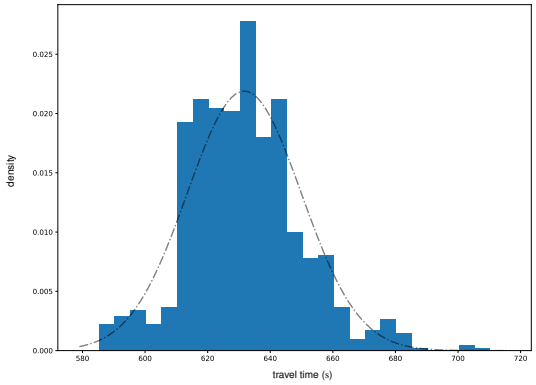


Fig. A.51-19. Density histogram of best travel time for vehicles, in seconds (s), during the simulation of a 24 h period, superimposing the normal density curve. The number of bins was calculated by the Freedman Diaconis rule.

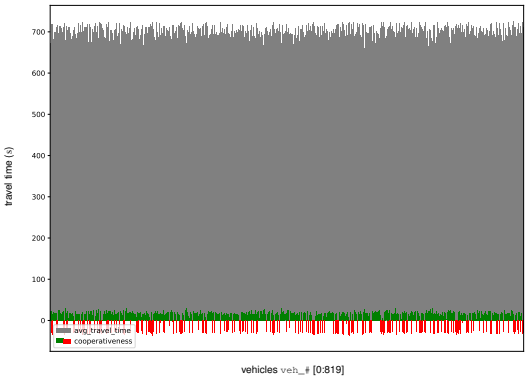


Fig. A.51-20. Average of the travel times, in seconds (s), of individual vehicles, during the simulation of a 24 h period. The bottom graph represents the *degree of cooperativeness**, downscaled by a normalization factor for the purpose of comparison with average times.

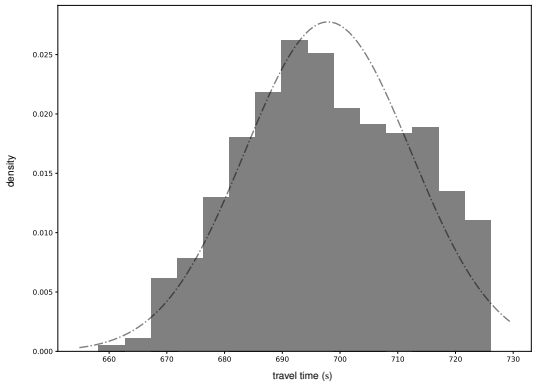


Fig. A.51-21. Density histogram of the average travel times, in seconds (s), of individual vehicles, during the simulation of a 24 h period, superimposing the normal density curve. The number of bins was calculated by the Freedman Diaconis rule.

* The *degree of cooperativeness* is a cumulative sum, calculated at each iteration, based on the complement of the ratio of cooperators, i.e., the higher the number of cooperators the less it increases, but the defectors are more penalized, and vice-versa. It varies inversely with the size of the group to which the player belongs.

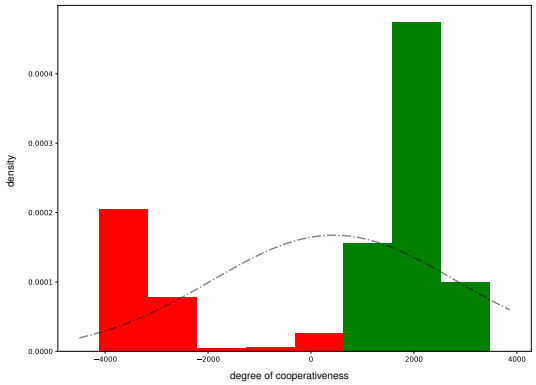


Fig. A.51-22. Density histogram of the *degree of cooperativeness** of individual vehicles, superimposing the normal density curve. The number of bins was calculated by the Freedman Diaconis rule. Generally, when strongly correlated with travel times, it presents a symmetric curve with respect to the *yy*-axis.

A.52 `820veh-24h-00049998`

```
Scenario: scenario-1
Timestamp: 20210521T214738Z
Number of vehicles: 820 vehs
Simulation time: 24.0 h
Warm up end time: 1866.6 s; step 18665
Vehicle selection strategy: roth_erev
RSU turned off: True
RSU strategy: travel_time_moving_average_product
Runner options:
   nogui: True
   step_length: 0.1
   seed: 19750808
   output_prefix: 820veh-24h-00049998
   sim_run_time: 24.0
   num_vehicles: 820
   warmup_speed: 13.96
   warmup_routes_weight: [473, 527]
   network_speed: 25.0
   change_behavior_probability: [100, 0]
   cooperation_probability: [50, 50]
   vehicle_selection_strategy: roth_erev
   turn_rsu_off: True
   rsu_dynamic_dissemination: False
   rsu_dissemination_interval: 5
   rsu_probabilistic_dissemination: False
   rsu_suggestion_strategy: travel_time_moving_average_product
   rsu_routes_weight: [460, 540]
   rsu_moving_avg_size: 5
   travel_times_ttl: 10
   rsu_dissemination_ttl: 0
   rsu_send_travel_time_info: False
   payoff_matrix: [180.0, 60.0, 0.0, -120.0]
   roth_erev_parameters: [0.1, 0.2]
Network Mean speed after warmup:
   Max: 12.12
   Min: 8.09
```

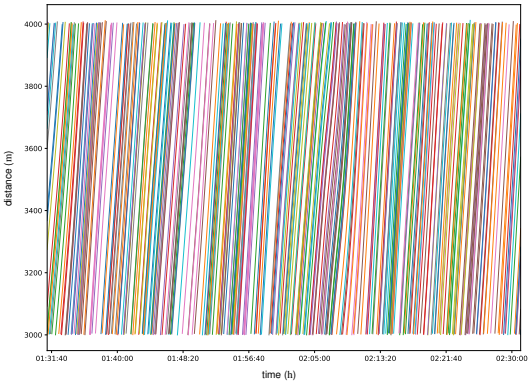


Fig. A.52-1. Time-Space diagram, for the one hour period after the end of the warmup, from 1:00:00 to 2:00:00 simulation time, plotted for the data from the sensor placed in the middle of the *direct* route (between 3000 m and 4000 m). In the case of an overloaded network, congestion shock waves can be observed.

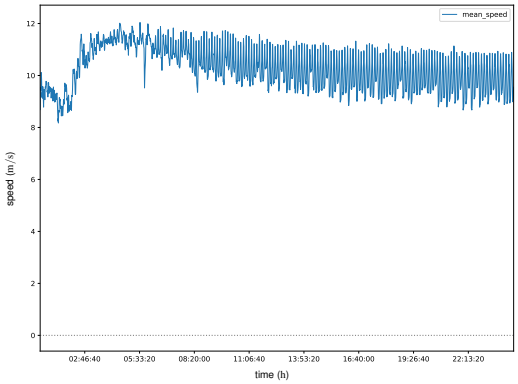


Fig. A.52-2. Mean speed in the network, in meters per second (m/s), over a 24 h period.

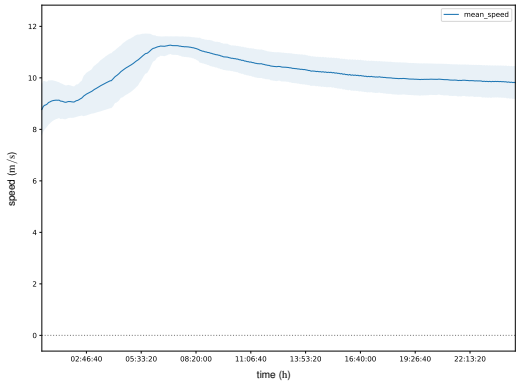


Fig. A.52-3. Mean speed in the network, in meters per second (m/s), over a 24 h period, 4 h Simple Moving Average, mean (line) and standard deviation (shaded).

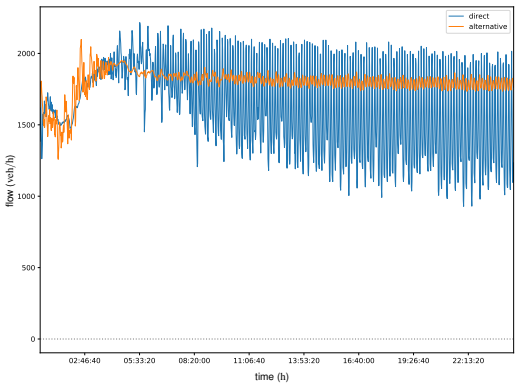


Fig. A.52-4. Traffic flow on each route, in vehicles per hour (veh/h), over a 24 h period.

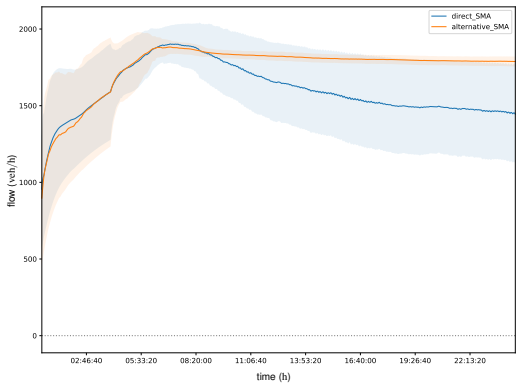


Fig. A.52-5. TrafficTraffic flow on each route, in vehicles per hour (veh/h), over a 24 h period, 4 h Simple Moving Average, mean (line) and standard deviation (shaded).

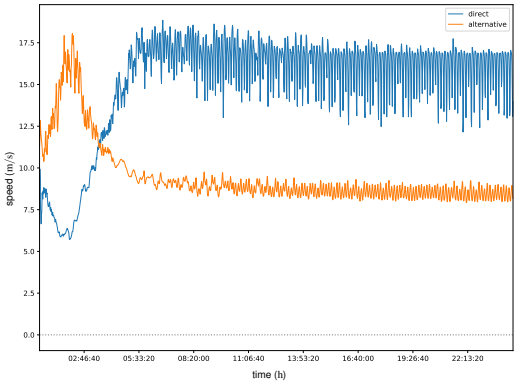


Fig. A.52-6. Mean speed on each route, in meters per second (m/s), aggregated to 1 min, over a 24 h period.

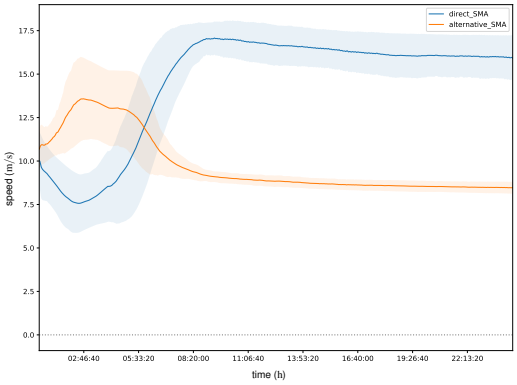


Fig. A.52-7. Mean speed on each route, in meters per second (m/s), aggregated to 1 min, over a 24 h period, 4 h Simple Moving Average, mean (line) and standard deviation (shaded).

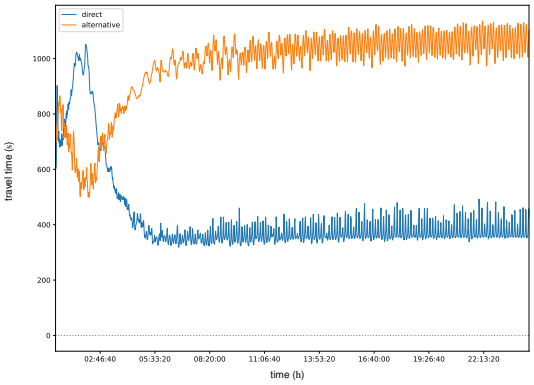


Fig. A.52-8. Travel times on each route, in seconds (s), aggregated to 1 min, over a 24 h period.

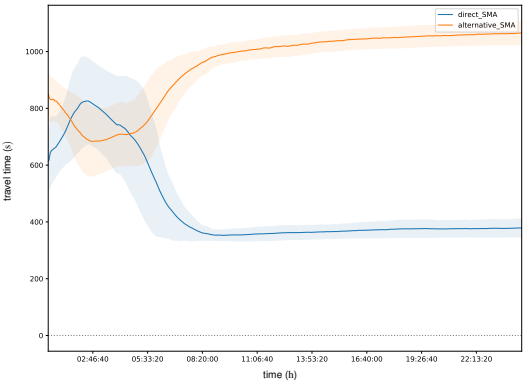


Fig. A.52-9. Travel times on each route, in seconds (s), aggregated to 1 min, over a 24 h period, 4 h Simple Moving Average, mean (line) and standard deviation (shaded).

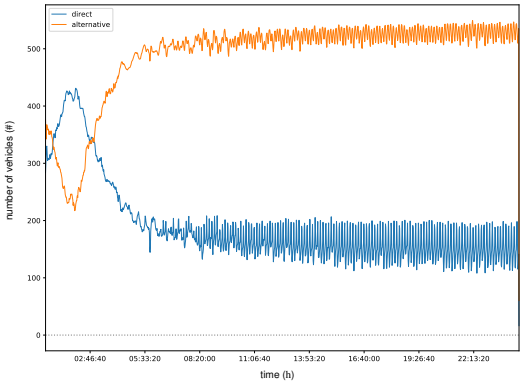


Fig. A.52-10. Average number of vehicles on each route, aggregated to 1 min, over a 24 h period.

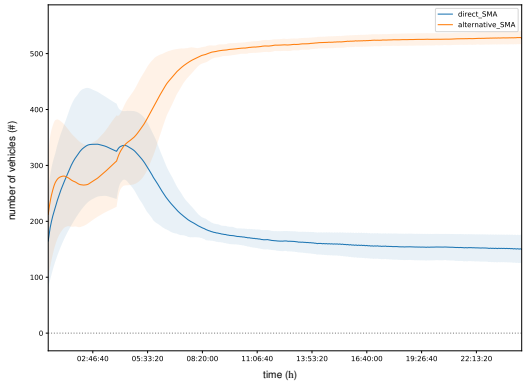


Fig. A.52-11. Average number of vehicles on each route, aggregated to 1 min, over a 24 h period, 4 h Simple Moving Average, mean (line) and standard deviation (shaded).

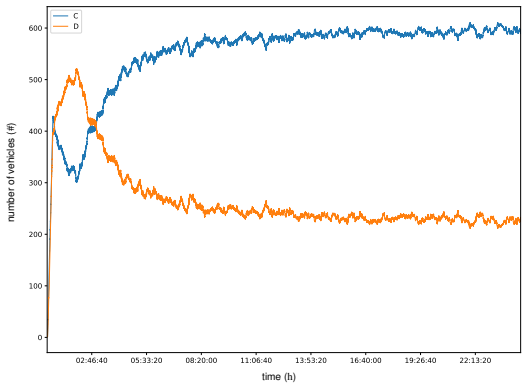


Fig. A.52-12. Evolution of the number of *Cooperators* and *Defectors* over a 24 h period.

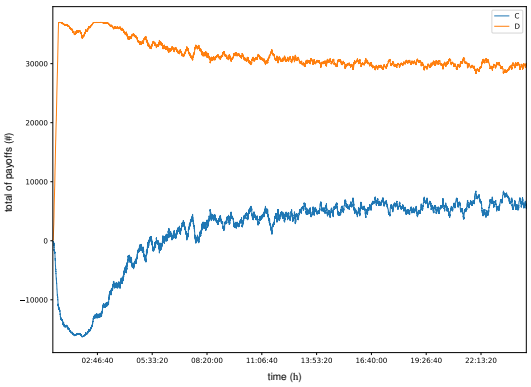


Fig. A.52-13. Evolution of total payoffs for *Cooperators* and *Defectors* (*individual payoff* times the *number of players receiving it*, $C(n) \times n$ and $D(n) \times (N-n)$, where n is the number of *Cooperators*), over a 24 h period.

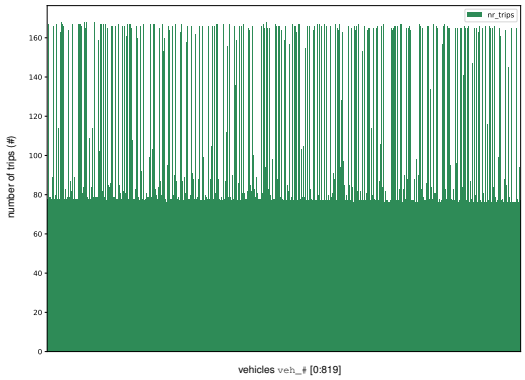


Fig. A.52-14. Number of trips made by each vehicle, during the simulation of a 24 h period.

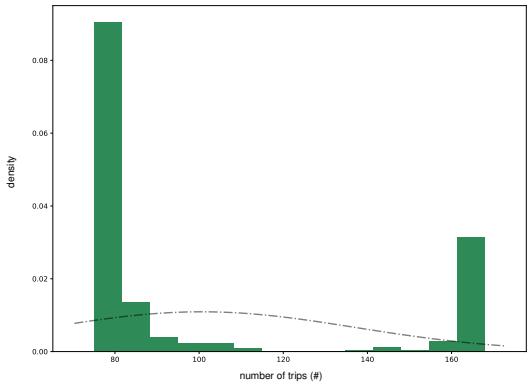


Fig. A.52-15. Density histogram of the number of trips made by each vehicle, during the simulation of a 24 h period, superimposing the normal density curve. The number of bins was calculated by the Freedman Diaconis rule.

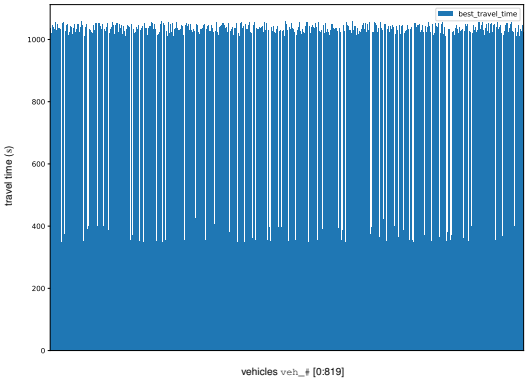


Fig. A.52-16. Best travel time for each vehicle, in seconds (s), during the simulation of a 24 h period.

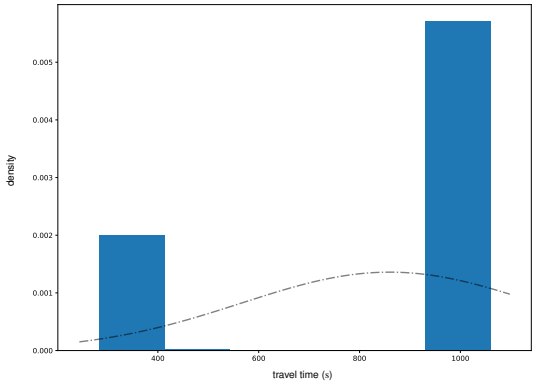


Fig. A.52-17. Density histogram of best travel time for vehicles, in seconds (s), during the simulation of a 24 h period, superimposing the normal density curve. The number of bins was calculated by the Freedman Diaconis rule.

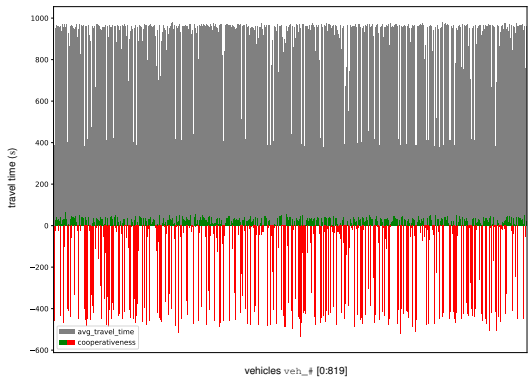


Fig. A.52-18. Average of the travel times, in seconds (s), of individual vehicles, during the simulation of a 24 h period. The bottom graph represents the *degree of cooperativeness**, downscaled by a normalization factor for the purpose of comparison with average times.

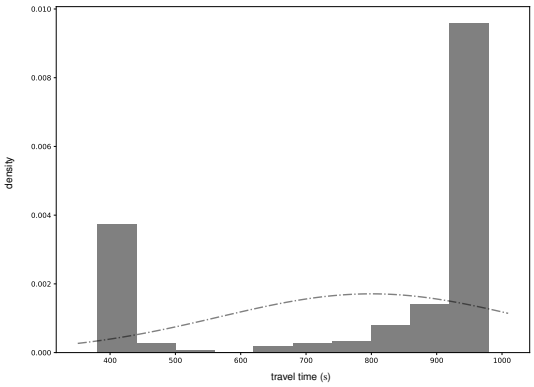


Fig. A.52-19. Density histogram of the average travel times, in seconds (s), of individual vehicles, during the simulation of a 24 h period, superimposing the normal density curve. The number of bins was calculated by the Freedman Diaconis rule.

* The *degree of cooperativeness* is a cumulative sum, calculated at each iteration, based on the complement of the ratio of cooperators, i.e., the higher the number of cooperators the less it increases, but the defectors are more penalized, and vice-versa. It varies inversely with the size of the group to which the player belongs.

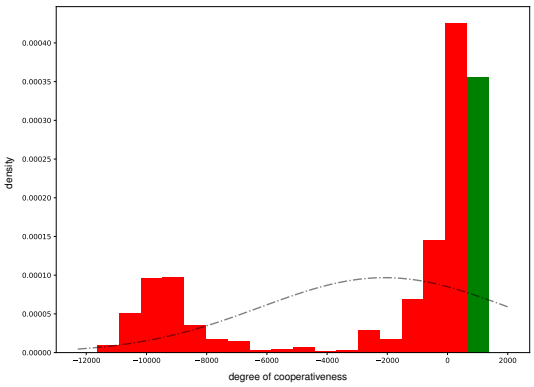


Fig. A.52-20. Density histogram of the *degree of cooperativeness** of individual vehicles, superimposing the normal density curve. The number of bins was calculated by the Freedman Diaconis rule. Generally, when strongly correlated with travel times, it presents a symmetric curve with respect to the *yy*-axis.

A.53 820veh-24h-19030003

```
Scenario: scenario-1
Timestamp: 20210618T105031Z
Number of vehicles: 820 vehs
Simulation time: 24.0 h
Warm up end time: 1866.6 s; step 18665
Vehicle selection strategy: mean_payoff
RSU turned off: False
RSU strategy: pigous_example_cooperation_weighted
Runner options:
   nogui: True
   step_length: 0.1
   seed: 19750808
   output_prefix: 820veh-24h-19030003
   sim_run_time: 24.0
   num_vehicles: 820
   warmup_speed: 13.96
   warmup_routes_weight: [473, 527]
   network_speed: 25.0
   change_behavior_probability: [80, 20]
   cooperation_probability: [50, 50]
   vehicle_selection_strategy: mean_payoff
   turn_rsu_off: False
   rsu_dynamic_dissemination: False
   rsu_dissemination_interval: 5
   rsu_probabilistic_dissemination: False
   rsu_suggestion_strategy: pigous_example_cooperation_weighted
   rsu_routes_weight: [460, 540]
   rsu_moving_avg_size: 5
   travel_times_ttl: 60
   rsu_dissemination_ttl: 0
   rsu_send_travel_time_info: True
   payoff_matrix: [180.0, 60.0, 0.0, -120.0]
   roth_erev_parameters: [0.1, 0.5]
   rsu_change_dissemination: False
   rsu_change_dissemination_steps: [14400, 28800, 43200, 57600, 72000]
   rsu_change_dissemination_intervals: [10, 20, 40, 80, 160]
Network Mean speed after warmup:
   Max: 11.81
   Min: 2.81
```

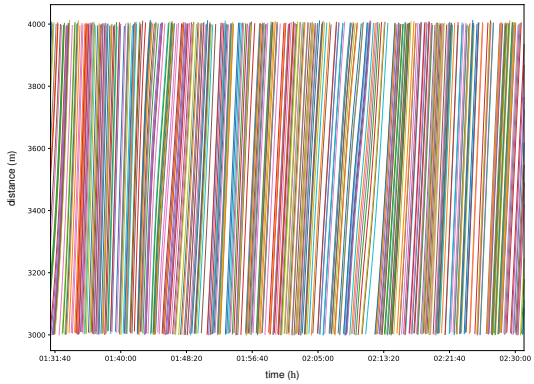


Fig. A.53-1. Time-Space diagram, for the one hour period after the end of the warmup, from 1:00:00 to 2:00:00 simulation time, plotted for the data from the sensor placed in the middle of the *direct* route (between 3000 m and 4000 m). In the case of an overloaded network, congestion shock waves can be observed.

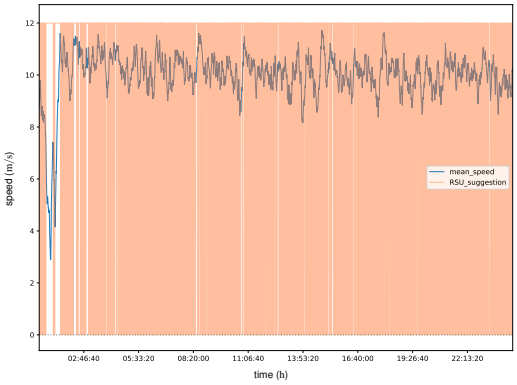


Fig. A.53-2. Mean speed in the network, in meters per second (m/s), over a 24 h period, superimposing (vertically, in orange) the time instants in which the RSU issued a recommendation to follow the *alternative* route.

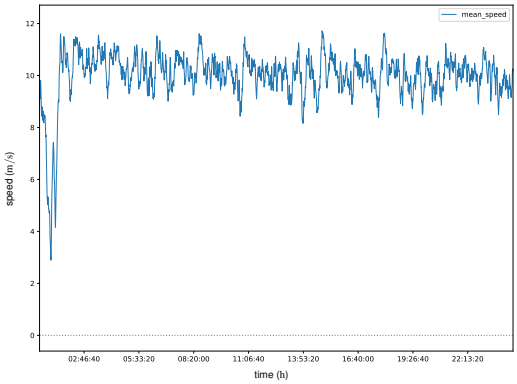


Fig. A.53-3. Mean speed in the network, in meters per second (m/s), over a 24 h period.

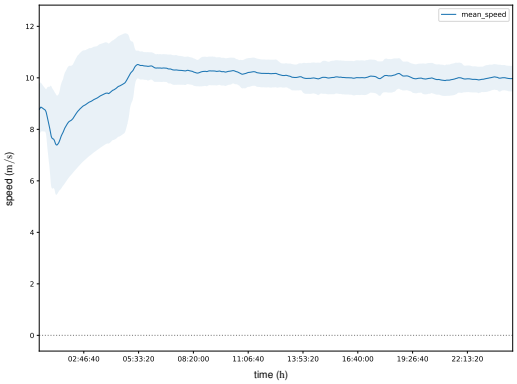


Fig. A.53-4. Mean speed in the network, in meters per second (m/s), over a 24 h period, 4 h Simple Moving Average, mean (line) and standard deviation (shaded).

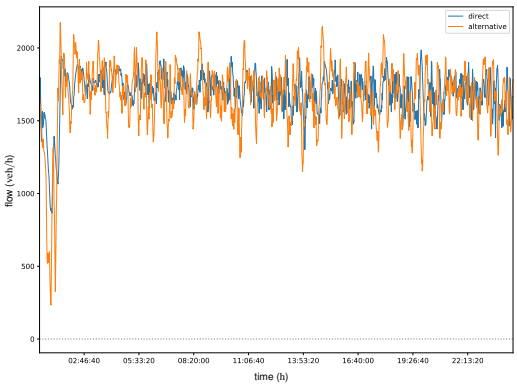


Fig. A.53-5. Traffic flow on each route, in vehicles per hour (veh/h), over a 24 h period.

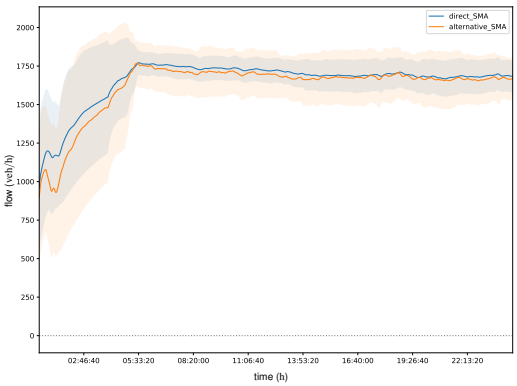


Fig. A.53-6. TrafficTraffic flow on each route, in vehicles per hour (veh/h), over a 24 h period, 4 h Simple Moving Average, mean (line) and standard deviation (shaded).

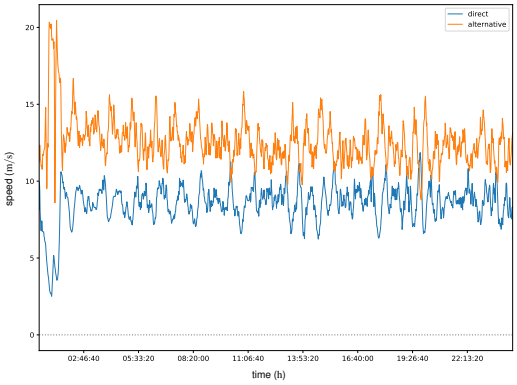


Fig. A.53-7. Mean speed on each route, in meters per second (m/s), aggregated to 1 min, over a 24 h period.

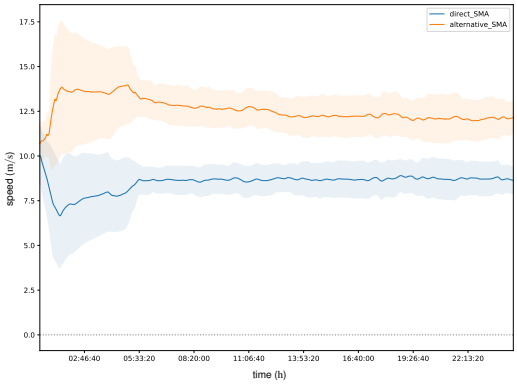


Fig. A.53-8. Mean speed on each route, in meters per second (m/s), aggregated to 1 min, over a 24 h period, 4 h Simple Moving Average, mean (line) and standard deviation (shaded).

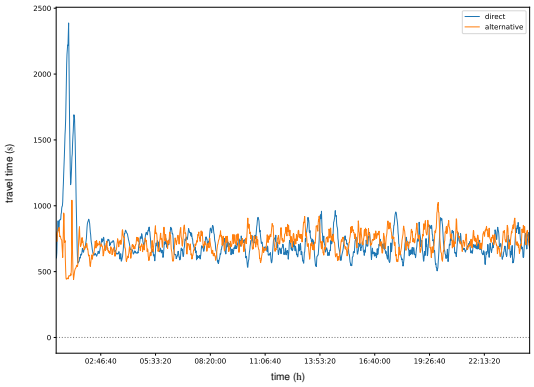


Fig. A.53-9. Travel times on each route, in seconds (s), aggregated to 1 min, over a 24 h period.

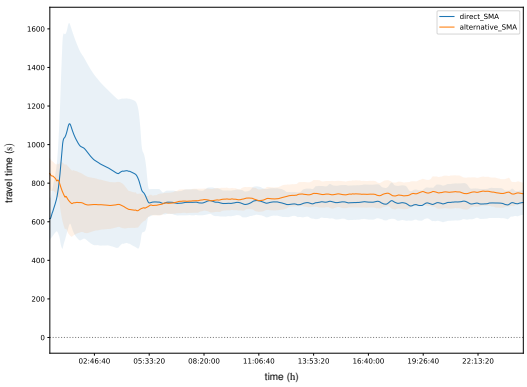


Fig. A.53-10. Travel times on each route, in seconds (s), aggregated to 1 min, over a 24 h period, 4 h Simple Moving Average, mean (line) and standard deviation (shaded).

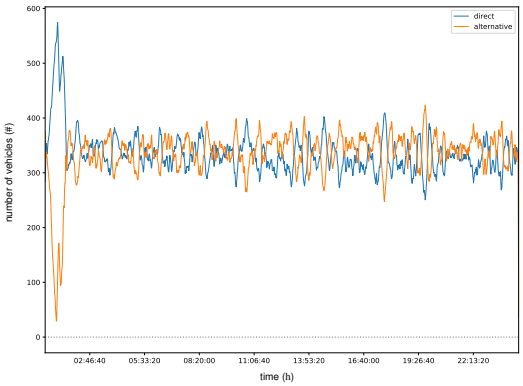


Fig. A.53-11. Average number of vehicles on each route, aggregated to 1 min, over a 24 h period.

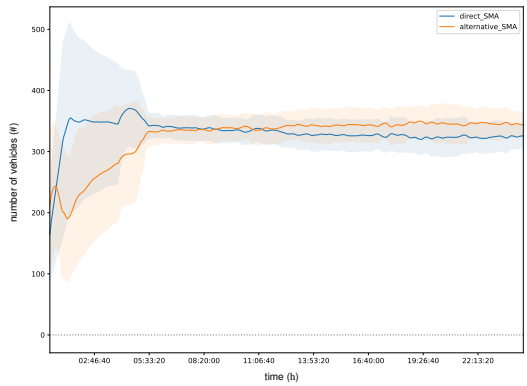


Fig. A.53-12. Average number of vehicles on each route, aggregated to 1 min, over a 24 h period, 4 h Simple Moving Average, mean (line) and standard deviation (shaded).

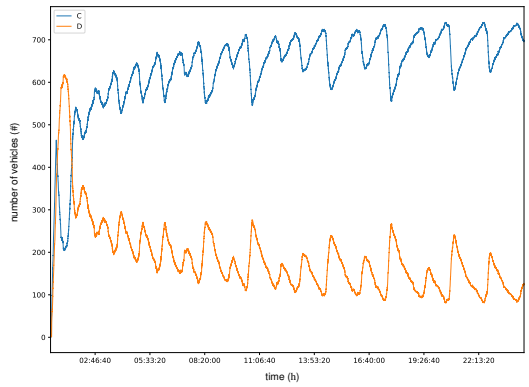


Fig. A.53-13. Evolution of the number of *Cooperators* and *Defectors* over a 24 h period.

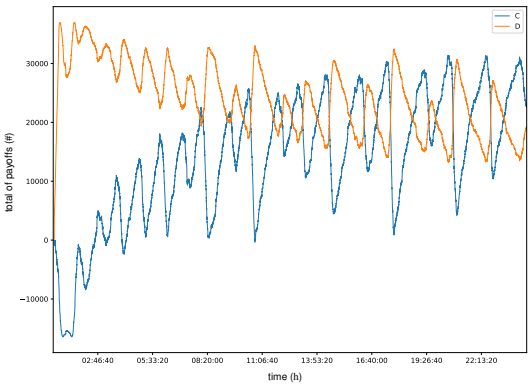


Fig. A.53-14. Evolution of total payoffs for *Cooperators* and *Defectors* (*individual payoff* times the *number of players receiving it*, $C(n) \times n$ and $D(n) \times (N-n)$, where n is the number of *Cooperators*), over a 24 h period.

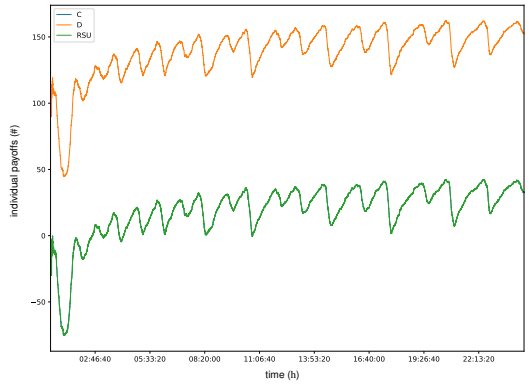


Fig. A.53-15. Evolution of the individual payoffs for *Cooperators, Defectors,* and *RSU* (always cooperating), over a 24 h period.

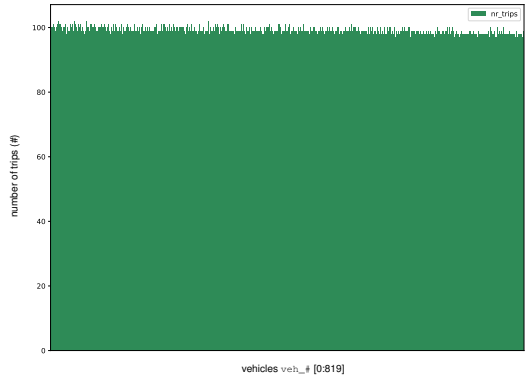


Fig. A.53-16. Number of trips made by each vehicle, during the simulation of a 24 h period.

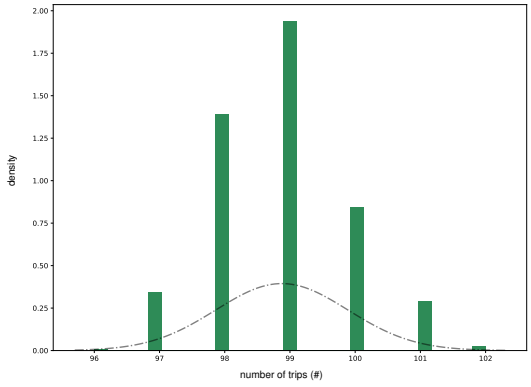


Fig. A.53-17. Density histogram of the number of trips made by each vehicle, during the simulation of a 24 h period, superimposing the normal density curve. The number of bins was calculated by the Freedman Diaconis rule.

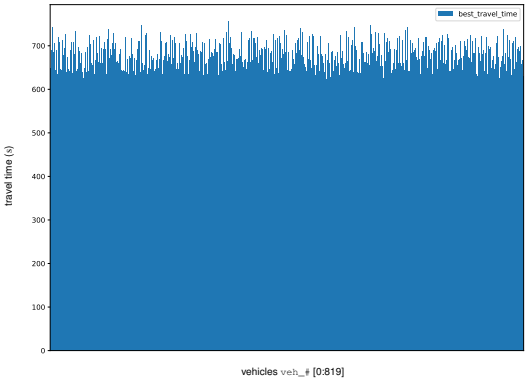


Fig. A.53-18. Best travel time for each vehicle, in seconds (s), during the simulation of a 24 h period.

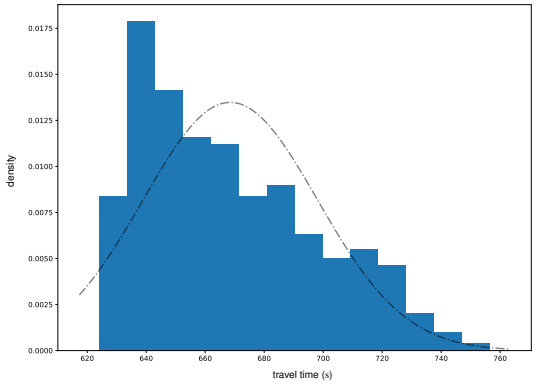


Fig. A.53-19. Density histogram of best travel time for vehicles, in seconds (s), during the simulation of a 24 h period, superimposing the normal density curve. The number of bins was calculated by the Freedman Diaconis rule.

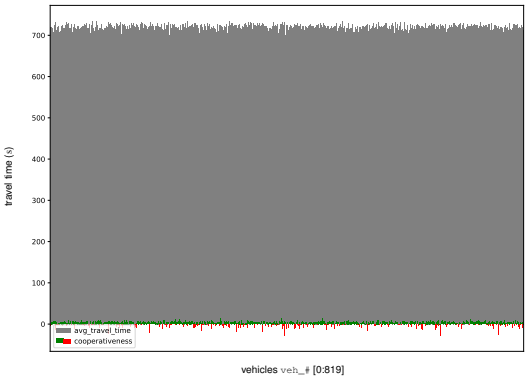


Fig. A.53-20. Average of the travel times, in seconds (s), of individual vehicles, during the simulation of a 24 h period. The bottom graph represents the *degree of cooperativeness**, downscaled by a normalization factor for the purpose of comparison with average times.

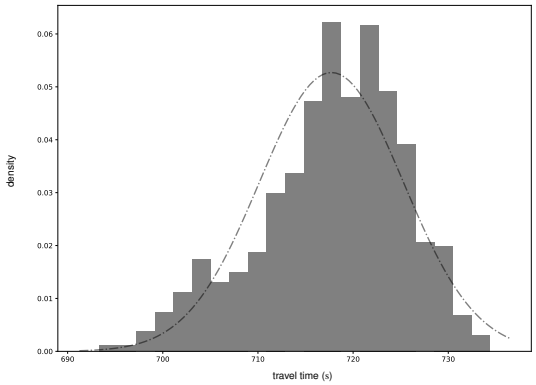


Fig. A.53-21. Density histogram of the average travel times, in seconds (s), of individual vehicles, during the simulation of a 24 h period, superimposing the normal density curve. The number of bins was calculated by the Freedman Diaconis rule.

* The *degree of cooperativeness* is a cumulative sum, calculated at each iteration, based on the complement of the ratio of cooperators, i.e., the higher the number of cooperators the less it increases, but the defectors are more penalized, and vice-versa. It varies inversely with the size of the group to which the player belongs.

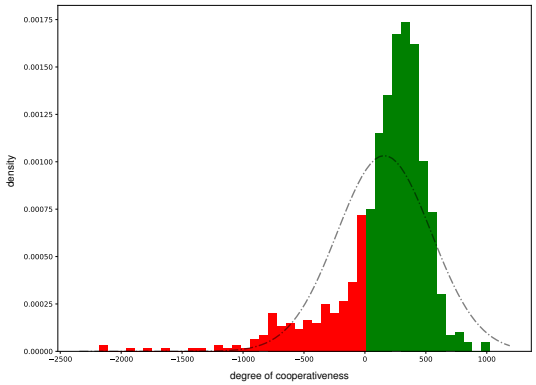


Fig. A.53-22. Density histogram of the *degree of cooperativeness** of individual vehicles, superimposing the normal density curve. The number of bins was calculated by the Freedman Diaconis rule. Generally, when strongly correlated with travel times, it presents a symmetric curve with respect to the *yy*-axis.

A.54 `570veh-24h-19040013`

```
Scenario: scenario-1
Timestamp: 20210620T112421Z
Number of vehicles: 570 vehs
Simulation time: 24.0 h
Warm up end time: 1494.2 s; step 14941
Vehicle selection strategy: roth_erev
RSU turned off: False
RSU strategy: pigous_example_cooperation_weighted
Runner options:
   nogui: True
   step_length: 0.1
   seed: 19750808
   output_prefix: 570veh-24h-19040013
   sim_run_time: 24.0
   num_vehicles: 570
   warmup_speed: 23.38
   warmup_routes_weight: [473, 527]
   network_speed: 25.0
   change_behavior_probability: [100, 0]
   cooperation_probability: [50, 50]
   vehicle_selection_strategy: roth_erev
   turn_rsu_off: False
   rsu_dynamic_dissemination: False
   rsu_dissemination_interval: 5
   rsu_probabilistic_dissemination: False
   rsu_suggestion_strategy: pigous_example_cooperation_weighted
   rsu_routes_weight: [471, 529]
   rsu_moving_avg_size: 5
   travel_times_ttl: 60
   rsu_dissemination_ttl: 0
   rsu_send_travel_time_info: False
   payoff_matrix: [180.0, 60.0, 0.0, -120.0]
   roth_erev_parameters: [0.5, 0.5]
   rsu_change_dissemination: True
   rsu_change_dissemination_steps: [14400, 28800, 43200, 57600, 72000]
   rsu_change_dissemination_intervals: [10, 20, 40, 80, 160]
Network Mean speed after warmup:
   Max: 16.92
   Min: 5.21
```

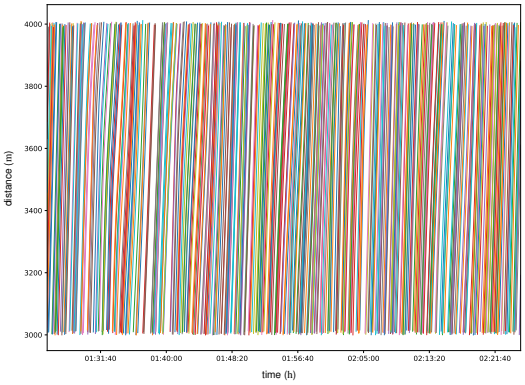


Fig. A.54-1. Time-Space diagram, for the one hour period after the end of the warmup, from 1:00:00 to 2:00:00 simulation time, plotted for the data from the sensor placed in the middle of the *direct* route (between 3000 m and 4000 m). In the case of an overloaded network, congestion shock waves can be observed.

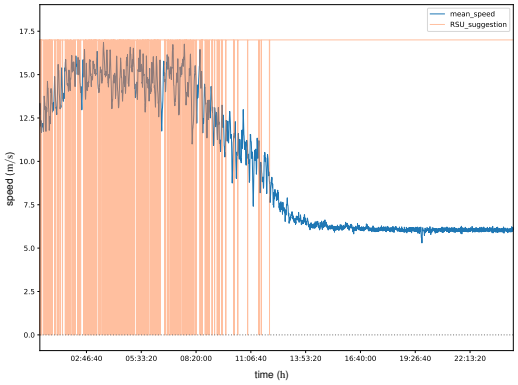


Fig. A.54-2. Mean speed in the network, in meters per second (m/s), over a 24 h period, superimposing (vertically, in orange) the time instants in which the RSU issued a recommendation to follow the *alternative* route.

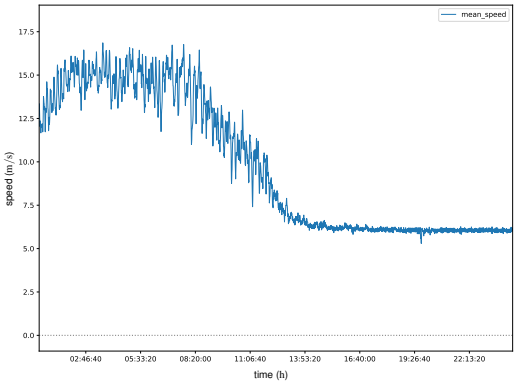


Fig. A.54-3. Mean speed in the network, in meters per second (m/s), over a 24 h period.

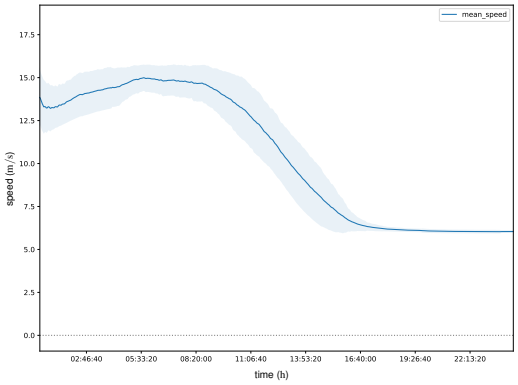


Fig. A.54-4. Mean speed in the network, in meters per second (m/s), over a 24 h period, 4 h Simple Moving Average, mean (line) and standard deviation (shaded).

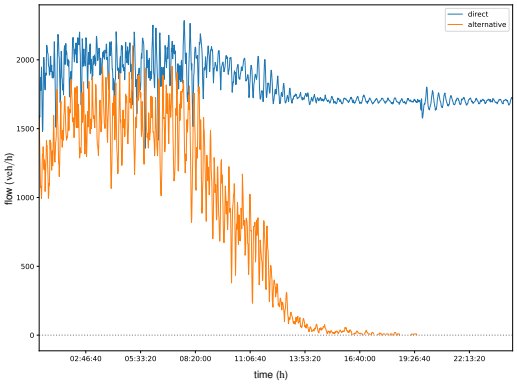


Fig. A.54-5. Traffic flow on each route, in vehicles per hour (veh/h), over a 24 h period.

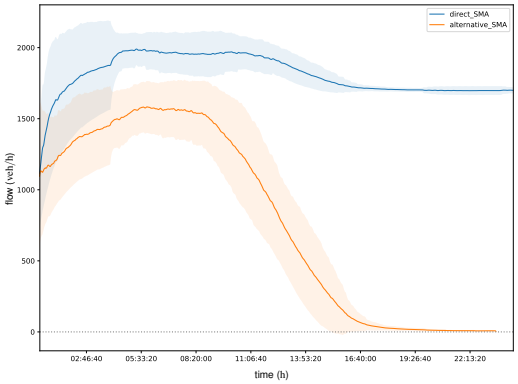


Fig. A.54-6. TrafficTraffic flow on each route, in vehicles per hour (veh/h), over a 24 h period, 4 h Simple Moving Average, mean (line) and standard deviation (shaded).

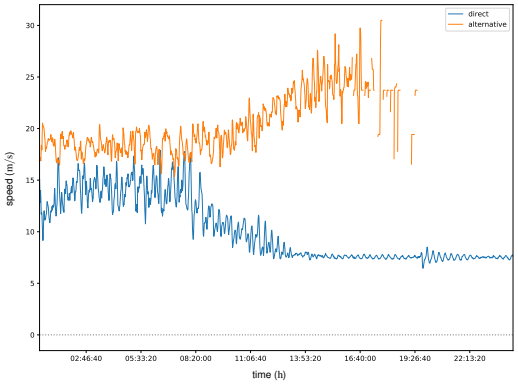


Fig. A.54-7. Mean speed on each route, in meters per second (m/s), aggregated to 1 min, over a 24 h period.

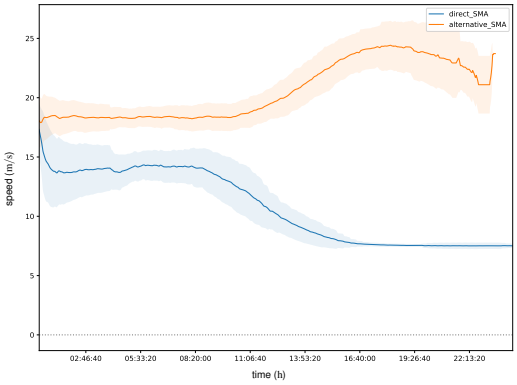


Fig. A.54-8. Mean speed on each route, in meters per second (m/s), aggregated to 1 min, over a 24 h period, 4 h Simple Moving Average, mean (line) and standard deviation (shaded).

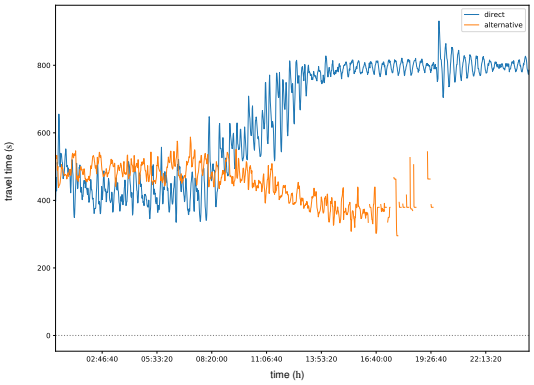


Fig. A.54-9. Travel times on each route, in seconds (s), aggregated to 1 min, over a 24 h period.

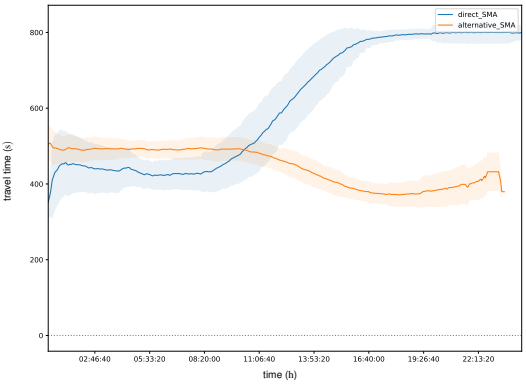


Fig. A.54-10. Travel times on each route, in seconds (s), aggregated to 1 min, over a 24 h period, 4 h Simple Moving Average, mean (line) and standard deviation (shaded).

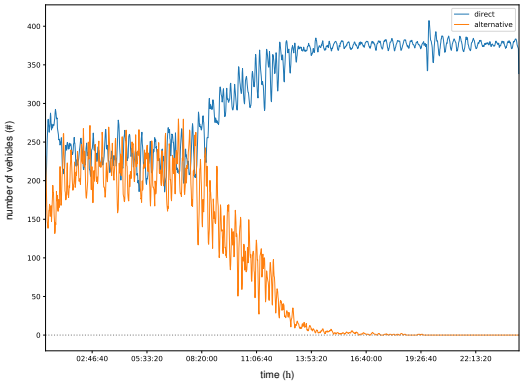


Fig. A.54-11. Average number of vehicles on each route, aggregated to 1 min, over a 24 h period.

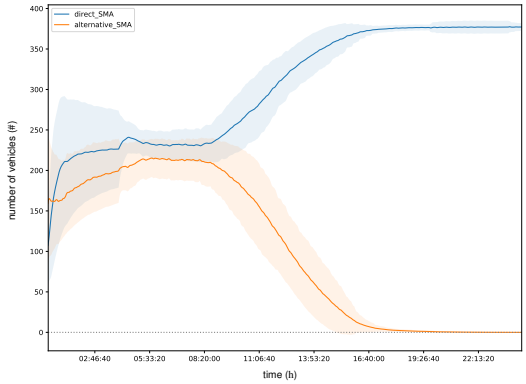


Fig. A.54-12. Average number of vehicles on each route, aggregated to 1 min, over a 24 h period, 4 h Simple Moving Average, mean (line) and standard deviation (shaded).

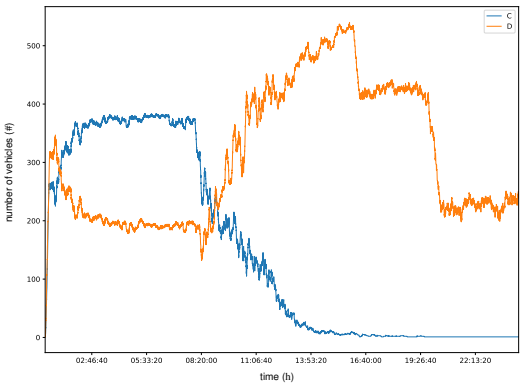


Fig. A.54-13. Evolution of the number of *Cooperators* and *Defectors* over a 24 h period.

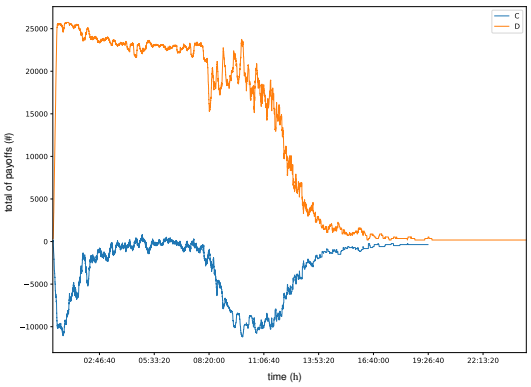


Fig. A.54-14. Evolution of total payoffs for *Cooperators* and *Defectors* (*individual payoff* times the *number of players receiving it*, $C(n) \times n$ and $D(n) \times (N-n)$, where n is the number of *Cooperators*), over a 24 h period.

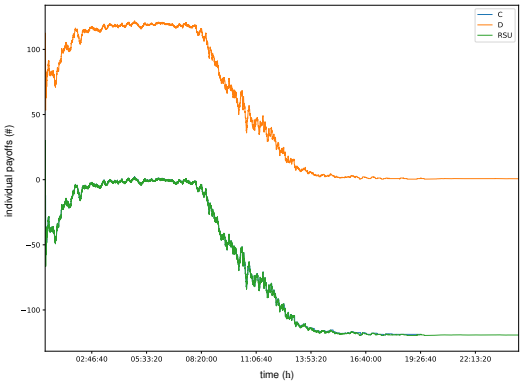


Fig. A.54-15. Evolution of the individual payoffs for *Cooperators, Defectors,* and *RSU* (always cooperating), over a 24 h period.

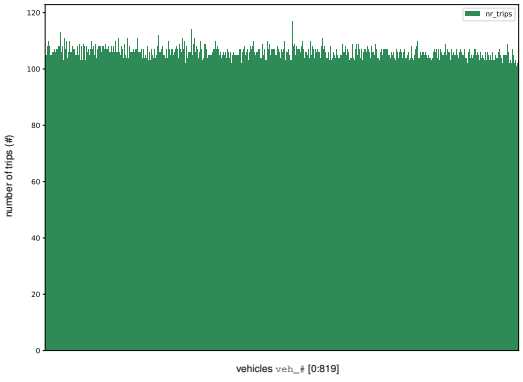


Fig. A.54-16. Number of trips made by each vehicle, during the simulation of a 24 h period.

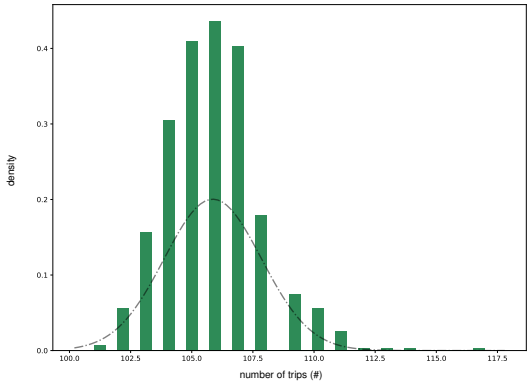


Fig. A.54-17. Density histogram of the number of trips made by each vehicle, during the simulation of a 24 h period, superimposing the normal density curve. The number of bins was calculated by the Freedman Diaconis rule.

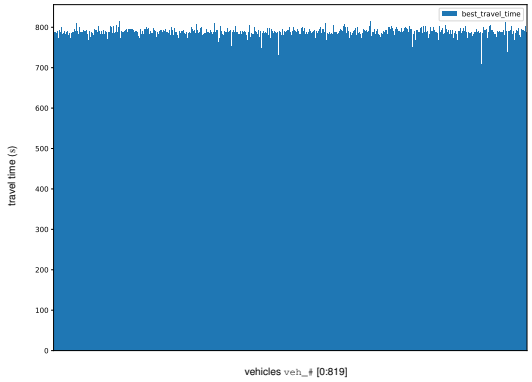


Fig. A.54-18. Best travel time for each vehicle, in seconds (s), during the simulation of a 24 h period.

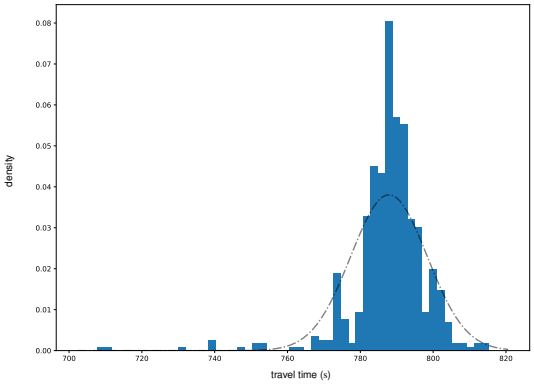


Fig. A.54-19. Density histogram of best travel time for vehicles, in seconds (s), during the simulation of a 24 h period, superimposing the normal density curve. The number of bins was calculated by the Freedman Diaconis rule.

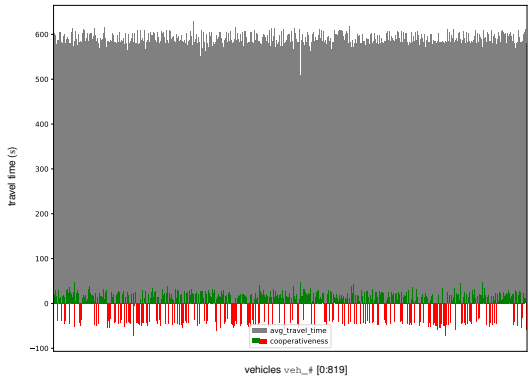


Fig. A.54-20. Average of the travel times, in seconds (s), of individual vehicles, during the simulation of a 24 h period. The bottom graph represents the *degree of cooperativeness**, downscaled by a normalization factor for the purpose of comparison with average times.

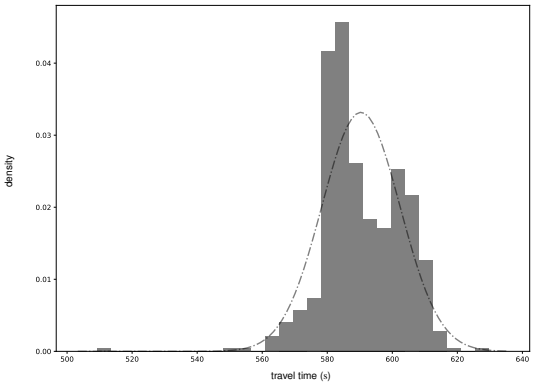


Fig. A.54-21. Density histogram of the average travel times, in seconds (s), of individual vehicles, during the simulation of a 24 h period, superimposing the normal density curve. The number of bins was calculated by the Freedman Diaconis rule.

* The *degree of cooperativeness* is a cumulative sum, calculated at each iteration, based on the complement of the ratio of cooperators, i.e., the higher the number of cooperators the less it increases, but the defectors are more penalized, and vice-versa. It varies inversely with the size of the group to which the player belongs.

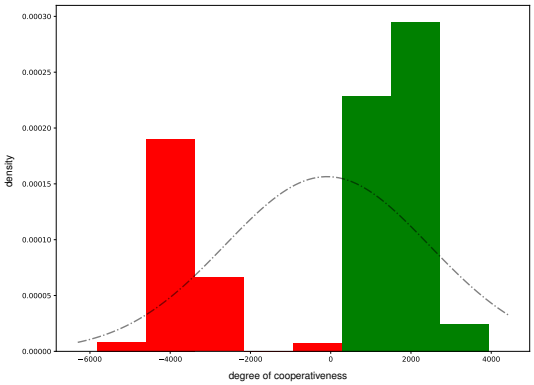


Fig. A.54-22. Density histogram of the *degree of cooperativeness** of individual vehicles, superimposing the normal density curve. The number of bins was calculated by the Freedman Diaconis rule. Generally, when strongly correlated with travel times, it presents a symmetric curve with respect to the *yy*-axis.

A.55 820veh-24h-19040013

```
Scenario: scenario-1
Timestamp: 20210611T140756Z
Number of vehicles: 820 vehs
Simulation time: 24.0 h
Warm up end time: 1866.6 s; step 18665
Vehicle selection strategy: roth_erev
RSU turned off: False
RSU strategy: pigous_example_cooperation_weighted
Runner options:
   nogui: True
   step_length: 0.1
   seed: 19750808
   output_prefix: 820veh-24h-19040013
   sim_run_time: 24.0
   num_vehicles: 820
   warmup_speed: 13.96
   warmup_routes_weight: [473, 527]
   network_speed: 25.0
   change_behavior_probability: [100, 0]
   cooperation_probability: [50, 50]
   vehicle_selection_strategy: roth_erev
   turn_rsu_off: False
   rsu_dynamic_dissemination: False
   rsu_dissemination_interval: 5
   rsu_probabilistic_dissemination: False
   rsu_suggestion_strategy: pigous_example_cooperation_weighted
   rsu_routes_weight: [460, 540]
   rsu_moving_avg_size: 5
   travel_times_ttl: 60
   rsu_dissemination_ttl: 0
   rsu_send_travel_time_info: False
   payoff_matrix: [180.0, 60.0, 0.0, -120.0]
   roth_erev_parameters: [0.5, 0.5]
   rsu_change_dissemination: True
   rsu_change_dissemination_steps: [14400, 28800, 43200, 57600, 72000]
   rsu_change_dissemination_intervals: [10, 20, 40, 80, 160]
Network Mean speed after warmup:
   Max: 11.91
   Min: 1.78
```

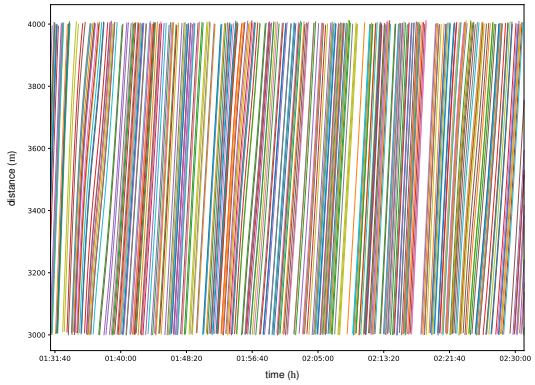


Fig. A.55-1. Time-Space diagram, for the one hour period after the end of the warmup, from 1:00:00 to 2:00:00 simulation time, plotted for the data from the sensor placed in the middle of the *direct* route (between 3000 m and 4000 m). In the case of an overloaded network, congestion shock waves can be observed.

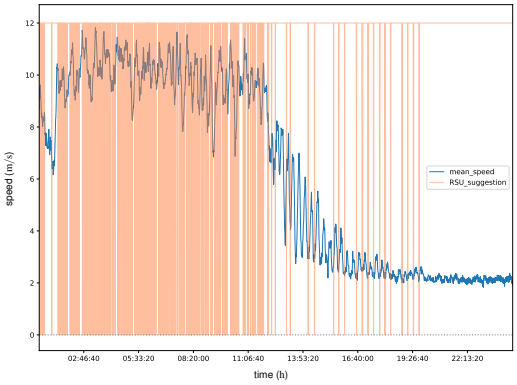


Fig. A.55-2. Mean speed in the network, in meters per second (m/s), over a 24 h period, superimposing (vertically, in orange) the time instants in which the RSU issued a recommendation to follow the *alternative* route.

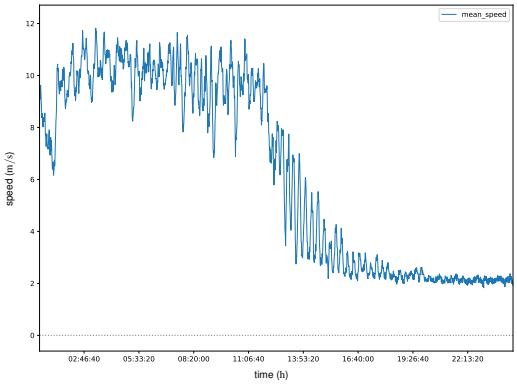


Fig. A.55-3. Mean speed in the network, in meters per second (m/s), over a 24 h period.

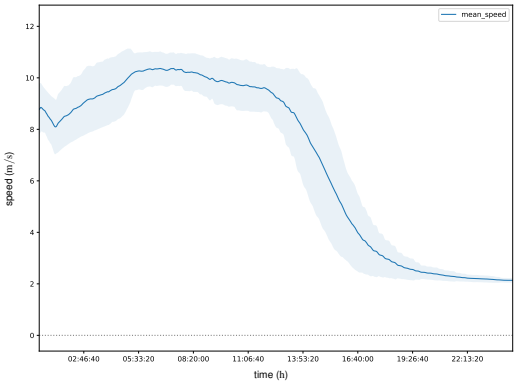


Fig. A.55-4. Mean speed in the network, in meters per second (m/s), over a 24 h period, 4 h Simple Moving Average, mean (line) and standard deviation (shaded).

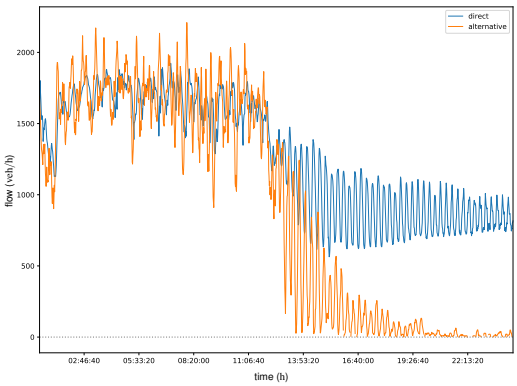


Fig. A.55-5. Traffic flow on each route, in vehicles per hour (veh/h), over a 24 h period.

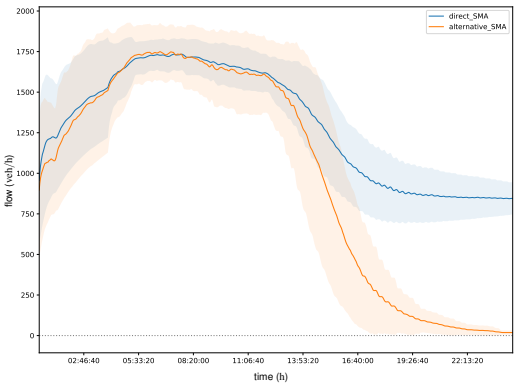


Fig. A.55-6. TrafficTraffic flow on each route, in vehicles per hour (veh/h), over a 24 h period, 4 h Simple Moving Average, mean (line) and standard deviation (shaded).

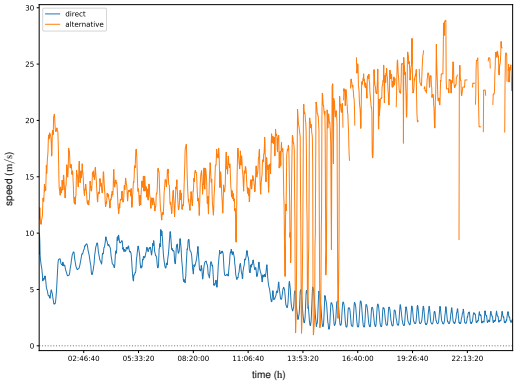


Fig. A.55-7. Mean speed on each route, in meters per second (m/s), aggregated to 1 min, over a 24 h period.

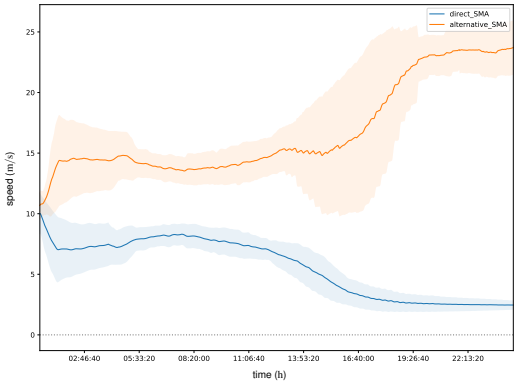


Fig. A.55-8. Mean speed on each route, in meters per second (m/s), aggregated to 1 min, over a 24 h period, 4 h Simple Moving Average, mean (line) and standard deviation (shaded).

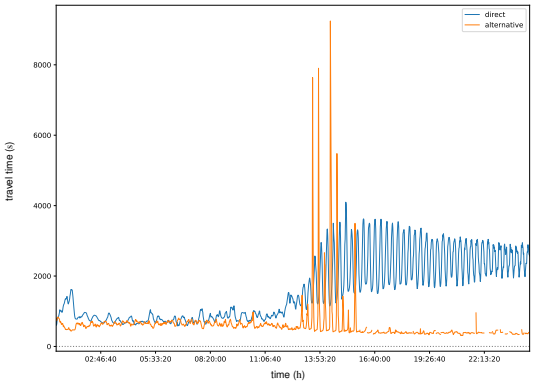


Fig. A.55-9. Travel times on each route, in seconds (s), aggregated to 1 min, over a 24 h period.

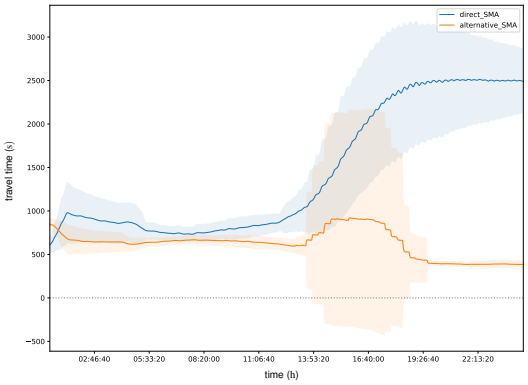


Fig. A.55-10. Travel times on each route, in seconds (s), aggregated to 1 min, over a 24 h period, 4 h Simple Moving Average, mean (line) and standard deviation (shaded).

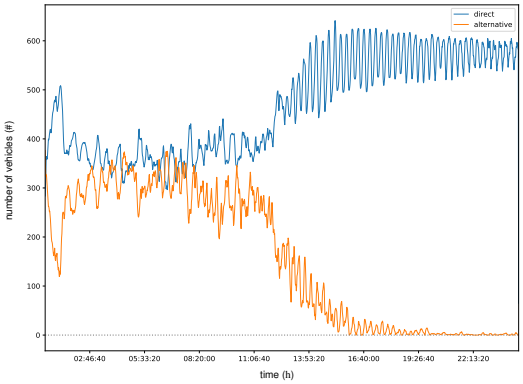


Fig. A.55-11. Average number of vehicles on each route, aggregated to 1 min, over a 24 h period.

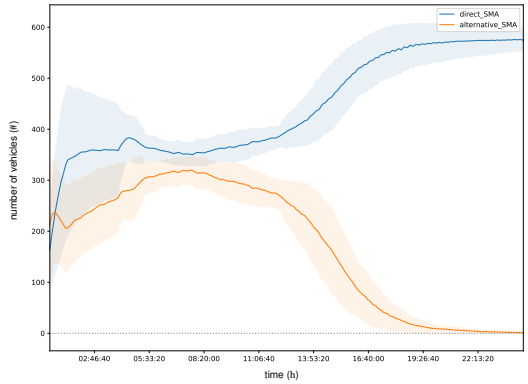


Fig. A.55-12. Average number of vehicles on each route, aggregated to 1 min, over a 24 h period, 4 h Simple Moving Average, mean (line) and standard deviation (shaded).

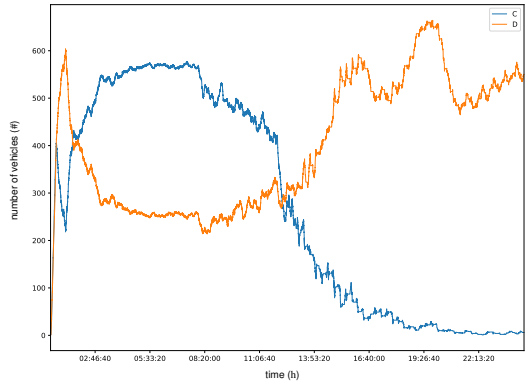


Fig. A.55-13. Evolution of the number of *Cooperators* and *Defectors* over a 24 h period.

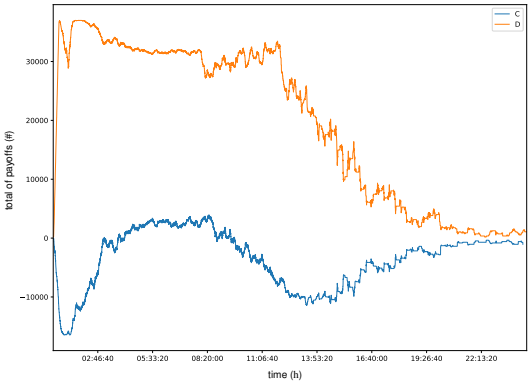


Fig. A.55-14. Evolution of total payoffs for *Cooperators* and *Defectors* (*individual payoff* times the *number of players receiving it*, $C(n) \times n$ and $D(n) \times (N-n)$, where n is the number of *Cooperators*), over a 24 h period.

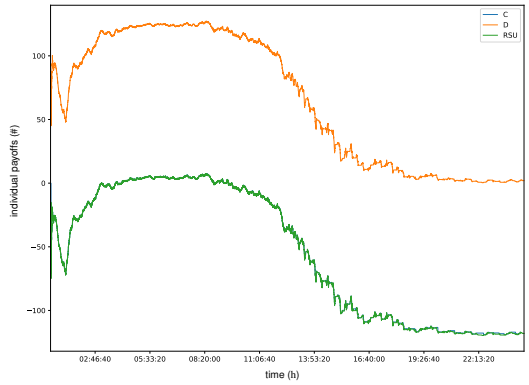


Fig. A.55-15. Evolution of the individual payoffs for *Cooperators, Defectors,* and *RSU* (always cooperating), over a 24 h period.

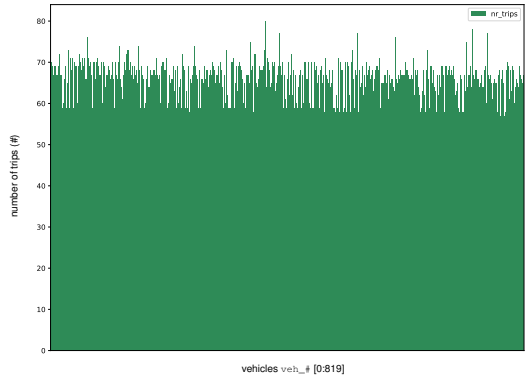


Fig. A.55-16. Number of trips made by each vehicle, during the simulation of a 24 h period.

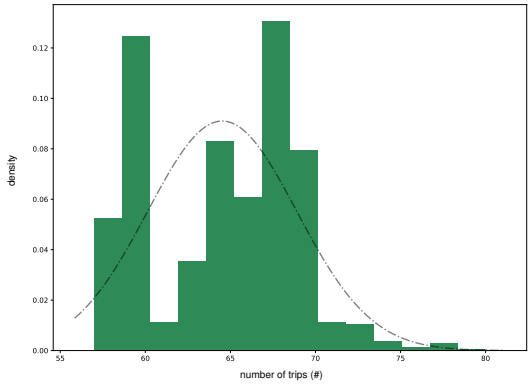


Fig. A.55-17. Density histogram of the number of trips made by each vehicle, during the simulation of a 24 h period, superimposing the normal density curve. The number of bins was calculated by the Freedman Diaconis rule.

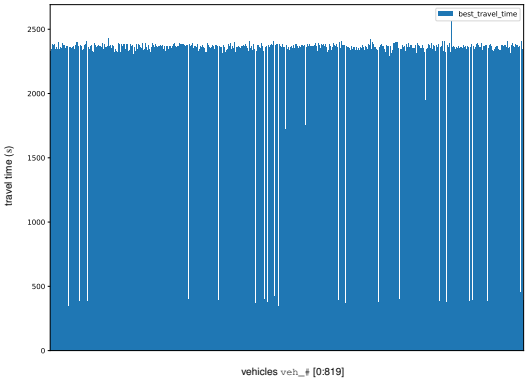


Fig. A.55-18. Best travel time for each vehicle, in seconds (s), during the simulation of a 24 h period.

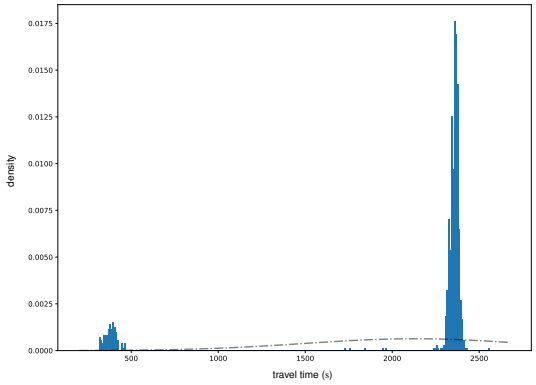


Fig. A.55-19. Density histogram of best travel time for vehicles, in seconds (s), during the simulation of a 24 h period, superimposing the normal density curve. The number of bins was calculated by the Freedman Diaconis rule.

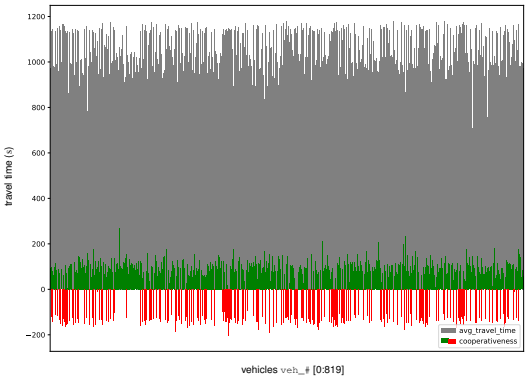


Fig. A.55-20. Average of the travel times, in seconds (s), of individual vehicles, during the simulation of a 24 h period. The bottom graph represents the *degree of cooperativeness**, downscaled by a normalization factor for the purpose of comparison with average times.

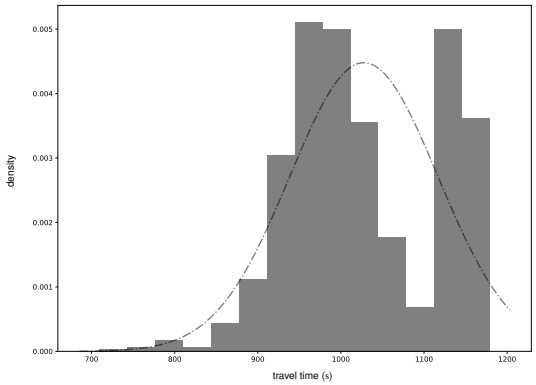


Fig. A.55-21. Density histogram of the average travel times, in seconds (s), of individual vehicles, during the simulation of a 24 h period, superimposing the normal density curve. The number of bins was calculated by the Freedman Diaconis rule.

* The *degree of cooperativeness* is a cumulative sum, calculated at each iteration, based on the complement of the ratio of cooperators, i.e., the higher the number of cooperators the less it increases, but the defectors are more penalized, and vice-versa. It varies inversely with the size of the group to which the player belongs.

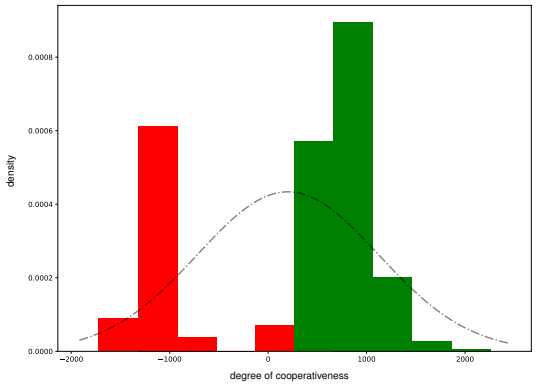


Fig. A.55-22. Density histogram of the *degree of cooperativeness** of individual vehicles, superimposing the normal density curve. The number of bins was calculated by the Freedman Diaconis rule. Generally, when strongly correlated with travel times, it presents a symmetric curve with respect to the *yy*-axis.

References

[1] Ghulam Abbas, Ziaul Haq Abbas, Shahab Haider, Thar Baker, Saadi Boudjit, and Fazal Muhammad. PDMAC: A Priority-Based Enhanced TDMA Protocol for Warning Message Dissemination in VANETs. *Sensors*, 20(1):45, January 2020.

[2] F. B. Abdesslem, H. Abrahamsson, and B. Ahlgren. Measuring Mobile Network Multi-Access for Time-Critical C-ITS Applications. In *2018 Network Traffic Measurement and Analysis Conference (TMA)*, pages 1–8, June 2018.

[3] O. T. Abdulhae, M. Ismail, M. A. Altahrawi, and M. A. Saad. Data Dissemination of Vehicular Ad-Hoc Network in Highway Scenario. In *2019 IEEE 14th Malaysia International Conference on Communication (MICC)*, pages 25–30, December 2019.

[4] Jeffrey L Adler and Victor J Blue. Toward the design of intelligent traveler information systems. *Transportation Research Part C: Emerging Technologies*, 6(3):157–172, June 1998.

[5] A. Ahmad, S. Din, A. Paul, G. Jeon, M. Aloqaily, and M. Ahmad. Real-Time Route Planning and Data Dissemination for Urban Scenarios Using the Internet of Things. *IEEE Wireless Communications*, 26(6):50–55, December 2019.

[6] S. A. Ahmad, A. Hajisami, H. Krishnan, F. Ahmed-Zaid, and E. Moradi-Pari. V2V System Congestion Control Validation and Performance. *IEEE Transactions on Vehicular Technology*, 68(3):2102–2110, March 2019.

[7] S. A. Ahmad and M. Shcherbakov. A Survey on Routing Protocols in Vehicular Adhoc Networks. In *2018 9th International Conference on Information, Intelligence, Systems and Applications (IISA)*, pages 1–8, July 2018.

[8] E. Ahmed and H. Gharavi. Cooperative Vehicular Networking: A Survey. *IEEE Transactions on Intelligent Transportation Systems*, 19(3):996–1014, March 2018.

[9] Vladimir Akimov and Mikhail Soutchanski. Automata Simulation of N-Person Social Dilemma Games. *The Journal of Conflict Resolution*, 38(1):138–148, 1994.

[10] A. Akinsanya, M. Nair, Y. Pan, and J. Wang. A Dynamic Resource Allocation Scheme in Vehicular Communications. In *IEEE INFOCOM 2020 - IEEE Conference on Computer Communications Workshops (INFOCOM WKSHPS)*, pages 127–131, July 2020.

[11] Ruqayah Al-ani, Bo Zhou, Qi Shi, and Ali Sagheer. A Survey on Secure Safety Applications in VANET. pages 1485–1490, June 2018.

[12] Duaa Zuhair Al-Hamid and Adnan Al-Anbuky. Vehicular Grouping and Network Formation: Virtualization of Network Self-healing. In Andrzej M.J. Skulimowski, Zhengguo Sheng, Sondès Khemiri-Kallel, Christophe Cérin, and Ching-Hsien Hsu, editors, *Internet of Vehicles.*

Technologies and Services Towards Smart City, Lecture Notes in Computer Science, pages 106–121, Cham, 2018. Springer International Publishing.

[13] H. D. R. Albonda and J. Pérez-Romero. A New Mode Selection and Resource Reuse Strategy for V2X in Future Cellular Networks. In *2020 IEEE 91st Vehicular Technology Conference (VTC2020-Spring)*, pages 1–6, May 2020.

[14] Sabri Allani, Taoufik Yeferny, and Richard Chbeir. A scalable data dissemination protocol based on vehicles trajectories analysis. *Ad Hoc Networks*, 71:31–44, March 2018.

[15] B. Amina and E. Mohamed. Performance Evaluation of VANETs Routing Protocols Using SUMO and NS3. In *2018 IEEE 5th International Congress on Information Science and Technology (CiSt)*, pages 525–530, October 2018.

[16] James Andreoni. Warm-Glow versus Cold-Prickle: The Effects of Positive and Negative Framing on Cooperation in Experiments*. *The Quarterly Journal of Economics*, 110(1):1–21, February 1995.

[17] K. Ansari. Cooperative Position Prediction: Beyond Vehicle-to-Vehicle Relative Positioning. *IEEE Transactions on Intelligent Transportation Systems*, 21(3):1121–1130, March 2020.

[18] S. Ansari, T. Boutaleb, S. Sinanovic, C. Gamio, and I. Krikidis. Vehicular multitier gateway selection algorithm for heterogeneous VANET architectures. In *2017 Advances in Wireless and Optical Communications (RTUWO)*, pages 180–185, November 2017.

[19] M. Aramrattana, T. Larsson, J. Jansson, and C. Englund. Dimensions of cooperative driving, its and automation. In *2015 IEEE Intelligent Vehicles Symposium (IV)*, pages 144–149, June 2015.

[20] Maytheewat Aramrattana, Tony Larsson, Jonas Jansson, and Arne Nåbo. Extended Driving Simulator for Evaluation of Cooperative Intelligent Transport Systems. In *Proceedings of the 2016 ACM SIGSIM Conference on Principles of Advanced Discrete Simulation*, SIGSIM-PADS '16, pages 255–258, New York, NY, USA, May 2016. Association for Computing Machinery.

[21] Fabio Arena and Giovanni Pau. An Overview of Vehicular Communications. *Future Internet*, 11(2):27, February 2019.

[22] Muhammad Arif, Guojun Wang, Md Zakirul Alam Bhuiyan, Tian Wang, and Jianer Chen. A survey on security attacks in VANETs: Communication, applications and challenges. *Vehicular Communications*, 19:100179, October 2019.

[23] Richard Arnott, Andre de Palma, and Robin Lindsey. Does providing information to drivers reduce traffic congestion? *Transportation Research Part A: General*, 25(5):309–318, September 1991.

[24] Richard Arnott, André de Palma, and Robin Lindsey. A Structural Model of Peak-Period Congestion: A Traffic Bottleneck with Elastic Demand. *The American Economic Review*, 83(1):161–179, 1993.

[25] Nick Asselin-Miller, Marius Biedka, Gena Gibson, Felix Kirsch, Nikolas Hill, Ben White, and Kotub Uddin. Study on the Deployment of C-ITS in Europe. Final Report ED60721, Ricardo Energy & Environment, London, UK, February 2016.

[26] G. Avino, M. Malinverno, C. Casetti, C. F. Chiasserini, F. Malandrino, M. Rapelli, and G. Zennaro. Support of Safety Services through Vehicular Communications: The Intersection Collision Avoidance Use Case. In *2018 International Conference of Electrical and Electronic Technologies for Automotive*, pages 1–6, July 2018.

[27] Robert M. Axelrod. *The Evolution of Cooperation*. Basic Books, New York, 1984.

[28] Robert M. Axelrod. *The Evolution of Cooperation*. Basic Books, New York, rev. ed edition, 2006.

[29] O. Baala, C. Boucetta, K. A. Ali, and A. Caminada. More Insights Into Communication Issues in the Internet of Vehicles. In *2018 15th International Symposium on Pervasive Systems, Algorithms and Networks (I-SPAN)*, pages 38–45, October 2018.

[30] Walter Balzano and Silvia Stranieri. Data Dissemination in Vehicular Ad Hoc Network: A Model to Improve Network Congestion. In Leonard Barolli, Makoto Takizawa, Fatos Xhafa, and Tomoya Enokido, editors, *Web, Artificial Intelligence and Network Applications*, Advances in Intelligent Systems and Computing, pages 851–859, Cham, 2019. Springer International Publishing.

[31] S. Bauk, J. A. L. Calvo, R. Mathar, and A. Schmeink. V2P/I communication for increasing occupational safety at a seaport. In *2017 International Symposium ELMAR*, pages 79–82, September 2017.

[32] Ana L. C. Bazzan and Franziska Klügl. A review on agent-based technology for traffic and transportation. *The Knowledge Engineering Review*, 29(3):375–403, June 2014.

[33] Ana L. C. Bazzan, Ana Peleteiro, and Juan C. Burguillo. Learning to cooperate in the Iterated Prisoner's Dilemma by means of social attachments. *Journal of the Brazilian Computer Society*, 17(3):163–174, October 2011.

[34] Tilman Becker, Michael Carter, and Jörg Naeve. *Experts Playing the Traveler's Dilemma*. February 2005.

[35] Moshe Ben-Akiva, Andre De Palma, and Kaysi Isam. Dynamic network models and driver information systems. *Transportation Research Part A: General*, 25(5):251–266, September 1991.

[36] Eran Ben-Elia and Erel Avineri. Response to Travel Information: A Behavioural Review. *Transport Reviews*, 35(3):352–377, May 2015.

[37] Eran Ben-Elia, Roberta Di Pace, Gennaro N. Bifulco, and Yoram Shiftan. The impact of travel information's accuracy on route-choice. *Transportation Research Part C: Emerging Technologies*, 26:146–159, January 2013.

[38] Eran Ben-Elia and Yoram Shiftan. Which road do I take? A learning-based model of route-choice behavior with real-time information. *Transportation Research Part A: Policy and Practice*, 44(4):249–264, May 2010.

[39] S. U. Bhover, A. Tugashetti, and P. Rashinkar. V2X communication protocol in VANET for co-operative intelligent transportation system. In *2017 International Conference on Innovative Mechanisms for Industry Applications (ICIMIA)*, pages 602–607, February 2017.

[40] F. Biral, G. Valenti, E. Bertolazzi, and A. Steccanella. Cooperative Safety Applications for C-ITS Equipped and Non-equipped Vehicles Supported by an Extended Local Dynamic Map built on SAFE STRIP Technology. In *2019 15th International Conference on Distributed Computing in Sensor Systems (DCOSS)*, pages 733–740, May 2019.

[41] Mate Boban and Andreas Festag. Service-actuated multi-channel operation for vehicular communications. *Computer Communications*, 93:17–26, November 2016.

[42] Phillip Bonacich, Gerald H. Shure, James P. Kahan, and Robert J. Meeker. Cooperation and Group Size in the N-Person Prisoners' Dilemma. *The Journal of Conflict Resolution*, 20(4):687–706, 1976.

[43] Marilisa Botte, Luigi Pariota, Luca D'Acierno, and Gennaro Nicola Bifulco. An Overview of Cooperative Driving in the European Union: Policies and Practices. *Electronics*, 8(6):616, June 2019.

[44] Robert Boyd and Peter J. Richerson. The evolution of reciprocity in sizable groups. *Journal of Theoretical Biology*, 132(3):337–356, June 1988.

[45] D. Braess. Über ein Paradoxon aus der Verkehrsplanung. *Unternehmensforschung*, 12(1):258–268, December 1968.

[46] M. B. Brahim and H. Menouar. Optimizing V2X Data Collection and Storage for a Better Cost and Quality Trade-off. In *2017 6th IEEE International Conference on Advanced Logistics and Transport (ICALT)*, pages 7–12, July 2017.

[47] M. Brambilla, M. Nicoli, G. Soatti, and F. Deflorio. Augmenting Vehicle Localization by Cooperative Sensing of the Driving Environment: Insight on Data Association in Urban Traffic Scenarios. *IEEE Transactions on Intelligent Transportation Systems*, 21(4):1646–1663, April 2020.

[48] Lindsay Browning and Andrew Colman. Evolution of coordinated alternating reciprocity in repeated dyadic games. *Journal of theoretical biology*, 229:549–57, September 2004.

[49] E. Bubeníková, M. Franeková, and P. Holečko. Conceptual design of driving lane-crossing alarm threshold in C-ITS applications and its implementation. In *2016 Cybernetics Informatics (K I)*, pages 1–6, February 2016.

[50] Andrew Butterfield, Gerard Ekembe Ngondi, and Anne Kerr. *A Dictionary of Computer Science*. Oxford University Press, Incorporated, Oxford, 2016.

[51] C-ITS Deployment Platform. C-ITS Platform. Final Report, EUROPEAN COMMISSION, Directorate-General for Mobility and Transport, January 2016.

[52] C-ITS Deployment Platform. C-ITS Platform Phase II. Final Report, EUROPEAN COMMISSION, Directorate-General for Mobility and Transport, September 2017.

[53] M. Cao, Q. Shuai, and V. O. K. Li. Navigation-Based Traffic Signal Control in Intelligent Transportation Systems. In *2018 IEEE Global Communications Conference (GLOBECOM)*, pages 1–7, December 2018.

[54] Valerio Capraro. A Model of Human Cooperation in Social Dilemmas. *PLOS ONE*, 8(8):e72427, August 2013.

[55] CAR 2 CAR Communication Consortium. Manifesto: Overview of the C2C-CC System. C2C-CC Manifesto, CAR 2 CAR Communication Consortium, August 2007.

[56] Fiona Carmichael. *A Guide to Game Theory*. Financial Times Prentice Hall, Harlow, Essex, England ; New York, 2005.

[57] J. Casademont, A. Calveras, D. Quiñones, M. Navarro, J. Arribas, and M. Catalan-Cid. Cooperative-Intelligent Transport Systems for Vulnerable Road Users Safety. In *2019 7th International Conference on Future Internet of Things and Cloud (FiCloud)*, pages 141–146, August 2019.

[58] Ennio Cascetta. *Transportation Systems Engineering: Theory and Methods*, volume 49 of *Applied Optimization*. Springer US, Boston, MA, 2001.

[59] Derek Caveney. Cooperative Vehicular Safety Applications. In *VANET*, chapter 2, pages 21–48. John Wiley & Sons, Ltd, 2010.

[60] Abdellah Chehri, Nordine Quadar, and Rachid Saadane. Communication and Localization Techniques in VANET Network for Intelligent Traffic System in Smart Cities: A Review. In Xiaobo Qu, Lu Zhen, Robert J. Howlett, and Lakhmi C. Jain, editors, *Smart Transportation Systems 2020*, Smart Innovation, Systems and Technologies, pages 167–177, Singapore, 2020. Springer.

[61] L. Chen and C. Englund. Cooperative ITS — EU standards to accelerate cooperative mobility. In *2014 International Conference on Connected Vehicles and Expo (ICCVE)*, pages 681–686, November 2014.

[62] L. Chen and C. Englund. Cooperative Intersection Management: A Survey. *IEEE Transactions on Intelligent Transportation Systems*, 17(2):570–586, February 2016.

[63] L. Chen, A. Habibovic, C. Englund, A. Voronov, and A. L. Walter. Coordinating dangerous goods vehicles: C-ITS applications for safe road tunnels. In *2015 IEEE Intelligent Vehicles Symposium (IV)*, pages 156–161, June 2015.

[64] Ho Ting Cheng, Hangguan Shan, and Weihua Zhuang. Infotainment and road safety service support in vehicular networking: From a communication perspective. *Mechanical Systems and Signal Processing*, 25(6):2020–2038, August 2011.

[65] S. Chiocchio, A. Persia, F. Valentini, E. Cinque, M. Pratesi, and F. Santucci. Integrated Simulation Environments for Vehicular Communications in Cooperative Road Transportation Systems. In *2018 2nd URSI Atlantic Radio Science Meeting (AT-RASC)*, pages 1–4, May 2018.

[66] Apratim Choudhury, Tomasz Maszczyk, Chetan B. Math, Hong Li, and Justin Dauwels. An Integrated Simulation Environment for Testing V2X Protocols and Applications. *Procedia Computer Science*, 80:2042–2052, January 2016.

[67] I. V. Chremos, L. E. Beaver, and A. A. Malikopoulos. A Game-Theoretic Analysis of the Social Impact of Connected and Automated Vehicles. In *2020 IEEE 23rd International Conference on Intelligent Transportation Systems (ITSC)*, pages 1–6, September 2020.

[68] A. Chtourou, P. Merdrignac, and O. Shagdar. Context-Aware Communication for V2V Collision Avoidance Applications. In *2020 International Wireless Communications and Mobile Computing (IWCMC)*, pages 1958–1963, June 2020.

[69] E. Cinque, F. Valentini, A. Iovine, and M. Pratesi. An adaptive strategy to mitigate instability in the ETSI DCC: Experimental validation. In *2017 15th International Conference on ITS Telecommunications (ITST)*, pages 1–6, May 2017.

[70] Andrew Colman and Lindsay Browning. Evolution of cooperative turn-taking. *Evolutionary Ecology Research*, 11, September 2009.

[71] Andrew M. Colman and Andrew M. Colman. *Game Theory and Its Applications in the Social and Biological Sciences*. International Series in Social Psychology. Butterworth-Heinemann, Oxford [England] ; Boston, Mass, 2nd ed edition, 1995.

[72] Russell Cooper, Douglas V. DeJong, Robert Forsythe, and Thomas W. Ross. Cooperation without Reputation: Experimental Evidence from Prisoner's Dilemma Games. *Games and Economic Behavior*, 12(2):187–218, February 1996.

[73] A. Correa, R. Alms, J. Gozalvez, M. Sepulcre, M. Rondinone, R. Blokpoel, L. Lücken, and G. Thandavarayan. Infrastructure Support for Cooperative Maneuvers in Connected and Automated Driving. In *2019 IEEE Intelligent Vehicles Symposium (IV)*, pages 20–25, June 2019.

[74] A. Costa, R. J. F. Rossetti, and Z. Kokkinogenis. Improving Route Choice: Communication Issues in Moving Variable Message Signs. In *2020 IEEE International Smart Cities Conference (ISC2)*, pages 1–8, September 2020.

[75] M. Covell, S. Baluja, and R. Sukthankar. Micro-Auction-Based Traffic-Light Control: Responsive, Local Decision Making. In *2015 IEEE 18th International Conference on Intelligent Transportation Systems*, pages 558–565, September 2015.

[76] A. Czyżewski, A. Sroczyński, T. Śmiałkowski, and P. Hoffmann. Development of Intelligent Road Signs with V2X Interface for Adaptive Traffic Controlling. In *2019 6th International Conference on Models and Technologies for Intelligent Transportation Systems (MT-ITS)*, pages 1–7, June 2019.

[77] Joahannes B. D. da Costa, Allan M. de Souza, Denis Rosário, Eduardo Cerqueira, and Leandro A. Villas. Efficient data dissemination protocol based on complex networks' metrics for urban vehicular networks. *Journal of Internet Services and Applications*, 10(1):15, August 2019.

[78] G. Daniel, M. Arce, and Todd Sandler. The Dilemma of the Prisoners' Dilemmas. *Kyklos*, 58(1):3–24, 2005.

[79] N. Dasanayaka, C. Wang, D. Jayalath, and Y. Feng. Publish-Subscribe Communications for V2I Safety Applications in Intelligent Transportation Systems. In *2019 IEEE 90th Vehicular Technology Conference (VTC2019-Fall)*, pages 1–6, September 2019.

[80] Nishanthi Dasanayaka, Khondokar Fida Hasan, Charles Wang, and Yanming Feng. Enhancing Vulnerable Road User Safety: A Survey of Existing Practices and Consideration for Using Mobile Devices for V2X Connections. *arXiv:2010.15502 [cs]*, October 2020.

[81] Fred D. Davis. Perceived Usefulness, Perceived Ease of Use, and User Acceptance of Information Technology. *MIS Quarterly*, 13(3):319–340, 1989.

[82] Fred D. Davis. User acceptance of information technology: System characteristics, user perceptions and behavioral impacts. *International Journal of Man-Machine Studies*, 38(3):475–487, March 1993.

[83] Fred D. Davis and Viswanath Venkatesh. A critical assessment of potential measurement biases in the technology acceptance model: Three experiments. *International Journal of Human-Computer Studies*, 45(1):19–45, July 1996.

[84] J H Davis, P R Laughlin, and S S Komorita. The Social Psychology of Small Groups: Cooperative and Mixed-Motive Interaction. *Annual Review of Psychology*, 27(1):501–541, 1976.

[85] R M Dawes. Social Dilemmas. *Annual Review of Psychology*, 31(1):169–193, January 1980.

[86] R M Dawes, J Delay, and W Chaplin. The Decision to Pollute. *Environment and Planning A: Economy and Space*, 6(1):3–10, February 1974.

[87] Mario De Felice, Ian Calcagni, Francesca Pesci, F. Cuomo, and Andrea Baiocchi. Self-Healing Infotainment and Safety Application for VANET dissemination. June 2015.

[88] Charles Desjardins, Julien Laumônier, and Brahim Chaib-draa. Learning Agents for Collaborative Driving. www.igi-global.com/chapter/learning-agents-collaborative-driving/26941, 2009.

[89] Kakan Chandra Dey, Anjan Rayamajhi, Mashrur Chowdhury, Parth Bhavsar, and James Martin. Vehicle-to-vehicle (V2V) and vehicle-to-infrastructure (V2I) communication in a heterogeneous wireless network – Performance evaluation. *Transportation Research Part C: Emerging Technologies*, 68:168–184, July 2016.

[90] G. Dimitrakopoulos and P. Demestichas. Intelligent Transportation Systems. *IEEE Vehicular Technology Magazine*, 5(1):77–84, March 2010.

[91] S. Din, A. Ahmad, A. Paul, M. Anisetti, G. Jeon, M. Imran, and N. Nasser. RTRD: Real-Time Route Discovery for Urban Scenarios Using Internet of Things. In *2019 IEEE Global Communications Conference (GLOBECOM)*, pages 1–5, December 2019.

[92] J. Ding, H. Xu, J. Hu, and Y. Zhang. The impact of centralized cooperative intersection control on traffic flow characteristics. In *2017 4th International Conference on Transportation Information and Safety (ICTIS)*, pages 858–864, August 2017.

[93] El Bachir Diop, Shengchuan Zhao, and Van Duy Tran. Modeling Travelers' Acceptance of Variable Message Signs: A Hierarchical Hybrid Choice Model. *Journal of Transportation Engineering, Part A: Systems*, 146(12):04020134, December 2020.

[94] N. Sree Divya and Dr Veeramallu Boddu. An Efficient Data Dissemination Method for VANET with the help of RSUs. *International Journal of Advanced Science and Technology*, 29(06):2010–2021, May 2020.

[95] Avinash K. Dixit, Susan Skeath, and David H. Reiley. *Games of Strategy*. W.W. Norton & Company, New York, fourth edition edition, 2015.

[96] Vinayak V. Dixit, Andreas Ortmann, E. Elisabet Rutström, and Satish V. Ukkusuri. Experimental Economics and choice in transportation: Incentives and context. *Transportation Research Part C: Emerging Technologies*, 77:161–184, April 2017.

[97] G. Domingues, J. Cabral, J. Mota, P. Pontes, Z. Kokkinogenis, and R. J. F. Rossetti. Traffic Simulation of Lane-Merging of Autonomous Vehicles in the Context of Platooning. In *2018 IEEE International Smart Cities Conference (ISC2)*, pages 1–6, September 2018.

[98] Anna Dreber, Tore Ellingsen, Magnus Johannesson, and David G. Rand. Do people care about social context? Framing effects in dictator games. *Experimental Economics*, 16(3):349–371, September 2013.

[99] Anna Dreber, David G. Rand, Drew Fudenberg, and Martin A. Nowak. Winners don't punish. *Nature*, 452(7185):348–351, March 2008.

[100] Eclipse SUMO. Eclipse SUMO - Simulation of Urban MObility. https://www.eclipse.org/sumo/.

[101] S. Edwards, G. Hill, P. Goodman, P. Blythe, P. Mitchell, and Y. Huebner. Quantifying the impact of a real world cooperative-ITS deployment across multiple cities. *Transportation Research Part A: Policy and Practice*, 115:102–113, September 2018.

[102] Thomas Eiter, Herbert Füreder, Fritz Kasslatter, Josiane Xavier Parreira, and Patrik Schneider. Towards a Semantically Enriched Local Dynamic Map. *International Journal of Intelligent Transportation Systems Research*, 17(1):32–48, January 2019.

[103] Lily Elefteriadou. Capacity. In Lily Elefteriadou, editor, *An Introduction to Traffic Flow Theory*, Springer Optimization and Its Applications, pages 93–110. Springer, New York, NY, 2014.

[104] Lily Elefteriadou. Flow, Speed, Density, and Their Relationships. In Lily Elefteriadou, editor, *An Introduction to Traffic Flow Theory*, Springer Optimization and Its Applications, pages 61–91. Springer, New York, NY, 2014.

[105] Lily Elefteriadou. Mathematical and Empirical Models. In Lily Elefteriadou, editor, *An Introduction to Traffic Flow Theory*, Springer Optimization and Its Applications, pages 129–135. Springer, New York, NY, 2014.

[106] Lily Elefteriadou. Modeling the Motion of a Single Vehicle. In Lily Elefteriadou, editor, *An Introduction to Traffic Flow Theory*, Springer Optimization and Its Applications, pages 3–30. Springer, New York, NY, 2014.

[107] Elsevier. Scopus - Document search. https://www.scopus.com/.

[108] J. Elster. Rational Choice Theory: Cultural Concerns. In Neil J. Smelser and Paul B. Baltes, editors, *International Encyclopedia of the Social & Behavioral Sciences*, pages 12763–12768. Pergamon, Oxford, January 2001.

[109] Joshua M. Epstein. Agent-based computational models and generative social science. *Complexity*, 4(5):41–60, 1999.

[110] Ido Erev and Alvin E. Roth. Predicting How People Play Games: Reinforcement Learning in Experimental Games with Unique, Mixed Strategy Equilibria. *The American Economic Review*, 88(4):848–881, 1998.

[111] ERTICO Task Force on Communication Technologies for C-ITS. Communication Technologies for future C-ITS service scenarios. Final Report, March 2015.

[112] ETSI Technical Committee Intelligent Transport System. Intelligent Transport Systems (ITS); Vehicular Communications; Basic Set of Applications; Definitions. Technical Report ETSI TR 102 638 V1.1.1, European Telecommunications Standards Institute, June 2009.

[113] ETSI Technical Committee Intelligent Transport System. Intelligent Transport Systems (ITS); Communications Architecture. European Standard ETSI EN 302 665 V1.1.1, European Telecommunications Standards Institute, September 2010.

[114] ETSI Technical Committee Intelligent Transport System. Intelligent Transport Systems (ITS); Vehicular Communications; Basic Set of Applications; Part 1: Functional Requirements. Technical Specification ETSI TS 102 637-1 V1.1.1, European Telecommunications Standards Institute, September 2010.

[115] Dick Ettema and Harry Timmermans. Costs of travel time uncertainty and benefits of travel time information: Conceptual model and numerical examples. *Transportation Research Part C: Emerging Technologies*, 14(5):335–350, October 2006.

[116] European Commission. A European strategy on Cooperative Intelligent Transport Systems, a milestone towards cooperative, connected and automated mobility. COM(2016) 766, November 2016.

[117] European Parliament, Council of the European Union. Directive 2010/41/EU of the European Parliament and of the Council of 7 July 2010 on the framework for the deployment of Intelligent Transport Systems in the field of road transport and for interfaces with other modes of transport. *Official Journal of the European Union*, L207:1–13, August 2010.

[118] European Transport Safety Council. *Briefing on Cooperative Intelligent Transport Systems C-ITS*. European Transport Safety Council, Brussels, November 2017.

[119] Elias C. Eze, Si-Jing Zhang, En-Jie Liu, and Joy C. Eze. Advances in vehicular ad-hoc networks (VANETs): Challenges and road-map for future development. *International Journal of Automation and Computing*, 13(1):1–18, February 2016.

[120] M. Fadda, M. Murroni, and V. Popescu. Interference Issues for VANET Communications in the TVWS in Urban Environments. *IEEE Transactions on Vehicular Technology*, 65(7):4952–4958, July 2016.

[121] Ernst Fehr and Simon Gächter. Altruistic punishment in humans. *Nature*, 415(6868):137–140, January 2002.

[122] Ernst Fehr and Klaus M. Schmidt. A Theory of Fairness, Competition, and Cooperation*. *The Quarterly Journal of Economics*, 114(3):817–868, August 1999.

[123] Elias Fernández-Domingos, Miguel Loureiro, Tamara Álvarez-López, Juan C. Burguillo, José Covelo, Ana Peleteiro, and Aleksander Byrski. Emerging Cooperation in N-Person Iterated Prisoner's Dilemma over Dynamic Complex Networks. *Computing and Informatics*, 36(3):493–516, 2017.

[124] J. Finocchiaro and H. D. Mathias. Evolutionary Optimization of Cooperative Strategies for the Iterated Prisoner's Dilemma. *IEEE Transactions on Games*, pages 1–1, 2020.

[125] Urs Fischbacher, Simon Gächter, and Ernst Fehr. Are people conditionally cooperative? Evidence from a public goods experiment. *Economics Letters*, 71(3):397–404, June 2001.

[126] Hans-Joachim Fischer. Standardization and Harmonization Activities Towards a Global C-ITS. In Claudia Campolo, Antonella Molinaro, and Riccardo Scopigno, editors, *Vehicular Ad Hoc Networks: Standards, Solutions, and Research*, pages 23–36. Springer International Publishing, Cham, 2015.

[127] Andreas Flache and Michael Macy. A More General Model of Cooperation Based on Reinforcement. July 2003.

[128] Andreas Flache and Michael W. Macy. Stochastic Collusion and the Power Law of Learning: A General Reinforcement Learning Model of Cooperation. *Journal of Conflict Resolution*, 46(5):629–653, October 2002.

[129] Marc Fleurbaey. *Fairness, Responsibility, and Welfare*. Oxford University Press, Oxford, 2012.

[130] Maede Fotros, Javad Rezazadeh, and Omid Ameri Sianaki. A Survey on VANETs Routing Protocols for IoT Intelligent Transportation Systems. In Leonard Barolli, Flora Amato, Francesco Moscato, Tomoya Enokido, and Makoto Takizawa, editors, *Web, Artificial Intelligence and Network Applications*, Advances in Intelligent Systems and Computing, pages 1097–1115, Cham, 2020. Springer International Publishing.

[131] James W. Friedman. A Non-cooperative Equilibrium for Supergames. *The Review of Economic Studies*, 38(1):1–12, January 1971.

[132] M. U. Ghazi, M. A. Khan Khattak, B. Shabir, A. W. Malik, and M. Sher Ramzan. Emergency Message Dissemination in Vehicular Networks: A Review. *IEEE Access*, 8:38606–38621, 2020.

[133] Amrita Ghosal and Mauro Conti. Security issues and challenges in V2X: A Survey. *Computer Networks*, 169:107093, March 2020.

[134] Dwight J. Goehring and James P. Kahan. The Uniform N-Person Prisoner's Dilemma Game: Construction and Test of an Index of Cooperation. *The Journal of Conflict Resolution*, 20(1):111–128, 1976.

[135] Jacob K. Goeree and Charles A. Holt. Ten Little Treasures of Game Theory and Ten Intuitive Contradictions. *American Economic Review*, 91(5):1402–1422, December 2001.

[136] B. D. Greenshields. A study of traffic capacity. In *Proceedings of the Highway Research Board*, volume 14, pages 448–477, 1935.

[137] Maxime Guériau, Romain Billot, Nour-Eddin El Faouzi, Julien Monteil, Frédéric Armetta, and Salima Hassas. How to assess the benefits of connected vehicles? A simulation framework for the design of cooperative traffic management strategies. *Transportation Research Part C: Emerging Technologies*, 67:266–279, June 2016.

[138] Mohammed I. Habelalmateen, A. H. Abbas, L. Audah, and N. a. M. Alduais. Dynamic multiagent method to avoid duplicated information at intersections in VANETs. *TELKOMNIKA (Telecommunication Computing Electronics and Control)*, 18(2):613–621, April 2020.

[139] Mohamed Hadded, Paul Muhlethaler, Anis Laouiti, and Leila Azzouz Saidane. A Novel Angle-Based Clustering Algorithm for Vehicular Ad Hoc Networks. In Anis Laouiti, Amir Qayyum, and Mohamad Naufal Mohamad Saad, editors, *Vehicular Ad-Hoc Networks for*

Smart Cities, Advances in Intelligent Systems and Computing, pages 27–38, Singapore, 2017. Springer.

[140] Henry Hamburger. N-person Prisoner's Dilemma. *Journal of Mathematical Sociology*, 3(1):27–48, 1973.

[141] M. Maad Hamdi, L. Audah, S. Abduljabbar Rashid, A. Hamid Mohammed, S. Alani, and A. Shamil Mustafa. A Review of Applications, Characteristics and Challenges in Vehicular Ad Hoc Networks (VANETs). In *2020 International Congress on Human-Computer Interaction, Optimization and Robotic Applications (HORA)*, pages 1–7, June 2020.

[142] Elyes Ben Hamida, Hassan Noura, and Wassim Znaidi. Security of Cooperative Intelligent Transport Systems: Standards, Threats Analysis and Cryptographic Countermeasures. *Electronics*, 4(3):380–423, September 2015.

[143] Badis Hammi, Houda Labiod, Gérard Segarra, Alain Servel, and Jean Philippe Monteuuis. CAM-Infrastructure: A novel solution for service advertisement in Cooperative Intelligent Transportation Systems. *Advances in Science, Technology and Engineering Systems Journal*, 2(3):1422–1431, August 2017.

[144] Garrett Hardin. The Tragedy of the Commons. *Science*, 162(3859):1243–1248, December 1968.

[145] Hannes Hartenstein and Kenneth P. Laberteaux, editors. *VANET: Vehicular Applications and Inter-Networking Technologies*. Intelligent Transportation Systems. Wiley, 2010.

[146] Syed Faraz Hasan, Nazmul Siddique, and Shyam Chakraborty. *Intelligent Transportation Systems*. Springer International Publishing, Cham, 2018.

[147] Dirk Helbing and Sergi Lozano. Phase transitions to cooperation in the prisoner's dilemma. *Physical Review E*, 81(5):057102, May 2010.

[148] Dirk Helbing, Martin Schönhof, Hans-Ulrich Stark, and Janusz Hołyst. How Individuals Learn to Take Turns: Emergence of Alternating Cooperation in a Congestion Game and the Prisoner's Dilemma. *Advances in Complex Systems (ACS)*, 08:87–116, February 2005.

[149] J. R. Hicks. The Foundations of Welfare Economics. *The Economic Journal*, 49(196):696–712, 1939.

[150] John J. Horton, David G. Rand, and Richard J. Zeckhauser. The online laboratory: Conducting experiments in a real labor market. *Experimental Economics*, 14(3):399–425, September 2011.

[151] C.-C. Hu. Peer-to-Peer Data Dissemination for Deadline-Sensitive Streaming in VANETs. *IEEE Access*, 8:136348–136360, 2020.

[152] C. Huang, M. Chiang, W. Su, and D. Dao. SDN-based V2V offloading for cellular network using the LifeTime-based network state routing (LT-NSR). In *2018 International Conference on Information Networking (ICOIN)*, pages 274–279, January 2018.

[153] Rodolfo I. Meneguette, Robson E. De Grande, and Antonio A. F. Loureiro. *Intelligent Transport System in Smart Cities: Aspects and Challenges of Vehicular Networks and Cloud*. Urban Computing. Springer International Publishing, Cham, 2018.

[154] Christian Iaione. The Tragedy of Urban Roads: Saving Cities from Choking, Calling on Citizens to Combat Climate Change. *Fordham Urban Law Journal*, 37(3):889, January 2010.

[155] R. Mark Isaac and James M. Walker. Group Size Effects in Public Goods Provision: The Voluntary Contributions Mechanism. *The Quarterly Journal of Economics*, 103(1):179–199, 1988.

[156] H. Ito, T. Murase, and K. Sasajima. Congestion control and energy savings for V2P communication crash warnings with proximity relying. In *2016 International Conference on Connected Vehicles and Expo (ICCVE)*, pages 43–48, September 2016.

[157] Krishna J. Efficient Information Dissemination in Vehicular Networks with Topological Approach. *International Journal of Advanced Trends in Computer Science and Engineering*, 9(3):3687–3694, June 2020.

[158] Olaf Jahn, Rolf H. Möhring, Andreas S. Schulz, and Nicolás E. Stier-Moses. System-Optimal Routing of Traffic Flows with User Constraints in Networks with Congestion. *Operations Research*, 53(4):600–616, August 2005.

[159] Farhan Jamil, Anam Javaid, Tariq Umer, and Mubashir Husain Rehmani. A comprehensive survey of network coding in vehicular ad-hoc networks. *Wireless Networks*, 23(8):2395–2414, November 2017.

[160] A. Jantošová, I. Dolnák, and M. Dado. An overview of vehicular ad hoc networks. In *2019 17th International Conference on Emerging eLearning Technologies and Applications (ICETA)*, pages 305–308, November 2019.

[161] Muhammad Awais Javed, Sherali Zeadally, and Elyes Ben Hamida. Data analytics for Cooperative Intelligent Transport Systems. *Vehicular Communications*, 15:63–72, January 2019.

[162] Mouna Jiber, Abdelilah Mbarek, Ali Yahyaouy, My Abdelouahed Sabri, and Jaouad Boumhidi. Road Traffic Prediction Model Using Extreme Learning Machine: The Case Study of Tangier, Morocco. *Information*, 11(12):542, December 2020.

[163] Wen-Long Jin. On the existence of stationary states in general road networks. *Transportation Research Part B: Methodological*, 81:917–929, November 2015.

[164] Y. Jin, W. Xu, P. Wang, and J. Wang. Route Planning of Rescue Vehicles in the Process of Dynamic Change of Traffic Volume under Emergency Conditions. In *2019 3rd International Symposium on Autonomous Systems (ISAS)*, pages 125–130, May 2019.

[165] Mary Sissons Joshi, Vijay Joshi, and Roger Lamb. The Prisoners' Dilemma and City-Centre Traffic. *Oxford Economic Papers*, 57(1):70–89, 2005.

[166] H. Jung, K. Lim, D. Shin, S. Yoon, S. Jin, S. Jang, and J. Kwak. Reliability Verification Procedure of Secured V2X Communication for Autonomous Cooperation Driving. In *2018 International Conference on Information and Communication Technology Convergence (ICTC)*, pages 1356–1360, October 2018.

[167] I. Kabashkin. Reliable v2x communications for safety-critical intelligent transport systems. In *2017 Advances in Wireless and Optical Communications (RTUWO)*, pages 251–255, November 2017.

[168] Z. Kailong, W. Min, S. Hang, Y. Ansheng, A. de La Fortelle, and M. Kejian. QoS-CITS: A simulator for service-oriented cooperative ITS of intelligent vehicles. In *2017 IEEE/ACIS 16th International Conference on Computer and Information Science (ICIS)*, pages 751–756, May 2017.

[169] Rahul Kala. Reaching destination on time with cooperative intelligent transportation systems. *Journal of Advanced Transportation*, 50(2):214–227, 2016.

[170] Nicholas Kaldor. Welfare Propositions of Economics and Interpersonal Comparisons of Utility. *The Economic Journal*, 49(195):549–552, 1939.

[171] Todd R. Kaplan and Bradley J. Ruffle. Which Way to Cooperate. SSRN Scholarly Paper ID 990942, Social Science Research Network, Rochester, NY, October 2011.

[172] Ramin Karimi and Saeed Shokrollahi. PGRP: Predictive geographic routing protocol for VANETs. *Computer Networks*, 141:67–81, August 2018.

[173] Emmanuel Kemel and Corina Paraschiv. Prospect Theory for joint time and money consequences in risk and ambiguity. *Transportation Research Part B: Methodological*, 56:81–95, October 2013.

[174] Boris S. Kerner. Definitions of The Three Traffic Phases. In Boris S. Kerner, editor, *Introduction to Modern Traffic Flow Theory and Control: The Long Road to Three-Phase Traffic Theory*, pages 9–40. Springer, Berlin, Heidelberg, 2009.

[175] Boris S. Kerner. Earlier Theoretical Basis of Transportation Engineering: Fundamental Diagram Approach. In Boris S. Kerner, editor, *Introduction to Modern Traffic Flow Theory and Control: The Long Road to Three-Phase Traffic Theory*, pages 173–219. Springer, Berlin, Heidelberg, 2009.

[176] Boris S. Kerner. Linking of Three-Phase Traffic Theory and Fundamental Diagram Approach to Traffic Flow Modeling. In Boris S. Kerner, editor, *Introduction to Modern Traffic Flow Theory and Control: The Long Road to Three-Phase Traffic Theory*, pages 245–252. Springer, Berlin, Heidelberg, 2009.

[177] Boris S. Kerner. Three-Phase Traffic Flow Models. In Boris S. Kerner, editor, *Introduction to Modern Traffic Flow Theory and Control: The Long Road to Three-Phase Traffic Theory*, pages 221–243. Springer, Berlin, Heidelberg, 2009.

[178] Femke Kessels. The Fundamental Diagram. In Femke Kessels, editor, *Traffic Flow Modelling: Introduction to Traffic Flow Theory Through a Genealogy of Models*, EURO Advanced Tutorials on Operational Research, pages 21–34. Springer International Publishing, Cham, 2019.

[179] Femke Kessels. Introduction to Traffic Flow Modelling. In Femke Kessels, editor, *Traffic Flow Modelling: Introduction to Traffic Flow Theory Through a Genealogy of Models*, EURO Advanced Tutorials on Operational Research, pages 1–19. Springer International Publishing, Cham, 2019.

[180] Femke Kessels. Macroscopic Models. In Femke Kessels, editor, *Traffic Flow Modelling: Introduction to Traffic Flow Theory Through a Genealogy of Models*, EURO Advanced Tutorials on Operational Research, pages 53–81. Springer International Publishing, Cham, 2019.

[181] Zahid Khan, Anis Koubaa, and Haleem Farman. Smart Route: Internet-of-Vehicles (IoV)-Based Congestion Detection and Avoidance (IoV-Based CDA) Using Rerouting Planning. *Applied Sciences*, 10(13):4541, January 2020.

[182] Sahil Khatri, Hrishikesh Vachhani, Shalin Shah, Jitendra Bhatia, Manish Chaturvedi, Sudeep Tanwar, and Neeraj Kumar. Machine learning models and techniques for VANET based traffic management: Implementation issues and challenges. *Peer-to-Peer Networking and Applications*, September 2020.

[183] T. Kimura, H. Saito, and H. Honda. Optimal transmission range for V2I communications on congested highways. In *2017 IEEE 28th Annual International Symposium on Personal, Indoor, and Mobile Radio Communications (PIMRC)*, pages 1–7, October 2017.

[184] T. Kitazato, M. Tsukada, H. Ochiai, and H. Esaki. Proxy cooperative awareness message: An infrastructure-assisted V2V messaging. In *2016 Ninth International Conference on Mobile Computing and Ubiquitous Networking (ICMU)*, pages 1–6, October 2016.

[185] Ido Klein and Eran Ben-Elia. Emergence of cooperation in congested road networks using ICT and future and emerging technologies: A game-based review. *Transportation Research Part C: Emerging Technologies*, 72:10–28, November 2016.

[186] Ido Klein and Eran Ben-Elia. Emergence of cooperative route-choice: A model and experiment of compliance with system-optimal ATIS. *Transportation Research Part F: Traffic Psychology and Behaviour*, 59:348–364, November 2018.

[187] Ido Klein, Nadav Levy, and Eran Ben-Elia. An Agent-Based Model of a System-Optimal ATIS. *Procedia Computer Science*, 109:893–898, January 2017.

[188] Ido Klein, Nadav Levy, and Eran Ben-Elia. An agent-based model of the emergence of cooperation and a fair and stable system optimum using ATIS on a simple road network. *Transportation Research Part C: Emerging Technologies*, 86:183–201, January 2018.

[189] Deddy P. Koesrindartoto. Discrete Double Auctions with Artificial Adaptive Agents: A Case Study of an Electricity Market Using a Double Auction Simulator. September 2002.

[190] Z. Kokkinogenis, M. Teixeira, P. M. d'Orey, and R. J. F. Rossetti. Tactical Level Decision-Making for Platoons of Autonomous Vehicles Using Auction Mechanisms. In *2019 IEEE Intelligent Vehicles Symposium (IV)*, pages 1632–1638, June 2019.

[191] Hariharan Krishnan, Fan Bai, and Gavin Holland. Commercial and Public Use Applications. In *Vehicular Networking*, chapter 1, pages 1–28. John Wiley & Sons, Ltd, 2010.

[192] Alexander Krylatov, Victor Zakharov, and Tero Tuovinen. Principles of Wardrop for Traffic Assignment in a Road Network. In Alexander Krylatov, Victor Zakharov, and Tero Tuovinen, editors, *Optimization Models and Methods for Equilibrium Traffic Assignment*, Springer Tracts on Transportation and Traffic, pages 17–43. Springer International Publishing, Cham, 2020.

[193] Steven Kuhn. Prisoner's Dilemma. In Edward N. Zalta, editor, *The Stanford Encyclopedia of Philosophy*. Metaphysics Research Lab, Stanford University, winter 2019 edition, 2019.

[194] Vishal Kumar, Narottam Chand, and Shailendra Mishra. Applications of VANETs: Present & future. In *Communications and Network*, volume 05, January 2013.

[195] H. Labiod, A. Servel, G. Seggara, B. Hammi, and J. P. Monteuuis. A New Service Advertisement Message for ETSI ITS Environments: CAM-Infrastructure. In *2016 8th IFIP International Conference on New Technologies, Mobility and Security (NTMS)*, pages 1–4, November 2016.

[196] Hanae Lahmiss and Abdellah Khatory. Trends and Applications of Cooperative Intelligent Transport Systems (C-ITS). In Abdelmjid Saka, Jean-Yves Choley, Jamel Louati, Zakaria Chalh, Maher Barkallah, Mohammed Alfidi, Mounir Ben Amar, Fakher Chaari, and Mohamed Haddar, editors, *Advances in Integrated Design and Production*, Lecture Notes in Mechanical Engineering, pages 527–536, Cham, 2021. Springer International Publishing.

[197] Paul A. M. Van Lange. *Social Dilemmas: The Psychology of Human Cooperation*. Oxford University Press, Oxford ; New York, 2014.

[198] Lucie Langer, Arndt Bonitz, Christoph Schmittner, and Stefan Ruehrup. Automated Right of Way for Emergency Vehicles in C-ITS: An Analysis of Cyber-Security Risks. In António Casimiro, Frank Ortmeier, Erwin Schoitsch, Friedemann Bitsch, and Pedro Ferreira, editors, *Computer Safety, Reliability, and Security. SAFECOMP 2020 Workshops*, Lecture Notes in Computer Science, pages 148–160, Cham, 2020. Springer International Publishing.

[199] B. Leblanc, S. Ercan, and C. d Runz. C-ITS data completion to improve unsupervised driving profile detection. In *2020 IEEE 91st Vehicular Technology Conference (VTC2020-Spring)*, pages 1–5, May 2020.

[200] Michael Lee and Travis Atkison. VANET applications: Past, present, and future. *Vehicular Communications*, October 2020.

[201] S. Lee. Structure of Enhanced QoS for Vehicular Network. In *2018 International Conference on Information and Communication Technology Convergence (ICTC)*, pages 1361–1363, October 2018.

[202] T.-K. Lee, J.-J. Chen, Y.-C. Tseng, and C.-K. Lin. Effect of Packet Loss and Delay on V2X Data Fusion. In *2020 21st Asia-Pacific Network Operations and Management Symposium (APNOMS)*, pages 302–305, September 2020.

[203] Uichin Lee and Mario Gerla. A survey of urban vehicular sensing platforms. *Computer Networks*, 54(4):527–544, March 2010.

[204] Wilhelm Leutzbach. The Motion of Several Vehicles on a Road. In Wilhelm Leutzbach, editor, *Introduction to the Theory of Traffic Flow*, pages 39–193. Springer, Berlin, Heidelberg, 1988.

[205] David Levinson. The value of advanced traveler information systems for route choice. *Transportation Research Part C: Emerging Technologies*, 11(1):75–87, February 2003.

[206] Nadav Levy and Eran Ben-Elia. Emergence of System Optimum: A Fair and Altruistic Agent-based Route-choice Model. *Procedia Computer Science*, 83:928–933, January 2016.

[207] Nadav Levy, Ido Klein, and Eran Ben-Elia. Emergence of cooperation and a fair system optimum in road networks: A game-theoretic and agent-based modelling approach. *Research in Transportation Economics*, 68:46–55, August 2018.

[208] X. Li, Y. Liu, and X. Yin. A Message-Oriented Message Dissemination and Authentication Scheme for Vehicular Ad Hoc Networks. In *2019 IEEE Intl Conf on Parallel Distributed Processing with Applications, Big Data Cloud Computing, Sustainable Computing Communications, Social Computing Networking (ISPA/BDCloud/SocialCom/SustainCom)*, pages 223–228, December 2019.

[209] L. Liang, H. Peng, G. Y. Li, and X. Shen. Vehicular Communications: A Physical Layer Perspective. *IEEE Transactions on Vehicular Technology*, 66(12):10647–10659, December 2017.

[210] Wim B.G. Liebrand. A Classification of Social Dilemma Games. *Simulation & Games*, 14(2):123–138, June 1983.

[211] J. Lin, Y. Huang, X. Su, Z. Su, and P. Zhao. An In-vehicle Camera Based Traffic Estimation in Smart Transportation. In *2019 IEEE 5th International Conference on Computer and Communications (ICCC)*, pages 2186–2192, December 2019.

[212] Robin Lindsey, Terry Daniel, Eyran Gisches, and Amnon Rapoport. Pre-trip information and route-choice decisions with stochastic travel conditions: Theory. *Transportation Research Part B: Methodological*, 67:187–207, September 2014.

[213] Xiaofeng Liu and Arunita Jaekel. Congestion Control in V2V Safety Communication: Problem, Analysis, Approaches. *Electronics*, 8(5):540, May 2019.

[214] Christian Lochert, Björn Scheuermann, and Martin Mauve. Information Dissemination in VANETs. In *VANET*, chapter 3, pages 49–80. John Wiley & Sons, Ltd, 2010.

[215] L. H. S. Lopes, R. A. F. Mini, and F. Cunha. A V2X Approach for Data Dissemination in Vehicular Ad Hoc Networks. In *2019 IEEE Symposium on Computers and Communications (ISCC)*, pages 1–6, June 2019.

[216] Pablo Alvarez Lopez, Evamarie Wiessner, Michael Behrisch, Laura Bieker-Walz, Jakob Erdmann, Yun-Pang Flotterod, Robert Hilbrich, Leonhard Lucken, Johannes Rummel, and Peter Wagner. Microscopic Traffic Simulation using SUMO. In *The 21st IEEE International Conference on Intelligent Transportation Systems*, 2019 IEEE Intelligent Transportation Systems Conference (ITSC), pages 2575–2582, Maui, HI, November 2018. IEEE.

[217] V.S.T.P.P.R.D. Luce, R.D. Luce, and H. Raiffa. *Games and Decisions: Introduction and Critical Survey*. Number vol. 10 in Dover Books on Mathematics. Dover Publications, 1957.

[218] Michael W. Macy and Andreas Flache. Learning dynamics in social dilemmas. *Proceedings of the National Academy of Sciences*, 99(suppl 3):7229–7236, May 2002.

[219] I. Mahjri, S. Faye, and D. Khadraoui. On Building Cooperative Intelligent Transportation Systems over Public Transports. In *2019 15th International Wireless Communications Mobile Computing Conference (IWCMC)*, pages 489–495, June 2019.

[220] Santa Maiti, Stephan Winter, and Lars Kulik. A conceptualization of vehicle platoons and platoon operations. *Transportation Research Part C: Emerging Technologies*, 80:1–19, July 2017.

[221] Suman Malik and Prasant Kumar Sahu. A comparative study on routing protocols for VANETs. *Heliyon*, 5(8):e02340, August 2019.

[222] Klaus Manhart and Andreas Diekmann. Kooperative Strategien im Gefangenendilemma: Computersimulation eines N-Personen-Spiels. *Analyse & Kritik - Zeitschrift für Sozialtheorie*, 11(2):134–153, 1989.

[223] M. Marques, C. Senna, and S. Sargento. Evaluation of Strategies for Emergency Message Dissemination in VANETs. In *2020 IEEE Symposium on Computers and Communications (ISCC)*, pages 1–6, July 2020.

[224] Vanessa Martins, João Rufino, Luis Silva, João Almeida, Bruno Miguel Fernandes Silva, Joaquim Ferreira, and José Fonseca. Towards Personal Virtual Traffic Lights. *Information*, 10(1):32, January 2019.

[225] Martin Mauve and Björn Scheuermann. VANET Convenience and Efficiency Applications. In *VANET*, chapter 4, pages 81–106. John Wiley & Sons, Ltd, 2010.

[226] Sebastiaan Meijer and Gert Jan Hofstede. Simulation games for improving the human orientation of production management. In *IFIP WG 5.7 Working Conference on Human Aspects in Production Management, October 5-9, 2003, Karlsruhe*. Shaker Verlag, 2003.

[227] A. Mejdoubi, H. Fouchal, O. Zytoune, and M. Ouadou. A Distributed Predictive Road Traffic Management System in Urban VANETs. In *2019 15th International Wireless Communications Mobile Computing Conference (IWCMC)*, pages 37–42, June 2019.

[228] P. Merdrignac, O. Shagdar, and F. Nashashibi. Fusion of Perception and V2P Communication Systems for the Safety of Vulnerable Road Users. *IEEE Transactions on Intelligent Transportation Systems*, 18(7):1740–1751, July 2017.

[229] Max-Arno Meyer, Christian Granrath, Günter Feyerl, Johannes Richenhagen, Jakob Kaths, and Jakob Andert. Closed-loop platoon simulation with cooperative intelligent transportation systems based on vehicle-to-X communication. *Simulation Modelling Practice and Theory*, 106:102173, January 2021.

[230] E. Mintsis, E. I. Vlahogianni, E. Mitsakis, and S. Ozkul. Evaluation of a cooperative speed advice service implemented along an urban arterial corridor. In *2017 5th IEEE International Conference on Models and Technologies for Intelligent Transportation Systems (MT-ITS)*, pages 232–237, June 2017.

[231] Evangelos Mintsis, Eleni I. Vlahogianni, Evangelos Mitsakis, and Seckin Ozkul. Enhanced speed advice for connected vehicles in the proximity of signalized intersections. *European Transport Research Review*, 13(1):2, January 2021.

[232] Asier Moreno, Enrique Onieva, Asier Perallos, Giovanni Iovino, and Pablo Fernández. Cooperative Decision-Making ITS Architecture Based on Distributed RSUs. In Juan M. García-Chamizo, Giancarlo Fortino, and Sergio F. Ochoa, editors, *Ubiquitous Computing and Ambient Intelligence. Sensing, Processing, and Using Environmental Information*, Lecture Notes in Computer Science, pages 84–90, Cham, 2015. Springer International Publishing.

[233] Boubakeur Moussaoui, Salah Merniz, Hacène Fouchal, and Marwane Ayaida. Routing over VANET in Urban Environments. In Günter Fahrnberger, Gerald Eichler, and Christian Erfurth, editors, *Innovations for Community Services*, Communications in Computer and Information Science, pages 143–152, Cham, 2016. Springer International Publishing.

[234] A. Mukhopadhyay and V. A. Bharadwaj. V2X based Road Safety Improvement in Blind Intersections. In *2020 Second International Conference on Inventive Research in Computing Applications (ICIRCA)*, pages 964–968, July 2020.

[235] John F. Nash. Equilibrium points in n-person games. *Proceedings of the National Academy of Sciences*, 36(1):48–49, January 1950.

[236] Meysam Nasimi, Mohammad Asif Habibi, and Hans D. Schotten. Platoon–assisted Vehicular Cloud in VANET: Vision and Challenges. *arXiv:2008.10928 [cs, eess]*, August 2020.

[237] Engineering National Academies of Sciences, and Medicine (U.S.) and Transportation Research Board. *Highway Capacity Manual: A Guide for Multimodal Mobility Analysis*. Transportation Research Board, Washington, D.C, 2016.

[238] National Research Council. *The Drama of the Commons*. National Academies Press, Washington, D.C., February 2002.

[239] Daniel B. Neill. Cooperation and coordination in the turn-taking dilemma. In *Proceedings of the 9th Conference on Theoretical Aspects of Rationality and Knowledge*, TARK '03, pages 231–244, New York, NY, USA, June 2003. Association for Computing Machinery.

[240] Daiheng Ni. Chapter 14 - general motors models. In Daiheng Ni, editor, *Traffic Flow Theory*, pages 197–212. Butterworth-Heinemann, 2016.

[241] Daiheng Ni. Chapter 2 - traffic flow characteristics I. In Daiheng Ni, editor, *Traffic Flow Theory*, pages 19–35. Butterworth-Heinemann, 2016.

[242] Daiheng Ni. Chapter 4 - equilibrium traffic flow models. In Daiheng Ni, editor, *Traffic Flow Theory*, pages 51–71. Butterworth-Heinemann, 2016.

[243] J. Nicolaisen, V. Petrov, and L. Tesfatsion. Market power and efficiency in a computational electricity market with discriminatory double-auction pricing. *IEEE Transactions on Evolutionary Computation*, 5(5):504–523, October 2001.

[244] Ko Nishihara. A Resolution of N-Person Prisoners' Dilemma. *Economic Theory*, 10(3):531–540, 1997.

[245] Ko Nishihara. Stability of the Cooperative Equilibrium in N-Person Prisoners' Dilemma with Sequential Moves. *Economic Theory*, 13(2):483–494, 1999.

[246] Mohammed Obaid and Zsolt Szalay. A Novel Model Representation Framework for Cooperative Intelligent Transport Systems. *Periodica Polytechnica Transportation Engineering*, 48(1):39–44, 2020.

[247] Kennedy John Offor, Lubos Vaci, and Lyudmila S. Mihaylova. Traffic Estimation for Large Urban Road Network with High Missing Data Ratio. *Sensors*, 19(12):2813, January 2019.

[248] Akira Okada. The Possibility of Cooperation in an N-Person Prisoners' Dilemma with Institutional Arrangements. *Public Choice*, 77(3):629–656, 1993.

[249] Renê Oliveira, Carlos Montez, Azzedine Boukerche, and Michelle S. Wangham. Reliable data dissemination protocol for VANET traffic safety applications. *Ad Hoc Networks*, 63:30–44, August 2017.

[250] Susan Oyama. Innate selfishness, innate sociality. *Behavioral and Brain Sciences*, 12(4):717–718, December 1989.

[251] P. K. Pandey, A. Swaroop, and V. Kansal. A Concise Survey on Recent Routing Protocols for Vehicular Ad hoc Networks (VANETs). In *2019 International Conference on Computing, Communication, and Intelligent Systems (ICCCIS)*, pages 188–193, October 2019.

[252] Anirudh Paranjothi, Mohammad S. Khan, and Sherali Zeadally. Survey on Congestion Detection and Control in Connected Vehicles. *Ad Hoc Networks*, 108:102277, November 2020.

[253] L. Pariota, L. D. Costanzo, A. Coppola, C. D'Aniello, and G. N. Bifulco. Green Light Optimal Speed Advisory: A C-ITS to improve mobility and pollution. In *2019 IEEE International Conference on Environment and Electrical Engineering and 2019 IEEE Industrial and Commercial Power Systems Europe (EEEIC / I CPS Europe)*, pages 1–6, June 2019.

[254] Anand Paul, Naveen Chilamkurti, Alfred Daniel, and Seungmin Rho. *Intelligent Vehicular Networks and Communications: Fundamentals, Architectures and Solutions*. Elsevier, Amsterdam Boston Heidelberg, 2017.

[255] T. Petrov, M. Dado, K. E. Ambrosch, and P. Holečko. Experimental topology for V2V communication based on Internet of Things. In *2016 ELEKTRO*, pages 72–76, May 2016.

[256] A. C. Pigou. *The Economics of Welfare*. Macmillan and Co., London, 1920.

[257] K. N. Porfyri, A. Kotsi, and E. Mitsakis. A microsimulation approach for the impact assessment of a Vehicle-to-Infrastructure based Road Hazard Warning system. In *2019 IEEE Intelligent Transportation Systems Conference (ITSC)*, pages 4443–4448, October 2019.

[258] Liqiang Qiao, Yan Shi, Shanzhi Chen, and Wei Gao. Modeling and Analysis of Safety Messages Propagation in Platoon-Based Vehicular Cyber-Physical Systems. *Wireless Communications and Mobile Computing*, 2018:e5641258, February 2018.

[259] Kashif Naseer Qureshi, Farooq Ul Islam, Omprakash Kaiwartya, Arvind Kumar, and Jaime Lloret. Improved Road Segment-Based Geographical Routing Protocol for Vehicular Ad-hoc Networks. *Electronics*, 9(8):1248, August 2020.

[260] Muddasir Rahim, Muhammad Awais Javed, Ahmad Naseem Alvi, and Muhammad Imran. An efficient caching policy for content retrieval in autonomous connected vehicles. *Transportation Research Part A: Policy and Practice*, 140:142–152, October 2020.

[261] A. U. Rahman, Y. Gupta, and G. Ghatak. On the Characterization of V2V Link Performance in Highway Vehicular Networks. In *2020 IEEE 3rd 5G World Forum (5GWF)*, pages 442–447, September 2020.

[262] G. Raja, A. Ganapathisubramaniyan, M. S. Selvakumar, T. Ayyarappan, and K. Mahadevan. Cognitive Intelligent Transportation System for Smart Cities. In *2018 Tenth International Conference on Advanced Computing (ICoAC)*, pages 146–152, December 2018.

[263] M. Randriamasy, A. Cabani, H. Chafouk, and G. Fremont. Reliable vehicle location in electronic toll collection service with cooperative intelligent transportation systems. In *2017 IEEE 28th Annual International Symposium on Personal, Indoor, and Mobile Radio Communications (PIMRC)*, pages 1–7, October 2017.

[264] Amnon Rapoport, Eyran J. Gisches, Terry Daniel, and Robin Lindsey. Pre-trip information and route-choice decisions with stochastic travel conditions: Experiment. *Transportation Research Part B: Methodological*, 68:154–172, October 2014.

[265] Asim Rasheed, Saira Gillani, Sana Ajmal, and Amir Qayyum. Vehicular Ad Hoc Network (VANET): A Survey, Challenges, and Applications. In Anis Laouiti, Amir Qayyum, and Mohamad Naufal Mohamad Saad, editors, *Vehicular Ad-Hoc Networks for Smart Cities*, Advances in Intelligent Systems and Computing, pages 39–51, Singapore, 2017. Springer.

[266] S. Abduljabbar Rashid, l Audah, M. Maad Hamdi, and S. Alani. An Overview on Quality of Service and Data Dissemination in VANETs. In *2020 International Congress on Human-Computer Interaction, Optimization and Robotic Applications (HORA)*, pages 1–5, June 2020.

[267] Mari Rege and Kjetil Telle. The impact of social approval and framing on cooperation in public good situations. *Journal of Public Economics*, 88(7):1625–1644, July 2004.

[268] Madlen Ringhand and Mark Vollrath. Make this detour and be unselfish! Influencing urban route choice by explaining traffic management. *Transportation Research Part F: Traffic Psychology and Behaviour*, 53:99–116, February 2018.

[269] Craig L. Robinson. Efficient Application Level Message Coding and Composition. In *VANET*, chapter 8, pages 273–297. John Wiley & Sons, Ltd, 2010.

[270] M. Röckl and P. Robertson. Data Dissemination in Cooperative ITS from an Information-Centric Perspective. In *2010 IEEE International Conference on Communications*, pages 1–6, May 2010.

[271] V. Díez Rodríguez, J. Detournay, A. Vinel, and N. Lyamin. An Approach for Receiver-Side Awareness Control in Vehicular Ad Hoc Networks. *IEEE Transactions on Intelligent Transportation Systems*, 19(4):1227–1236, April 2018.

[272] Roger P. Roess and Elena S. Prassas. The Fundamental Concept of Capacity. In Roger . P Roess and Elena . S Prassas, editors, *The Highway Capacity Manual: A Conceptual and Research History: Volume 1: Uninterrupted Flow*, Springer Tracts on Transportation and Traffic, pages 27–47. Springer International Publishing, Cham, 2014.

[273] Roger P. Roess and Elena S. Prassas. The Fundamental Concept of Level of Service. In Roger . P Roess and Elena . S Prassas, editors, *The Highway Capacity Manual: A Conceptual and Research History: Volume 1: Uninterrupted Flow*, Springer Tracts on Transportation and Traffic, pages 49–76. Springer International Publishing, Cham, 2014.

[274] M. Rondinone, T. Walter, R. Blokpoel, and J. Schindler. V2X Communications for Infrastructure-Assisted Automated Driving. In *2018 IEEE 19th International Symposium on "A World of Wireless, Mobile and Multimedia Networks" (WoWMoM)*, pages 14–19, June 2018.

[275] Óscar Rosas-Jaimes and Luis Alvarez-Icaza. Density and Velocity Estimation in Traffic Flow. *IFAC Proceedings Volumes*, 38(1):144–149, January 2005.

[276] Rosaldo J. F Rossetti, Rafael H Bordini, Ana L. C Bazzan, Sergio Bampi, Ronghui Liu, and Dirck Van Vliet. Using BDI agents to improve driver modelling in a commuter scenario. *Transportation Research Part C: Emerging Technologies*, 10(5):373–398, October 2002.

[277] Rosaldo J. F. Rossetti and Ronghui Liu. An Agent-Based Approach to Assess Drivers' Interaction with Pre-Trip Information Systems. *Journal of Intelligent Transportation Systems*, 9(1):1–10, March 2005.

[278] Alvin E. Roth and Ido Erev. Learning in extensive-form games: Experimental data and simple dynamic models in the intermediate term. *Games and Economic Behavior*, 8(1):164–212, January 1995.

[279] Casey G. Rothschild. The evolution of reciprocity in sizable human groups. *Journal of Theoretical Biology*, 257(4):609–617, April 2009.

[280] Tim Roughgarden. *Selfish Routing and the Price of Anarchy*. MIT Press, Cambridge, Mass, 2005.

[281] Intae Ryoo, Wonshik Na, and Seokhoon Kim. Information exchange architecture based on software defined networking for cooperative intelligent transportation systems. *Cluster Computing*, 18(2):771–782, June 2015.

[282] M. S and S. P. Performance Comparison of Communication Technologies for V2X Applications. In *2020 5th International Conference on Communication and Electronics Systems (ICCES)*, pages 356–362, June 2020.

[283] A. H. Sakr, G. Bansal, V. Vladimerou, and M. Johnson. Lane Change Detection Using V2V Safety Messages. In *2018 21st International Conference on Intelligent Transportation Systems (ITSC)*, pages 3967–3973, November 2018.

[284] Norman Salazar, Juan A. Rodriguez-Aguilar, Josep Ll. Arcos, Ana Peleteiro, and Juan C. Burguillo-Rial. Emerging cooperation on complex networks. In *The 10th International Conference on Autonomous Agents and Multiagent Systems - Volume 2*, AAMAS '11, pages 669–676, Richland, SC, May 2011. International Foundation for Autonomous Agents and Multiagent Systems.

[285] H. H. Saleh and S. T. Hasson. A Survey of Routing Algorithms in Vehicular Networks. In *2019 International Conference on Advanced Science and Engineering (ICOASE)*, pages 159–164, April 2019.

[286] R. J. Salter. The relationship between speed, flow and density of a highway traffic stream. In R. J. Salter, editor, *Highway Traffic Analysis and Design*, pages 119–130. Macmillan Education UK, London, 1996.

[287] Ghassan Samara. Intelligent Reputation System for Safety Messages in VANET. *IAES International Journal of Artificial Intelligence (IJ-AI)*, 9(3):439, September 2020.

[288] Julio A. Sanguesa, Manuel Fogue, Piedad Garrido, Francisco J. Martinez, Juan-Carlos Cano, Carlos T. Calafate, and Pietro Manzoni. RTAD: A real-time adaptive dissemination system for VANETs. *Computer Communications*, 60:53–70, April 2015.

[289] José-Antonio Santos, Alberto Fernández, Mar Moreno-Rebato, Holger Billhardt, José-A. Rodríguez-García, and Sascha Ossowski. Legal and ethical implications of applications based on agreement technologies: The case of auction-based road intersections. *Artificial Intelligence and Law*, 28(4):385–414, December 2020.

[290] Thomas C. Schelling. Hockey Helmets, Concealed Weapons, and Daylight Saving: A Study of Binary Choices with Externalities. *The Journal of Conflict Resolution*, 17(3):381–428, 1973.

[291] E. Schoch, F. Kargl, M. Weber, and T. Leinmuller. Communication patterns in VANETs. *IEEE Communications Magazine*, 46(11):119–125, November 2008.

[292] Johan Scholliers, Marcel van Sambeek, and Kees Moerman. Integration of vulnerable road users in cooperative ITS systems. *European Transport Research Review*, 9(2):15, March 2017.

[293] R. Selten, T. Chmura, T. Pitz, S. Kube, and M. Schreckenberg. Commuters route choice behaviour. *Games and Economic Behavior*, 58(2):394–406, February 2007.

[294] M. Seredynski and F. Viti. A survey of cooperative ITS for next generation public transport systems. In *2016 IEEE 19th International Conference on Intelligent Transportation Systems (ITSC)*, pages 1229–1234, November 2016.

[295] Cosma Rohilla Shalizi. Methods and Techniques of Complex Systems Science: An Overview. In Thomas S. Deisboeck and J. Yasha Kresh, editors, *Complex Systems Science in Biomedicine*, Topics in Biomedical Engineering International Book Series, pages 33–114. Springer US, Boston, MA, 2006.

[296] Wenlong Shang, Ke Han, Washington Ochieng, and Panagiotis Angeloudis. Agent-based day-to-day traffic network model with information percolation. *Transportmetrica A: Transport Science*, 13(1):38–66, January 2017.

[297] A. Sharma and L. K. Awasthi. A Comparative Survey on Information Dissemination in Heterogeneous Vehicular Communication Networks. In *2018 First International Conference on Secure Cyber Computing and Communication (ICSCCC)*, pages 556–560, December 2018.

[298] Surbhi Sharma and Baijnath Kaushik. A survey on internet of vehicles: Applications, security issues & solutions. *Vehicular Communications*, 20:100182, December 2019.

[299] Yossi Sheffi. *Urban Transportation Networks: Equilibrium Analysis With Mathematical Programming Methods*. Prentice Hall, Englewood Cliffs, NJ, USA, 1984.

[300] Prashant Kumar Shrivastava, Priya Srivastava, and Dr Rachana Dubey. Detailed Study On Data Dissemination with Cluster-based Data Dissemination in VANET. 8(10):5, 2019.

[301] Pranav Kumar Singh, Sunit Kumar Nandi, and Sukumar Nandi. A tutorial survey on vehicular communication state of the art, and future research directions. *Vehicular Communications*, 18:100164, August 2019.

[302] Alexander Smith. Group composition and conditional cooperation. *The Journal of Socio-Economics*, 40(5):616–622, October 2011.

[303] G. S. Snoddy. Learning and stability: A psychophysiological analysis of a case of motor learning with clinical applications. *Journal of Applied Psychology*, 10(1):1–36, 1926.

[304] G. Soatti, M. Nicoli, N. Garcia, B. Denis, R. Raulefs, and H. Wymeersch. Enhanced vehicle positioning in cooperative ITS by joint sensing of passive features. In *2017 IEEE 20th International Conference on Intelligent Transportation Systems (ITSC)*, pages 1–6, October 2017.

[305] Sripada Soumya and V. A. Sankar Ponnapalli. A Survey—Vanets and Protocols. In Amit Kumar, Marcin Paprzycki, and Vinit Kumar Gunjan, editors, *ICDSMLA 2019*, Lecture Notes in Electrical Engineering, pages 413–419, Singapore, 2020. Springer.

[306] Pietro Spadaccino, Francesca Cuomo, and Andrea Baiocchi. Epidemic and Timer-Based Message Dissemination in VANETs: A Performance Comparison. *Electronics*, 9(4):595, April 2020.

[307] M. Srotyr, T. Zelinka, and Z. Lokaj. Hybrid communication solution for C-ITS and its evaluation. In *2017 Smart City Symposium Prague (SCSP)*, pages 1–7, May 2017.

[308] Hans-Ulrich Stark. Dilemmas of Partial Cooperation. *Evolution*, 64(8):2458–2465, 2010.

[309] Ulrich Stark, Dirk Helbing, Martin Schönhof, Janusz Hołyst, Hans-Ulrich Stark, and Janusz Lyst. Alternating cooperation strategies in a Route Choice Game: Theory, experiments, and effects of a learning scenario. pages 256–273, January 2008.

[310] D. Su and S. Ahn. Autonomous platoon formation for VANET-enabled vehicles. In *2016 International Conference on Information and Communication Technology Convergence (ICTC)*, pages 247–250, October 2016.

[311] Junjie Sun and Leigh Tesfatsion. Dynamic Testing of Wholesale Power Market Designs: An Open-Source Agent-Based Framework. *Computational Economics*, 30(3):291–327, October 2007.

[312] Ling Sun, Yameng Li, and Jian Gao. Architecture and Application Research of Cooperative Intelligent Transport Systems. *Procedia Engineering*, 137:747–753, January 2016.

[313] M. Szilagyi. An Investigation of N-person Prisoners' Dilemmas. *Complex Syst.*, 2003.

[314] Miklos N. Szilagyi. Investigation of N-Person Games by Agent-Based Modeling. *Complex Systems*, 21(3):201–243, October 2012.

[315] Seji Takanashi and Makoto Yokoo. Two-stage N-person Prisoner's Dilemma with Social Preferences. In *Proceedings of the 18th International Conference on Autonomous Agents and MultiAgent Systems*, AAMAS '19, pages 2206–2208, Richland, SC, May 2019. International Foundation for Autonomous Agents and Multiagent Systems.

[316] Jun Tanimoto. Social Dilemma Analysis for Modeling Traffic Flow. In Jun Tanimoto, editor, *Evolutionary Games with Sociophysics: Analysis of Traffic Flow and Epidemics*, Evolutionary Economics and Social Complexity Science, pages 105–154. Springer, Singapore, 2018.

[317] Jun Tanimoto, Shinji Kukida, and Aya Hagishima. Social dilemma structures hidden behind traffic flow with lane changes. *Journal of Statistical Mechanics: Theory and Experiment*, 2014:P07019, July 2014.

[318] Jun Tanimoto and Hiroki Sagara. A study on emergence of alternating reciprocity in a 2×2 game with 2-length memory strategy. *Biosystems*, 90(3):728–737, November 2007.

[319] Michael Taylor. *The Possibility of Cooperation*. Studies in Rationality and Social Change. Cambridge Univ. Press [u.a.], Cambridge, repr edition, 1997.

[320] A. I. TEI, Z. DOUKHA, and Y. ZAFOUNE. Multi-criteria-based relay election for Data Dissemination in urban VANET. In *2019 International Conference on Theoretical and Applicative Aspects of Computer Science (ICTAACS)*, volume 1, pages 1–8, December 2019.

[321] L. H. Teixeira and Á Huszák. Preemptive Network Selection for V2V Communication. In *2019 42nd International Conference on Telecommunications and Signal Processing (TSP)*, pages 436–439, July 2019.

[322] L. H. Teixeira and Á Huszák. Service-based Interface Selection Scheme for V2V Network Communication. In *IEEE EUROCON 2019 -18th International Conference on Smart Technologies*, pages 1–6, July 2019.

[323] Dušan Teodorović and Milan Janić. Chapter 4 - Traffic Flow Theory. In Dušan Teodorović and Milan Janić, editors, *Transportation Engineering*, pages 163–196. Butterworth-Heinemann, January 2017.

[324] Dušan Teodorović and Milan Janić. Chapter 5 - Capacity and Level of Service. In Dušan Teodorović and Milan Janić, editors, *Transportation Engineering*, pages 197–292. Butterworth-Heinemann, January 2017.

[325] G. Thandavarayan, M. Sepulcre, and J. Gozalvez. Analysis of Message Generation Rules for Collective Perception in Connected and Automated Driving. In *2019 IEEE Intelligent Vehicles Symposium (IV)*, pages 134–139, June 2019.

[326] Edward L. Thorndike. *Animal Intelligence: Experimental Studies*. The Macmillan company, New York, 1911.

[327] C.-K. Toh. *Ad Hoc Wireless Networks: Protocols and Systems*. Prentice Hall PTR, USA, 1st edition, 2001.

[328] Ravi Tomar, Manish Prateek, and Hanumat G.Sastry. Simulation of Information Dissemination using Flooding in VANET. *Journal of Communications Technology, Electronics and Computer Science*, 19(0):1–4, October 2018.

[329] Ravi Tomar, Hanumat G. Sastry, and Manish Prateek. A Novel Protocol for Information Dissemination in Vehicular Networks. In Ching-Hsien Hsu, Sondès Kallel, Kun-Chan Lan, and Zibin Zheng, editors, *Internet of Vehicles. Technologies and Services Toward Smart Cities*, Lecture Notes in Computer Science, pages 1–14, Cham, 2020. Springer International Publishing.

[330] Y. Toor, P. Muhlethaler, A. Laouiti, and A. D. La Fortelle. Vehicle Ad Hoc networks: Applications and related technical issues. *IEEE Communications Surveys Tutorials*, 10(3):74–88, Third 2008.

[331] Kagan Tumer, Zachary T. Welch, and A. Agogino. Traffic congestion management as a learning agent coordination problem. In *Multi-Agent Systems for Traffic and Transportation Engineering*, 2009.

[332] United Nations, Department of Economic and Social Affairs, Population Division. *World Urbanization Prospects: The 2018 Revision*. 2019.

[333] Odilbek Urmonov and HyungWon Kim. A Multi-Hop Data Dissemination Algorithm for Vehicular Communication. *Computers*, 9(2):25, June 2020.

[334] Eric van Dijk. Social Dilemmas, Psychology of. In James D. Wright, editor, *International Encyclopedia of the Social & Behavioral Sciences (Second Edition)*, pages 245–249. Elsevier, Oxford, January 2015.

[335] Mariska van Essen, Tom Thomas, Eric van Berkum, and Caspar Chorus. From user equilibrium to system optimum: A literature review on the role of travel information, bounded rationality and non-selfish behaviour at the network and individual levels. *Transport Reviews*, 36(4):527–548, July 2016.

[336] Paul A. M. Van Lange, Jeff Joireman, Craig D. Parks, and Eric Van Dijk. The psychology of social dilemmas: A review. *Organizational Behavior and Human Decision Processes*, 120(2):125–141, March 2013.

[337] N. Varga, L. Bokor, A. Takács, J. Kovács, and L. Virág. An architecture proposal for V2X communication-centric traffic light controller systems. In *2017 15th International Conference on ITS Telecommunications (ITST)*, pages 1–7, May 2017.

[338] V. Vibin, P. Sivraj, and V. Vanitha. Implementation of In-Vehicle and V2V Communication with Basic Safety Message Format. In *2018 International Conference on Inventive Research in Computing Applications (ICIRCA)*, pages 637–642, July 2018.

[339] R. Vilalta, R. Casellas, R. Sedar, F. Vázquez-Gallego, R. Martínez, S. K. Datta, M. Lefebvre, F. Gardes, J.-M. Odinot, J. Härri, J. Alonso-Zarate, and R. Muñoz. Vehicular Message Exchange in Cross-border Scenarios Using Public Cloud Infrastructure. In *2020 IEEE 3rd 5G World Forum (5GWF)*, pages 251–256, September 2020.

[340] A. Vinel, N. Lyamin, and P. Isachenkov. Modeling of V2V Communications for C-ITS Safety Applications: A CPS Perspective. *IEEE Communications Letters*, 22(8):1600–1603, August 2018.

[341] Jana Vyrastekova and Yukihiko Funaki. Cooperation in a sequential N-person prisoner's dilemma: The role of information and reciprocity, October 2010.

[342] J. Wahle and M. Schreckenberg. Information in Intelligent Transportation System. In Heike Emmerich, Britta Nestler, and Michael Schreckenberg, editors, *Interface and Transport Dynamics*, Lecture Notes in Computational Science and Engineering, pages 301–316, Berlin, Heidelberg, 2003. Springer.

[343] Joachim Wahle, Ana Lúcia C Bazzan, Franziska Klügl, and Michael Schreckenberg. The impact of real-time information in a two-route scenario using agent-based simulation. *Transportation Research Part C: Emerging Technologies*, 10(5):399–417, October 2002.

[344] S. Wang, T. Wang, and S. Wang. Effective gateway association schemes for performance improvement of V2I communications in heterogeneous vehicular networks. In *2017 IEEE/CIC International Conference on Communications in China (ICCC)*, pages 1–4, October 2017.

[345] J G Wardrop. Some theoretical aspects of road traffic research. *Proceedings of the Institution of Civil Engineers*, 1(3):325–362, May 1952.

[346] Anke Weidlich and Daniel Veit. A critical survey of agent-based wholesale electricity market models. *Energy Economics*, 30(4):1728–1759, July 2008.

[347] Roman L. Weil. The N-person Prisoner's dilemma: Some theory and a computer-oriented approach. *Behavioral Science*, 11(3):227–234, 1966.

[348] W. K. Wolterink, G. Heijenk, and G. Karagiannis. Constrained geocast to support Cooperative Adaptive Cruise Control (CACC) merging. In *2010 IEEE Vehicular Networking Conference*, pages 41–48, December 2010.

[349] N. Yakusheva, A. Proletarsky, and M. Basarab. Implemented Vehicular Communication Systems: Overview and Comparative Analysis. In *2019 27th Telecommunications Forum (TELFOR)*, pages 1–4, November 2019.

[350] N. Yakusheva, A. Proletarsky, and M. Basarab. State of the art and trends of Vehicle Communication: Overview. In *2019 27th Telecommunications Forum (TELFOR)*, pages 1–4, November 2019.

[351] Xin Yao and Paul J. Darwen. An Experimental Study of N-Person Iterated Prisoner's Dilemma Games. *Informatica*, 18:435–450, 1994.

[352] Alisson Yury, Everaldo Andrade, Michele Nogueira, Aldri Santos, and Fernando Matos. Social-based Cooperation of Vehicles for Data Dissemination of Critical Urban Events. *arXiv:2009.04315 [cs]*, September 2020.

[353] M. M. Zanjireh and H. Larijani. A Survey on Centralised and Distributed Clustering Routing Algorithms for WSNs. In *2015 IEEE 81st Vehicular Technology Conference (VTC Spring)*, pages 1–6, May 2015.

[354] S. Zeadally, J. Guerrero, and J. Contreras. A tutorial survey on vehicle-to-vehicle communications. *Telecommunication Systems*, 73(3):469–489, March 2020.

[355] S. Zeadally, M. A. Javed, and E. B. Hamida. Vehicular Communications for ITS: Standardization and Challenges. *IEEE Communications Standards Magazine*, 4(1):11–17, March 2020.

[356] Sherali Zeadally, Ray Hunt, Yuh-Shyan Chen, Angela Irwin, and Aamir Hassan. Vehicular ad hoc networks (VANETS): Status, results, and challenges. *Telecommunication Systems*, 50(4):217–241, August 2012.

[357] Chunbo Zhang, Nasser R. Sabar, Edward Chung, Ashish Bhaskar, and Xiucheng Guo. Optimisation of lane-changing advisory at the motorway lane drop bottleneck. *Transportation Research Part C: Emerging Technologies*, 106:303–316, September 2019.

[358] Kailong Zhang, Ce Xie, Yujia Wang, Min Wang, Arnaud De La Fortelle, Weibin Zhang, and Zongtao Duan. Service-Oriented Cooperation Policies for Intelligent Ground Vehicles Approaching Intersections. *Applied Sciences*, 8(9):1647, September 2018.

[359] M. Zhang and R. S. Wolff. Routing protocols for vehicular Ad Hoc networks in rural areas. *IEEE Communications Magazine*, 46(11):126–131, November 2008.

[360] Feng Zhu and Satish V. Ukkusuri. Efficient and fair system states in dynamic transportation networks. *Transportation Research Part B: Methodological*, 104:272–289, October 2017.

[361] Markus Zimmermann, David Schopf, Niklas Lütteken, Zhengzhenni Liu, Konrad Storost, Martin Baumann, Riender Happee, and Klaus J. Bengler. Carrot and stick: A game-theoretic approach to motivate cooperative driving through social interaction. *Transportation Research Part C: Emerging Technologies*, 88:159–175, March 2018.

[362] Johannes Zschache. *The Matching Law and Melioration Learning: From Individual Decision-Making to Social Interaction*. PhD thesis, January 2017.